

**The archaeology of the lower Sundays River
Valley, Eastern Cape Province, South Africa: an
assessment of Earlier Stone Age alluvial terrace
sites**

Matt Geoffrey Lotter

A thesis submitted to the Faculty of Science, University of the Witwatersrand,
Johannesburg, in fulfillment of the requirements for the degree of Doctor of
Philosophy

Johannesburg, 2016

Declaration

I declare that this thesis is my own, unaided work, except where otherwise acknowledged. It is being submitted for the Degree of Doctor of Philosophy at the University of the Witwatersrand, Johannesburg. It has not been submitted before for any degree or examination at any other university.

Signed this ____ day of _____ 20 ____

Matt Geoffrey Lotter

Abstract

The lower Sundays River Valley, within the Eastern Cape Province of South Africa, has featured in a range of papers over the last century. A large portion of these focuses on improving our understanding of a series of river terraces that border the present channel. Earlier Stone Age (ESA) artefacts were first noted to occur in these deposits in the 1950s, but since this initial research there has been no attempt to investigate these further.

Our understanding of the Eastern Cape's early archaeology is poor and this can be attributed to a lack of research. Only a single ESA site, Amanzi Springs, has been fully excavated for the entire province, and although the artefacts here provide some indication as to what characterises this region's early archaeology, the significance of this site is limited by our inability to date it. Well-dated ESA sites are thus completely absent in the Eastern Cape.

More recently, a study has provided a series of dates for the Sundays River terraces. Most importantly, this research confirmed the presence of these ESA – more specifically Acheulean – artefacts within three of these dated deposits, namely: Atmar Farm dated to 0.65 ± 0.12 Ma (millions of years ago), Bernol Farm dated to 1.14 ± 0.2 Ma, and Penhill Farm date to $<1.37 \pm 0.16$ Ma and more recently constrained by this research to $>0.485 \pm 0.051$ Ma. Accordingly, it has been the purpose of this research to investigate these deposits through both survey and excavation, and to provide details on this archaeology.

This research thus provides the first ever comprehensively described and dated ESA sites for this region, and from this we can now begin to construct our understanding of the local Acheulean Tradition. This research also provides a contextual assessment for the formation of these deposits and what processes have influenced their formation and modification. Furthermore, from the detailed analysis of the artefacts, we can begin to understand the strategies employed in their production.

Our investigations have shown that largely different contextual conditions are present at each of the three sites. This has had significant impacts on the integrity of these assemblages, and the preservation and retention of assemblage components are highly variable between them. All of the artefact assemblages show the following characteristics: simple strategies in core reduction, low levels of reduction in both cores and formal tools, simple and expedient production of retouched artefacts with little emphasis on careful edge modification, and large cutting tools (LCTs) that are flaked bifacially but have limited shaping overall.

For the first time in half a century our research now provides comparative material from three dated sites that can be used to help understand variability in the local Acheulean Tradition. This has important implications for not only the Eastern Cape, but also to sites elsewhere in the interior.

Acknowledgements

This research was only made possible by the significant contributions of others. I am indebted to the people mentioned here and I thank you all sincerely, from the bottom of my heart, for the role you have played in my life over the last few years.

First and foremost I would like to thank my family. You have all been so supportive of my desires to study further and to follow my passion. I cannot thank you enough for this, and your encouragement and interest in my work has helped me to get through some of the most challenging times, of which there have been many!

To my partner, Nicole, I cannot even begin to describe how grateful I am to have you in my life. Not only have you been fully supportive of my research, but you have also provided me with invaluable advice throughout the duration of my studies at Wits. I have never come across another person who is able to see the solution in the problem as quickly as you do, and had it not been for your wise words of wisdom over the last few years I would still be trying to complete this work. I thank you for standing by me through both the easy and difficult times.

To my supervisor, Kathy, thank you for all of your patience, guidance and encouragement. Thank you for sharing your knowledge and thank you for all of your hard work. I am so happy we had the opportunity to work together over the last few years and you have taught me an invaluable set of skills. Thank you for leading by example and for sharing your passion.

To Ryan Gibbon and Darryl Granger, had it not been for your initial encouragement this study would not have happened. Thank you for helping us set up this project and for your invaluable input, both in and out of the field. Ryan, thank you for all your advice and assistance over the last few years.

A very special mention must be given to Kudu Ridge. Brian, Jenny and Andrew (and all the pets), words cannot begin to express my gratitude. Thank you for letting me into your home and for providing me with a base from which I could conduct my

research. You allowed me to come and go as I needed, and without your gracious hospitality (and that wonderful noodle salad) I would definitely not have finished my excavations.

I have been fortunate enough to work with several very talented and inspiring researchers. I am both privileged and honoured to call these gentlemen my friends. Tim Forssman, George Leader, Dominic Stratford, Matt Caruana, Raymond Couzens and Hao Li, thank you for sharing your knowledge and for always lending a listening ear. Your advice and guidance has been indispensable. Thank you for all the laughs, discussions, braais, and ping pong battles.

The following individuals provided additional assistance: Frédéric Doucet at the Council for Geosciences (sediment analysis), Marion Bamford (phytolith and pollen analysis), Geeske Langejans (residue and use-wear analysis) and Wendy Voorvelt (artefact drawings). I would also like to thank SAHRA, ECPHRA and the Albany Museum. For assistance in the field and lab I thank Vicky Gibbon, Natasha Phillips, Teekay, Spelo, John, Sia, and Thando.

I wish to thank the landowners for allowing us onto their properties. Without your cooperation and willingness none of this would have been possible. In this regard special thanks must go to Andre and Ronel Serfontein (Atmar Farm), Adrian and Noel Walton (Bernol Farm) and Errol and Lindi Hewson (Penhill Farm).

Thank you for financial support that was provided by: the Palaeontological Scientific Trust (PAST) and its Scatterlings of Africa Programs, the National Research Foundation, the University of the Witwatersrand and the Carstens Trust.

Contents

Declaration	ii
Abstract	iii
Acknowledgements	v
Contents	vii
List of Figures	xv
List of Tables	xxiii

Chapter 1 – Introduction

1.1 Introduction to the research	1
1.2 Organisation of the thesis	5

Chapter 2 – Literature review

2.1 The Acheulean Tradition: classification, chronological trends and hominids

2.1.1 Introduction	6
2.1.2 Classification	7
2.1.2.1 Advent of Large Cutting Tools (LCTs)	7
2.1.2.2 Large flake Acheulean	9
2.1.2.3 Improved core reduction	10
2.1.3 The earliest Acheulean assemblages	11
2.1.4 Site location and distribution	13
2.1.5 Hominid ranging abilities	13
2.1.6 Controlled use of fire	14
2.1.7 Social evolution through time	14
2.1.7.1 Standardised design	14
2.1.7.2 Subsistence strategies	15
2.1.8 Acheulean hominids	16

2.2 Acheulean sites of Africa: a review

2.2.1 Introduction	18
2.2.2 Part One	19

2.2.2.1	Olduvai Gorge	23
2.2.2.2	Peninj	26
2.2.2.3	Ologesailie	29
2.2.3	Part Two	33
2.2.3.1	Canteen Kopje	36
2.2.3.2	Wonderwerk Cave	39
2.2.3.3	Amanzi Springs	42
2.2.3.4	Cave of Hearths	44
2.2.3.5	Montagu Cave	47
2.2.4	Concluding discussion	50
2.3	Localised site formation and transformation: a review of relevant deposit modification and sedimentary processes	
2.3.1	Introduction	55
2.3.2	The significance of site formation and transformation studies	55
2.3.3	Experimental research: actualistic studies	57
2.3.3.1	Assemblage size profiles	58
2.3.3.2	Artefact scatter patterns	60
2.3.3.3	Artefact spatial distribution patterns	61
	<i>Trampling disturbance</i>	62
	<i>Fluvial forces</i>	62
	<i>Aeolian processes</i>	64
	<i>Bioturbation</i>	64
	<i>Termites</i>	65
	<i>Earthworms</i>	65
	<i>Plant roots</i>	65
	<i>Burrowing animals</i>	66
	<i>Downslope dispersal</i>	66
	<i>Rain splash and sheetwash/flow erosion</i>	67
	<i>Rill and gully erosion</i>	68
	<i>Mass movement/wasting</i>	70
	<i>a. Debris flow</i>	73
	<i>b. Earth slide/flow</i>	74
	<i>The influence of sediment characteristics</i>	75
2.3.3.4	Artefact condition	75

2.4 Summary	79
--------------------	----

Chapter 3 – Study sites and methods

3.1 A history of research in the lower Sundays River Valley	
3.1.1 Introduction	80
3.1.2 An introduction to the lower Sundays River Valley	80
3.1.3 Studies on fluvial geomorphology and terrace formation, composition and description	82
3.1.3.1 A summary of the model proposed by Hattingh and Rust (1999) and Hattingh (2008) for the evolution of the Sundays River terraces	85
3.1.4 Dating of the preserved terraces	90
3.1.5 The Stone Age archaeology of the Sundays River Valley in relation to the wider Eastern Cape region	92
3.2 Study sites of the lower Sundays River Valley	
3.2.1 Introduction	96
3.2.2 Atmar Farm	96
3.2.3 Bernol Farm	101
3.2.4 Penhill Farm	105
3.3 Excavation methods	
3.3.1 Introduction	113
3.3.2 Excavations: site specifics	116
3.3.2.1 Atmar Farm	116
3.3.2.2 Bernol Farm	118
3.3.2.3 Penhill Farm	119
3.4 Lithic analysis	
3.4.1 Introduction	125
3.4.2 Typology	126
3.4.2.1 Flaking debris	126
3.4.2.2 Complete flakes (≥ 20 mm)	126
3.4.2.3 Cores (≥ 20 mm)	127
3.4.2.4 Formal tools (≥ 20 mm)	129
3.4.2.5 Other (≥ 20 mm)	131

3.4.3	Raw material classification	132
3.4.4	Artefact condition	133
3.4.5	Additional notes	134
3.4.6	Technology	134
3.4.6.1	Introduction	134
3.4.6.2	Incomplete and complete flake attributes	137
3.4.6.3	Core attributes	144
3.4.6.4	Retouched piece attributes	147
3.4.6.5	LCT attributes	152
3.4.6.6	Other attributes	156
3.4.7	Additional analysis	156
3.5	Non-lithic analysis and sampling	
3.5.1	Introduction	158
3.5.2	Sediment sampling	158
3.5.3	Dating samples	164
3.5.4	Non-lithic analysis	165
 Chapter 4 – Results		
4.1	Introduction	166
4.2	Atmar Farm	167
4.2.1	Introduction	167
4.2.2	Site context	
4.2.2.1	Artefact size distributions	167
4.2.2.2	Artefact condition and raw material data	169
4.2.3	Typology	171
4.2.4	Summary	181
4.3	Bernol Farm	
4.3.1	Introduction	182
4.3.2	Site context	182
4.3.2.1	Artefact size distributions	182
4.3.2.2	Artefact condition and raw material data	182
4.3.3	Typology	184
4.3.4	Technology	194

4.3.4.1 LCT size and shape	194
4.3.4.2 LCT reduction	197
4.3.5 Residue and use-wear analysis	203
4.3.6 Non-lithic material	204
4.3.7 Summary	205
4.4 Penhill Farm	
4.4.1 Introduction	208
4.4.2 Site context	209
4.4.2.1 Sediment PSD analysis	209
4.4.2.2 Artefact size distributions	221
4.4.2.3 Artefact condition and raw material data	225
4.4.2.4 Artefact spatial distributions	233
4.4.2.5 Artefact depositional (fabric) data	243
4.4.2.6 Debris flow dating results	247
4.4.2.7 Summary	248
4.4.3 Typology	252
4.4.3.1 Flaking debris	255
4.4.3.2 Complete flakes	259
4.4.3.3 Cores	266
4.4.3.4 Formal tools	277
<i>Scrapers</i>	284
<i>LCTs</i>	290
4.4.3.5 Other	304
4.4.3.6 Additional features	304
4.4.3.7 Summary	313
4.4.4 Technology	316
4.4.4.1 Flaking debris and complete flakes	316
<i>Flaking debris and complete flake dimensions/size</i>	317
<i>Flaking strategy</i>	324
<i>Level of reduction</i>	333
<i>Summary</i>	343
4.4.4.2 Cores	347
<i>Core dimensions/size</i>	347
<i>Flaking strategy</i>	350

<i>Level of reduction</i>	362
<i>Summary</i>	367
4.4.4.3 Formal tools	370
<i>Retouched pieces</i>	370
<i>Retouched piece dimensions/size</i>	370
<i>Flaking strategy</i>	371
<i>Level of reduction</i>	378
<i>Summary</i>	381
<i>LCTs</i>	383
<i>LCT size and shape</i>	383
<i>LCT reduction</i>	391
<i>Summary</i>	403
4.4.4.4 Modified and split cobbles (Other)	406
4.4.5 Residue and use-wear analysis	407
4.4.6 Non-lithic material	407

Chapter 5 – Discussion

5.1 Introduction	410
5.2 Atmar Farm	411
5.2.1 Site context	411
5.2.2 Typology	413
5.2.3 Final comments	415
5.3 Bernol Farm	417
5.3.1 Site context	417
5.3.2 Typology	417
5.3.3 Technology	418
5.3.3.1 LCT size and shape	418
5.3.3.2 LCT reduction	419
5.3.4 Use-wear and residue analysis	422
5.3.5 Final comments	422
5.4 Penhill Farm	423
5.4.1 Site context	423
5.4.1.1 Sediment PSD analysis	423

5.4.1.2	Artefact size distributions	424
5.4.1.3	Artefact condition and raw material data	427
5.4.1.4	Artefact spatial distributions	428
5.4.1.5	Artefact depositional (fabric) data	430
5.4.1.6	Debris flow dating results	431
5.4.1.7	Final comments	434
5.4.2	Typology	436
5.4.2.1	Flaking debris	436
5.4.2.2	Complete flakes	437
5.4.2.3	Cores	439
5.4.2.4	Formals tools	440
	<i>Scrapers</i>	441
	<i>LCTs</i>	441
5.4.2.5	Other	442
5.4.2.6	Additional features	443
5.4.3	Technology	444
5.4.3.1	Flaking debris and complete flakes	444
	<i>Flaking debris and complete flake dimensions/size</i>	444
	<i>Flaking strategy</i>	446
	<i>Level of reduction</i>	449
5.4.3.2	Cores	454
	<i>Core dimensions/size</i>	454
	<i>Flaking strategy</i>	455
	<i>Level of reduction</i>	457
5.4.3.3	Formal tools	458
	<i>Retouched pieces</i>	458
	<i>Retouched piece dimensions/size</i>	458
	<i>Flaking strategy</i>	459
	<i>Level of reduction</i>	460
	<i>LCTs</i>	461
	<i>LCT size and shape</i>	462
	<i>LCT reduction</i>	464
5.4.4	Residue and use-wear analysis	468
5.4.5	Non-lithic	468

5.4.6 Final comments	469
5.5 Atmar, Bernol and Penhill Farm inter-site comparison	470
5.5.1 Atmar and Penhill Farm artefact typology	470
5.5.2 Bernol and Penhill Farm LCT technology	473
5.6 Comparison between the lower Sundays River sites and other local and international sites	476
5.6.1 Core reduction	477
5.6.2 Retouched piece frequency and reduction	478
5.6.3 LCT frequency and reduction	480
 Chapter 6 – Final summary and conclusion	
6.1 Research question 1	486
6.1.1 Atmar Farm	487
6.1.2 Bernol Farm	487
6.1.3 Penhill Farm	488
6.2 Research question 2	491
6.2.1 Atmar Farm	492
6.2.2 Bernol Farm	493
6.2.3 Penhill Farm	494
6.2.4 Key features	500
6.3 Research question 3	500
6.4 Research question 4	503
6.5 Future work	505
 References	507
Appendices	551

List of Figures

Chapter 1

1.1:

Figure 1.1. Location of the study area, Eastern Cape Province, South Africa.	1
--	---

Chapter 2

2.2:

Figure 2.2.1. LCTs from Olduvai Gorge.	24
Figure 2.2.2. ST-69 handaxe on flake from Peninj.	28
Figure 2.2.3. Member 1 Site I3 artefacts from Olorgesailie.	31
Figure 2.2.4. Pit 6 Victoria West cores, Canteen Kopje.	37
Figure 2.2.5. Bifaces from Wonderwerk Cave, Excavation 1.	41
Figure 2.2.6. Cores and LCTs from Amanzi Springs.	43
Figure 2.2.7. A selection of handaxes and cleavers from Cave of Hearths.	46
Figure 2.2.8. LCTs from Montagu Cave, all made on quartzite.	48

2.3:

Figure 2.3.1. Gully erosion showing a cut and fill sequence.	70
Figure 2.3.2. Types of mass movement.	72
Figure 2.3.3. Classification of slope processes.	72
Figure 2.3.4. Debris flow deposits.	74

Chapter 3

3.1:

Figure 3.1.1. Important features of the lower Sundays River Valley.	82
Figure 3.1.2. Lower Sundays River Valley terraces.	84
Figure 3.1.3. Knick point development causing terrace formation.	86
Figure 3.1.4. Artistic reconstruction of the lower Sundays River Valley.	87
Figure 3.1.5. Large alluvial fan south of the Klein Winterhoek Mountains.	87
Figure 3.1.6. Preserved higher terraces west of the present Sundays River.	88
Figure 3.1.7. Lower Sundays River terrace map.	91
Figure 3.1.8. Southern African Early Acheulean sites.	93
Figure 3.1.9. Sundays and Coega River Valley sites.	93

Figure 3.1.10. ESA artefacts from a large surface site.	95
Figure 3.1.11. Artefacts recovered from the lower Sundays River Valley.	95
3.2:	
Figure 3.2.1. Study sites within the lower Sundays River Valley.	96
Figure 3.2.2. Atmar Farm site plan view.	97
Figure 3.2.3. Atmar Farm Terrace 10 exposure.	98
Figure 3.2.4. Profile of the Atmar Farm deposits from Excavation 1.	99
Figure 3.2.5. Cut and fill deposit in upper fines, Atmar Farm.	99
Figure 3.2.6. Excavation 1 west wall.	100
Figure 3.2.7. Bernol Farm site plan view.	102
Figure 3.2.8. Profile of the Bernol Farm terrace exposure.	103
Figure 3.2.9. Terrace 9 exposure at the dated location.	103
Figure 3.2.10. Survey site 4.	104
Figure 3.2.11. Survey site 2.	104
Figure 3.2.12. Penhill Farm site plan view.	106
Figure 3.2.13. Facing east, the Penhill Farm borrow pit deposit exposure.	107
Figure 3.2.14. Stratigraphic sequence at Penhill Farm.	107
Figure 3.2.15. Debris flow exposure in east face of borrow pit.	108
Figure 3.2.16. Penhill Farm Excavation 1 stratigraphic sequence.	109
Figure 3.2.17. Excavation 1 west wall square DD.	110
Figure 3.2.18. Plan view of the exposed debris flow in Excavation 1.	111
3.3:	
Figure 3.3.1. Atmar Farm Excavation 1 stepped trench.	116
Figure 3.3.2. Excavation 1 with squares A1 and A2 dropped into the gravels.	117
Figure 3.3.3. Atmar Farm test pit excavation due north of Excavation 1.	118
Figure 3.3.4. Bernol Farm test pit excavation at survey site 2.	119
Figure 3.3.5. Penhill Farm 1 X 3 m grid prior to excavation.	120
Figure 3.3.6. Excavation 1 full grid established.	122
Figure 3.3.7. Flood damage to the Penhill Farm Excavation 1.	123
Figure 3.3.8. Exposing the debris flow in square DD1, Excavation 1.	124
3.4:	
Figure 3.4.1. Technological flake measurement methods.	137
Figure 3.4.2. Flake platform measurements.	138
Figure 3.4.3. Dorsal flake scar patterns.	141

Figure 3.4.4. Flake termination types.	142
Figure 3.4.5. Technological flake classification.	143
Figure 3.4.6. Flake dorsal cortex locations.	144
Figure 3.4.7. Length, width and thickness measurement method.	144
Figure 3.4.8. Free-hand core flaking strategies.	146
Figure 3.4.9. Retouch position classification.	148
Figure 3.4.10. Retouch localisation classification.	149
Figure 3.4.11. Retouch distribution classification.	149
Figure 3.4.12. Edge delineation classification.	150
Figure 3.4.13. Retouch invasiveness.	151
Figure 3.4.14. Angle classification.	152
Figure 3.4.15. Technological measurements for LCTs.	153
Figure 3.4.16. LCT tip shape.	155
Figure 3.4.17. Butt shape.	155
Figure 3.4.18. Microscope work at the University of Johannesburg.	157
3.5:	
Figure 3.5.1. Penhill Farm Excavation 1 east wall sample locations.	161
Figure 3.5.2. Penhill Farm Excavation 1 north wall sample locations.	161
Figure 3.5.3. Penhill Farm Excavation 1 south wall sample locations.	162
Figure 3.5.4. Penhill Farm Excavation 1 west wall sample locations.	162
Figure 3.5.5. Penhill Farm borrow pit sample locations.	163
Figure 3.5.6. Penhill Farm borrow pit sample locations.	163
Figure 3.5.7. Penhill Farm samples from the surrounding area.	164
Chapter 4	
4.2:	
Figure 4.2.1. Assemblage profile for Atmar Farm.	169
Figure 4.2.2. Atmar Farm raw material types.	170
Figure 4.2.3. Atmar Farm artefact condition.	171
Figure 4.2.4. Frequency of the five different artefact types at Atmar Farm.	173
Figure 4.2.5. Percentages of the four flaking debris types at Atmar Farm.	173
Figure 4.2.6. Complete flake types.	174
Figure 4.2.7. Core type classification.	175
Figure 4.2.8. Atmar Farm cores made on quartzite cobbles.	178

Figure 4.2.9. Atmar Farm formal tools on quartzite complete flakes.	179
Figure 4.2.10. Atmar Farm LCTs, on large flakes, all poorly preserved.	180
4.3:	
Figure 4.3.1. Bernol Farm artefact raw material types.	184
Figure 4.3.2. Bernol Farm artefact preservation states.	184
Figure 4.3.3. Artefact percentages at Bernol Farm.	186
Figure 4.3.4. Boulder-core found near the dated location at Bernol Farm.	187
Figure 4.3.5. LCTs sampled from Bernol Farm.	188
Figure 4.3.6. Bernol Farm LCTs.	190
Figure 4.3.7. Handaxes from Bernol Farm, all on quartzite flake blanks.	191
Figure 4.3.8. Cleavers from Bernol Farm.	192
Figure 4.3.9. Cleavers from Bernol Farm.	193
Figure 4.3.10. Bernol Farm LCT tip shape.	197
Figure 4.3.11. Average number of flake scars, by type.	199
Figure 4.3.12. Negative flake scar termination types on the LCT assemblage.	199
Figure 4.3.13. Flaking location for the Bernol Farm LCT sample.	201
Figure 4.3.14. Percentage remaining cortex on the LCT sample.	203
Figure 4.3.15. Use-wear and residue analysis on a handaxe from Bernol Farm.	204
Figure 4.3.16. Non-lithic material obtained from Bernol Farm.	205
4.4:	
Figure 4.4.1. Particle size distribution for the alluvium.	210
Figure 4.4.2. Particle size distribution for the debris flow sediment.	212
Figure 4.4.3. Particle size distribution for the colluvium.	213
Figure 4.4.4. Particle size distribution for the channel flow sediment.	214
Figure 4.4.5. Particle size distribution for the bedrock samples.	215
Figure 4.4.6. Grain size distribution curves for the main deposits.	217
Figure 4.4.7. Alluvium grain size distribution curves in red.	218
Figure 4.4.8. Debris flow grain size distribution curves in red.	219
Figure 4.4.9. Colluvium grain size distribution curves in red.	220
Figure 4.4.10. Artefact size distribution for the colluvial assemblage.	222
Figure 4.4.11. Debris flow assemblage artefact size distribution.	223
Figure 4.4.12. Artefact size by depth for the debris flow assemblage.	224
Figure 4.4.13. Raw material percentages for the colluvial assemblage.	226
Figure 4.4.14. Debris flow assemblage raw material distribution.	228

Figure 4.4.15. Debris flow assemblage raw material changes, by depth.	229
Figure 4.4.16. Artefact condition for the ≥ 20 mm colluvial sample.	231
Figure 4.4.17. Artefact condition for the ≥ 20 mm debris flow sample.	231
Figure 4.4.18. Artefact condition for the ≥ 20 mm debris flow sample, by depth.	232
Figure 4.4.19. Number of artefacts by depth at Penhill Farm.	234
Figure 4.4.20. Artefact number by square for the debris flow assemblage.	235
Figure 4.4.21. Horizontal spatial distribution of artefacts, by size.	237
Figure 4.4.22. Horizontal spatial distribution of artefacts, by condition.	238
Figure 4.4.23. Horizontal spatial distribution of artefacts, by type.	239
Figure 4.4.24. Vertical artefact distribution by size, looking east.	240
Figure 4.4.25. Vertical artefact distribution by condition, looking east.	241
Figure 4.4.26. Vertical artefact distribution by type, looking east.	242
Figure 4.4.27. Excavation 1 artefact orientation.	245
Figure 4.4.28. Excavation 1 dip angle data.	246
Figure 4.4.29. Unrefined dating results for the Excavation 1 debris flow.	247
Figure 4.4.30. Refined dating results for the debris flow.	248
Figure 4.4.31. Colluvial assemblage artefact types.	254
Figure 4.4.32. Debris flow assemblage artefact types.	254
Figure 4.4.33. Flaking debris by type for the colluvial assemblage.	256
Figure 4.4.34. Flaking debris by type for the debris flow assemblage.	256
Figure 4.4.35. Quartzite bipolar flaking debris from the colluvial assemblage.	257
Figure 4.4.36. Quartzite bipolar flaking debris from the debris flow.	258
Figure 4.4.37. Colluvial assemblage complete flake types.	260
Figure 4.4.38. Debris flow assemblage complete flake types.	260
Figure 4.4.39. Colluvial assemblage complete flakes.	261
Figure 4.4.40. Debris flow assemblage end-struck quartzite complete flakes.	262
Figure 4.4.41. Debris flow assemblage end-struck quartzite complete flakes.	263
Figure 4.4.42. Debris flow bipolar complete flakes made on quartzite.	264
Figure 4.4.43. Debris flow assemblage large quartzite complete flakes.	265
Figure 4.4.44. Core type classification for the colluvial assemblage.	267
Figure 4.4.45. Debris flow assemblage core types.	268
Figure 4.4.46. Colluvial assemblage cores.	269
Figure 4.4.47. Colluvial assemblage cores.	270
Figure 4.4.48. Debris flow assemblage cores on cobbles.	271

Figure 4.4.49. Debris flow assemblage discoidal cores.	272
Figure 4.4.50. Debris flow assemblage chopper-cores.	273
Figure 4.4.51. Debris flow assemblage cores.	274
Figure 4.4.52. Debris flow assemblage quartzite cores.	275
Figure 4.4.53. Debris flow assemblage cores on cobbles with large scars.	276
Figure 4.4.54. Formal tool types for the colluvial assemblage.	278
Figure 4.4.55. Debris flow assemblage formal tool types.	278
Figure 4.4.56. Colluvial assemblage quartzite formal tools.	279
Figure 4.4.57. Debris flow formal tools.	280
Figure 4.4.58. Debris flow assemblage formal tools.	281
Figure 4.4.59. Debris flow assemblage denticulates.	282
Figure 4.4.60. Debris flow quartzite flake composite pieces.	283
Figure 4.4.61. Scraper types for the colluvial assemblage.	284
Figure 4.4.62. Scraper types for the debris flow assemblage.	285
Figure 4.4.63. Colluvial assemblage scrapers.	286
Figure 4.4.64. Debris flow assemblage quartzite scrapers.	287
Figure 4.4.65. Debris flow scrapers.	288
Figure 4.4.66. Debris flow scrapers.	289
Figure 4.4.67. LCT type distribution for the colluvial assemblage.	290
Figure 4.4.68. Debris flow assemblage LCT types.	291
Figure 4.4.69. Colluvial assemblage handaxe.	291
Figure 4.4.70. Colluvial assemblage LCTs.	292
Figure 4.4.71. Colluvial assemblage LCTs.	293
Figure 4.4.72. Debris flow assemblage cleavers.	294
Figure 4.4.73. Debris flow assemblage cleavers.	295
Figure 4.4.74. Debris flow assemblage cleavers.	296
Figure 4.4.75. Debris flow assemblage LCTs.	297
Figure 4.4.76. Debris flow assemblage handaxes.	298
Figure 4.4.77. Debris flow assemblage quartzite handaxes on flakes.	299
Figure 4.4.78. Debris flow quartzite broken handaxes/LCTs.	300
Figure 4.4.79. Picks from the debris flow assemblage.	301
Figure 4.4.80. Debris flow LCTs.	302
Figure 4.4.81. Debris flow assemblage LCTs.	303
Figure 4.4.82. Debris flow cobbles.	305

Figure 4.4.83. Colluvial assemblage utilised and recycled pieces.	306
Figure 4.4.84. Debris flow assemblage utilised and recycled pieces.	307
Figure 4.4.85. Colluvial assemblage flake size distribution, by flaking axis.	322
Figure 4.4.86. Debris flow assemblage flake size distribution, by flaking axis.	323
Figure 4.4.87. Colluvial assemblage flaking axis distribution.	325
Figure 4.4.88. Debris flow assemblage flaking axis distribution.	326
Figure 4.4.89. Colluvial assemblage dorsal scar directions.	328
Figure 4.4.90. Debris flow assemblage dorsal scar directions.	328
Figure 4.4.91. Complete flake dorsal scar patterns.	329
Figure 4.4.92. Technological flake types for the colluvial assemblage.	334
Figure 4.4.93. Technological flake types for the debris flow assemblage.	334
Figure 4.4.94. Colluvial assemblage flake platform facets.	336
Figure 4.4.95. Debris flow assemblage flake platform facets.	336
Figure 4.4.96. Colluvial assemblage dorsal scar number.	338
Figure 4.4.97. Debris flow assemblage dorsal scar number.	338
Figure 4.4.98. Colluvial complete flake dorsal cortex.	340
Figure 4.4.99. Debris flow complete flake dorsal cortex.	340
Figure 4.4.100. Dorsal cortex location for the colluvial complete flakes.	342
Figure 4.4.101. Dorsal cortex location for the debris flow complete flakes.	342
Figure 4.4.102. Directionality of core flaking for the colluvial assemblage.	352
Figure 4.4.103. Directionality of core flaking for the debris flow assemblage.	352
Figure 4.4.104. Blank type distribution for the colluvial assemblage cores.	355
Figure 4.4.105. Blank type distribution for the debris flow assemblage cores.	355
Figure 4.4.106. Scar length comparison for the colluvial assemblage.	359
Figure 4.4.107. Scar length comparison for the debris flow assemblage.	360
Figure 4.4.108. Flake scar negatives for the colluvial assemblage cores.	361
Figure 4.4.109. Flake scar negatives for the debris flow cores.	362
Figure 4.4.110. Number of flake scars on the colluvial cores.	363
Figure 4.4.111. Number of flake scars on the debris flow cores.	363
Figure 4.4.112. Remaining cortex on the colluvial cores.	366
Figure 4.4.113. Remaining cortex on the debris flow cores.	366
Figure 4.4.114. Blank type distribution for the colluvial assemblage.	372
Figure 4.4.115. Blank type distribution for the debris flow assemblage.	372
Figure 4.4.116. Retouch position for the colluvial assemblage formal tools.	374

Figure 4.4.117. Debris flow formal tool retouch position.	374
Figure 4.4.118. Colluvial assemblage retouch classification, by localisation.	375
Figure 4.4.119. Debris flow assemblage retouch classification, by localisation.	375
Figure 4.4.120. Retouched edge shape classification for the colluvial sample.	376
Figure 4.4.121. Retouched edge shape classification for the debris flow sample.	376
Figure 4.4.122. Edge angle classification for the colluvial assemblage.	377
Figure 4.4.123. Edge angle classification for the debris flow assemblage.	377
Figure 4.4.124. Retouch continuity for the colluvial formal tools.	378
Figure 4.4.125. Debris flow formal tool retouch continuity.	378
Figure 4.4.126. Invasiveness of edge retouch for the colluvial assemblage.	379
Figure 4.4.127. The extent of artefact retouch for the debris flow assemblage.	379
Figure 4.4.128. Cortex preservation on the colluvial retouched pieces.	380
Figure 4.4.129. Debris flow assemblage cortex preservation.	380
Figure 4.4.130. Colluvial assemblage LCT tip shape.	390
Figure 4.4.131. Debris flow assemblage LCT tip shape.	390
Figure 4.4.132. Average number of flake scars, by colluvial LCT type.	394
Figure 4.4.133. Average number of flake scars, by debris flow LCT type.	395
Figure 4.4.134. Negative termination types on the colluvial LCTs.	396
Figure 4.4.135. Negative termination types on the debris flow LCTs.	396
Figure 4.4.136. Flaking location for the colluvial LCT sample.	399
Figure 4.4.137. Flaking location for the debris flow LCT sample.	400
Figure 4.4.138. Percentage remaining cortex on the colluvial LCT sample.	402
Figure 4.4.139. Percentage remaining cortex on the debris flow LCT sample.	402
Figure 4.4.140. Use-wear and residue analysis on a complete flake.	407
Figure 4.4.141. Non-lithic material obtained from Penhill Farm.	409

List of Tables

Chapter 2

2.2:

Table 2.2.1. Achuelean sites from North and East Africa, and Malawi.	19
Table 2.2.2. Basic comparative data from Olduvai Gorge.	25
Table 2.2.3. Basic comparative data for sites from Peninj.	28
Table 2.2.4. Basic comparative data for sites from Olorgesailie.	32
Table 2.2.5. South African Acheulean sites.	33
Table 2.2.6. Basic comparative data from Canteen Kopje.	38
Table 2.2.7. Basic comparative data for Wonderwerk Cave.	41
Table 2.2.8. Basic comparative data for Amanzi Springs.	43
Table 2.2.9. Basic comparative data for Cave of Hearths.	46
Table 2.2.10. Basic comparative data for Montagu Cave.	49

Chapter 3

3.1:

Table 3.1.1. Terrace dates for the lower Sundays River Valley.	90
--	----

3.3:

Table 3.3.1. Excavation techniques applied at the three investigated sites.	113
---	-----

3.4:

Table 3.4.1. Data obtained from the Bernol and Penhill Farm artefacts.	135
--	-----

3.5:

Table 3.5.1. Phytolith and pollen sediment sample information.	159
Table 3.5.2. Sediment samples from Penhill Farm.	159

Chapter 4

4.2:

Table 4.2.1. Artefact size distribution data for Atmar Farm.	168
Table 4.2.2. Raw material and artefact condition data for Atmar Farm.	169
Table 4.2.3. Assemblage classification for Atmar Farm.	172
Table 4.2.4. Raw material use at Atmar Farm.	177

4.3:

Table 4.3.1. Artefact size distribution data for Bernol Farm.	183
Table 4.3.2. Raw material and artefact condition data for Bernol Farm.	183
Table 4.3.3. Assemblage classification for Bernol Farm.	185
Table 4.3.4. Location/site of sampled artefacts from Bernol Farm.	186
Table 4.3.5. Raw material use at Bernol Farm.	189
Table 4.3.6. LCT size data averages.	195
Table 4.3.7. LCT damage, by type.	196
Table 4.3.8. Bernol Farm LCT tip shape, by type.	196
Table 4.3.9. Cleaver butt plan shape.	197
Table 4.3.10. Bernol Farm LCT blank types.	198
Table 4.3.11. Average number of flake scars on the Bernol Farm LCTs.	198
Table 4.3.12. Shaping data for the Bernol Farm LCT sample.	200
Table 4.3.13. Mean flaking coverage in the 12 sectors.	202
Table 4.3.14. Percentage cortex on the Bernol Farm LCTs, by type.	202

4.4:

Table 4.4.1. Penhill Farm assemblage samples.	209
Table 4.4.2. Colluvial assemblage artefact size distribution.	221
Table 4.4.3. Debris flow assemblage artefact size distribution.	223
Table 4.4.4. Raw material and condition data for the colluvial assemblage.	225
Table 4.4.5. Raw material and condition data for the debris flow assemblage.	227
Table 4.4.6. Rayleigh test statistical data.	244
Table 4.4.7. Colluvial assemblage artefact classification.	252
Table 4.4.8. Debris flow assemblage artefact classification.	253
Table 4.4.9. Raw material use, by artefact type, for the colluvial assemblage.	308
Table 4.4.10. Raw material use, by artefact type, for the debris flow assemblage.	310
Table 4.4.11. SFD and flaking debris >20 mm sample weights.	317
Table 4.4.12. Colluvial assemblage flake measurements, by raw material.	318
Table 4.4.13. Debris flow flake measurements, by raw material.	319
Table 4.4.14. Colluvial complete flake measurements, by flaking axis.	320
Table 4.4.15. Debris flow complete flake measurements, by flaking axis.	321
Table 4.4.16. Colluvial assemblage flaking axis, by raw material.	327
Table 4.4.17. Debris flow assemblage flaking axis, by raw material.	327
Table 4.4.18. Colluvial assemblage dorsal scar pattern, by raw material.	330

Table 4.4.19. Debris flow assemblage dorsal scar pattern, by raw material.	331
Table 4.4.20. Colluvial complete flake termination types, by raw material.	332
Table 4.4.21. Debris flow complete flake termination types, by raw material.	332
Table 4.4.22. Colluvial technological flake type, by raw material.	335
Table 4.4.23. Debris flow technological flake type, by raw material.	335
Table 4.4.24. Colluvial assemblage flake facets, by raw material.	337
Table 4.4.25. Debris flow assemblage flake facets, by raw material.	337
Table 4.4.26. Colluvial assemblage complete flake scars, by raw material.	339
Table 4.4.27. Debris flow assemblage complete flake scars, by raw material.	339
Table 4.4.28. Colluvial complete flake dorsal cortex, by raw material.	341
Table 4.4.29. Debris flow complete flake dorsal cortex, by raw material.	341
Table 4.4.30. Complete flake interior and exterior platform angles.	343
Table 4.4.31. Colluvial assemblage core measurements, by raw material.	348
Table 4.4.32. Debris flow assemblage core measurements, by raw material.	348
Table 4.4.33. Colluvial assemblage core measurements, by core type.	349
Table 4.4.34. Debris flow assemblage core measurements, by core type.	350
Table 4.4.35. Core flaking pattern, by raw material, for the colluvial sample.	353
Table 4.4.36. Core flaking pattern, by raw material, for the debris flow sample.	354
Table 4.4.37. Colluvial core blank type, by raw material and core type.	357
Table 4.4.38. Debris flow core blank type, by raw material and core type.	358
Table 4.4.39. Core flake scar number, by raw material and core type.	365
Table 4.4.40. Remaining cortex, by raw material, for the colluvial cores.	367
Table 4.4.41. Remaining cortex, by raw material, for the debris flow cores.	367
Table 4.4.42. Formal tool measurements for the colluvial assemblage.	371
Table 4.4.43. Formal tool measurements for the debris flow assemblage.	371
Table 4.4.44. Blank type by raw material for the colluvial sample.	373
Table 4.4.45. Debris flow sample blank type, by raw material.	373
Table 4.4.46. Colluvial assemblage remaining cortex, by raw material.	381
Table 4.4.47. Debris flow assemblage remaining cortex, by raw material.	381
Table 4.4.48. Colluvial LCT data, by type and raw material.	384
Table 4.4.49. Debris flow LCT data, by type and raw material.	386
Table 4.4.50. Colluvial assemblage LCT damage, by type.	388
Table 4.4.51. Debris flow assemblage LCT damage, by type.	388
Table 4.4.52. Colluvial assemblage LCT tip shape, by type.	389

Table 4.4.53. Debris flow assemblage LCT tip shape, by type.	389
Table 4.4.54. Colluvial assemblage cleaver butt plan shape.	391
Table 4.4.55. Debris flow assemblage cleaver butt plan shape.	391
Table 4.4.56. Colluvial LCT blank type, by raw material and type.	392
Table 4.4.57. Debris flow LCT blank type, by raw material and type.	392
Table 4.4.58. Average number of flake scars for the colluvial LCTs.	393
Table 4.4.59. Average number of flake scars for the debris flow LCTs.	393
Table 4.4.60. Shaping data for the colluvial LCT sample.	397
Table 4.4.61. Shaping data for the debris flow LCT sample.	397
Table 4.4.62. Mean flaking coverage in the 12 sectors for the colluvial LCTs.	401
Table 4.4.63. Mean flaking coverage in the 12 sectors for the debris flow LCTs.	401
Table 4.4.64. Remaining cortex on the colluvial LCTs.	401
Table 4.4.65. Remaining cortex on the debris flow LCTs.	402
Table 4.4.66. Split and modified cobble data from Penhill Farm.	406
Table 4.4.67. Colluvial assemblage non-lithic material.	408
Table 4.4.68. Debris flow assemblage non-lithic material.	408

Chapter 1

Introduction

1.1 Introduction to the research

The lower Sundays River Valley is situated within the Eastern Cape Province of South Africa (Fig. 1.1). Alluvial (river) terrace deposits found within this lower valley have been the subject of a range of studies; these have explored: terrace origin, composition, age, preserved paleontological remains, river ecology, and their significance with reference to the topographical evolution of southern Africa (Ruddock 1948, 1957, 1968; Forbes & Allanson 1970; Partridge & Maud 1987; Hattingh 1994, 1996, 2008; Hattingh & Goedhart 1997; Dollar 1998; Hattingh & Rust 1999; Ross *et al.* 1999; Erlanger 2010; Erlanger *et al.* 2012). However, no study addresses the cultural stratigraphy of these terraces in terms of associated Earlier Stone Age (ESA) – more specifically Acheulean – artefact occurrences, within a dated framework.

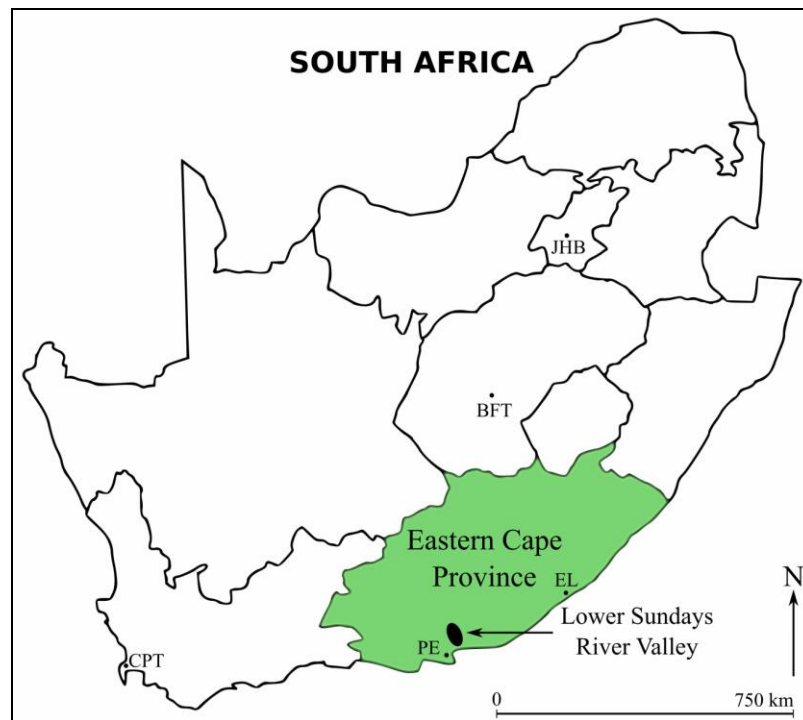


Figure 1.1. Location of the study area, Eastern Cape Province, South Africa.

For southern Africa the majority of preserved Acheulean sites occurs within secondary contexts (predominantly underground cave infills and reworked alluvial terraces) and most of these are confined to the interior of the region (the Vaal River and the Cradle of Humankind, with a few exceptions; Kuman 2007). Southern African ESA sites are also plagued by the absence of datable materials and the (frequent) poor quality of assemblages, especially for sites in and around 1 Ma (millions of years ago) and younger. Many of the typological and technological descriptions for these assemblages are also largely inadequate and dating has remained questionable. For the Eastern Cape it is widely recognised that there is a significant dearth of information pertaining to its ESA archaeology (Sampson 1974; Klein 2000a; Mitchell 2002; Phillipson 2005; Herries 2011; Lombard *et al.* 2012), and the majority of sites is poor-context surface scatters. There are only a limited number of studies (excluding Heritage Impact Assessments conducted by Binneman in 2010 and 2011) that note the presence of this early material within the entire province (Laidler 1947; Ruddock 1957; Inskeep 1965; Deacon 1970; Erlanger 2010; Erlanger *et al.* 2012). For southern Africa, the total number of sites from which we can construct our earliest understandings of hominid culture, technology, and subsistence during the Acheulean is low. There is therefore a need to conduct research elsewhere, from a range of different sites and contexts, to reach a more holistic understanding of the regions where Acheulean archaeology occurs. The need to conduct research at sites in datable contexts is also extremely vital.

Recent research conducted within the lower Sundays River Valley by D. Granger, R. Gibbon and E. Erlanger has provided cosmogenic nuclide burial dates of between 4.26-0.26 Ma for the preserved alluvial terrace deposits (Erlanger *et al.* 2012). This research has highlighted that within three of these dated deposits ESA artefacts are preserved: Penhill Farm dated to $<1.37 \pm 0.16$ Ma, and more recently constrained to $>0.485 \pm 0.051$ Ma by this research; Bernol Farm dated to 1.14 ± 0.20 Ma; and Atmar Farm dated to 0.65 ± 0.12 Ma (Granger *et al.* 2013).

Accordingly, the aim of this project has been to investigate these preserved assemblages in an attempt to improve our understanding of the Eastern Cape ESA sequence. This study therefore provides a unique opportunity to assess ESA artefact assemblages within a dated chronological sequence.

It is the goal of this research to address the following questions:

1. What specific site formation conditions can be established for the artefact-bearing horizons within these deposits, and how have these affected site integrity and context?
2. What is the typological and technological nature of the lower Sundays River Valley ESA archaeology?
3. What significance do these ESA sites have with regard to the wider archaeological record of the Eastern Cape?
4. Where does the Eastern Cape archaeological sequence 'fit in' with regard to the wider ESA sequence of southern Africa and beyond, and what basic comparisons can be made between these assemblages and those elsewhere?

In order to address these questions several key methods were employed at each of the three sites. Excavations in the form of full-scale (large) or small test pits formed the basis for most of this research. These excavations were conducted in such a way so as to provide as much contextual information as possible; the careful assessment of artefact spatial and depositional characteristics was performed. The sampling of sediments for phytolith and pollen analysis was also conducted, along with particle sizing for the Penhill Farm site. The typological and technological assessment of each assemblage involved a detailed set of measurements and a comprehensive attribute analysis.

Data obtained from this research shows that the lower Sundays River Valley has an extremely rich ESA record. Since Amanzi Springs (Inskeep 1965; Deacon 1970), the only other ESA site in the Eastern Cape to have been excavated, this project provides the first detailed documentation of an additional three sites that fall within the Acheulean. Although assemblage preservation varies greatly between the three sites due to very different site formation conditions, these sites nonetheless provide an important glimpse into this region's early archaeology. In particular, Penhill Farm provides one of the most well-preserved southern African ESA assemblages, and through the detailed analysis implemented by this research, it is now one of the most well-described.

It is clear that hominids have frequented the lower Sundays River Valley from at least 1.1 Ma (Bernol Farm) up until 0.485 Ma, to carry out their daily activities. This, coupled with additional surface finds of Middle and Later Stone Age (MSA and LSA) material throughout this lower valley, attests to the long-term use of the area for subsistence activities. As a result, the potential for this region in contributing to discussions concerning hominid complexity in subsistence strategies and artefact manufacturing through time is great. There is also the potential in future work to study hominid behaviour across the dated landscape of the lower Sundays River Valley.

1.2 Organisation of the Thesis

Chapter 1 provides a brief introduction to the chosen research area. It also highlights the questions guiding this research. Chapter 2 provides a discussion of all literature pertinent to the topics of this research. Accordingly, an introduction to the Acheulean Tradition, which focuses on general trends, classification, changes through time and the hominids responsible for its production, is provided, followed thereafter by a summary of the relevant African Acheulean sites >0.5 Ma, for industrial and chronological comparisons. The goal here is to understand the Acheulean Tradition, where it occurs, what characterises this material, and the quality of the sites and assemblages from which it has been described. A detailed discussion concerning all site formation and transformation processes that may have affected the lower Sundays River archaeological sites, at a more local scale, is provided in the latter half of this chapter.

Chapter 3 contextualises the research area by discussing all studies conducted within the lower Sundays River Valley, providing an important regional scale background for understanding the formation and preservation of the alluvial terrace deposits. Following this is a description of the three excavated sites and a discussion of the methodological approaches that have been employed throughout this study. This will include detailed discussions of excavation methods and post-excavation lab analysis techniques used to assess artefact typology and technology. Chapter 4 provides all of the results for data obtained during the analysis of the assemblages, dealing first with site context, then followed by assemblage typology and technology. Chapter 5 provides a discussion of these results and a comparison with data obtained from sites elsewhere. Chapter 6 is a summary with the final conclusions of this research.

Chapter 2

Literature Review

2.1 The Acheulean Tradition: classification, chronological trends and hominids

2.1.1 Introduction

The Acheulean Tradition is regarded as the most significant technological development that occurred during the evolution of the ESA, which encompasses the Lomekwian, Oldowan and Acheulean Traditions and is found between 3.3 and 0.3/0.25 Ma in Africa (Harris *et al.* 2007; Diez-Martín & Eren 2012; Harmand *et al.* 2015). Although the Lomekwian is the earliest industry at 3.3 Ma, it is currently known from only one small assemblage (Harmand *et al.* 2015). In contrast, the Oldowan has long been recognised as a persistent but variable, primarily core- and flake-based technology (Mode 1) that changed very little over its near 1 million years of existence from 2.6 to 1.7 Ma (Semaw *et al.* 2009). This persistence, however, is a testament to its simple applicability to perform whatever tasks were required during these early developmental stages. At 1.7 Ma, a new stone tool technology (Mode 2) presents itself (Semaw *et al.* 2009; Diez-Martín *et al.* 2015). This change in technology marks the start of the Acheulean and this Tradition is widely recognised as the longest persisting and most widespread Stone Age technology in the world (Mitchell 2002), one that is inherently variable across both space and time (Sharon *et al.* 2011). As a result of this longevity, it is frequently divided into three different phases (Kuman 2014b): an Early Acheulean (which starts at 1.7 Ma and continues until 1 Ma), a Middle Acheulean (from 1 Ma to 0.6 Ma), and a Later Acheulean (from 0.6 Ma to 0.3 Ma).

2.1.2 Classification

2.1.2.1 Advent of Large Cutting Tools (LCTs)

The first detailed descriptions of the Acheulean were presented by Mary Leakey (1971) based on assemblages retrieved from Olduvai Gorge (type site EF-HR). From this it was clear that the most diagnostic Acheulean artefacts included Large Cutting Tools (or LCTs), which distinguish it from the Oldowan (Semaw *et al.* 2009; Sharon 2010; Sharon *et al.* 2011). These types, including handaxes, cleavers and picks, are found in Acheulean assemblages in association with various other core and flake forms, similar to those found in the Oldowan (McNabb & Beaumont 2011b). At certain sites (e.g., Peninj and Olduvai Gorge type site EF-HR), these LCTs are frequently retouched and take on the form of large scrapers with pointed distal ends (de la Torre & Mora 2005; de la Torre *et al.* 2008).

Handaxes, cleavers and picks occur in a variety of shapes, sizes and forms. Generally speaking handaxes are tools shaped through primary flaking to a convergent distal end (Kuman *et al.* 2014), either through unifacial and/or bifacial working (Li *et al.* 2014). Primary flaking involves the removal of large flakes that shape the blank (either a cobble or a flake); secondary shaping consists of small removals around the peripheries of a tool to make the edges regular (Kuman *et al.* 2014). Early examples place emphasis upon creating a sharp distal end or tip (Kuman *et al.* 2014), whereas later in time more emphasis is placed upon creating sharp cutting edges around the lateral margins of the tool (Kuman 2014b). The functional uses of handaxes (and LCTs in general) are debated (see Machin *et al.* 2007; Semaw *et al.* 2009; Beyene *et al.* 2013; Diez-Martín *et al.* 2015); however, it appears that primary uses would have included some form of heavy-duty butchery, wood working, and digging (Kuman 2014b; Beyene *et al.* 2013; Diez-Martín *et al.* 2015). Cleavers require a different strategy of production and frequently have less working along the lateral edges of the piece. Emphasis rather is placed upon creating a single broad sharp cutting edge, or 'bit', at the distal or lateral portion of the piece; this edge is rarely retouched (Kuman *et al.* 2014; Li *et al.* 2014). Blank types also vary (flakes, cobbles and split cobbles) and shaping generally occurs on one or both of the lateral edges, frequently thinning

the bulbar area (when made on large side-, corner-, or end-struck flakes; Kuman *et al.* 2014). This tool could then have been used for heavy-duty chopping, cutting, hacking, and perhaps scraping wood (Kuman 2014b; Diez-Martín *et al.* 2015). Pick and pick-like tools have shaping focused on the distal end of the piece with much less emphasis on the body (Li *et al.* 2014). It would appear that these tools were most suitable for digging tasks (Beyene *et al.* 2013; Diez-Martín *et al.* 2015). Although Leakey's (1971) use of the term 'biface' implies a less 'functional subjectivity' to handaxes and cleavers, more recently Kuman (2014b) highlights that often handaxes are not bifacial, and that some pieces, especially in the earliest Acheulean, are frequently trihedral and pick-like. Accordingly, the term LCT is regarded as the best generic term today for these pieces.

Through time, these characteristic LCTs vary in appearance and form. Generally speaking, LCTs in most early assemblages are unrefined and robust (thicker), are frequently referred to as being large and pick-like (e.g., pick-like handaxes), and the amount of preparation and shaping (trimming) can be minimal (Lepre *et al.* 2011; Beyene *et al.* 2013). Flake scars are frequently large and deep suggesting the exclusive use of hard (stone) hammer percussion (Klein 2000a), as seen at Olduvai Gorge in the early Bed II assemblages (de la Torre & Mora 2014). Later in time, during the following Middle and Later Acheulean phases, LCTs tend to take on a much more refined appearance. Roe (1994a) was able to characterise changes in technology at Olduvai Gorge following the Early Acheulean; these later LCTs are thinner in profile and more regular in shape, and this could be considered a Middle Acheulean technology (Kuman 2014b). In addition to this, overall artefact symmetry is improved and the increase in thinner forms is due to a greater use of large flakes as blank types, followed by more refined trimming and shaping techniques (e.g., soft-hammer percussion, as documented by de la Torre & Mora 2014 on later Bed II, III and IV assemblages). The well-known 'classic' and 'refined' looking handaxes and cleavers occur during the Later Acheulean, after 0.6 Ma (Kuman 2014b).

Although this trend towards greater LCT refinement occurs during the three Acheulean phases, variability that occurs during the Later Acheulean is most likely due to differences in raw materials and environments (Clark 2001). There can be more refined or crude forms that occur throughout any of these phases, and it is not

uncommon to see extremely crude ‘early’ looking LCTs in the Sangoan Industry (a terminal industry of the late ESA; Kuman *et al.* 2005) and some more refined LCTs during the Early Acheulean as well. Furthermore, tool standardisation was not the desired outcome of hominids during the Acheulean as artefact production was more focused on creating functional tools (Kuman 2014b). Although this may be the case, during later phases in the Acheulean, however, the increase in LCT symmetry and standardisation may indeed be the result of some kind of aesthetic consideration (for those especially well made pieces; Klein 2000b; McNabb *et al.* 2004), the improved technological competence of the producers, or the acquisition of better raw materials from distant sources (Kuman 2014b).

The presence of these LCTs, even if just a single specimen within a site, is argued by some (Kuman 2007) to represent an Acheulean assemblage, whereas others in the past have argued that a much higher percentage (at least 40%; Leakey 1971) is required to make such classifications. More recently Goren-Inbar and Sharon (2006) discuss Acheulean site classification if handaxes in an assemblage are largely absent. In this regard site classification based purely upon handaxe frequencies is of little use now. Handaxes will seldom be produced ‘evenly’ across space, and the functional uses of these tools, as well as their role in mobility patterns, must be considered (Goren-Inbar & Sharon 2006). It is likely that individual site variation is based on the requirements of a given group, the raw materials available in a given area, or even transporting of artefacts off-site, hence giving rise to variable LCT frequencies.

2.1.2.2 Large flake Acheulean

Another important component of the Acheulean is the production of large flakes >100 mm in length (Sharon 2006, 2008, 2010; Mishra *et al.* 2010). Although many of the core forms present in most Acheulean assemblages are largely similar to those in the Oldowan, the production of large flakes in the Oldowan is absent (Mishra *et al.* 2010). Mishra *et al.* (2010) describe this difference according to strategies in core reduction: the Oldowan is characterised by small cores giving rise to small flakes, and the Acheulean, which also retains small cores and flakes, is also characterised by the addition of larger cores that are used to produce larger flakes (along with new flaking strategies to reduce these larger cores; McNabb & Beaumont 2011b). Accordingly, it

appears that with the advent of LCTs, a major technological barrier had been broken and the emphasis then shifted to producing these large flake blanks upon which handaxes, cleavers and picks could be produced (Mishra *et al.* 2010; Sharon 2010).

2.1.2.3 Improved core reduction

For the Early Acheulean there is only limited documentation of Prepared Core Technology (akin to the Levallois technique), but improved knapping strategies have been identified in several earlier assemblages (see Texier 1995; Semaw 2000; Delagnes & Roche 2005). Most notable though is the hierarchical bifacial centripetal method. This is a fairly complex flaking process that maintains bifacial working through a differential treatment of the upper and lower planes of the core (one surface will form a subordinate plane from which the principal surface can be exploited; de la Torre 2009). This process is geared towards core surface preparation, which prepares a core in such a way that flake detachment is carefully controlled (de la Torre 2009).

Identifying the Levallois technique, and what can be defined as ‘Levallois,’ has been dealt with by several authors (Boëda 1988, 1993, 1994, 1995; Van Peer 1992; Chazan 1997; Brantingham & Kuhn 2001); the latter is still a topic of much debate (de la Torre *et al.* 2003; Lycett *et al.* 2010; Eren *et al.* 2011; Herries 2011; Lycett & Eren 2013). Irrespective of these debates, the presence of more ‘organised’ strategies of flake removal attests to the evolutionary development of Prepared Core Technology within and from the Early Acheulean (White *et al.* 2011).

Prepared Core Technology first appears during the later stages of the Early Acheulean and is now recognised as forming a component in several early assemblages (Kuman 2001; McNabb 2001; Fluck 2002; Sharon 2006; Sharon & Beaumont 2006; Lycett 2009b; Lycett *et al.* 2010; McNabb & Beaumont 2011b; Leader 2014). One example of this more advanced core reduction is the Victoria West Industry, well represented at many Early Acheulean sites across southern Africa (most specifically in the interior, dated at Canteen Kopje to >1 Ma; Gibbon *et al.* 2013; Leader 2014). Victoria West cores document an advanced system of preferential flake detachment. The emphasis is on maintaining the overall shape of the core (with differential emphasis placed upon both the upper and lower surfaces) such that a single preferential removal

can be struck with a predetermined shape and size (Sharon 2006; Sharon & Beaumont 2006; Leader 2014). Other techniques of core preparation occur elsewhere in Africa in the Sahara (the Tabalbala-Tachengit technique, with no absolute dates; Tixier 1957; Biberson 1961; Clark 1992, 2001; Sharon 2006; Sharon & Beaumont 2006), and in Kenya and elsewhere with the Kombewa Core Method (>1 Ma; Clark 1998; Chavaillon & Berthelet 2004; Sharon 2006).

Although it is both extremely difficult and frequently problematic to create a list of diagnostic ‘Acheulean tool/artefact types’, McNabb and Beaumont (2011b) in this regard state that the basic Acheulean ‘package’ therefore includes the advent of LCTs, the production of large flakes from cores (through improved core preparation strategies) and core and flake forms synonymous to those found during the Oldowan.

2.1.3 The earliest Acheulean assemblages

At present, East and South Africa contain the earliest Acheulean sites. In South Africa the Cradle of Humankind with its karst topographic landscape has, until recently, provided the only datable Early Acheulean sites in southern Africa (Kuman in press). Most notable is the Sterkfontein Member 5 assemblage, which is accompanied by a faunal age estimate of 1.6 Ma (the assemblage itself could range anywhere between 1.7 to 1.4 Ma; Kuman 1994, in press; Kuman & Clarke 2000). Swartkrans Member 2 at 1.5 Ma and Member 3 at 0.96 Ma (Brain & Watson 1992; Brain 1993a; Sutton 2012; Gibbon *et al.* 2014; Kuman in press) and Kromdraai A (Kuman *et al.* 1997; Pickering 2006) at 1.5 Ma are also dated by age estimates provided by fauna. Research outside of the Cradle, in the Northern Cape Province of South Africa, has yielded assemblages ranging between 1.7 to 1.3 Ma, dated through the application of the cosmogenic burial dating method (Rietputs 15 Formation; Gibbon *et al.* 2009a; Leader 2009, 2014). Canteen Kopje, also in the Northern Cape Province, has become the focus of new research since 2007 and excavations in Pit 6 have yielded an Early Acheulean assemblage dating to 1.51 ± 0.08 Ma (for alluvial gravels, also using cosmogenics; Gibbon *et al.* 2013; Leader 2014). Elsewhere in the Northern Cape, Stratum 11 at the site of Wonderwerk Cave has been dated through the application of

palaeomagnetism and cosmogenics and has provided an age of 1.5 Ma (Chazan 2015).

East Africa contains a number of sites dating to the Early Acheulean. Recent work at the site of Kokiselei 4, within the Nachukui Formation (West Turkana, Kenya), provides an age of 1.76 Ma for the first appearance of the Early Acheulean (Lepre *et al.* 2011). Recent work by Beyene *et al.* (2013: 1), for the site of Konso, provides an age of 1.75 Ma and it is argued that this assemblage is “...chronologically indistinguishable...” from that found at Kokiselei 4. The site of Gona, in Ethiopia, has Early Acheulean sites preserved at ca. 1.6 Ma (Quade *et al.* 2004). Elsewhere, at Olduvai Gorge in Tanzania, Middle and Upper Bed II sites are dated to between 1.79 and 1.15 Ma (Hay 1976; Leakey 1976; Kimura 2002). Peninj, at Lake Natron, Tanzania has its earliest Acheulean sites dating within the range of 1.5-1.4 Ma (Isaac & Curtis 1974; de la Torre *et al.* 2008; Peters *et al.* 2008). Braun *et al.* (2009) highlight that the Okote Member of the Koobi Fora Formation, East Lake Turkana, dates to between 1.6-1.4 Ma (and sites here are seen as being contemporaneous with those from Olduvai Gorge Bed II; Isaac 1997). The age of Melka Kunture, within the Middle Awash, Ethiopia has recently been revised to 1.5 Ma (Gallotti 2013). Gadeb sites, most specifically the Gadeb 2 sites, date to <1.45 Ma (de la Torre 2011; these are also seen as being contemporaneous with those from Olduvai Gorge in the Middle-Upper Bed II sites). It is clear from the distribution and age of these sites that the Early Acheulean appears as early in East Africa as it does in South Africa (Kuman 2014b). However, Herries (2011), in reviewing all of southern Africa’s earliest Acheulean sites, suggests that the East African Acheulean sequence precedes that found in southern Africa.

The earliest Acheulean sites outside of the African continent include Ubeidiya, situated in the Jordan Valley, Israel (Bar-Yosef & Goren-Inbar 1993) and Attirampakkam, in Tamil Nadu, India (Pappu *et al.* 2011). The former site has been dated to 1.5 Ma (Bar-Yosef & Goren-Inbar 1993), and the latter site has recently had its age revised to 1.51 Ma (Pappu *et al.* 2011).

2.1.4 Site location and distribution

It is at the start of the Acheulean that one sees drastic changes in hominid behaviour. In terms of the size and distribution of sites there is a shift from very few sites (during the Oldowan) to a far greater number during the Acheulean, and especially during the Later Acheulean (Clark 2001; Harris *et al.* 2007). Although this may be related to site age and preservation, during the Acheulean there is a far greater expansion of sites into a wider range of environments; most significant is the repeated use of certain areas for seasonal resource abundance (Rogers *et al.* 1994; Klein 2000a; Harris *et al.* 2007). Coupled with this increase in site abundance is the overall trend toward larger individual sites and greater densities of lithic material within these sites (Kuman 2014b). This emphasises the increase in habitual use of stone artefacts for daily subsistence in the Acheulean, in contrast to the more sporadic and expedient use of stone technologies during the Oldowan (Harris *et al.* 2007; Kuman 2014b). Sites also tend to occur in areas where resources were plentiful (e.g., tethering to raw material outcrops), and Harris *et al.* (2007) note that the majority of sites is situated at or near to a body of water (especially during drier climates). Deacon and Deacon (1999) highlight that it is within these types of environments that both plant and animal yields are highest.

2.1.5 Hominid ranging abilities

Although tethering to important resource areas is evident during the Acheulean, most notable is the increase in hominid ranging abilities (Clark 1994; Rogers *et al.* 1994; Harris *et al.* 2007). Establishing Acheulean territory sizes is problematic, and it is clear from modern hunter-gatherer populations that large areas are required from which the necessary resources can be extracted to survive (Klein 2000a). One way of establishing these ranging abilities during the Acheulean is by looking at the raw materials used for artefact production, and from where these have been sourced. For the interior of South Africa (specifically Vaal River Basin sites), most sites occur on what would have been the banks of the Vaal River; raw materials in the form of river cobbles and boulders were readily available close by. In this regard Klein (2000a) states that for most known southern African localities, raw materials were available

within only a few kilometers. However, at Elandsfontein within the Western Cape of South Africa, Deacon & Deacon (1999) highlight that raw material sourcing may have occurred over distances of between 10-30 km, perhaps upwards of 40 km (Braun *et al.* 2013). In relation to modern hunter-gatherers, Klein (2000a) suggests that Acheulean hominid territories were most likely not comparable or as extensive. However, this increased ranging attests to the use of more varied landscapes during the Acheulean (Kuman 2014b).

2.1.6 Controlled use of fire

One of the most significant technological developments of the Acheulean is the controlled use of fire. The use of fire brought with it behavioural changes connected to social interactions and the ability to control aspects of diet, bodily warmth, and protection from predators (Alperson-Afil *et al.* 2007). Evidence suggesting this controlled use of fire, however, is highly contested and frequently difficult to interpret as many sites are only poorly preserved and occur in open-air localities (see reviews by James 1989 and Alperson-Afil *et al.* 2007). In South Africa two sites retain early evidence for burning: Swartkrans, at 0.96 Ma, contains bone which appears to have been burnt in a campfire and was then subsequently washed into an underground cave deposit (Brain & Watson 1992; Brain 1993b); Wonderwerk Cave contains burnt bone and vegetation from a single horizon dated to 1.1 Ma and is regarded as indicating *in situ* burning (Beaumont & Vogel 2006; Beaumont 2011; Berna *et al.* 2012). Elsewhere in Israel, at the site of Gesher Benot Ya'akov, evidence dating to 0.8-0.7 Ma provides the clearest evidence for the use of hearths (Alperson-Afil *et al.* 2007; Alperson-Afil & Goren-Inbar 2010).

2.1.7 Social evolution through time

2.1.7.1 Standardised design

Additional social, technological, conceptual and organisational developments took place during the Acheulean. Lithic technology during the entire Acheulean changes very little, suggesting the development of a standard 'conceptual and purposeful'

design for LCTs (McNabb *et al.* 2004; Sharon *et al.* 2011). Although there is variation in LCTs between sites, due to raw material differences, preferences by individual hominid groups, and even (immeasurable) factors concerning hominid age and skill level (Clark 2001), most pertinent is the consistency in their overall form through time. Irrespective of whether this standardisation in tool manufacture was intentional or not, the proliferation and abundance of LCTs throughout Acheulean sites suggests that a level of social interaction and cohesion had developed that was not as advanced during the preceding Oldowan (McNabb *et al.* 2004). It would be difficult to assume that a 'standardised' design could proliferate and be replicated across continents without a 'social dissemination' of these ideas (McNabb *et al.* 2004). McNabb *et al.* (2004) in this regard discuss the possibility of 'social traditions' within the Acheulean.

2.1.7.2 Subsistence strategies

This increase in overall social organisation may also be related to improved subsistence strategies. Klein (2000a,b) discusses whether Acheulean hominids had either primary or secondary access to resources, most specifically, to animals. Were Acheulean hominids hunters or scavengers? At Wonderwerk Cave and Cave of Hearths, faunal remains from Acheulean levels may help answer this question; however, the limited number of bones preserved and the presence of carnivores at Cave of Hearths suggest that hominids were not the primary accumulators at this later Acheulean site (Klein 2000a,b). More recently at Cave of Hearths, Ogola (2009b) has shown that these bones have a complex accumulation history and hominids appear to have been the accumulators whilst carnivores the modifiers of assemblage components.

New research by Wilkins and Chazan (2012) at the site of Kathu Pan, Northern Cape Province, South Africa provides compelling evidence for blade production, as well as the development of hafted points (Wilkins *et al.* 2012) during the later Acheulean. These technological adaptations are most frequently associated with the Middle Stone Age (MSA) and they brought with it an improved ability for hominids to hunt and injure game. At ca. 500 ka at Kathu Pan, this pushes back the earliest forms of hafting by 200 ka; this directly implies that the proliferation of hafting during the MSA was

not a unique ‘MSA invention’, but rather, one which developed towards the terminal point of the world’s longest lasting stone tool tradition, the Acheulean (Wilkins *et al.* 2012). However, more recently Rots and Plisson (2014) provide a critique of this study and call this finding into question based upon methodological and interpretive differences. A response by Wilkins *et al.* (2015) asserts that their findings are robust, based upon a combination of evidence. Irrespective of these recent debates this research hints at the possibility of improved hunting proficiency during the Acheulean and that hominids were actively seeking out game for capture.

2.1.8 Acheulean hominids

The term ‘hominid’ is used in this research to refer only to humans and their ancestral kin going as far back as their divergence from the great apes or ‘pongids’ (see discussions by Underdown 2006; Wood & Harrison 2011; Clarke 2014). The significant changes that occur within the archaeological record at the start of the Acheulean were most likely brought on by the arrival of a new African hominid species called *Homo ergaster* (also known as African *Homo erectus*; Rightmire 1990; Klein 2000a,b; Coolidge & Wynn 2009; Grine *et al.* 2009; de la Torre & Mora 2014). The earliest appearance of this hominid occurs in East Africa, Kenya, at 1.7 Ma at the site of Koobi Fora (Lepre & Kent 2010). In South Africa, *ergaster* specimens are found in direct association with Acheulean artefacts at Sterkfontein, in the Member 5 levels, estimated to 1.6 Ma (Kuman & Clarke 2000); but at Swartkrans, *ergaster* fossils are dated to >1.7 Ma (Pickering *et al.* 2012). *Homo ergaster* is characterised by more sapient (human-like) traits, and these include: an increase in cranial capacity, modern body proportions (long legs and arms), reduced sexual dimorphism (size differences between male and females), an improved ability to walk long distances (increased ranging), better adaption to heat, higher quality diet, more complex social structures (sharing, cooperating, colonizing, organizing), and the skillful use of stone technologies (Bar-Yosef & Belfer-Cohen 2001).

Stone artefact production during later phases of the Acheulean is frequently associated with several other hominid species. Although there is much debate as to the classification of these specimens (see discussions by McBrearty & Tryon 2006;

Coolidge & Wynn 2009; Herries 2011; Dusseldorp *et al.* 2013; Wadley 2015), it is clear that a more evolved form of *Homo* is responsible for these advanced developments during the Middle and Later Acheulean. For the Middle Acheulean, at around 1 Ma, hominid remains are preserved within the Bouri Formation (Daka Member, Middle Awash, Ethiopia; Asfaw *et al.* 2002) and Danakil Formation (Buia, Eritrea; Abbate *et al.* 1998). The former represents *Homo ergaster*, interestingly showing intermediacy between both earlier and later African fossils; its temporal and geographic position indicates that *Homo ergaster* was the ancestor of *Homo sapiens* (Asfaw *et al.* 2002). The well-preserved *Homo* cranium from Buia provides an interesting mixture of characters typical of both *Homo ergaster* and *Homo sapiens* (Abbate *et al.* 1998). This mix of traits provides crucial data on the morphological variation of early-middle Pleistocene *Homo* crania, suggesting morphology similar to that of *Homo sapiens* had begun to differentiate in Africa at 1 Ma (Abbate *et al.* 1998).

Hominids responsible for the Later Acheulean include archaic forms of *Homo sapiens* (the term ‘archaic’ is used to refer to all sub-species under and including *Homo heidelbergensis* and *rhodesiensis*). Fossil specimens for these hominids include: the Bodo cranium, Ethiopia, at 0.65-0.55 Ma (Clark *et al.* 1994); a skullcap from the site of Elandsfontein, South Africa, at ca. 0.5 Ma (Drennan 1953; Singer 1954; Klein *et al.* 2007); the Ndutu cranium, Tanzania, at 0.4 Ma (Rightmire 1983; Clarke 1990); and the Kabwe cranium, Zambia, at >0.4 Ma (Rightmire 1998).

Artefact refinement during the middle and later Acheulean phases is linked to the slower maturation rate of more advanced *Homo* by Kuman (2014b). Hominids learned to make stone tools by watching and learning their group’s tradition (Kuman 2014b). Early *Homo ergaster* is well recognised as having a faster maturation rate compared to that of modern humans, based primarily on differences in dental development (e.g., tooth eruption, but see also discussions by Smith 1993; Dean *et al.* 2001; Dean & Smith 2009; Graves *et al.* 2010; Antón & Snodgrass 2012; Schwartz 2012). With the advent of archaic *Homo*, maturation rates were slowed and this may have allowed more time to be spent on observing and interacting with other group members, promoting improvements in artefact technology.

2.2 Acheulean sites of Africa: a review

2.2.1 Introduction

The purpose of this review is to provide a brief background to the Acheulean sites of Africa that are >0.5 Ma. This review will provide basic information that relates specifically to site context, chronology (age) and assemblages, with a focus on stone tools only. Little mention will be given to other preserved items, e.g., bone, due to the scarcity of this material within the Sundays River assemblages.

Tables 2.2.1 (Part One) and 2.2.5 (Part Two) provide a list of the African Acheulean sites, and key publications. Not all of the sites and assemblages listed in these tables are relevant for comparison, and only a sample of these will be discussed (three from East Africa in Part One and five from South Africa in Part Two). For each site, comparative information will be presented that relates to three of the most informative assemblage components, namely: cores, retouched pieces and LCTs (here meaning handaxes, cleavers, picks and bifaces).

This review is not intended to be completely inclusive of all research, or all sites, but rather, it is structured to provide current explanations for the most relevant sites in relation to the three aforementioned topics. Although there are numerous sites that could have been discussed here, this review is limited to focusing only on those that would be the most informative for assemblage comparisons. In addition, emphasis is placed only on those sites located in Africa as these are well-known and widely referred to in numerous papers, thus serving as a good proxy against which comparisons can be made.

A final concluding discussion will summarise general trends in assemblage integrity, site quality, and site significance for the African Acheulean Tradition.

2.2.2 Part One

Table 2.2.1. Achuelean sites from North and East Africa, and Malawi.

Part One						
Site name:	Country:	Age (Ma):	Age estimate:	Stratigraphic context:	Cultural industry:	Key references:
Kokiselei 4	Kenya	1.76	Argon-Argon; palaeomagnetism	Nachukui Formation	Early Acheulean	Roche & Kibunjia 1994; Roche <i>et al.</i> 2003; Harmand 2007; Lepre <i>et al.</i> 2011; Quinn <i>et al.</i> 2013
Konso	Ethiopia	1.75	Argon-Argon; palaeomagnetism	Konso Formation	Early Acheulean	Asfaw <i>et al.</i> 1992; Beyene 2003; Suwa <i>et al.</i> 2007; Beyene <i>et al.</i> 2013
Olduvai Gorge	Tanzania	1.79-1.15	Potassium-Argon; palaeomagnetism	Upper and Middle Bed II	Early Acheulean	Leakey 1971, 1976, 1979; Hay 1976; Stiles 1979; Cerling & Hay 1986; Petraglia & Potts 1994; Roe 1994a; Tamrat <i>et al.</i> 1995; Kimura 2002; Egeland <i>et al.</i> 2004; de la Torre & Mora 2005; Mora & de la Torre 2005; Egeland & Domínguez-Rodrigo 2008; Lycett 2008; Lycett & von Cramon-Taubadel 2008; Peters <i>et al.</i> 2008; Diez-Martín <i>et al.</i> 2009a; Domínguez-Rodrigo <i>et al.</i> 2009c; Semaw <i>et al.</i> 2009; Ashley <i>et al.</i> 2010; Shipton & Petraglia 2010; Diez-Martín <i>et al.</i> 2015
Gona	Ethiopia	1.6	Argon-Argon	Upper Busidima Formation	Early Acheulean	Quade <i>et al.</i> 2004; Semaw <i>et al.</i> 2009
Mwanganda	Malawi	1.6	Fauna; artefacts	Palaeosol formed on Chiwondo Formation	Early Acheulean	Clark & Haynes 1970; Kaufulu & Stern 1987; Clark 1990
Konso	Ethiopia	<1.6	Argon-Argon; palaeomagnetism	Konso Formation	Early to Middle Acheulean	Asfaw <i>et al.</i> 1992; Beyene 2003; Suwa <i>et al.</i> 2007; Beyene <i>et al.</i> 2013
Melka-Kunture	Ethiopia	1.5	Argon-Argon	Melka Kunture Formation; Garba IV	Early Acheulean	Chavaillon <i>et al.</i> 1979; D'Andrea <i>et al.</i> 2002; Chavaillon & Piperno 2004; Raynal <i>et al.</i> 2004a; Negash <i>et al.</i> 2006; Morgan <i>et al.</i> 2012; Gallotti 2013

Table 2.2.1 continued...

Site name:	Country:	Age (Ma):	Age estimate:	Stratigraphic context:	Cultural industry:	Key references:
Peninj	Tanzania	1.5	Potassium-Argon; Argon-Argon; palaeomagnetism; biostratigraphy	Humbu Formation	Early Acheulean	Isaac & Curtis 1974; Domínguez-Rodrigo <i>et al.</i> 2001a; Domínguez-Rodrigo <i>et al.</i> 2001b; Domínguez-Rodrigo <i>et al.</i> 2002; de la Torre <i>et al.</i> 2003; Egeland <i>et al.</i> 2004; de la Torre <i>et al.</i> 2008; de la Torre 2009; de la Torre & Mora 2009; Domínguez-Rodrigo <i>et al.</i> 2009a; Domínguez-Rodrigo <i>et al.</i> 2009b; Domínguez-Rodrigo <i>et al.</i> 2009d; Diez-Martín <i>et al.</i> 2012
Eastern Middle Awash	Ethiopia	1.5-1.3	Fauna; artefacts	Middle Bodo Beds; Maka lag deposit	Early Acheulean	Clark & Schick 2000
Gadeb	Ethiopia	<1.45	Potassium-Argon; palaeomagnetism	Mio Goro Formation	Early Acheulean	Clark & Kurashina 1979; Clark 1980, 1987; de la Torre 2011
Chitimwe	Malawi	>1.4	Artefacts	Chitimwe Formation	Early Acheulean	Clark 1990
Koobi Fora	Kenya	<1.4	Argon-Argon	Chari Member	Early Acheulean	Isaac & Harris 1978; Schick 1987, 1991, 1997; Toth 1987; Bunn 1994; Rogers <i>et al.</i> 1994; Isaac 1997; Isaac & Behrensmeyer 1997; Isaac & Harris 1997; Ludwig & Harris 1998; McDougall & Brown 2006
Peninj	Tanzania	1.3-1.2	Potassium-Argon; Argon-Argon; palaeomagnetism; biostratigraphy	Moinik Formation	Early Acheulean	Isaac & Curtis 1974; Diez-Martín <i>et al.</i> 2009b; Domínguez-Rodrigo <i>et al.</i> 2009a; Domínguez-Rodrigo <i>et al.</i> 2009b; Domínguez-Rodrigo <i>et al.</i> 2009d; Diez-Martín <i>et al.</i> 2012
Olduvai Gorge	Tanzania	1.15-0.95	Palaeomagnetism	Bed III	Later Acheulean	Leakey 1979, 1994a,f; Jones 1980, 1994; Cerling & Hay 1986; Hay 1994; Leakey & Roe 1994; Roe 1994a,b; Tamrat <i>et al.</i> 1995; Peters <i>et al.</i> 2008
Melka-Kunture	Ethiopia	1.1-0.8	Argon-Argon	Melka Kunture Formation; Garba XIII and XII	Early to Middle Acheulean	Chavaillon <i>et al.</i> 1979; Chavaillon & Berthelet 2004; Chavaillon & Piperno 2004; Morgan <i>et al.</i> 2012
Western Middle Awash	Ethiopia	<1.042	Argo-Argon; palaeomagnetism	Bouri Formation; Daka Member	Early Acheulean	Schick & Clark 2000; WoldeGabriel <i>et al.</i> 2008

Table 2.2.1 continued...

Site name:	Country:	Age (Ma):	Age estimate:	Stratigraphic context:	Cultural industry:	Key references:
Sidi Abderrahman	Morocco	1	Fauna; artefacts; palaeomagnetism; OSL	Thomas Quarry 1; Unit L	Early Acheulean	Raynal & Texier 1989; Raynal <i>et al.</i> 2001; Raynal <i>et al.</i> 2004b
Olorgesailie	Kenya	0.99	Argon-Argon	Olorgesailie Formation; Member 1	Acheulean	Kleindienst 1961; Isaac 1977; Bye <i>et al.</i> 1987; Potts 1989; Deino & Potts 1990; Blumenschine 1991; Potts <i>et al.</i> 1999; Sikes <i>et al.</i> 1999; Noll 2000; Noll & Petraglia 2003; Potts <i>et al.</i> 2004; Shipton & Petraglia 2010; Tryon & Potts 2011; Durkee & Brown 2014
Olorgesailie	Kenya	0.97-0.78	Argon-Argon; palaeomagnetism	Olorgesailie Formation; Members 6 and 7	Acheulean	Kleindienst 1961; Isaac 1977; Bye <i>et al.</i> 1987; Potts 1989; Deino & Potts 1990; Potts <i>et al.</i> 1999; Noll 2000; Noll & Petraglia 2003; Potts <i>et al.</i> 2004; Shipton & Petraglia 2010; Walter & Trauth 2013; Durkee & Brown 2014
Kariandusi	Kenya	0.96-0.78	Argon-Argon	Fluvial deposits bordering lake margin	Later Acheulean	Gowlett 1979, 2006, 2011; Gowlett & Crompton 1994; Phillipson 1997; Deino <i>et al.</i> 2004; Lycett 2008, 2009a; Lycett & von Cramon-Taubadel 2008; Shipton & Petraglia 2010; Shipton 2011; Walter & Trauth 2013; Durkee & Brown 2014; Munga 2014
Olduvai Gorge	Tanzania	0.95-0.78	Palaeomagnetism	Bed IV	Later Acheulean	Jones 1979; 1980, 1994; Leakey 1979, 1994b,c,d,f; Cerling & Hay 1986; Callow 1994; Hay 1994; Leakey & Roe 1994; Roe 1994a,b; Tamrat <i>et al.</i> 1995; Peters <i>et al.</i> 2008
Melka-Kunture	Ethiopia	0.88-0.4	Argo-Argon; palaeomagnetism; artefacts	Melka Kunture Formation; Simbiro III; Gombore II; Garba I; Garba III	Middle to Later Acheulean	Chavaillon <i>et al.</i> 1979; Chavaillon & Berthelet 2004; Chavaillon & Piperno 2004; Negash <i>et al.</i> 2006; Morgan <i>et al.</i> 2012
Olduvai Gorge	Tanzania	0.78-0.5	Palaeomagnetism	Masek Beds	Later Acheulean	Leakey 1979, 1994e,f; Cerling & Hay 1986; Callow 1994; Roe 1994a,b; Leakey & Roe 1994; Tamrat <i>et al.</i> 1995; Peters <i>et al.</i> 2008

Table 2.2.1 continued...

Site name:	Country:	Age (Ma):	Age estimate:	Stratigraphic context:	Cultural industry:	Key references:
Kilombe	Kenya	>0.7	Palaeomagnetism	Single surface preserved within infilled sedimentary basin	Later Acheulean	Bishop 1978; Gowlett 1978, 1979, 1988, 1991, 2006, 2011; Crompton & Gowlett 1993; Gowlett & Crompton 1994
Olorgesailie	Kenya	0.66-0.6	Argon-Argon	Olorgesailie Formation; Members 10 and 11	Acheulean	Kleindienst 1961; Isaac 1977; Bye <i>et al.</i> 1987; Potts 1989; Deino & Potts 1990; Noll 2000; Tryon & Potts 2011; Durkee & Brown 2014
Eastern Middle Awash	Ethiopia	<0.64	Argon-Argon; fauna; artefacts	Dawaitoli Formation; Member U-2/U-3 interface, U-3 and U-T	Middle Acheulean	Clark & Schick 2000
Lake Baringo; Kenyan Rift Valley	Kenya	0.55-0.5 <0.52	Palaeomagnetism; ESR; Argon-Argon	Kapthurin Formation Member K3; Member K4	Late Acheulean	Tallon 1976, 1978; Cornelissen <i>et al.</i> 1990; Cornelissen 1992; McBrearty <i>et al.</i> 1996; McBrearty 1999; Deino & McBrearty 2002; Tryon & McBrearty 2002, 2006; Tryon 2003, 2006; Tryon <i>et al.</i> 2005; McBrearty & Tryon 2006; Johnson <i>et al.</i> 2009; Johnson & McBrearty 2010, 2012

2.2.2.1 Olduvai Gorge

Olduvai Gorge, situated in northern Tanzania, forms part of the East African Rift System. Sites in the Upper and Middle Bed II deposits belong to the early Acheulean and have featured prominently in literature over the last five decades. Most relevant though is the synthesis provided by Leakey and Roe (1994) for Acheulean material in Beds III (1.15-0.95 Ma), IV (0.95-0.78 Ma) and the Masek Beds (0.78-0.5 Ma; see Table 2.2.1 for references). Olduvai Gorge sites are preserved within fluvial-lacustrine sediments comprised of clays, silts and sands, which form part of an ancient lake basin (Petraglia & Potts 1994); the majority of sites was located at or near to a body of water (lake shores, rivers/streams, and springs; Hay 1976; Leakey 1976; Ashley *et al.* 2010), with others occurring in a variety of ecological settings at distances away from these water sources (Egeland & Domínguez-Rodrigo 2008).

The context of the Olduvai sites has been widely discussed over several decades. Leakey (1976) originally grouped all Bed II (and Bed I) sites into four categories; these categories included: living floors (minimally disturbed deposits), butchering or kill sites (tools found associated with faunal remains), sites with diffused material (or large vertical distributions), and river or stream channel sites. Additional site formation models have been proposed but are beyond the scope of this review (Domínguez-Rodrigo *et al.* 2007). Irrespective of these different models most researchers agree, however, on two fundamental concepts. The first is that the Olduvai assemblages represent areas where hominids purposefully transported in food items, and second is that items (stone tools) were transported in to process those foods (Kimura 2002). Research by Petraglia and Potts (1994) has helped to document the influence of water flow and how this affected site formation, thus allowing sites to be ranked in order of disturbance. Leakey and Roe (1994) state that sites excavated in Beds III, IV and the Masek Beds all occur within river or stream channels, where artefacts and faunal remains were redistributed by fluvial action.

Excavations conducted in the more recent Acheulean Beds (III, IV and Masek; Table 2.2.1) illustrate trends in artefact production and the treatment of raw materials, and Table 2.2.2 provides some basic information for each of these deposits. However, this information must be treated with caution for two reasons. First, no synthesis for Beds

III, IV and the Masek Beds is provided by Leakey and Roe (1994), and thus the notes supplied in Table 2.2.2 focus on only the most important trends for sites within these Beds. Second, de la Torre and Mora (2005) have provided a revision of the typological classification system originally developed by Leakey (1971). Artefacts from these later Beds (III, IV and Masek, discussed here) still follow this original, unrevised, classification.

Bed III provides assemblages that are not very informative of general trends during this period, and only two (from JK) are large enough to use for comparison (Tables 2.2.1 & 2.2.2; Roe 1994b). Bed IV, on the other hand, provides a range of assemblages (from areas WK, PDK and HEB) comprised almost entirely of lithic debris. From these sites it is clear that raw materials were differentially and preferentially sourced for the production of bifaces (e.g., green phonolite at area HEB, sourced from 9 km away; Fig. 2.2.1), and these were subsequently reduced using a consistent technological process (Roe 1994b); biface morphology shows that items in Bed IV are highly finished (Roe 1994a). The Masek Beds provided only a single site (FLK) worth excavating, yet the assemblages illustrate an almost exclusive use of white quartzite. The many large bifaces from these levels therefore illustrate great knapping proficiency and a unique specialisation in the reduction of this material (Table 2.2.2; Roe 1994b).

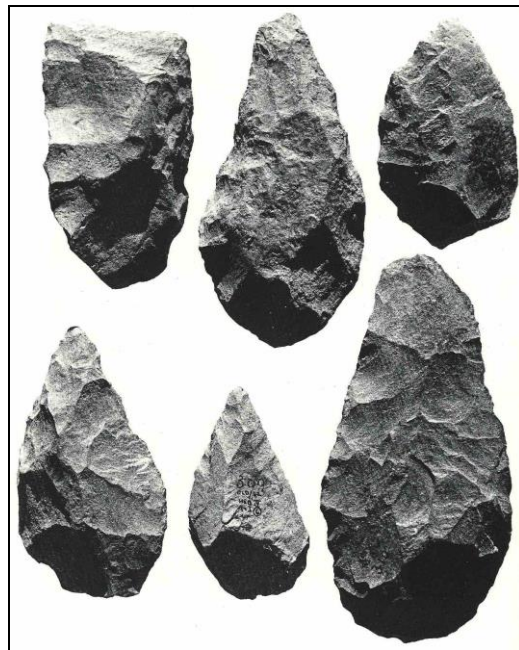


Figure 2.2.1. LCTs from Olduvai Gorge (from Leakey & Roe 1994). Cleaver (top left) and handaxes from Bed IV, area HEB, made on green phonolite.

Table 2.2.2. Basic comparative data from Olduvai Gorge (Leakey & Roe 1994).

Site name: Olduvai Gorge Beds III, IV and Masek		
Artefact:	Data:	Key points:
Cores	Flaking strategy/ reduction	<p><u>Bed III</u>: Radial and multi-directional core reduction strategies most frequent. Simple reduction strategies dominate. One core shows radial core preparation for a single large removal.</p> <p><u>Bed IV</u>: Radial and multi-directional core reduction strategies most frequent. Bipolar reduction infrequent.</p> <p><u>Masek Beds</u>: Limited core sample. Radial reduction most common; remaining types irregular.</p>
Retouched pieces	Number of retouched pieces	<p><u>Bed III</u>: Scrapers are the most frequent retouched tools; light-duty side scrapers are the most common.</p> <p><u>Bed IV</u>: Scrapers are the most frequent retouched tools; light-duty side scrapers are the most common. End scrapers follow thereafter, but sometimes hollow and notched types are more frequent.</p> <p><u>Masek Beds</u>: A limited sample shows a preference for light-duty side scrapers.</p>
	Flaking strategy/ reduction	<p><u>Bed III</u>: Retouch gives rise to both regular and irregular worked edges, with frequent indentations in the latter that occur as notches. Retouch is mostly steep and noninvasive.</p> <p><u>Bed IV</u>: Retouched edges range from straight to convex to concave shapes. Trimming is generally irregular and discontinuous along edges; continuous retouch is rare.</p> <p><u>Masek Beds</u>: Retouch creates edges that are generally straight or convex, usually uneven. Trimming is irregular.</p>
LCTs	Number of LCTs	<p><u>Bed III</u>: Handaxes are the dominant LCT; cleavers and picks follow thereafter.</p> <p><u>Bed IV</u>: Notable abundance of handaxes, followed by cleavers. Picks are few and a large percentage of the LCT sample includes broken and/or unfinished pieces.</p> <p><u>Masek Beds</u>: Cleavers are very few. Handaxes are well represented.</p>

Table 2.2.2 continued...

Site name: Olduvai Gorge Beds III, IV and Masek		
Artefact:	Data:	Key points:
LCTs	Flaking strategy/ reduction	<p><u>Bed III</u>: Highly variable shaping of LCTs that are generally produced on large flake blanks (not exclusively). Some exhibit trimming across entire tool circumference, yet overall, tool shaping is minimal. Some flaking occurs to reduce butt thickness.</p> <p><u>Bed IV</u>: Handaxe shapes and flatness are more regular, as are the cutting edges; cleavers are more frequent and are elegantly made. However, exceptions do occur and technology is highly variable.</p> <p><u>Masek Beds</u>: Handaxes show greatest technological competency with good control over raw materials. Preferred shapes give rise to form and size similarities. Cutting edges carefully shaped, as are the tool tips.</p>

2.2.2.2 Peninj

Peninj is situated on the western shore of Lake Natron, Tanzania. The majority (not all) of sites occurs in what are termed the Upper Sandy Clays (USC) of the Humbu Formation (Domínguez-Rodrigo *et al.* 2001b; de la Torre *et al.* 2008). Peninj is comprised of three main areas within which Acheulean sites have been found (de la Torre 2009). This includes the North Escarpment (Domínguez-Rodrigo *et al.* 2009b), the South Escarpment (Domínguez-Rodrigo *et al.* 2009d) and the Type Section (Diez-Martín *et al.* 2009b; de la Torre 2009).

Deposits in the North and South Escarpments are characterised by a fluvial environment, with the former being further away from the lake and nearer to the Peninj River, and the latter in a similar riverine setting but also within an alluvial fan depositional environment (Domínguez-Rodrigo *et al.* 2009b; Domínguez-Rodrigo *et al.* 2009d). The alluvial and deltaic environment deposits in the Type Section have been more affected by tectonic activity, and subsequent erosion has created a complex exposure of these deposits (Domínguez-Rodrigo *et al.* 2002). The dating of these deposits (see Table 2.2.1) has been constrained within ages provided for the overlying Moinik Formation (1.37-1.33 Ma) and the Main Tuff of the USC within the Humbu

Formation (dated to >1.5 Ma; de la Torre *et al.* 2008). A single Early Acheulean site (ST69) also occurs within the Moinik Formation and is constrained to near 1.2 Ma (Diez-Martín *et al.* 2009b).

A complex distribution of sites at Peninj allows for a comprehensive spatial and temporal understanding of the Acheulean Tradition. Summarising the details and individual variability of each site in this region is beyond the scope of this review; however, emphasis here will be placed upon more general trends for sites strictly within the Moinik Formation (1.3-1.2 Ma; Table 2.2.3).

Deposits of site ST-69 of the Type Section were formed during low lake levels, within a lacustrine plain (Diez-Martín *et al.* 2009b). This assemblage is largely different from the earlier sites of the Type Section in that bifaces dominate (handaxes and cleavers; Diez-Martín *et al.* 2009b). These are generally made on large side-struck flakes struck off locally and semi-locally available volcanic rocks (Fig. 2.2.2; Diez-Martín *et al.* 2009b). Core reduction is dominated by centripetal exploitation, and bifaces transported into the site were already pre-formed (Diez-Martín *et al.* 2009b). Retouch is common and is utilised frequently to improve biface tip shape and to reduce striking platform thickness (Diez-Martín *et al.* 2009b). Bifaces are generally symmetrical in appearance and differences in size are generally due to flaking/reduction intensity (Diez-Martín *et al.* 2009b).

South Escarpment sites are discussed by Domínguez-Rodrigo *et al.* (2009d). One such site (MHS, now termed PEES2; Table 2.2.3) provides a unique deposit, which suggests very low energy conditions for deposit formation, evidenced by the distribution of material, a lack of orientations and concentrations by raw material, and no edge abrasion (Domínguez-Rodrigo *et al.* 2009d). This assemblage is dominated by small flakes, and the early stages of core knapping (as well as of heavy-duty tools) appear to have taken place off-site (Domínguez-Rodrigo *et al.* 2009d). LCTs (handaxes) and knives are common and have been transported in (often from far, ≥ 5 km), although flakes indicative of their re-sharpening and maintenance on-site do occur; the transporting and prevalence of these pieces supports their importance (Domínguez-Rodrigo *et al.* 2009d). These flake-based tools show clear use-wear, and many edges have been retouched and damaged. Retouching is generally constrained

to the thinnest part of the flake, at the opposite end of the flake platform (Domínguez-Rodrigo *et al.* 2009d).

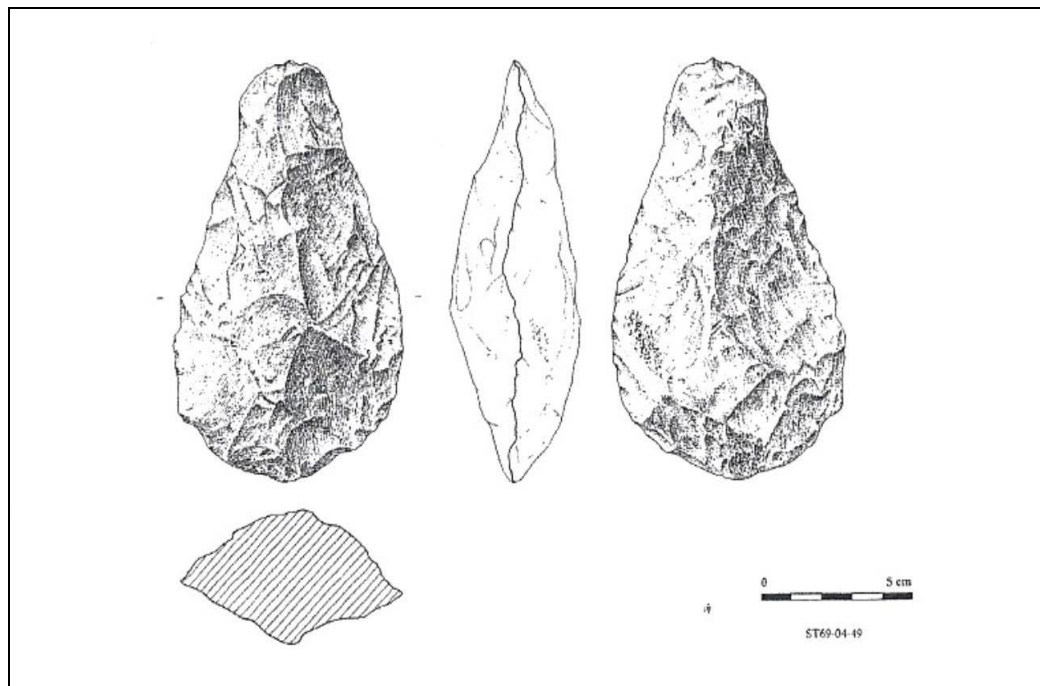


Figure 2.2.2. ST-69 handaxe on flake from Peninj (from Diez-Martín *et al.* 2009b).

Table 2.2.3. Basic comparative data for sites from Peninj. Information for site ST-69 is from Diez-Martín *et al.* (2009b) and for site PEES2 is from Domínguez-Rodrigo *et al.* (2009d).

Site name: Peninj sites from the Moinik Formation		
Artefact:	Data:	Key points:
Cores	Flaking strategy/reduction	<p><u>ST-69</u>: Shows a limited sample of cores but those that do occur show a preference for radial reduction strategies (centripetal exploitation). This reduction occurs on both faces and no hierarchisation occurs.</p> <p><u>PEES2</u>: Limited core sample of 15 pieces, classified as polyhedrons/cores. This suggests a preference for multi-directional core reduction strategies.</p>
Retouched pieces	Number of retouched pieces	<p><u>ST-69</u>: Retouched LCTs are the most common retouched tools; a single scraper occurs on a retouched flake.</p> <p><u>PEES2</u>: Little information on retouched items; however, LCTs appear to be the most abundant.</p>
	Flaking strategy/reduction	<p><u>ST-69</u>: Retouch is generally simple and marginal, the majority of which is bifacial. Retouch to create a notched edge is uncommon.</p> <p><u>PEES2</u>: Some LCTs show extensive retouched edges, some of which occur bifacially.</p>

Table 2.2.3 continued...

Site name: Peninj sites from the Moinik Formation		
Artefact:	Data:	Key points:
LCTs	Number of LCTs	<p><u>ST-69</u>: Handaxes are the most abundant LCT, followed by cleavers.</p> <p><u>PEES2</u>: Handaxes (and knives) are the most abundant LCTs.</p>
	Flaking strategy/reduction	<p><u>ST-69</u>: LCTs are most frequently made on thick, large, heavy flake blanks obtained through radial flaking. These are then invasively flaked/retouched (centripetally) to reduce ventral thickness, improve cutting edges, reduce platform thickness, and improve tip shapes. Edge retouch is common in the majority of the LCTs (simple and marginal), most of which is discontinuous or partial. LCTs are symmetrical (horizontal view) and shapes are quite standardised.</p> <p><u>PEES2</u>: LCTs generally produced on large flakes from boulder cores. Retouch is not always common and LCT edges are frequently irregular. Generally, the thickest part of the LCT (flake platform) is opposite to the thinnest part, where the edges are shaped and retouched. Unifacial retouch is most frequent.</p>

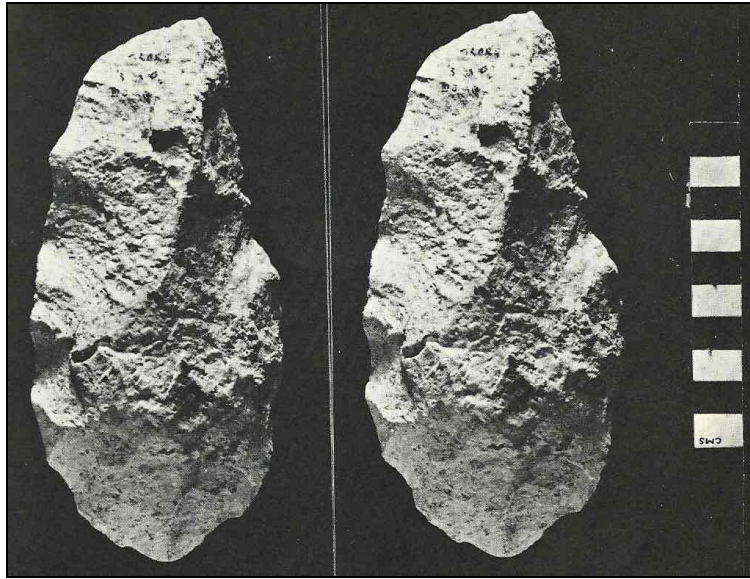
2.2.2.3 Olorgesailie

The Olorgesailie Formation documents an important period of human evolution between 0.99-0.6 Ma (Table 2.2.1). These deposits occur in the Olorgesailie Basin, found in the southern Kenya Rift Valley (Potts *et al.* 1999). They preserve a unique sequence of lacustrine, fluvial, low energy floodplain, and volcanigenic sediments, all of which occur beneath the overlying late Pleistocene Oltepesi beds (Potts *et al.* 1999). The Olorgesailie Formation represents approximately 80 m worth of palaeolandscape evolution, divided into 14 different members due to lithological and stratigraphical positions (Potts 1989). Most of the archaeological assemblages at Olorgesailie occur within Members 1 (0.99 Ma), 6 and 7 (0.97-0.78 Ma), and 10 and 11 (0.66-0.6 Ma; Deino & Potts 1990); Isaac (1977) provides a detailed account of the sites and assemblages within these members (see Table 2.2.4 for a summary of general trends in artefact production). All sites occur within fine-grained diatomaceous volcanic sands and silts. This suggests they are floodplain deposits

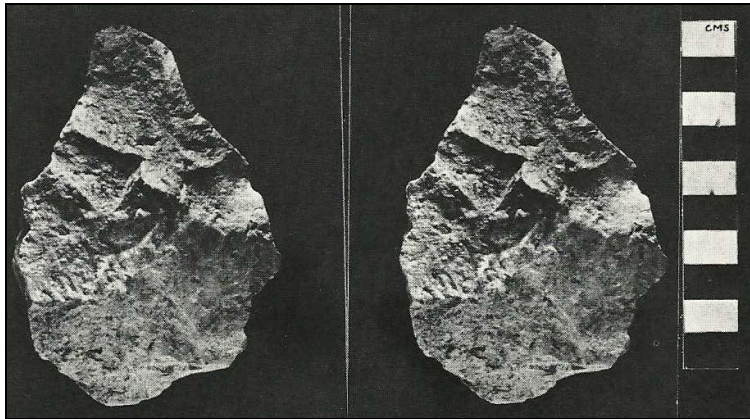
marginal to a lake, subjected to occasional re-working when lake levels increased and temporary flooding occurred (Isaac 1977).

One layer near the top of Member 1 preserves a yellow-brown palaeosol of silts and clays yielding an extremely rich array of fauna and artefacts (Potts 1989; Potts *et al.* 1999). Although artefacts occur lower down in Member 1 their distribution is scarce, whereas exposures of the palaeosol show an almost continuous spread of fauna and artefacts (with varied concentrations) across two kilometers (Potts 1989). This palaeosol appears to preserve evidence for animal butchery (numerous cut-marked bones occur within this horizon; Potts 1989). Interestingly the assemblages from the palaeosol are comprised almost exclusively of sharp flakes, scrapers and Oldowan-type cores (Fig. 2.2.3c). This may indicate a differential use of the environment and these assemblages may indicate a functional response to the desired butchery activities (Potts 1989). Handaxes within such contexts are notably rare (<5%; Fig. 2.2.3b) further supporting a differentiation of activities between lake margin contexts and channel sites elsewhere in the Basin (Potts 1989). Handaxes are extremely abundant in Member 7 (Isaac 1977).

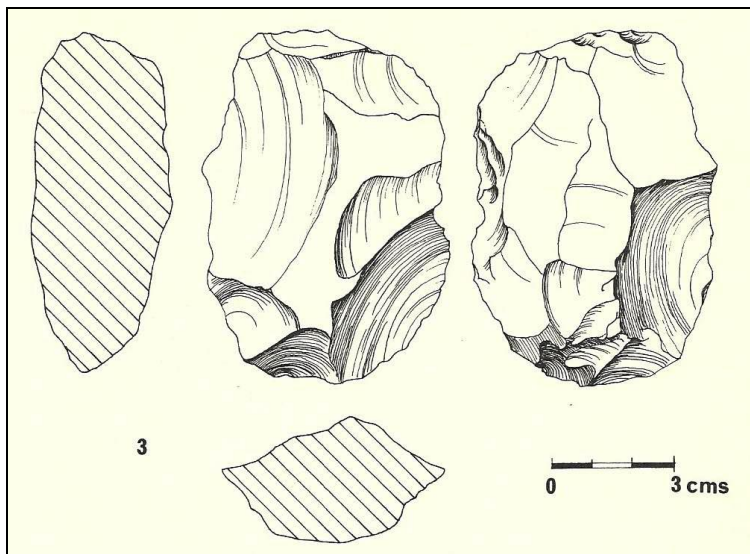
Raw material use in the Olorgesailie Basin is reliant on the transport of suitable lava clasts from distant sources (mainly from the highland) as local rivers/streams lacked an ability to transport items of a suitable size (Tryon & Potts 2011). LCT morphology suggests intensive flake reduction, which may indicate the overall scarcity of suitable raw materials within the Basin (Tryon & Potts 2011). This is further supported by additional flake and core data, which supports the economisation of lithic material due to a scarcity during Member 1 times (Tryon & Potts 2011). Members 1 and 6/7 indicate that raw materials were specifically selected for the production of LCTs primarily based on the mechanical and physical properties of these materials to maintain usable edges (Noll 2000). Raw material variability, through time, also caused differences in the lithic assemblages (especially relevant for Members 6/7; Noll 2000).



a



b



c

Figure 2.2.3. Member 1 Site I3 artefacts from Olorgesailie (from Isaac 1977). Cleaver on side-struck flake (a), handaxe (b) and core (c).

Table 2.2.4. Basic comparative data for sites from Olorgesailie (Isaac 1977).

Site name: sites from the Olorgesailie Formation		
Artefact:	Data:	Key points:
Cores	Flaking strategy/ reduction	<u>All</u> : Almost all cores can be classified as discoidal cores, with a centripetal (radial) strategy of reduction. In addition, these cores show bifacial working, and scars on opposite faces are largely comparable in size. Other core forms occur but are infrequent (e.g., prismatic blade cores, casual cores, multi-directional cores).
Retouched pieces	Number of retouched pieces	<u>All</u> : Overall scraper form shows a preference for nosed types, and a large percentage of the remaining types have retouch along a single edge giving rise to side and end types.
	Flaking strategy/ reduction	<u>All</u> : Flake blanks are favoured for tool production. Little standardisation occurs in the scraper sample. Retouched scrapers are casually shaped; this gives rise to irregular (somewhat serrated) edges with intermittent scars that are only marginal.
LCTs	Number of LCTs	<u>Member 1</u> : Handaxes are the most common LCT. <u>Members 6/7</u> : Handaxes are most frequent in the majority of the assemblages, followed by cleavers. However, there is a high prevalence of robust pick-like forms. <u>Members 10/11</u> : Handaxes and cleavers account for the majority of all large bifacial tools; handaxes dominate.
	Flaking strategy/ reduction	<u>All</u> : Large flake blanks favoured for LCT production, showing simple dorsal scar arrangement. Ventral trimming to reduce platform thickness common. LCT trimming highly variable with shallow/noninvasive to deep/bold scars. <u>Member 1</u> : Overall size of LCTs is smaller and thicker than those from the other Members. LCT trimming shows an abundance of large deep scars, and the overall number is few. Overall LCT shapes are pick and core-like, and 'classic' looking handaxes and cleavers are infrequent. <u>Members 6/7</u> : Overall variance in LCT dimensions is low. LCT shapes tend towards robust, thick, pick-like forms, showing crude patterns in flake reduction/shaping (deep flake scars with a low total count). LCTs are generally asymmetrical in cross-section. Retouch is infrequent. <u>Members 10/11</u> : Overall refinement in LCT shape and trimming is increased. A single piece resembles a Lupemban lanceolate (elongate and thin). Cleavers are generally more elongated and retain chisel-like distals.

2.2.3 Part Two

Table 2.2.5. South African Acheulean sites (see also Kuman 2007).

Part 2					
Site name:	Age (Ma):	Age estimate:	Stratigraphic context:	Cultural industry:	Key references:
Coopers Cave	1.9-1.6	Fauna	Coopers D; cave infill	Early Acheulean?	Steininger & Berger 2001; Berger <i>et al.</i> 2003; Kuman 2003, 2007; Hall 2004; de Ruiter <i>et al.</i> 2009
Sterkfontein	1.7-1.4	Fauna; artefacts	Members 5 East and West; cave infills	Early Acheulean	Vrba 1975; Stiles 1979; Clarke 1994a; Kuman 1994, 1998, 2003, 2007, 2014b, in press; Reed 1997; Field 1999; Kuman & Clarke 2000; Avery 2001; Luyt & Lee-Thorp 2003; Smith & Grine 2008; Ogola 2009a; Pickering & Kramers 2010; Stratford 2011; Clarke 2012
Rietputs 15	1.7-1.3	Cosmogenics	Alluvial gravels; Rietputs 15 Formation	Early Acheulean	Kuman 2007, 2014b, in press; Gibbon <i>et al.</i> 2009a; Leader 2009; Couzens 2012
Canteen Kopje	>1.5	Cosmogenics	Alluvial gravels; Pit 6	Early Acheulean	De Wit 1996, 2008; Beaumont & McNabb 2000; Beaumont 2004; Gibbon <i>et al.</i> 2008, 2009b; McNabb & Beaumont 2011a,b; Gibbon <i>et al.</i> 2013; Leader 2014; Kuman in press
Canteen Kopje	1.51	Cosmogenics	Alluvial gravels; Pit 6	Early Acheulean	De Wit 1996, 2008; Beaumont & McNabb 2000; Beaumont 2004; Gibbon <i>et al.</i> 2008, 2009b; McNabb & Beaumont 2011a,b; Gibbon <i>et al.</i> 2013; Leader 2014; Kuman in press
Wonderwerk Cave	1.5-1.1	Cosmogenics; palaeomagnetism	Stratum 11	Early Acheulean	Chazan <i>et al.</i> 2008; Beaumont 2011; Matmon <i>et al.</i> 2012; Chazan 2015; Goldberg <i>et al.</i> 2015
Kromdraai A	1.5-1.0	Fauna	Cave deposits; miners dump	Early Acheulean	Kuman <i>et al.</i> 1997; Field 1999; Kuman 2003, 2007, in press

Table 2.2.5 continued...

Site name:	Age (Ma):	Age estimate:	Stratigraphic context:	Cultural industry:	Key references:
Swartkrans	1.5 0.96	Fauna; cosmogenics	Members 2 and 3; cave infills	Early Acheulean Middle Acheulean	Leakey 1970; Vrba 1975; Brain & Sillen 1988; Clark 1991, 1993; Brain & Watson 1992; Brain 1993a,b; Watson 1993; Clarke 1994b; Field 1999; Susman <i>et al.</i> 2001; Backwell & d'Errico 2003; Kuman 2003, 2007, 2014b, in press; Egeland <i>et al.</i> 2004; Pickering <i>et al.</i> 2004, 2007; Pickering <i>et al.</i> 2008; Sutton 2012; Gibbon <i>et al.</i> 2014
Canteen Kopje	>1	Cosmogenics	Alluvial gravels; Pit 6	Early Acheulean; Victoria West	McNabb 2001; Sharon & Beaumont 2006; McNabb & Beaumont 2011a,b; Gibbon <i>et al.</i> 2013; Leader 2014; Kuman in press
Goldsmiths	>1	Fauna; artefacts	Miners dump of disturbed cave infills	Early Acheulean	Mokokwe 2005; Kuman 2007, in press; Jacoby <i>et al.</i> 2013
Maropeng	>1	Artefacts	Open-air site of colluvial pavement	Early Acheulean	Pollarolo <i>et al.</i> 2010; Kuman in press
Three Rivers	>1	Artefacts	Alluvial gravels	Early Acheulean	Mason 1962a
Cornelia	1.07-0.99	Palaeomagnetism; biostratigraphy	Valley fill; alluvial and colluvial gravels and clays	Acheulean	Brink <i>et al.</i> 2012; Kuman in press
Wonderwerk Cave	1.07-0.99	Cosmogenics; palaeomagnetism	Strata 8-10	Acheulean	Beaumont & Vogel 2006; Chazan <i>et al.</i> 2008; Berna <i>et al.</i> 2012; Matmon <i>et al.</i> 2012; Chazan <i>et al.</i> 2015; Goldberg <i>et al.</i> 2015
Wonderwerk Cave	<1	Cosmogenics; Palaeomagnetism	Strata 5-8	Later Acheulean Fauresmith	Binneman & Beaumont 1992; Beaumont & Vogel 2006; Chazan <i>et al.</i> 2008; Beaumont 2011; Matmon <i>et al.</i> 2012; Chazan <i>et al.</i> 2015; Goldberg <i>et al.</i> 2015

Table 2.2.5 continued...

Site name:	Age (Ma):	Age estimate:	Stratigraphic context:	Cultural industry:	Key references:
Elandsfontein	1.0-0.6	Palaeomagnetism; fauna; artefacts	Preserved palaeosurface in dune sands	Later Acheulean	Singer & Crawford 1958; Netterberg 1974; Klein 1978; Avery 1988; Klein & Cruz-Urbe 1991; Deacon 1998; Luyt <i>et al.</i> 2000; McNabb <i>et al.</i> 2004; Klein <i>et al.</i> 2007; Archer & Braun 2010; Braun <i>et al.</i> 2013
Doornlaagte	1.0-0.5 (Middle Pleistocene)	Artefacts	Living floor near pan periphery	Later Acheulean	Butzer 1974; Netterberg 1974; Deacon 1988; Mason 1988; Beaumont 1990; McNabb <i>et al.</i> 2004
Amanzi Springs	Middle Pleistocene	Artefacts	Disturbed spring mound	Later? Acheulean	Inskeep 1965; Deacon 1970; McNabb <i>et al.</i> 2004
Cave of Hearths	<0.78	Palaeomagnetism; ESR	Cave Breccias; Beds 1, 2 and 3	Later Acheulean	van Riet Lowe 1954; Mason 1962b, 1988; Latham & Herries 2004, 2009; McNabb <i>et al.</i> 2004; Underhill 2007; Curnoe 2009; Herries & Latham 2009; Maguire 2009; McNabb 2009; McNabb & Sinclair 2009a,b; McNabb <i>et al.</i> 2009; Ogola 2009b; Couzens 2012; Li <i>et al.</i> submitted
Montagu Cave	<0.6	Artefacts	Cave strata; Layers 3 and 5	Later Acheulean	Keller 1973; McNabb <i>et al.</i> 2004
Kathu Pan 1	0.682-0.435	OSL; ESR	Stratum 4a	Late/final Acheulean; Fauresmith	Porat <i>et al.</i> 2010; Herries 2011; Wilkins & Chazan 2012; Wilkins <i>et al.</i> 2012

2.2.3.1 Canteen Kopje

Canteen Kopje is a Vaal River Basin site found within the Northern Cape Province, close to the town of Barkly West. Recent studies (see Table 2.2.5 for references) provide an improved understanding of the formation of the site and the preserved Early Acheulean assemblages. Excavations in Areas 1 and 2 (Beaumont & McNabb 2000; McNabb 2001; McNabb & Beaumont 2011a,b), and Pit 6 (Leader 2014), provide details on the stratified gravels and sands found across this site, however, the depositional units between these areas are not entirely comparable (De Wit 2008).

Although this may be the case, deposits in Pit 6 preserve two Early Acheulean assemblages, overlain by Victoria West Acheulean material (Leader 2014). Through the application of the cosmogenic nuclide burial dating method, the two lower units have been dated to 1.51 Ma (Organised Core Acheulean assemblage) and >1.5 Ma (Basal Early Acheulean assemblage); the Victoria West Prepared Core assemblage is >1 Ma (Table 2.2.5; Gibbon *et al.* 2013; Leader 2014; Kuman in press). These gravels at Canteen Kopje form part of the Rietputs Formation (McNabb & Beaumont 2011a,b).

A detailed analysis of the Pit 6 assemblages is provided by Leader (2014; see summary in Table 2.2.6). As the assemblage names suggest, the difference between the two basal units is primarily related to core reduction, of which the Basal Early Acheulean lacks both prepared and organised cores, whereas the overlying Acheulean levels contain organised cores (those with more organised knapping techniques in the form of asymmetrical control; Leader 2014). The Basal Early Acheulean assemblage is comprised mainly of flakes and flaking debris, with simple cores (casual and irregular, 55%); bifaces (n=33) are dominated by cleavers and other tools include flaked-flakes and scrapers (Leader 2014). Andesite is the most favoured raw material, with a small amount of hornfels. The overlying Organised Core assemblage is similar in composition, with the addition of bifacial chopping tools. Improved core reduction strategies here are seen as an important advancement over the older underlying Basal Acheulean levels (Leader 2014). The uppermost Victoria West Prepared Core assemblage provides the most advanced core reduction strategy at the site as a small component among the cores (Fig. 2.2.4; Table 2.2.6).

It is suggested, by Leader (2014), that this assemblage represents the earliest representation of Prepared Core Technology (PCT) in the world.

Canteen Kopje provides a unique Acheulean sequence. The catchment area of the Vaal River sampled at this site was clearly utilised over a very long period of time, most likely due to its favourable location and proximity to good quality raw materials, especially in the form of large andesite boulders (McNabb & Beaumont 2011b). These boulders were then reduced as cores, from which large flakes could be obtained that could then serve as blanks for LCT production (especially relevant for the Victoria West cores; Table 2.2.6; McNabb & Beaumont 2011b).

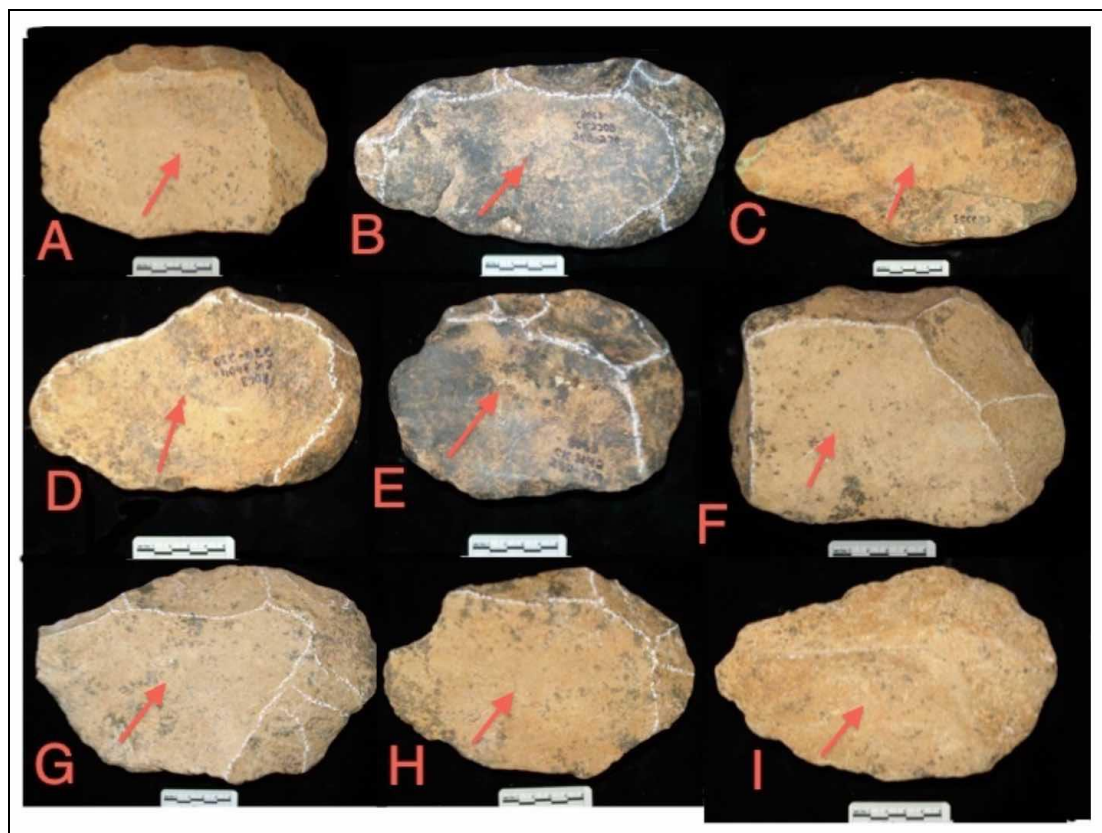


Figure 2.2.4. Pit 6 Victoria West cores, Canteen Kopje (from Leader 2014). Note the consistent direction of preferential removals in relation to the narrow end of the core.

Table 2.2.6. Basic comparative data from Canteen Kopje. All information is from Leader (2014) unless otherwise indicated. LCT information from McNabb and Beaumont (2011b) relates to Stratum 2a and 2b in Areas 1 and 2; Stratum 2a is comparable to the Pit 6 Victoria West levels.

Site name: Canteen Kopje Pit 6 Victoria West levels		
Artefact:	Data:	Key points:
Cores	Flaking strategy/reduction	Simple core reduction strategies are most common. Casual cores with only one or two removals are the most frequent type. Thereafter, notable samples of irregular, chopper-core, polyhedral and discoidal/radial types occur. Most notable is the sample of organised cores, all of which show some form of asymmetry and/or shaping to exploit a preferential or elongated core surface. In addition to these types occur the asymmetrical Victoria West 'hoenderbek' prepared cores; these types account for 9% of all reduction strategies. Scar counts are greatest on these Victoria West cores and the largest scars occur on boulder cores, where the largest surface has been exploited. Scar size on the Victoria West cores is also large relative to total core size.
Retouched pieces	Number of retouched pieces	Scrapers are the most common retouched tools. These are broken down into a general 'scraper' category (those with consistent retouch on one or more edges), and denticulated/notched, heavy-duty, and convergent types. General types are the most common; however, denticulated/notched types account for approximately 17% of the total scraper sample.
	Flaking strategy/reduction	There is little mention of how retouch has been performed and what characterises it, most likely due to the extremely abraded state of the artefacts. Where mention has been made, this retouch appears restricted to specific edges on tools and is fairly consistent along these edges. Notched and denticulated retouch is uncommon.
LCTs	Number of LCTs	The Victoria West levels show a large sample of LCTs (n=118, here excluding LCT flakes). Cleavers are the most frequent type, followed thereafter by handaxes. More robust LCTs (picks and pick-like handaxes) are less common.

Table 2.2.6 continued...

Site name: Canteen Kopje Pit 6 Victoria West levels		
Artefact:	Data:	Key points:
LCTs	Flaking strategy/ reduction	Only very basic information is provided concerning the reduction of LCTs and this relates mainly to blank type. Again, this is likely due to the poor state of artefact preservation that limited any detailed analysis. Overall, large flake blanks are favoured for LCT production; only a single handaxe and cleaver were made on cobble blanks. By size, cleavers are notably smaller than handaxes (especially those on andesite). <u>McNabb & Beaumont 2011b</u> : Handaxes and cleavers are predominantly asymmetrical in plan view (with a few exceptions). There is no standardised/formalised outline for LCT shapes. Cleavers show less thinning and shaping than handaxes, and for the former most of this is restricted to the lateral edges of the tool and the butt (for removal). In addition, cleaver shaping frequently involves any strategy that requires the least amount of working. Handaxe thinning and shaping is more invasive and covers more of the LCT, due mainly to an emphasis on shaping the converging tip. Handaxes therefore show greater symmetry overall.

2.2.3.2 Wonderwerk Cave

Wonderwerk Cave is situated on the eastern flank of the Kuruman Hills, in the Northern Cape Province. The site is comprised of deposits filling a phreatic tube, approximately 10-20 m in height, that extends inwards 140 m at the base of a hillside (Chazan *et al.* 2008). The cave formed in the dolomites of the Late Archean-Early Proterozoic Ghaap Group, found underlying the Banded Ironstone Formation of the Griqualand West Sequence (Beaumont & Vogel 2006; Matmon *et al.* 2012).

At present, the longest ESA sequence at the site occurs in the (approx.) 2 m deep sequence of Excavation 1 (Berna *et al.* 2012). This sequence has been divided into different archaeological and lithostratigraphic strata; the correspondence between these strata is limited. Most relevant here are the assemblages pertaining to archaeological Strata 5-11 (see Table 2.2.5 for ages and references). Sedimentological details summarised by Beaumont and Vogel (2006) for the Wonderwerk excavations highlight three main constituents for all the ESA levels, which include: a well-sorted

reddish fine silt and sand comprised of sub-rounded quartz grains (with extraneous origin; Chazan *et al.* 2012), roof debris (of varying quantities between the strata), and organic residues (e.g., wood ash) introduced through humans, porcupines and birds. Water transport from the cave entrance and aeolian action are possible sources for the introduction of the extraneous sands (Beaumont & Vogel 2006; Chazan *et al.* 2008). Overall, Wonderwerk Cave provides a unique sequence of extremely dry deposits, which most likely accounts for the high preservation of organics (Beaumont & Vogel 2006). This sequence also provides one of the longest records of *in situ* ESA and ESA/MSA transitional material (Chazan *et al.* 2008).

The earliest assemblages from Strata 10 and 11 are small (Beaumont & Vogel 2006; Chazan *et al.* 2012). However, in general the upper Strata (5-11) from Excavation 1 all represent a Mode 2 Acheulean technology, dominated by bifaces and a limited number of cores and flakes (Fig. 2.2.5; Chazan *et al.* 2008). Other characteristic features of the local Acheulean, such as Victoria West technology and cleavers, are poorly represented (Chazan *et al.* 2008). Basal Stratum 11 marks the advent of bifacial technology with two crude asymmetrical bifaces, shifting in Stratum 10 to bifaces with noninvasive retouch (Fig. 2.2.5; Table 2.2.7; Chazan *et al.* 2008; Berna *et al.* 2012; Chazan 2015).

Previous research has classified the upper Strata (5-7) assemblages as Fauresmith (Late, Middle and Early; Beaumont & Vogel 2006), although there is a lack of both large flake-blade (or Levallois) production and prepared core technology for these levels. More recently though, Chazan (2015) suggests there is the possibility that these artefacts are typologically 'Fauresmith.'

Basic trends in biface shape and size are summarised in Table 2.2.7, from Chazan (2015). These notes discuss technological progression in the LCT sample from Strata 5-10, and these new data show a refinement in LCTs through time. Specifically, there is a progression in the systematic production of LCTs using noninvasive removals in Strata 8-10, with a shift towards more invasive removals in Strata 5-8.

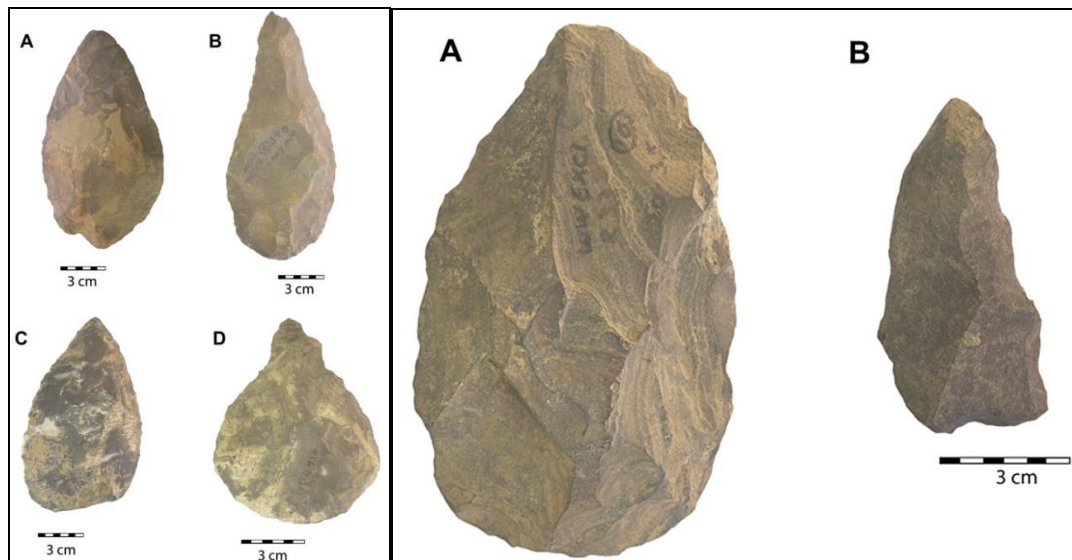


Figure 2.2.5. Bifaces from Wonderwerk Cave, Excavation 1 (from Chazan *et al.* 2008). Left image: Stratum 8 (a-b) and Stratum 9 (c-d); Right image: Stratum 10 (a) and Stratum 11 (b).

Table 2.2.7. Basic comparative data for Wonderwerk Cave, from Chazan (2015).

Site name: Wonderwerk Cave Strata 8-10 and 5-8		
Artefact:	Data:	Key points:
Cores	Flaking strategy/ reduction	The core sample is limited for all strata. Those that are present show no elaborate production, and only a small sample (5) has greater than five removals. Although several pieces appear to show slightly more organised knapping (e.g., a radial arrangement), Chazan (2015) concludes that there are no discernible trends in core reduction at the current stage of analysis.
Retouched pieces	Number of retouched pieces	Little data is provided that addresses the frequency of retouched tools, and what characterises this retouch. However, this form of tool modification is most frequent on LCTs and it is addressed below.
	Flaking strategy/ reduction	
LCTs	Number of LCTs	Handaxes are the most frequent LCT, followed thereafter by infrequent cleavers.

Table 2.2.7 continued...

Site name: Wonderwerk Cave Strata 8-10 and 5-8		
Artefact:	Data:	Key points:
LCTs	Flaking strategy/ reduction	<p><u>Strata 8-10</u>: Systematic production of handaxes with shaping that is noninvasive. These pieces are highly variable in morphology, the amount of cortex retained, and the positioning of the distal edge/tip. Retouch to regularise these working edges is absent. Tip shapes are commonly pointed or rounded. Butts are mostly cortical and unworked. The production of cleavers on large flakes develops during this period.</p> <p><u>Strata 5-8</u>: Handaxe reduction shows a shift towards invasive removals. Retouch is more prevalent and is frequently used to create and regularise working edges and to enhance the distal tips. Some pieces show retouch around the entire circumference of the tool, albeit infrequently. Shaping occurs throughout all portions of the tools.</p>

2.2.3.3 Amanzi Springs

Amanzi Springs is the only ESA site in the Eastern Cape to be sufficiently documented through excavation. Located within the Uitenhage District, on a hillside overlooking the Coega River Valley, the site is associated with a series of spring deposits (Amanzi Springs Formation) corresponding to two separate phases of artefact accumulation (the two lower members preserve the Acheulean material – the Enqhura and Rietheuvel Members; Deacon 1970). Although there are other ESA sites within the Eastern Cape (e.g., Geelhoutboom; Laidler 1947), the majority is surface scatters and contextually are of minimal value. It appears that Amanzi Springs was most likely a favoured point on the local landscape, due to its availability of fresh water and its vantage point over the Coega Valley (Deacon 1970). The preserved deposits also appear to represent multiple occupations, through time.

Studies at Amanzi Springs by Inskeep (1965) and Deacon (1970) investigate the stratigraphy of the site, artefact typology, the presence of organic remains, the extent of the deposits, and the duration of site occupation. Our understanding of this site, however, is still limited (Deacon 1970). Overall the site is of secondary context and contains a rich sample of diagnostic Acheulean material including handaxes, cleavers,

large bifacial tools, flakes and retouched pieces, all of which were described as heavy and unstandardised in form (Table 2.2.8; Fig. 2.2.6; Inskeep 1965; Deacon 1970). The site has not been dated, but based on the LCT study by McNabb *et al.* (2004), a roughly Middle Pleistocene age would be appropriate (Table 2.2.5).

Amanzi Springs serves as the only proxy with which new ESA material can be compared for the rest of the Eastern Cape (Table 2.2.8).

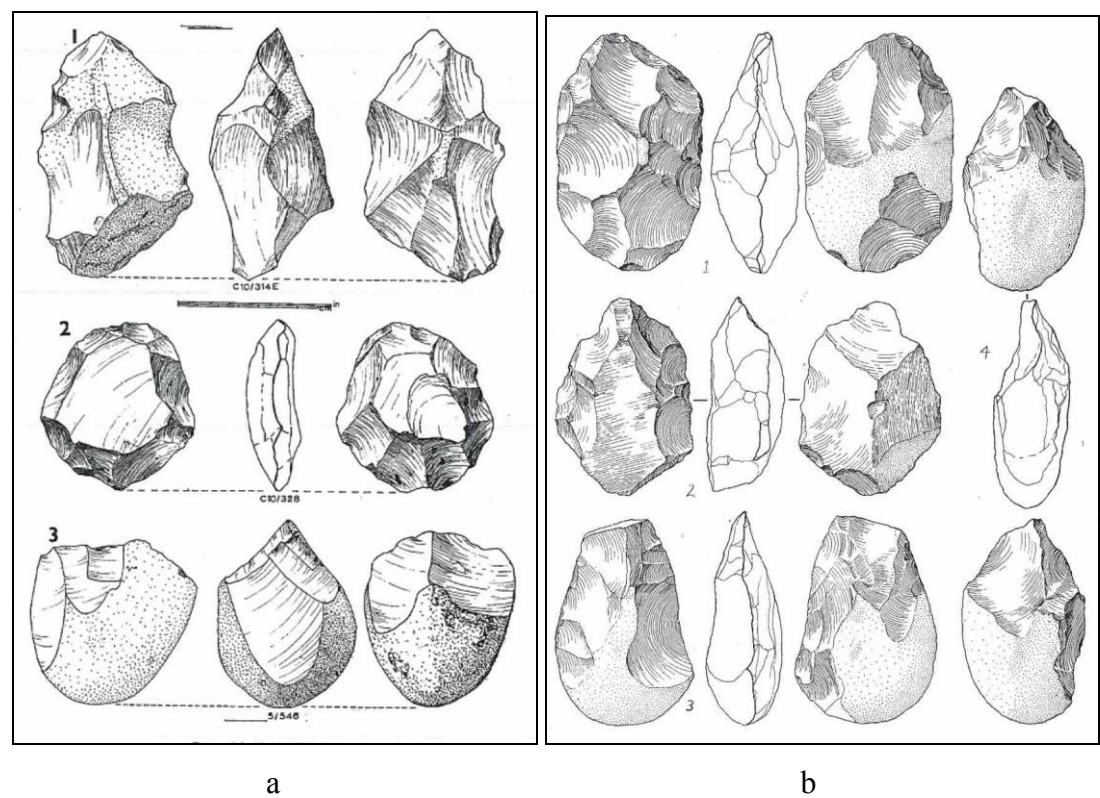


Figure 2.2.6. Cores and LCTs from Amanzi Springs; a: discoidal cores (1 & 2) and irregular core (3; from Deacon 1970); b: cleaver (1), handaxe (3) and picks (2 & 4; from Inskeep 1965).

Table 2.2.8. Basic comparative data for Amanzi Springs from Deacon (1970). Additional LCT information is from McNabb *et al.* (2004).

Site name: Amanzi Springs		
Artefact:	Data:	Key points:
Cores	Flaking strategy/reduction	The majority of all cores are classified as discoidal/radial. This suggests that radial core reduction strategies are most frequent; however, a notable sample of cores has only a single or maximum of two removals, suggesting that casual core reduction is also common. In addition to these, a number of irregular cores shows a multi-directional reduction strategy.

Table 2.2.8 continued...

Site name: Amanzi Springs		
Artefact:	Data:	Key points:
Retouched pieces	Number of retouched pieces	Scrapers are the most common type of retouched tool, most notably informal side scrapers, thereafter followed by end types.
	Flaking strategy/reduction	Only limited information is provided which speaks to both the type and character of retouch on modified pieces. Overall, flakes are favoured for reduction and retouch is minimal. Retouch is more extensive and prevalent on larger flakes. Based on artefact images supplied by Deacon (1970), retouch appears to range from discontinuous, to partial, continuous and total, for artefacts in the illustrated sample. Although notching appears infrequent, edge denticulation is common. Retouch appears short and noninvasive and is restricted to blank margins.
LCTs	Number of LCTs	Handaxes and other large bifaces are the most common LCTs; cleavers are poorly represented and picks are rare.
LCTs	Flaking strategy/reduction	<p>Overall LCT shapes and finishes are highly variable. Cobble blanks are most favoured for LCT production, which are frequently split longitudinally. Flakes are also utilised but infrequently.</p> <p>Handaxes are generally pear-shaped and show minimal flaking. There is little trimming and shaping of both the edges and pointed distals, although more refined examples do occur. Where edge trimming is present this is variable, as is edge thinness. Butts are normally cortical.</p> <p>Cleavers are poorly represented but where they do occur their plan forms are highly variable.</p> <p>Bifaces are common and are divided into several sub-types. Most common are elongated types that lack any tip emphasis but have edge trimming. Some retouch can be found on the points.</p> <p><u>McNabb <i>et al.</i> 2004</u>: A sample of analysed LCTs shows an abundance of convergent generalised tip shapes. A visual assessment indicates a lack of symmetry in all three portions (tip, medial and distal) of the LCTs.</p>

2.2.3.4 Cave of Hearths

Situated within the Limpopo Province the Cave of Hearths site is found within the Makapan Valley, an area preserving ancient sediments within caves found along its

margin (Maguire 2009). The surrounding landscape is characterised by high lying quartzites and dolomites, of which the dissolution of the latter has given rise to a complex cave system preserving three Beds (1-3) with ESA artefacts (Latham & Herries 2004, 2009 provide detail on the development of these beds). Although no absolute dates have been obtained for these beds, Herries and Latham (2009) provide a maximum age of 0.78 Ma, with a best age estimate at 0.5 Ma (Table 2.2.5). Mason (1988) originally envisioned occupation within the cave, along with the preservation of primary *in-situ* knapping activities, but McNabb (2009) has shown that the assemblages have been disturbed and are of secondary context. McNabb (2009) also concludes that the assemblages do not appear to represent an intensive long-term accumulation or one by a large group of hominids.

Originally excavated in the 1950s by Mason (1962; 1988), updated details of the assemblages are presented by McNabb (2009; see Table 2.2.9), with LCT refinement studies more recently provided by Couzens (2012) and Li *et al.* (submitted). A sample of 2212 artefacts occurs within a sloping talus cone, comprising a range of LCTs (cleavers dominate), cores (non-prepared), flakes (some retouched) and various unknapped elements (hammerstones, manuports and spheroids; McNabb 2009). Raw materials vary, yet quartzite is the most favoured and well-preserved material; its influence on tool production and behaviour though is negligible (McNabb 2009). Blank type selection followed strict rules for specific artefact types (e.g., size for LCTs), and these blanks were sourced from suitable outcrops in the surrounding landscape (McNabb 2009). For LCTs, large side-struck flakes are most common and these were then reduced (mostly off-site) according to a highly standardised knapping strategy (McNabb 2009). Although this strategic reduction was employed, individual variation in the morphology of LCTs suggests an unstandardised final form (Fig. 2.2.7; Table 2.2.9; McNabb 2009). Cores and flakes are also dominated by quartzite, yet the lack of small debitage (chunks, chips and flakes) in the cave suggests off-site knapping (McNabb 2009). As with LCTs, blanks for core reduction were chosen primarily on size, and an abundance of discoids in the assemblages suggests an emphasis on the reduction of flat blanks that are thin in cross-section; McNabb (2009) proposes that discoids may have served both as cores and as tools.

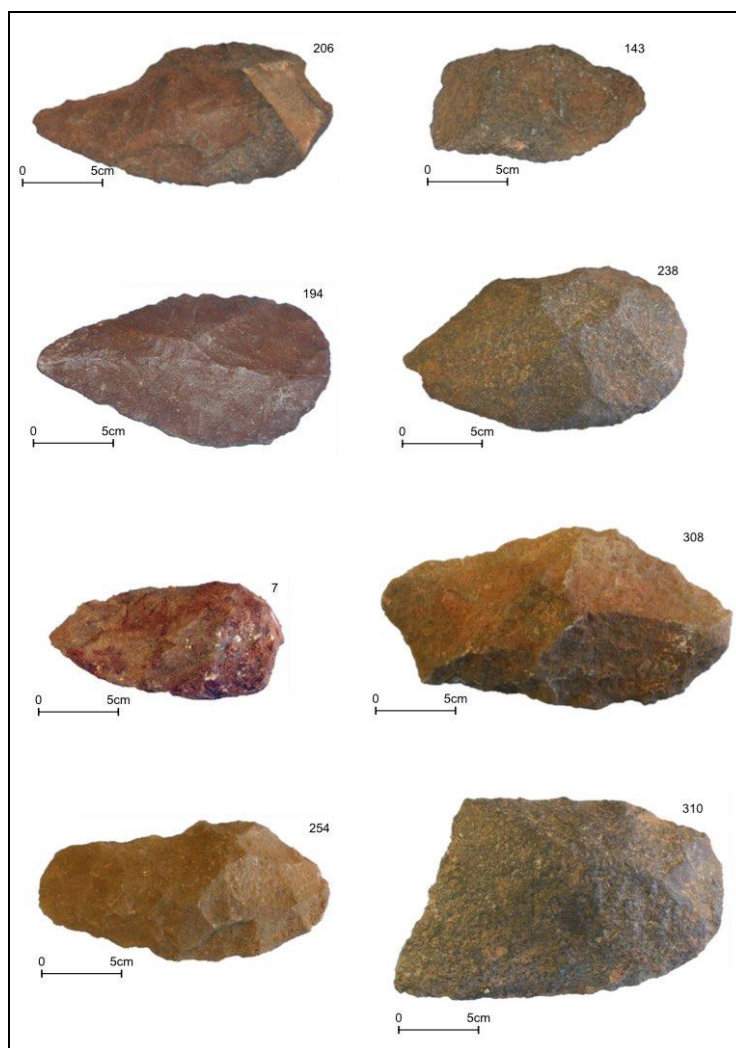


Figure 2.2.7. A selection of handaxes and cleavers from Cave of Hearths (Beds 1-3; from McNabb 2009).

Table 2.2.9. Basic comparative data for Cave of Hearths, from McNabb (2009).

Site name: Cave of Hearths Beds 1-3		
Artefact:	Data:	Key points:
Cores	Flaking strategy/reduction	Discoidal cores are the most frequent core type, reduced by alternate flaking applied in a centripetal manner. However, a range of other core types (and hence reduction strategies) occurs.
Retouched pieces	Number of retouched pieces	Flaked-flakes, a range of scrapers, denticulates and composite pieces (those with two different types of retouch on different artefact edges) are the most common retouched tools. For scrapers, transverse types are the most frequent.

Table 2.2.9 continued...

Site name: Cave of Hearths Beds 1-3		
Artefact:	Data:	Key points:
Retouched pieces	Flaking strategy/ reduction	Flake blanks are favoured for retouching. Overall standardisation in tool retouching is minimal. Scrapers are highly variable in form and retouch appears to occur only on flake edges that were suitable; retouch therefore follows the natural shape of the flake edge. Retouch is frequently continuous.
LCTs	Number of LCTs	Bifaces and cleavers are the most frequent LCT types (where bifaces here refer to LCTs with a variety of converging tip shapes). Cleavers are notably more abundant.
	Flaking strategy/ reduction	Flake blanks are most favoured for LCT production. Overall LCT symmetry is low and there is little standardisation in final forms. Exceptions do occur but these appear to be sporadic. There is no consistent strategy in biface thinning and shaping; however, partial marginal flaking is most common, yet opposite faces are frequently knapped differently. As for cleavers the pattern is slightly different, where partial marginal flaking on both faces is most favoured (least effort strategy). Overall, cleavers show less reduction than bifaces, and refinement in the LCTs is low. Even though several pieces occur that are more elegantly shaped and thinned the emphasis on this is minimal.

2.2.3.5 Montagu Cave

The Montagu Cave site is located near to the town of Montagu, in the Western Cape Province. Found within the valley of the Little Karoo, flanked by the Cape Fold Mountains of the Swartberg (to the North) and the Langeberg (to the South), this cave is located along the southern boundary of the valley within Table Mountain Sandstones (Keller 1973). Comprised of two chambers, an inner and an outer, excavations have only been conducted in the outer chamber where archaeological material is preserved in a series of cave strata (Keller 1973). Based on the morphology and dimensions of this chamber and its opening, occupations of the cave appear to have been most intense towards the rear (Keller 1973). The cave was formed by the dissolution of weaker strata in the exposed Table Mountain Sandstones, causing roof collapse and an overall expansion of the cave system (Keller 1973).

Keller (1973) provides a detailed account of the stratigraphy and associated assemblages preserved at the site, of which later Acheulean material is described from Layers 3 and 5 (Tables 2.2.5 & 2.2.10). A comparison of these assemblages shows that both are dominated by a high percentage of waste debris (Keller 1973). Overall, the distribution of LCTs (Fig. 2.2.8), minimally trimmed pieces, cores and scrapers is similar; however, differences in the types of scrapers, the range of core types, and types of waste do occur between the layers. Scrapers are smaller in Layer 3 whereas large scrapers appear in Layer 5; discoidal cores dominate both layers, with a higher prevalence of plano-convex cores in Layer 5 (Keller 1973). These are described as being similar to unstruck Victoria West cores (Keller 1973); however McNabb *et al.* (2004) state that illustrations of the cores do not indicate this.

Keller (1973) interprets the site as a workshop where hominids were sourcing locally available quartzite cobbles, from the nearby valley, upon which artefacts were then produced. Occupation of the cave took place over multiple periods, evidenced by the preservation of what appear to be horizons of flaking debris and tools, suggesting knapping floors (McNabb *et al.* 2004). The site remains undated (Table 2.2.5).

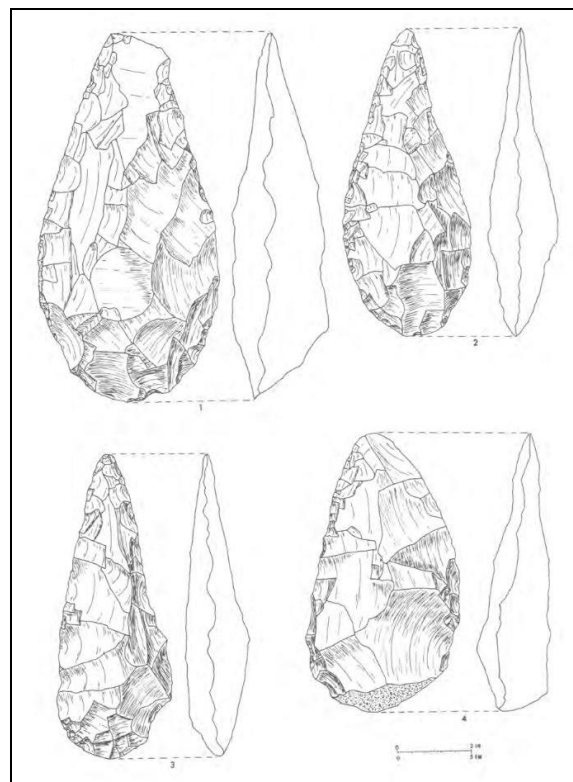


Figure 2.2.8. LCTs from Montagu Cave, all made on quartzite (from Keller 1973).

Table 2.2.10. Basic comparative data for Montagu Cave, from Keller (1973). Additional LCT information is from McNabb *et al.* 2004.

Site name: Montagu Cave Layers 3 and 5		
Artefact:	Data:	Key points:
Cores	Flaking strategy/ reduction	Discoidal cores are the most common core type, the majority of which are trimmed bifacially. This gives rise to cores with mostly round and ovoid plan shapes. Additional core types do occur that show a range of reduction strategies, but these are infrequent.
Retouched pieces	Number of retouched pieces	The most common retouched tools include an abundance of small scrapers, with multiple forms. These also include small samples of heavier-duty core scrapers. A range of minimally trimmed flakes, chips and chunks also occur, but are less common.
	Flaking strategy/ reduction	Only basic information is provided that characterises retouched items. Overall, chunks are the most favoured blank for retouching. Thereafter, retouch is mostly unifacial along a single edge (one side), giving rise to a steep edge. The retouched edges are generally irregular in shape.
LCTs	Number of LCTs	Handaxes and cleavers are the most common LCTs. Handaxes are only marginally more abundant than cleavers in both layers. A notable sample of variable bifaces is also present.
LCTs	Flaking strategy/ reduction	<p>The majority of blanks utilised for LCT production is indeterminate, but where these can be determined there is a preference for large side-struck flakes (especially for cleavers). Handaxes are predominantly bifacial and this trimming continues to the base of the tools where the butts are shaped/trimmed. The majority of handaxes are only coarsely finished, yet finer types do occur infrequently. Handaxe shapes that are most common include ovate, long ovate and lanceolate shapes. Cleavers have parallel sides with distal bits that are straight or slightly angled (termed guillotine). For those on flakes the platforms show either some reduction or complete removal, which would account for the high percentage of bifacial butt trimming. Butts are mostly U-shaped. The majority of cleavers shows coarse finishing, yet more refined examples do occur.</p> <p><u>McNabb <i>et al.</i> 2004:</u> Convergent with a generalised tip and wide/divergent tips are the most common tip shapes for a random sample of LCTs. In addition to this a visual symmetry assessment shows that LCTs are predominantly asymmetrical throughout all portions (tip, medial and base).</p>

2.2.4 Concluding discussion

The distribution and quantity of Acheulean sites >0.5 Ma in Africa appears to be extensive (Tables 2.2.1 & 2.2.5); however, not all sites contribute equally to our understanding of the Acheulean Tradition. The following discussion will highlight several pertinent themes through which all of these sites and assemblages can be assessed, and these will relate to site context, preservation, description, and deposit dating.

Almost all southern African Acheulean assemblages occur within disturbed, secondary context, open-air locations (Mitchell 2002). Although an extensive distribution of surface sites covers most of South Africa, the majority of these lacks stratigraphic context and conditions for early site preservation are rarely met (Kuman 1998; Klein 2000a). The southern African landscape has been dominated by erosion and planation for millions of years, thus occasional sediment traps within which ESA artefacts could be buried are extremely limited; where sites do occur these are restricted to occasional caves (e.g., Cave of Hearths, Montagu Cave and Wonderwerk Cave, and the Cradle of Humankind sites), fluvial deposits (sites along the Vaal and Orange Rivers and elsewhere), seasonal lake basins (pans or playas, e.g., Kathu Pan), sporadic spring mounds (Amanzi Springs), and coastal sites within aeolian environments (e.g., Elandsfontein). In reality there are no sites in South Africa with rich sedimentary sequences, with artefacts and fossils, like those found in East Africa (Clark 1990).

Site preservation within many of these environments is extremely limited. High energy alluvial gravel sites (e.g., Rietputs 15, Canteen Kopje, Three Rivers) contain heavily abraded time-averaged assemblages. Furthermore, assessing the behavioural and technological complexity of these assemblages is limited due to the non-existent retention of vital site spatial information, as well as fauna. Any interpretations about behavioural complexity are based purely upon the artefacts themselves; however, these sites do document the widespread distribution and proliferation of the Acheulean Tradition across the sub-continent (Kuman 2007). Locating more of these sites within finer silts and sands (low energy environments) is needed (Kuman 2007).

Artefact-bearing sites located in the Cradle of Humankind in Gauteng (e.g., Swartkrans, Kromdraai A, Coopers Cave, Sterkfontein and Goldsmiths) are located within a few kilometers of each other, all within the same geological formation (Kuman 1998). Until recently, some of these sites have provided the only early datable deposits with stone tools for the whole country, thus highlighting the limited distribution and preservation of early sites elsewhere (Kuman 1998). Although they occur preserved within cave infills (and occasional dumps), none (except Swartkrans during Member 3 times) is a living site, but rather, areas where surface occupation material was channeled (through surface wash/flow) into cave entrances (Kuman 1998, 2003). As a result all but one of these assemblages are incomplete due to sporadic site capture, and all possibilities of understanding landscape-use patterns are limited. From a behavioural perspective it is clear that cave entrances would have provided shelter or shade, possible standing water, and favourable vantage points, yet this is the limit of our interpretations (Kuman 1998). Cave deposits are also extremely difficult to interpret due to re-working, dissolution, solution cavities, collapses and mixing (Kuman 2003).

Slightly more favourable lower energy deposits include those found at Amanzi Springs, Doornlaagte, Kathu Pan, Maropeng and Elandsfontein, as well as the cave sites Wonderwerk Cave, Cave of Hearths and Montagu Cave. Some of the best and most informative sequences are preserved at pan sites, which document repeated visits to the area by hominids sourcing both game and water (Kuman 2007). The coastal dune and cave sites provide some of the best conditions for faunal preservation (e.g., Elandsfontein and Cave of Hearths; Kuman 2007); however, the latter are often comprised of extremely complex stratigraphical sequences that are difficult to interpret and correlate (Kuman 2007).

The majority of southern African sites also contains little datable material (volcanics and fauna) and developing a reliable chronology is therefore difficult (Klein 2000a; Mitchell 2002; Phillipson 2005; Kuman 2007). This is in stark contrast to the sites of East Africa where the preservation of volcanic sediments and ash, interspersed between depositional units, allows for direct dating and regional inter-site correlations (Klein 2000a). Stratigraphy and dating in South Africa is therefore heavily reliant on the documented East African sequence, and no site can be correlated to any well-

dated external stratigraphy (Klein 2000a). Well-dated Acheulean sites in southern Africa are therefore few in number (especially between 1.3-0.78 Ma; Kuman 2014b), due primarily to the poor conditions of site preservation (discussed above) and the limit of reliable means of dating within such contexts (Herries 2011). Amanzi Springs and Doornlaagte are two important sites that cannot at present be placed anywhere in time (no absolute ages; Klein 1983), and a host of other sites are dated purely through climate fluctuations, faunal correlations or at worst, artefact comparisons (Phillipson 2005). Cave sites provide the best potential for dating in this region (see especially recent work at Wonderwerk Cave by Matmon *et al.* 2012 and Goldberg *et al.* 2015), and more recently, alluvial gravel sites are being dated through the cosmogenic nuclide burial dating method (albeit with large error margins; Kuman 2007, 2014b). If more sites in favourable, datable, contexts are not found, South Africa will always trail East Africa as a source of information regarding the earliest tool-makers (Klein 1983). For the Eastern Cape specifically there is a need to provide more ESA sites along the coastal periphery of the country so that we can understand crucial aspects of hominid behaviour within these sorts of ecological, climatological, and environmental contexts.

Generally speaking then, southern Africa has an extensive range of early sites, yet our overall understanding is limited by the absence of sites in fine sediments and in datable open-air contexts (Kuman in press). These keyhole sites of secondary context are generally found within favoured points on the landscape that are close to raw material and water sources (Kuman 2007, in press). Kuman (2003) suggests that most sites only occur where sediment was able to accumulate, and not all sites may therefore indicate the tethering of hominids to resources (e.g., water). We therefore cannot study hominid behaviour across dated landscapes, as can be done in East Africa (Mitchell 2002; Kuman in press). Many of the South African assemblages also lack adequate description, due either to the limited quantity of material recovered (e.g., Coopers Cave), or, emphasis upon other issues (e.g., basic typologies, dating, site formation and palaeoenvironments). There is a need to locate and describe (both typologically and technologically) new sites for this region.

Further afield in Africa, sites are characterised by an array of depositional environments found within a range of geographical contexts. The majority of these

sites, however, is closely associated with fluvial action (spring deposits or some kind of fluvial and/or lacustrine system; Diez-Martín & Eren 2012). Early studies addressing the associations between bone and stone for these sites frequently overlooked the multitude of processes (anthropogenic or natural) that may have affected site formation and transformation, and we have therefore had a limited understanding of the behavioural integrity of these sites until more recently (Harris *et al.* 2007; Diez-Martín & Eren 2012). Although Schick (1987) sees floodplain or lacustrine sites preserving some of the best information on hominid behaviours (as disturbances are moderate to low), Harris *et al.* (2007) suggest that sites with winnowed and/or transported elements seldom have the integrity to question such issues. The only other site to come from a largely different depositional environment is the marine beach locality of Sidi Abderrahman (Harris *et al.* 2007).

A notable difference between the southern African and other African sites is the more abundant presence of fauna at the latter. Extensive faunal assemblages occur at: Sidi Abderrahman, Melka-Kunture, Gadeb, Konso, Kapthurin Formation, Kariandusi, Kilombe, Olorgesailie, Olduvai Gorge Beds 3 and 4, Middle Awash Valley, Peninj and the Malawi Rift Valley sites (Clark 1990; Harris *et al.* 2007). Our behavioural interpretation of these sites though is weak as the majority occurs in secondary context (Harris *et al.* 2007). One site with a unique faunal assemblage is that from Mwanganda (Clark 1990), and other notable assemblages are found in the Middle Awash Valley, in both primary and secondary context, with some bifaces found associated with modified bone (Harris *et al.* 2007). The Lake Malawi sites (Chitimwe and Mwanganda) provide vital fauna for comparison with the southern African sites of Sterkfontein and Swartkrans (Clark 1990).

Although the sites of East and North Africa provide some of the most detailed information on hominid behaviour and technological complexity during the Acheulean, several issues are still apparent. Many of the assemblage descriptions for these African sites are still seen as being largely inadequate (Diez-Martín & Eren 2012). Specifically for the earliest sites, small assemblages and a lack of technological treatment has given rise to only brief and basic summaries (Diez-Martín & Eren 2012). In contrast, Peninj has one of the most detailed technological studies and regional inter-site comparisons; the study of Olorgesailie has also provided vital

data (Diez-Martín & Eren 2012). In addition to this Olduvai Gorge has long been used as a proxy against which early assemblages could be compared, based on the work of Leakey (1971); more recent work by de la Torre and Mora (2005) has provided important updates to this classification and provided vital technological data.

Overall, our understanding of the archaeological evidence in relation to the more regional environmental contexts is also limited (Diez-Martín & Eren 2012). Experimental studies for the Acheulean are also far more limited when compared to earlier (Oldowan) and later periods (Diez-Martín & Eren 2012). It is suggested that there is a need for more integrative technological, regional, economical, and functional studies to better our understanding of the Acheulean Tradition (Diez-Martín & Eren 2012). This is not only pertinent to studies occurring further north of South Africa but a prerequisite for all Stone Age studies taking place on the African continent.

2.3 Localised site formation and transformation: a review of relevant deposit modification and sedimentary processes

2.3.1 Introduction

There has been no study in the Sundays River Valley that takes into account both the archaeological assemblages in these river terraces and the respective conditions that have led to their preservation and/or modification. There has also been little discussion concerning the fluvial terraces and how they may have been modified over time through their exposure. It is thus important to summarise here the list of possible processes that may have played a role in assemblage preservation and modification in the lower Sundays River Valley.

2.3.2 The significance of site formation and transformation studies

It is widely accepted that in order to fully understand archaeological deposits, site formation and transformation processes need to be investigated (Schiffer 1983; Hofman 1986; Hull 1987; Schick 1987, 1991; Deacon & Geleijnse 1988; Stein & Teltser 1989; Stern 1993; Karkanas *et al.* 2000; Stein 2001; Morton 2004). Although early archaeological sites provide us with a unique ‘window into the past’ through which we can investigate hominid behaviours and activities (Schick 1991), until these materials are viewed in light of their respective chronological, spatial and functional contexts, they are meaningless (Morton 2004). Because our understanding of any site is inherently reliant on the (correct) interpretation of these site contexts, and because the natural environment is one that is constantly being re-shaped and re-worked, to the point that the archaeological record is never unchanging or ‘static,’ the application of site formation studies allows one to develop a more holistic understanding of assemblage preservation and modification prior to behavioural interpretation (Schiffer 1983; Schick 1991; Stein 2001; Morton 2004).

Schick (1991) illustrates that site formation studies are concerned with identifying patterns produced by hominid activities, patterns produced by non-cultural forces, and

distinguishing the relative contribution of these two primary patterns when applicable. Hominid activities create archaeological materials, all of which have at one point in time operated within a specific social, cultural, and behavioural context (Schiffer 1983). Artefacts therefore play a role in establishing organisational norms and structuring social interactions (Schiffer 1983). Contextually, patterns are thus created as these materials are transferred and handled within the landscape. However, because these materials fall within open ‘ever-changing’ landscapes, these archaeological deposits and site contexts are constantly being re-patterned and transformed by non-cultural forces. These forces serve to distort and transform deposits within which archaeological occurrences are preserved. As a result, site formation studies place careful emphasis on distinguishing between these cultural and non-cultural ‘pattern-forming’ processes.

Site formation studies are still limited by the fact that there will always be variability in both these processes (cultural and natural) and, how they influence deposit formation (Morton 2004). McPherron (2005) states that any number of processes may have combined to create a specific pattern in the record, and it may be difficult to understand the complexities of the processes involved. Most important is that site contexts, which archaeologists wish to understand, are frequently far removed from reality, ancient in age, and have been exposed to a multitude of formational and transformational processes, through time.

In this regard Morton (2004) states that the past will forever be unknowable. Site formation studies will very seldom be able to provide a complete understanding of all the natural and/or cultural processes that have played a role in deposit formation (Morton 2004). A fundamental concept in all site formation studies is therefore that the original archaeological occurrence will never be attainable, even after all the depositional patterns have been fully understood (Morton 2004). Rather, site formation studies at best provide a model which enables researchers in the present to establish the extent to which the archaeological record has been affected in the past (Morton 2004). These models have been created through the application of experimental studies, which aim to recreate the processes involved in both deposit genesis and degeneration.

2.3.3 Experimental research: actualistic studies

The theoretical understanding of site formation has only been made possible through the application of actualistic studies. It is through these studies that formation and transformational patterns can be identified, along with how these may have affected site context. Actualistic studies include those that address:

- Assemblage size profiles (Bunn *et al.* 1980; Schiffer 1983; Schick 1984, 1987, 1991, 1997; Petraglia & Potts 1994; Kandel *et al.* 2003; Kuman & Field 2009)
- Artefact scatter patterns (Schick 1984, 1991, 1997; Petraglia & Potts 1994; Morton 2004)
- Artefact condition (Shackley 1974; Kuman 1989; Nielsen 1991; Pappu 1996; McBrearty *et al.* 1998; Shea 1999; Holmes *et al.* 2008; Kuman & Field 2009; Thompson 2009)
- Artefact spatial distribution patterns, both horizontal and vertical, affected through the processes of:
 - Animal trampling (Schiffer 1983; Villa & Courtin 1983; Gonzales *et al.* 1985; Nielsen 1991; Vermeersch & Bubel 1997; McBrearty *et al.* 1998; Morton 2004; Forssman & Pargeter 2014)
 - Fluvial forces (Schiffer 1983; Schick 1984, 1987, 1991, 1997; Petraglia & Potts 1994; Morton 2004; McPherron 2005)
 - Aeolian forces (Kandel *et al.* 2003)
 - Bioturbation (Cahen & Moeyersons 1977; Moeyersons 1978; Schiffer 1983; Stein 1983; Erlandson 1984; Hofman 1986; McBrearty 1990; Vermeersch & Bubel 1997; Morton 2004; Anderson & Anderson 2010; Lotter *et al.* 2016)
 - Downslope dispersals and movements due to *slope detachment* (Stern 1993; Morton 2004), *hydrological processes such as rain splash, sheetwash/flow erosion* (Quansah 1981; El-Swaify *et al.* 1982; Slattery & Bryan 1992; Brown 1997; de Jong *et al.* 1999; Lal 2001; Ventura *et al.* 2002; Zhang *et al.* 2003; Goldberg & Macphail 2006; Charlton 2008; Anderson & Anderson 2010) and *rill and gully erosion* (El-Swaify *et al.* 1982; Ballantyne & Benn 1994; Botha *et al.* 1994; Brown 1997; de Jong *et al.* 1999; Lal 2001; Ventura *et al.* 2001; Zhang *et al.*

2003; Grab & Deschamps 2004; Goldberg & Macphail 2006; Charlton 2008; Anderson & Anderson 2010; Boardman *et al.* 2012), and mass movements/wasting (Culling 1963; Albjar *et al.* 1979; Lowe 1982; Wright & Anderson 1982; Akerman 1984; Mills 1984; Abrahams *et al.* 1985; Postma 1986; Abrahams *et al.* 1990; Mosher *et al.* 1994; Bertran & Texier 1995, 1999; Armanini & Michiue 1997; Bertran *et al.* 1997; Hand 1997; Major 1997, 1998, 2000; Shimokawa 1997; Curry & Ballantyne 1999; Fannin & Wise 2001; Parsons *et al.* 2001; Malet *et al.* 2002; Dasgupta 2003; Mills & Grab 2005; Obanawa & Matsukura 2006; Sass & Krautblatter 2007; Charlton 2008; Mills *et al.* 2009; Anderson & Anderson 2010; Muir *et al.* 2015)

- Sediment wetting and drying cycles (Cahen & Moeyersons 1977; Moeyersons 1978)

The following discussion will highlight those studies most relevant to assessing site context and integrity for this study.

2.3.3.1 Assemblage size profiles

Assessing the size distribution of artefactual material, within an archaeological context, is extremely important when assessing site integrity; this can only be investigated when archaeological samples are compared against modern analogies. These analogies allow researchers to assess the representation of all artefacts (of all sizes) within deposits in relation to specific cultural activities. Studies by Schick (1987, 1991, 1997) at Koobi Fora and Kuman and Field (2009) at Sterkfontein have been fundamental in this regard, and through experimental knapping demonstrations these authors have developed a modern analogy that accounts for the specific artefact sizes, types and distributions that should characterise a site of primary knapping activity. These studies also highlight that rock fracture, although different for each material, is consistent enough to establish predictable flake versus small flaking debris (SFD<20 mm) percentages. This enables researchers to: assess the given distribution of flaked material, within a given context; establish deviations away from a regular distribution of material; and, to question the possible reasons for variation (Schick 1984, 1987, 1991, 1997; Kuman & Field 2009).

A high percentage of SFD (60-87%) should characterise a site of primary knapping activity, and deviations away from this distribution could be the result of several factors. If knapping did not take place on-site, or if the deposit has been exposed to natural processes, then a range of different distributions should be expected (Schick 1997; Kuman & Field 2009). With reference to the former, Schick (1991) suggests that already manufactured lithics can be brought into a site by hominids, thereby eliminating the need for on-site production. Natural processes may include some form of fluvial or hydrological processes, causing winnowing and leading to a removal of the smallest assemblage components (SFD), or re-concentrations, where sites are created through the re-deposition of material from one or more other areas (often causing high concentrations of SFD elsewhere; Schick 1991).

The distribution of SFD or the presence and/or absence of on-site knapping activities should not be used alone, however to represent good site integrity and preservation. The following two examples from Koobi Fora and Sterkfontein provide an explanation:

- Koobi Fora assemblages at several sites are characterised by a lack of SFD, but artefacts >20 mm are well represented (Schick 1987, 1991, 1997). This distribution of material would appear to suggest a lack of on-site knapping. However, Schick (1987, 1991, 1997) has shown that fluvial forces have affected many of these sites, causing a re-distribution (winnowing) of this SFD off-site and a re-concentration of it elsewhere. Knapping is therefore likely to have occurred but its direct representation on-site has been distorted.
- The Oldowan assemblage at Sterkfontein has a more than-complete size profile, especially relevant for both quartz and chert, which are sourced locally and then flaked expediently on-site (Kuman & Field 2009). It would appear then that site context is good; however, this secondary context cave infill assemblage formed as a result of surface/slope wash in and around the cave entrance. These natural processes had a significant influence on the retention of assemblage components during deposit formation (Kuman & Field 2009).

On- versus off-site lithic manufacture can be established by looking at both the size range of lithic material and the individual character of the pieces. A low quantity of

SFD on-site coupled with artefacts >20 mm can be used to indicate the preferential transport of raw materials as these large (>20 mm) pieces would have been brought in, which at Sterkfontein applies to quartzite artefacts (Kuman & Field 2009). In addition to this, both cortical flakes and cores provide vital information for this purpose; a high representation of the former suggests on-site knapping (possibly even primary knapping locales), whereas a presence of the latter bearing primary flake removals (but an absence of these flakes on-site) suggests the initial phases of core reduction took place elsewhere (Kuman & Field 2009).

Additional processes that cause altered assemblage profiles may also include aeolian and/or less intense hydrological processes, such as sheetwash (Schiffer 1983; Schick 1984, 1987, 1991, 1997; Kandel *et al.* 2003; Morton 2004). The Geelbek Object Movement Experiment (GOME) has provided important data on how aeolian wind processes and the movement of sand mantles leads to the differential movement and/or removal of certain assemblage components (Kandel *et al.* 2003). This is primarily dependent on both the density and shape of the individual artefacts, and it is suggested here that size (hence affecting the smallest assemblage components – SFD) would also play an important role in assemblage modification.

2.3.3.2 Artefact scatter patterns

A site may be characterised by both a high distribution of SFD and pieces suggesting on-site knapping; however a spatial analysis of these pieces (of all sizes) must also be considered. Through the experimental work of Schick (1984, 1991, 1997) on sites where knapping is conducted, the spread of artefacts of a specific size outwards from a central area can be used as a modern comparative model. This enables researchers to answer important questions about site integrity (seen in the retention, or absence, of artefact spatial patterns) and the postures utilised during core/tool reduction (i.e., standing versus sitting or kneeling; Schick 1984, 1991, 1997; Morton 2004). Knapping closer to the ground causes a more localised and concentrated scatter of debris, whereas knapping while standing causes a wider spatial distribution of material away from the central knapping locale (Schick 1984, 1991).

Although this is the case, very seldom do archaeological sites preserve such scatter patterns without some form of modified distribution. At Olduvai Gorge, for example, Petraglia and Potts (1994) provide a detailed account of how assemblages have been modified by fluvial forces, causing a re-distribution of artefacts away from knapping locales. This is clearly seen in the ‘stretching out’ of the site, where small material occurs at a distance downstream away from the knapping area (Petraglia & Potts 1994). These authors have shown that this does not relate to a higher posture (standing) that was utilised while knapping, thus causing increased scatter distances, but rather, the influence of fluvial flow differentially removing small assemblage components and re-depositing them elsewhere, towards the site periphery (Petraglia & Potts 1994).

The refitting of artefacts is another crucial aspect of all spatial studies, most pertinent when assessing the feasibility of on-site knapping (and establishing knapping locales) even within secondary context deposits (Schick 1991; Morton 2004). It seems logical to assume that if any area has had some form of on-site knapping, the pieces that remain should refit. Although visually some sites may appear to suggest localised knapping, very often the distribution of material is a result of lithic influx, either through a preferential transport of material or through natural processes, or some form of post-depositional disturbance that has re-shaped the site (Schick 1991). Conjoining artefact analysis is therefore crucial when assessing site integrity.

2.3.3.3 Artefact spatial distribution patterns

The displacement and re-arrangement of artefacts within archaeological horizons is well-documented. Because a large number of ESA archaeological occurrences comprise of open-air sites, often their exposure to processes affecting the vertical and horizontal distribution of artefacts is extensive (Schick 1984). Processes affecting these distributions include: animal trampling, fluvial and less intense hydrological forces, aeolian winds, bioturbation, dispersal due to downslope gradients, or through other factors affecting sediments such as wetting and drying cycles. A summary of each follows.

Trampling disturbance:

Several studies have investigated the effect of both human and animal induced trampling disturbance, as well as the 'patterns' such disturbances create (Schiffer 1983; Villa & Courtin 1983; Gonzales *et al.* 1985; Nielsen 1991; Vermeersch & Bubel 1997; McBrearty *et al.* 1998; Morton 2004; Forssman & Pargeter 2014). Irrespective of the cause of this disturbance, 'patterns' are due mainly to the nature of the sediments within which artefacts are deposited, and the nature of the artefacts themselves (densities, shapes and sizes; Gonzales *et al.* 1985; Nielsen 1991; Vermeersch & Bubel 1997; McBrearty *et al.* 1998). Loose, unconsolidated sediments allow artefacts to move downwards easily, and it is most often that the smallest pieces become buried the quickest, limiting horizontal displacement; in contrast, larger artefacts remain at the surface for longer and tend to be more displaced horizontally (frequently through kicking) to lower traffic areas. Nielsen (1991) in this regard suggests that both a horizontal and vertical size sorting of material can occur due to trampling disturbance. Although such disturbance can lead to pronounced deposit modification, trampling seldom results in the removal of material altogether, but rather, a spatial displacement of it elsewhere (Morton 2004).

Fluvial forces:

Schick (1984, 1991, 1997), and Petraglia and Potts (1994) examine the effects of fluvial forces, whereas Morton (2004) investigates lacustrine and lakeshore processes related to fluvial forces. Artefact depositional patterns that are created by these forces depend upon the following factors: the specific shape, size and weight of the artefacts, the degree and intensity of fluvial flow, and the initial concentration of the artefacts within the deposit (Schick 1984; Petraglia & Potts 1994; Morton 2004). In relation to these factors, Schick (1991) provides a detailed account of which patterns will be caused by high energy versus low energy flow within any site. Accordingly, Schick (1991) demonstrates that smaller material (SFD) will more easily be removed and spread horizontally across a site, and it will also be deposited the greatest distance away (Schick 1984, 1991, 1997). In contrast, larger material will remain closest to its original position, depending on flow velocities (Schick 1984, 1991, 1997).

The movement of artefacts away from a site means that re-deposition and re-accumulation has to occur elsewhere. This is most frequently in an area where flow velocity is reduced, either as a result of an obstruction (tree, root or boulder) or some form of erosional hollow/depression where flow depth is increased (i.e., where water begins to pool; Schick 1991). These re-accumulations therefore comprise mixed assemblages where pieces may be derived from some considerable distance away, versus those pieces that have been sourced more locally (Schick 1991); deposits can be matrix-supported, clast-supported, or form thin lenses of material (e.g., stringers; Goldberg & Macphail 2006). A large number of Acheulean sites has formed in this way (Schick 1984, 1991). Artefact conjoining (refit) studies can play a vital role in assessing the degree to which site modification has occurred through such forces.

Another way to assess the severity of these forces is through the analysis of artefact dip angles and orientations (imbrication, or fabric), of both clasts and artefacts; these can reveal specific patterns that indicate the final stages of deposition in a range of process-derived contexts (Krumbein 1939; Andrews & Smithson 1966; Tandon & Kumar 1981; Butler 1982; Schiffer 1983; Yagishita & Jopling 1983; Petts & Foster 1985; Bluck 1987; Dietrich 1987; Naden & Brayshaw 1987; Schick 1991, 1997; Petraglia & Potts 1994; Evans 2000; Bridge 2003; Morton 2004; Millane *et al.* 2006; Kostic & Aigner 2007; Hodge *et al.* 2009; Benito-Calvo & de la Torre 2011). This patterning is often used to establish the direction of flow when artefacts were deposited and to suggest that a portion of the assemblage may have been removed as a result of such flow across a site (provided imbrication patterns occur coupled with the removal of assemblage components within a given context; Butler 1982; Schiffer 1983; Petts & Foster 1985; Schick 1991, 1997; Petraglia & Potts 1994; Morton 2004; Millane *et al.* 2006). While these patterns are evident in most alluvial contexts (Petts & Foster 1985; Bluck 1987; Dietrich 1987; Bridge 2003), Dietrich (1987) illustrates that if the force of flow is low enough, imbrications will be absent. Benito-Calvo and de la Torre (2011) have applied GIS techniques at Olduvai Gorge to show that the presence of non-random orientations can be used to question original assumptions (i.e., undisturbed assemblages; Leakey 1971) about site integrity.

Additional studies by Bridge (2003), Schick (1991) and Morton (2004) provide detailed discussions of how imbrication patterns are dependent upon artefact or clast

morphology (such as size, shape and long axis length) and the intensity of fluvial flow. Accordingly, shapes that are more tabular, flat and/or discoidal will create orientations (dip directions) that indicate the upstream pattern of flow, whereas elongated pieces will do one of the following: align parallel to the flow provided that no obstructions have hampered the rotation or movements of the piece or, if movements have been obstructed, a perpendicular orientation to the direction of flow will develop (Petts & Foster 1985; Bridge 2003; Millane *et al.* 2006). Long axis orientation is regarded as being the primary indicator of fluvial flow (Schick 1991).

Large artefacts tend to develop an upstream dip angle as sediments are scoured out from underneath the upstream base of the piece (Morton 2004). Sediments that are easily erodible and unconsolidated therefore facilitate this process. Larger pieces also tend to align perpendicular to the direction of flow, whereas smaller artefacts align parallel (Schick 1991, 1997). By assessing dips and orientations, not only can flow direction be investigated, but so can the intensity of fluvial flow and what assemblage components are likely to have been removed (Schick 1991, 1997; Petraglia & Potts 1994).

Aeolian processes:

The GOME project, already mentioned in the assemblage profile section, provides data that shows how artefacts can be relocated within a site due to aeolian-related processes (Kandel *et al.* 2003). Because the Geelbek site is located within a dune field of minimal vegetated cover, movement of sediments due to dominant wind directions occurs, causing the migration of assemblage components over time through slope and slope instability processes (Kandel *et al.* 2003). This study has shown that artefacts will migrate in the direction of the dominant wind flow, and again, although there is little mention of artefact size (but rather density and shape), it would appear that the smallest assemblage components are most susceptible to this re-location.

Bioturbation:

Four primary agents are responsible for the majority of bioturbated deposits in almost all archaeological contexts and these include: termites, earthworms, plant roots and burrowing animals. Each of these, however, will ‘pattern’ a deposit in a specific way.

Termites:

Studies by McBrearty (1990) and Morton (2004) have shown there are three primary features that characterise termite-modified deposits. An obvious indicator would be the preservation of any form of termite remains (fossil termitia – burrows and channels). This may also include termite activity that occurs in the present. Another feature is a lack of site stratigraphy, due mainly to the pronounced mixing of sediments from different levels and horizons. If artefact concentrations occur with marked upper and lower contacts, and/or if there is a dispersal of artefacts within a given horizon (upward and downward stretching), this too can indicate the influence of termites. Although artefact displacement does occur, this is mostly restricted to vertical movements.

Earthworms:

Studies that address the influence of earthworms highlight that they create minimal disruption to the vertical and horizontal distributions of artefacts (Stein 1983; Morton 2004). The disruptions that do occur cause only microstratigraphic changes and changes to the organic component of the soils within which artefacts are preserved (Morton 2004). Stein (1983) provides parameters (temperature, moisture, soil acidity) that can be used to establish whether a site faces potential disruption from earthworms, or whether conditions in the past have been suitable for such disturbance.

Plant roots:

Although the disturbance of roots is often equated to that of earthworms (minimal artefact displacement and a mixing of sediments; Morton 2004), it is suggested here that plant roots can play a major role in vertical artefact displacement as well. A recent study at Canteen Kopje has proposed the mixing of artefact horizons through possible tree falls/collapses (tree-throw; Lotter *et al.* 2016). Root systems often contain cobbles, pebbles and occasional artefacts, and the upheaval of these ‘root wads’ through tree death, for example, can cause the localised upward displacement of this material (Anderson & Anderson 2010). Morton (2004) suggests that root activity is an important process that needs to be investigated when assessing the integrity of a site, but more studies are needed to fully document its level of influence.

Burrowing animals:

Burrowing animals can cause pronounced disruptions in deposits, primarily through the mixing of sediments, the displacement of archaeological horizons (specific portions of a horizon), and creation of a bimodal pattern of artefact distribution vertically (Erlandson 1984; Morton 2004). However, establishing the extent to which deposits have been modified in the past is extremely difficult, and determining which agent is responsible is dependent upon several factors such as climate, temperatures, and moisture (Erlandson 1984), as these factors will determine which kinds of flora and fauna will influence a given deposit. In general, artefacts can be considerably displaced both vertically and horizontally.

Downslope dispersal:

The movement of site contents or sediments downslope is dependent upon several key factors, most pertinent of which is the slope gradient (Morton 2004). Although steep slopes lead to the pronounced movement of pieces through detachment, additional factors relating to the density of vegetation and character of the sediments can also greatly influence the nature and severity of artefact displacement irrespective of the slope gradient (Morton 2004). Furthermore, artefacts are differentially re-organised downslope due to differences in shape, size and density (Stern 1993; Morton 2004). Large pieces tend to travel downslope at a faster rate than small pieces, yet if these pieces are blade (elongated and thin) and/or disc-like in shape, transport rates will be slower (Morton 2004). Spherical pieces generally have high rates of downslope dispersal.

Additional mention must be given here to surface erosive processes affected by slope gradients, causing the deposition of colluvially accumulated sediments. All surface erosion is dependent upon two important factors, erosivity and erodibility (Charlton 2008). The former relates specifically to the ability of any agent to erode, such as rainfall, and how it can remove surface sediments; this ability is dependent upon the amount of available kinetic energy (Charlton 2008). Erodibility refers to the susceptibility of a given medium, or substrate, to erode. This is again influenced by several factors, most of which relate to the characteristics of the medium itself (e.g., fine-grained and high in cohesive clay versus loose and unconsolidated coarser sands; Charlton 2008). Two forms of unconcentrated surface flow erosion will be discussed

here, namely rain splash and sheetwash/flow erosion, as well as two concentrated forms, including rill and gully erosion. A final mention will be given to larger scale downslope mass movement events.

Rain splash and sheetwash/flow erosion:

Downslope erosion of surface sediments through both rain splash and sheetwash (hydrological processes) has been noted in many studies (Quansah 1981; El-Swaify *et al.* 1982; Slattery & Bryan 1992; Brown 1997; de Jong *et al.* 1999; Lal 2001; Ventura *et al.* 2002; Zhang *et al.* 2003; Goldberg & Macphail 2006; Charlton 2008; Anderson & Anderson 2010). Several factors determine the extent and rate of this downslope movement and these are primarily concerned with rainfall and the character of the impacted medium. From a purely meteorological perspective, rainfall will vary due to: drop size, velocity, distribution, angle and direction, as well as with rain intensity, frequency and duration (Charlton 2008). The erosive capability of this rainfall is also determined by factors influencing runoff. Runoff is governed by the water supply rate, the depth of flow that develops, flow velocity, frequency, magnitude, duration and the sediment content (Charlton 2008). Even if these conditions are favourable, sediment characteristics also play an equally important role in facilitating the erosive process; this is affected by: particle sizes, porosity, cohesiveness, and pre-existing soil moisture content, along with any vegetated (dense or sparse) cover (Goldberg & Macphail 2006; Charlton 2008). As a result, rain splash erosion is most effective on bare sloped surfaces where sediments have poor cohesive strength (Charlton 2008). Additional land use practices such as ploughing and terracing can influence surface erodibility (Charlton 2008).

Rain splash concerns the detachment of soil particles through the impact of individual drops upon a given surface (Anderson & Anderson 2010). Each raindrop possesses kinetic energy, most of which is expelled upon impact. However, these impacts are sufficient enough to eject soil particles, and when this occurs on slopes, a net downslope movement of particles/sediment develops as ejected particles travel longer distances downhill than uphill (Anderson & Anderson 2010). This is most pronounced on steeply sloped surfaces (Charlton 2008).

Where the intensity and duration of rain exceeds the infiltration capacity of the underlying sediments, overland flow develops (Goldberg & Macphail 2006; Charlton 2008). Where this occurs as surface flow in thin sheets, this is what can be called ‘sheetwash or sheetflow.’ This flow is seldom of uniform depth, due mainly to surface irregularities that promote flow channeling (Charlton 2008). This downslope flow exerts a shear stress on the surface sediments, and when this stress exceeds the cohesive resistance of the sediments, soil erosion occurs (Charlton 2008). Due to pre-existing surface irregularities, sheetwash is generally unable to cause significant surface erosion; however, where slopes are steep and surface sediments are smooth and non-cohesive, this erosion can be extensive (Charlton 2008).

Through the combined action of (initial) rain splash particle detachment and (secondary) sheetwash, large volumes of sediment can be eroded from areas of sloping land (Charlton 2008). Rain splash provides a perfect mechanism where drop impact leads to the dislodging of sediment particles. Subsequent overland flow allows for the pronounced downslope transportation of these detached particles, creating a water and particle rich abrasive medium (Charlton 2008).

Rill and gully erosion:

Where concentrated and channeled sheetwash occurs, rill and gully erosion develops. This occurs when surface water can no longer move along in thin sheets but instead occurs within favoured lines of drainage (Goldberg & Macphail 2006). It is in fact through the development of rills and gullies that the most obvious effects of surface runoff flow can be seen (Boardman *et al.* 2012). The effect, character, description and classification of these features have been dealt with in many papers (El-Swaify *et al.* 1982; Ballantyne & Benn 1994; Botha *et al.* 1994; Brown 1997; de Jong *et al.* 1999; Lal 2001; Ventura *et al.* 2001; Zhang *et al.* 2003; Grab & Deschamps 2004; Goldberg & Macphail 2006; Charlton 2008; Anderson & Anderson 2010; Boardman *et al.* 2012).

Rills are small surface channels, or micro-channels, that begin to form when surface flow is able to overcome a critical shear stress for the underlying sediments (Charlton 2008). They vary in size with widths of between 50-300 mm and depths of 30 mm (Charlton 2008). The dominant processes that act within a rill include particle

detachment and concentrated flow (Zhang *et al.* 2003). Through these processes, eroded sediment is carried downslope and deposited lower down where flow velocity is reduced (Charlton 2008). The presence of these features on a slope is largely dictated by the erodibility of the underlying sediments, surface topography and slope steepness (Charlton 2008). Overall, through the combined action of rain splash detachment, sheetwash, and rill erosion, large volumes of sediment, and even small rock fragments, can be redistributed (Charlton 2008).

Larger more permanent features include gullies, ranging in size from a few centimeters to many meters in length and width. These are frequently associated with dry, poorly vegetated arid landscapes where sporadic rainfall leads to significant sediment erosion events (Boardman *et al.* 2012). However, they can occur anywhere that slope, sediment, vegetation and surface flow characteristics are favourable. Gullies provide an important link between riverbanks and upland areas, supplying vast amounts of sediment and rock (eroded material) to downslope river systems (Charlton 2008).

Gully extension and development follows a similar sequence to that seen in normal rivers and streams, although sidewalls are frequently steeper and channels are narrower (Charlton 2008). These steep sides are highly susceptible to mass movements, especially when sediment moisture is high after rainfall (Charlton 2008). Landslides are also commonly associated with gully development (Charlton 2008). Active headward erosion occurs at the top of the gully, causing the removal of sediment by undercutting the gully system upslope (Goldberg & Macphail 2006; Charlton 2008). Gully extension can take place rapidly if conditions are favourable and large volumes of sediment can be removed from the landscape; the rate of gully extension is controlled by slope steepness, upstream sediment supply, and the size of the upstream drainage catchment (Charlton 2008). Deposition in the base of gullies will also occur where flow is reduced. This will frequently give rise to the formation of 'cut and fill' structures (Fig. 2.3.1), characterised by a build up of colluvial sediments from several different depositional events (Boardman *et al.* 2012). Gully deposits containing larger particles (rocks and cobbles) can frequently be winnowed of their finer material (clays, silts and/or sands; supporting matrix), causing the formation of lag deposits (Goldberg & Macphail 2006).



Figure 2.3.1. Gully erosion showing a cut and fill sequence (from Boardman *et al.* 2012).

Mass movement/wasting:

Involved with the downslope movement of sediments and rocks under the influence of gravity (alternatively called ‘sediment gravity flows’), a range of papers has dealt with the effects, types, definitions and characteristics of these processes (Culling 1963; Albjar *et al.* 1979; Lowe 1982; Wright & Anderson 1982; Akerman 1984; Mills 1984; Abrahams *et al.* 1985; Postma 1986; Abrahams *et al.* 1990; Mosher *et al.* 1994; Bertran & Texier 1995, 1999; Armanini & Michiue 1997; Bertran *et al.* 1997; Hand 1997; Major 1997, 1998, 2000; Shimokawa 1997; Curry & Ballantyne 1999; Fannin & Wise 2001; Parsons *et al.* 2001; Malet *et al.* 2002; Dasgupta 2003; Mills & Grab 2005; Obanawa & Matsukura 2006; Sass & Krautblatter 2007; Charlton 2008; Mills *et al.* 2009; Anderson & Anderson 2010; Muir *et al.* 2015). The mass movement of sediment and rock is not a direct result of moving water, air or ice, but rather these serve as the lubricating mediums (Charlton 2008). The spatial and temporal scales at which these processes operate is highly variable, ranging from the small-scale movement of a few centimeters of sediment over hundreds of years to the removal of whole mountainsides in a matter of seconds (Charlton 2008).

The classification and terminology used to describe these movements has been a debated topic for many years (see Postma 1986 and Dasgupta 2003 for descriptions), and this is due primarily to differences in deposit and process description, identification, and a lack of concern for the spatial variability of a single deposit. Irrespective of these issues, mass movement events are influenced by a few key factors. The first relates to the force acting upon a given body of sediment, a downslope shear stress (Charlton 2008). A second force is the frictional resistance of the underlying sediment (Charlton 2008). Additional factors that greatly influence the type and rate of downslope movement relate to the cohesive strength of the sediment body (governed by particle size and shape), sediment moisture content (providing lubrication), slope steepness, and the prevalence of trigger mechanisms (Charlton 2008). Trigger mechanisms can include earthquakes, heavy rainfall, wildfires, changes in vegetation cover, and slope steepening and loading (caused by accumulating debris; Charlton 2008). Describing mass movement deposits generally includes the analysis of the following sediment characteristics: composition (distribution, sorting, support, packing of grains); clast morphology, shape and roundness; deposit stratification; graded or ungraded bedding; and the orientations of clasts within the deposit (Major 1998).

Several different types of mass movement have been described and the terminology here will follow that from Bertran and Texier (1999) and Charlton (2008). Figure 2.3.2 illustrates that in terms of movement, these events generally occur as slides, flows, or falls. Slide movements occur where a shear plane exists between a given sediment body and the underlying surface (parallel for a translational slide and concave for a rotational slide, shown in Figure 2.3.2a & b, respectively; Charlton 2008). Flows do not retain a shear plane and the deposit is more fluid in composition (highly variable); flows are frequently channelised (following pre-existing gullies), have well-defined boundaries, and terminate with a debris accumulation zone (Fig. 2.3.2c; Charlton 2008). The vertical displacement of material (sediment or boulders) occurs as a fall (Fig. 2.3.2d; Charlton 2008).

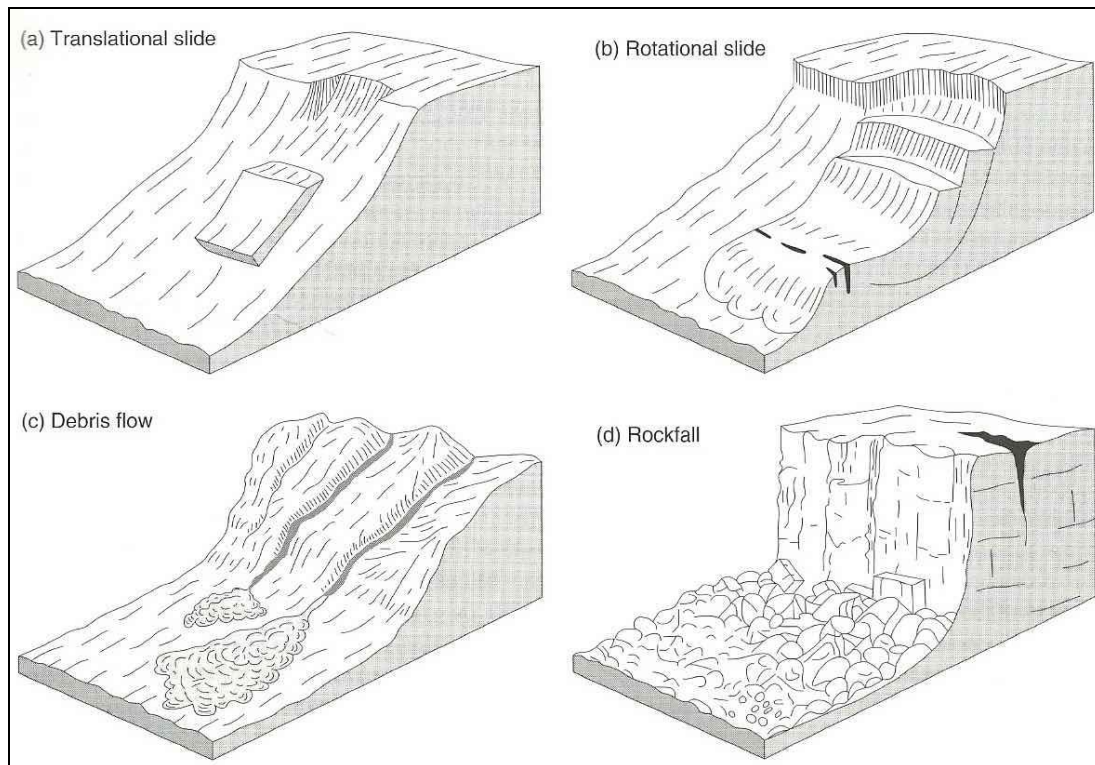


Figure 2.3.2. Types of mass movement (from Charlton 2008). Translational slide (a); rotational slide (b); debris flow (c); rockfall (d).

A detailed description of mass movements based on the composition of moving material is provided by Bertran and Texier (1999; Fig. 2.3.3). A summary here will address debris and earth slides/flows (water and fines). Based on the work of Dasgupta (2003), it must be noted that the description of these deposits is difficult. Even within a single deposit, flow transformation can lead to the presence of several types, due to differing quantities of sediment and water within the flow (Fig. 2.3.3), and each of these slope processes occurs as a segment of a continuous spectrum of sediment gravity flows.

Sediment concentration	Low		Intermediate	High	
Main interstitial fluid	air	water	water + fines	air	water + fines
Process	Rockfall	Runoff Streamflow	Hyperconcentrated Flow	Grain flow Rock-avalanche (>10 ³ m ³)	Debris flow (liquefaction) Solifluction Earth slide / flow (distinct sliding planes)

Figure 2.3.3. Classification of slope processes (from Bertran & Texier 1999).

a. Debris flow:

Debris flows are highly concentrated mixtures of liquefied sediment and water (Major 1997). Sediments can include rocks, soil, organic matter and additional debris, all of which are deposited downslope *en masse*, giving rise to a poorly sorted, matrix- or clast-supported mixture of sediment ranging in size from clay to boulders (Fig. 2.3.4; Major 1997; Anderson & Anderson 2010). The supporting matrix bears a finite cohesive strength, which allows for the transport of large items (in contrast to other sediment gravity flows, such as hyperconcentrated flow; Dasgupta 2003). This strength, however, will still give rise to an upper limit in terms of cobble or boulder size, suggesting that large items exceeding this strength will settle through the matrix during flow (Lowe 1982). Deposit grading is generally absent, although normal or reverse grading can occur (Major 1997). Clast depositional fabric within the flow generally shows no or only weakly preferred orientations, and the highest strength occurs at the lateral margins of the deposit (Bertran & Texier 1999).

Debris flows are characterised by a three-phase lifecycle, including initiation, flow, and deposition (Shimokawa 1997). Initiation is generally in response to the upslope accumulation of debris on steep slopes or valley beds, and subsequent saturation by water causes a downslope slumping and sliding of this material (Shimokawa 1997). They can also be initiated by the removal of loose debris that has accumulated in upslope rills and gullies (lag deposits), and/or by the transformation of a landslide, into a watery slurry sediment mixture, due to rainfall (Bertran & Texier 1999). Deposit lubrication that overcomes clast weight and frictional resistance may be provided by a clay-water matrix that comprises of as little as 5% of the total flow volume (Lowe 1982). This will initiate flow downslope causing the erosion of valley and gully bottoms and sidewalls, and a great deal of sediment can be transported in a single event (Shimokawa 1997). Importantly, debris flows will collect surface debris that occurs downslope and incorporate it into the deposit through mixing. Deposition will occur downslope due to a reduction in flow momentum (most commonly caused by changes in flow area and/or reduction in slope gradients). Although some debris will remain from the flow, upslope, the majority is deposited in a fan, with a lobate cone- or tongue-shaped termination (Fig. 2.3.2c; Shimokawa 1997). Multiple flows in a given area are difficult to differentiate as individual events (Lowe 1982; Major 1997, 2000).

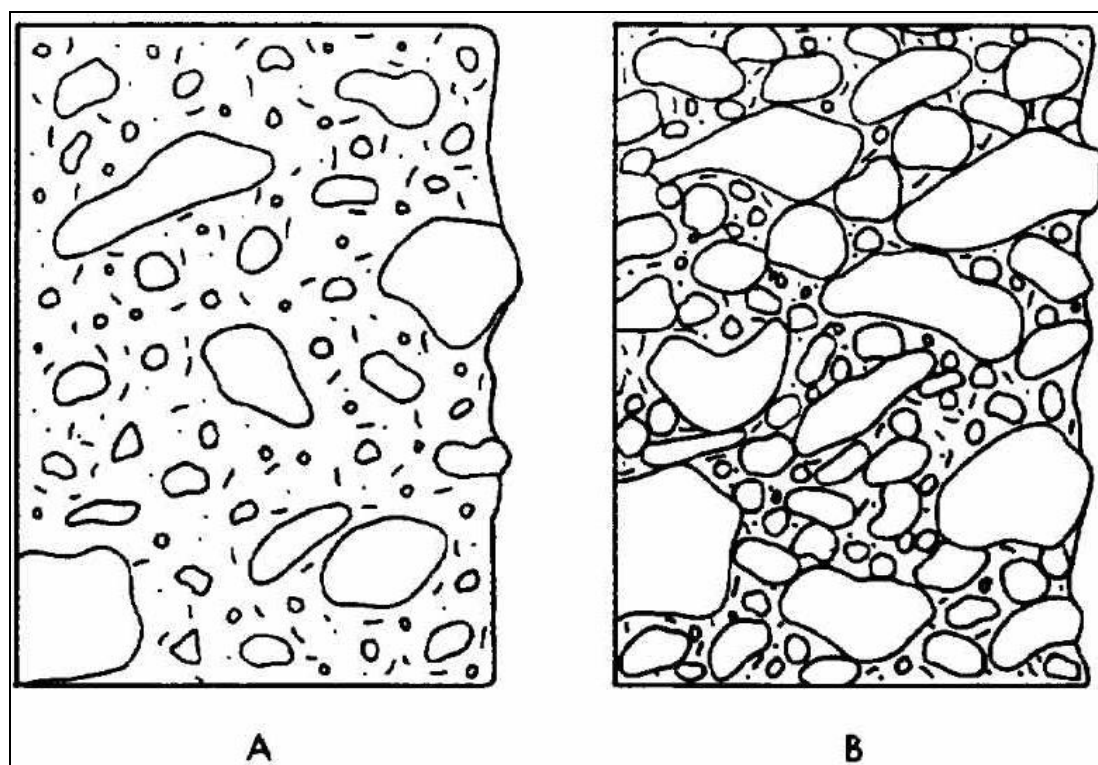


Figure 2.3.4. Debris flow deposits (modified from Lowe 1982). Massive, structureless, matrix-supported deposit (a); massive, structureless, clast-supported deposit (b).

b. Earth slide/flow:

Earth slides or flows are characterised by the displacement of sediments along a shear plane (Fig. 2.3.2a & b). Generally the blocks of sediment (containing a range of particle sizes, but generally fine) will break away in whole pieces and will disintegrate downslope as movement occurs (Bertran & Texier 1999). This initial movement downslope will be the result of forces overcoming the cohesive strength of the sediments (Bertran & Texier 1999). The rate of movement is dependent upon the moisture content of the moving mass and/or the surface upon which downslope movement occurs.

These deposits are characterised by a homogenised mass containing a brecciated structure, especially where deformation is weak (Bertran & Texier 1999). Any bedding that may have been retained in the block of material is either completely removed or deformed through folding and/or stretching (Fig. 2.3.2b). An upslope bedding of material is frequently used to identify these features (Bertran & Texier 1999).

The influence of sediment characteristics:

Subsurface artefact movements occur within sediments where both re-consolidation and wetting and drying cycles affect a given deposit (Cahen & Moeyersons 1977; Moeyersons 1978). Sediments that promote artefact creep through wetting and drying cycles have a high clay fraction (Cahen & Moeyersons 1977; Moeyersons 1978). Re-consolidating sediments cause the vertical displacement of artefacts, stretching the distribution of pieces over a larger area, as sediment structures change. The rate of artefact movement depends upon the frequency of sediment contraction and expansion events, the size, orientation and weight of the artefacts, and the number of biogenic agents that cause the mixing and continual re-consolidation of sediments (Cahen & Moeyersons 1977; Moeyersons 1978). Although movements through artefact creep occur more gradually, when a clay-rich sediment is affected by both bioturbation and wetting and drying cycles, the combination of these processes can lead to significant artefact displacements (Cahen & Moeyersons 1977; Moeyersons 1978). This is especially evident where bioturbation forms burrows and holes, and the subsequent collapse of these subsurface structures promotes significant sediment re-consolidation (Cahen & Moeyersons 1977; Moeyersons 1978).

Vertical artefact movements within these sediments will often lead to a re-concentration of pieces lower down, frequently along a depositional unconformity (e.g., bedrock, or a different deposit type such as gravel; Moeyerson 1978). These concentrations may therefore represent time-averaged assemblages where the mixing of overlying horizons, with assemblages from different periods, causes the downward migration of pieces. These deposits generally lack any form of stratigraphy (Moeyersons 1978).

2.3.3.4 Artefact condition

Research concerned with artefact condition focuses on the effects of trampling, weathering, abrasion, and the specific composition of the raw material upon which the artefact is made (Shackley 1974; Kuman 1989; Nielsen 1991; Pappu 1996; McBrearty *et al.* 1998; Shea 1999; Holmes *et al.* 2008; Kuman & Field 2009; Thompson 2009). Assessing the condition of artefacts within archaeological sites is fundamentally important when explaining site context and formation.

Kuman (1989) and McBrearty *et al.* (1998) note that trampling often leads to the damage of artefacts. Nielsen (1991) shows that trampling-induced artefact damage occurs in three ways, including breakage, micro-flaking and abrasion. The extent of this damage is determined by three additional factors, namely the duration of trampling disturbance affecting the site/deposit, the nature of the sediments within which artefacts are preserved, and the size of the individual artefacts (Nielsen 1991). Kuman (1989) has also shown that the type of artefact damage is highly correlated with the thickness of the artefact edge. Breaks or micro-fractures are created along the edges of thin unretouched artefacts, such as flakes, whereas crushing of artefact edges is more common on thicker-edged retouched tools (Kuman 1989). When viewing final artefact form, an assessment of artefact damage through trampling processes must be conducted as some damage that may appear to be intentional tool retouch or secondary modification could in fact be the result of naturally induced processes (Kuman 1989; McBrearty *et al.* 1998; Kuman & Field 2009).

Artefact weathering has been dealt with in several studies, most of which emphasise two key issues: the first is that raw materials each weather a specific way (usually dependent upon the strength of the material), and second, the rate and type of weathering reflects the type and intensity of erosive process that has acted upon the material (Shackley 1974; Pappu 1996; Shea 1999; Holmes *et al.* 2008; Thompson 2009). Within an archaeological context very often there are different raw materials utilised for lithic production. Each of these materials has formed in a specific way (e.g., sedimentary sandstone or metamorphosed quartzites), yet the chemical, mechanical and physical weathering potential of each material is different (Shea 1999). Artefacts will then reflect this weathering potential, in final form, in response to a given process. An example illustrating this would be artefacts from an alluvial context, with progressive edge rounding and modification. Final artefact form is therefore crucial when assessing not only the context of an assemblage and/or site, but also to estimate the severity of the weathering process/es involved (Shea 1999; Thompson 2009).

The following two examples provide an illustration:

- At the ESA site of Ubeidiya, Shea (1999) has shown that artefacts comprise a mix of fresh to heavily abraded pieces, yet the context and

formation/accumulation history of the deposit has remained the same throughout its development (formed by moderate fluvial forces). Looking purely at the range of weathering states would appear to suggest differences in accumulation histories. However, it is shown that the differential chemical break down of artefacts *in-situ* is responsible for the wide range of conditions (Shea 1999). Furthermore, Shea (1999) was able to assess the level of fluvial influence by establishing which abrasion state was most common (slightly abraded). Intense fluvial action would have caused more progressive rounding of artefact edges, whereas minimal influence would have resulted in a completely fresh assemblage, provided there was an absence of any other form of weathering (Shea 1999). Although the artefacts reacted differently to their homogenous depositional environments, weathering states can still be used to question the extent to which site formational processes such as fluvial forces have affected the artefacts themselves (Shea 1999).

- Pinnacle Point in the Western Cape also provides a sample of artefacts with a range of conditions, both horizontally and vertically, within a single deposit (Thompson 2009). Interestingly, in contrast to the example above, these varied conditions are not the result of *in-situ* chemical decay but rather a differential exposure of the artefacts through time as the site formed. These exposures, at varying periods for different lengths of time, meant that artefacts became differentially rounded, polished and patinated through abrasion from the accumulating sands (Thompson 2009). Those artefacts exposed more frequently than others, either through sediment re-working or differential surface exposures due to slow burial, obtained the poorest condition (Thompson 2009). Based on these weathering states it is proposed that the deposit formed through periodic depositional events, which lead to alternated periods of artefact reburial and exposure (Thompson 2009).

A final mention of how to quantify artefact abrasion caused by fluvial processes is worth noting here. Shackley (1974) developed a system of measurements by analysing ridge widths and patterns of abrasion on flint implements. Accordingly, a seven-level scale of wear for artefacts, ranging from mint condition to very heavily abraded, was proposed. Shackley (1974) also distinguished between wear caused by chipping versus grinding (rounding) of edges based on the size of the artefact, the

particle size distribution of the material within the transporting medium, and the flow velocity of this medium. This important study provides a quantitative method to assess artefact edge modification, contrasting with more subjective studies that employ only visual assessments.

2.4 Summary

The information provided by the first half of this chapter has helped to explain the nature and characteristics of the Acheulean Tradition within Africa, and at which sites this technology occurs. From the review of sites it is clear that locating and excavating well-dated ‘contextually sound sites’ is one of the greatest challenges that faces ESA archaeologists today. Providing adequate assemblage descriptions and accounting for the full range of processes that may or may not have had an influence on deposit formation and transformation are also of great importance.

The final section of this chapter provided a detailed account of all processes that may have played a role in deposit formation and transformation, affecting both the primary deposition of artefacts and post-burial secondary modification, at a more local scale. From both the range and variability of these processes it is clear that assessing the influence of these within a given deposit is crucial to overall site interpretations. Excavations in the lower Sundays River Valley have provided important assemblages from which we can address important cultural questions regarding assemblage typology and technology. However, contextual interpretations must precede these.

Chapter 3 will provide a background to research that has been conducted in the Sundays River Valley. From this a comprehensive understanding of the regional scale fluvial landscape will be provided. This chapter will also provide the details of all methods employed during this study, including a description of the three study sites: Atmar, Bernol and Penhill Farm.

Chapter 3

Study sites and methods

3.1 A history of research in the lower Sundays River Valley

3.1.1 Introduction

The lower Sundays River Valley has been noted in a range of papers dealing with:

- Palaeontological remains (fauna and flora, as well as present flora; Brenner & Oertli 1976; Brown & Gow 1976; Brown 1977; Shone 1978, 1986; Cooper 1979, 1981, 1983; Cowling 1983; Rich *et al.* 1983; Bamford 1986; Hoffman & Cowling 1990, 1991; Moolman & Cowling 1994; Forster *et al.* 1995; Frost 1996; De Klerk *et al.* 1997, 1998; McMillan 1999, 2003; Ross *et al.* 1999; De Klerk *et al.* 2000; Gomez *et al.* 2002a; Gomez *et al.* 2002b; Almond *et al.* 2009; Choiniere *et al.* 2012; Galton & Molnar 2012; Muir *et al.* 2015)
- River ecology (Forbes & Allanson 1970)
- Stone Age archaeology (Ruddock 1957)
- Fluvial geomorphology and river terrace formation and dating (Haughton 1928, 1935; Ruddock 1948, 1968; Dingle & Scrutton 1974; Partridge & Maud 1987; Hattingh 1994, 1996, 2008; Hattingh & Goedhart 1997; Dollar 1998; Hattingh & Rust 1999; Bridgland & Westaway 2008; Erlanger 2010; Erlanger *et al.* 2012)

A summary is found below; palaeontological work, however, is not relevant and will not be discussed further (a more inclusive reference list is provided by Almond *et al.* 2009).

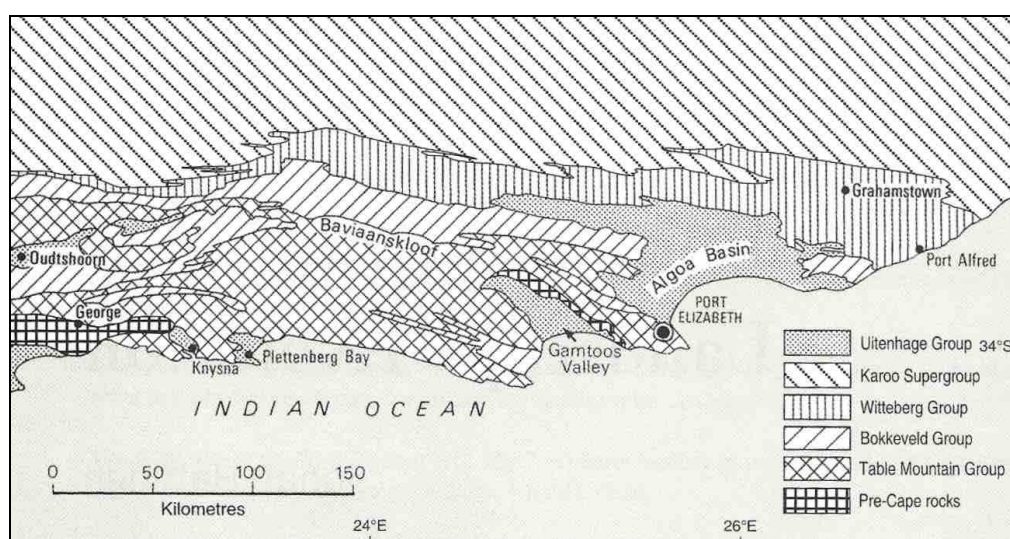
3.1.2 An introduction to the lower Sundays River Valley

The present-day Sundays River originates along the edge of the Great Escarpment, north of the town of Graaff-Rienet. The river then flows south over Karoo Supergroup

shale and sandstone, towards the Indian Ocean, intersecting the Klein Winterhoek Mountains about 80 km from the coast (Fig. 3.1.1a & b; Hattingh & Rust 1999). These mountains form the eastern-most limit of the Cape Fold Belt and they are comprised of well-indurated quartzites and sandstones of the Palaeozoic Witteberg Group; these quartzites and sandstones account for more than 95% of the clasts downstream (Fig. 3.1.1a & b; Ruddock 1948; Hattingh 1994; Hattingh & Rust 1999). Additional clasts are in the form of Dwyka Group diamictites (a further 3%) and Karoo dolerites and hornfels (Hattingh 1994). A limited number of clasts from the Zuurberg basalt and Enon, Kirkwood, and Sundays River Formations are also present in the deposits of the lower valley (Fig. 3.1.1d; Hattingh 1994).

Where the Sundays River intersects these erosion-resistant quartzites and sandstones (at Korhaans Drift, forming a fixed knick point), this demarcates the upper (north) and lower (south) valleys (Hattingh & Rust 1999). Flowing south from these mountains the lower Sundays River enters the Algoa Basin, comprised of highly erodible shale and mudstones of the Uitenhage Series (Ruddock 1948; Hattingh & Rust 1999). The Algoa Basin is a half-graben with an east-west striking fault forming the north and east margin of the basin (Fig. 3.1.1c; Hattingh & Rust 1999).

The unique underlying geology of this region has enabled the lower Sundays River Valley to record changes in drainage evolution in the form of preserved fluvial terrace deposits (Hattingh & Rust 1999). These deposits unconformably overlie the deposits of the Algoa Basin (Hattingh 1994).



a

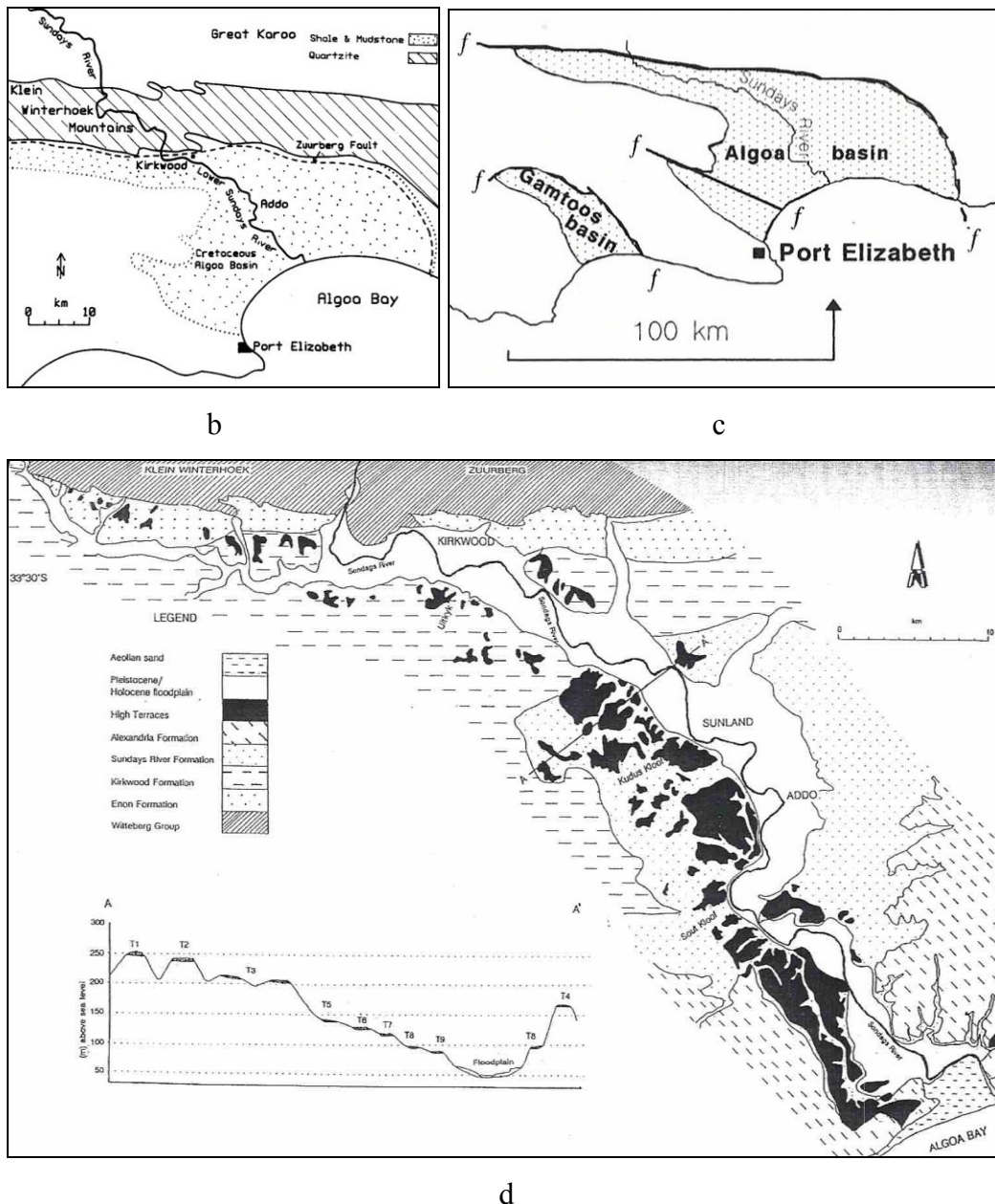


Figure 3.1.1. Important features of the lower Sundays River Valley. Main geological members of part of the Eastern Cape, showing relevant basins (a; from Hattingh 2008); location of the Sundays River in relation to the Klein Winterhoek Mountains (b; from Hattingh 1996); distribution of faults (f) in relation to the lower valley (c; from Hattingh & Rust 1999); detailed geological formations of the lower valley (d; from Hattingh 1994).

3.1.3 Studies on fluvial geomorphology and terrace formation, composition and description

The majority of rivers in the Eastern Cape originated approximately 120 Ma, due primarily to the development of the southern African sub-continent after the

fragmentation of Gondwanaland (Hattingh 2008). As a result the rivers of this region illustrate a very complex and lengthy evolutionary history. However, emphasis here will be placed only upon the period encompassing the formation and evolution of the lower Sundays River Valley fluvial terrace deposits (Hattingh and Rust 1999 and Hattingh 2008 discuss the river's earlier development).

Haughton (1928, 1935) was the first to identify fluvial gravel deposits bordering the current Sundays River, which are most developed in the lower valley on the western side of the present river channel. Later research by Ruddock (1948) sought to provide a more detailed understanding of the terraces and their major physiographic features. In order to do so a map of the terraces was prepared, using heights along their length, allowing one to establish a length-profile for each. Also of interest was establishing terrace thickness (Ruddock 1948).

As a result Ruddock (1948) was able to identify both lower (primarily comprised of fine sand and silt, below 100 ft) and higher (primarily comprised of gravel, at and above 170 ft) terraces, four of which he termed 'principal terraces,' as they have similar heights throughout the lower valley. These principal terraces are (highest to lowest): Kirkwood, Harveyton, Addo and Colchester, respectively. They were seen to document sea level changes related to what were termed 'Major' and 'Minor' Emergences (by Krige 1927); however, Ruddock (1948) was unable to determine the precise sea levels that corresponded to the terraces. This was due to an inability to determine exactly where the Sundays River mouth was during each stage of sea level rise (Ruddock 1948). However, based on pre-existing palaeontological and archaeological data at the time, Ruddock (1957) concluded that the terraces preserved a record spanning the middle to the end of the Pleistocene.

Later work by Ruddock (1968) also suggested that three phases of seaward tilting and warping in the Algoa Basin were responsible for terrace formation in the lower valley – one in the late Tertiary (probably Miocene), one in the Pliocene and one in the Plio-Pleistocene. During these shifts, transgressive events led to a reduction in channel gradients (increase in sea level through base-level rises) and aggradation, whereas regressions (lowering of sea level) led to an increase in stream power and downward incision through steeper river gradients (Ruddock 1968).

More recent work on the lower Sundays River Valley has been provided by Hattingh (1994, 1996, 2008), Hattingh and Goedhart (1997) and Hattingh and Rust (1999). These studies have provided a more accurate separation of the terraces based on their heights and on morphological, compositional and topographical differences (Dollar 1998). These authors demonstrate that a total of 13 terraces occurs, of which the upper nine (seen to be from the Late Miocene through Pliocene, 180-40 m above the present river level and primarily comprised of gravel deposits) can be distinguished from the lower four (Pleistocene through Holocene, 25-3 m above the present river level, primarily comprised of fine silt and sand; Fig. 3.1.2; Hattingh 1994, 1996, 2008). The highest and oldest of these (Terrace 1) occurs 180 m above the present river level and the lowest (Terrace 13) occurs only a few meters above this present level (Hattingh 2008). The upper terraces (1-9) are collectively known as the Kudus Kloof Formation and the lower terraces (10-13) the Sunland Formation (Hattingh 1994). The majority of the upper terraces now occurs as discontinuous and sporadic gravel-capped hills, due mainly to their dissection by tributaries of the Sundays River (Hattingh 1994). These upper gravel deposits are frequently calcretised, giving rise to well-cemented conglomerates; it is suggested that calcium for this calcretisation is derived from weathered Dwyka diamictite and Karoo dolerite (Hattingh 1994). Overall, these terrace deposits range in thickness from 3-12 meters (Hattingh 1996).

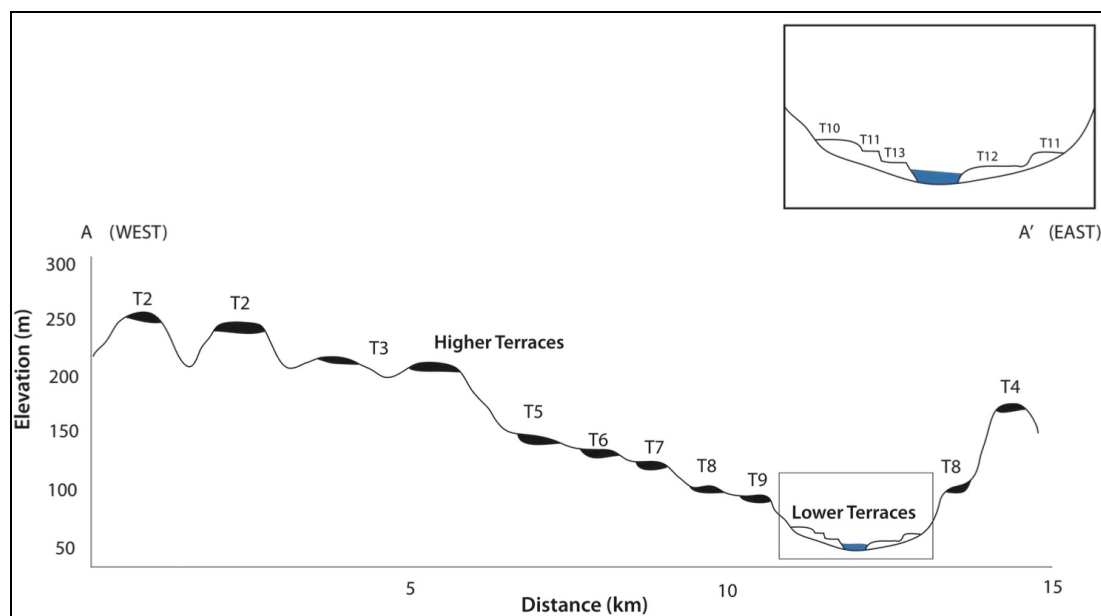


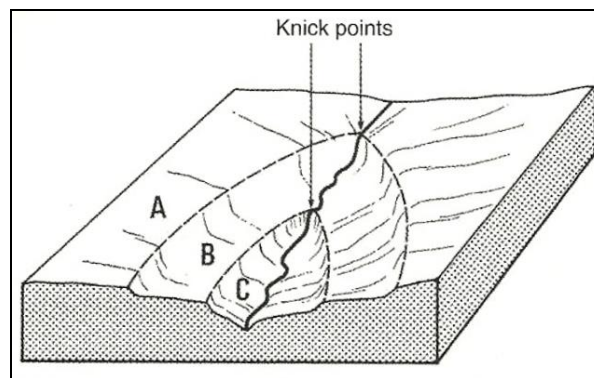
Figure 3.1.2. Lower Sundays River Valley terraces (from Erlanger 2010), Upper (Terraces 1-9) and lower (Terraces 10-13). Note west to east descent of terraces. Terraces are best preserved on the western side of the river due to the eastward migration of the river through time.

Debate concerning terrace development has invoked various explanations, including climate change, neotectonic activity, marine transgressive and regressive events, and associated geological controls (Ruddock 1957; Hattingh 1994, 1996, 2008; Hattingh & Goedhart 1997; Dollar 1998; Hattingh & Rust 1999). Detailed accounts by Hattingh (2008) and Hattingh and Rust (1999) provide some understanding for the formation of these terraces.

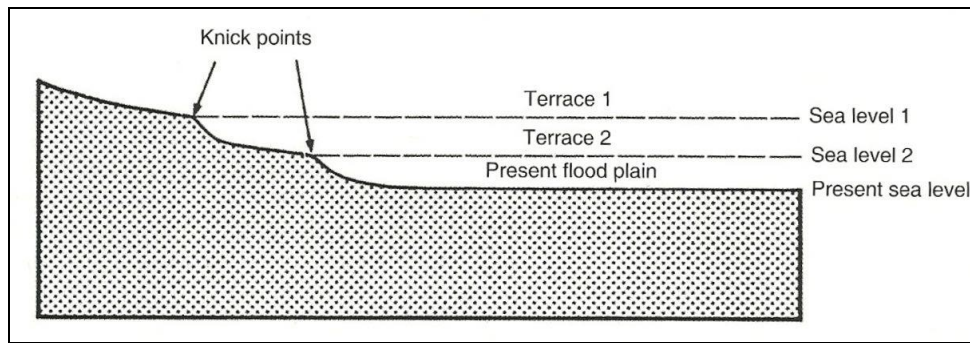
3.1.3.1 A summary of the model proposed by Hattingh and Rust (1999) and Hattingh (2008) for the evolution of the Sundays River terraces

In the past the Sundays River has flowed at several different levels above and below the present river level. By 5 Ma however, sea levels were approximately 200 m higher than at present and the Sundays River flowed 180 m above its present level. Since then there has been an overall decline in sea level.

Sea level forms a permanent base level of erosion for all streams and rivers. By lowering the base level of erosion a stream will begin to erode vertically downwards in order to compensate for such a change. This leads to the creation of a knick point. Originating at the most distal end of the river (where it meets the coastline) these knick points then migrate upstream as the river continues to lengthen its profile, through active headward erosion, in an attempt to create erosional and depositional stability/equilibrium (Fig. 3.1.3a). Multiple decreases in sea level will cause a series of knick points to develop and as these migrate upwards a new river profile is formed below the level of the previous floodplain (Fig. 3.1.3). The preservation of these older river profiles, above the level of the new riverbed, is what forms these terraces (Fig. 3.1.3b).



a



b

Figure 3.1.3. Knick point development causing terrace formation (from Hattingh 2008). Knick points migrate upstream through active headward erosion (a); longitudinal river profile highlighting terrace preservation in relation to sea level changes (b).

The higher Miocene to Pliocene period terraces (1-9) illustrate that stream energy during their formation was high. During this period there was a constant decline in sea level, forcing the river to vertically incise and steepen its profile. The presence of large boulder-sized clasts within these upper terraces attests to the constant declining of sea level, maintaining high energy flow downstream through the steep gradients.

Climatic conditions during this time indicate a much warmer, tropical environment with very high rainfall. This, coupled with the decreasing sea level, led to heightened sediment transport and the weathering and erosion of the local drainage basin. Hattingh (1994) suggests that these higher terrace deposits could be derived primarily from extreme flooding events brought on by cyclonic rainstorms.

Prevailing conditions during this early period also led to the formation of large alluvial fans along the margins of nearby mountains (Figs. 3.1.4 & 3.1.5; Hattingh 1994). These fans then supplied large quantities of sediment and water to the lower valley (mass flow deposits), and through time, a large floodplain formed during periods of aggradation and reduced river incision. Subsequent down cutting of the river into this floodplain gave rise to the terraces preserved today (Fig. 3.1.4). A combination of steep mountain slopes and high precipitation and sediment accumulation rates produced ideal conditions for debris flow and sheet-flood conditions (Hattingh 1994). Overall, between 5 and 1 Ma, the Sundays River Valley

comprised of a wide valley floor with braided channels yielding a very high sediment load (Fig. 3.1.4; Hattingh 1996).

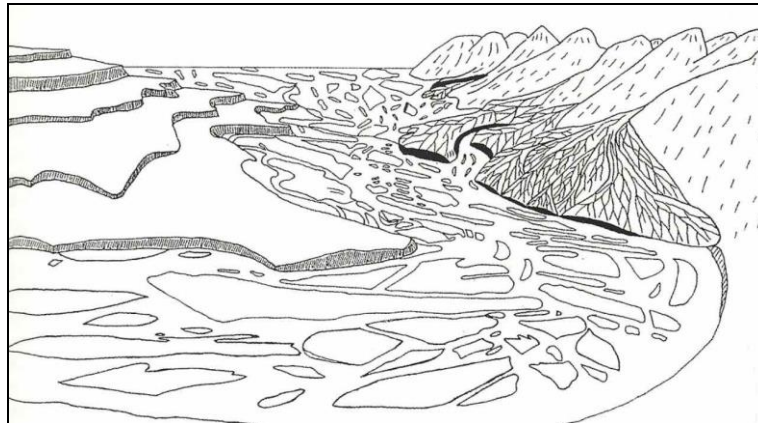


Figure 3.1.4. Artistic reconstruction of the lower Sundays River Valley (from Hattingh 2008). Alluvial fan development took place along mountain margins, coupled with terrace formation. These fans would then have supplied sediment to the lower valley.

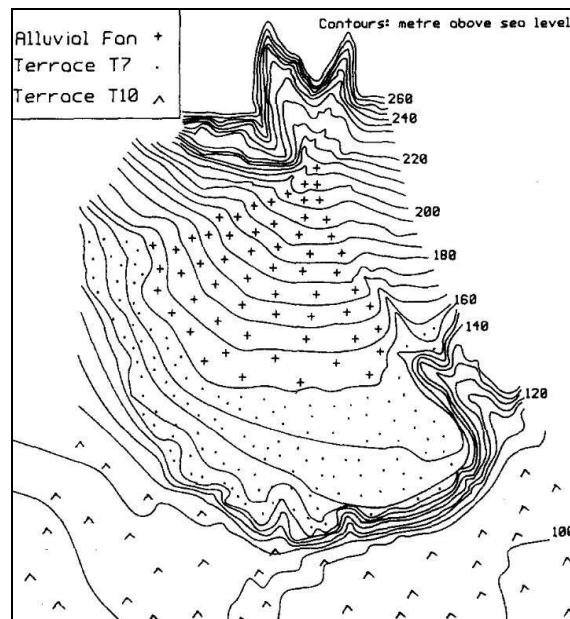


Figure 3.1.5. Large alluvial fan south of the Klein Winterhoek Mountains (from Hattingh 1996).

Crustal displacement in the Algoa Basin caused the Sundays River to migrate eastwards during its evolution, seen in the asymmetry and unpaired terraces of the lower valley today (Fig. 3.1.2). Additional evidence supporting this displacement is river capture that took place during the development of the palaeo-Sundays River (Hattingh 1996). Terrace deposits occur south of the Klein Winterhoek Mountains, up to 25 km west of the present river valley, indicating that a portion of the lower Sundays River Valley was originally found 118 km to the west (Fig. 3.1.6).

Neotectonic faults to the east of the Sundays River Valley, which are believed to have developed due to the rejuvenation of the Zuurberg fault along the northern and eastern margin of the Algoa Basin, were the epicentres for crustal movements (Fig. 3.1.1b & c; Hattingh 1996; see Hattingh & Goedhart 1997 for a detailed discussion of these faults).

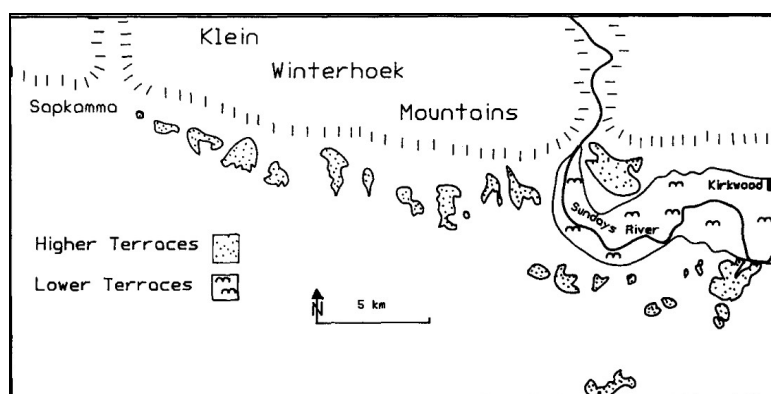


Figure 3.1.6. Preserved higher terraces west of the present Sundays River (from Hattingh 1996). These indicate stream capture (pre-middle Pliocene) and the eastward migration of the valley. Since the middle Pliocene, the Sundays River has received the majority of its water and sediment via the gorge at Korhaans Poort.

This tilting in the Algoa Basin caused the Sundays River to migrate laterally up to at least 12 km since the late Miocene. Based on the current spatial arrangement of the Sundays River terraces though, this migration appears to have been episodic (during times of heightened crustal movement; Hattingh 1996). This tilting has occurred frequently from the late Pleistocene up until more recently; lower terrace (10-13) morphology and spatial arrangement, coupled with the position of the present Sundays River mouth at the eastern most limit of the terminal valley, supports this (Hattingh 1996). This tilting played a vital role in the widespread preservation of the lower Sundays River terraces on the western flank of the valley (Hattingh & Rust 1999).

In summary, the upper Late Miocene-Pliocene terraces are seen to represent both falling sea levels and tectonic activity that caused a steepening of the river profile and heightening of fluvial flow and energy (Dollar 1998; Hattingh 2008). These upper terraces are comprised primarily of gravel-rich deposits, which have been described in detail elsewhere by Hattingh (1994, 1996), Hattingh and Goedhart (1997) and Hattingh and Rust (1999). Parts of the higher terraces that formed during marine

transgressive events, causing the deposition of fine sediments, are generally absent due to their removal through erosion (Hattingh 1996).

In contrast to the upper terraces, Hattingh (2008) and Hattingh and Rust (1999) highlight that temperature changes during the Pleistocene played a pivotal role in the formation of the lower terraces. Glacial and interglacial periods caused fluctuations in sea levels. Declining sea levels led to pronounced river incision in the lower valley, giving rise to a steep river profile. The regional climate shifted towards cooler and drier conditions (more moderate), and tropical rainstorms became infrequent. This lowered the sediment transporting competence of the river. However, pebble sized gravel clasts were still transported during these times as the steep river profile facilitated this.

Interglacials caused a rise in sea level and a backing up (choking) of the Sundays River mouth, causing a build up of sediments towards the distal portion of the lower valley. As a result of lowered river energy, and a shift towards aridification, sediment transport was restricted to fine silt and sand only (floodplain sediments). Increased sea levels also led to a regionally higher water table, causing valley side saturation. Through mass failure events the Sundays River Valley expanded laterally (creating a wide valley).

In summary, the lower Pleistocene-Holocene terraces are regarded as having been formed during marine transgressive events which led to a reduced river profile, lower energy flow towards the sea, and the deposition of finer silts and sands further down valley (Hattingh 1994, 1996, 2008; Hattingh & Goedhart 1997). These fine-grained deposits are better preserved than those within the higher terraces as their exposure to erosion has been much shorter and the prevailing climatic conditions since their formation have been far more moderate (Hattingh 1996). Discontinuous gravel lags and beds within these lower terraces are seen to indicate heightened tectonic activity causing intermittent higher energy flows and gravel deposition (Hattingh & Goedhart 1997).

According to Hattingh and Rust (1999) and Hattingh (2008), the terraces of the lower Sundays River therefore record the development and evolution of the Sundays River

from the Miocene to the Holocene and are widely recognised as being extremely sensitive indicators of sea level changes, climate change and neotectonic activity, all of which were crucial in the formation and preservation of these terraces (Hattingh 1994). However, recent dating work on these terraces, discussed below, suggests a revision is needed to assess the significance of these factors in their contribution to regional landscape evolution.

3.1.4 Dating of the preserved terraces

The most recent studies engaging with the lower Sundays River Valley by Erlanger (2010) and Erlanger *et al.* (2012) focus on providing a better understanding of the topographical evolution of South Africa. This work has sought to provide a chronology for these fluvial terraces such that uplift mechanisms and erosion rates can be questioned. Numerous debates regarding the evolution of the southern African high plateau, since the formation of the sub-continent, have questioned whether it is regionally stable or one that is continually uplifting due to ascending mantle flow (Erlanger *et al.* 2012). As a result, establishing river incision and rock uplift rates are crucial in determining the conditions and character for possible Neogene uplift (Erlanger *et al.* 2012). In order to do this, these authors determine uplift rates through cosmogenic ^{26}Al and ^{10}Be dating of the preserved terraces along the lower Sundays River Valley and an uplifted marine terrace near Durban (Fig. 3.1.7). Dating results, summarised by Erlanger 2010, Erlanger *et al.* (2012) and Granger *et al.* (2013), formed the chronological basis for this study (Table 3.1.1).

Table 3.1.1. Terrace dates for the lower Sundays River Valley. Here Canal (CL) refers to Atmar Farm, Lower Lookout (LL) to Bernol Farm, and Borrow Pit (BRW) to Penhill Farm.

Site	Terrace	Age (Ma)
Unilow (UL)	13	0.23 ± 0.15
Jagylak (JV)	11	0.26 ± 0.15
Unifrutti (UF)	11	0.37 ± 0.19
Canal (CL)	10	0.65 ± 0.06
Lower Lookout (LL)	9	1.14 ± 0.2
Borrow Pit (BRW)	9	1.37 ± 0.16
Railroad Cut (RRC)	8	3.20 ± 0.49
Uitkyk (UK)	7	4.06 ± 0.62
Kirkwood (KCS)	5	n.d.

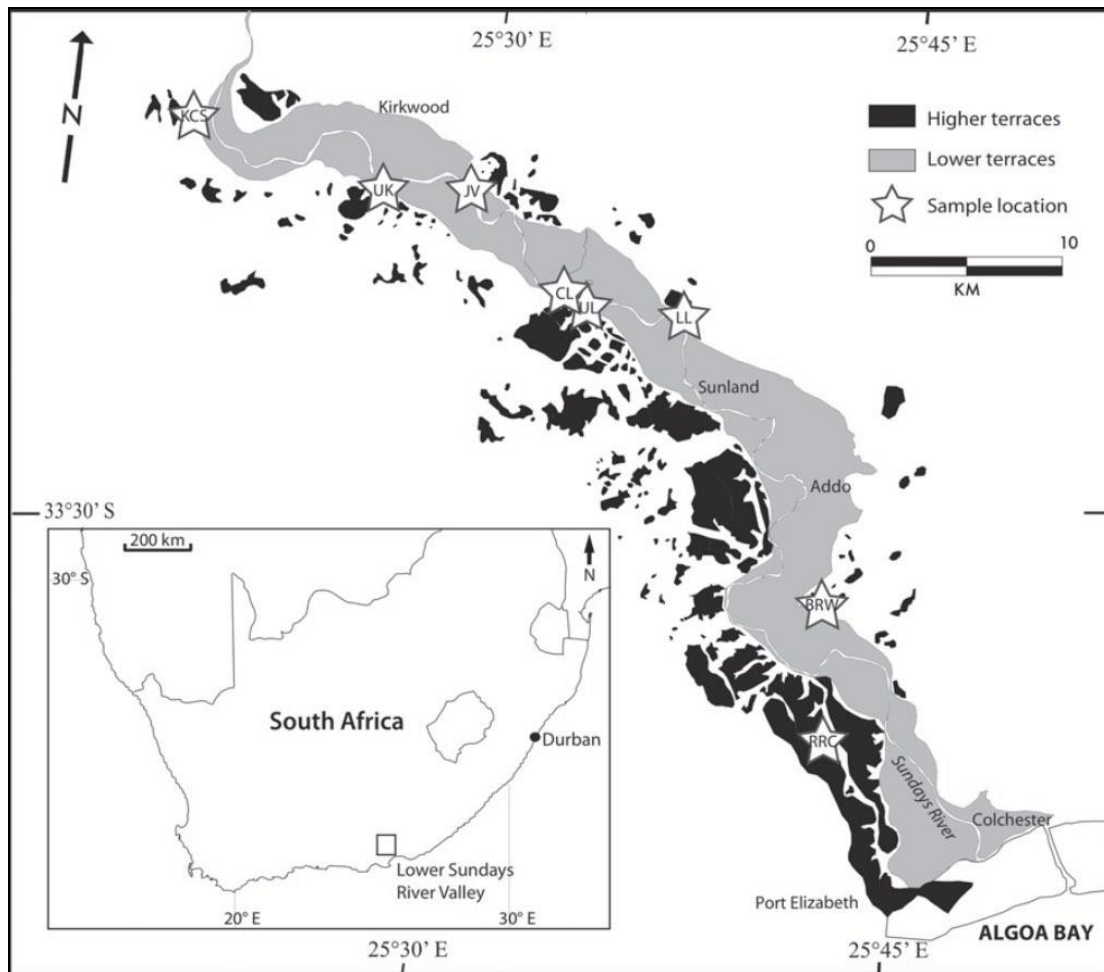


Figure 3.1.7. Lower Sundays River terrace map (from Erlanger *et al.* 2012). Terrace sampling locations indicated by stars. Site names follow those presented in Table 3.1.1.

Several important conclusions are presented by this research; a summary is as follows (Erlanger 2010; Erlanger *et al.* 2012):

1. Proposed rates of Neogene/Quaternary uplift for southern Africa have ranged between 0-200 m/My (million years). Based on the long-term rate of river incision, an uplift rate of 16.9 ± 1.2 m/My is provided for the Sundays River.
2. Importantly, river incision has remained constant over the Plio-Pleistocene, which contradicts those who have proposed fluctuating river incision during this period (Bridgland & Westaway 2008).
3. The age of the Alexandria Formation in the Algoa Bay, standing 400 m above sea level, has been debated by several authors (Partridge & Maud 1987; Hattingh & Rust 1999; Bridgland & Westaway 2008). A new age of between 22-25 Ma (Early Miocene) is provided based on this long-term rate of river incision. This contradicts the estimated age of 3.3 Ma based on microfaunal

remains (McMillan 1990) and suggests the implausibility of rapid uplift along the coast in South Africa during the Pliocene, as proposed by several authors (Partridge & Maud 1987, Partridge 1997, 1998; Bridgland & Westaway 2008) based on this original age estimate.

4. Climate has had little influence on terrace formation based on the steady erosion rate of the Sundays River (6 m/My over the last 4 My). Although a shift towards drier climates has been proposed for the Plio-Pleistocene (seen in the shift from gravels to sands in the valley – Hattingh 1996), constant and steady erosion rates over this period suggest a lack of climatic influence on erosion.
5. Tectonic rock uplift rates presented by Erlanger (2010) and Erlanger *et al.* (2012) are incompatible with models proposing rapid and recent Pliocene uplift. Rather, these rates are in accordance with slow mantle-driven uplift.
6. The highest terraces in the Sundays River Valley may correlate with the Alexandria Formation, thereby documenting 20 My of rock uplift for this region. This contradicts original age estimates (Hattingh 1994, 1996, 2008; Hattingh & Goedhart 1997; Hattingh & Rust 1999) of Late Miocene to Pliocene for the upper terraces (1-9) and the Pleistocene through Holocene for the lower terraces (10-13). These upper terraces are now seen to span the Early Miocene to Middle Pleistocene, with the lower terraces now spanning the Late Pleistocene to Holocene.

3.1.5 The Stone Age archaeology of the Sundays River Valley in relation to the wider Eastern Cape region

Reviews of southern Africa's Stone Age archaeology are provided by Sampson (1974), Phillipson (2005), Klein (2000a), Mitchell (2002), Phillipson (2005), Herries (2011) and Lombard *et al.* (2012), but all these reviews illustrate a dearth of information pertaining to the ESA of the Eastern Cape. Although Sampson (1974) provides a detailed Early Acheulean site map for the Eastern Cape (Fig. 3.1.8), of which the majority of sites consists of unnamed surface scatters (save for Geelhoutboom), Amanzi is (as noted in Mitchell 2002) the only ESA site to be excavated and named for this entire region (see Chapter 2.2, Part Two; Inskeep 1965; Deacon 1970).

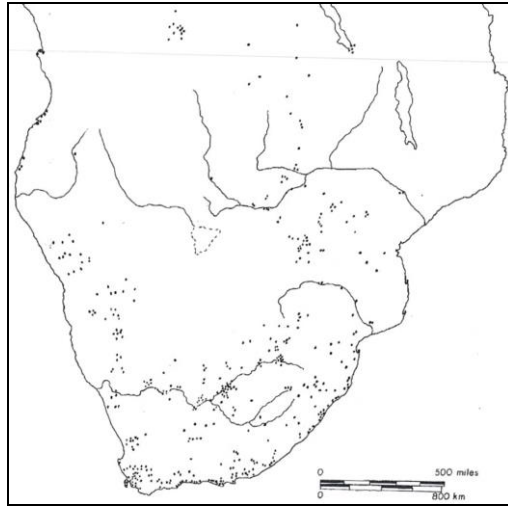


Figure 3.1.8. Southern African Early Acheulean sites (those recorded up to 1965; from Sampson 1974). The majority is poor context surface scatters. Note the high distribution of sites within the Eastern Cape.

Early descriptive work by Ruddock (1957), assisted by the Abbé Breuil and Clarence van Riet Lowe, was the first to note the presence of (surface) Stone Age implements in the terraces bordering the Sundays River, as well as in the neighbouring Coega River Valley (Fig. 3.1.9). The purpose of this research was to correlate known artefact-bearing deposits in the Sundays Valley to the preserved terraces, and hence, to Quaternary sea levels (Ruddock 1957).

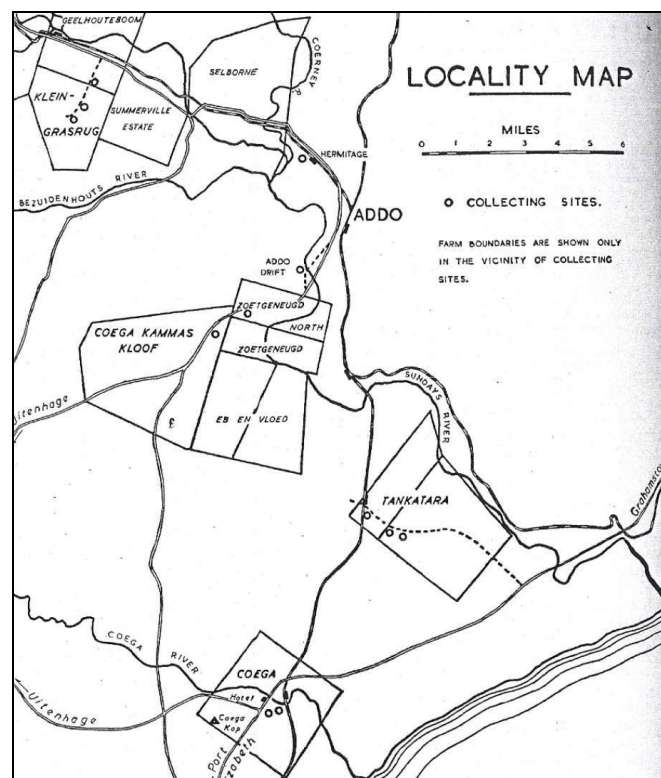


Figure 3.1.9. Sundays and Coega River Valley sites (from Ruddock 1957).

Sampling was conducted mainly on the Sundays River Valley higher terraces (linked to the Major Emergence), with artefacts being found in the bottom of gravel pits, the sides of road cuttings or atop terrace outcroppings (Ruddock 1957). No record was kept for those artefacts obtained from *in situ* positions within the gravel deposits. The sampled terraces, as noted by Ruddock (1957), depict sea levels ranging in height from 190 to 300 ft above present sea level. Coega Valley sites occur at a similar height above sea level and it is proposed these relate to the same period as those in the neighboring Sundays Valley (Ruddock 1957).

Artefacts generally retained a varied condition (weathering/abrasion state) and a range of 'Stone Age cultures' occurred (Acheulean, Fauresmith, MSA and LSA; Ruddock 1957). The younger artefacts generally retained a fresher condition (less worn/damaged). Artefacts were subsequently divided, based on their condition, into six different weathering categories in an effort to differentiate between assemblages that might have been of different ages. A five-stage typological classification system was also utilised in this regard, but the details are not provided. Based on the analysis of 271 artefacts, a clear trend in artefact typology and condition emerged, with the typologically youngest pieces being the most unworn. Overall, based on this classification, an Early, Middle and Late Acheulean (the Stellenbosch, an earlier term for the Acheulean at the time) was proposed, tying in with the condition of the artefacts as worn to fresh, respectively (Ruddock 1957).

These authors also attempted to determine an age for the artefacts, based on this typological and weathering state classification. Worn pieces were regarded as having been influenced by fluvial processes (many of which showed clear clast imbrication), or by some form of downslope movement along terrace outcrops, friction from nearby cobbles, bioturbation, movements within the gravels, or animal trampling (Ruddock 1957). However, due to the lack of stratigraphic control on all the samples obtained, ages can only remain tentative; van Riet Lowe suggested that the Sundays River assemblages could be synonymous with those Early and Middle Acheulean occurrences in the Vaal River (Ruddock 1957).

More recently, Heritage Impact Assessments conducted by Binneman (2010, 2011) in the district of Humansdorp report frequent ESA artefact occurrences (Fig. 3.1.10);

these are mostly surface sites, which contextually are of minimal value with low research potential. However, as shown by Sampson (1974; Fig. 3.1.8), there is a clear prevalence for and widespread surface distribution of ESA artefacts with the Eastern Cape. This is further supported by the rich surface concentrations of artefacts found at Geelhoutboom (Laidler 1947).



Figure 3.1.10. ESA artefacts from a large surface site (from Binneman 2010). The site is claimed to be the largest exposed ESA site in the Eastern Cape, found at the confluence of the Krom and Diep Rivers. Artefacts include handaxes, cleavers, cores, flaked cobbles, and flakes, all on quartzite cobbles. Some appear MSA-like.

Most relevant is the dating work conducted by Erlanger (2010) and Erlanger *et al.* (2012), and subsequent work conducted by Granger *et al.* (2013). During their investigation of the lower Sundays River Valley terraces these authors noted the presence of ESA artefacts within three of the terrace deposits, hence providing the necessary basis within which this project was framed. Only brief mention of the archaeology in these terraces is provided; however, artefacts recovered included flakes, cores, and Acheulean bifaces (Fig. 3.1.11 a & b; Erlanger 2010).

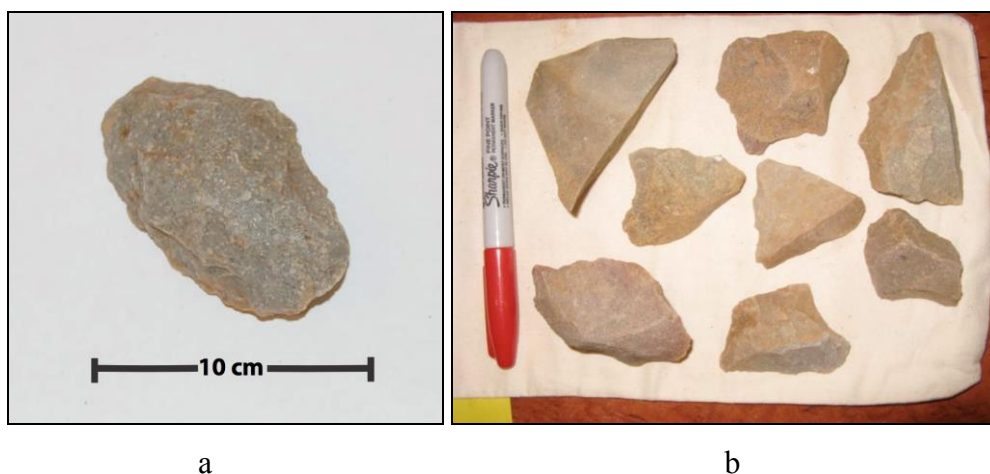


Figure 3.1.11. Artefacts recovered from the lower Sundays River Valley (from Erlanger 2010). *In situ* handaxe collected from the Bernol Farm 'Lower Lookout' Terrace 9 exposure (a); a selection of *in situ* lithics from the Penhill Farm 'Borrow Pit' Terrace 9 exposure (b).

3.2 Study sites of the lower Sundays River Valley

3.2.1 Introduction

Excavations in the lower Sundays River Valley have been conducted on three separate farms, namely Atmar, Bernol and Penhill (Fig. 3.2.1). A discussion of each site, which focuses on site context, location and dating, is found below. Thereafter, all methods that were applied at these sites or to the excavated material will be presented.

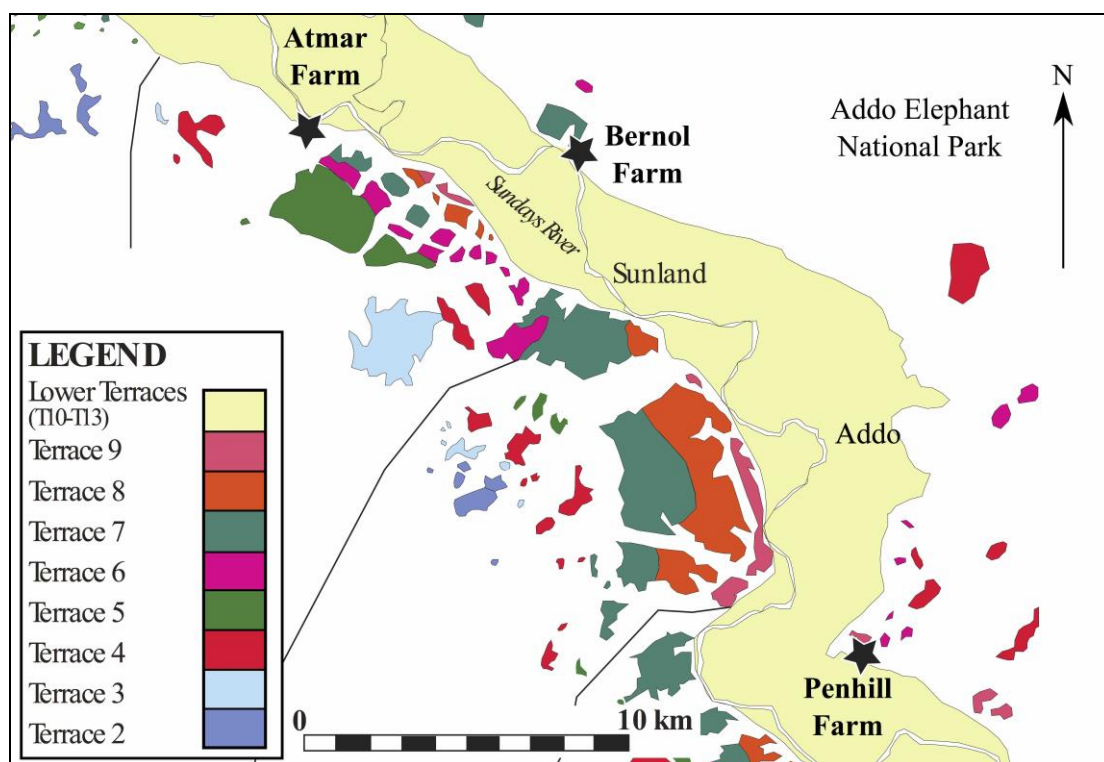


Figure 3.2.1. Study sites within the lower Sundays River Valley (modified from Erlanger 2010).

3.2.2 Atmar Farm

Atmar Farm ($33^{\circ}28'1.87''S$; $25^{\circ}31'41.59''E$) is a citrus producing establishment found just outside of Kirkwood on the R336. The site occurs behind a tree line that serves as a windbreak for the nearby orchards and along the edge of a working canal, which diverts water from the Sundays River for irrigation purposes (Figs. 3.2.2 & 3.2.3). Diggings for the placement of this canal have exposed gravel and fine sediment alluvium from Terrace 10 (Fig. 3.2.3).

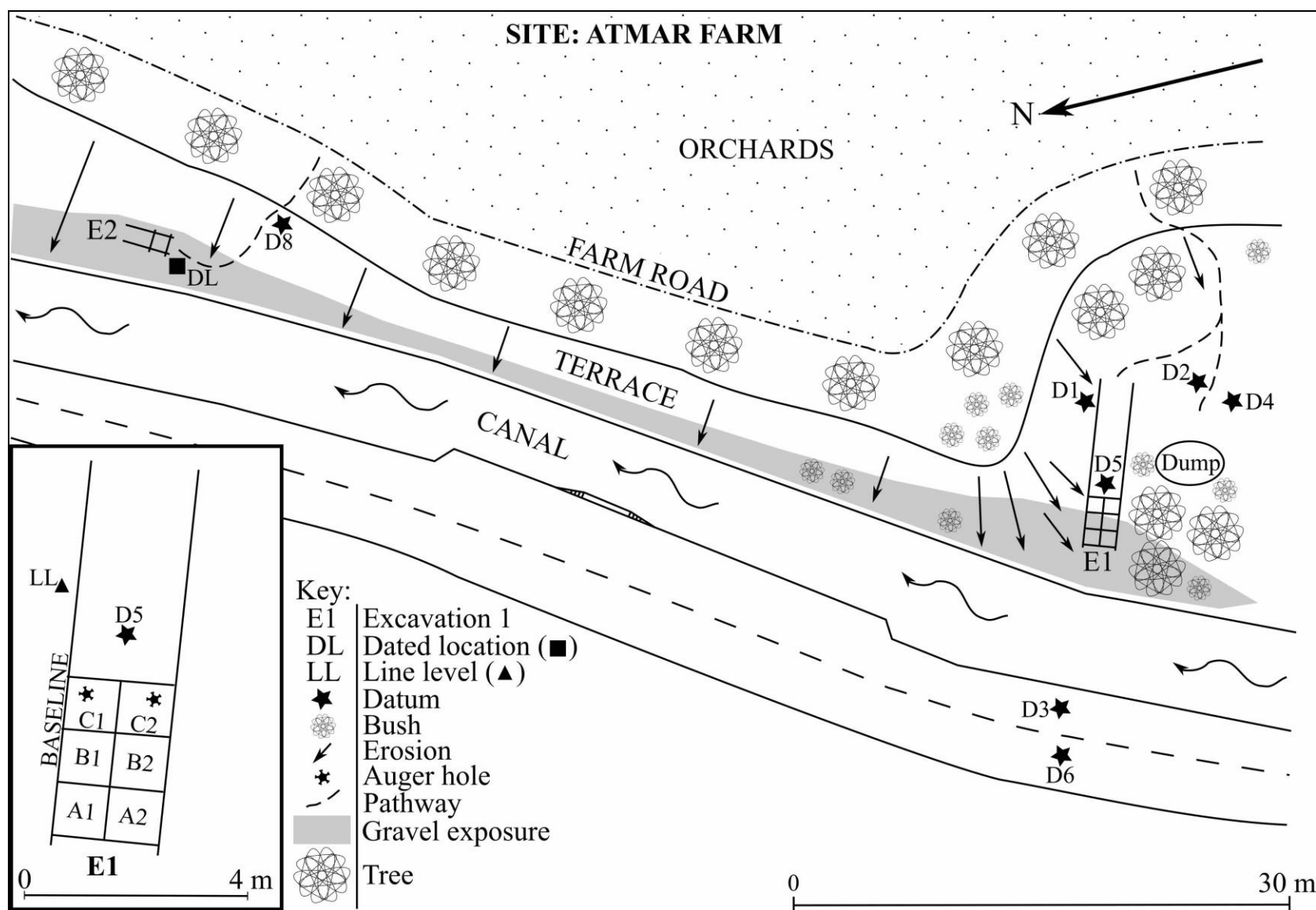


Figure 3.2.2. Atmar Farm site plan view. Enlarged area shows main excavation.



Figure 3.2.3. Atmar Farm Terrace 10 exposure. Note fine sediments overlying discontinuous gravels, and canal in foreground with eroded terrace exposure in the background.

The Atmar Farm stratigraphic sequence is simple (Fig. 3.2.4). The lightly coloured fine sediments are comprised of overbank sands and silts and dominate the upper portion of this terrace exposure (Fig. 3.2.3), preserving sporadic Stone Age artefacts in good condition. Some of these appear MSA-like, especially in the upper fines, but they are most likely derived from the surface. This capping of fine sediment varies in thickness from greater than three meters to less than one meter, depending on deposit removal through surface erosion. In places, extensive surface erosion has led to the formation of rills and gullies (dongas; see Chapter 2.3; Charlton 2008; Boardman *et al.* 2012) that have subsequently been infilled, often with modern material, e.g., glass and tin (Fig. 3.2.5). Overall, the overbank fines are massive, structureless and bioturbated. Calcretised root casts are common, and occasional nodules of calcrete and gravels are found within the deposit.

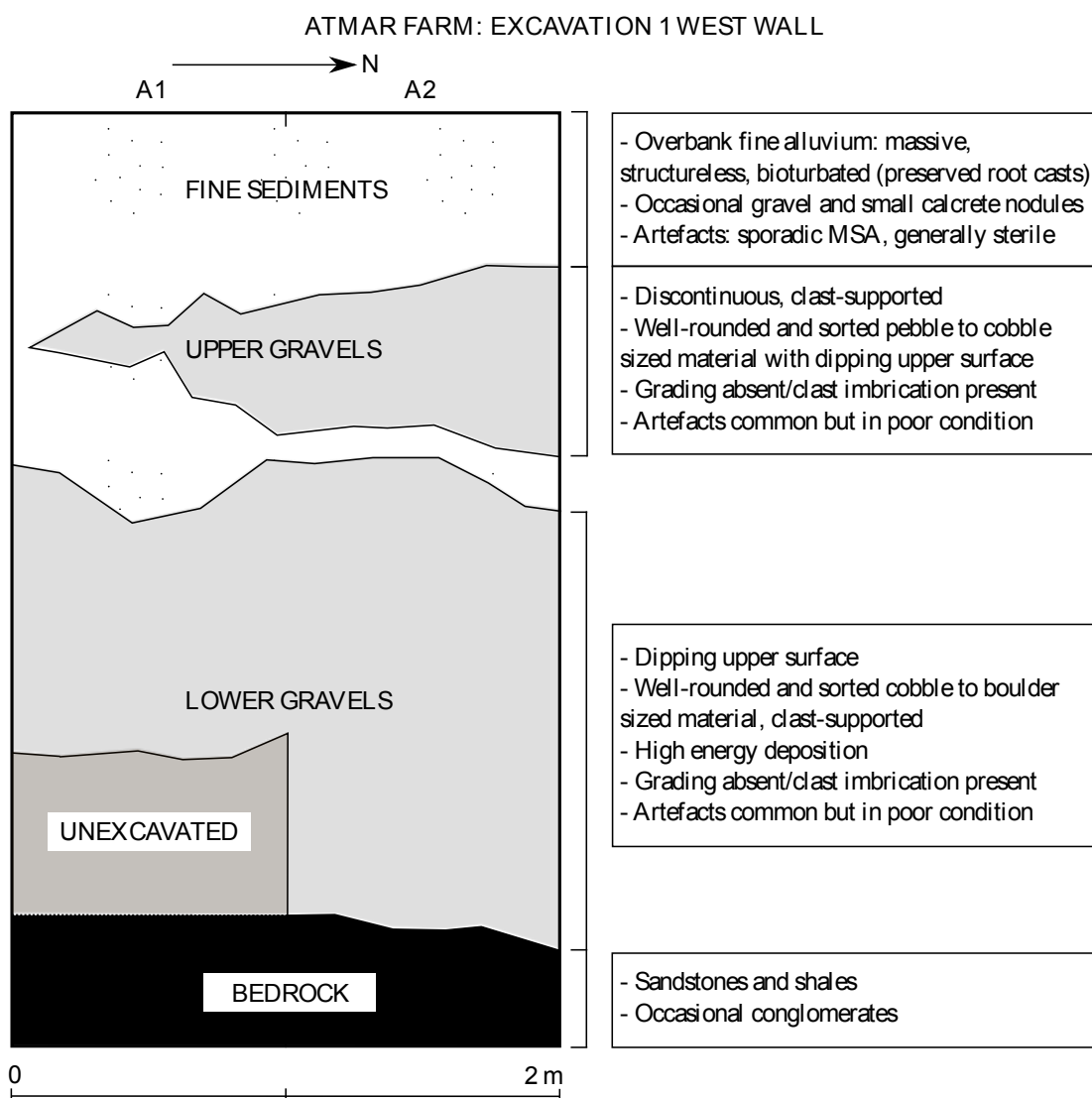


Figure 3.2.4. Profile of the Atmar Farm deposits from Excavation 1. Scale applicable to both axes.



Figure 3.2.5. Cut and fill deposit (see Chapter 2.3; Boardman *et al.* 2012) in upper fines, Atmar Farm (Excavation 1 east wall in squares C1 and C2). Scale bar is 30 cm.

Underlying these fines occur discontinuous clast-supported gravels (see Chapter 2.3; Goldberg & Macphail 2006) that vary in thickness (<1 m to approximately 2 m). These contain the bulk of the ESA artefactual material (although still very diffuse) and a range of pebble, cobble and boulder sized clasts, most of which are imbricated (see Chapter 2.3; Schick 1991, 1997; Petraglia & Potts 1994; Hodge *et al.* 2009) and well-rounded (some sub-angular); the interstitial matrix is comprised of sand, and calcrete is largely absent (Fig. 3.2.4). The upper surface of these gravels has a distinct dip. Figure 3.2.6 illustrates that in Excavation 1, both an upper and a lower bed of gravels occurs, each of which varies in thickness and composition. Bedrock in this excavation was clay-like (mudstone or shale) but there are additional exposures of sandstone and conglomerate in the local area (Fig. 3.2.4).

Based on work conducted by Erlanger *et al.* (2012), this west facing terrace exposure has been dated to 0.65 ± 0.06 Ma using the cosmogenic burial dating method (Table 3.1.1). This age, obtained through the sampling of clasts from the gravels, dates when the overbank fines were deposited.



Figure 3.2.6. Excavation 1 west wall (squares A1 and A2). Note upper and lower gravels (see Fig. 3.2.4). Spade for scale.

3.2.3 Bernol Farm

Bernol Farm (33°28'30.30"S; 25°36'24.00"E) preserves a southwest facing exposure of Terrace 9, found above an abandoned sand-filled canal that runs parallel to the Sundays River (Fig. 3.2.7). The site is found to the north of the R336 and is located near to the monument called 'The Look Out'.

This site is characterised by a complex exposure, across several hundred meters, of bedded overbank fine sediments and gravels (alluvium) sitting atop sandstone bedrock (Figs. 3.2.7-3.2.9). At the dated location (Fig. 3.2.9), the fine sediments (silts and sands) are greater than three meters in thickness and imbricated gravels, as well as calcrete and silcrete, occur sporadically in the upper portion of the exposure as thin, discontinuous matrix-supported gravel stringers (10-15 cm thick; see Chapter 2.3; Goldberg & Macphail 2006). Outsized clasts have been sourced from a higher terrace nearby (Granger *et al.* 2013). Towards the base of this exposure occurs a larger discontinuous graded gravel deposit (1-1.5 m thick, clast-supported), within which ESA artefacts and bone are preserved, along with additional gravel material (all imbricated and rounded to sub-angular in shape, shown in Figure 3.2.9). Sporadic bone and artefacts here and in the overlying thin stringers represent deposition on the floodplain with minor re-working and sorting by river flow (Granger *et al.* 2013); the bone is only partially mineralised.

The date for this exposure is provided by Granger *et al.* (2013) and is 1.14 ± 0.2 Ma (Table 3.1.1). This was obtained through clast sampling from the gravels and thus dates the deposition of the overbank fines (Fig. 3.2.9).

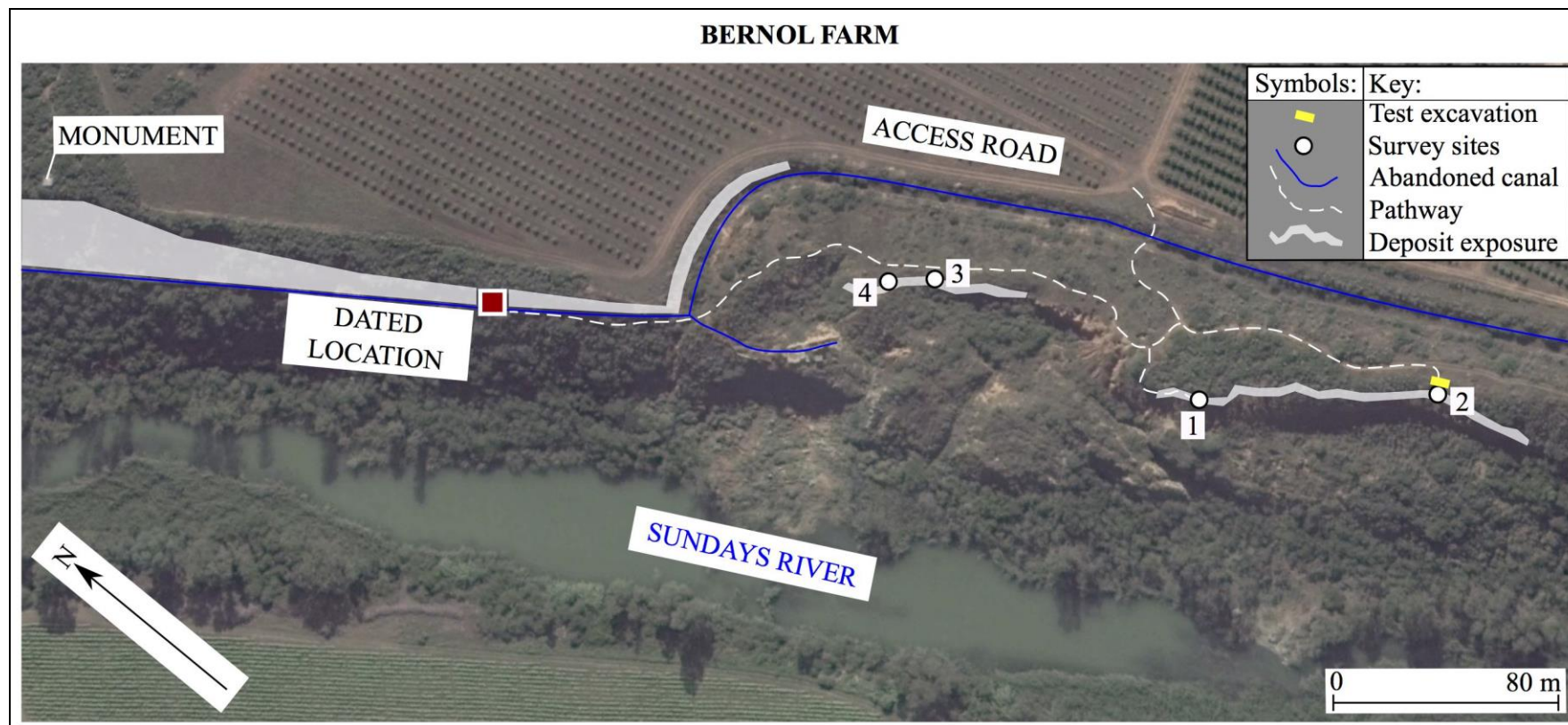


Figure 3.2.7. Bernol Farm site plan view.

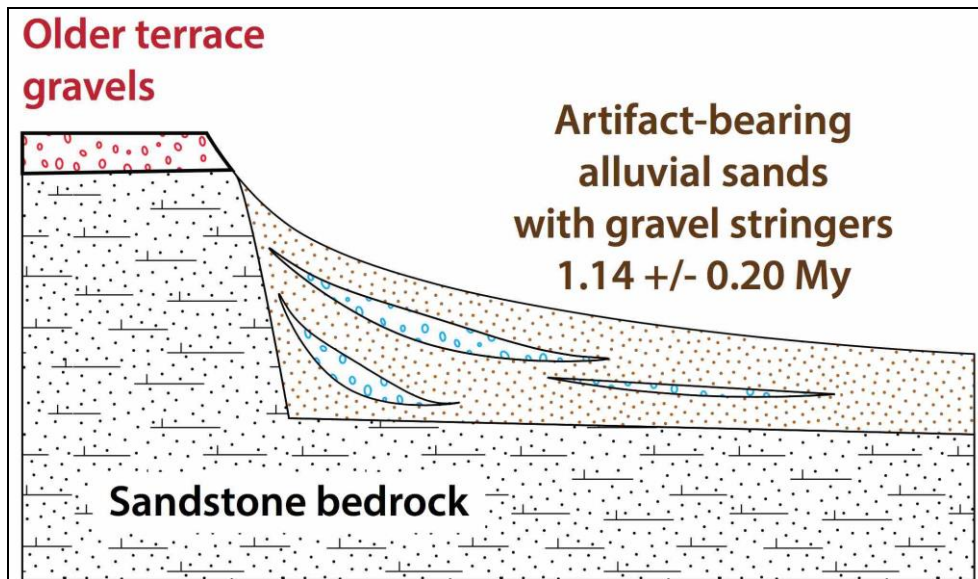


Figure 3.2.8. Profile of the Bernol Farm terrace exposure (from Granger *et al.* 2013). Note source of clasts from older terrace higher upslope



Figure 3.2.9. Terrace 9 exposure at the dated location. Note upper fines with sporadic lenses (stringers; see Chapter 2.3; Goldberg & Macphail 2006) and lower unit with gravels.

Elsewhere, additional areas (survey sites 1-4, Fig. 3.2.7) contain deposits with preserved shell, bone, gravels and ESA artefacts (Figs. 3.2.10 & 3.2.11). Within these areas artefacts are abundant and there appears to be a mix of both ESA and MSA technology (the latter of which is most likely derived from the surface). However, it is unclear how exactly these exposures relate to the dated location and whether they are

alluvial and/or colluvial in origin. Survey sites 3 and 4 (Fig. 3.2.10) are ‘lag-like’ and appear to occur within the host alluvium; it is unclear though whether this deposit is overlain by colluvium or alluvium. The shell rich horizons at sites 1 and 2 are deeply weathered, nodular, and silcretised, and chunks of soil are found suspended above in fine sands that are sorted (and possibly even wind blown, shown in Figure 3.2.11). Based on elevation readings though, obtained on clasts from the dated deposit (Fig. 3.2.7), the survey sites all occur at the same height (except for site 3 which is approximately 0.6 m lower than the lowest point of the dated gravels).



Figure 3.2.10. Survey site 4. Deposit contains gravels, bone, stone and shell (image courtesy of R.J. Gibbon).



Figure 3.2.11. Survey site 2. Deposit is silcretised and contains shell, bone, and artefacts. Scale bar is 10 cm.

3.2.4 Penhill Farm

Located south of the town of Addo, off a dirt road that runs roughly parallel to the R335, Penhill Farm (33°35'46.90"S; 25°41'18.20"E) preserves a circular (amphitheater-like) exposure of Terrace 9 deposits at the southern-most boundary of the property (Fig. 3.2.12). It appears to be a borrow pit quarry that in the past was used to supply sand, gravel and calcrete for the production and maintenance of the dirt road nearby. As a result, what remains is a continuous vertical exposure of fine sediments and gravels that varies in height (Figs. 3.2.12 & 3.2.13).

From the top of this exposure occur several meters of fine lightly coloured sterile overbank sands and silt (alluvium), which are massive and structureless. At the southern most portion of the borrow pit, underlying this exposed wall of fines, is a gravel horizon of unknown thickness (at least >0.5 m and up to 1.5 m elsewhere, shown in Figure 3.2.12). This layer of imbricated gravel appears lightly calcretised and contains a clast-supported matrix of pebbles and cobbles; the interstitial matrix is sand. It is from this area (dated location 1; Fig. 3.2.12) that clasts were selected and dated using the cosmogenic nuclide burial method, providing an age of 1.37 ± 0.16 Ma for overbank fine deposition (Granger *et al.* 2013). Stone Age artefacts have not been found in these gravels.

Underneath this gravel horizon occurs bedded fluvial sediments with well-sorted and rounded medium- to coarse-grained sand, also of unknown thickness. Although bedrock is not visible underneath these gravels, gravel conglomerate that occurs towards the deepest point of the borrow pit may form part of the local bedrock.

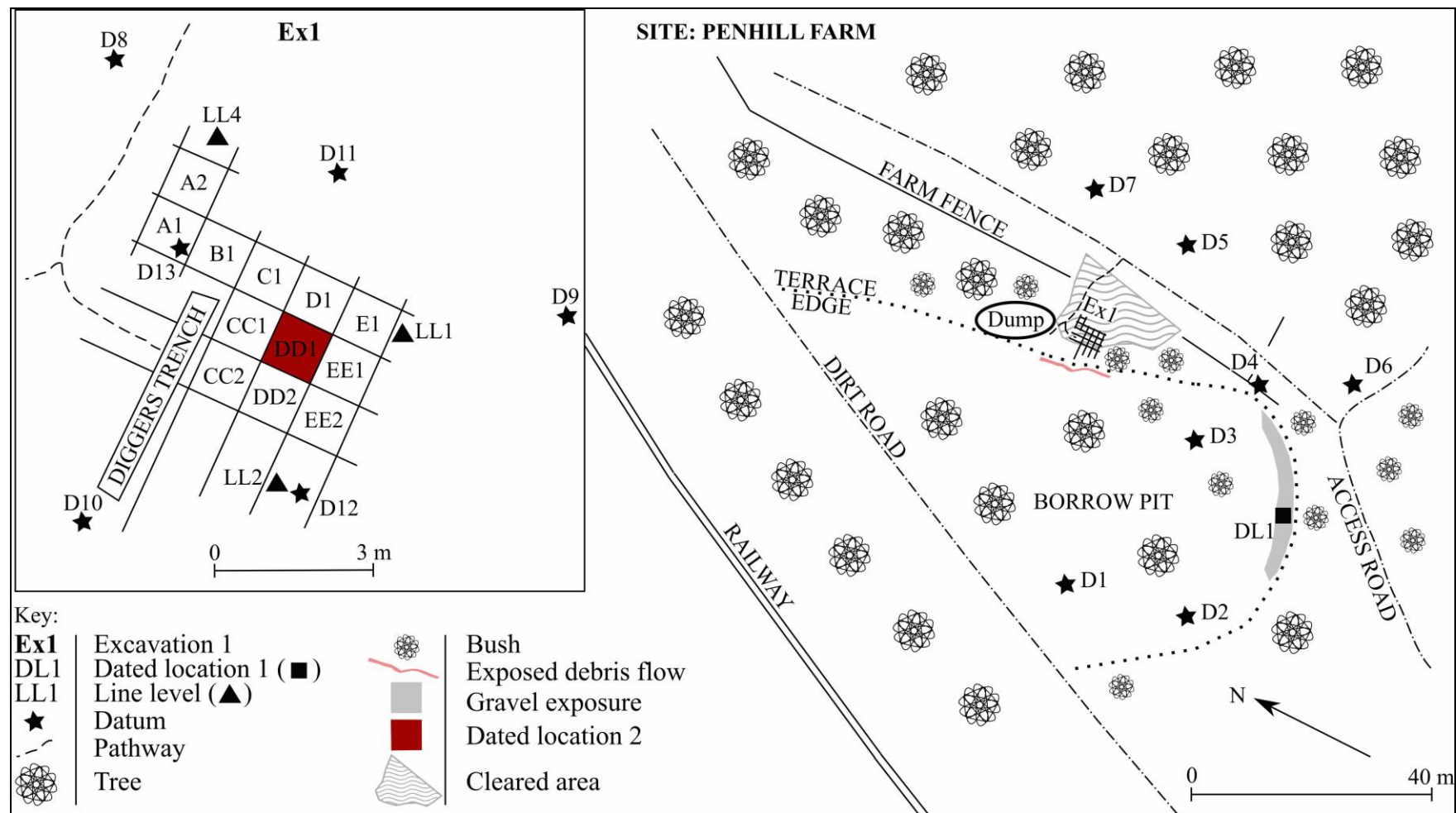


Figure 3.2.12. Penhill Farm site plan view. Enlarged area shows main excavation.



Figure 3.2.13. Facing east, the Penhill Farm borrow pit deposit exposure. Note extensive overbank fines (image courtesy of R.J. Gibbon).

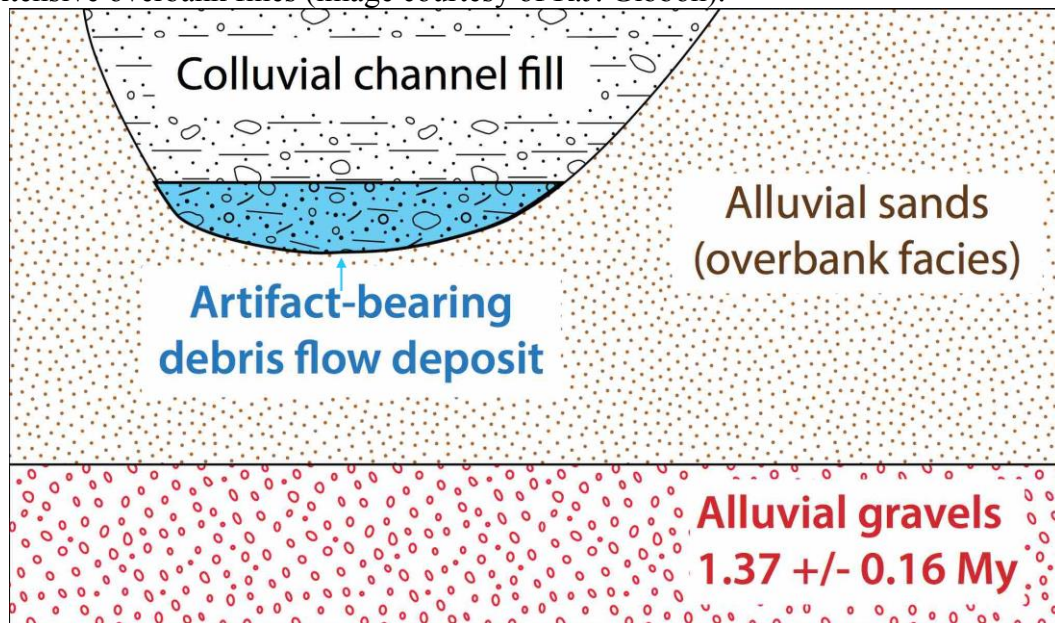


Figure 3.2.14. Stratigraphic sequence at Penhill Farm (as shown in Figure 3.2.15). Erosion channel is cut into overbank fines (modified from Granger *et al.* 2013).

Towards the east of the borrow pit occurs an erosion channel that has been cut into the fine alluvium (Figs. 3.2.14 & 3.2.15). This has subsequently been filled with poorly sorted colluvium that is derived from sediments occurring upslope. At the base of this channel occurs a debris flow deposit (originally and incorrectly defined as a

gravel stringer by Erlanger 2010 and Erlanger *et al.* 2012). The debris flow deposit (see discussion in Chapter 2.3) is discontinuous, occurring only within the base of the cut channel, and it rises towards the surface at its southern boundary (Fig. 3.2.15). This southern boundary is not an ‘extension’ of the debris flow deposit upslope, but rather it represents a hill slope lag where clasts are preferentially orientated parallel to the slope (Fig. 3.2.15).

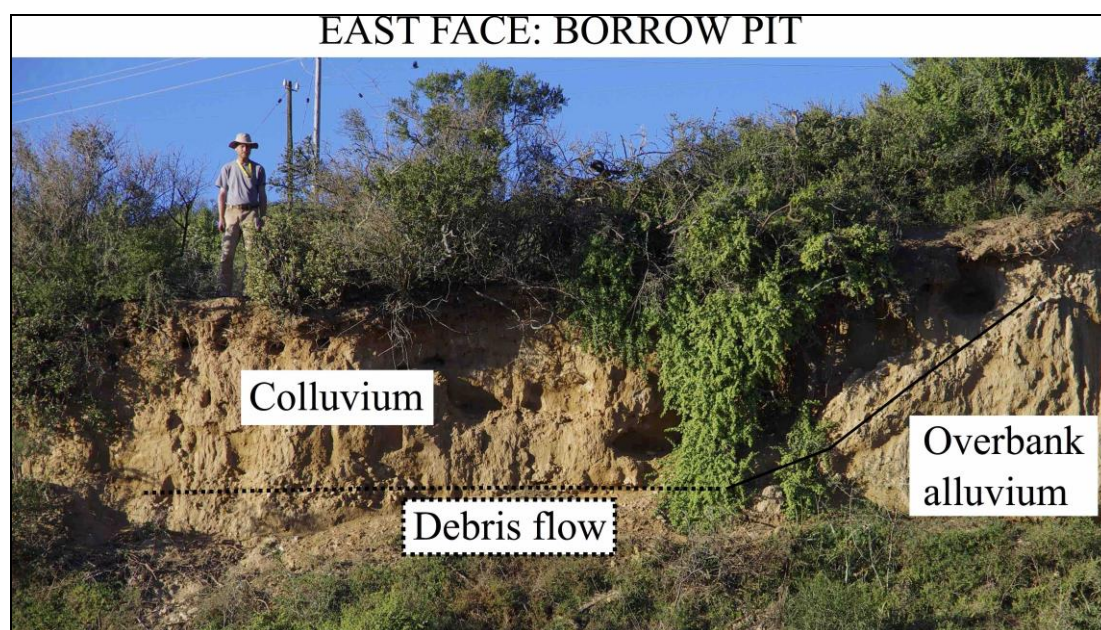


Figure 3.2.15. Debris flow exposure in east face of borrow pit. Note underlying fine alluvium and overlying colluvium, and rise of deposit (hill slope lag) towards the south (modified from original image courtesy of R.J. Gibbon).

Excavations at Penhill Farm have revealed the true complexity of the colluvium (silts and sands) found overlying the debris flow, and although the stratigraphy varies per square, some general trends are described here (Fig. 3.2.16). Starting from the top of the sequence, the upper 0.2 m of deposit comprises a dark organic rich horizon. Root activity here is abundant and this continues down to approximately 1 m (Fig. 3.2.16). However, root activity is generally at its highest concentration from the surface to 0.5 m and thereafter it occurs down to depths > 2 m (even within the debris flow, shown in Figure 3.2.16). Artefacts in the upper 1 m are sporadic and nodules of calcrete and gravel occur, along with preserved root casts. Although not all the artefacts in this upper part of the deposit may be colluvial, the abraded condition of the pieces suggests their long-term surface exposure at some point and the possibility of re-working by roots (causing their displacement; see Chapter 2.3; Lotter *et al.* 2016).

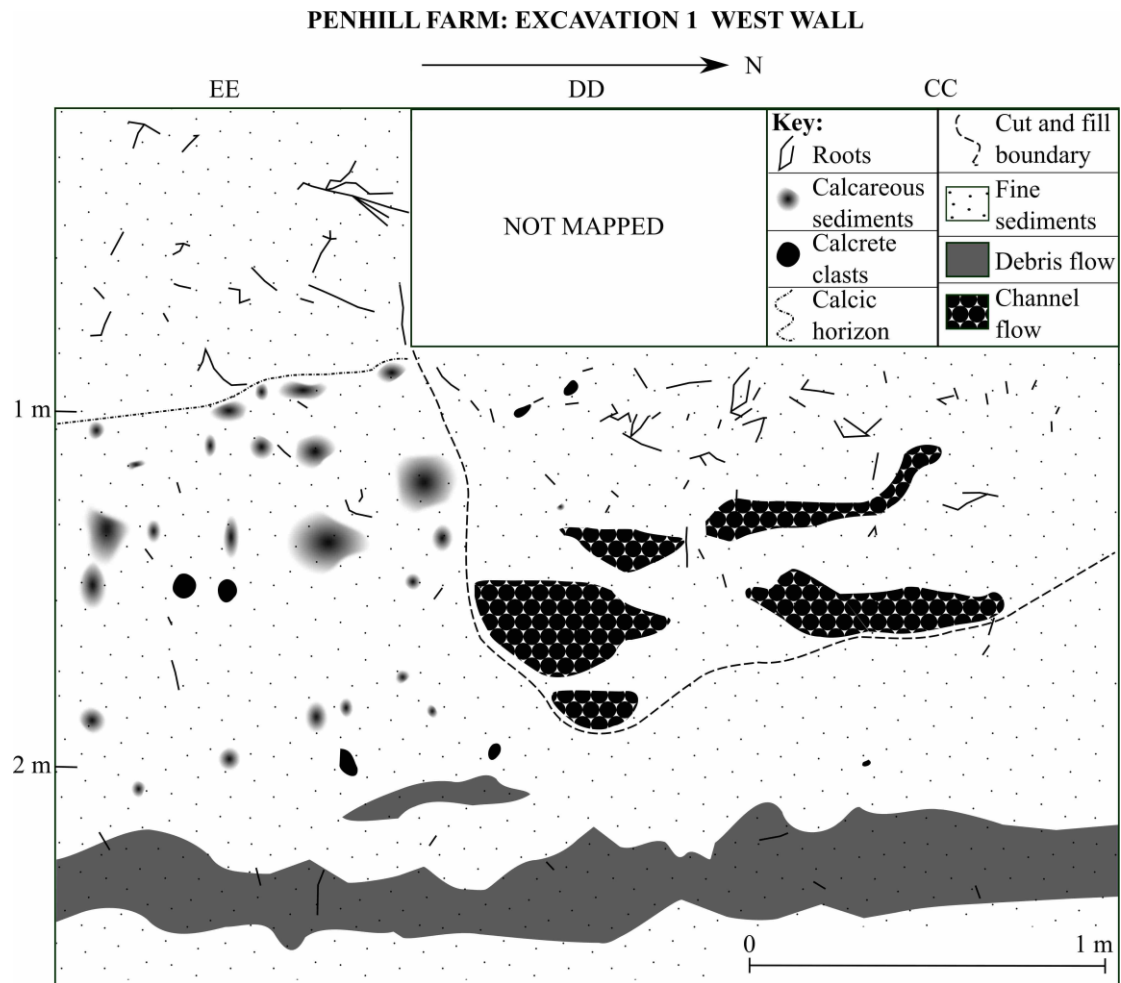


Figure 3.2.16. Penhill Farm Excavation 1 stratigraphic sequence. Sterile fine alluvium underlies the debris flow and poorly sorted colluvium occurs above. Channel flow is detailed in Figure 3.2.17.

Beneath the upper 1 m of deposit the silts and sands are generally sterile and featureless until reaching the debris flow. Several areas where calcretisation of the sediments seems to be taking place *in situ* occur, and occasional calcrete nodules can also be found (Fig. 3.2.16). This calcretisation appears to take place beneath a ‘calcic horizon’ that can be found at variable depths along each of the excavation walls. This horizon is most commonly found, however, towards the base of the most active root zone. Preserved root casts are also common here and occur down to the debris flow.

In the east and west (Fig. 3.2.16) walls of Excavation 1, several distinct features are present within the colluvium overlying the debris flow. A cut and fill deposit is exposed in the west wall and this has been further eroded by five distinct channels (Figs. 3.2.16 & 3.2.17). These channels preserve rounded nodules of silcrete and calcrete, rounded pebbles and cobbles, and sporadic artefacts. This material is sorted,

imbricated, and occurs within a (primarily) clast-supported matrix (Fig. 3.2.17). Grading of the fine sediments also occurs in some of these features. The east wall of the excavation also exposes the cut and fill and channel deposits and, based on the differences in height of these features between the walls, it appears that these channels eroded the cut and fill deposit in a downslope east to west direction.

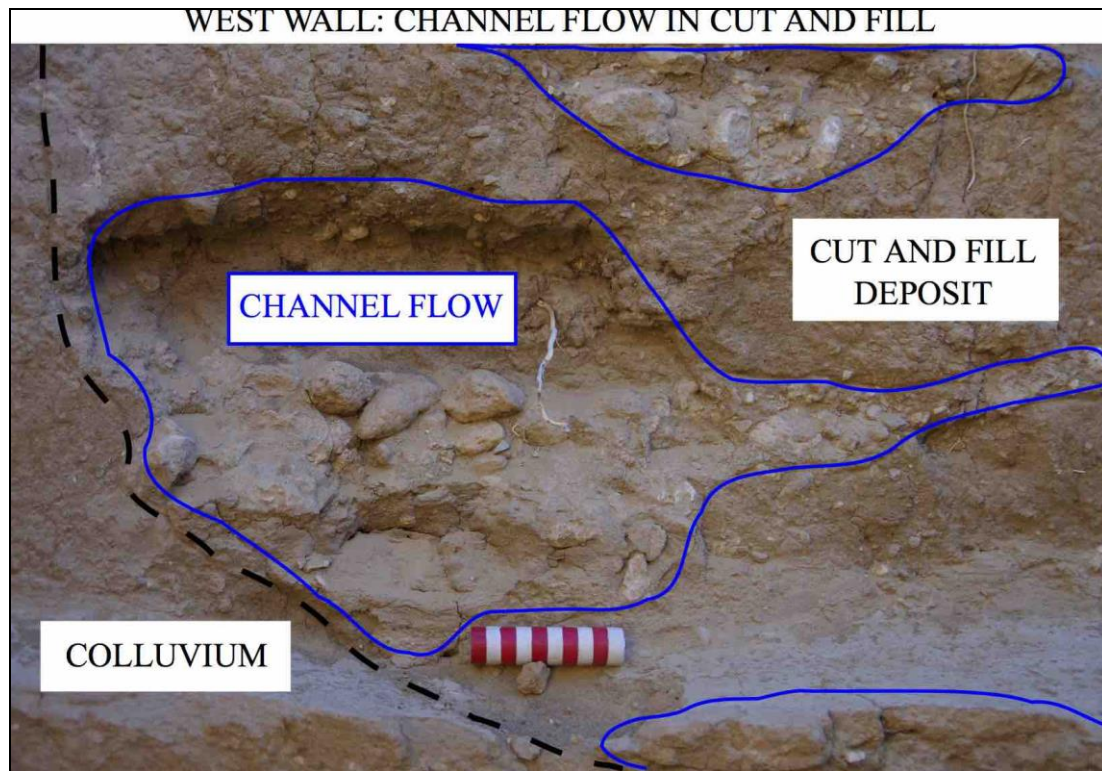


Figure 3.2.17. Excavation 1 west wall square DD. Note cut and fill boundary (dashed line) in colluvium and infill with channelised flow, and sorting and clast imbrication. Bedding of sediments occurs in some of these features (modified from original image courtesy of R.J. Gibbon).

At the base of the erosion channel cut into the fine alluvium (Figs. 3.2.14 & 3.2.16) occurs the debris flow, which preserves an extremely abundant collection of well-preserved ESA artefacts. This flow is wedged out and is thickest in the east and thinnest in the west. Overall deposit thickness also varies due to the irregular upper and lower surface of the flow, but it ranges from approximately <20 to >50 cm; the depth of the surface/top of the debris flow varies between the squares as well, with a minimum of 1.8 m and a maximum depth of 2.25 m. The base of the flow also varies from 2.4-2.5 m.

This debris flow swept a lag of nodules, gravels and artefacts into a cone, likely from a nearby source upslope only several meters away (Granger *et al.* 2013). This flow

was then deposited into the base of the erosion channel. The flow is matrix-supported with silts and sands (almost clast-supported in places) and preserves an abundance of re-worked calcrete and silcrete, and gravels, none of which show any sorting, grading, or imbrication patterns (Fig. 3.2.18). The calcrete and silcrete nodules vary greatly in size from only a few centimetres to infrequent boulder sized pieces, all of which show edge rounding and damage due to re-working (rolling). The composition of these nodules is silty/sandy, suggesting their growth *in situ* in fine sediments higher upslope, thereafter being eroded and concentrated into a lag downslope from their original position. Their composition is also in contrast to those calcretes exposed elsewhere in the local area, which are much purer and whiter. In addition to this, no calcrete is found preserved on any of the artefacts, which suggests their formation and point of origin is different from that of the artefacts.

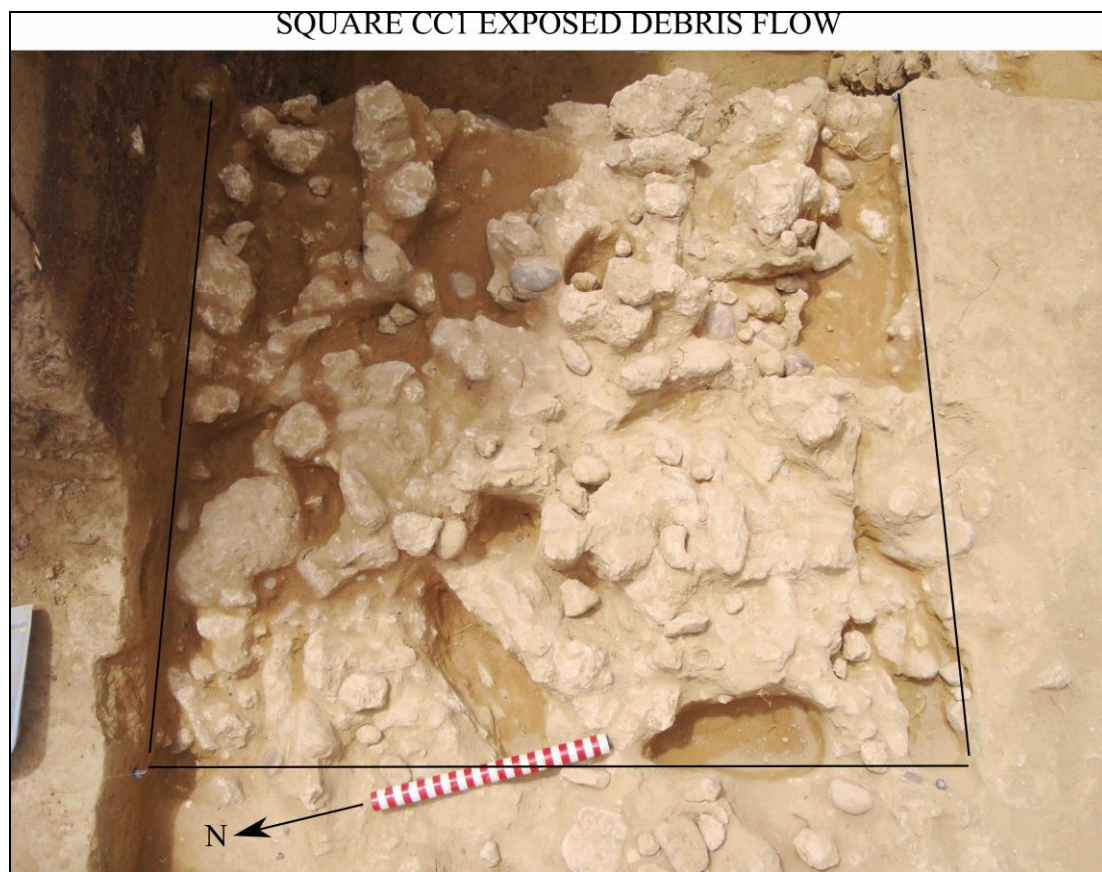


Figure 3.2.18. Plan view of the exposed debris flow in Excavation 1. Note matrix-supported calcrete and silcrete nodules with artefacts and gravels. Scale bar is 30 cm.

Pebbles and cobbles found within the flow have a low frequency. This suggests that the upslope channel, which concentrated the debris flow, had not fully tapped into the gravel-rich colluvial wedge coming off the older, higher terrace upslope.

Underlying the debris flow at approximately 2.5 m are the sterile overbank silts and sands (Fig. 3.2.16), presumably continuing down to the dated gravels, which may be at a similar depth to those dated gravels in the southern portion of the borrow pit (Fig. 3.2.12).

It must be emphasised here that the date provided by Granger *et al.* (2013) now has a questionable association with the debris flow deposit as it would have taken some time for the erosion channel to form after the deposition of the overbank fines. The infilling of this channel, with the poorly sorted colluvium, would also have taken some time to occur as the upslope lag of calcrete, silcrete and gravels needed to form prior to the debris flow event.

3.3 Excavation methods

3.3.1 Introduction

Excavations in the lower Sundays River Valley have followed protocols that allowed for the detailed recording of each site (Table 3.3.1).

Table 3.3.1. Excavation techniques applied at the three investigated sites.

Excavation techniques:	Atmar Farm	Bernol Farm	Penhill Farm
Large-scale excavation	X	-	X
Test pit excavation	X	X	-
5 cm spits	-	X	X
10 cm spits	X	X	X
>10 cm spits	X	X	X
Artefact spatial recording	-	-	X
Spatial survey	X	X	X
Fabric analysis	-	-	X
2 mm sieve	X	X	X
4 mm sieve	X	X	X
Auger testing	X	-	X

Site formation studies employ the use of several techniques, each aimed at extracting as much data as possible about the deposit of interest. Maximum data extraction is thus vital for all site formation studies, as it is this data that enables researchers to question and possibly infer first, the reasons for why deposits have come to be shaped a specific way, and second, what processes (cultural or natural) have facilitated in the production of such deposits (Morton 2004). Accordingly, the following methods proposed by Schick (1991) are argued to provide the necessary high-resolution data that these studies require:

- Screening of excavation sediment that allows for a thorough recovery of lithic (or other) debris, preferably using a fine mesh (5 mm or smaller)
- Assessing the size distribution of debitage
- Recording of artefact spatial distributions
- Artefact refitting and a spatial assessment of refitted pieces

- Recording of artefact depositional characteristics (e.g., fabric)

Although Schick (1991) originally formulated these methods to assess the depositional patterns created by fluvial forces, they are widely applicable to a range of conditions. A brief description of each of the techniques shown in Table 3.3.1 is provided below:

- Large-scale excavation: this involves any excavation larger than a single 1 X 1 m square. Where specific site conditions dictate, these excavations were utilised to provide an extensive sample of material and to provide a detailed understanding of site context.
- Test pit excavation: this refers to the excavation of a single 1 X 1 m square, normally performed as a precursor to more detailed large-scale work (as above). The purpose of this excavation is to provide only a preliminary understanding of site context.
- Excavation spits: this refers to the thickness of the levels dug whilst conducting excavations at a given site. These are listed here as 5, 10 and >10 cm as site-specific conditions dictated the need to interchange between these depths for any number of reasons (e.g., time restraints, changes in deposit type, ease of excavation). These spits were dug primarily with trowels, but hand chisels, spades and picks were also utilised where necessary. These spits were also dug in a way that was sensitive to deposit stratigraphy.
- Artefact spatial recording and spatial survey: recording of all site spatial information was performed using an EDM total station (Nikon NPL-302). Within excavations, individual artefacts (lithics) ≥ 20 mm in maximum length were point plotted (but not natural pieces). A single reading obtained from the midpoint of the top of each artefact was recorded. Spatial surveying involved the recording of important information pertaining to excavation stratigraphy, surrounding landscape features, and points of interest. The number of readings recorded for each feature was dictated by the nature of the feature and the level of accuracy required.
- Fabric analysis (see Chapter 2.3; Bertran & Texier 1995, 1999): this was performed, *in situ*, on both artefactual and natural material using a Brunton

compass. However, to ensure accuracy in recordings, restrictions were put in place to ensure the selection of suitable samples. As such, only flat or elongated pieces were selected (Major 1998). Flat pieces have an A-axis (thickness) that is less than half of the B-axis (width). Elongated pieces have a C-axis that is two times the B-axis, where the C-axis represents the total length. Samples also needed to have a flat base with no concavities or convexities. For each sample, the following steps were employed:

1. The sample was measured in millimeters (A and B axes for flat pieces and C and B axes for elongated pieces), to determine if suitable, and the shape was recorded.
 2. A board was placed where the original piece lay to average out the underlying depositional surface.
 3. For flat pieces a line level was rotated on the surface of the board, until level, to establish the strike. Aligning the Brunton compass parallel to the line level, a degree reading was then read off the magnetic north arrow and recorded. Perpendicular to the strike is the dip angle (degrees), measured using the Brunton compass clinometer resting atop the dipping board. The direction of this dip was also recorded using the nearest cardinal point (e.g., north, southwest).
 4. For elongated pieces the Brunton compass was aligned parallel to the long axis and the bearing in degrees (always in line with the plunge downwards) was obtained whilst *in situ*, measuring off the magnetic north arrow. Thereafter, the piece was removed and the board was placed upon the underlying depositional surface. The plunge (degrees) was then calculated using the clinometer (as above).
- Sieving: in order to ensure the complete capture of all assemblage components (e.g., bone, stone, and other organic matter), both 2 and 4 mm sieves were utilised. Although the use of these sieves in conjunction with each other is most effective, the specific conditions at each site dictated the need to use either of them interchangeably. Deposit type and moisture content of the sieved medium also played a major role in the use of the fine 2 mm sieve (see following discussion below). All material obtained from the sieve was carefully bagged and tagged for the respective square and depth.

- Auger testing: an auger was used at times to obtain sediment samples, or (more frequently) to assess deposit morphology and depth. By sinking an auger hole at strategic points, either in an excavation or the surrounding landscape, survey and excavation work become more informed.

3.3.2 Excavations: site-specifics

3.3.2.1 Atmar Farm

In order to gain access to the Terrace 10 exposure it was decided that a stepped trench, set roughly perpendicular to the canal, would be best. Because sampling of this terrace exposure was focused on the gravels, found under the fine overbank alluvium, an area where this overburden was at a minimum was chosen (along the edge of a donga where the majority of the fine alluvium had been eroded away). A 3 X 2 m trench was then established (Excavation 1, shown in Figure 3.3.1).

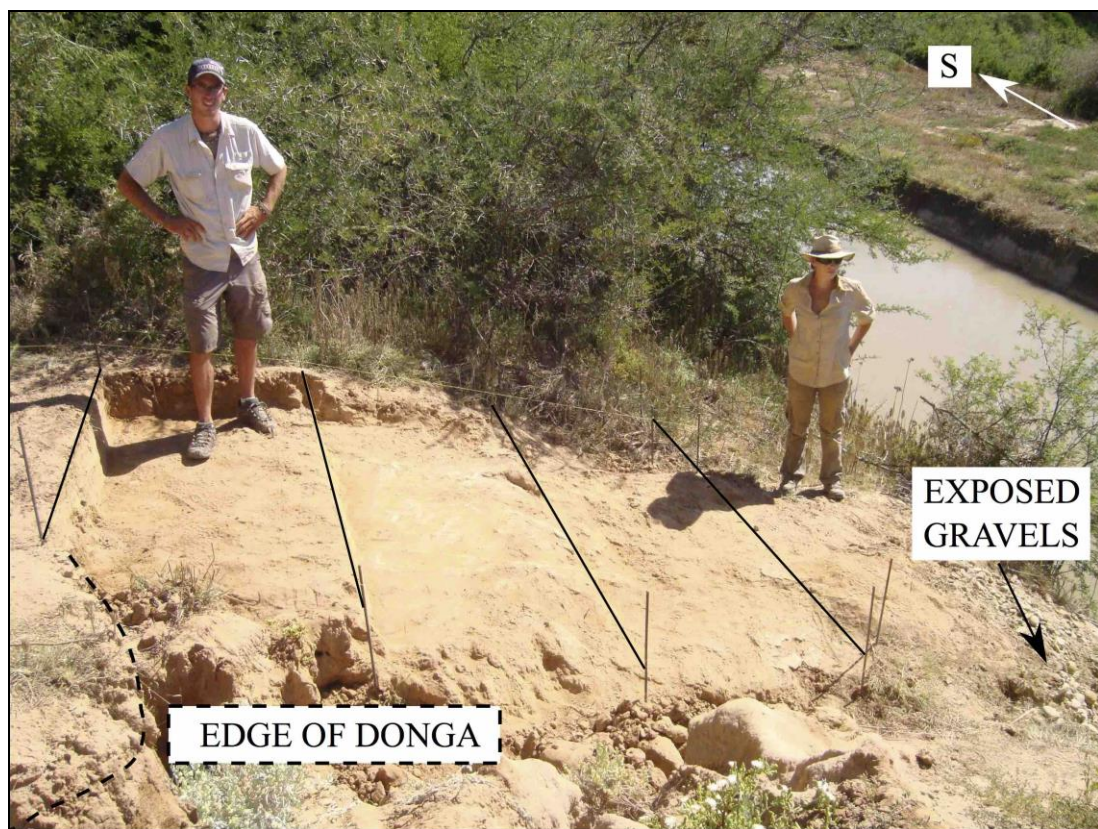


Figure 3.3.1. Atmar Farm Excavation 1 stepped trench. Note canal at right of image and exposed gravels at bottom right. The donga edge can be seen in the foreground.

Excavations here proceeded in spits of 10 cm within the fine overbank alluvium. These were thickened once hitting the gravels due to the large size of the clasts. Spits were dug primarily with spades, due to the extremely hard nature of the deposit. In the gravels a pick was used to loosen the material prior to removal by spades for sieving. Sieving with both 2 and 4 mm mesh was used within the fines, yet the general absence of material later dictated the need for only the 4 mm. This was also carried out for the gravels due to the almost complete absence of SFD.

Spatial and depositional data on artefacts within the gravels was not recorded. This is because the deposit type preserved no spatial information and the clearly imbricated nature of the clasts would only have provided (depositional) data that would confirm, contextually, what we already knew about the deposit.

Although the intention was to take all squares down into the gravels, based on the low frequency of artefacts obtained from the first two excavated squares (A1 & A2, shown in Figure 3.3.2), there was no need to continue with the excavations here.



Figure 3.3.2. Excavation 1 with squares A1 and A2 dropped into the gravels. Squares B1 and B2 sit atop the surface of the gravels.

A smaller test pit excavation (Excavation 2, shown in Figure 3.3.3) was opened up to assess the artefact frequency at the dated location (Fig. 3.2.2). This excavation was also placed along the edge of a donga, except here this needed to be cut back to provide an area large enough to excavate from. In terms of technique, excavations here followed the same protocol as that applied to Excavation 1, the only difference being the use of 20 cm spits throughout. Once a sufficient sample of material had been obtained, for comparison with Excavation 1, the test pit was closed.

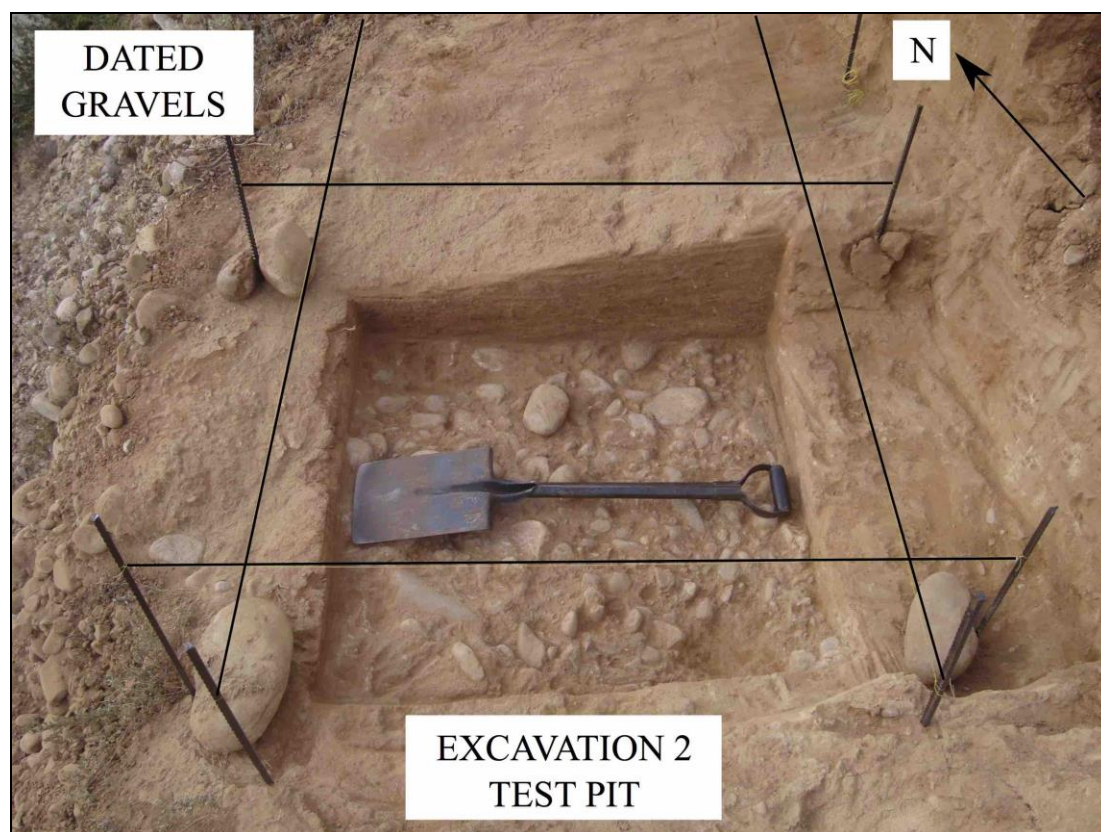


Figure 3.3.3. Atmar Farm test pit excavation due north of Excavation 1. Note dated gravels at left of image and cut back donga to the right. Spade for scale.

3.3.2.2 Bernol Farm

Survey work on Bernol Farm has shown the Terrace 9 exposure to be extremely complex. Most important is the extreme difficulty getting into the deposits to conduct sampling where artefacts are abundant at the dated location (Fig. 3.2.9), as an extremely thick overburden is found with no access to it from the top. As a result the bulk of work here has only been preliminary and artefacts retrieved from this property are mainly surface finds and those found eroding from *in situ* positions at the survey sites and near the dated location. However, a single test pit excavation was opened up

at survey site 2 (Figs. 3.2.7 & 3.3.4). The goal of this excavation was to sample the artefact, bone and shell-rich horizon found exposed along the edge of the survey site. The excavation was placed as close to this as possible.

Excavations here proceeded in 10 cm spits until reaching a grey horizon that appeared to be the start of the artefact rich layer. Thereafter 5 cm spits were utilised. Sieving was conducted using both 2 and 4 mm mesh. No spatial or depositional data was obtained on the artefacts. Excavations were completed at approximately 1.5 m and the pit was then closed.

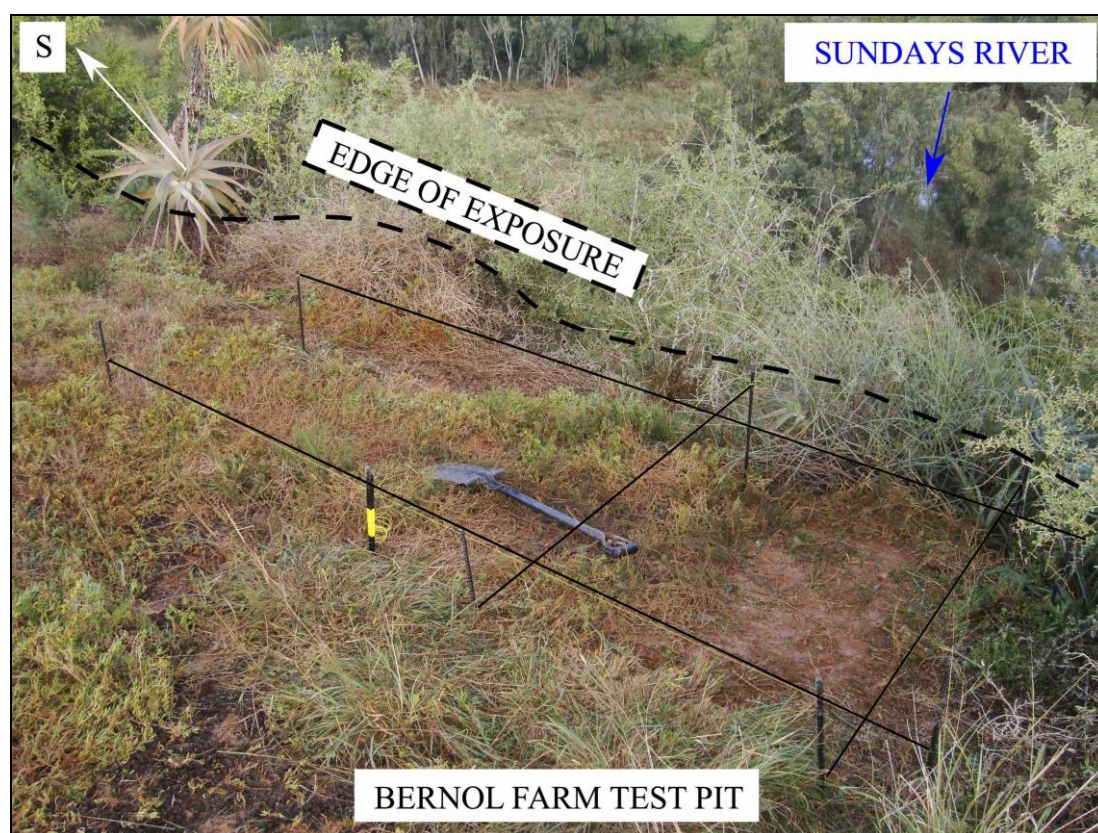


Figure 3.3.4. Bernol Farm test pit excavation at survey site 2. Shell, bone, and artefact rich horizon is found beneath the edge of this exposure towards the right of the image. Spade for scale.

3.3.2.3 Penhill Farm

From basic survey work on the Penhill Farm property it was clear that excavations needed to focus on sampling the debris flow. The artefacts here are extremely concentrated and well preserved, in contrast to the sporadic pieces that occur in the overlying colluvium. However, gaining access to this deposit from within the borrow

pit would have proven troublesome due to the steep sloping surface leading up to the exposure. It was therefore decided that excavation would take place above the exposure, east from the edge of the terrace (shown in Figure 3.2.12 and where the person is standing in Figure 3.2.15). Dense vegetation growth along and back from the terrace edge further restricted access to this area. With the kind assistance of the landowner, a portion of this vegetation was then cleared using a grader (see Figure 3.2.12 for cleared area). This opened up a sufficiently large area within which the excavation could be established. In order to confirm the extent of the debris flow deposit and whether it extended back (east) into the terrace, with the landowner's assistance, a trench (2 X 0.3 m, see Figure 3.2.12) was dug (with a back hoe) perpendicular to the terrace edge down (approximately 1.7 m) towards the debris flow. This trench also provided us with an estimation of the ratio of artefacts to a given volume, which assisted in future planning for the excavation grid.

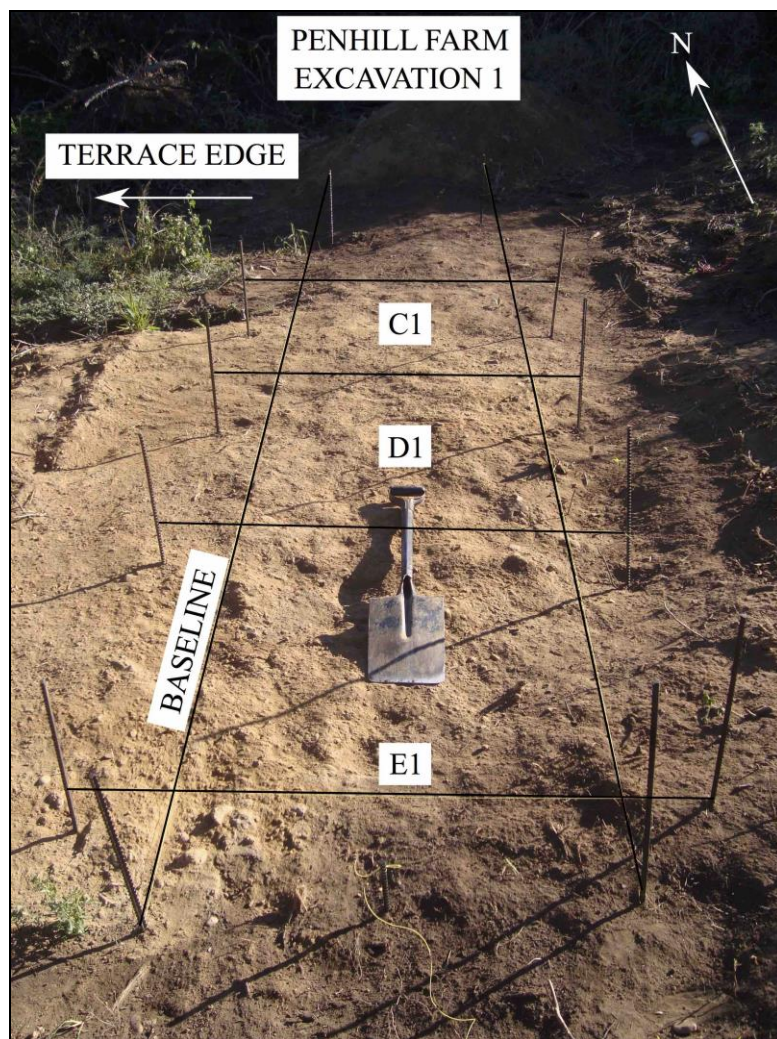


Figure 3.3.5. Penhill Farm 1 X 3 m grid prior to excavation. Squares A1 and B1 (not shown) were not excavated at any point. Spade for scale.

Once we were confident the debris flow extended back from the terrace edge, an adaptable grid was established (Excavation 1, initially a 1 X 3 m grid that could be expanded in any direction, shown in Figure 3.3.5). Squares C1 and E1 were excavated first using 5 cm spits and both 2 and 4 mm sieve mesh, and a good sample of material from the debris flow was obtained from below 1.9 m. Spatial and depositional data was also obtained on all suitable pieces. From these squares it became clear that the debris flow extended back from where it was exposed at the terrace edge and towards the excavation grid (east); however, after excavating these squares it was clear that the debris flow occurred in only half of each square. This suggested that the debris flow was discontinuous towards the east. To test this, another square (A2, further to the northeast away from the terrace edge, see Figure 3.2.12) was opened up and excavated down to 2.6 m, during which time the debris flow was not found. In order to enlarge the excavation and provide a sufficient sample of material it was therefore decided that the grid be extended towards the terrace edge (in a west direction).

Due to the generally sterile nature of the overlying fines in the three excavated squares, and because of time restraints in the field, it was decided that this overburden should be cleared so as to reach the debris flow as quickly as possible (Fig. 3.3.6). This overburden was cleared to a depth of 1.75 m, safely above the highest point of exposure for the flow. Excavations took place with spade and pick and all sediments were screened using 2 and 4 mm sieve mesh. All excavated artefacts were carefully bagged and tagged for the respective clearing. Although several smaller channel flow deposits have already been described and shown to occur in this overburden (Figs. 3.2.16 & 3.2.17), the sporadic nature of the artefacts preserved here did not at the time warrant their careful exposure and excavation. The goal was to focus on sampling the debris flow deposit as this contained the highest abundance of well preserved artefacts. Had time permitted, the careful excavation of these upper levels using fine spits and the recording of spatial and depositional data would have been more favourable.

Once the overburden had been removed the original grid (with 3 m² excavated, squares A2, E1 and C1) was expanded by another 7 m², giving a total of 10 m² (squares A1 and B1 remained unexcavated throughout, Figures 3.2.12 and 3.3.6).

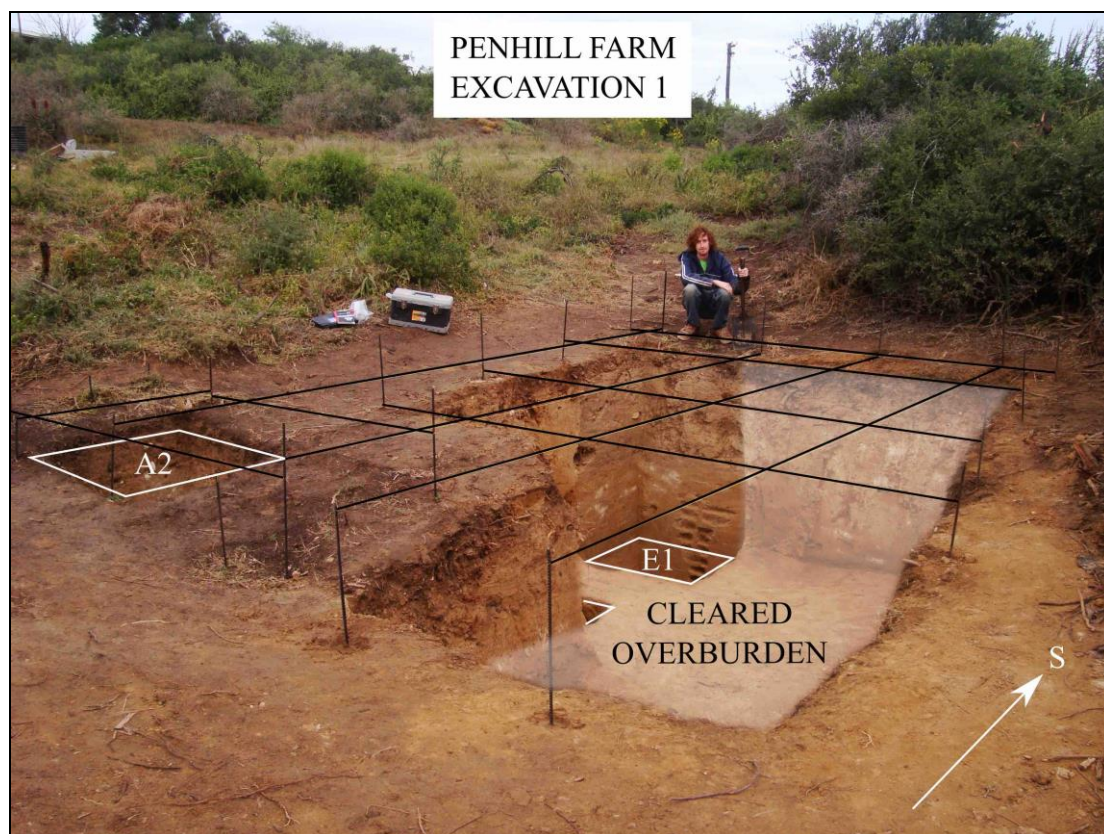


Figure 3.3.6. Excavation 1 full grid established. Note overburden clearing (lightened area) also for square D1. Spade for scale.

Immediately after expanding the grid an extreme flooding event took place. This event caused 2012 to be the second wettest year on record for the Eastern Cape since 1955 (the first being 1968; Spies 2012). In excess of 200 mm of rain fell locally over the Addo area overnight (potentially more), and not only did this cause considerable damage to the excavation (Fig. 3.3.7) but many parts of the Eastern Cape were affected (Mortimer 2012; Spies 2012). An extensive site clean up was therefore needed and all infilled sediments were removed. The majority of these infilled sediments though was from upslope of the excavation and from wall collapses of the colluvium found above the debris flow, both of which do not contain any significant concentrations of lithic debris. Due to the moisture content of the removed sediment, neither 2 or 4 mm mesh could be used to retrieve any material. Fortunately, only minor erosion of the debris flow took place in squares D1, CC1 and EE1, due primarily to the layer (\pm 5-15 cm) of overburden that protected it from erosion. Where minor erosion did occur, there is the possibility that some of the assemblage components were lost as this wet sediment had to be discarded. This was unavoidable.

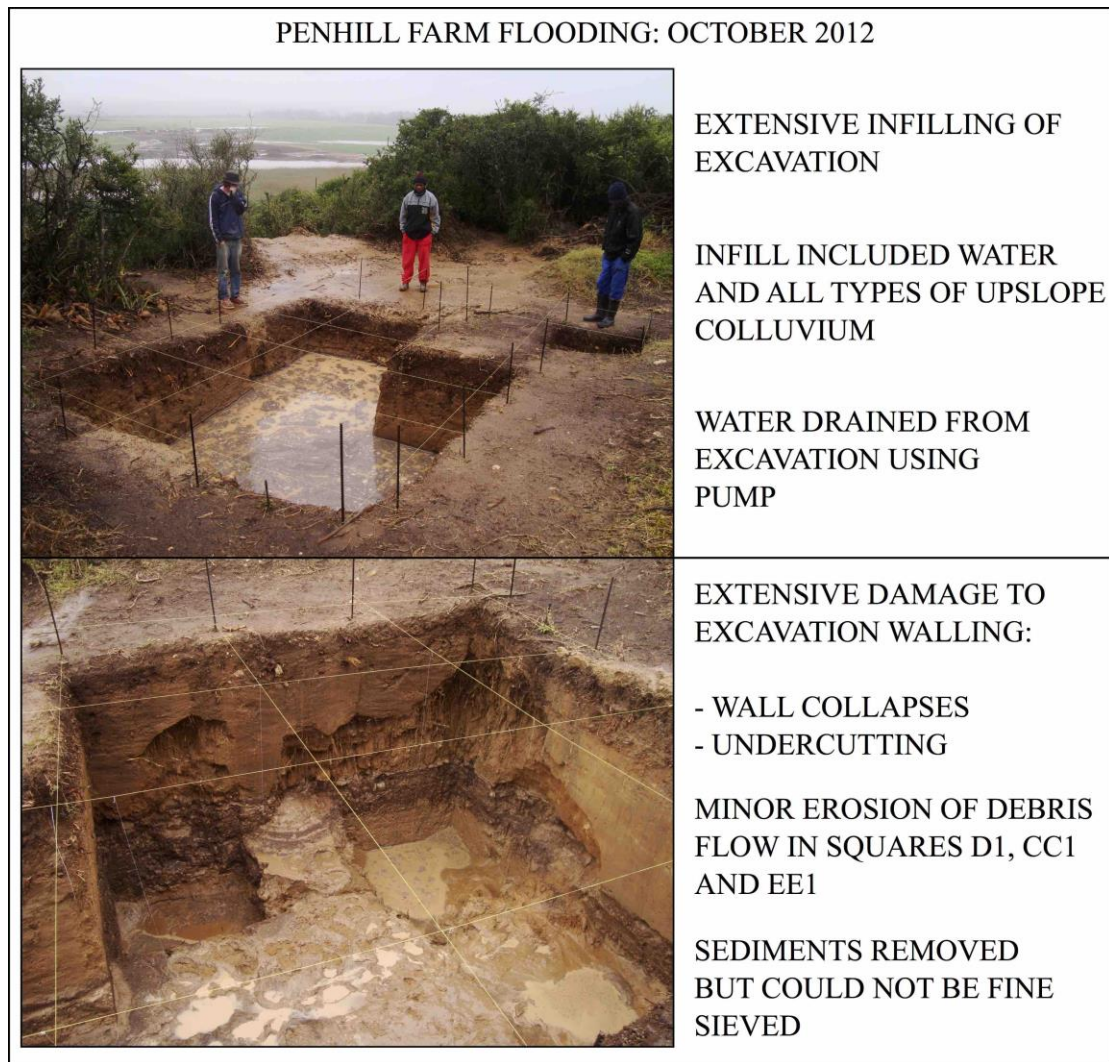


Figure 3.3.7. Flood damage to the Penhill Farm Excavation 1.

Thereafter, excavations proceeded following the same protocol as had been applied in the previous three squares. The debris flow was carefully exposed in each square and mapped before being taken down in 5 cm spits (Fig. 3.3.8). Artefacts were mapped in spatially and depositional data on suitable pieces was recorded. Unfortunately the moisture content of the excavation remained high as several smaller rainfall events occurred. As a result the 2 mm sieve could not be used at certain times. As soon as the sediments became dry enough both sieves were used.

Excavations concluded when reaching the sterile fine alluvium found underlying the debris flow.



Figure 3.3.8. Exposing the debris flow in square DD1, Excavation 1.

3.4 Lithic analysis

3.4.1 Introduction

The approaches used during the lithic analysis are discussed in this section. This includes a detailed account of the typological classification used and the technological measurements employed to record artefact features. Below is a list of items that were recorded for all artefacts obtained from survey work and excavation:

1. Material type: this denotes the actual type of material (of the artefact). Lithics were recorded as stone. Although not to be discussed in this section, other types included: bone, charcoal, shell, ostrich egg shell (OES), tin, glass and metal.
2. Maximum length: a measurement obtained in millimeters using a pair of digital calipers along the longest axis of the artefact.
3. Weight (mass in grams): individual artefacts ≥ 20 mm (complete flakes, cores, formal tools and other) were each weighed on a digital scale, to the nearest 100th of a gram. Flaking debris ≥ 20 mm (see below for types) was combined into a single sample (for each excavation bag) and weighed collectively; SFD was also measured collectively per excavation bag, although this was divided into <10 mm and <20 mm samples (and each was then weighed separately). Weight data was not recorded for the Atmar Farm assemblage.
4. Artefact type (typology): in order to account for the different artefacts a list of types was developed, according to five main categories. This included: flaking debris, complete flakes, cores, formal tools, and 'other' types (see following discussion).
5. Raw material: a range of raw material types is found in the lower Sundays River Valley. The careful study of each and every artefact to correctly identify these materials was pursued (see following discussions).
6. Artefact condition: assessing the preservation of artefacts is crucial when investigating the formation of a site. Condition relates to the exterior of the artefact and what processes modify these surfaces. This analysis was performed on each and every artefact ≥ 20 mm (see following discussions).

3.4.2 Typology

Detailed artefact descriptions are found below, modified from those presented by Kleindienst (1962), Leakey (1971), Clark and Kleindienst (2001) and Kuman (2001).

3.4.2.1 Flaking debris

- Small flaking debris (SFD): all lithics <20 mm in maximum length that are the smallest by-products of the flaking process. These include all chunks, chips and portions of flakes.
- Chunks (≥ 20 mm): these are pieces that are usually angular and thick and they do not retain any flake-like features. They cannot be related to any specific portion of a flake either (e.g., proximal or distal end).
- Incomplete flakes (≥ 20 mm): broken flakes that lack one or more distal or lateral portions but retain all or most of the striking platform (proximal portion of the piece). They frequently possess a clear dorsal and ventral surface and bulb of percussion.
- Flake fragments (≥ 20 mm): broken pieces of flakes that do not possess the striking platform (proximal end). They possess a clear dorsal and ventral surface and sometimes preserve a portion of the bulbar scar.
- Split flakes (≥ 20 mm): flakes that have broken through the centre of the bulb of percussion (perpendicular to the platform) during the knapping process.
- Bipolar incomplete flakes, fragments and chunks (≥ 20 mm, no split flakes): broken flakes removed from a bipolar core, or chunks and flakes with recognisable bipolar features (impact marks, thin/crushed platforms, lack of a clear bulb, and spalled pieces).

3.4.2.2 Complete flakes (≥ 20 mm)

- Complete flakes: freehand produced flakes with complete striking platform and bulb of percussion. The piece is complete to the lateral boundaries of termination and no breakage occurs at the distal end. These are further divided into:

- End-struck: striking platform is proximal, perpendicular to artefact long axis.
- Side-struck: striking platform is lateral, parallel to artefact long axis.
- Corner-struck: striking platform at approximately 45° to artefact long axis.
- Kombewa: flake with two ventral surfaces and possibly two bulbs of percussion.
- Core trimming: flakes from a core removed with the intention of adjusting a striking platform or removing an angular edge. Frequently triangular in cross-section (not exclusively), forming part of the core edge, however can be flat, tabular or chunky.
- Bipolar: flakes from a bipolar core that normally show two points of percussion, at opposite poles, or a single point of percussion. Crushing/powdering of the polar ends is common. Flake features appear less pronounced (bulb of percussion and ripples). Large portions of the original core often remain.
- Handaxe/LCT trimming (HATF) or periphery shaping: flake that appears to have a very angled platform (in relation to the angle of the removal). Suggests the flake has been removed from the periphery of a LCT (secondary shaping removal/flake).
- Bi-bulb: flake that retains two bulbs of percussion on a single ventral surface.
- Core rejuvenation: an elongated flake that contains a platform along the core surface/edge, removed so that a new platform can be exposed from which to flake (different from a core tablet which removes the whole upper surface of a core).

3.4.2.3 Cores (≥ 20 mm)

- Core fragments: an incomplete broken core, or pieces of a core, that must show evidence of some working. As it is broken it is difficult to assign it to a specific core type. They contain no clear bulb or platform, normally are very angular, and retain the edge of a core.

- Casual: a core that has one or two removals. These cores appear to suggest the testing of raw material suitability.
- Bipolar: a core with opposed platforms, though only one may be preserved. These cores are created through the bipolar method of flaking, between a hammer and an anvil. Flakes can be removed from both platforms on one or both faces.
- Chopper-core: either bifacial or unifacial. A series of removals adjacent to one another along a given edge gives rise to a jagged chopping/cutting edge. The artefact, however, shows no signs of use and is thus called a core (versus a tool, i.e., a chopper). The focus of all core work has thus been to provide a series of flake removals.
- Discoidal: a core that is worked in a radial fashion with all removals being worked from the outside of the core inwards (centripetally). This gives rise to a core that is frequently quite round in plan view and disc-like in profile, but cross-sectional thicknesses may vary and discoidal cores can also be elongated. Portions of cortex are frequently found in the centre of the core on both faces. Discoids can be unifacial or bifacial. A single atypical discoidal core was recovered from Penhill Farm showing a single large removal, but lacking asymmetry.
- Irregular: a core that has been worked in a completely unorganised fashion. The shape is more irregular and flatter than a polyhedral core. Characterised by only a few removals from any given direction.
- Polyhedral/multi-platform: a core in which every possible flaking platform has been worked (more than 2 striking platforms) and eventually exhausted (hence it is discarded). These cores are frequently spherical in shape but can be completely irregular. The core is worked from multiple directions wherever a platform presents itself.
- Single platform: a core that has a series of removals from a single platform edge/face, all trending in the same direction. The angle of the platform is close to 90°. These single platform cores differ from unifacial choppers/chopper-cores as the flaking angle is far steeper. The goal is to produce flakes and no use-wear is evident.

- Boulder-core: a core ≥ 256 mm where large flakes have been removed. These large flake blanks may have subsequently served as tool blanks.

3.4.2.4 Formal tools (≥ 20 mm)

- Handaxe (LCT): tool with a convergent distal end and cutting edges around the margins of the piece. Shaping is therefore not limited to the distal end but a significant amount occurs over the body of the tool, with generally less towards the base. Produced on cobbles or large flakes and usually trend towards some degree of symmetry in shape. Can be unifacial, partly bifacial or bifacial.
- Cleaver (LCT): a large shaped tool (either bifacial, partly bifacial or unifacial) with a sharp distal cutting edge (or bit, usually unflaked) at a right angle or slightly oblique position to the long axis of the piece. Shaping is common on the laterals, often to reduce the thickness of the bulb when made on large flakes. Also made on cobbles.
- Pick (LCT): shaped tool that appears similar to handaxes, but with emphasis on shaping/retouch at the tip of the piece to produce a strong pointed end. Can be unifacial, partly bifacial, bifacial, or even trihedral. Frequently largely cortical with less overall shaping towards the base of the tool (generally less symmetrical than most handaxes). Made on both flakes and cobbles.
- Biface (LCT): artefact made on a flake or cobble blank that has been minimally worked bifacially (or partly bifacially) but which lacks a clearly convergent distal end; some appear to be intermediate between handaxes and cleavers. Due to a lack of emphasis on a convergent distal end or the peripheral cutting edges, these are called bifaces to distinguish them from handaxes which are more markedly convergent.
- Broken Handaxe/LCT: any broken portion (either distal or proximal) of an LCT.
- Knife: artefact that has a single long cutting edge with either unifacial, bifacial or no retouch. Edge is sharp and knife-like, not scraper-like (which has a steeper edge). The tools opposite edge is either naturally blunt or roughly backed (retouched) by the tool-makers.

- Chopper: either bifacial or unifacial. A series of primary shaping removals along a given edge gives rise to a jagged chopping/cutting edge; secondary working is generally absent. This edge shows clear use-wear or crushing indicating its use as a tool and not just as a core (e.g., chopper-core). Use-wear presents itself in the form of small edge chipping or abrasion, causing edge blunting. Rounded cortex frequently forms the butt end. These are further divided into:
 - Side: chopper edge occurs at 90° to long axis of tool.
 - End: chopper edge occurs parallel (in line with) the long axis of the tool.
 - Chopper: multiple chopper edges.
- Flaked-flake: a flake that has then been flaked, one or more times on one or more edges, to create a notch. This notch is not retouched.
- Retouched flake: flakes with more than minimal or discontinuous retouch (that would then be a miscellaneous retouched piece, see below), which cannot be readily assigned to a more formal type (e.g., a scraper).
- Scraper: a flake or core serves as the blank and these show several unifacial removals (retouch) in one or more areas of the tool, which were used for scraping purposes (steep edged; >45°). These are further divided into:
 - Composite: multiple scraper edges on one tool with at least two different types (e.g., side and end, side and convex).
 - Concave: continuous removals occur with a clear emphasis on creating a wide concavely curved edge.
 - Convex: removals that occur along a face which is slightly convex in shape.
 - End: removals occur parallel to the long axis of the artefact (at a polar end).
 - Side: removals occur 90° to the long axis of the artefact, forming a fairly straight scraping edge.
 - Double side and end: continuous retouch all around the distal and lateral edges of the tool.

- Notched: removals appear as separate notches in one or more locations on the tool. Discontinuous and often isolated for the specific creation of a localised scraper edge.
- Convergent: a pointed tool resembling a retouched point but with steep edges that suggest it was used as a scraper. The retouch may also form small notches.
- Denticulated: removals are relatively steep and are interspaced yet continuous for a given length. This retouch creates a steep jagged edge.
- Heavy-duty/core: unifacial removals focused on one or more steep edges of a core, block or chunk. Flaking geared towards edge shaping for use as a tool versus flaking for core reduction.
- Miscellaneous retouched piece (MRP): artefacts with minimal areas of discontinuous retouch, insufficient to define the tool as any particular type. There can be several different areas of retouch, each of which is isolated from the other.
- Burin: frequently made on broken or spalled edges of a flake. The spall creates an angular edge that has little to no retouch.
- Awl: tool with a narrow worked/retouched tip forming a pointed distal end; either unifacially or bifacially retouched.
- Denticulate: artefact with retouch that produces a sharp serrated cutting edge. Retouch is less steep ($<45^\circ$) than for a denticulated scraper.
- Composite piece: artefacts that show at least two different shaping patterns (e.g., denticulate and scraper), created through retouch.

3.4.2.5 Other (≥ 20 mm)

- Modified cobble: a cobble that shows evidence of repeated bashing/pounding. Shallow flake scars occur around the percussed area.
- Split cobble: a cobble or boulder that is split either into two or more portions. This may be the result of the anvil technique (bipolar core working) or damage to a hammerstone during flaking.

3.4.3 Raw material classification

The lower Sundays River Valley is characterised by an abundance of quartzite clasts, due primarily to the composition of the upstream Klein Winterhoek mountain range. However, several other raw materials were also identified during the analysis of the lithic assemblages. These are briefly described below, following definitions from Bell and Wright (1985) and Norman and Whitfield (2006):

- Quartz: one of the most abundant minerals in the Earth's crust, chemically classified as a silicate (Norman & Whitfield 2006). They are extremely resistant to weathering and often retain a fresh condition (Bell & Wright 1985). Locally they are clear to milky white in colouration.
- Quartzite (fine and coarse): a rock that is comprised of metamorphosed sandstone (Bell & Wright 1985). It contains small sand-sized sedimentary quartz grains that are re-crystallised together into larger interlocking crystals (Norman & Whitfield 2006). Quartzites have a 'sugary and grainy' appearance and locally they vary in colour from white to grey to dark red. During classification quartzites were divided into both fine- and coarser-grained types.
- Siltstone: a sedimentary rock that contains silt-sized particles, which can include minerals quartz, feldspar, mica, and calcite (Bell & Wright 1985). These are then compacted and cemented (lithified) to form the rock.
- Silt-quartzite: a unique but rare high quality raw material with visible quartz grains set amongst a fine matrix of silt-sized particles (matrix-supported). Presumably a sedimentary rock but the high-quality suggests a metamorphic origin.
- Hornfels: a fine-grained rock that is comprised of a metamorphosed mudstone or shale (Norman & Whitfield 2006). These are extremely suitable for knapping and locally colours occur in a range of greys to black.
- Crypto-crystalline (CCS): sedimentary rocks with forms of silica that are extremely fine-grained, generally grey or white in colour (Norman & Whitfield 2006). Varieties include chert, agate, chalcedony, and jasper, all with variable colours.

- Lava: a general term used here to describe any kind of hard igneous rock that is fine- to medium-grained (Norman & Whitfield 2006).
- Silcrete: a sedimentary rock comprised of fine chemical sediments of carbonate (forming calcrete) or silica (forming silcrete). They are formed by the accumulation of these sediments near the surface of the soil, frequently forming a hard capping (Norman & Whitfield 2006).
- Claystone: a fine-grained sedimentary rock comprised of clay-sized particles formed through hardened and compacted clay. These are different from shales in that they have no bedding laminations (Norman & Whitfield 2006).
- Indeterminate: any raw material that could not be confidently identified due to excessive weathering, abrasion or chemical breakdown.

3.4.4 Artefact condition

The study of artefact condition can be a somewhat subjective undertaking, especially if several different researchers are to assess the same or separate parts of a given assemblage. To minimise this subjectivity and to ensure consistency this analysis was performed solely by the author. Following the discussion presented in Chapter 2.3 on artefact condition it is necessary to clarify the definitions of both weathering and abrasion. Weathering refers to the chemical breakdown/decay of a given raw material (Schiffer 1983; Thompson 2009), whereas abrasion refers to a ‘wearing down’ of artefact surfaces/edges (Shackley 1974; Schiffer 1983; Shea 1999; Holmes *et al.* 2008; Thompson 2009). This abrasion is caused by either an abrasive medium passing over the surface of the artefact or by the movement of the artefact over an abrasive surface/medium. The following categories were utilised:

- Fresh/unabraded: artefacts with very sharp edges and prominent dorsal ridges/scars. No modification to the external surfaces of the piece occurs.
- Slightly abraded: minor abrasion causing a slight blunting of artefact edges and/or dorsal scar ridges. Modification is only slight.
- Heavily abraded or rolled: pronounced abrasion across a considerable portion (if not all) of the artefact. This leads to worn edges that are dull to the touch. Rolled artefacts have clearly been influenced by fluvial forces, causing a significant modification to all artefact edges/surfaces. This damage is

normally extensive (affecting the whole piece). No effort was made to distinguish between heavily abraded and rolled pieces.

- Weathered (decay of raw material): where specific conditions dictate certain raw materials are susceptible to a chemical breakdown either at the surface or during burial.
- Varnishing: as described by Thompson (2009, termed ‘polish,’ and different from patination), these are artefacts that possess a change in the reflective property of the artefact (either restricted or extensive). Where varnishing is incomplete, this suggests a differential exposure of artefact faces to natural elements (abrasive mediums), which would cause the ‘smoothing’ of an artefact surface. This was recorded in conjunction with the above (4) types.

3.4.5 Additional notes

A final mention must be given here to any atypical features that were identified on the Sundays River artefacts. This involved keeping a basic record of any kind of obvious recycling or utilisation damage. Recycling suggests the re-use of an artefact across both space and time, either for the same purpose or for a completely different task (Assaf *et al.* 2015; Parush *et al.* 2015). For this research artefact recycling was identified by a difference in condition between scars or surfaces (termed ‘double patina’; Barkai *et al.* 2015; Vaquero *et al.* 2015), or by two successive tool uses that differ functionally (Vaquero *et al.* 2015); a heavily abraded artefact with newer, fresher removals, or a core that has been retouched for use as a scraper, provides some illustration. Artefact utilisation included cutting (chipping along specific thin artefact/tool edges), percussion/pounding (surface pitting that suggests repeated bashing), and scraping (chipping along steep artefact/tool edges) damage.

3.4.6 Technology

3.4.6.1 Introduction

A detailed technological analysis was conducted on both the Penhill Farm assemblages and all the LCTs obtained from Bernol Farm; the poor preservation of

artefacts from Atmar Farm meant that detailed technological analysis could not be pursued. Table 3.4.1 provides a summarised list of all the attributes recorded on each of the five main artefact types (formal tools include both retouched pieces and LCTs). The way in which these attributes were recorded is discussed below. However, a brief note regarding the recording of this data must be presented first.

Table 3.4.1. Data obtained from the Bernol and Penhill Farm artefacts ('comp.' refers to complete).

Data	Incomp. flakes	Comp. flakes	Cores	Retouched pieces	LCT	Other
Length	X	X	X	X	X	X
Width	X	X	X	X	X	X
Thickness	-	X	X	X	X	X
Platform thickness	X	X	-	-	-	-
Platform width	X	X	-	-	-	-
Platform facets	X	X	-	-	-	-
Platform angles	-	X	-	-	-	-
Flaking axis	-	X	-	-	-	-
Flake scars	-	X	X	-	X	-
Flaking pattern	-	X	X	-	X	-
Termination type	-	X	X	-	X	-
Remaining cortex	-	X	X	X	X	-
Toth type	-	X	-	-	-	-
Cortex location	-	X	-	-	-	-
Flake scar length	-	-	X	-	-	-
Core size	-	-	X	-	-	-
Blank type	-	-	X	X	X	-
Retouch position	-	-	-	X	-	-
Retouch localisation	-	-	-	X	-	-
Retouch distribution	-	-	-	X	-	-
Retouch delineation	-	-	-	X	-	-
Retouch extent	-	-	-	X	-	-
Retouch angle	-	-	-	X	-	-
Edge length	-	-	-	-	X	-
Tip shape	-	-	-	-	X	-
Cleaver butt plan	-	-	-	-	X	-
Damage/breakage	-	-	-	-	X	-
Refitting	-	-	-	-	-	-
Residues/use-wear	-	X	-	-	X	-

Technological data that could be reliably and correctly recorded on artefacts (even those possessing breaks) was included in this study. Some clarification on this is needed and the following points provide an illustration:

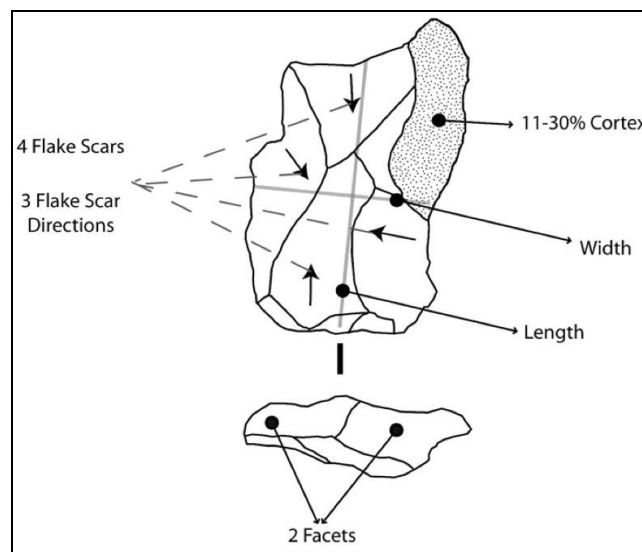
- Technological flake length and width, including platform thickness, width and facet count, were recorded on complete and incomplete flakes where possible, and on retouched pieces made on either of these blank types. These data were only recorded if the measurements/features were unaffected by tool retouch and/or any kind of edge damage/breakage, and remained accurately preserved. For example, if all the edges on a complete flake were retouched (excluding the platform area) then no length or width measurements were recorded. But, all data that could be obtained on the unaltered platform area were recorded.
- A single core was retouched (unifacial discoid), with another three showing use-wear (choppers). Where possible, the retouched core was analysed in both the core and formal tool (retouch) sections, whereas the three choppers were included in the core analysis. Once again only measurements that could be correctly and reliably recorded were included. Accordingly, all core fragments were excluded from the core analysis.

For certain flake measurements two methods are used to record the same or very similar artefact features. The primary reason for this was to ensure that the Sundays River data could be compared to that from sites elsewhere, which have been recorded using multiple approaches. Some more specific reasons are listed below:

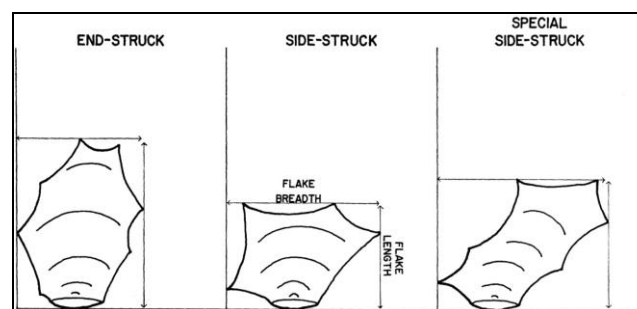
- Flaking axis: measurements following both Mason's (1965) and Isaac and Keller's (1968) methods were recorded. The sole purpose here was to consider the percentage of corner-struck types (Mason 1965) as these are not defined using Isaac and Keller's (1968) approach.
- Flake cortex preservation: two methods were used to record dorsal and platform cortex preservation. Toth's (1985) technological flake classification involves six flake categories that take into account both platform and dorsal cortex preservation. The method developed by Nishimura (2005) and Marwick (2008) was used to provide a more accurate representation of the exact location of this dorsal cortex.

3.4.6.2 Incomplete and complete flake attributes

- Technological flake length and width (following Braun *et al.* 2008, shown in Figure 3.4.1a): length refers to the distance between the distal termination of the flake and the point of percussion, along the technological axis (perpendicular to the platform). Width, measured perpendicular to the midpoint of the length, refers to the distance between the lateral edges of the flake on the ventral surface.
- Technological flake length and width (following Isaac & Keller 1968, shown in Figure 3.4.1b): length refers to the most distal tip of the artefact that occurs within the smallest encompassing rectangle, measured whilst the striking platform of the artefact is aligned on the horizontal. Following this orientation width refers to the distance between the lateral margins of the piece within the smallest encompassing rectangle.



a (from Braun *et al.* 2008)



b (from Isaac & Keller 1968)

Figure 3.4.1. Technological flake measurement methods.

- Technological flake thickness at midpoint (following Dibble 1997): this is the thickness of the flake where the width and length axes intersect.
- Flake maximum thickness (following Andrefsky 2005): this is the greatest distance between the dorsal and ventral surfaces.
- Platform maximum thickness (following Andrefsky 2005, shown in Figure 3.4.2): this is the greatest distance between the dorsal and ventral surfaces at the striking platform.
- Platform thickness at point of percussion (following Dibble 1997): this is the distance between the dorsal and ventral surfaces of the flake platform at the point of percussion (perpendicular to the platform width axis).
- Platform width (following Andrefsky 2005, shown in Figure 3.4.2): this is the total length of the platform measured from one lateral edge to another.

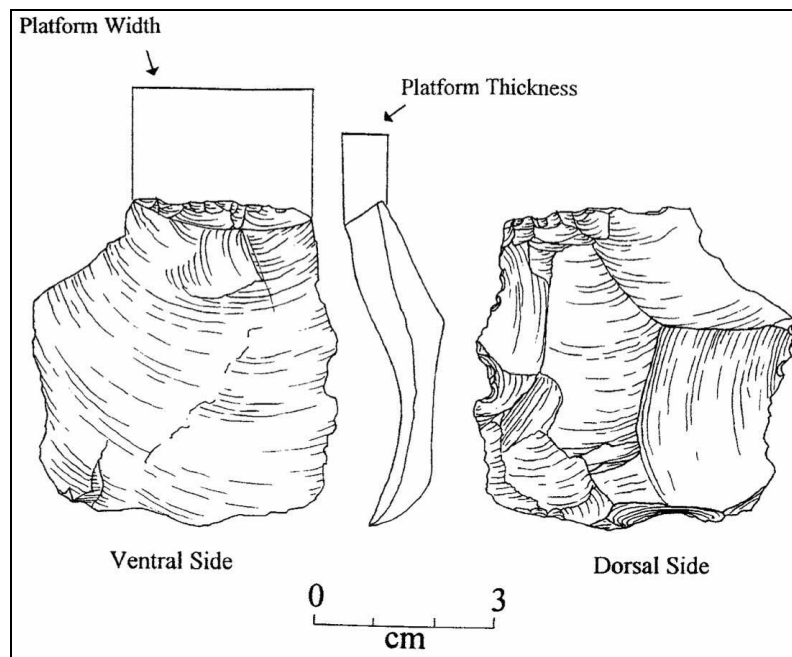


Figure 3.4.2. Flake platform measurements (from Andrefsky 2005).

- Number of platform facets (Fig. 3.4.1a): this refers to the number of flat surfaces or planes that occur along the flake platform. The following numbers were recorded:

0. Cortical	4. Multi-faceted
1. Plain	5. Partly cortical (where a portion of cortex is retained)
2. Dihedral	
3. Facetted	

- Interior platform angle (following Marwick 2008): this is the angle between the striking platform surface, at the point of percussion, and the flake ventral surface, measured using a goniometer.
- Exterior platform angle (following Dibble 1997): this is the angle between the striking platform surface, at the point of percussion, and the exterior (dorsal) flake surface.
- Technological flaking axis (following Isaac & Keller 1968, shown in Figure 3.4.1b): a side-struck flake is one that is wide or wider than it is long (breadth/length ratio is ≥ 1). An end-struck flake has a breadth/length ratio < 1 .
- Technological flaking axis (following Mason 1965): this is determined by aligning the long axis of the flake on the vertical axis and determining the position of the striking platform as:
 - Corner-struck: platform is intermediate between the proximal and lateral positions (see below).
 - Side-struck: platform is lateral and perpendicular to the long axis.
 - End-struck: platform is proximal and in line with the long axis.
- Dorsal flake scar count (following Braun *et al.* 2008, shown in Figure 3.4.1a): this refers to the number of negative flake scars, greater than 10 mm, found on the dorsal surface of the flake. Those that appeared to represent the edge of the core, or some pre-existing surface, were excluded.
- Dorsal scar directions (following Braun *et al.* 2008, shown in Figure 3.4.1a): this refers to the number of different flaking directions found on the flake dorsal surface. Directions need be separated by at least 30° to be termed different. Only those where a direction could be established were counted.
- Dorsal scar pattern (modified from Kuman 2001, shown in Figure 3.4.3): this refers to the general pattern of flake reduction, visible on a flake dorsal surface. The number of removals per direction were not quantified. The following patterns were utilised:

Indeterminate: no discernable pattern can be identified.

0. None: completely cortical.

1. Unidirectional-proximal: only a single direction moving away from the proximal end.

2. Unidirectional-distal: only a single direction moving towards the proximal end.
3. Unidirectional-transverse-proximal: two directions, one moving away from the proximal end and another that is perpendicular (transverse, from a lateral) to this direction.
4. Convergent-proximal: two intermediate directions from the proximal end (corners) that converge distally.
5. Convergent-distal: two intermediate directions from the distal end (corners) that converge proximally.
6. Radial: three or more directions moving centripetally towards the centre.
7. Transverse-opposed: two directions from either lateral moving towards and intersecting at the middle of the piece.
8. Parallel-opposed: two directions with one occurring away from the proximal end and the other occurring away from the distal end, causing an intersection at the middle of the piece.
9. Complex: two directions including one main direction (any that is either 90° or 180° to the platform) and one intermediate direction (corner).
10. Transverse: one direction, perpendicular to the platform, that is from the lateral.
11. Intermediate-proximal: one intermediate direction that is moving away from the proximal end.
12. Unidirectional-transverse-distal: two directions, one moving towards the proximal end and another that is perpendicular (transverse, from a lateral) to this direction.
13. Intermediate-distal: one intermediate direction that is moving towards the proximal end.

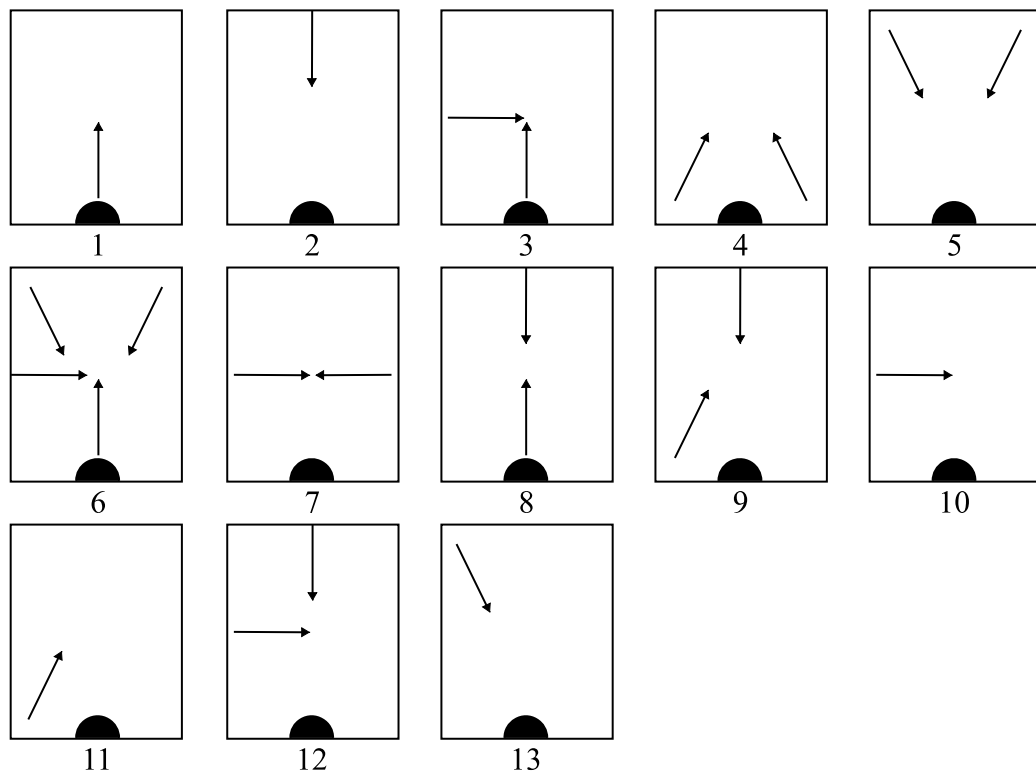


Figure 3.4.3. Dorsal flake scar patterns. Note platform (black semicircle) is always placed at bottom (proximal) for correct orientation.

- Flake termination types (following Andrefsky 2005, shown in Figure 3.4.4): this refers to the manner in which the flake detaches itself from the core. The following termination types were identified:
 - Feather: flake separates from the core smoothly and retains a thin edge around the periphery of the piece.
 - Step: flake that breaks during removal, creating a perpendicular angle between the distal surface of the flake and the flake ventral surface.
 - Hinge: flake where the distal end (fracture surface) turns upwards, resulting in a hinge.
 - Plunging/overshoot: a flake that is longer than usual and one that removes a portion of the core.

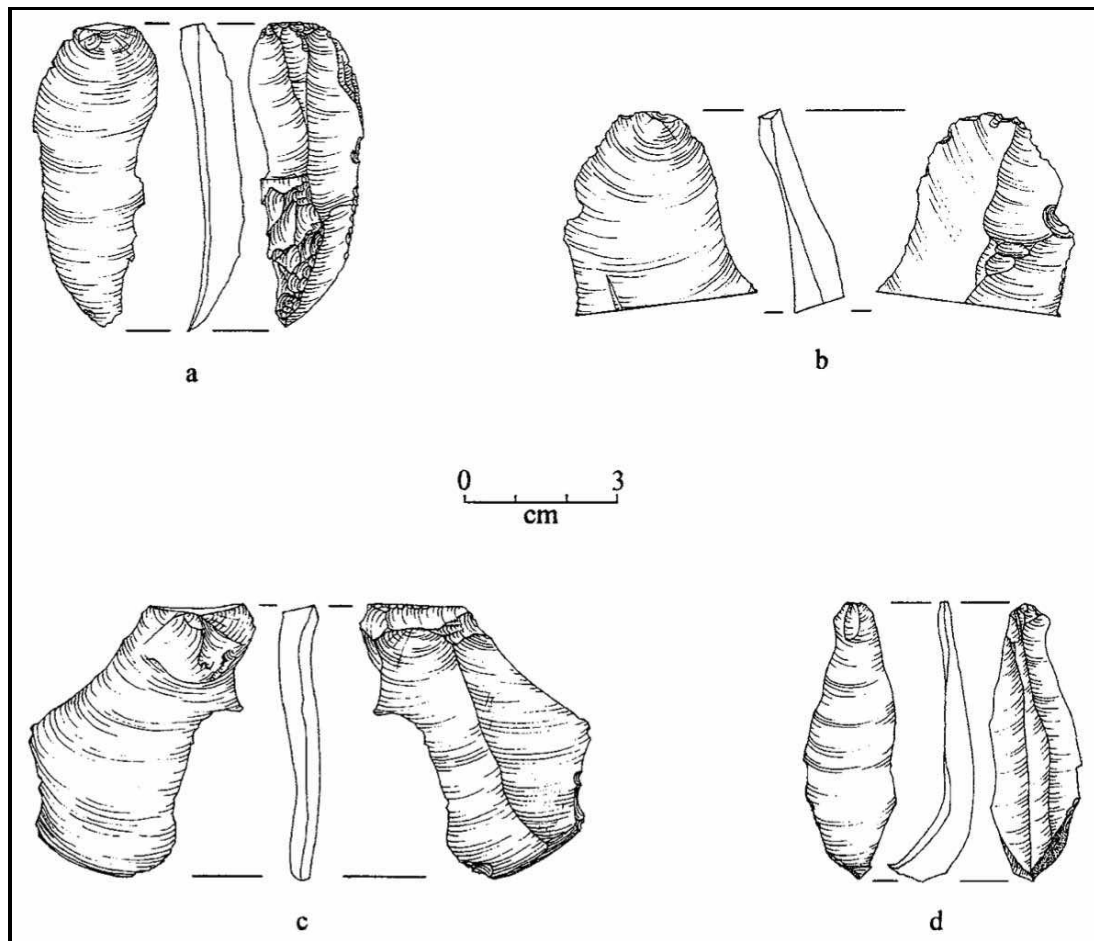


Figure 3.4.4. Flake termination types (from Andrefsky 2005). Feather (a), step (b), hinge (c) and plunging/overshoot (d).

- Percentage dorsal cortex (following Braun *et al.* 2008): this refers to the percentage of remaining cortex found on the flake dorsal surface. An eight stage system is used:

1. 100% (all cortex)	5. 31-50%
2. 91-99%	6. 11-30%
3. 71-90%	7. 1-10%
4. 51-70%	8. 0% (no cortex)
- Technological flake categories (following Toth 1985, shown in Figure 3.4.5): based on the six stage flake classification system developed by Toth (1985), this categorises flakes based on the percentage (presence, partial absence or complete absence) of cortex found on both the flake dorsal surface and

platform area. In general, flakes that are completely non-cortical tend to represent later stages of core knapping. The types are as follows:

- I. Cortical platform and dorsal surface.
- II. Cortical platform and partially cortical dorsal surface.
- III. Cortical platform with no dorsal cortex.
- IV. Non-cortical platform and cortical dorsal surface.
- V. Non-cortical platform and partially cortical dorsal surface.
- VI. Non-cortical platform and non-cortical dorsal surface.

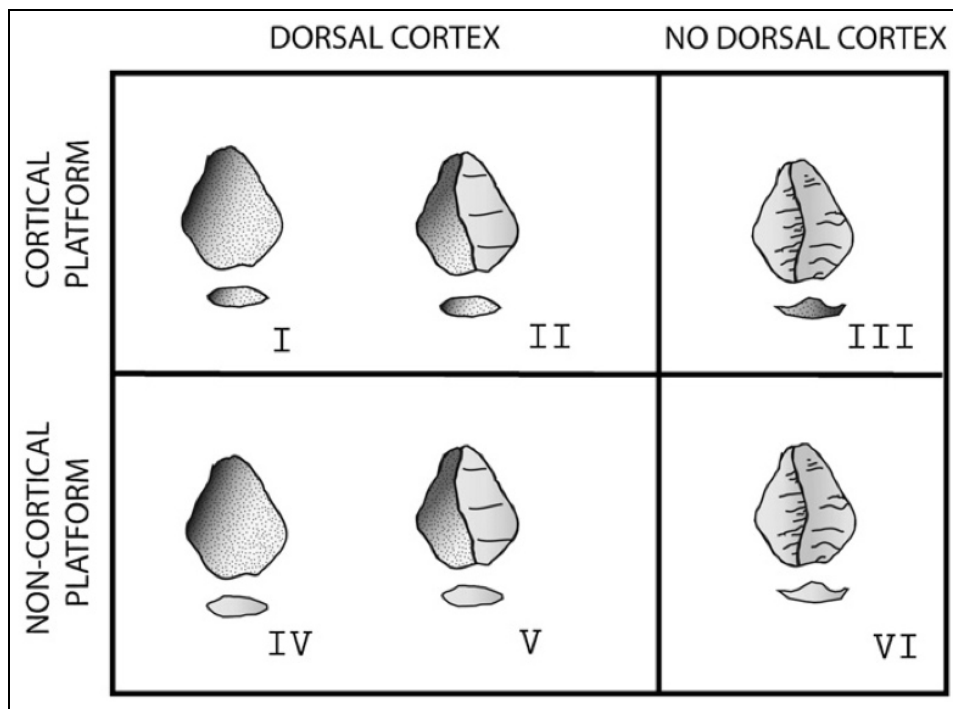


Figure 3.4.5. Technological flake classification (Toth 1985; from Braun *et al.* 2008).

- Dorsal cortex location (modified from Nishimura 2005 and Marwick 2008, shown in Figure 3.4.6): this refers to the area of the flake dorsal surface where cortex is preserved. Six primary areas have been identified:
 1. Primary removal
 2. Crescent shaped
 3. Distal
 4. Tertiary removal
 5. Proximal
 6. Central

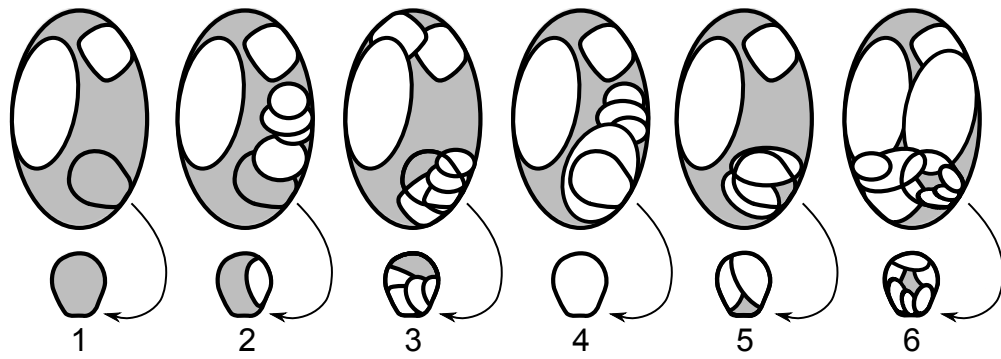


Figure 3.4.6. Flake dorsal cortex (grey) locations (redrawn and modified from Marwick 2008).

3.4.6.3 Core attributes

- Length, width and thickness measurements (Fig. 3.4.7): an artefact was placed within a box such that the long axis was parallel to the base of the box (X-axis). The length measurement then refers to this distance measured along the X-axis (not necessarily a maximum distance). The width measurement refers to the distance measured along the Y-axis (90° to the X-axis length measurement). Flipping the artefact from a horizontal to a vertical position the thickness measurement then refers to the distance measured along the Y-axis.

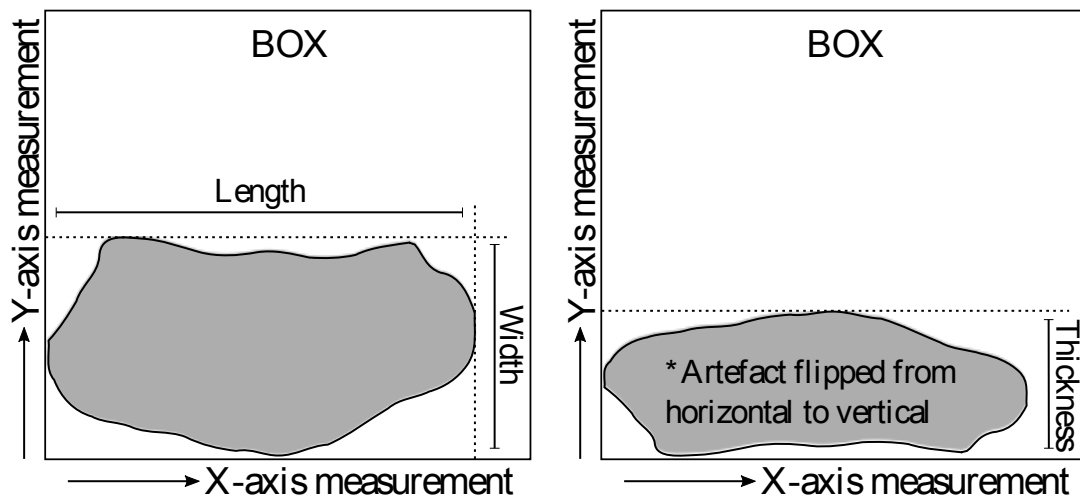


Figure 3.4.7. Length, width and thickness measurement method (for cores, retouched pieces and other cobbles).

- Core size (following Andrefsky 2005): this is the artefact maximum length multiplied by the weight.

- Total number of flake scars: this refers to the total number of removals found on the core. A cut off size of 10 mm was used; modern damage to any piece was not counted.
- Largest flake scar length: a single maximum length measurement was obtained from the largest flake removal (negative scar).
- Directionality of the flaking strategy (following de la Torre 2011, shown in Figure 3.4.8): this refers to the flaking strategy employed during core reduction. The following types were recorded (after de la Torre 2011):
 1. USP: unifacial simple partial exploitation
 2. BSP: bifacial simple partial exploitation
 3. UAU1: unidirectional abrupt unifacial exploitation on one knapping surface
 4. UAU2: unidirectional abrupt unifacial exploitation on two independent knapping surfaces
 5. UAUT: unifacial abrupt unidirectional total exploitation
 6. UABI: unifacial abrupt bidirectional exploitation
 7. BAP: bifacial abrupt partial exploitation
 8. BALP: bifacial alternating partial exploitation
 9. BALT: bifacial alternating total exploitation
 10. UP: unifacial peripheral exploitation
 11. BP: bifacial peripheral
 12. UC: unifacial centripetal exploitation
 13. BHC: bifacial hierarchical centripetal
 14. Discoid
 15. Polyhedral
 16. Multifacial/irregular
 17. Casual (included here as a modified category)
 18. Bipolar (included here as a modified category)

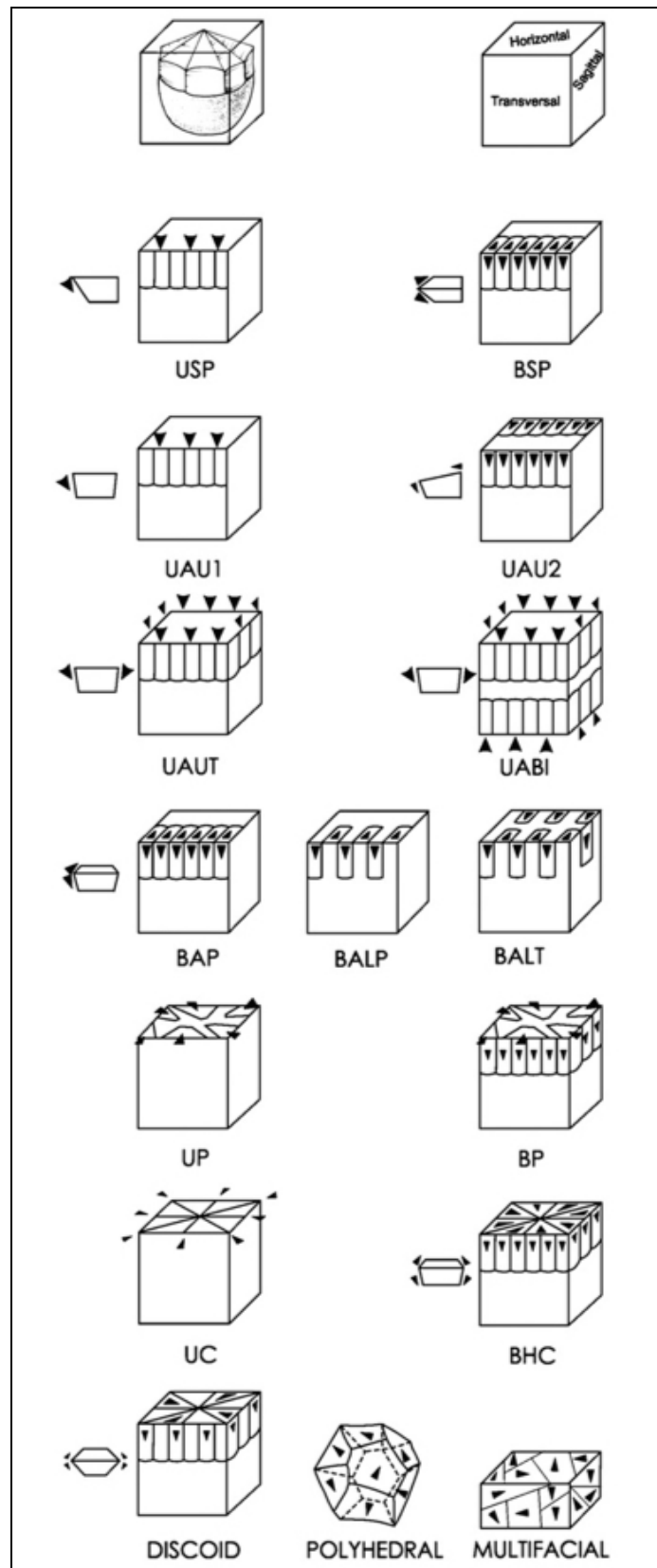


Figure 3.4.8. Free-hand core flaking strategies (from de la Torre 2011).

- Flake negative termination types: as per those listed above for the complete flake analysis (following Andrefsky 2005, shown in Figure 3.4.4), this is the nature of the detached flake negatives across the core. This is an experimental approach to quantifying the knapping proficiency of hominids (and influence of raw material).
- Percentage remaining cortex: this was quantified collectively for both the upper and lower surfaces (total surface area) and rated according to the following scale:

0. No cortex	3. 50-74% cortex
1. 1-24% cortex	4. 75-100% cortex
2. 25-49% cortex	
- Blank type: this refers to the piece from which a core is made. Eight types were identified as follows:
 1. Block: piece of raw material with angular edges that is exploited due to its angularities. Frequently tabular in form.
 2. Fragment: this appears derived from a large flake.
 3. Flake: a clear flake that has been removed (frequently large) and then reduced. The bulb, or a portion of the platform, is often retained.
 4. Cobble: rounded river cobble that is 64-256 mm in size.
 5. Pebble: rounded river pebble that is 4-64 mm in size.
 6. Indeterminate: no diagnostic features. Included all pieces that may have been from any of the remaining seven categories but could not be confidently classified as such.
 7. Split cobble: a cobble that has been split prior to reduction.
 8. Bipolar split cobble/pebble: a cobble/pebble that has been split using the bipolar method and then flaked.

3.4.6.4 Retouched piece attributes

- Length, width and thickness measurements: the method here follows that for cores, shown in Figure 3.4.7. For retouched flakes see the methods listed in the incomplete and complete flake section.
- Blank type: as recorded for cores with the addition of two extra categories:

9. Chunk: clear chunk that has then been purposefully retouched or re-shaped.
 10. Discoidal core: a core that has been retouched for a secondary purpose.
- Percentage remaining cortex: as recorded for cores (scale from 0-4).
 - Retouch position (following Inizan *et al.* 1999, shown in Figure 3.4.9): this was only recorded where the blank could be clearly orientated (e.g., a complete flake). This was not recorded on chunks or fragments. The following positions were identified:
 1. Direct: removals originate from the lower face.
 2. Inverse: removals originate from the upper face.
 3. Alternate: removals from face along one edge and from the opposite face along the other edge.
 4. Alternating: removals originating from both faces in an alternating sequence along the same edge.
 5. Bifacial: removals occur as above but exactly opposite to one another on the two faces. On one face it occurs first, then the other follows.
 6. Crossed: as above, except here removals occur from either face at any point along the edge.

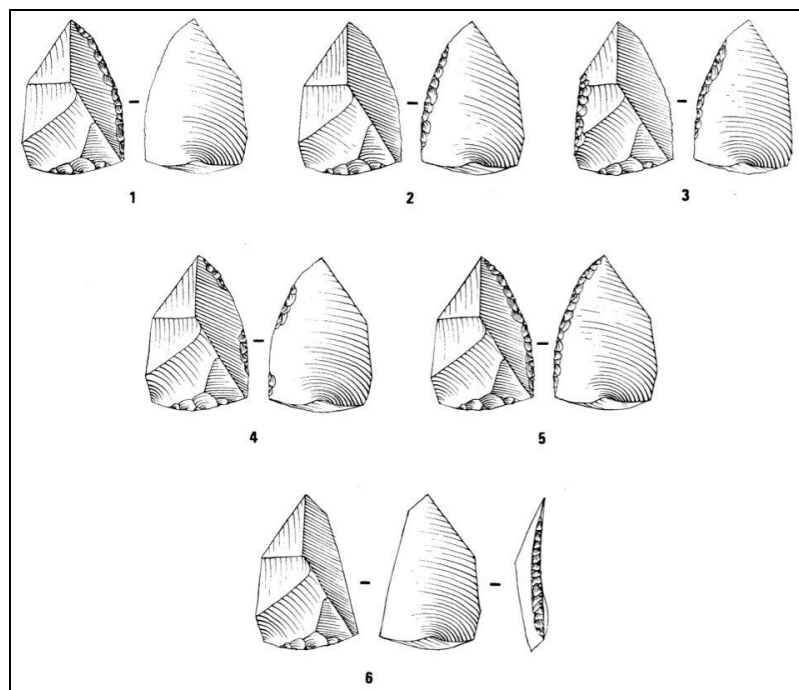


Figure 3.4.9. Retouch position classification (from Inizan *et al.* 1999). Direct (1), inverse (2), alternate (3), alternating (4), bifacial (5) and crossed (6).

- Retouch localisation (following Inizan *et al.* 1999, shown in Figure 3.4.10): this defines the place occupied by retouch relative to a specific orientation. This was recorded only on pieces where an orientation could be determined (e.g., complete or incomplete flakes). The following areas were recorded:
 1. Proximal
 2. Mesial
 3. Distal
 4. Basal

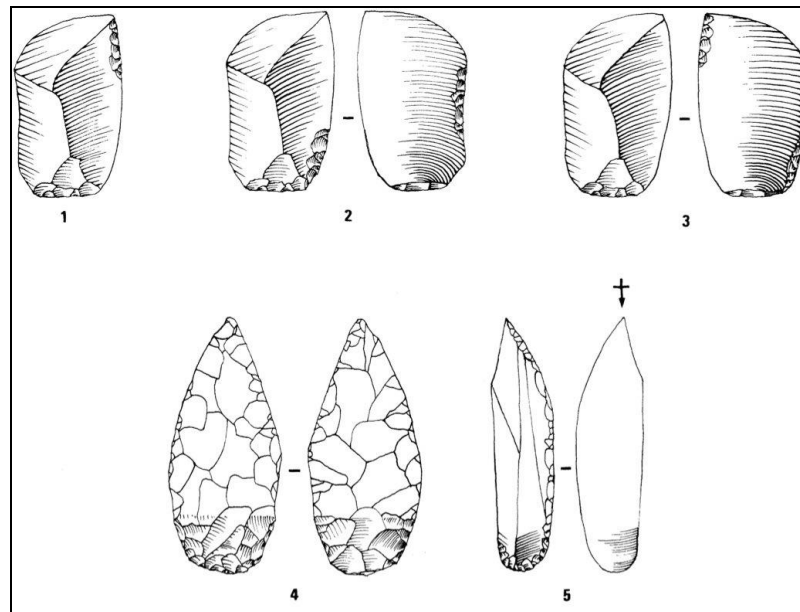


Figure 3.4.10. Retouch localisation classification (from Inizan *et al.* 1999). Distal (1), mesial and proximal (2), proximal and distal (3) and basal (4 & 5).

- Retouch distribution (following Inizan *et al.* 1999, shown in Figure 3.4.11): the continuity of removals along a given edge is described as either:
 1. Discontinuous: gaps between removals on a given edge.
 2. Continuous: no gaps between removals on a given edge.
 3. Partial: as above yet only across a portion of a given edge.
 4. Total: continuous and across the full length of a given edge.

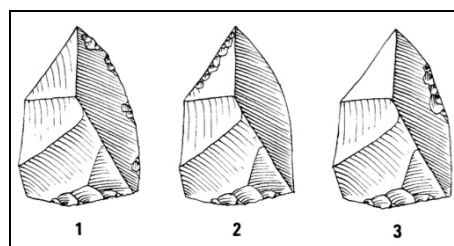


Figure 3.4.11. Retouch distribution classification (from Inizan *et al.* 1999). Discontinuous (1), total (2) and partial (3).

- Retouch delineation (following Inizan *et al.* 1999, shown in Figure 3.4.12): the shape of the edge (outline) created by a series of removals is classified here.

The following shapes were identified:

- | | |
|-------------------------|--|
| 1. Rectilinear/straight | 12. Tang |
| 2. Convex | 13. Long narrow tang |
| 3. Concave | 14. Irregular |
| 4. Notched | 15. Regular |
| 5. Denticulated | 16. Unusual (burin/awl
specific, included here as a
modified category) |
| 6. Serrated | 17. Convergent (e.g.,
convergent scraper,
included here as a modified
category) |
| 7. Cran | |
| 8. Shoulder | |
| 9. Nose | |
| 10. Tongue | |
| 11. Tang | |

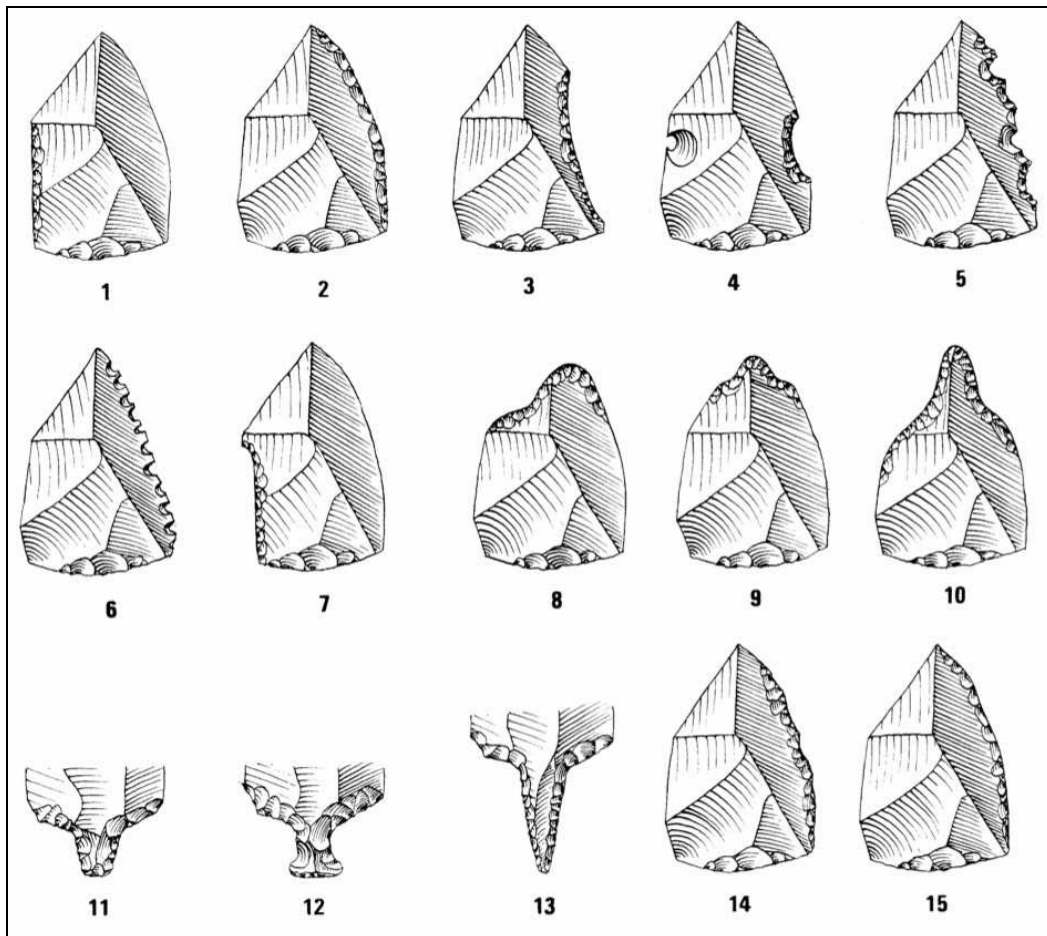


Figure 3.4.12. Edge delineation classification (from Inizan *et al.* 1999). Numbers (1-15) relate directly to those listed above (excluding 16 & 17).

- Retouch invasiveness (or ‘extent’ following Inizan *et al.* 1999, shown in Figure 3.4.13): the invasiveness of the retouch along a given edge is termed:
 1. Short: affects only a small portion of the edge.
 2. Long: affecting a larger portion of the edge.
 3. Invasive: if removals cover a large portion of a face.
 4. Covering: removals cover an entire face.

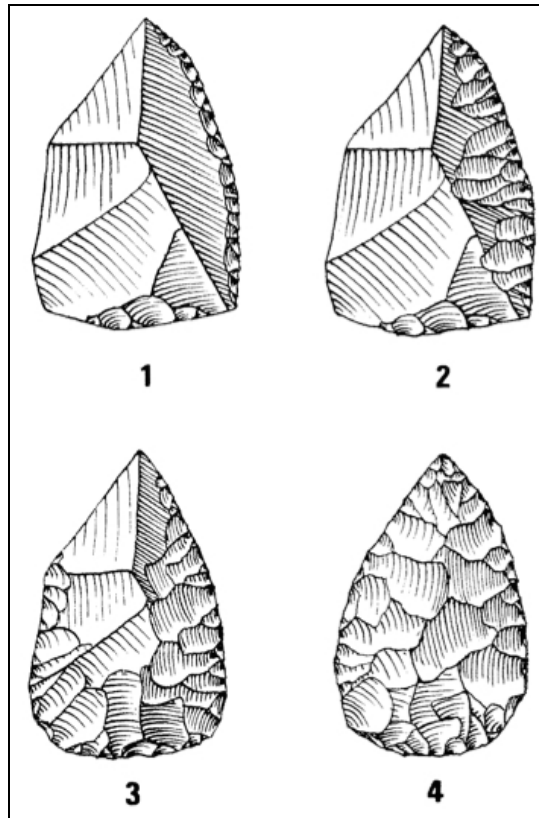


Figure 3.4.13. Retouch invasiveness (from Inizan *et al.* 1999). Short (1), long (2), invasive (3) and covering (4).

- Retouch angle (following Inizan *et al.* 1999, shown in Figure 3.4.14): the steepness of the removals along a given edge is classified as follows:
 1. Abrupt: approximately 90°.
 2. Crossed abrupt: approximately 90°, with removals from both faces.
 3. Semi-abrupt: an intermediate angle close to 45°.
 4. Low: an acute angle of around 10°.

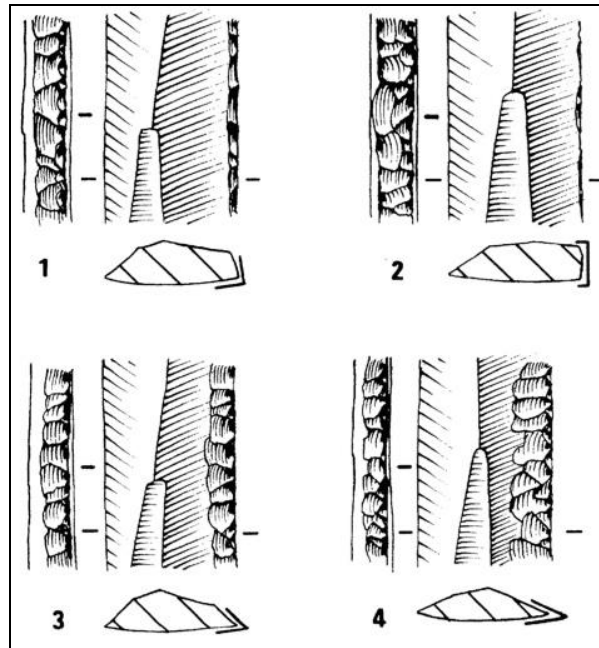


Figure 3.4.14. Angle classification (from Inizan *et al.* 1999). Abrupt (1 & 2), semi-abrupt (3) and low (4).

3.4.6.5 LCT attributes

- Technological measurements (following Roe 1964 and redrawn by Sharon 2008, shown in Figure 3.4.15): following the LCT orientation in Figure 3.4.15, a series of measurements were obtained on all LCTs, excluding broken LCTs and LCT fragments. These measurements are listed below:

Handaxe/biface/pick (Fig. 3.4.15a)~

1. Length: maximum length from tip to base.
2. Maximum width: greatest distance from lateral edge to lateral edge.
3. Location of maximum width: measured from tip of base up to the maximum width line.
4. Width: at upper fifth.
5. Width: at half length.
6. Width: at lower fifth.
7. Thickness: at upper fifth.
8. Thickness: at half length.
9. Maximum thickness: greatest distance between the upper and lower face.
10. Thickness: at lower fifth.

11. Location of maximum thickness: measured from tip of base up to the maximum thickness line.

Cleaver (Fig. 3.4.15b)~

1. Length: maximum length from tip to base.
2. Maximum width: greatest distance from lateral edge to lateral edge.
3. Edge length: total length of cleaver edge (business end). Often a curved measurement.
4. Maximum thickness: greatest distance between the upper and lower face.

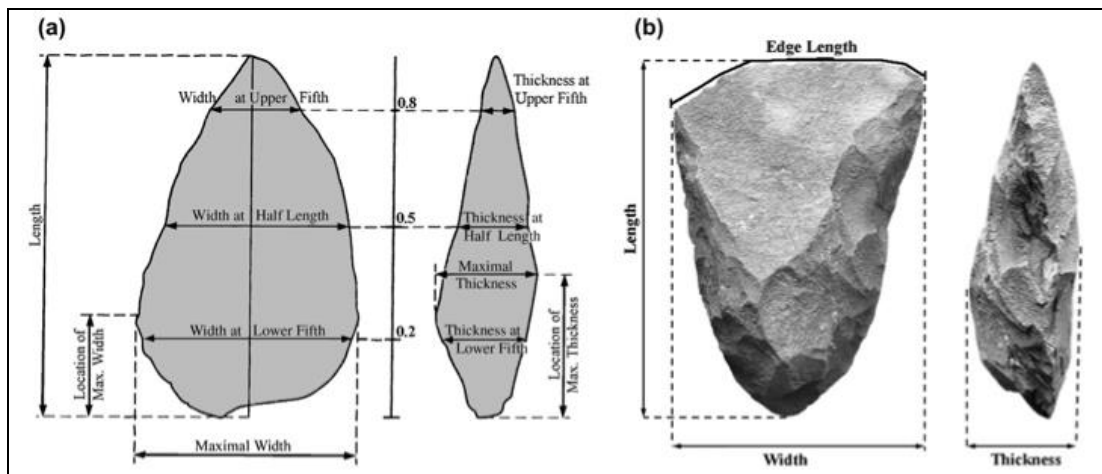


Figure 3.4.15. Technological measurements for LCTs (following Roe 1964, redrawn by Sharon 2008). Figure from Sharon (2008).

- Total number of flake scars: this refers to the total number of removals found on both faces of an LCT. A cut off size of 10 mm was used; modern damage to any piece was not counted. These removals were also classified and quantified as either primary or secondary removals. Following Kuman *et al.* (2014), primary flaking consists of large removals that shape the cobble or flake blank after it has been detached from the core, whereas secondary flaking is used to regularise and refine tool edges (through smaller removals, or retouch).
- Flaking location using the 12 sector method (following Kuman *et al.* 2014): this quantifies both the location and type of flaking (as described above) on both faces of an LCT. Each face of an LCT is divided along its long axis into distal, medial and proximal sectors of equal length, giving rise to six equal sectors (hence a total of twelve with both faces combined). Thereafter, each sector is classified as either cortical (C), primary (P), secondary (S) or

ventral/no working (V), provided that feature takes up at least 50% of the sector. For artefacts on flake blanks the dorsal surface is recorded first. Following Kuman *et al.* (2014): a bifacial piece has flaking in half or more of the sectors on both faces. A unifacial piece has flaking on only one face or in a maximum of one sector on the opposite face. A partly bifacial piece has at least two to three sectors flaked on the lesser worked face (between 16.6% and 50%).

- Flake negative termination types: as recorded for cores, those types shown in Figure 3.4.4 (following Andrefsky 2005).
- Percentage remaining cortex: as recorded for cores and retouched pieces (scale from 0-4).
- Blank type: this refers to the piece from which an LCT is made. Recorded as per those listed for cores (1-8).
- LCT tip shape (following McNabb & Sinclair 2009a, shown in Figure 3.4.16): tip shapes were divided into seven main types. These are as follows:
 1. Markedly convergent: lateral edges converge forming a sharp to slightly rounded distal tip.
 2. Convergent square: lateral edges converge but has a square distal tip, resembling a narrow cleaver edge.
 3. Convergent oblique: lateral edges converge but has a distal edge that is at an oblique angle to the long axis of the LCT.
 4. Generalised convergent: lateral edges converge but tip takes on an irregular shape (different from those described above).
 5. Divergent with square tip: lateral edges are either parallel or slightly divergent with a flat square distal tip.
 6. Divergent with oblique tip: lateral edges are either parallel or slightly divergent and the tip occurs at an oblique angle to the artefact mid-line.
 7. Wide with convex tip: the lateral edges and the distal edge have no distinct break in slope.








1		MARKEDLY CONVERGENT
2		CONVERGENT SQUARE
3		CONVERGENT OBLIQUE
4		GENERALISED CONVERGENT
5		DIVERGENT OR PARALLEL SIDED WITH A SQUARE TIP
6		DIVERGENT OR PARALLEL SIDED WITH OBLIQUE CLEAVER EDGE
7		WIDE WITH CONVEX TIP

Figure 3.4.16. LCT tip shape (redrawn from McNabb & Sinclair 2009a).

- Cleaver butt plan (following Clark & Kleindienst 1974, shown in Figure 3.4.17): three primary butt shapes were identified during the analysis of LCTs. These included rounded, squared and pointed bases.

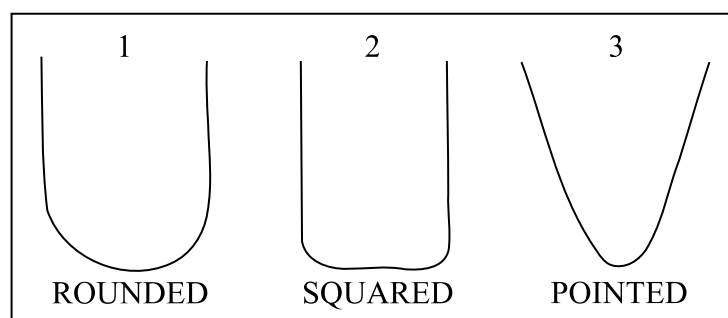


Figure 3.4.17. Butt shape (redrawn from Clark and Kleindienst 1974).

- LCT damage or breaks: this refers to an LCT with damage that has not been the intentional result of flaking. Damage/breaks were classified as:
 1. Partial tip/cleaver edge break: any break found above the mid-length line (handaxes/picks/bifaces/unifaces); anywhere along the cleaver edge, or bit (cleavers).
 2. Partial lateral edge break: with the face divided in two equal halves, any break that occurs beneath the mid-length line, towards the laterals (handaxes, picks, bifaces, unifaces); anywhere along the lateral edges (cleavers)
 3. Partial butt break: damage that occurs below the lower fifth width line (handaxes only).

3.4.6.6 Other attributes

These atypical pieces (modified and split cobbles) were measured to provide lengths, widths and thicknesses, following the method shown in Figure 3.4.7.

3.4.7 Additional analysis

- Refitting: the value of refitting is immense, not only for site formation interpretations but also for the lithic assemblage and what technological strategies were implemented on-site. This analysis, however, is extremely time consuming and as a result it could not be pursued. It must be noted here though that the Penhill Farm assemblage appears to have a high potential for this analysis.
- Residues and use-wear: an exploratory investigation into this analysis was conducted with the assistance of Dr. Geeske Langejans (University of Johannesburg, South Africa). Due to time constraints only a single LCT from Bernol Farm and a single utilised complete flake from Penhill Farm could be analysed. These were viewed and photographed using an Olympus SZX16 stereo microscope using a model DP72 digital camera, with Olympus CellSens imaging software at several magnifications between 12.5 to 115 times (Fig. 3.4.18).



Figure 3.4.18. Microscope work at the University of Johannesburg.

3.5 Non-lithic analysis and sampling

3.5.1 Introduction

This section provides a summary of all sampling and analysis that occurred on non-lithic material. This primarily concerns the collection of:

- Sediment samples, post-excavation, for particle size distribution (PSD) classification and an assessment of phytolith and pollen preservation.
- Dating samples, which are natural cobbles.

Additional analysis on all non-lithic material (e.g., shell and bone) obtained from the Sundays River sites will be outlined here.

3.5.2 Sediment sampling

Sediment samples were obtained from all three properties to assess the preservation of phytoliths and/or pollen remains (Table 3.5.1). This analysis was conducted in the hope of providing vital palaeoenvironmental data (through palaeoflora) for the Sundays River Valley during the ESA. These samples were analysed by Prof. Marion Bamford at the University of the Witwatersrand.

An extensive sediment sampling survey was conducted on Penhill Farm, the purpose of which was to strengthen our contextual understanding of the debris flow deposit, and to better understand the nature and character of sediments in the surrounding landscape (through a PSD analysis; Table 3.5.2).

PSD classification has long been used to differentiate between deposits of different origin (Thomas 1987) through assessing the proportions of three sediment fractions (namely sand, silt and clay; Blott & Pye 2012). The character of sediment and the proportional frequency of each of these size fractions can provide vital information that pertains to the origin, transport, formation, and deposition of sediment (see examples and discussions by Perez 1989; Blair & McPherson 1999; Blott & Pye 2001, 2012; Goldberg & Macphail 2006; Germaine & Germaine 2009).

Table 3.5.1. Phytolith and pollen sediment sample information.

Site:	Number of samples:	Sample locations:
Atmar Farm	6	1) Excavation 1 square A2 west wall: two from above the basal gravels and two from above the upper gravels, all within the fine overbank alluvium. 2) An additional two samples were collected from above the gravels (fine alluvium) at the dated location.
Bernol Farm	6	1) Survey site 2: two samples obtained from within the shell rich horizon. 2) Survey site 4: two samples obtained within and beneath the shell/artefact rich horizon. 3) Dated location: two samples obtained, one within the thick basal gravels and another from a thin stringer in the fine overbank alluvium.
Penhill Farm	8	1) Dated location 1: two samples obtained from the fine alluvium overlying the dated gravels. 2) Exposed debris flow in east face of borrow pit: three samples obtained, below, above and within the debris flow. 3) Excavation 1 square CC2 north wall: three samples obtained, below, above and within the debris flow.

Accordingly, 45 samples were collected from across Penhill Farm and within Excavation 1 (Table 3.5.2; Figs. 3.5.1-3.5.7). Alluvium, colluvium, and the debris flow are the three main deposit types found at Penhill Farm. Samples were carefully selected so that each of these sediment types could be analysed and characterised.

Table 3.5.2. Sediment samples from Penhill Farm (survey and excavation). See sample location Figures 3.5.1-3.5.7.

Sample:	Wall:	Square:	Sample location and description:
1	East	E1	At side of channel cut into the fine overbank alluvium.
2	East	E1	Infilled channel colluvium.
3	East	D1	Beneath base of channel cut into the fine overbank alluvium, directly under the debris flow.
4	East	D1	Sediment from within debris flow.
5	East	D1	Sediment from channel flow feature.
6	East	D1	Infilled channel colluvium.
7	East	C1	Beneath base of channel cut into the fine overbank alluvium, directly under the debris flow.
8	East	C1	Sediment from within debris flow.
9	East	C1	Infilled channel colluvium.
10	East	C1	Sediment from channel flow feature.
11	North	N/A	Beneath base of channel cut into the fine overbank alluvium, directly under the debris flow.

Table 3.5.2 continued...

Sample:	Wall:	Square:	Sample location and description:
12	North	N/A	Sediment from within debris flow.
13	North	N/A	Infilled channel colluvium.
14	South	EE1	Beneath base of channel cut into the fine overbank alluvium, directly under the debris flow.
15	South	EE1	Sediment from within debris flow.
16	South	EE1	Sediment between (separate?) debris flow.
17	South	EE1	Infilled channel colluvium.
18	South	EE2	Sandy colluvial infill.
19	West	EE2	Beneath base of channel cut into the fine overbank alluvium, directly under the debris flow.
20	West	CC2	Beneath base of channel cut into the fine overbank alluvium, directly under the debris flow.
21	West	EE2	Sediment from within debris flow.
22	West	DD2	Sediment between (separate?) debris flow.
23	West	DD2	Sediment from channel flow feature.
24	West	EE2	Infilled channel colluvium.
25	West	EE2	Infilled channel colluvium. Calcic horizon sediment.
26	West	DD3/4	Infilled channel colluvium in cut and fill feature.
27	West	CC3/4	Infilled channel colluvium in cut and fill feature.
28	N/A	N/A	Alluvium from dated location 1.
29	N/A	N/A	Sediment from under base of debris flow exposed at edge of terrace, south of Excavation 1 (borrow pit southeast face).
30	N/A	N/A	Sediment from within debris flow (borrow pit southeast face).
31	N/A	N/A	Exposed debris flow in borrow pit east wall: sediment beneath riser.
32	N/A	N/A	Exposed debris flow in borrow pit east wall: sediment within riser.
33	N/A	N/A	Exposed debris flow in borrow pit east wall: sediment above riser.
34	SURVEY 2		Upslope colluvium.
35	SURVEY 3		Upslope colluvium.
36	SURVEY 5		Exposed bedrock sample (crushed).
37	SURVEY 6		Upslope colluvium.
38	SURVEY 7		Gravel colluvium, upslope.
39	N/A	N/A	Borrow pit south face fine overbank alluvium.
40	N/A	N/A	Colluvium from top of adjacent field.
41	N/A	N/A	Fine alluvium from above dated gravels (dated location 1).
42	N/A	N/A	Exposed bedrock sample (crushed).
43	N/A	N/A	Exposed bedrock sample (crushed).
44	N/A	N/A	Exposed bedrock sample (crushed).
45	N/A	N/A	Exposed bedrock sample (crushed).

These samples were then prepared for analysis by following these procedures:

1. Each sample was sieved using 2 mm mesh (all organic material was removed).
2. Particles larger than 2 mm (calcrete nodules, artefacts and natural gravels) were removed from the sample and weighed.
3. Sediment aggregates (clumps >2 mm) were gently broken down to ensure they passed through the sieve.

4. The total sample (< and >2 mm fractions) was then weighed.

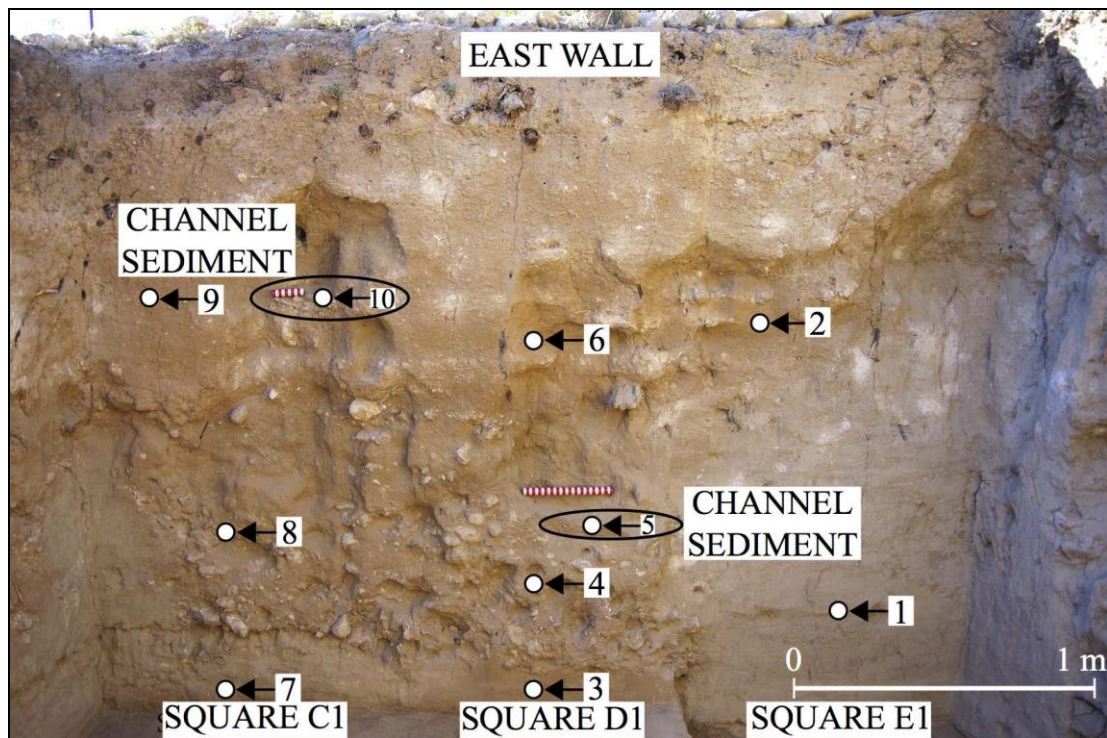


Figure 3.5.1. Penhill Farm Excavation 1 east wall sample locations. Note channel features in upper colluvium. Also note discontinuous nature of debris flow in squares C1 and E1. Modified from original image courtesy of R.J. Gibbon.

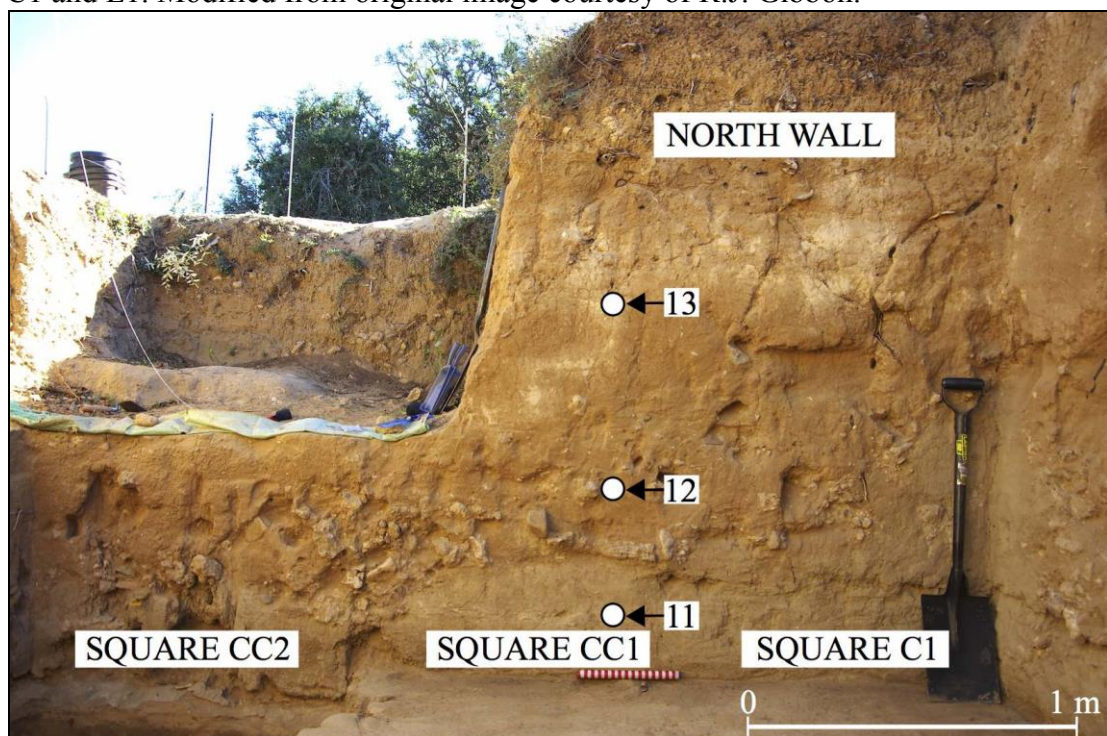


Figure 3.5.2. Penhill Farm Excavation 1 north wall sample locations. Note sterile colluvium above debris flow and overburden clearing at left of image. Modified from original image courtesy of R.J. Gibbon.

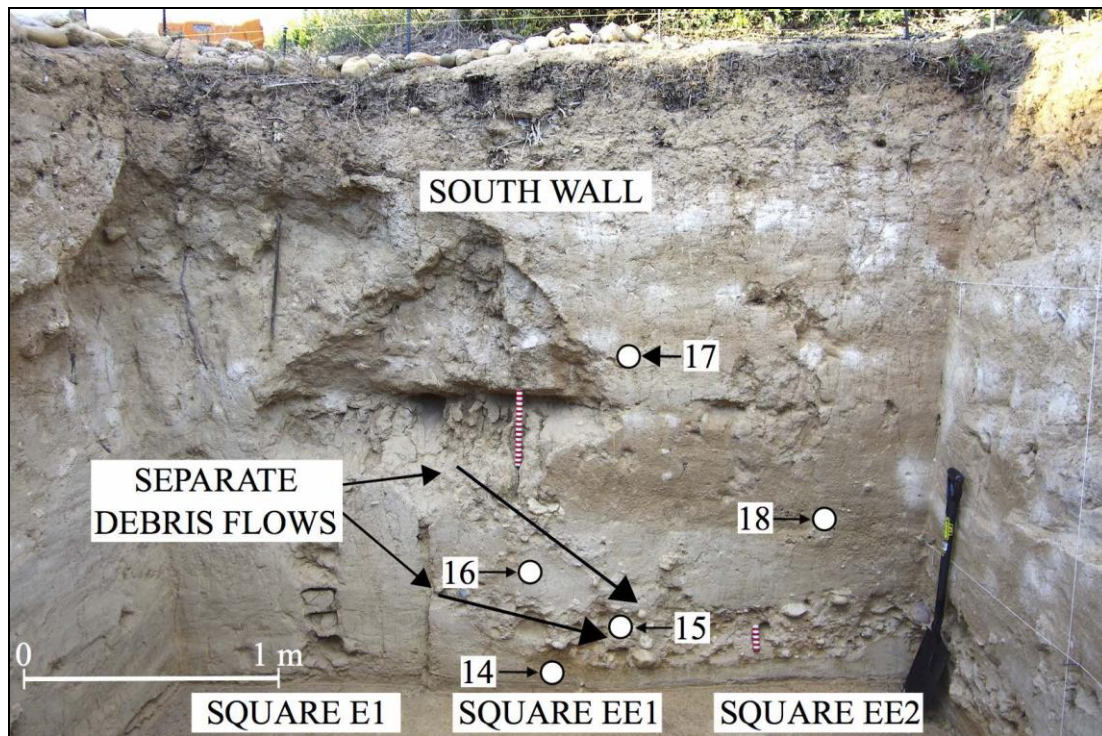


Figure 3.5.3. Penhill Farm Excavation 1 south wall sample locations. Note discontinuous debris flow in Square E1. Note damage to wall due to rain (see Chapter 3.3). Modified from original image courtesy of R.J. Gibbon.

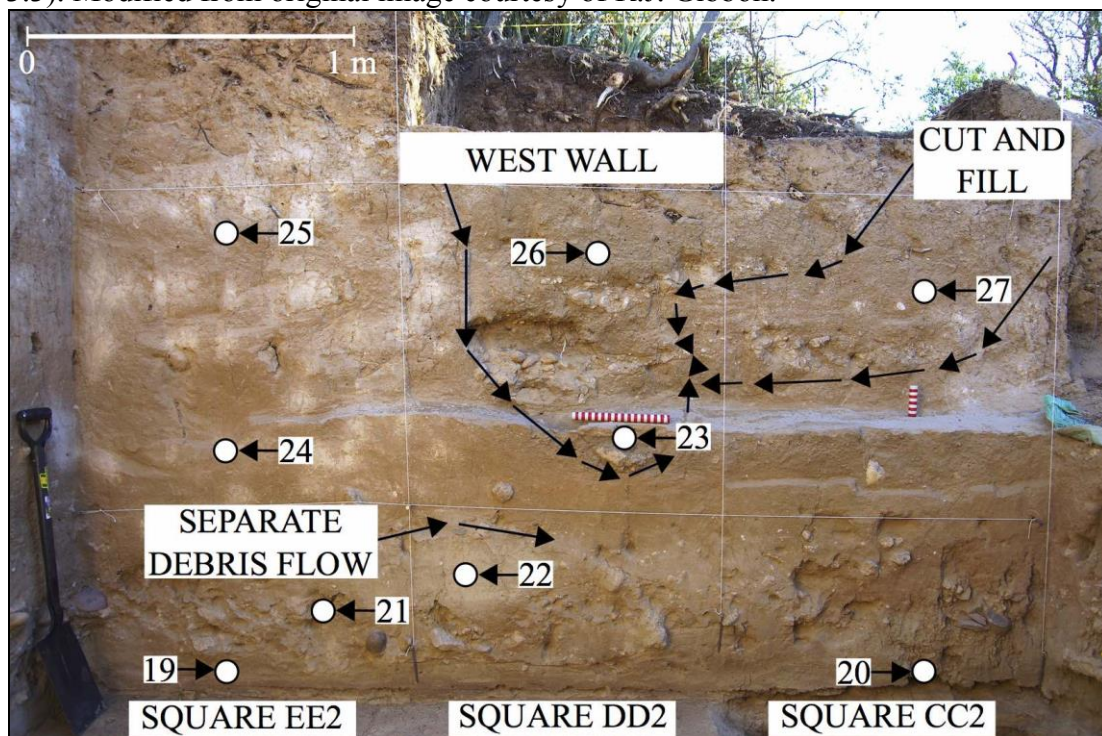


Figure 3.5.4. Penhill Farm Excavation 1 west wall sample locations. Note cut and fill deposit, with channel feature (sample 23), found above the debris flow. Modified from original image courtesy of R.J. Gibbon.

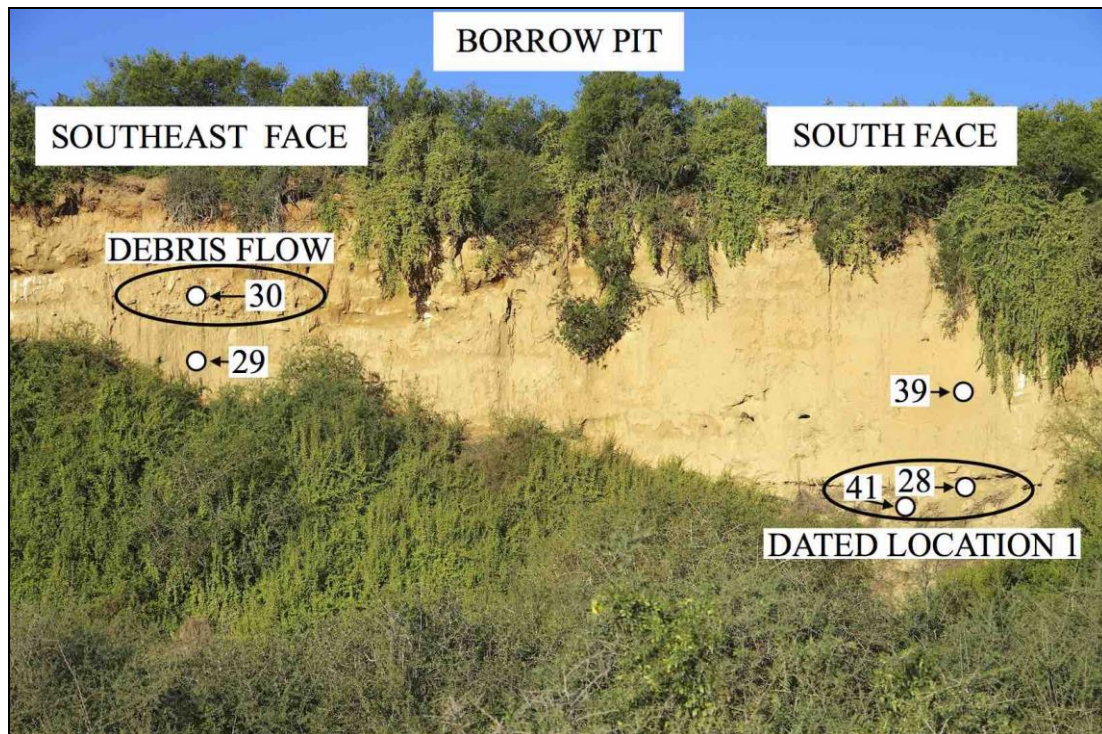


Figure 3.5.5. Penhill Farm borrow pit sample locations. Note exposure of massive overbank fines, within which another channel has been filled (with a debris flow, southeast face). Modified from original image courtesy of R.J. Gibbon.

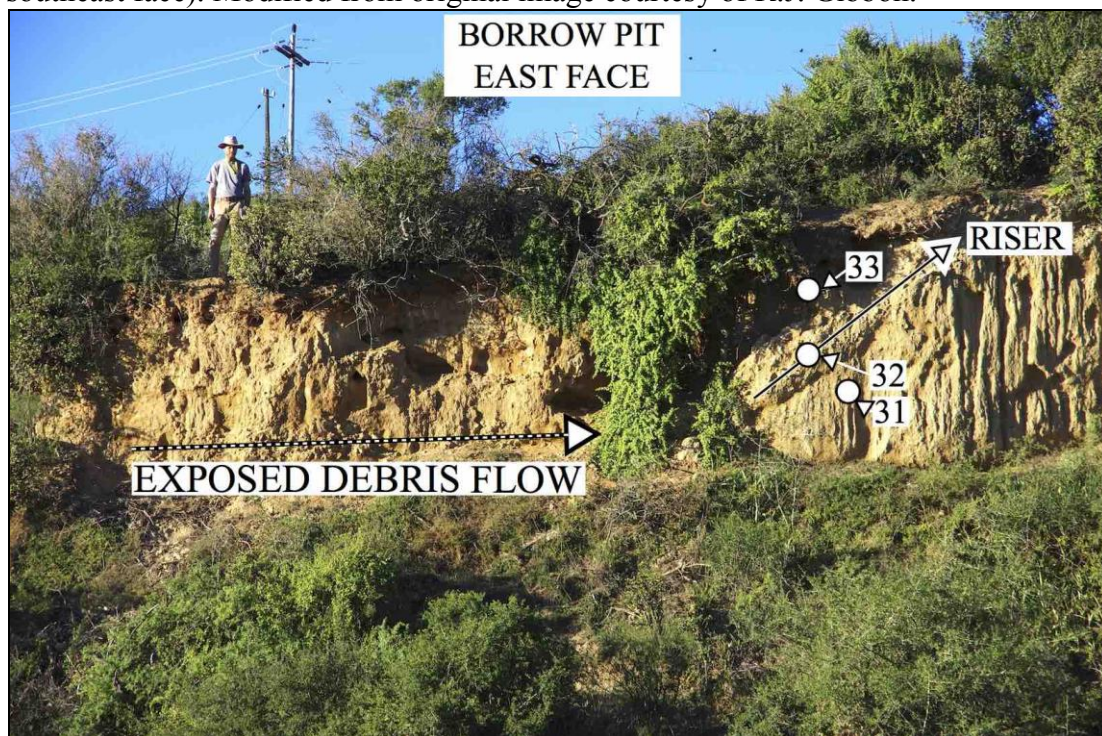


Figure 3.5.6. Penhill Farm borrow pit sample locations. Sampling of sediments beneath, within, and above the hill slope lag south of the exposed debris flow. Modified from original image courtesy of R.J. Gibbon.

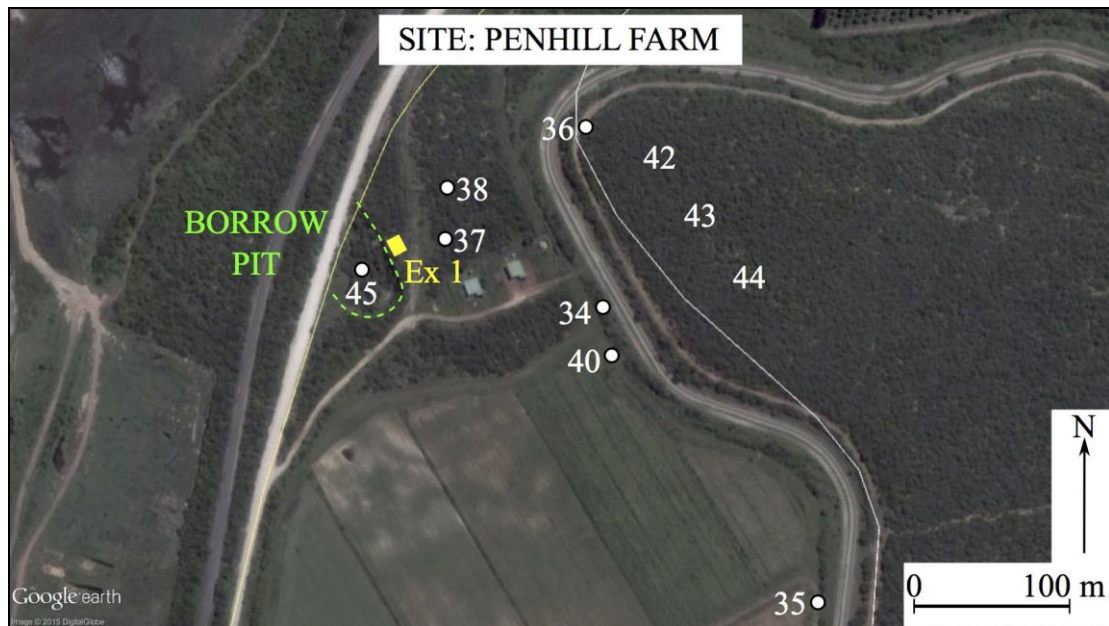


Figure 3.5.7. Penhill Farm samples from the surrounding area. Note position of Excavation 1 (Ex 1). Exact GPS positions of samples 42, 43 and 44 were not recorded.

Each <2 mm sample was then submitted to the Council for Geoscience (CGS) in Pretoria for PSD analysis. This was conducted by Dr. Frederic Doucet at the Laboratory of Applied Mineralogy and Industrial Chemistry. Sediment sizing was obtained by laser diffraction using a Malvern Mastersizer 2000, following the method outlined in Doucet (2010). PSD curves for clay, silt, and sand were then produced for each sample.

3.5.3 Dating samples

In order to provide better resolution on the age of the debris flow deposit at Penhill Farm, quartzite clasts were selected (n=9) for dating using the cosmogenic nuclide burial method. This method is reviewed in detail by Granger & Muzikar (2001) and Granger (2006) and has been applied at several South African sites (see Gibbon *et al.* 2009a; Gibbon *et al.* 2014; Leader 2014; Granger *et al.* 2015). This method is based upon the build-up and decay of cosmogenic ^{26}Al and ^{10}Be , which is stored in the mineral quartz before burial. This method therefore dates the burial of quartz, within a deposit overlain by sufficient depth, and its application is suitable for many sites that have previously been undatable (Gibbon *et al.* 2009a).

For analysis, the selected clasts consisted of nine cobbles and pebbles (Excavation 1 square DD1, dated location 2, shown in Figure 3.2.12) sourced directly from the debris flow deposit; samples were all within 20 cm of each other (vertically) and occurred at least 2.2 m below the main site datum, with a local overburden depth of maximum 2.09 m. These samples were sent directly to our collaborating dating specialist, Prof. Darryl Granger, at the Purdue Rare Isotope Measurement Laboratory (PRIME), Department of Earth, Atmospheric and Planetary Sciences, Purdue University (Indiana, USA).

3.5.4 Non-lithic analysis

A basic analysis was conducted on all non-lithic components from Penhill Farm, which included fragments of bone, shell and charcoal (excavations at Atmar and Bernol Farm did not yield any non-lithic assemblages worthy of analysis). Each fragment was weighed individually on a digital scale, to the nearest 100th of a gram, and a count of the fragments, per bag and spit, was conducted.

Unfortunately the fragmented nature of the bone meant that the identification of faunal taxa was impossible. Isotope analysis on the fragments could also not be pursued due to the (likely) contamination of the samples by water.

Chapter 4

Results

4.1 Introduction

Excavation and survey work in the lower Sundays River Valley has provided important data for each of the three sites. Although this is the case, the poor preservation of artefacts at Atmar Farm, coupled with the extremely sporadic occurrence of the artefacts, and the limited access to deposits at Bernol Farm meant that the majority of research work was conducted at Penhill Farm. Penhill Farm was also an extremely productive site and it was decided to focus work there. As a result, only basic data can be presented for both Atmar and Bernol Farm.

Data below are first presented by site, addressing site context and preservation (and dating where relevant), and thereafter focus is on the preserved assemblages (artefact typology and technology). Single assemblages are discussed for both Atmar and Bernol Farm. For Penhill Farm, however, two assemblages are discussed together, with results presented separately within sections dealing with site context, typology and technology.

For convenience, summaries are placed at the end of each major data section. These highlight the most important trends in the data that will be points for discussion in the following sections. It must be emphasised here that the significance of all data in Chapter 4 will be discussed in detail in Chapter 5.

4.2 Atmar Farm

4.2.1 Introduction

Excavations 1 and 2 at Atmar Farm have provided a small, poorly preserved, lithic assemblage of 345 pieces from the gravel deposit. Assemblage data from the two excavations are combined here as the gravel deposit between Excavations 1 and 2 is comprised of the same continuous exposure. This assemblage includes all lithic material that is both larger and smaller than 20 mm, obtained from within the gravels, but excludes all material obtained from the thin fine sediment overburden found above the gravels. However, the total number of excluded items from the fine overburden is only 68 pieces (7<20 mm, 61>20 mm).

Non-lithic material was extremely scarce in both excavations. Bone comprised of only two small fragments, one of which was obtained from the gravels in Excavation 2. In addition, modern items including tin/metal (2 fragments), glass (9 fragments) and a land snail shell (1 fragment) were recovered from the fine overburden, in association with the excluded lithics (above), suggesting the disturbed nature of these fine deposits (locally) above the gravels. For this reason, these lithics were excluded from analysis.

Phytolith and pollen analysis proved to be unsuccessful within both excavations, due to the complete absence of this material within the fine overbank alluvial sediments.

4.2.2 Site context

4.2.2.1 Artefact size distributions

The range of artefact sizes at Atmar Farm is presented in Table 4.2.1 and Figure 4.2.1. A full size range of pieces occurs, with varying quantities for each, except for material in the <170 and <190 mm size categories. A limited number (n=2) of pieces occurs that are <10 mm in maximum length, and a combined SFD total includes 45

pieces (collectively just over 13%). The largest quantity of material (n=238, 69%) is larger than 20 mm and smaller than 80 mm, with the highest frequency of material (n=63, 18.3%) in the <40 mm category.

Table 4.2.1. Artefact size distribution data for Atmar Farm.

Artefact size	Number	Percentage
<10 mm	2	0.6
<20 mm	43	12.5
<30 mm	49	14.2
<40 mm	63	18.3
<50 mm	42	12.2
<60 mm	34	9.9
<70 mm	29	8.4
<80 mm	21	6.1
<90 mm	7	2
<100 mm	14	4.1
<110 mm	6	1.7
<120 mm	14	4.1
<130 mm	3	0.9
<140 mm	4	1.2
<150 mm	4	1.2
<160 mm	4	1.2
<170 mm	0	0
<180 mm	3	0.9
<190 mm	0	0
<200 mm	1	0.3
>200 mm	2	0.6
Total	345	100

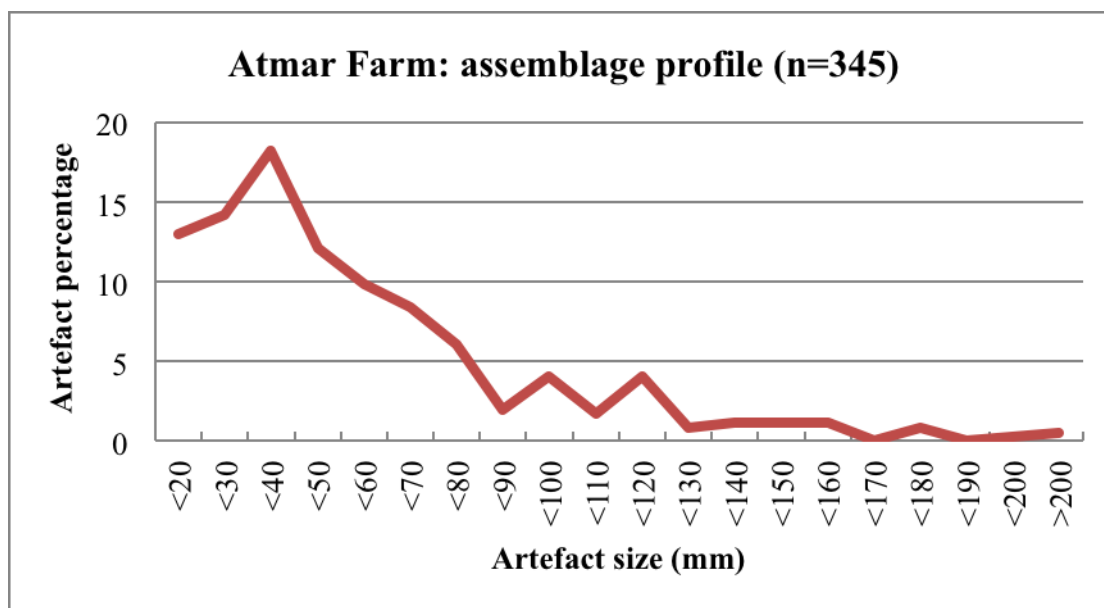


Figure 4.2.1. Assemblage profile for Atmar Farm.

4.2.2.2 Artefact condition and raw material data

These data are presented in Table 4.2.2 and Figures 4.2.2 and 4.2.3. Quartzite is clearly the dominant raw material type in the Atmar Farm assemblage, accounting for 97.7% of all raw materials (n=293); there is a clear preference for fine-grained quartzite (n=279). Other materials are rare: hornfels (n=4), quartz (n=1), siltstone (n=1), and a single specimen of heavily abraded/rolled indeterminate material (n=1; Table 4.2.2). No artefacts are made on crypto-crystalline material, lava or silcrete.

Table 4.2.2. Raw material and artefact condition data for Atmar Farm. Bracketed values indicate percentages. Quartzite is divided into coarse (C) and fine (F) types.

Raw material	Artefact condition				Total
	Fresh/unabraded	Slightly abraded	Heavily abraded/rolled	Weathered	
Quartz	1 (0.3)	0	0	0	1 (0.3)
C Quartzite	1 (0.3)	7 (2.3)	6 (2)	0	14 (4.7)
F Quartzite	61 (20.3)	67 (22.3)	151 (50.3)	0	279 (93)
Siltstone	1 (0.3)	0	0	0	1 (0.3)
Hornfels	0	0	0	4 (1.3)	4 (1.3)
CCS	0	0	0	0	0
Lava	0	0	0	0	0
Silcrete	0	0	0	0	0
Indet.	0	0	1 (0.3)	0	1 (0.3)
Total	64 (21.3)	74 (24.7)	158 (52.7)	4 (1.3)	300 (100%)

For condition, the single quartz specimen retains a fresh/unabraded state, due mainly to the resistive qualities of the material (Table 4.2.2). In contrast, all hornfels pieces are weathered, highlighting the susceptibility of this material to *in situ* decay/breakdown. Interestingly, the fine quartzite sample (n=279, 100%) appears to show a greater resistance to abrasion as 22% of specimens (n=61) retain a fresh/unabraded condition; collectively, 78% are slightly to heavily abraded/rolled (n=218). In contrast, only 7% of coarser quartzites (n=1) retain a fresh/unabraded condition with the majority occurring as slightly to heavily abraded/rolled (collectively 93%, n=13).

No artefacts from the Atmar Farm excavations retain an exterior surface varnish. Overall, the assemblage is dominated by heavily abraded/rolled pieces (53%), and only 21% retain a fresh/unabraded condition (Fig. 4.2.3). Collectively, 78% of the assemblage possesses some form of artefact damage and natural edge modification (Fig. 4.2.3).

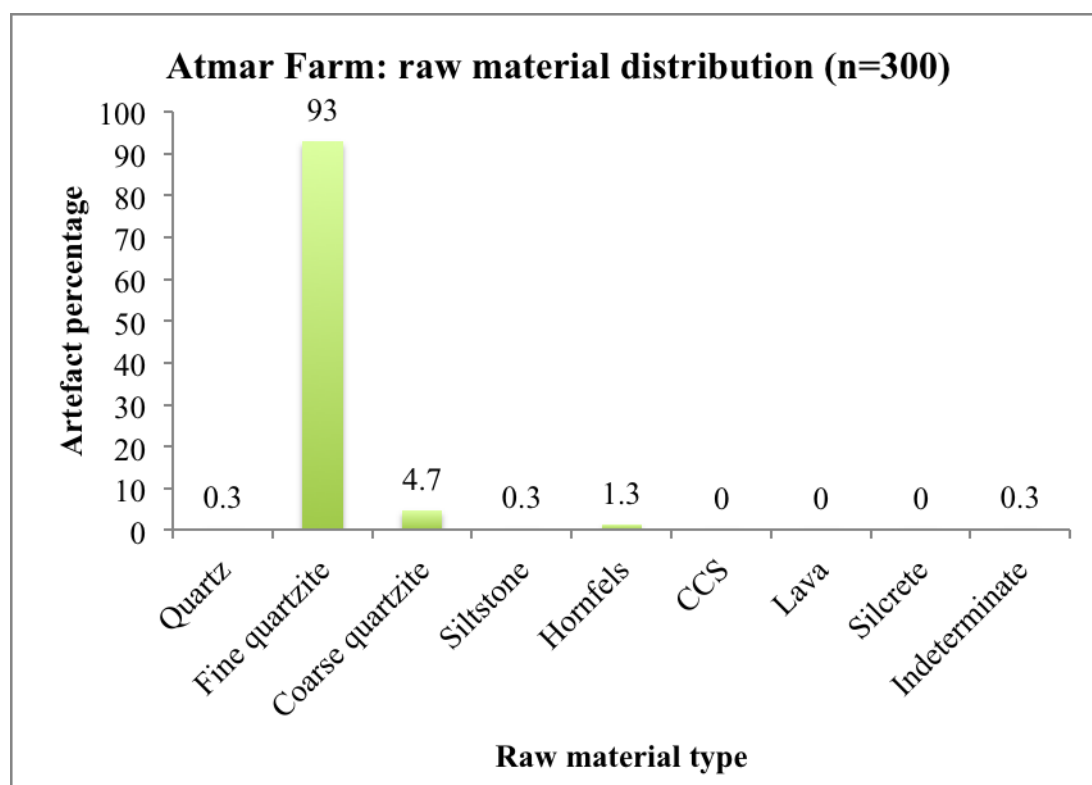


Figure 4.2.2. Atmar Farm raw material types (≥ 20 mm sample).

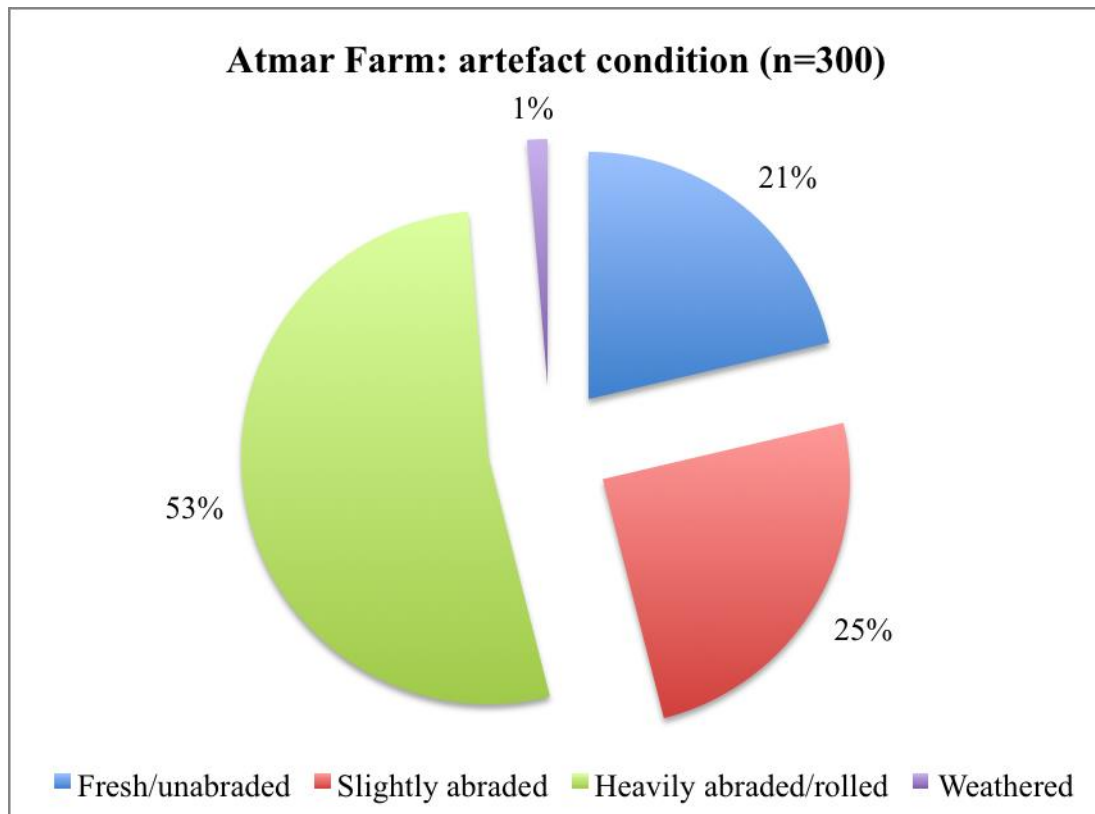


Figure 4.2.3. Atmar Farm artefact condition (≥ 20 mm sample).

4.2.3 Typology

A typological assessment of the Atmar Farm assemblage is presented in Figures 4.2.4-4.2.10 and Tables 4.2.3 and 4.2.4, with summaries provided by Table 4.2.3 and Figure 4.2.4.

The Atmar Farm assemblage (Table 4.2.3) provides a limited sample of formal tools ($n=7$, 2%), cores ($n=26$, 7.5%, of which 12 are casual) and complete flakes ($n=35$, 10.1%). The majority of material (79.4%) is comprised of flaking debris (Fig. 4.2.4), and split and modified cobbles (other types; $n=3$, 0.9%) were also recovered.

Flaking debris (Fig. 4.2.5) is comprised of SFD (16.4%), chunks (3.3%), incomplete flakes (56.6%) and flake fragments (23.7%); split flakes and bipolar debris were not recovered.

Table 4.2.3. Assemblage classification for Atmar Farm (n=345).

Flaking debris:	N	%
SFD	45	13
Chunk	9	2.6
Incomplete flake	155	44.9
Flake fragment	65	18.8
Split flake	0	0
Bipolar	0	0
Total	274	79.4
Formal tools:		
Handaxe	1	0.3
Broken LCT	0	0
Cleaver	1	0.3
Pick	0	0
Biface	1	0.3
Knife	0	0
Chopper	1	0.3
Side chopper	0	0
End chopper	0	0
Flaked-flake	1	0.3
Retouched flake	0	0
Scraper~		
<i>Composite</i>	0	0
<i>Concave</i>	0	0
<i>Convex</i>	0	0
<i>End</i>	0	0
<i>Side</i>	0	0
<i>Double side & end</i>	0	0
<i>Notched</i>	0	0
<i>Convergent</i>	0	0
<i>Denticulated</i>	1	0.3
<i>Heavy-duty/core</i>	0	0
MRP	0	0
Burin	0	0
Awl	0	0
Denticulate	1	0.3
Composite piece	0	0
Total	7	2.0
Complete flakes:	N	%
End-struck	8	2.3
Side-struck	14	4.1
Corner-struck	12	3.5
Kombewa	0	0
Core trimming	1	0.3
Bipolar	0	0
Handaxe trimming	0	0
Bi-bulb	0	0
Core rejuvenation	0	0
Total	35	10.1
Cores:		
Core fragment	3	0.9
Casual	12	3.5
Bipolar	0	0
Chopper-core	6	1.7
Discoidal	2	0.6
Irregular	3	0.9
Polyhedral	0	0
Single platform	0	0
Boulder-core	0	0
Total	26	7.5
Other:		
Modified cobble	0	0
Split cobble	3	0.9
Total:	3	0.9
Assemblage total	345	100

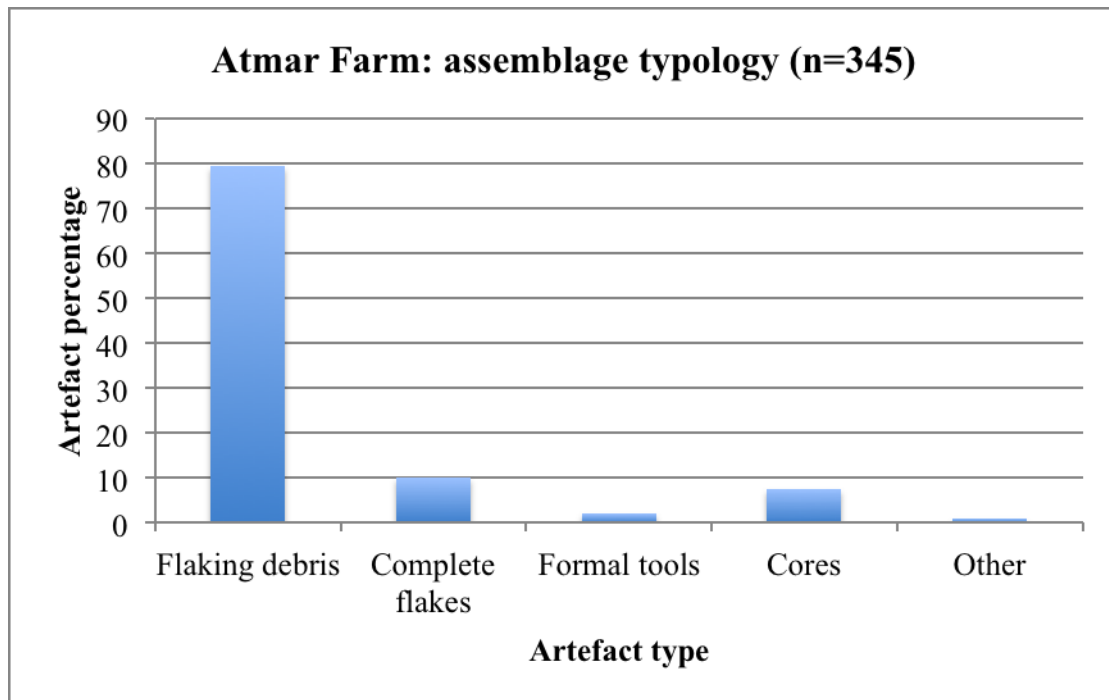


Figure 4.2.4. Frequency of the five different artefact types at Atmar Farm.

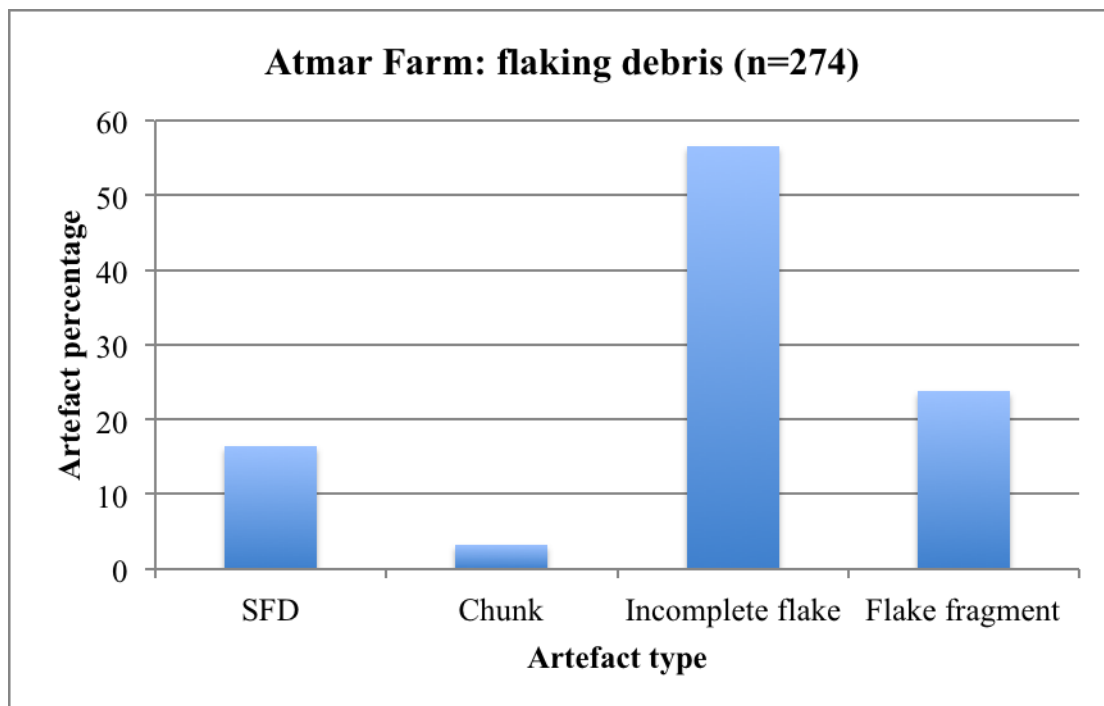


Figure 4.2.5. Percentages of the four flaking debris types at Atmar Farm.

Complete flakes (n=35) have a higher proportion of side-struck specimens (n=14, 40%; Table 4.2.3; Fig. 4.2.6). Corner-struck types account for 34.3% (n=12) and end-struck types for 23% (n=8); a single core trimming flake was also recovered.

Raw material data in Table 4.2.4 highlights the preferential use of quartzite, with 97.2% (n=34) of the complete flake sample made on this material. A single end-struck flake is made on hornfels.

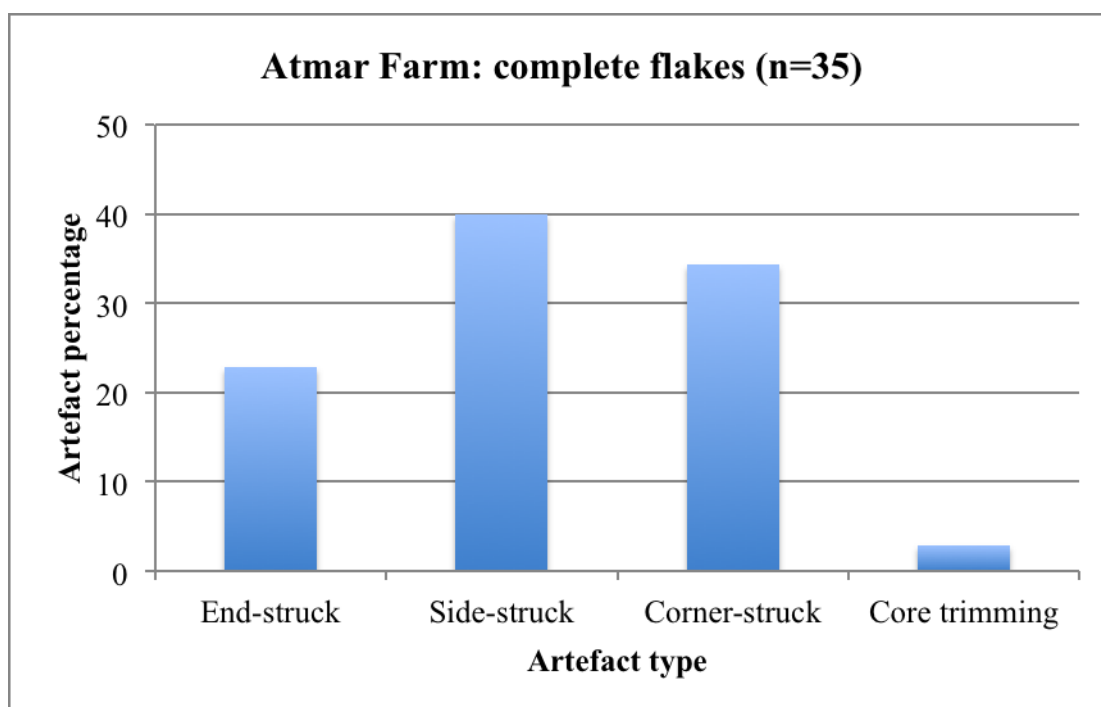


Figure 4.2.6. Complete flake types.

The core sample (n=26; Tables 4.2.3 & 4.2.4) at Atmar Farm is dominated by simple reduction strategies involving the knapping of quartzite cobbles. The majority of all cores has only a single to a maximum of two removals (casual cores; n=12, 46.2%; Fig. 4.2.7). Chopper-cores (n=6, 23.1%; Fig. 4.2.7) that are both unifacially and bifacially worked are shown in Figure 4.2.8, highlighting the limited number of flakes removed from the core edges (>3 but ≤ 10).

More structured knapping is present in only two cores (discoids; 7.7%), and three cores with an unstructured knapping strategy are also present (irregular; 11.5%; Fig. 4.2.7). Pieces that indicate some form of core working but that are damaged and difficult to assign to a given core type are classified as core fragments (n=3, 11.5%; Fig. 4.2.7).

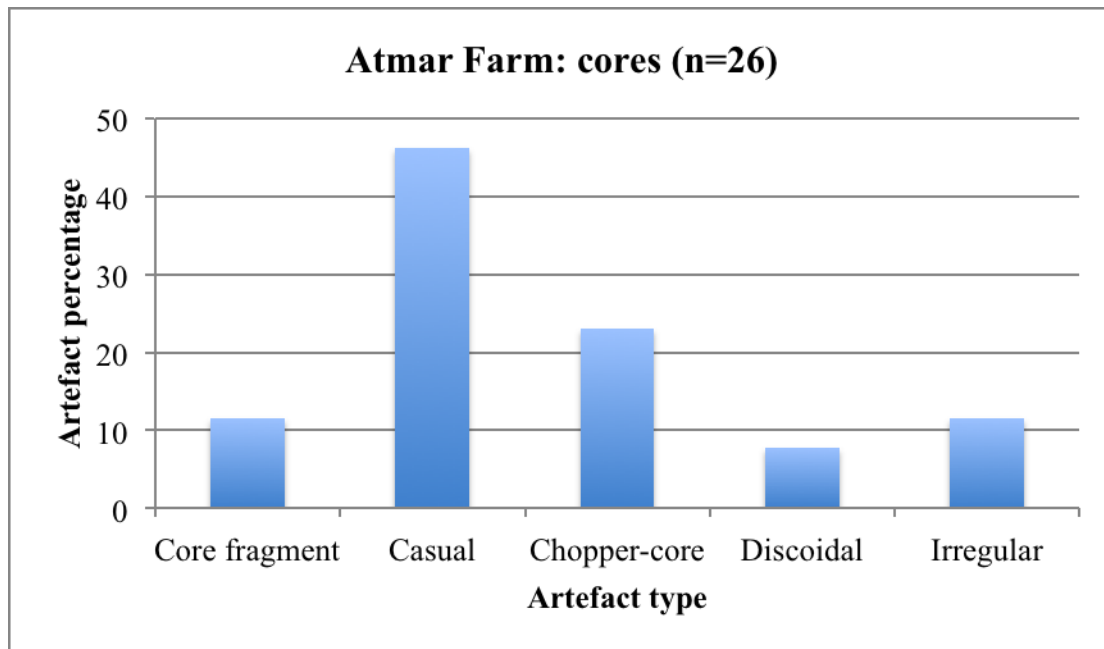


Figure 4.2.7. Core type classification.

The formal tool assemblage at Atmar Farm is comprised of only seven pieces, six of which are shown in Figures 4.2.9 and 4.2.10. LCTs (n=3; Table 4.2.3) consist of a single cleaver, a biface and a handaxe, all of which are produced on large flake blanks (Fig. 4.2.10). A single bifacial chopper (Fig. 4.2.9c), a flaked-flake, and two retouched pieces (denticulate and denticulated scraper, shown in Figure 4.2.9a and 4.2.9b, respectively) make up the remaining formal tool assemblage. Table 4.2.4 highlights the dominant use of quartzite in formal tool manufacture, but it also shows that a single LCT (unifacial handaxe; Fig. 4.2.10a) was produced on hornfels.

Retouched pieces and the chopper are made on complete flake blanks in quartzite (>10 cm in maximum length for the chopper, Figure 4.2.9c). A tertiary flake (no cortex on the dorsal surface or platform) was used to produce the chopper and the chopping edge is characterised by several bifacial removals at the distal end of the piece. For the retouched flakes cortex is present on both dorsal surfaces, and the retouch position (alternate) and localisation (distal and mesial right) is the same for both specimens (Fig. 4.2.9a & b). The retouch distribution for Figure 4.2.9b is partial on the distal edge and discontinuous on the mesial right, whereas Figure 4.2.9a is total on the distal edge and partial on the mesial right portion of the specimen. Retouch delineation and extent (invasiveness) is denticulated and short, respectively, in each of

the pieces, whereas the retouch angle for Figure 4.2.9b is abrupt and semi-abrupt for Figure 4.2.9a.

The extremely poor preservation state of the LCTs restricts detailed analysis; however, some basic conclusions can be made. Large flakes are favoured as LCT blanks, all of which are corner-struck and retain a portion of the outer cortex of the knapped cobbles (Fig. 4.2.10). These flakes all exceed 10 cm in maximum length and the number of flakes removed is kept to a minimum but provides some degree of edge shaping; removals in the bulbar area of the flake (to reduce tool thickness) are not present and the majority of removals is towards the lateral edges of the pieces. It appears that the flake blanks utilised for LCT production were already thin and of the necessary shape prior to any subsequent shaping (primary and secondary working). Although secondary working is difficult to identify due to artefact condition, where it does appear it is in conjunction with larger primary removals (along lateral edges, see Figure 4.2.10a ventral surface). Tip shape for the unifacial handaxe and biface is generalised convergent and convergent oblique for the cleaver; butt shape for the cleaver is pointed.

Artefacts that are classified under other types include three quartzite split cobbles (Table 4.2.3). No modified cobbles were found within the excavations.

Evidence to suggest the recycling of tools was not identified on any of the lithics at Atmar Farm, nor was any obvious use-wear (utilisation) damage (except for the chopper).

Table 4.2.4. Raw material use at Atmar Farm (excluding flaking debris and other artefact samples).

Complete flakes:	Total	Raw material type															
		Quartz		Quartzite		Siltstone		Hornfels		CCS		Lava		Silcrete		Indet.	
		N	%	N	%	N	%	N	%	N	%	N	%	N	%	N	%
End-struck	8	0	0	7	20	0	0	1	2.9	0	0	0	0	0	0	0	0
Side-struck	14	0	0	14	40	0	0	0	0	0	0	0	0	0	0	0	0
Corner-struck	12	0	0	12	34.3	0	0	0	0	0	0	0	0	0	0	0	0
Core trimming	1	0	0	1	2.9	0	0	0	0	0	0	0	0	0	0	0	0
Total	35	0	0	34	97.2	0	0	1	2.9	0	0	0	0	0	0	0	0

Cores:	Total	Quartz		Quartzite		Siltstone		Hornfels		CCS		Lava		Silcrete		Indet.	
		N	%	N	%	N	%	N	%	N	%	N	%	N	%	N	%
		N	%	N	%	N	%	N	%	N	%	N	%	N	%	N	%
Core fragment	3	0	0	3	11.5	0	0	0	0	0	0	0	0	0	0	0	0
Casual	12	0	0	12	46.2	0	0	0	0	0	0	0	0	0	0	0	0
Chopper-core	6	0	0	6	23.1	0	0	0	0	0	0	0	0	0	0	0	0
Discoidal	2	0	0	2	7.7	0	0	0	0	0	0	0	0	0	0	0	0
Irregular	3	0	0	3	11.5	0	0	0	0	0	0	0	0	0	0	0	0
Total	26	0	0	26	100	0	0	0	0	0	0	0	0	0	0	0	0

Formal tools:	Total	Quartz		Quartzite		Siltstone		Hornfels		CCS		Lava		Silcrete		Indet.	
		N	%	N	%	N	%	N	%	N	%	N	%	N	%	N	%
		N	%	N	%	N	%	N	%	N	%	N	%	N	%	N	%
Handaxe	1	0	0	0	0	0	0	1	14.3	0	0	0	0	0	0	0	0
Cleaver	1	0	0	1	14.3	0	0	0	0	0	0	0	0	0	0	0	0
Biface	1	0	0	1	14.3	0	0	0	0	0	0	0	0	0	0	0	0
Chopper	1	0	0	1	14.3	0	0	0	0	0	0	0	0	0	0	0	0
Flaked-flake	1	0	0	1	14.3	0	0	0	0	0	0	0	0	0	0	0	0
Denticulated scraper	1	0	0	1	14.3	0	0	0	0	0	0	0	0	0	0	0	0
Denticulate	1	0	0	1	14.3	0	0	0	0	0	0	0	0	0	0	0	0
Total	7	0	0	6	85.8	0	0	1	14.3	0	0	0	0	0	0	0	0



Figure 4.2.8. Atmar Farm cores made on quartzite cobbles. Bifacial chopper-cores (a and c) and a unifacial chopper-core (b) are shown.



Figure 4.2.9. Atmar Farm formal tools on quartzite complete flakes. Denticulate (a), denticulated scraper (b), and bifacial chopper (c).

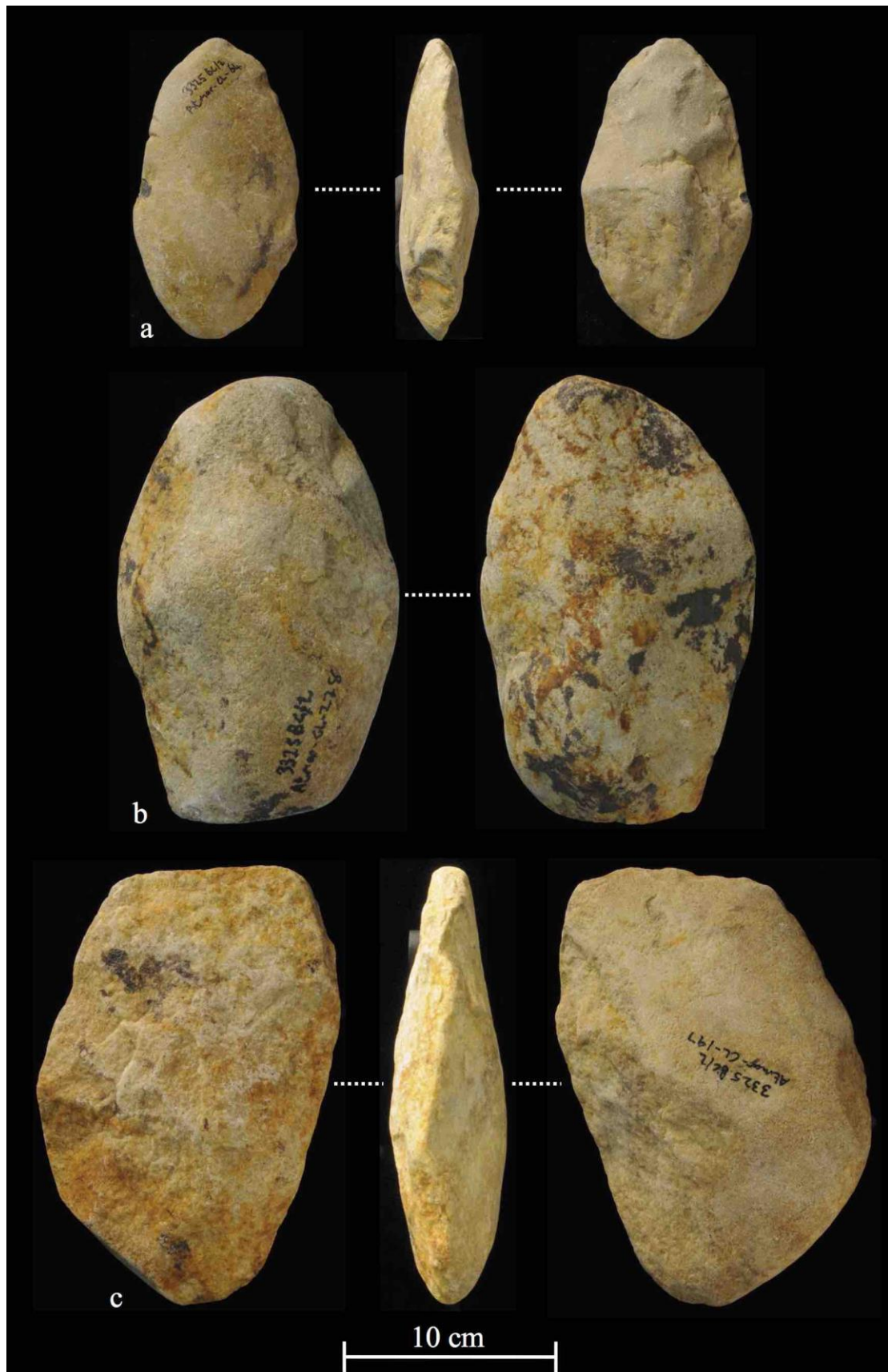


Figure 4.2.10. Atmar Farm LCTs, on large flakes, all poorly preserved. Hornfels unifacial handaxe (a), biface on quartzite (b) and cleaver on quartzite (c).

4.2.4 Summary

Atmar Farm provides a small assemblage of sporadic, poorly preserved lithic artefacts coupled with a general absence of all non-lithic material. An assessment of site context shows that a full size range of artefacts occurs, yet very little SFD is retained within the assemblage (13%). The majority of all material is larger than 20 mm and smaller than 80 mm (69%). Almost all of these artefacts are produced on quartzite, comprising 97.7% of the entire sample, and finer-grained types are favoured. All other raw materials are rare or completely absent.

The majority of the Atmar Farm artefacts shows some form of artefact damage or natural edge modification (collectively 78% are slightly to heavily abraded/rolled), and none retains any form of surface varnish. By material quartz and quartzite show a greater resistance to abrasion, whereas hornfels shows a greater susceptibility to weathering.

A basic typological classification of the lithic assemblage shows that formal tools are uncommon (n=7), as are cores (n=26) and complete flakes (n=35). Flaking debris comprises the majority of the assemblage (79.4%), yet none is bipolar. Quartzite complete flakes are the most abundant, with only a single flake made on hornfels; corner- and end-struck types dominate and no bipolar pieces were recovered. Cores show simple reduction strategies focused on the knapping of quartzite cobble blanks. Accordingly, casual cores (46.2%) dominate the sample and the remaining cores show a limited number of removals; discoids are uncommon (n=2). The small formal tool sample comprises only three poorly preserved LCTs, all of which are made on large corner-struck flake blanks with only minimal flaking to provide some basic edge shaping. A flaked-flake and two retouched pieces make up the remaining formal tool sample, the latter of which have denticulated retouch that is minimally invasive. Other types include three split cobbles.

Tool recycling and utilisation damage is not evident on the majority of the Atmar Farm artefacts, except for minor edge damage that occurs on the quartzite bifacial chopper.

4.3 Bernol Farm

4.3.1 Introduction

Survey work at Bernol Farm has provided a small, well-preserved assemblage of 19 pieces that only provides preliminary information. Unfortunately our excavation to sample the artefact, bone, and shell rich horizon at survey site 2 (Fig. 3.3.4) proved to be unsuccessful. As a result data here are obtained from artefacts that were sampled from the surface near to eroded artefact-bearing deposits or from *in situ* positions, at either the dated location or the survey sites (1-4, Figure 3.2.7; see typology discussion below for the location of the recovered artefacts). This sample therefore represents a biased collection.

In addition to lithics, bone and shell fragments were found at both the survey sites and the dated location, both at the surface and from *in situ* positions. The fragmented and poorly preserved nature of this bone meant that detailed analysis could not be pursued. Additional attempts to obtain phytolith and pollen remains from the fine alluvium proved to be unsuccessful.

4.3.2 Site context

4.3.2.1 Artefact size distributions

The range of artefact sizes at Bernol Farm is presented in Table 4.3.1. Because the sample represents a biased collection an assemblage profile is not presented here.

4.3.2.2 Artefact condition and raw material data

These data are presented in Table 4.3.2 and Figures 4.3.1 and 4.3.2. All of the selected artefacts are made on fine quartzite. By condition this fine quartzite contains both a fresh/unabraded portion (n=14; 73.7%) and slightly abraded component (n=5;

26.3%; Table 4.3.2). No artefacts obtained from Bernol Farm retain an exterior surface varnish, and none is weathered or heavily abraded/rolled (Fig. 4.3.2).

Table 4.3.1. Artefact size distribution data for Bernol Farm.

Artefact size	Number	Percentage
<10 mm	0	0
<20 mm	0	0
<30 mm	0	0
<40 mm	0	0
<50 mm	1	5.3
<60 mm	0	0
<70 mm	3	15.8
<80 mm	1	5.3
<90 mm	1	5.3
<100 mm	3	15.8
<110 mm	2	10.5
<120 mm	0	0
<130 mm	1	5.3
<140 mm	3	15.8
<150 mm	0	0
<160 mm	0	0
<170 mm	4	21.1
<180 mm	0	0
<190 mm	0	0
<200 mm	0	0
>200 mm	0	0
Total	19	100

Table 4.3.2. Raw material and artefact condition data for Bernol Farm. Bracketed values indicate percentages. Quartzite is divided in coarse (C) and fine (F) types.

Raw material	Artefact condition				Total
	Fresh/unabraded	Slightly abraded	Heavily abraded/rolled	Weathered	
Quartz	0	0	0	0	0
C Quartzite	0	0	0	0	0
F Quartzite	14 (73.7)	5 (26.3)	0	0	19 (100)
Siltstone	0	0	0	0	0
Hornfels	0	0	0	0	0
CCS	0	0	0	0	0
Lava	0	0	0	0	0
Silcrete	0	0	0	0	0
Indet.	0	0	0	0	0
Total	14 (73.7)	5 (26.3)	0	0	19 (100%)

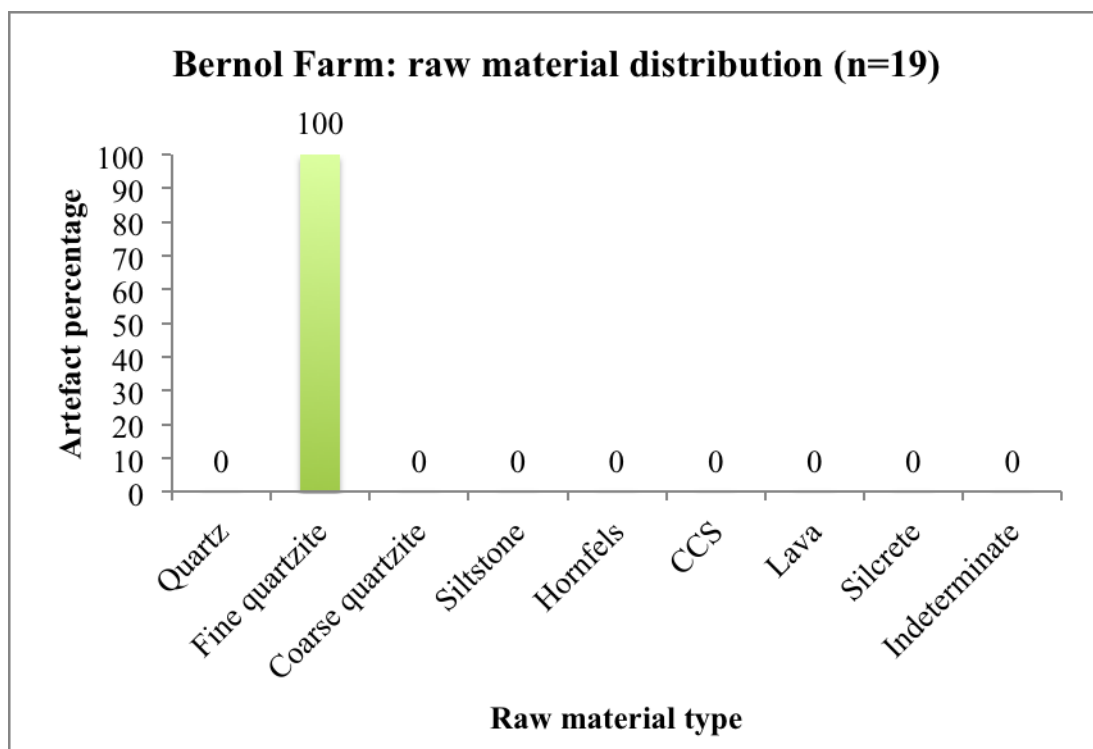


Figure 4.3.1. Bernol Farm artefact raw material types.

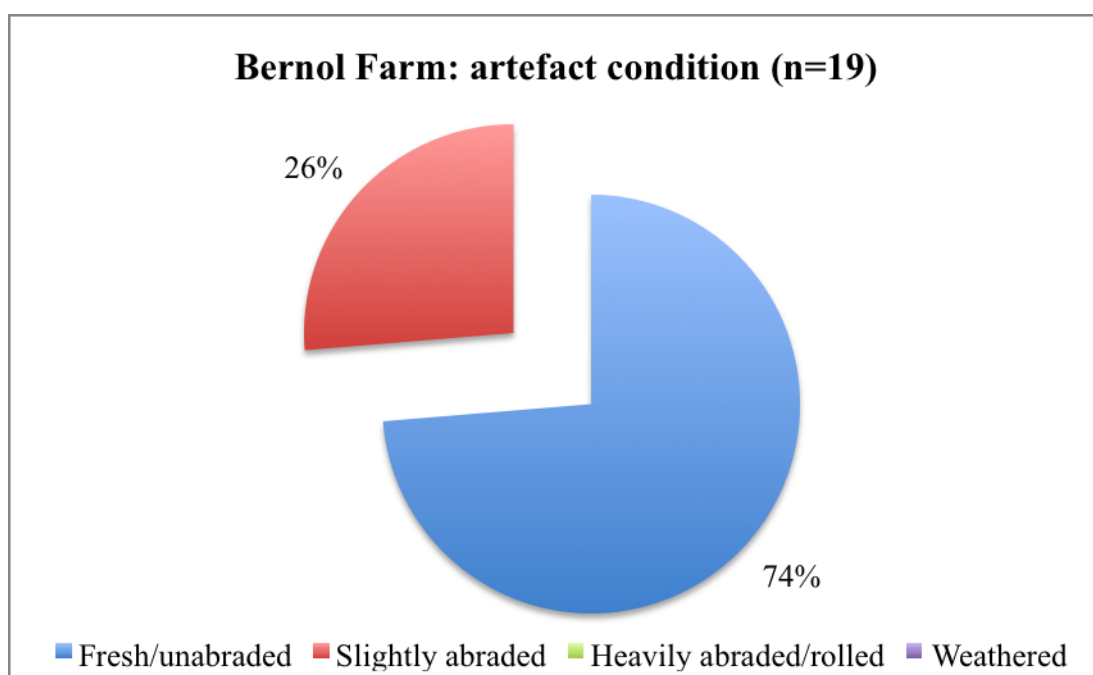


Figure 4.3.2. Bernol Farm artefact preservation states.

4.3.3 Typology

The Bernol Farm assemblage is presented in Figures 4.3.3-4.3.9 and Tables 4.3.3-4.3.5, with summaries provided by Table 4.3.3 and Figure 4.3.3.

Table 4.3.3. Assemblage classification for Bernol Farm (n=19).

Flaking debris:	N	%
SFD	0	0
Chunk	0	0
Incomplete flake	3	15.8
Flake fragment	0	0
Split flake	0	0
Bipolar	0	0
Total	3	15.8

Formal tools:

Handaxe	3	15.8
Broken handaxe/LCT	0	0
Cleaver	6	31.6
Pick	1	5.3
Biface	1	5.3
Uniface	0	0
Knife	0	0
Chopper	0	0
Side chopper	0	0
End chopper	0	0
Flaked-flake	0	0
Retouched flake	0	0
Scraper~		
<i>Composite</i>	0	0
<i>Concave</i>	0	0
<i>Convex</i>	0	0
<i>End</i>	0	0
<i>Side</i>	0	0
<i>Double side and end</i>	0	0
<i>Notched</i>	0	0
<i>Convergent</i>	0	0
<i>Denticulated</i>	0	0
<i>Heavy-duty/core</i>	0	0
MRP	0	0
Burin	0	0
Awl	0	0
Denticulate	0	0
Composite piece	0	0
Total	11	57.9

Complete flakes:	N	%
End-struck	1	5.3
Side-struck	0	0
Corner-struck	0	0
Kombewa	0	0
Core trimming	0	0
Bipolar	0	0
Handaxe trimming	0	0
Bi-bulb	0	0
Core rejuvenation	0	0
Total	1	5.3

Cores:

Core fragment	0	0
Casual	0	0
Bipolar	0	0
Chopper-core	2	10.5
Discoidal	2	10.5
Irregular	0	0
Polyhedral	0	0
Single platform	0	0
Boulder-core	0	0
Total	4	21.1

Other:

Modified cobble	0	0
Split cobble	0	0
Total:	0	0

Assemblage total	19	100
-------------------------	-----------	------------

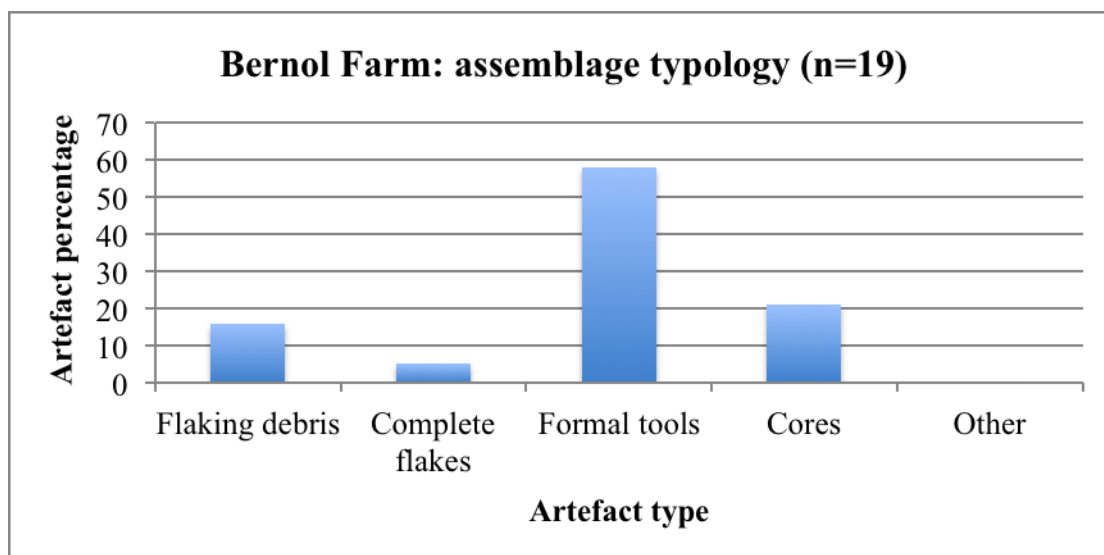


Figure 4.3.3. Artefact percentages at Bernol Farm.

The Bernol Farm assemblage provides a good sample of formal tools (LCTs), due mainly to the nature of our survey and our intention to select diagnostic pieces (n=11, 57.9%; Table 4.3.3; Fig. 4.3.3). A small sample of cores (n=4, 21.1%), flaking debris (n=3, 15.8%) and a single end-struck complete flake (5.3%) make up the remaining parts of the assemblage. No split or modified cobbles were recovered. Table 4.3.4 provides the location for the sampled artefacts.

Table 4.3.4. Location/site of sampled artefacts from Bernol Farm. Where the location is not recorded these pieces are from either the dated location or the survey sites. Merged cells indicate artefacts were retrieved from one of a possible two sites. HA refers to handaxes, 'comp.' refers to complete, and 'disc.' to discoidal.

Loc/site	Incomp. flake	Comp. flake	Chopper-core	Disc. core	HA	Cleaver	Pick	Biface
Dated location	-	-	-	-	-	-	-	-
Survey 1	1	-	-	1	2	2	-	-
Survey 2	-	-	2	-	-	-	-	-
Survey 3	2	-	-	-	1	-	-	1
Survey 4		-	-	-	-	-	-	
Not recorded	-	1	-	1	-	4	1	-

Although the core and flake sample is limited, the large size of these pieces is notable. The single end-struck complete flake has a maximum length of 132.5 mm, and one of the discoidal cores has a maximum length of 168 mm; a single chopper-core measures 136 mm. Although not collected, a boulder-core (Fig. 4.3.4) was found in the abandoned sand-filled canal at the dated location (Fig. 3.2.7), having eroded out of the adjacent deposit (Fig. 3.2.9). It clearly illustrates the use of boulder-cores for obtaining large flakes (presumably for use as tool blanks). Table 4.3.5 highlights the exclusive use of quartzite in the core and flake samples.



Figure 4.3.4. Boulder-core found near the dated location at Bernol Farm. Core shows numerous large (>10 cm) flake removals. Shoe for scale (30 cm).

The formal tool assemblage at Bernol Farm is comprised of 11 LCTs (Table 4.3.3), all of which are produced on quartzite (Table 4.3.5). Cleavers dominate the sample ($n=6$, 54.5%), followed thereafter by handaxes ($n=3$, 27.3%) and a single pick and biface

(collectively 18.2%; Table 4.3.3; Fig. 4.3.5). These LCTs are illustrated in Figures 4.3.6-4.3.9.

A detailed analysis and description of the LCT sample is presented in the following section.

None of the artefacts from the Bernol Farm property appeared to suggest any kind of tool recycling.

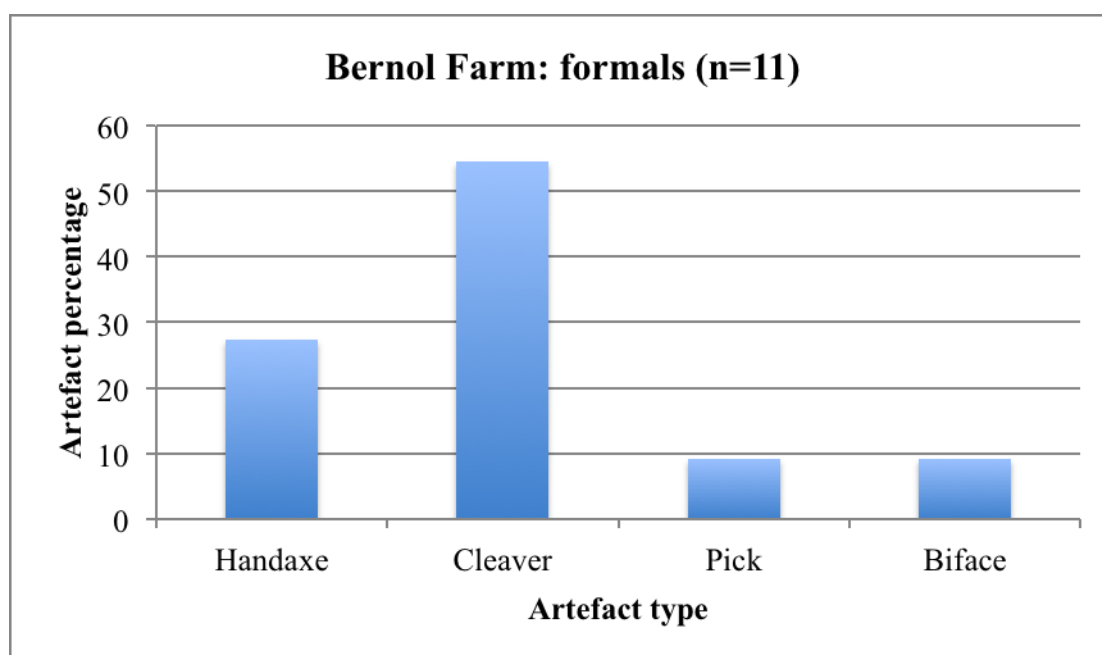


Figure 4.3.5. LCTs sampled from Bernol Farm.

Table 4.3.5. Raw material use at Bernol Farm (excluding flaking debris).

Complete flakes:	Total	Raw material type															
		Quartz		Quartzite		Siltstone		Hornfels		CCS		Lava		Silcrete		Indet.	
		N	%	N	%	N	%	N	%	N	%	N	%	N	%	N	%
End-struck	1	0	0	1	100	0	0	0	0	0	0	0	0	0	0	0	0
Total	1	0	0	1	100	0	0	0	0	0	0	0	0	0	0	0	0

Cores:	Total	Raw material type															
		Quartz		Quartzite		Siltstone		Hornfels		CCS		Lava		Silcrete		Indet.	
		N	%	N	%	N	%	N	%	N	%	N	%	N	%	N	%
Chopper-core	2	0	0	2	50	0	0	0	0	0	0	0	0	0	0	0	0
Discoidal	2	0	0	2	50	0	0	0	0	0	0	0	0	0	0	0	0
Total	4	0	0	4	100	0	0	0	0	0	0	0	0	0	0	0	0

Formal tools:	Total	Raw material type															
		Quartz		Quartzite		Siltstone		Hornfels		CCS		Lava		Silcrete		Indet.	
		N	%	N	%	N	%	N	%	N	%	N	%	N	%	N	%
Handaxe	3	0	0	3	27.3	0	0	0	0	0	0	0	0	0	0	0	0
Cleaver	6	0	0	6	54.5	0	0	0	0	0	0	0	0	0	0	0	0
Pick	1	0	0	1	9.1	0	0	0	0	0	0	0	0	0	0	0	0
Biface	1	0	0	1	9.1	0	0	0	0	0	0	0	0	0	0	0	0
Total	11	0	0	11	100	0	0	0	0	0	0	0	0	0	0	0	0

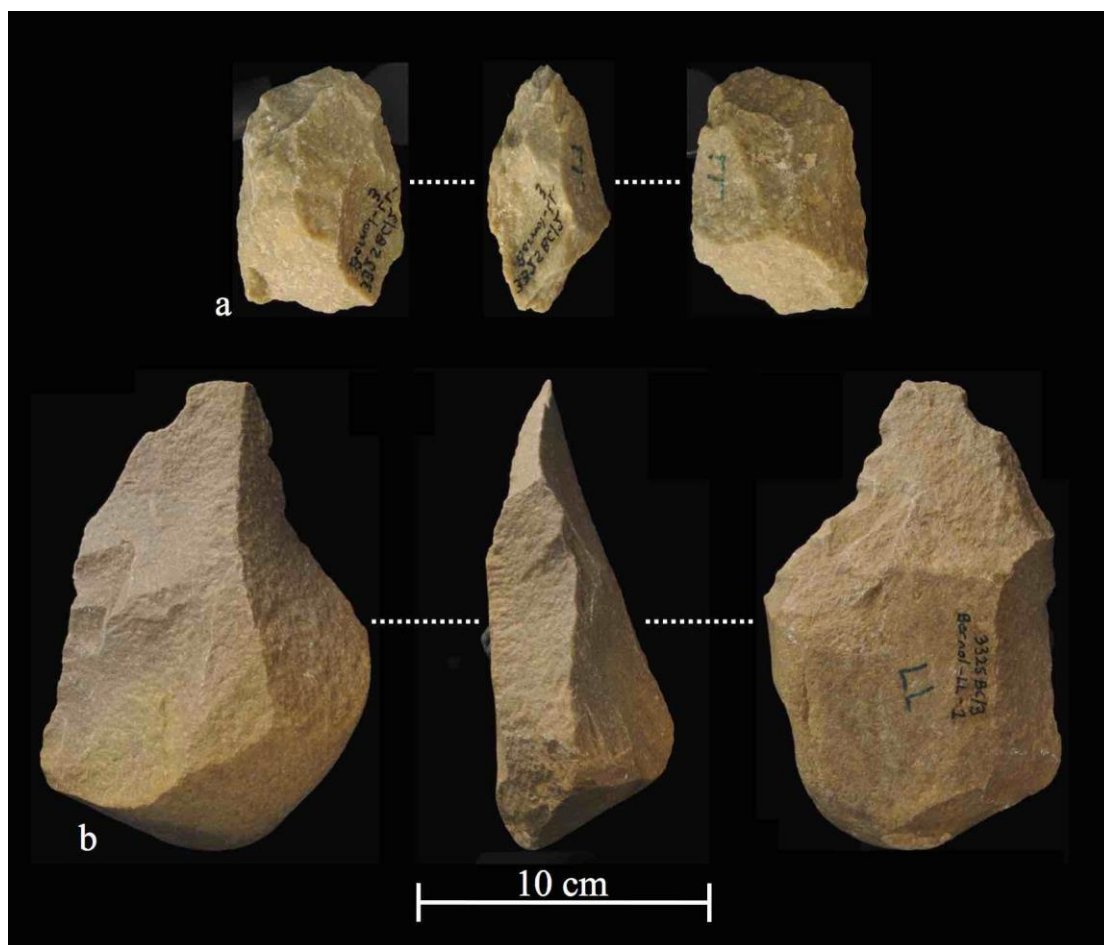


Figure 4.3.6. Bernol Farm LCTs. Biface on an indeterminate quartzite blank (a), showing a non-convergent distal end and an unclear emphasis on the distal or peripheral edges; pick on a large, thick, corner-struck cortical flake (b).

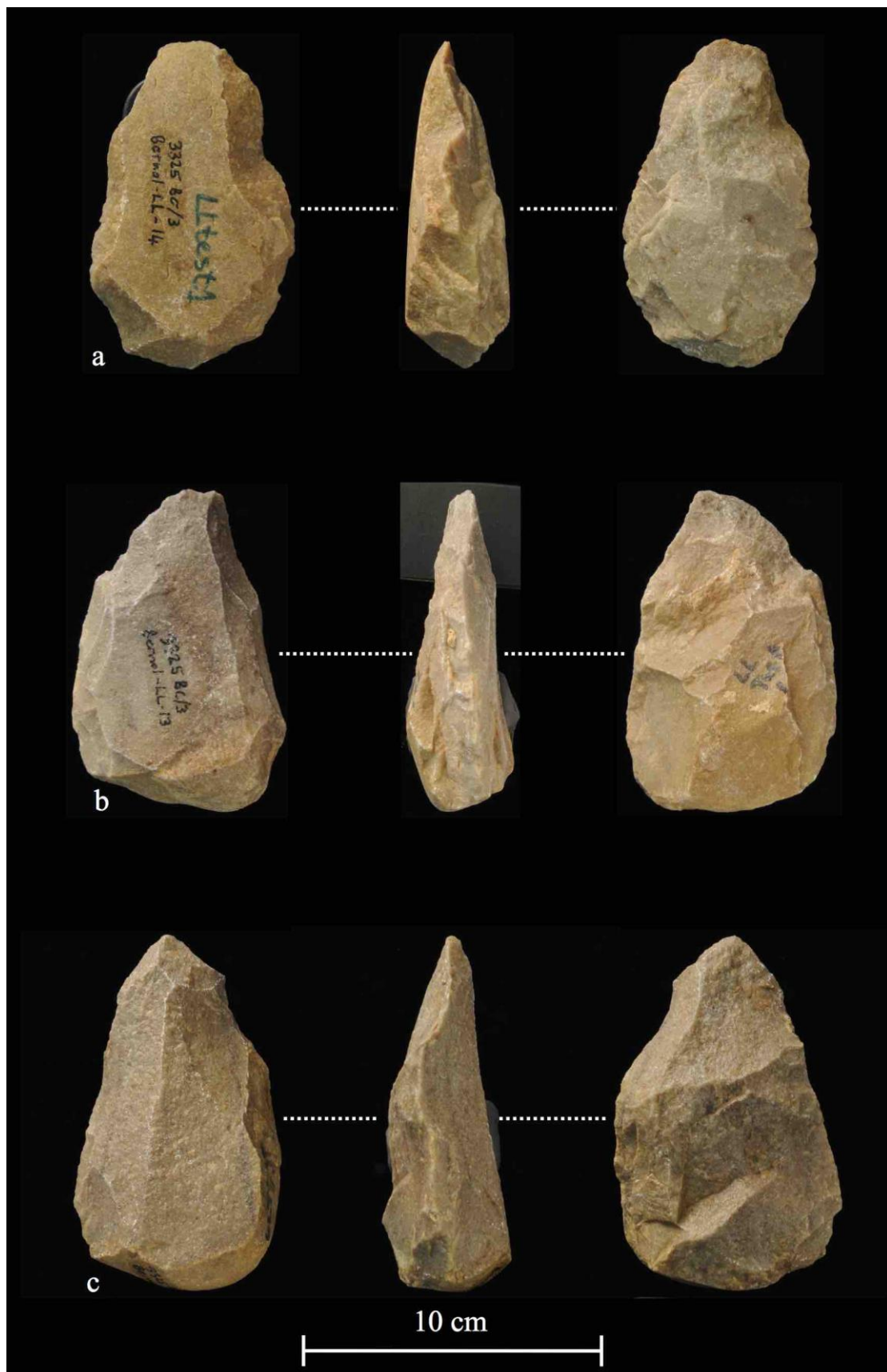


Figure 4.3.7. Handaxes from Bernol Farm, all on quartzite flake blanks. Note cortical dorsal surface (a), cortical butt (b) and cortical butt and lateral edge (c).

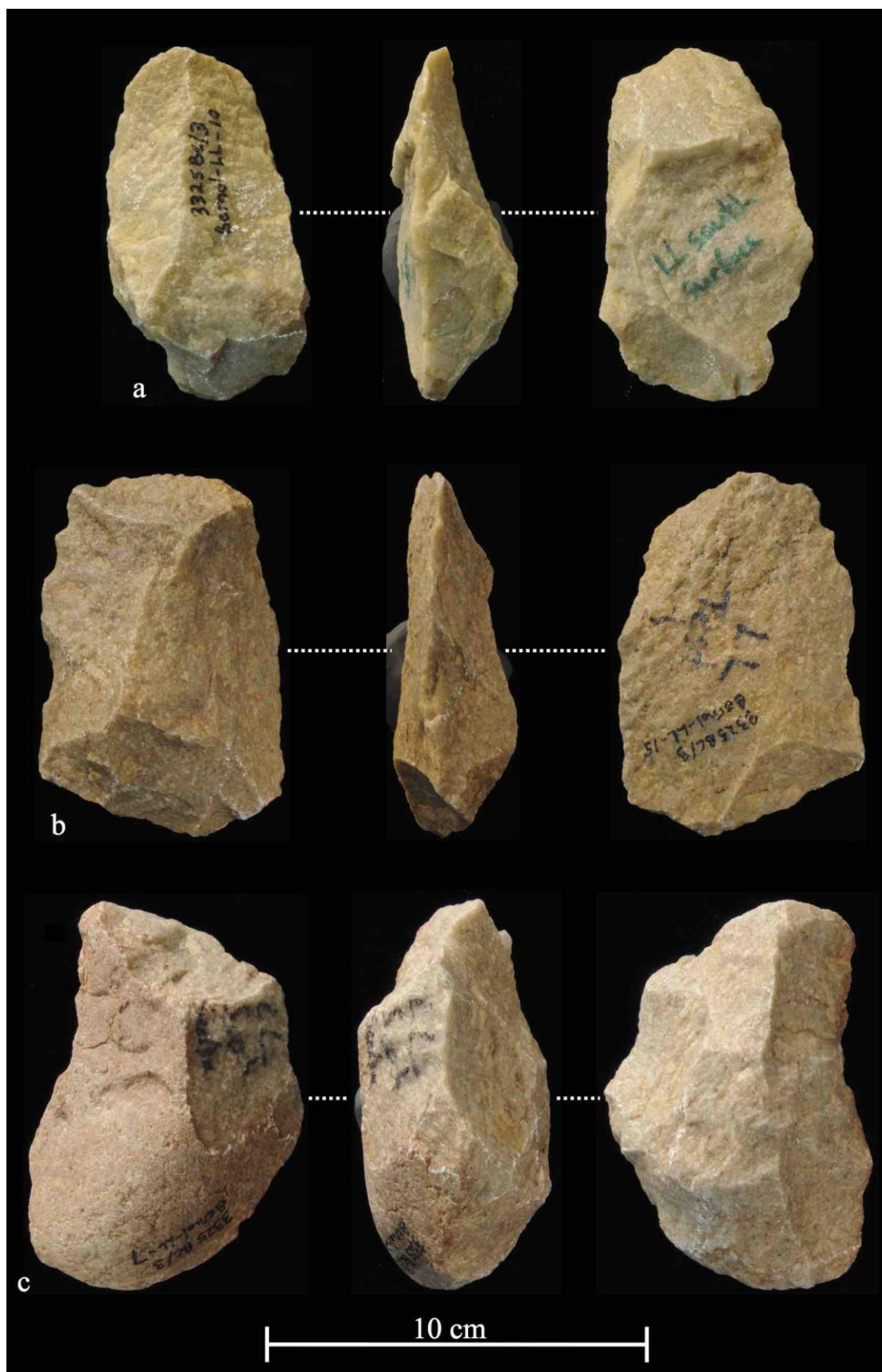


Figure 4.3.8. Cleavers from Bernol Farm. These are made on flake blanks (a and b) and an indeterminate blank (c).

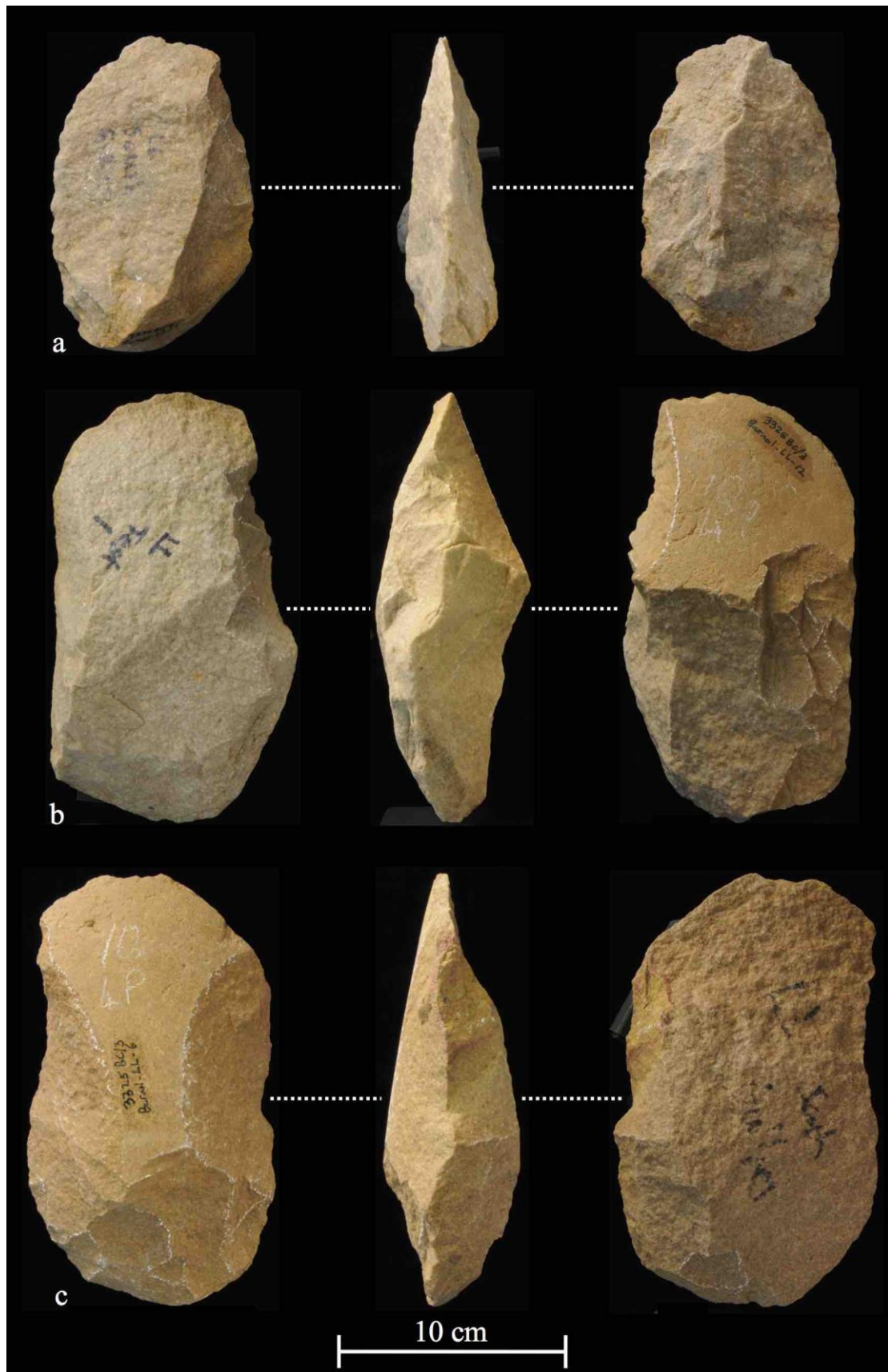


Figure 4.3.9. Cleavers from Bernol Farm. The flake blanks utilised are corner-struck (a and c) and side-struck (b).

4.3.4 Technology

Data for the Bernol Farm LCT assemblage (n=11) will first address size and shape (through technological measurements, including weight) and then reduction. It must be emphasised here that the overall significance of this data is limited because it is based on a small sample of selected pieces.

4.3.4.1 LCT size and shape

Averages for LCT size data are presented in Table 4.3.6 (see Appendix A Tables 1 and 2 for individual LCT data, and Table 3 for additional LCT measurement averages). By weight, cleavers and the single pick account for the heaviest pieces (maximum weights). However, the lightest piece is also a cleaver at 119.9 g. The variation (SD) in cleaver weight is the greatest at 381.41 g with a mean weight of 474.68 g. Handaxe weight varies far less (SD=82.64 g), with a mean weight of 268.84 g.

Length, width and thickness data illustrate that the pick is one of the largest pieces with the second largest length (165 mm), largest width (108 mm) and the second largest thickness measurement (62 mm). By length, handaxes range in size from 102-120 mm, with a mean of 108.67 mm. Cleaver length ranges from 90-173 mm, with a mean of 126.83 mm, again showing the greatest variation (SD=38.7 mm). Cleaver width has a mean of 78 mm, followed thereafter by handaxes (68.33 mm) and the biface (53 mm). Excluding the pick, LCT thickness is greatest for the cleavers (mean=44.93 mm).

LCT elongation (L/W ratio) data illustrates that cleavers are the most elongated (high L/W ratio, with a mean of 1.62). Handaxes follow thereafter with a mean ratio of 1.59; the pick and biface are the shortest (low L/W ratio) pieces in the assemblage (with values of 1.53 and 1.49 respectively).

LCT refinement (T/W ratio) data shows that the handaxes have the lowest ratio (mean=0.55). Cleavers are not too dissimilar with a mean ratio of 0.57, equal to that

of the pick. The standard deviation between the handaxes and cleavers differs by only 0.03, and the biface has the largest T/W ratio (0.75).

Table 4.3.6. LCT size data averages. See Appendix A Table 3 for additional measurement averages.

Bernol Farm LCTs (n=11)		Pick (n=1)	Biface (n=1)	Handaxe (n=3)	Cleaver (n=6)
Weight (g)	Min	963.47	148.91	220.31	119.90
	Median	-	-	221.96	317.66
	Max	963.47	148.91	364.26	999.28
	Mean	-	-	268.84	474.68
	SD	-	-	82.64	381.41
Length (mm)	Min	165.00	79.00	102.00	90.00
	Median	-	-	104.00	116.00
	Max	165.00	79.00	120.00	173.00
	Mean	-	-	108.67	126.83
	SD	-	-	9.87	38.70
Width (mm)	Min	108.00	53.00	64.00	51.00
	Median	-	-	67.00	77.50
	Max	108.00	53.00	74.00	102.00
	Mean	-	-	68.33	78.00
	SD	-	-	5.13	20.23
Thickness (mm)	Min	62.00	40.00	32.00	27.00
	Median	-	-	33.00	41.00
	Max	62.00	40.00	48.00	72.60
	Mean	-	-	37.67	44.93
	SD	-	-	8.96	17.43
L/W (elongation)	Min	1.53	1.49	1.52	1.42
	Median	-	-	1.62	1.61
	Max	1.53	1.49	1.63	1.80
	Mean	-	-	1.59	1.62
	SD	-	-	0.06	0.15
T/W (refinement)	Min	0.57	0.75	0.48	0.44
	Median	-	-	0.52	0.55
	Max	0.57	0.75	0.65	0.76
	Mean	-	-	0.55	0.57
	SD	-	-	0.09	0.12

Additional morphological (and breakage) data is presented in Tables 4.3.7-4.3.9 and Figure 4.3.10. Table 4.3.7 illustrates that only a single handaxe retained any kind of edge damage, in this case on the distal portion of the piece (minor partial tip break). All the other LCTs are complete and undamaged.

Table 4.3.7. LCT damage, by type.

Type	Damage/break		
	Partial tip/cleaver edge	Partial lateral edge	Partial butt
Pick (n=1)	0	0	N/A
Biface (n=1)	0	0	N/A
Handaxe (n=3)	1	0	0
Cleaver (n=6)	0	0	N/A

An analysis of LCT tip shape (Table 4.3.8; Fig. 4.3.10) shows a clear dominance of generalised convergent types (n=7). By type this includes 83.3% of the cleaver sample, 33.3% of the handaxe sample and 100% of the biface sample. Only a single cleaver has a convergent oblique tip shape (16.7%), and the remaining shapes comprise of markedly convergent pieces (n=1 pick and 2 handaxes). Types 2 (convergent square) and 5-7 (square tip, oblique tip and wide convex tip) are not represented.

Table 4.3.8. Bernol Farm LCT tip shape, by type.

Tip shape	Type			
	Pick (n=1)	Biface (n=1)	Handaxe (n=3)	Cleaver (n=6)
1) Markedly convergent	1 (100%)	0	2 (66.7%)	0
2) Convergent square	0	0	0	0
3) Convergent oblique	0	0	0	1 (16.7%)
4) Generalised convergent	0	1 (100%)	1 (33.3%)	5 (83.3%)
5) Square tip: divergent/parallel sided	0	0	0	0
6) Oblique tip: divergent/parallel sided	0	0	0	0
7) Wide with convex tip	0	0	0	0
Total	1 (100%)	1 (100%)	3 (100%)	6 (100%)

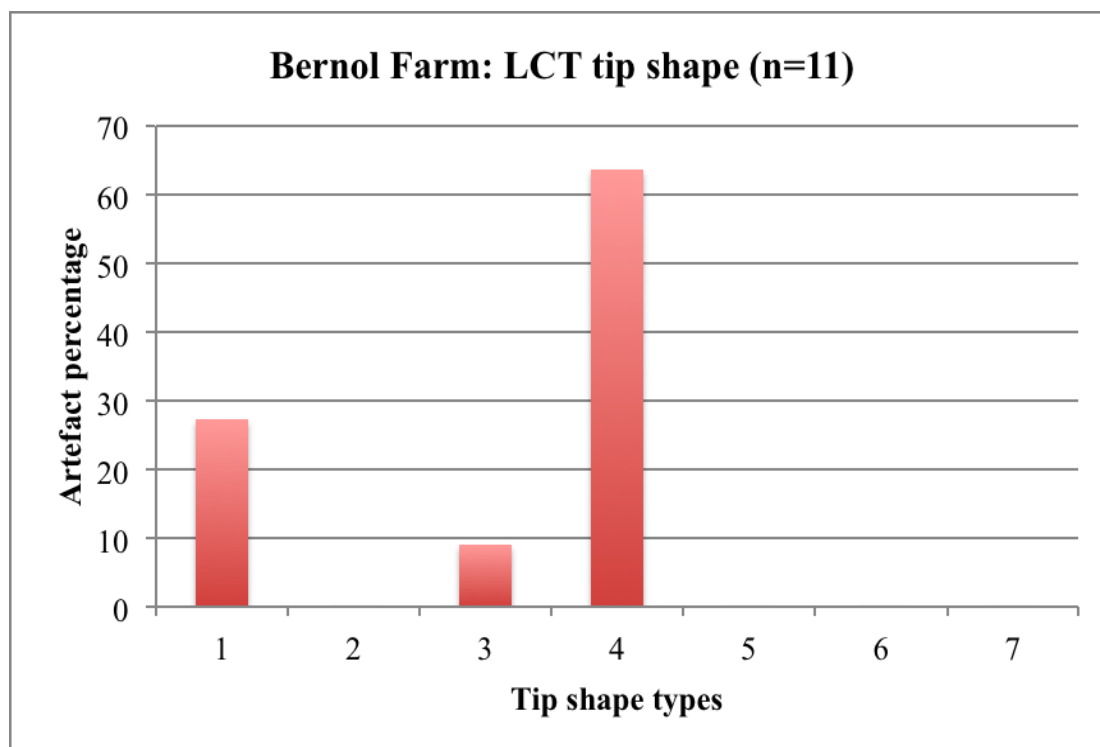


Figure 4.3.10. Bernol Farm LCT tip shape. Numbers 1-7 as per those listed in Table 4.3.8.

Cleaver butt plan shape shows that none is pointed (Table 4.3.9). An equal number of rounded and squared butts occurs (each n=3, 50%).

Table 4.3.9. Cleaver butt plan shape.

Type	Butt plan			Total
	Rounded	Squared	Pointed	
Cleaver (n=6)	3 (50%)	3 (50%)	0	6 (100%)

4.3.4.2 LCT reduction

Blank type plays an important role in the production of artefacts. Table 4.3.10 illustrates that flake blanks at Bernol Farm are favoured for LCT production (n=9, 81.8%). The blank types for a single cleaver and the biface could not be identified with certainty (n=2, 18.2%), but they appear possibly to also be thick flakes. An inability to distinguish between different blank types for these specimens meant that a more conservative 'indeterminate' designation was appropriate.

Table 4.3.10. Bernol Farm LCT blank types.

Blank type	Type				Total
	Pick (n=1)	Biface (n=1)	Handaxe (n=3)	Cleaver (n=6)	
Block	0	0	0	0	0
Fragment	0	0	0	0	0
Flake	1	0	3	5	9 (81.8%)
Cobble	0	0	0	0	0
Pebble	0	0	0	0	0
Indeterminate	0	1	0	1	2 (18.2%)
Split cobble	0	0	0	0	0
Bipolar split	0	0	0	0	0
Total	1 (9.1%)	1 (9.1%)	3 (27.3%)	6 (54.5%)	11 (100%)

The average number of removals on the Bernol Farm LCTs is presented in Table 4.3.11 and Figure 4.3.11. The biface and handaxe samples show the greatest flake scar numbers (19 and 18.67 scars, respectively). The cleavers and the pick have a lower flake scar count, and for the former the standard deviation is 2.93. Handaxes show a greater standard deviation at 6.43 for the mean flake scar number.

The number of primary flake scars is highest for the handaxe sample and biface (10 and 7, respectively); the pick and cleavers are lower at 4 and 5.33, respectively. Interestingly, the secondary flake scar counts are greatest for the pick and biface. Cleavers retain the lowest mean secondary flake scar number (6.83). In all samples except for the handaxes, secondary flaking exceeds that of primary flaking.

Table 4.3.11. Average number of flake scars on the Bernol Farm LCTs. Where n=1 the mean value here does not refer to an average but rather the total scar count for each piece (pri=primary; sec=secondary).

Type	Sample	Scar counts					
		Mean	SD	Mean pri.	SD	Mean sec.	SD
Pick	1	14.00	-	4.00	-	10.00	-
Biface	1	19.00	-	7.00	-	12.00	-
Handaxe	3	18.67	6.43	10.00	3.00	8.67	3.79
Cleaver	6	12.17	2.93	5.33	1.51	6.83	3.71

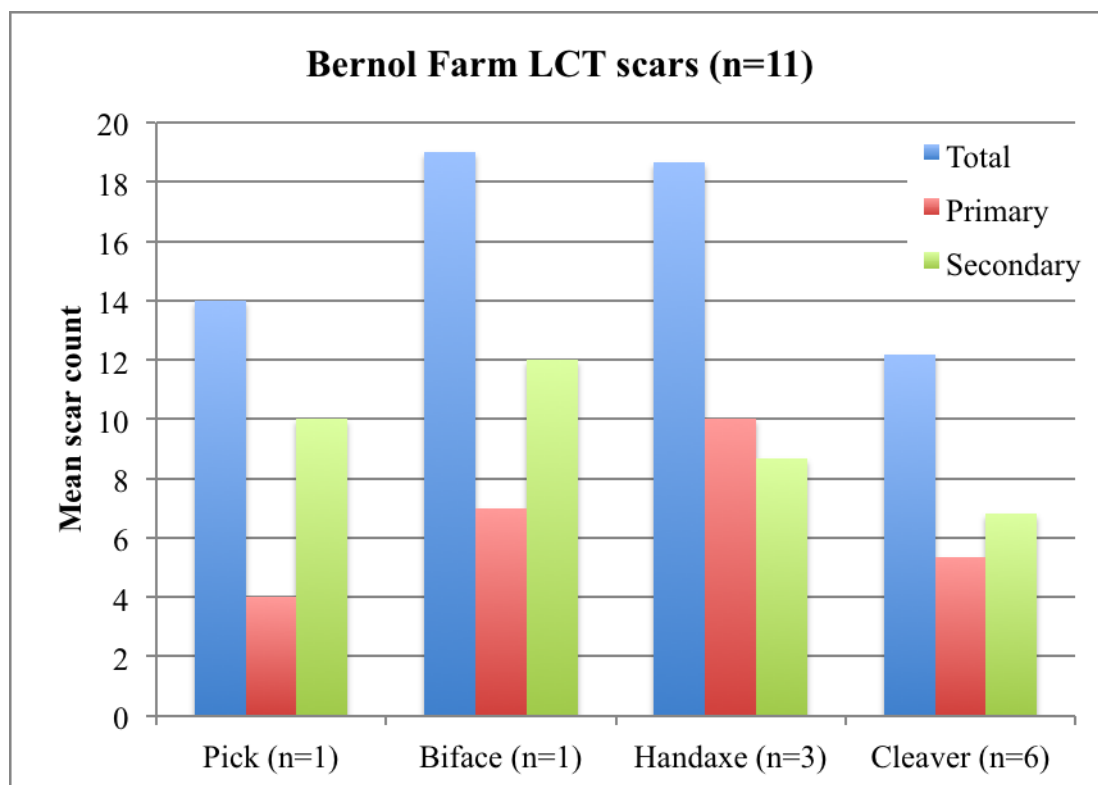


Figure 4.3.11. Average number of flake scars, by type.

The type and quantity of flake scar negatives on LCTs is shown in Figure 4.3.12. For the LCTs the number of step terminations exceeds the number of feather terminations. The number of hinge terminations is lower than both the feather and step types. No overshoot flake scar negatives were identified on any of the LCTs.

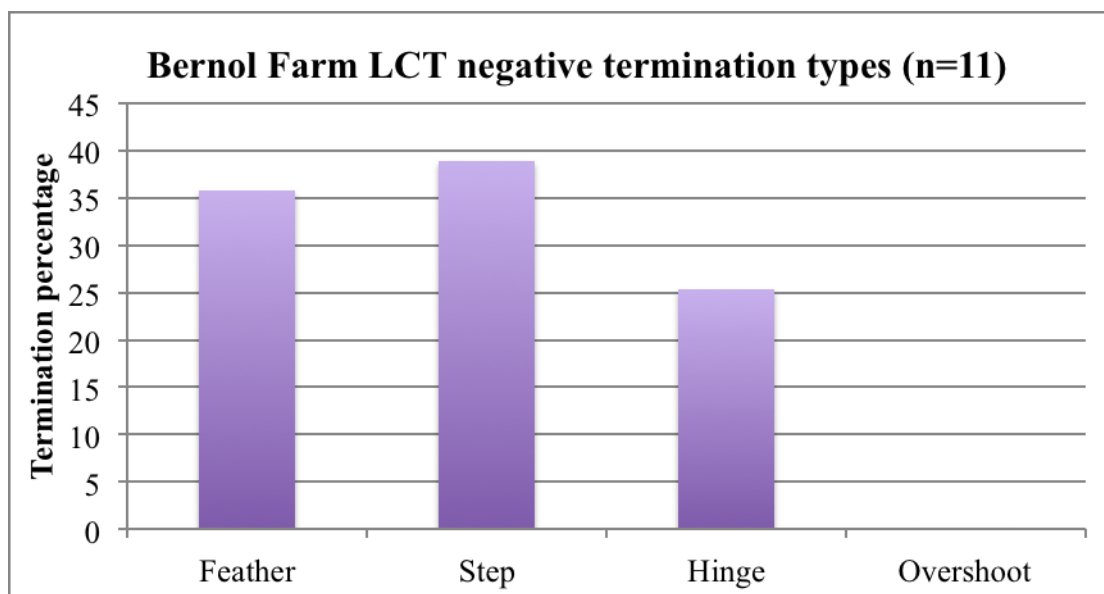


Figure 4.3.12. Negative flake scar termination types on the LCT assemblage.

Table 4.3.12 and Figure 4.3.13 provide an assessment of LCT flaking location. From this analysis the Bernol Farm LCT sample is dominated by bifacial pieces (n=8, 72.7%), including one pick, one biface, three handaxes and three cleavers. Partly bifacial pieces account for 18.2% of the total sample (n=2 cleavers) and a single unifacial cleaver was also recovered (9.1%). Overall, cleavers are the only tool to show all three types in this limited sample.

Table 4.3.12. Shaping data for the Bernol Farm LCT sample.

Type	Bifacial	Partly bifacial	Unifacial	Sample
Pick	1	0	0	1 (9.1%)
Biface	1	0	0	1 (9.1%)
Handaxe	3	0	0	3 (27.3%)
Cleaver	3	2	1	6 (54.5%)
Total	8 (72.7%)	2 (18.2%)	1 (9.1%)	11 (100%)

The location of flaking for all the LCTs (n=11), by sector, is presented in Figure 4.3.13 and Table 4.3.13 (see Appendix A Figures 1 and 2 for the flaking location of the handaxes and cleavers). Figure 4.3.13 shows that the percentage of primary flaking is high for all the sectors across both faces (proximal, medial and distal portions). However, primary flaking is marginally more abundant on the right side of both faces, whereas secondary flaking is more common on the opposite side (left) on either face. This primary flaking is also more common towards the medial and distal portions of both faces. To be expected, cortex is proportionally more common towards the proximal end of the LCTs.

Overall, the attention paid to secondary flaking (edge refinement) is low for the total LCT sample (13% of sectors; Table 4.3.13). Cleavers retain the lowest proportion of primary and secondary (65%) and secondary (11%) flaking, whereas handaxes retain the highest (72% and 17%, respectively). This suggests a clear preference for tool shaping versus tool edge refinement at Bernol Farm.

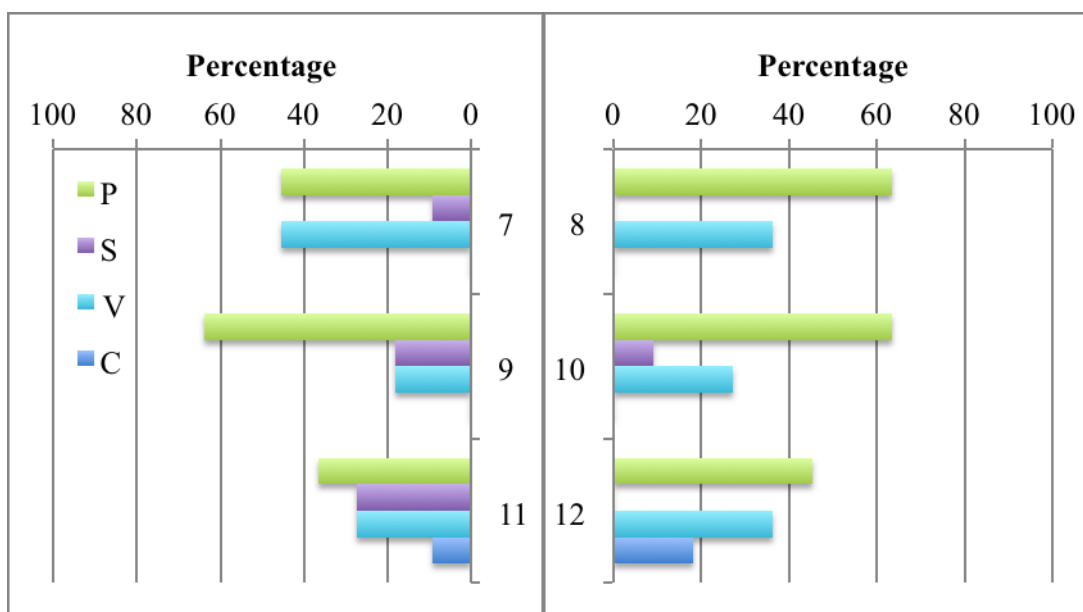
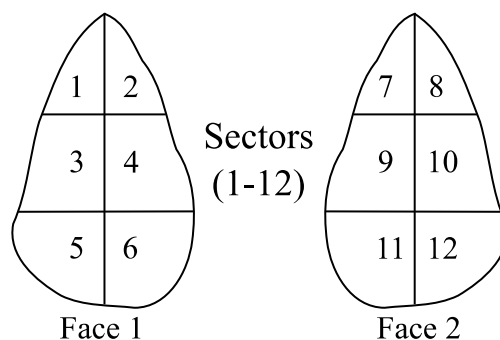
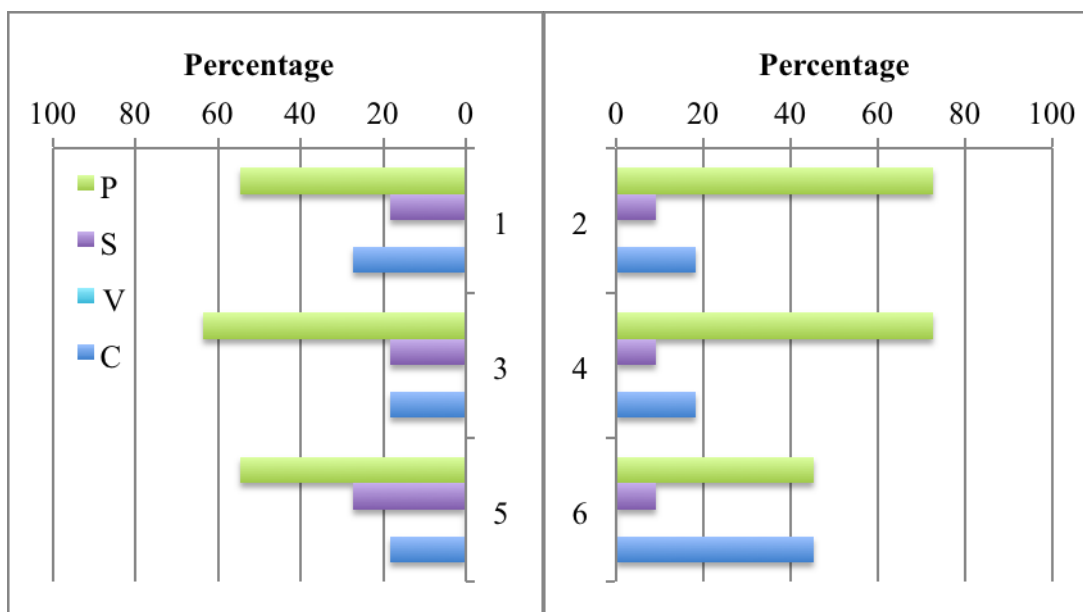


Figure 4.3.13. Flaking location for the Bernol Farm LCT sample (n=11). P: primary; S: secondary; V: ventral/no working; C: cortical. For flake blanks the dorsal surface is recorded first (face 1, upper graphs) and the ventral second (face 2, lower graphs).

Table 4.3.13. Mean flaking coverage in the 12 sectors. Pick and biface excluded. Values below are discussed as percentages.

LCT sample	Sector sample	Mean flaking coverage		
		Type	Primary and secondary	Secondary
n=11	n=132	All	0.70	0.13
n=3	n=36	Handaxe	0.72	0.17
n=6	n=72	Cleaver	0.65	0.11

The percentage of remaining cortex that is left on the Bernol Farm LCTs, subsequent to primary and secondary flaking, is shown in Table 4.3.14 and Figure 4.3.14. No artefacts retain greater than 49% cortex. The majority is therefore not cortical at all (0% cortex, n=3), or, ranges from 1-49% (n=8). Figure 4.3.14 illustrates that the proportion of LCTs with 1-24% and 25-49% is equal (36.4%); 27.3% preserve no remaining cortex.

By type, the single biface preserves no remaining cortex (0%) ,whereas the pick preserves 25-49% (Table 4.3.14). The majority of handaxes is 25-49% cortical (n=2) and the majority of cleavers is 1-24% cortical (n=3). None of the handaxes preserve 0% cortex whereas 33.3% of the cleaver sample does (n=2).

Table 4.3.14. Percentage cortex on the Bernol Farm LCTs, by type.

Type	Remaining cortex (%)					Total
	0	1-24	25-49	50-74	75-100	
Pick (n=1)	0	0	1 (100%)	0	0	1 (100%)
Biface (n=1)	1 (100%)	0	0	0	0	1 (100%)
Handaxe (n=3)	0	1 (33.3%)	2 (66.7%)	0	0	3 (100%)
Cleaver (n=6)	2 (33.3%)	3 (50%)	1 (16.7%)	0	0	6 (100%)

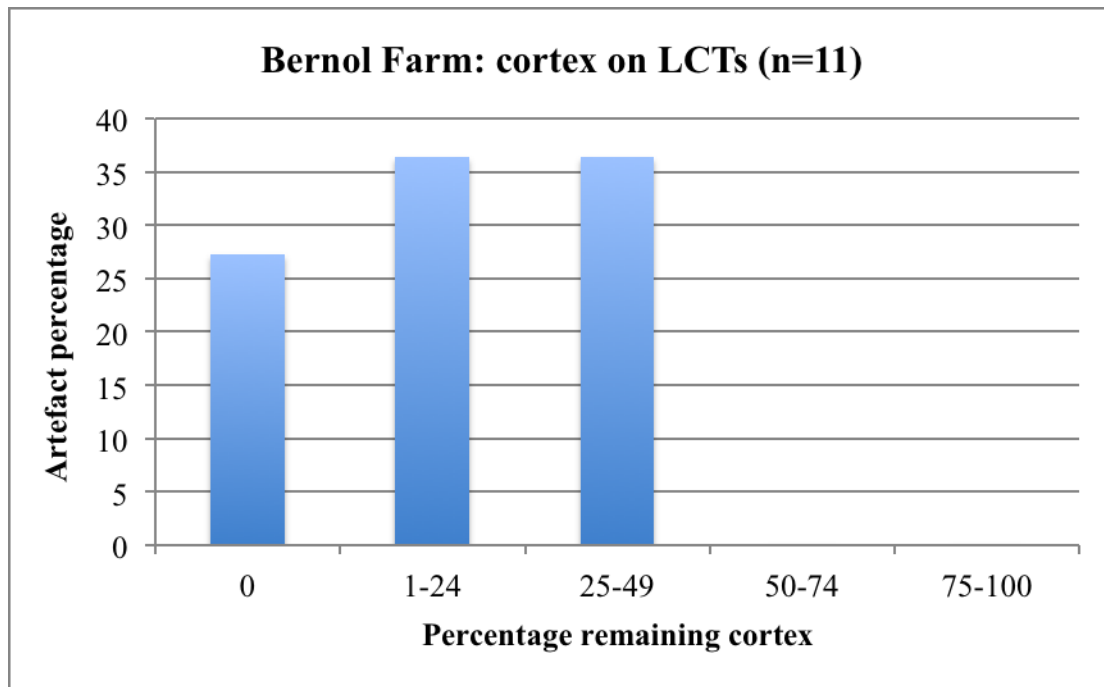


Figure 4.3.14. Percentage remaining cortex on the LCT sample (n=11).

4.3.5 Residue and use-wear analysis

Although only a single artefact from Bernol Farm could be assessed for the preservation of organic residues and use-wear damage, some interesting results obtained by Geeske Langejans' study can be presented (Fig. 4.3.15). Three types of organic residue are located along the edge and interior of the analysed handaxe, and these include: organic drops (of unidentifiable constituents), a green surface-deposit that may likely be some kind of bacterial/algal growth, and fibres (likely derived from a cloth/clothing).

However, the possibility of edge damage through use is suggested by edge rounding that occurs on only certain edges of the handaxe. Although the context of this artefact is unknown (from the survey sites, therefore either alluvial or colluvial), the possibility of this edge rounding being cultural, versus natural, is indicated by its discontinuous nature and its concentration at specific points along the edge of the handaxe. Without analysing a larger sample of artefacts though this finding cannot be confirmed and must be treated with caution.

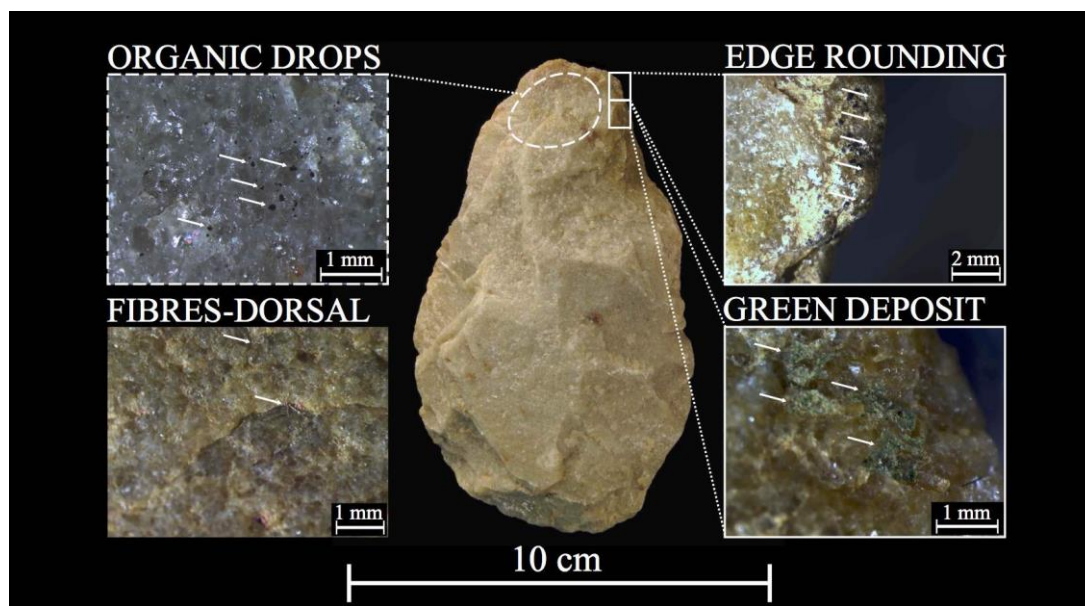


Figure 4.3.15. Use-wear and residue analysis on a handaxe from Bernol Farm (Bernol-LL-14). Magnified images courtesy of G. Langejans.

4.3.6 Non-lithic material

The Terrace 9 exposure at Bernol Farm and the survey sites (1-4) preserve fragmented bone and shell (Fig. 4.3.16). The bone fragment (Fig. 4.3.16a) was found eroding out from the base of the Terrace 9 exposure, near to the dated location. Elsewhere at Bernol Farm similar fragments are quite common.

The types of analysis that one can apply to such pieces are limited due to their highly fragmented nature and likely contamination by water (limiting chemical analysis). However, more extensive sampling and excavation of the property may uncover more worthwhile samples.

Shell fragments were found to be prolific at the survey sites (Fig. 4.3.16b). The context of these survey sites is not fully understood and these shells may rather be from more modern times. An investigation into these preserved shells is needed.

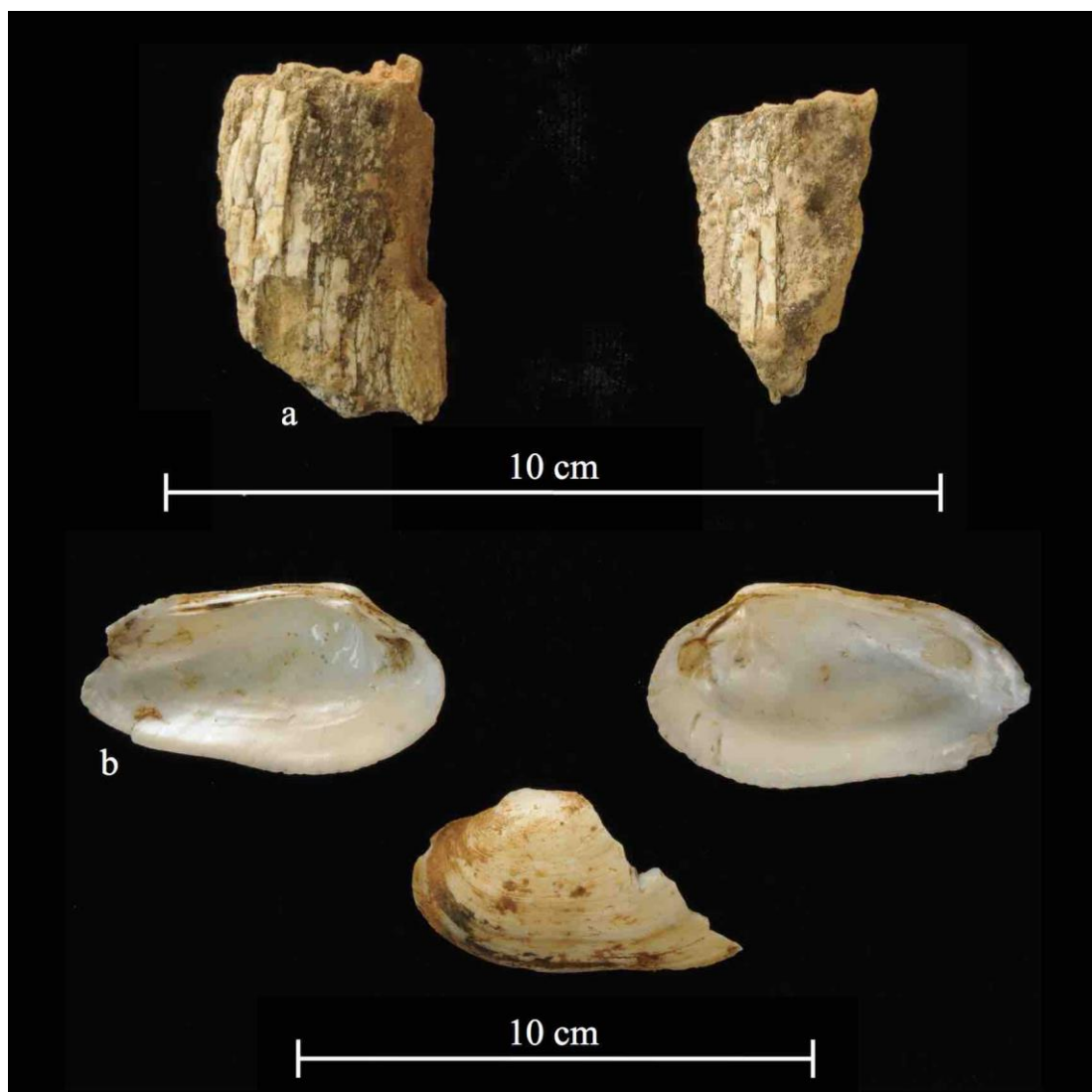


Figure 4.3.16. Non-lithic material obtained from Bernol Farm. Partially fossilised bone fragments (a) found eroding out of the fine overbank alluvium near to the dated location, and shells (b; likely of the *Lutrariidae* family) from survey site 2.

4.3.7 Summary

Bernol Farm provides a small (n=19) sample of well-preserved quartzite artefacts comprised primarily of formal tools (n=11 LCTs). Both bone and shell are common on Bernol Farm, yet only a limited sample was obtained during this research. In addition, no phytolith and pollen remains were recovered from the sampled sediments.

Although only basic information regarding the context of the site is presented most notable is the fresh appearance of the majority (74%) of the artefacts. In addition to

this, none of the artefacts retain any kind of surface varnish and none is weathered or heavily abraded/rolled.

A basic typological analysis of the cores and flakes suggests that large flake production is pursued at Bernol Farm. This is also supported by the LCT sample as these pieces are all made on large flake blanks (except for two indeterminate blanks).

A technological analysis of the Bernol Farm LCTs shows some interesting trends. LCT size and shape data show that, by weight, cleavers and picks are the heaviest pieces. Cleavers also account for the lightest piece and thus they show the greatest variation for this attribute. Length, width and thickness measurements show that the pick and cleavers are the largest pieces, followed thereafter by the smaller biface and handaxes. Tool elongation (L/W ratio) is greatest for the cleavers (most elongated) and lowest for the pick and biface, and LCT refinement (T/W ratio) shows that the handaxe sample is the most refined (mean=0.55). Generalised convergent shapes are the most common tip type for the LCTs (n=7).

Flake blanks are favoured for LCT production at Bernol Farm. LCT reduction shows that for almost all of the LCTs the quantity of secondary flake scars exceeds that of primary scars. The biface and handaxes retain the highest combined primary and secondary scar counts, followed by the picks and cleavers. Primary flaking is most abundant on the handaxes (10 scars), whereas secondary shaping is most abundant on the pick and biface. An assessment of LCT flake negative termination types was largely uninformative.

The location of these flake scars shows that the majority of the LCT sample (n=8) is flaked bifacially. A single cleaver is unifacial and another is partly bifacial, thus showing that cleavers have multiple flaking patterns. To be expected the distribution of cortex is most common towards the base of the LCTs, with progressively more primary and secondary removals towards the medial and distal portions on both faces. This cortex, however, does not exceed 50% on any of the LCTs. Overall flaking patterns show that secondary flaking along edges is limited, which suggests a preference for tool shaping versus edge refinement.

A single handaxe shows the residues of three surface deposits, all of which appear to have been introduced onto the artefact surfaces post-excavation. Discontinuous rounding along the edges of the handaxe suggests possible use-wear damage.

The small sample of non-lithic material shows that bone is partially fossilised at Bernol Farm. A chemical analysis of this material could not be pursued due to the likely contamination of the samples by water. More abundant shell remains show good preservation but these are likely from more modern times.

4.4 Penhill Farm

4.4.1 Introduction

Excavation 1 at Penhill Farm has provided a large, extremely well-preserved lithic assemblage of 9904 pieces, including a large component of small flaking debris <20 mm (Table 4.4.1). As discussed in Chapter 3.3 excavations at this site were focused on careful sampling of the extremely rich artefact-bearing debris flow deposit, and our stratigraphic resolution for the upper 1.8 m of deposit is less refined. Although both deposits are colluvial by nature, results here will be grouped into two assemblages, one for the overlying colluvium (from the surface down to 1.8 m; n=1258, 12.7% of all material) and one for the debris flow (found beneath 1.8 m and down to 2.5 m; n=8646, 87.3% of all material; Table 4.4.1).

The colluvial assemblage also includes all lithic material obtained from the digger trench excavation nearby (n=233, 25<20 mm, 208>20 mm; see Fig. 3.2.12 and Chapter 3.3). The debris flow assemblage also contains a small sample of lithics that was obtained directly from the exposed deposit within the east face of the borrow pit (thus outside of the excavation, n=11, all >20 mm; see Fig. 3.2.15).

Contextual data by depth will not be presented for the colluvial assemblage but will be for the debris flow; however, only artefacts where the specific spit depth was recorded will be included in this analysis. As a result the sample discussed above (n=11) from outside the excavation will not be included, along with artefacts that were obtained from wall cleans and surface sweeps (poor contexts) within Excavation 1 (n=65, 24<20 mm, 41>20 mm). A final assemblage of 8570 pieces (4742<20 mm, 3828>20 mm) will therefore be used in the debris flow assemblage analysis by depth.

In the following typological and technological sections, no data will be presented by depth due to the nature of the deposit (see following site context discussion). A detailed analysis of the two assemblages is presented in the technological data section.

Non-lithic material is extremely scarce in Excavation 1 and the small fragments (i.e., bone and shell) that were preserved limited detailed analysis. Phytolith and pollen analysis was unsuccessful within Excavation 1 and from the nearby sample sites.

Table 4.4.1. Penhill Farm assemblage samples.

Penhill Farm	Sample		
Assemblage	<20 mm	>20 mm	Total
Colluvium	279	979	1258
Debris flow	4767	3879	8646
			9904

4.4.2 Site context

Results for the particle size distribution of sediments will be presented first, followed thereafter by contextual data that relates specifically to the Excavation 1 assemblages. Dating results are discussed at the end of this section.

4.4.2.1 Sediment PSD analysis

These results are grouped together according to five main deposit types, namely: alluvium (Fig. 4.4.1), debris flow sediment (Fig. 4.4.2), colluvium (Fig. 4.4.3), channel flow sediment (Fig. 4.4.4) and crushed bedrock (Fig. 4.4.5; see also Table 3.5.2 and Figs. 3.5.1-3.5.7).

The alluvium is dominated by medium silt to fine sands (Fig. 4.4.1). Those that are the most sorted include samples 28, 39 and 41 (borrow pit alluvium; see Fig. 3.5.5), all of which peak in the coarse silt to very fine sand size classes (7.9-9%); these samples also retain the least amount of fine (clay to medium silt) and coarser sediment (>100 microns). Trimodal distributions can be seen in samples 1 and 3 with peaks in the very fine silt, coarse silt and very fine sand size classes, respectively. The distribution curves for samples 1 and 3 are similar, perhaps due to the close proximity of the two samples. Bimodal distributions occur in samples 14, 19, 28 and 39 and the remaining samples are all unimodal. These unimodal samples have similar size distribution curves and the largest mode occurs between 50-200 microns (coarse silt to fine sand).

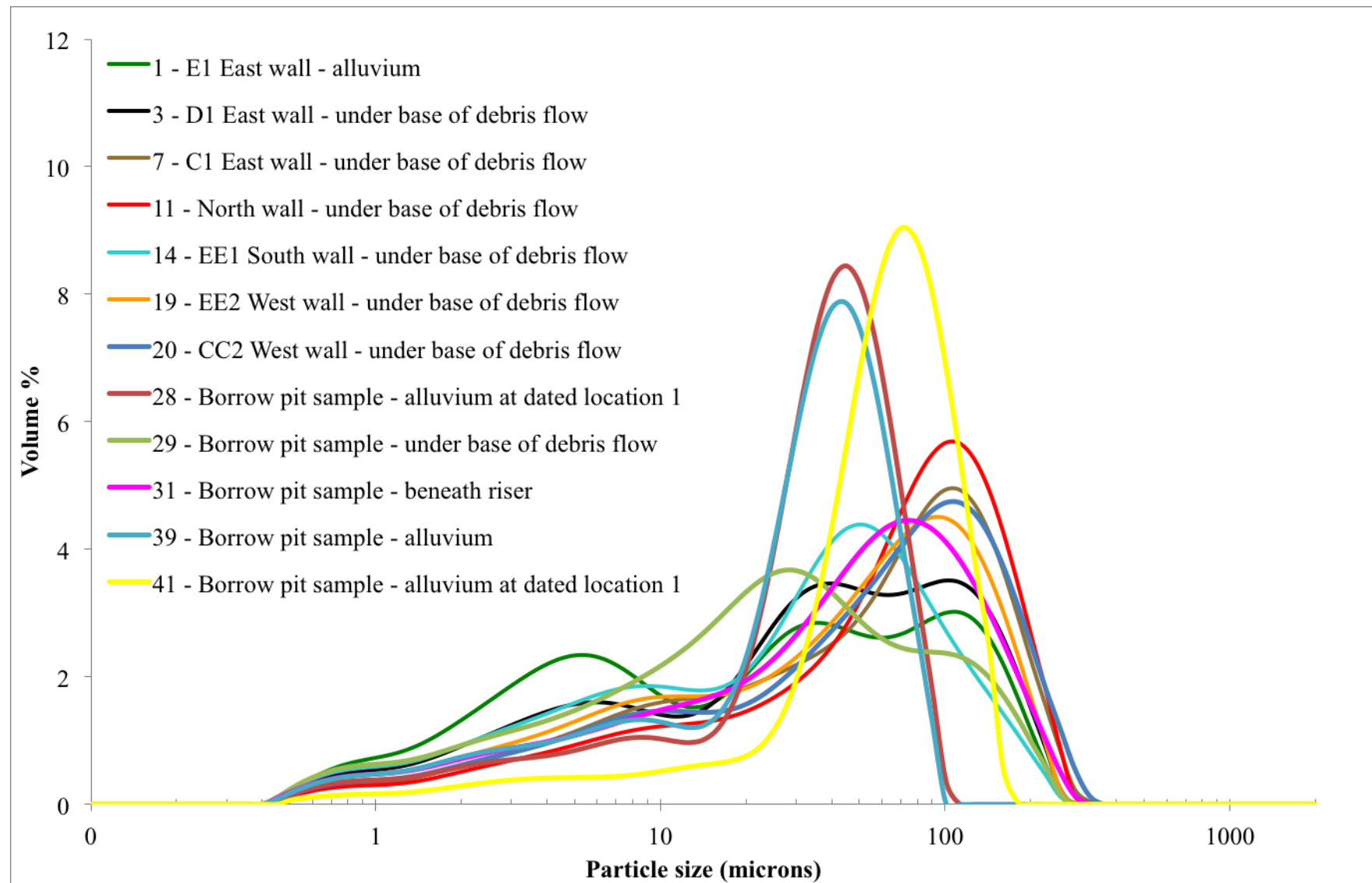


Figure 4.4.1. Particle size distribution for the alluvium.

The debris flow sediment is poorly sorted (Fig. 4.4.2). The grain size distribution curves for all the samples are largely similar, except for samples 16 and 22, both of which occur within fine sediments located between horizons within the debris flow (see Figs. 3.5.3 & 3.5.4). The latter sample (22) has a trimodal distribution, with peaks in the very fine silt, medium to coarse silt, and fine sand size classes, respectively. The highest percentage of fine sediment is found in samples 16 and 22 (clay to fine silt). Bimodal distributions occur in samples 4, 30 and 32. For all the samples the greatest percentage of sediment occurs from 20-200 microns (medium silt to fine sand).

Grain size distribution curves for the colluvial sediments (Fig. 4.4.3) are similar to those presented for the debris flow (Fig. 4.4.2), illustrating a lack of grain sorting. However, one sample from the cut and fill colluvium (26) indicates greater sorting (6.6% peak in the very fine sand size class). The remaining samples are all unimodal to bimodal in distribution, all of which show an extremely low percentage of fine clays. The highest percentage of sediment for all the samples occurs in the fine silt to fine sand size classes.

Sediment samples obtained from the channel flow features indicate a high level of grain sorting (Fig. 4.4.4), especially sample 23 (DD2 west wall). The three samples all retain a very low percentage of fine clays, and peak percentages occur from 40-150 microns (coarse silt to fine sand). The grain size distribution curves for samples 10 and 23 are notably similar, both of which have a bimodal distribution with a peak in the fine to medium silt size class (10-20 microns).

Bedrock samples provide an interesting mix of sediments, most of which are well-sorted (samples 36, 42, 43 and 45; Fig. 4.4.5). The distribution curves for samples 36, 43 and 45 are remarkably similar, all of which have a very low percentage of clay and very fine silt. These samples also have a bimodal distribution, with peaks in the fine to medium silt and coarse silt to very fine sand size classes, respectively. Sample 43, however, differs in its higher percentage of sediment that is larger than 200 microns, also evident in sample 44. Sample 42 has its highest percentage (6.4%) of sediment in the medium silt size class, and the bimodal distribution evident in sample 44 illustrates peaks in the coarse silt (4.1%) and fine sand (3.3%) size classes.

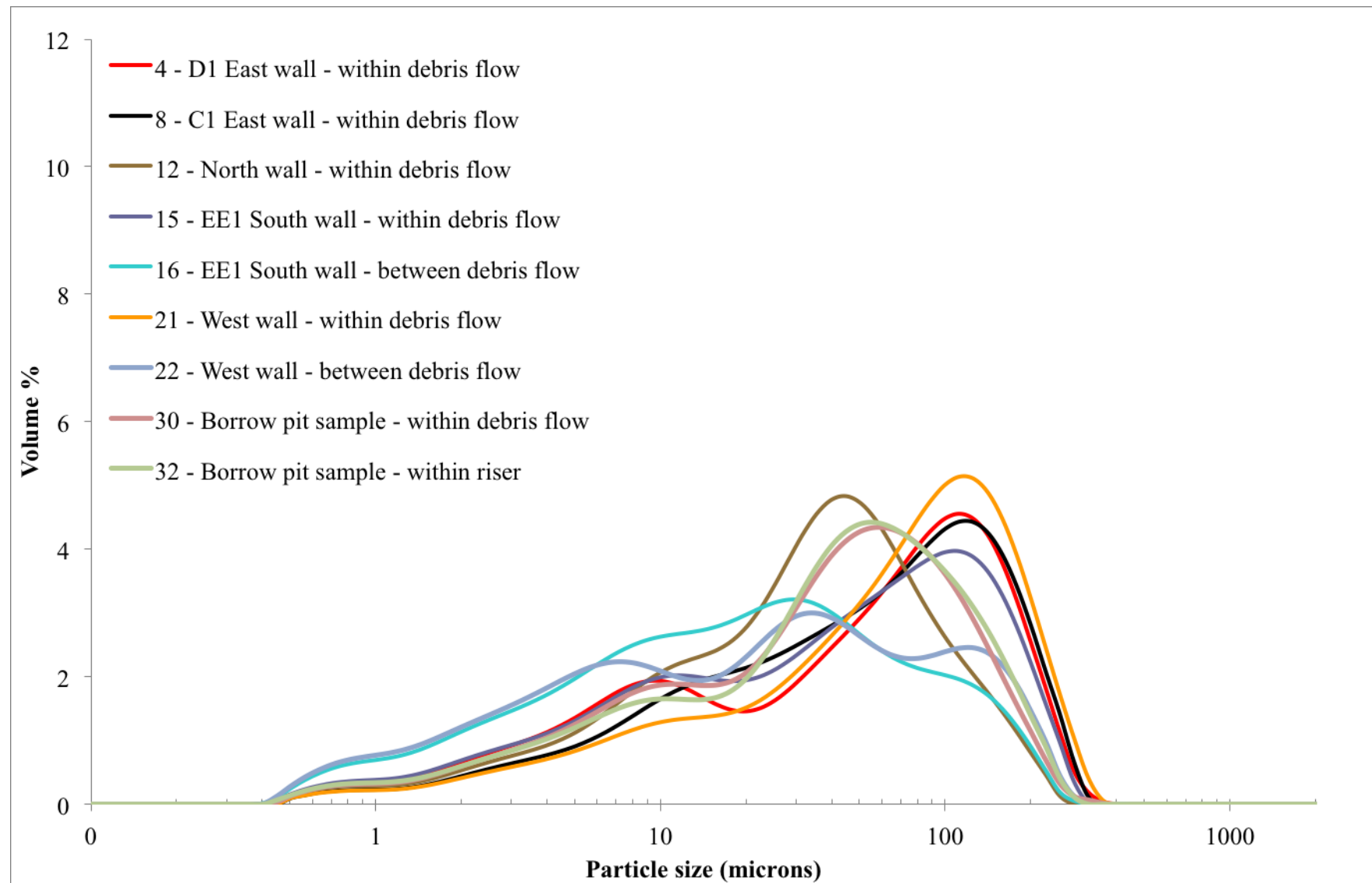


Figure 4.4.2. Particle size distribution for the debris flow sediment.

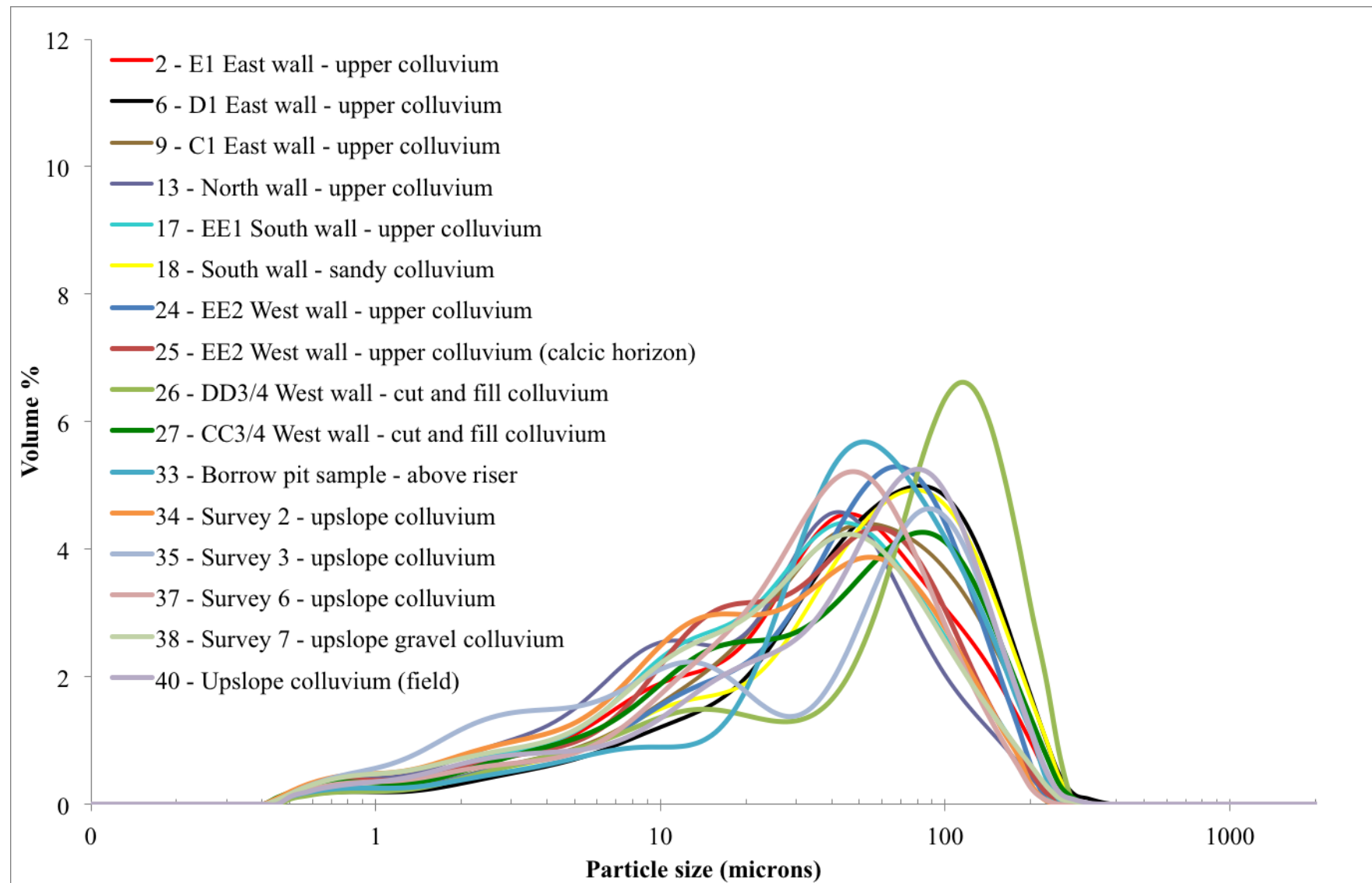


Figure 4.4.3. Particle size distribution for the colluvium.

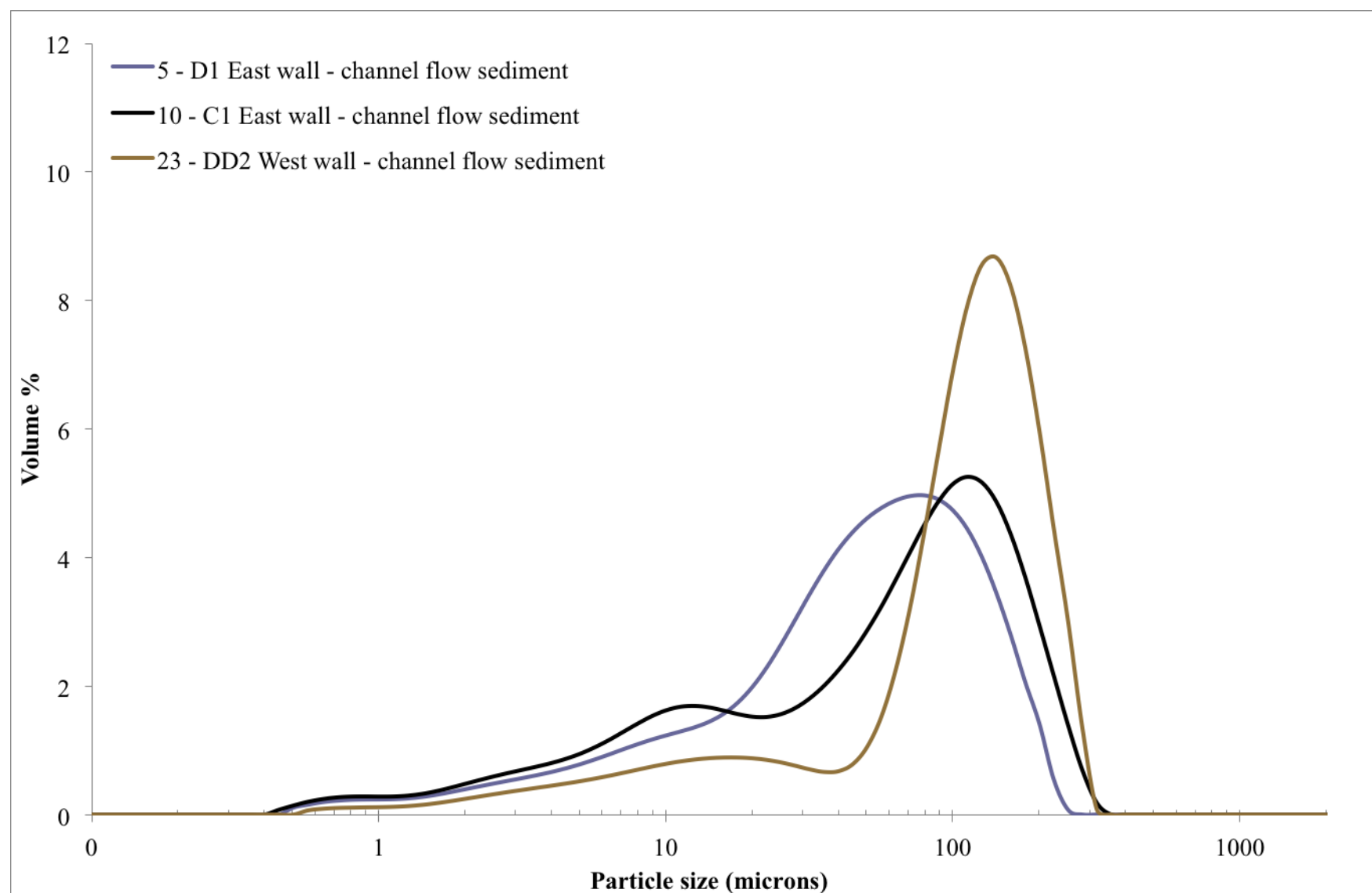


Figure 4.4.4. Particle size distribution for the channel flow sediment.

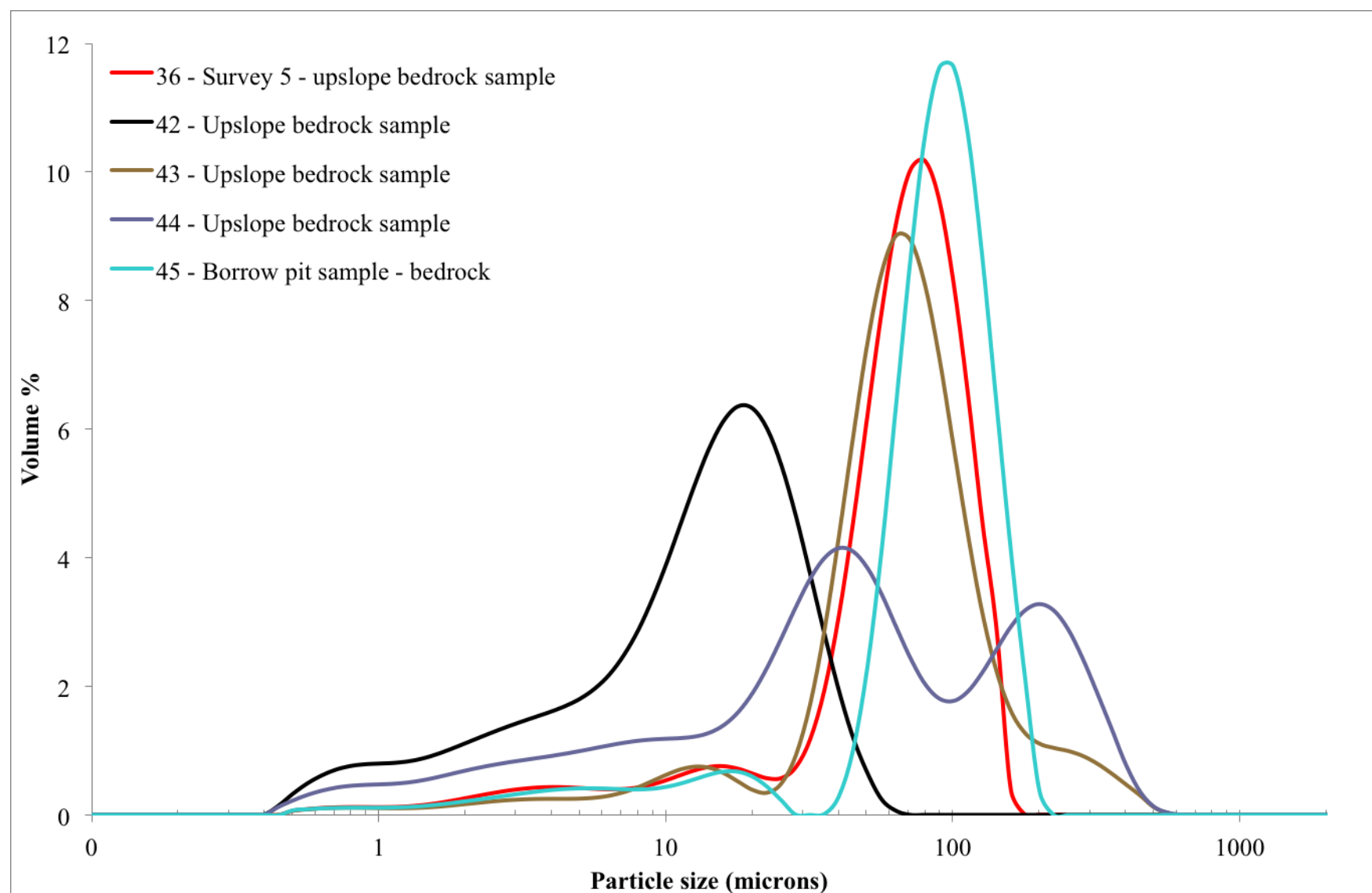


Figure 4.4.5. Particle size distribution for the bedrock samples.

Summary graphs are presented in Figures 4.4.6-4.4.9. By grouping the samples according to the main deposit types one can see that the bedrock (brown), alluvium (red) and channel flow sediments (yellow) account for the most well-sorted samples. The alluvium also has the highest representation of fines (clays to fine silts; Fig. 4.4.6). The colluvium and debris flow sediments have notably similar distribution curves, highlighting their poor sorting. Both the alluvium and colluvium overlap in the coarser fraction, showing that their peaks are similarly distributed (Fig. 4.4.6). The primary defining feature in these sediments is the percentage of fines.

By excluding the bedrock and channel flow samples, Figure 4.4.7 clearly indicates the greater level of sorting within the alluvium. The high percentage of fine material (clays) is also clear. Figures 4.4.8 and 4.4.9 indicate that both the debris flow and colluvial sediments have a lower percentage of fines (clays) and the grain size distribution curves are largely similar (poorly sorted).

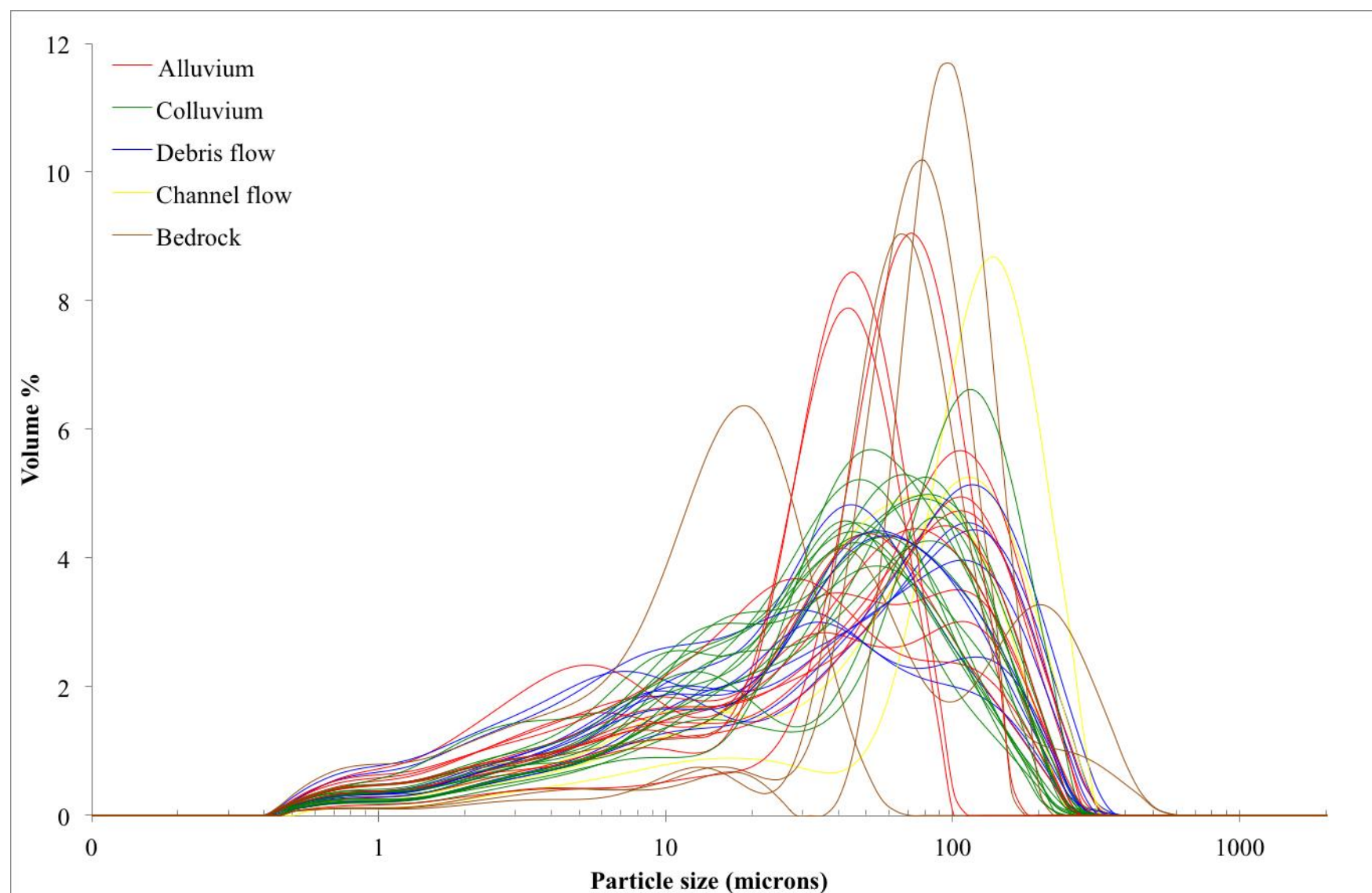


Figure 4.4.6. Grain size distribution curves for the main deposits (grouped and colour coded).

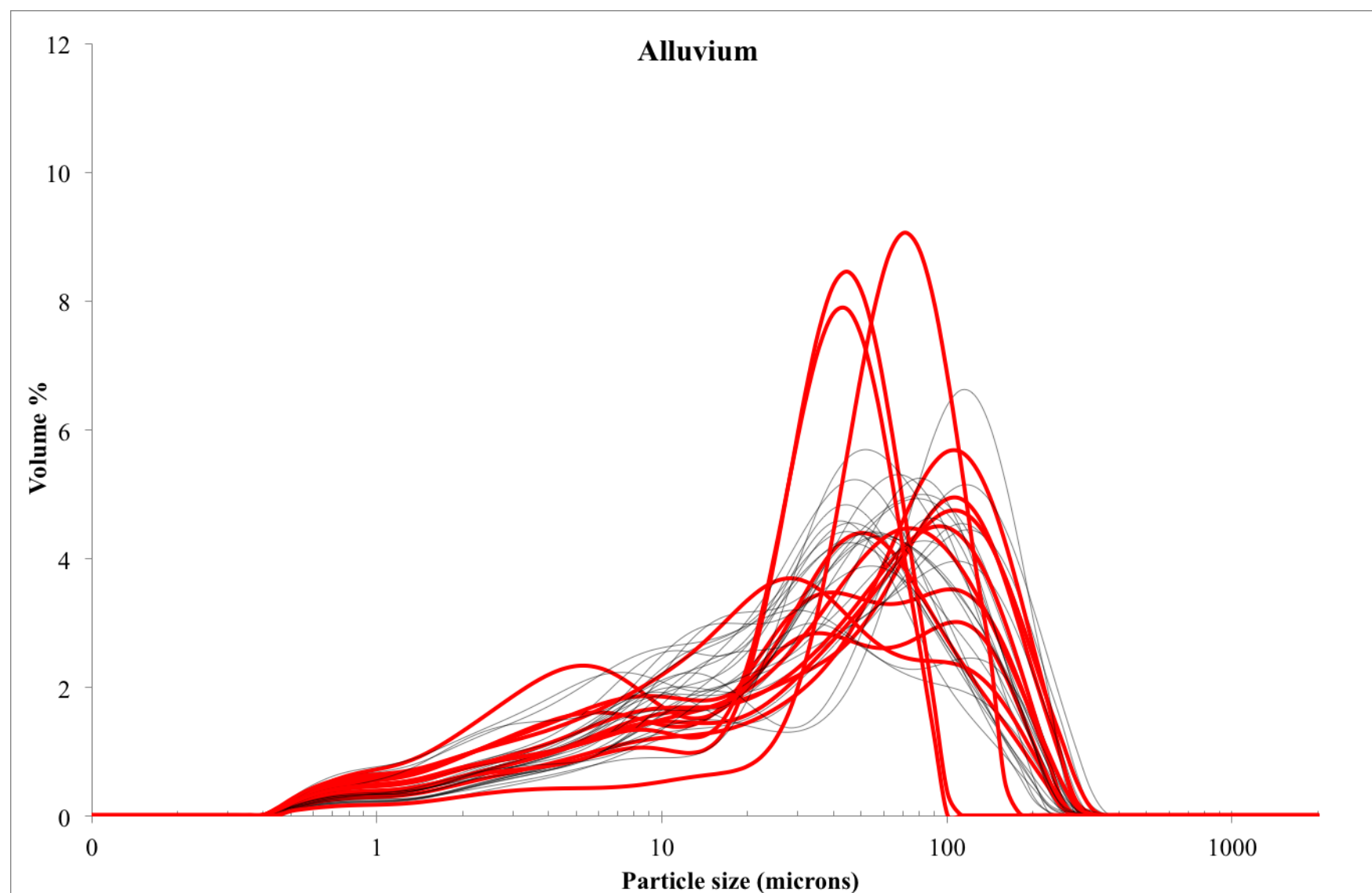


Figure 4.4.7. Alluvium grain size distribution curves in red (over the colluvium and debris flow sediments in grey).

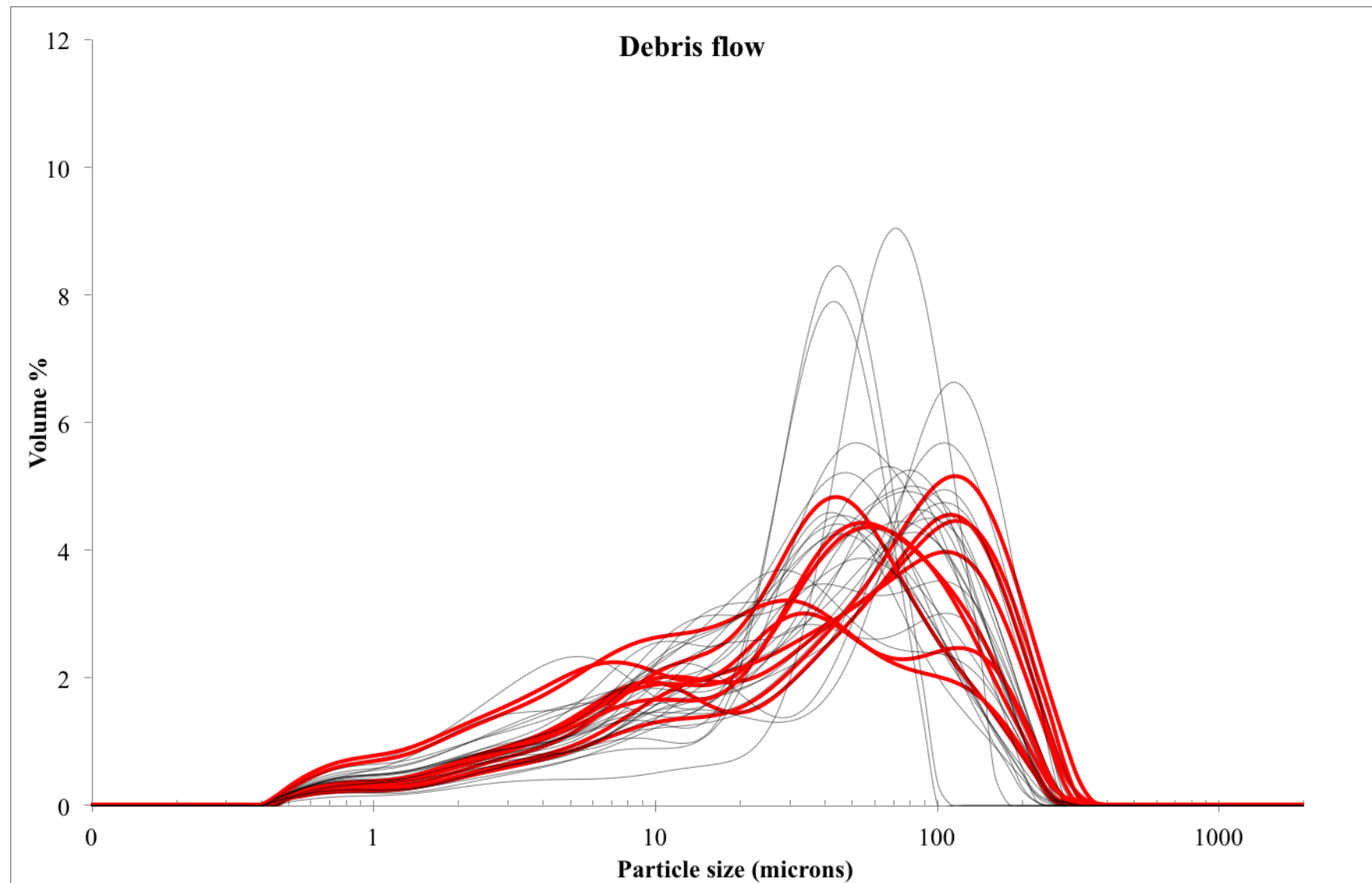


Figure 4.4.8. Debris flow grain size distribution curves in red (over the colluvium and alluvium in grey).

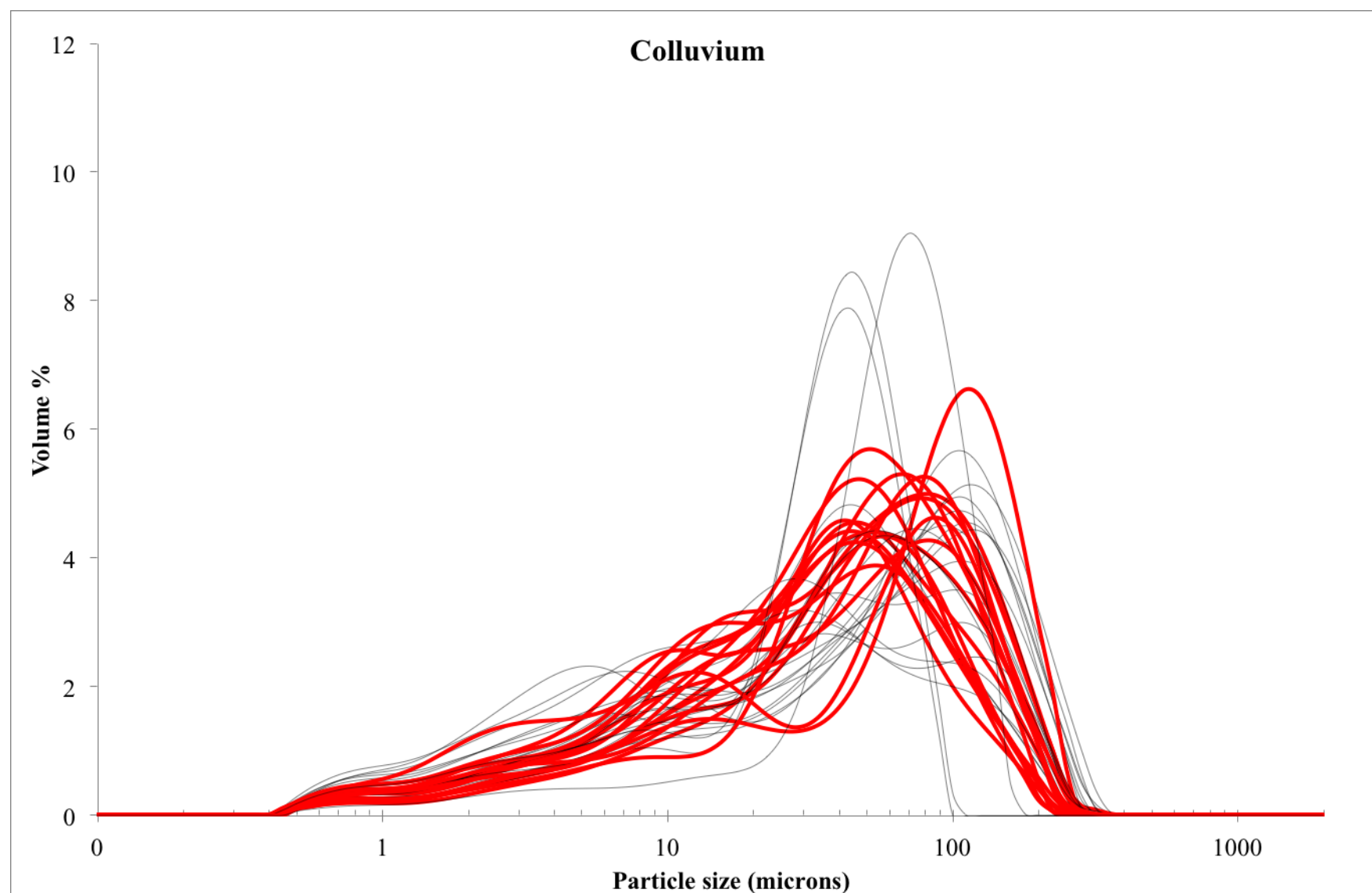


Figure 4.4.9. Colluvium grain size distribution curves in red (over the debris flow and alluvial sediments in grey).

4.4.2.2 Artefact size distributions

Artefact sizes for the Penhill Farm assemblages are presented in Tables 4.4.2 and 4.4.3 and Figures 4.4.10 and 4.4.11 Both assemblages have a full range of artefact sizes represented, except for pieces in the <180 and <190 mm size categories for the colluvial and debris flow assemblages, respectively (Tables 4.4.2 & 4.4.3).

The greatest quantity of material for the colluvial assemblage falls within the <30 mm size category (n=296, 23.5%; Table 4.4.2; Fig. 4.4.10). Collectively SFD <20 mm in size (n=279) only accounts for 22% of the assemblage. Thereafter, the greatest quantity of material occurs in the size categories larger than 30 mm and smaller than 100 mm (n=653, 52%). A limited quantity of material occurs that is larger than 100 mm (n=29, 2%). Only a single artefact exceeds 200 mm in length (Table 4.4.2).

Table 4.4.2. Colluvial assemblage artefact size distribution.

Artefact size	Number	Percentage
<10 mm	51	4.1
<20 mm	228	18.1
<30 mm	296	23.5
<40 mm	237	18.8
<50 mm	164	13.0
<60 mm	82	6.5
<70 mm	76	6.0
<80 mm	35	2.8
<90 mm	34	2.7
<100 mm	25	2.0
<110 mm	9	0.7
<120 mm	6	0.5
<130 mm	3	0.2
<140 mm	4	0.3
<150 mm	1	0.1
<160 mm	2	0.2
<170 mm	1	0.1
<180 mm	0	0
<190 mm	2	0.2
<200 mm	1	0.1
>200 mm	1	0.1
Total	1258	100

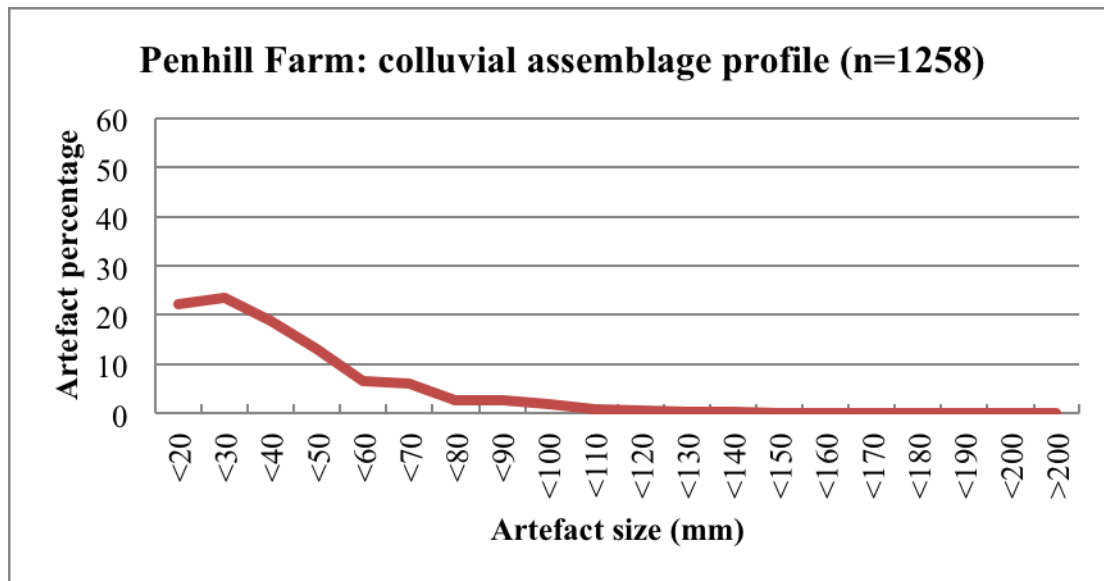


Figure 4.4.10. Artefact size distribution for the colluvial assemblage.

The underlying debris flow assemblage shows a contrasting pattern in artefact size distributions (Table 4.4.3; Fig. 4.4.11). Most noticeable is the high quantity of material that occurs in both the <10 and <20 mm size categories (n=4767, 55%). Collectively, over 73% of the entire assemblage is less than 30 mm in size (n=6321) and a high percentage of the remaining assemblage (n=2116, 24.5%) occurs that is larger than 30 mm and smaller than 80 mm. Artefacts larger than 100 mm provide only a small percentage (1%, n=113) of the total sample.

Artefact size by depth for the debris flow assemblage is shown in Figure 4.4.12. From this only minor variation can be seen in the size distribution of material across the excavated levels, and no sorting or grading occurs. Although there is some variation, notably between 180-190 cm, thereafter from 190-250 cm the size distribution of lithics appears to remain similar for all of the depths. SFD ranges from 52-62% for these levels, interestingly showing a trend for the lowest quantity (marginally) towards the upper surface of the debris flow and the greatest quantity towards the base. However, notably low SFD percentages also occur towards the middle of the flow between 210-225 cm (52-53%), thus suggesting that no trend, but rather variation, occurs between the depths.

Table 4.4.3. Debris flow assemblage artefact size distribution.

Artefact size	Number	Percentage
<10 mm	1952	22.6
<20 mm	2815	32.6
<30 mm	1554	18.0
<40 mm	848	9.8
<50 mm	525	6.1
<60 mm	363	4.2
<70 mm	230	2.7
<80 mm	150	1.7
<90 mm	55	0.6
<100 mm	41	0.5
<110 mm	33	0.4
<120 mm	29	0.3
<130 mm	13	0.2
<140 mm	14	0.2
<150 mm	6	0.1
<160 mm	4	0.05
<170 mm	1	0.01
<180 mm	3	0.03
<190 mm	0	0
<200 mm	5	0.1
>200 mm	5	0.1
Total	8646	100

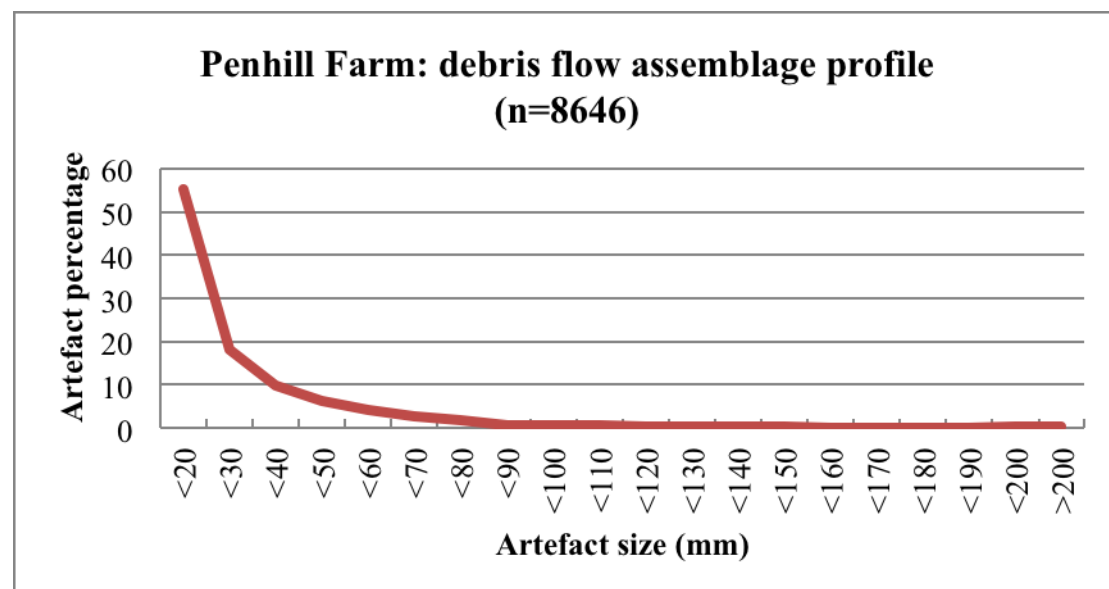


Figure 4.4.11. Debris flow assemblage artefact size distribution.

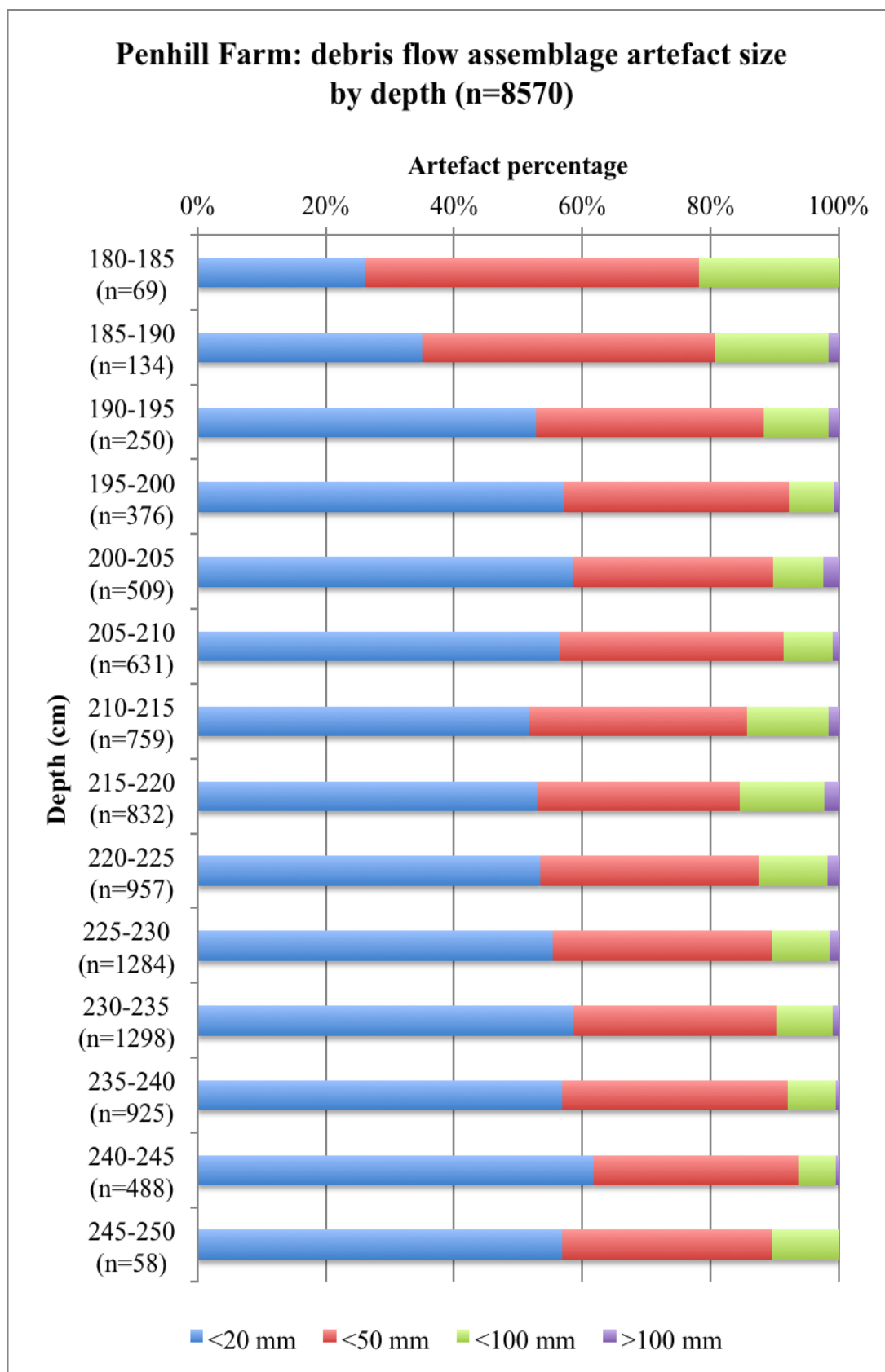


Figure 4.4.12. Artefact size by depth for the debris flow assemblage.

4.4.2.3 Artefact condition and raw material data

These data for Penhill Farm are presented in Tables 4.4.4 (colluvial assemblage) and 4.4.5 (debris flow assemblage) and Figures 4.4.13-4.4.18. The ≥ 20 mm colluvial assemblage is dominated by fine-grained quartzites (n=828, 84.6%) and only a limited number of artefacts is produced on coarser-grained types (n=32, 3.2%; Table 4.4.4). Siltstone and hornfels account for 11.2% of the total assemblage, and lava, silcrete and claystone were also utilised during lithic production.

By condition all raw materials have the highest frequency of pieces in the fresh/unabraded state (Table 4.4.4). Overall this accounts for 69.1% of the total sample (n=676). However, a high amount of pieces (n=261, 26.7%) retains a slightly abraded condition, most notably 26% (n=217) of the fine quartzite sample, 36% (n=23) of the siltstone sample, and 39% (n=12) of the coarse quartzite sample. Only 34 pieces retain a heavily abraded/rolled condition, the majority of which comprise of siltstone and fine quartzite. Weathered artefacts are few, yet 13% (n=6) of the hornfels sample accounts for 75% of the total weathered sample (n=8).

Table 4.4.4. Raw material and condition data for the colluvial assemblage. Bracketed values indicate percentages. Quartzite (qzte) is divided into coarse (C) and fine (F) types.

Raw material	Artefact condition				Total	Varnished
	Fresh/unabraded	Slightly abraded	Heavily abraded/rolled	Weathered		
Quartz	0	0	0	0	0	0
C Qzte	18 (1.8)	12 (1.2)	1 (0.1)	0	31 (3.2)	1 (0.1)
F Qzte	587 (60)	217 (22.2)	24 (2.5)	0	828 (84.6)	19 (1.9)
Siltstone	33 (3.4)	23 (2.3)	7 (0.7)	1 (0.1)	64 (6.5)	0
Silt-qzte	0	0	0	0	0	0
Hornfels	31 (3.2)	8 (0.8)	1 (0.1)	6 (0.6)	46 (4.7)	0
CCS	0	0	0	0	0	0
Lava	1 (0.1)	0	0	0	1 (0.1)	0
Silcrete	3 (0.3)	0	0	0	3 (0.3)	0
Claystone	3 (0.3)	1 (0.1)	1 (0.1)	1 (0.1)	6 (0.6)	0
Indet.	0	0	0	0	0	0
Total	676 (69.1)	261 (26.7)	34 (3.5)	8 (0.8)	979 (100%)	20 (2)

Varnished pieces comprise of 19 fine quartzite artefacts and a single coarse quartzite artefact, collectively 2% of the entire sample (Table 4.4.4).

The complete colluvial assemblage (n=1258) raw material distribution is shown by Figure 4.4.13. These distributions are similar to those presented in Table 4.4.4; however, quartz comprises 0.2% of this total sample. Collectively, quartzites account for 88.1% of the colluvial assemblage. No artefacts are produced on silt-quartzite and crypto-crystalline material.

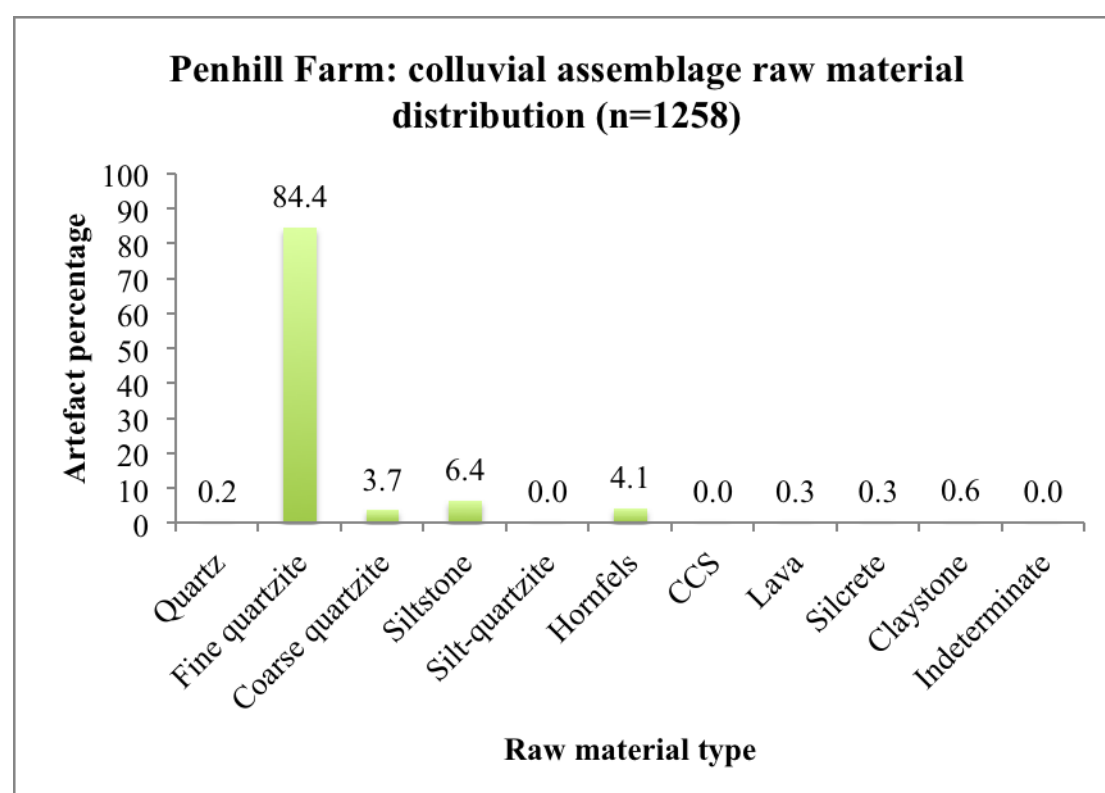


Figure 4.4.13. Raw material percentages for the colluvial assemblage.

The debris flow assemblage (Table 4.4.5) shows a similar preference for fine-grained quartzites, and crypto-crystalline materials are again absent from the sample. Silt-quartzite is present, however, and accounts for 0.2% of the ≥ 20 mm sample (n=8). Siltstone, coarse quartzites and hornfels also account for notable (ranging between 5.3-7.7%) samples, collectively 18.4% (n=715) of the total sample.

By condition the debris flow artefacts are better preserved than those in the overlying colluvial assemblage (Table 4.4.5). Collectively 96.7% (n=3752) of the assemblage is fresh/unabraded to only slightly abraded, and heavily abraded types only account for

1.2% of the sample (n=46). Interestingly though the percentage of weathered pieces is higher for this assemblage, accounting for 2.1% of the total sample (n=81). Once again hornfels provides the highest proportion of this weathered material (n=43, 53%), followed thereafter by fine quartzite and siltstone (n=16, 20% each). A total of 161 pieces (4.2% of the total sample) retained some form of surface varnish, which is most evident on the fine quartzite sample (n=146, 91%). Coarse quartzite, siltstone, silt-quartzite, hornfels and claystone raw materials account for the remaining varnished sample (collectively 15 pieces, 9%).

Table 4.4.5. Raw material and condition data for the debris flow assemblage. Bracketed values indicate percentages. Quartzite (qzte) is divided into coarse (C) and fine (F) types.

Raw material	Artefact condition				Total	Varnished
	Fresh/unabraded	Slightly abraded	Heavily abraded/rolled	Weathered		
Quartz	0	0	0	0	0	0
C Qzte	147 (3.8)	53 (1.4)	5 (0.1)	2 (0.1)	207 (5.3)	9 (0.2)
F Qzte	2498 (64.4)	559 (14.4)	28 (0.7)	16 (0.4)	3101 (79.9)	146 (3.8)
Siltstone	212 (5.5)	64 (1.6)	7 (0.2)	16 (0.4)	299 (7.7)	2 (0.1)
Silt-qzte	7 (0.2)	1 (0.03)	0	0	8 (0.2)	1 (0.03)
Hornfels	122 (3.1)	40 (1)	4 (0.1)	43 (1.1)	209 (5.4)	1 (0.03)
CCS	0	0	0	0	0	0
Lava	7 (0.2)	2 (0.1)	0	0	9 (0.2)	0
Silcrete	3 (0.1)	2 (0.1)	1 (0.03)	2 (0.1)	8 (0.2)	0
Claystone	27 (0.7)	8 (0.2)	1 (0.03)	2 (0.1)	38 (1)	2 (0.1)
Indet.	0	0	0	0	0	0
Total	3023 (77.9)	729 (18.8)	46 (1.2)	81 (2.1)	3879 (100%)	161 (4.2)

The raw material distribution for the total debris flow sample (n=8646) is shown in Figure 4.4.14 and these trends are similar to those presented in Table 4.4.5. Quartzite, specifically fine quartzite, is clearly the most favoured raw material type (79.6%), followed thereafter by siltstone (8.2%). In contrast to the colluvial assemblage, hornfels (4.2%) is less abundant in relation to coarse quartzites (5.5%) even though it is a finer-grained raw material. Small samples of quartz, silt-quartzite, lava, silcrete, and claystone all occur (collectively 2.4%), and crypto-crystalline materials are absent from the assemblage.

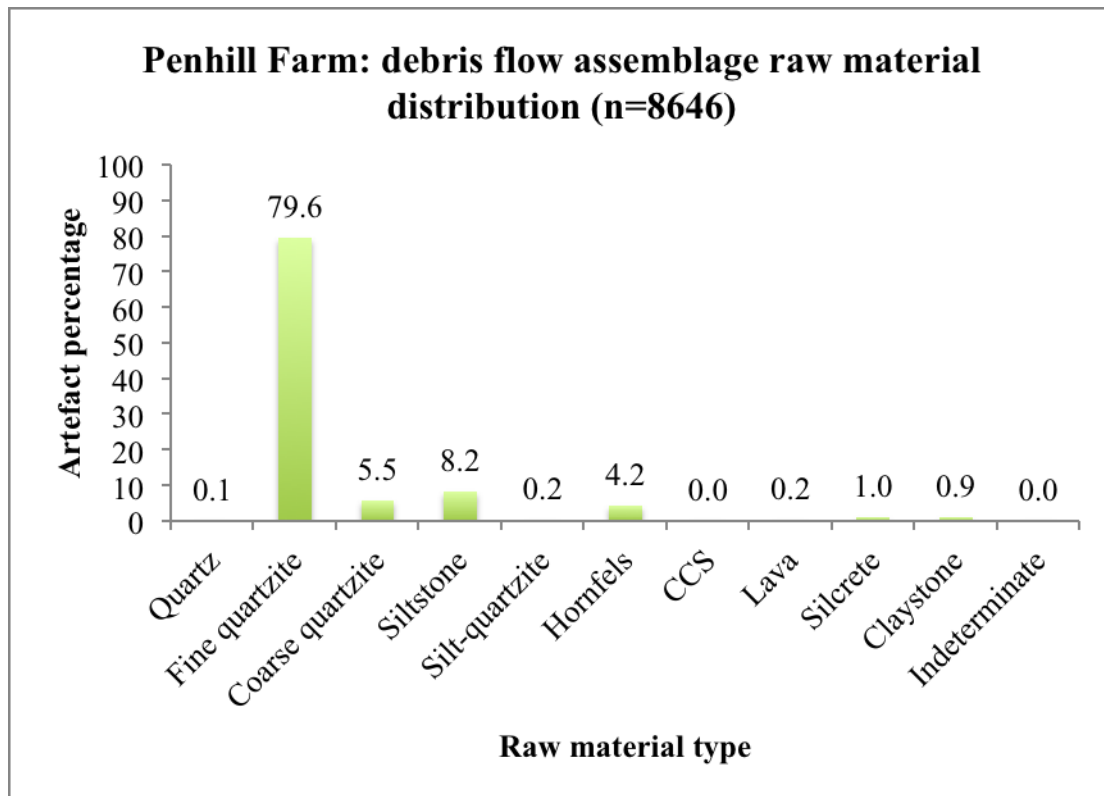


Figure 4.4.14. Debris flow assemblage raw material distribution.

Figure 4.4.15 illustrates that only minor variation occurs by depth in raw material distributions within the debris flow assemblage. Quartzites account for over 80% of the raw materials across all the excavated depths (except for level 245-250 cm, 79%), and siltstone and hornfels are the only other raw materials that can be found across these depths as well (ranging between 4-12% for the former and 2.6-6% for the latter). The remaining raw materials have a very limited distribution throughout the excavated depths. Lava appears more abundant between 180-200 cm and claystone only occurs from 195-245 cm. Interestingly, the highest percentage (5%) of silcrete occurs at the base of the debris flow (245-250 cm).

Artefact preservation states for the ≥ 20 mm colluvial and debris flow assemblage samples are presented in Figures 4.4.16 and 4.4.17. From these data it is clear that both assemblages retain a large percentage of fresh/unabraded material, collectively 69% for the colluvial assemblage and 78% for the debris flow (Figs. 4.4.16 & 4.4.17); artefact condition is notably fresher for the latter (differing by 9%). In addition to this an 8% percentage difference occurs, in the amount of slightly abraded material,

between the two assemblages (lowest for the debris flow assemblage at 19%; Figs. 4.4.16 & 4.4.17).

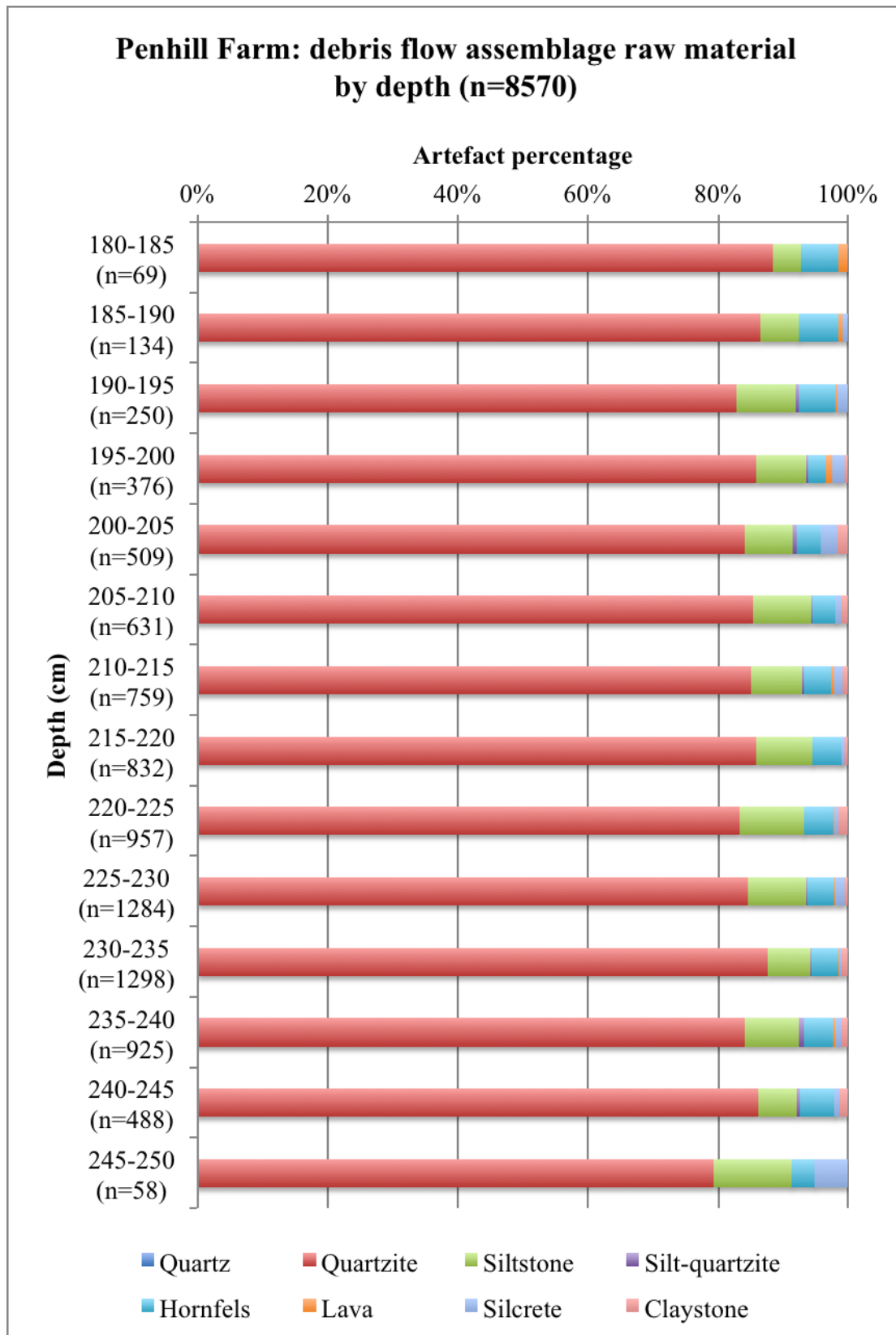


Figure 4.4.15. Debris flow assemblage raw material changes, by depth (combined <20 mm and ≥20 mm samples).

Most important is the difference in heavily abraded/rolled material between the assemblages. Although this material only accounts for small percentages of the total samples, the highest (3%) occurs in the colluvial assemblage (Fig. 4.4.16). Interestingly though the percentage of weathered pieces is highest for the debris flow assemblage at 2% of the total sample (Fig. 4.4.17). Collectively, 31% of the colluvial assemblage artefacts retain a modified exterior condition, in contrast to the 22% of the total debris flow sample (Figs. 4.4.16 & 4.4.17).

Artefact condition by depth for the debris flow assemblage is presented in Figure 4.4.18, showing that only minor variation occurs across the excavated levels. However, these data clearly illustrate the abundance of fresh/unabraded pieces throughout. The highest percentage (88%) of fresh/unabraded pieces occurs in the final spit (245-250 cm), with the lowest (73%) between 220-225 cm. Where a lower percentage of fresh/unabraded pieces occur the percentage of slightly abraded pieces increases, most evident from 205-235 cm, where slightly abraded pieces range from 18-23%.

Most interesting though is the distribution of heavily abraded/rolled and weathered pieces, both of which occur throughout the excavation from 185-240 cm (Fig. 4.4.18). However, both of these types are completely absent from the final spit of 245-250 cm (although the small sample size must be considered here), and only weathered pieces (in conjunction with fresh/unabraded and slightly abraded pieces) are found at 180-185 and 240-245 cm. The highest percentage (4%) of weathered pieces occurs at the top of the debris flow (180-185 cm), along with a notable percentage (3%) at 210-215 cm. Also at this depth (210-125 cm) occurs the highest percentage of heavily abraded/rolled pieces (2%).

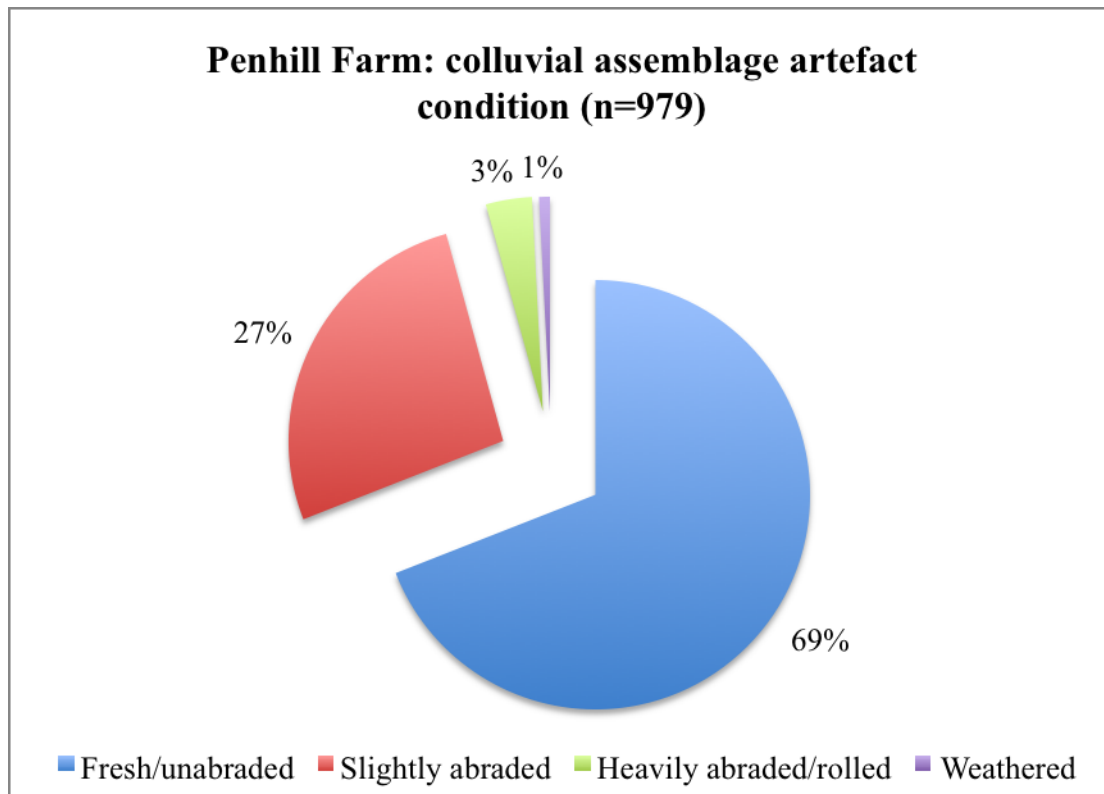


Figure 4.4.16. Artefact condition for the ≥ 20 mm colluvial sample.

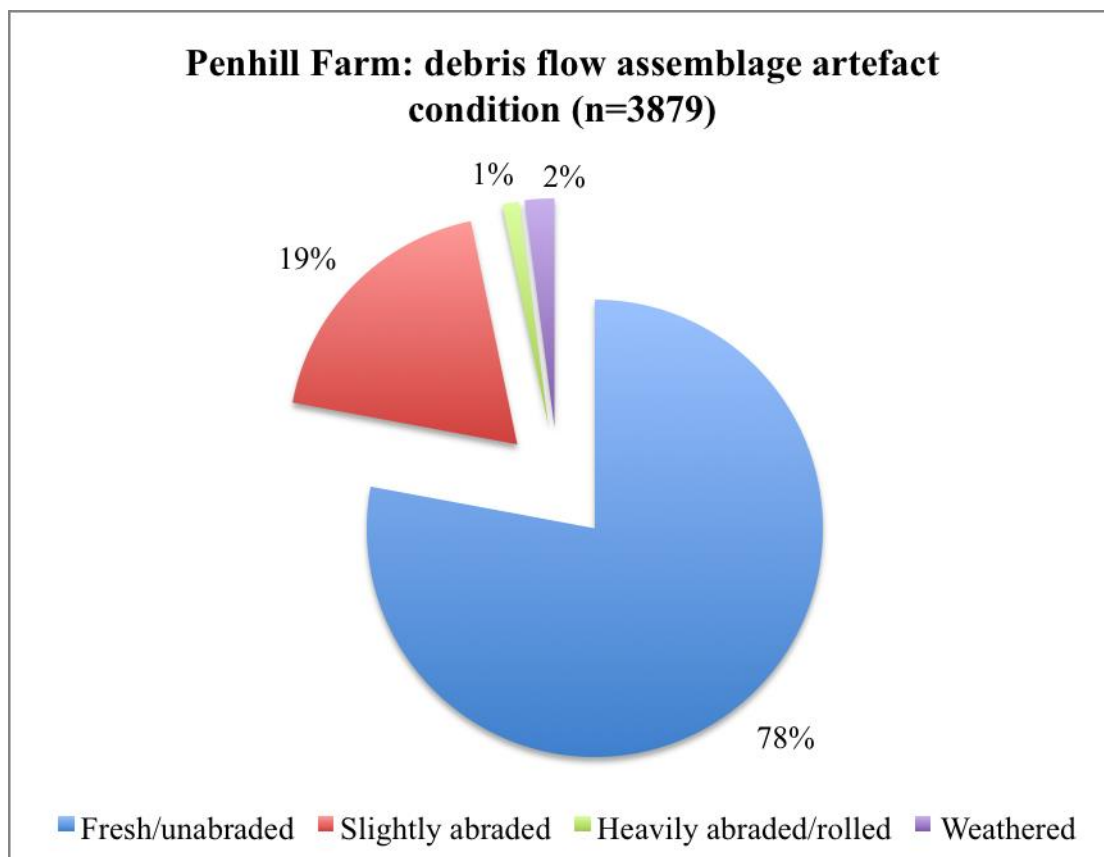


Figure 4.4.17. Artefact condition for the ≥ 20 mm debris flow sample.

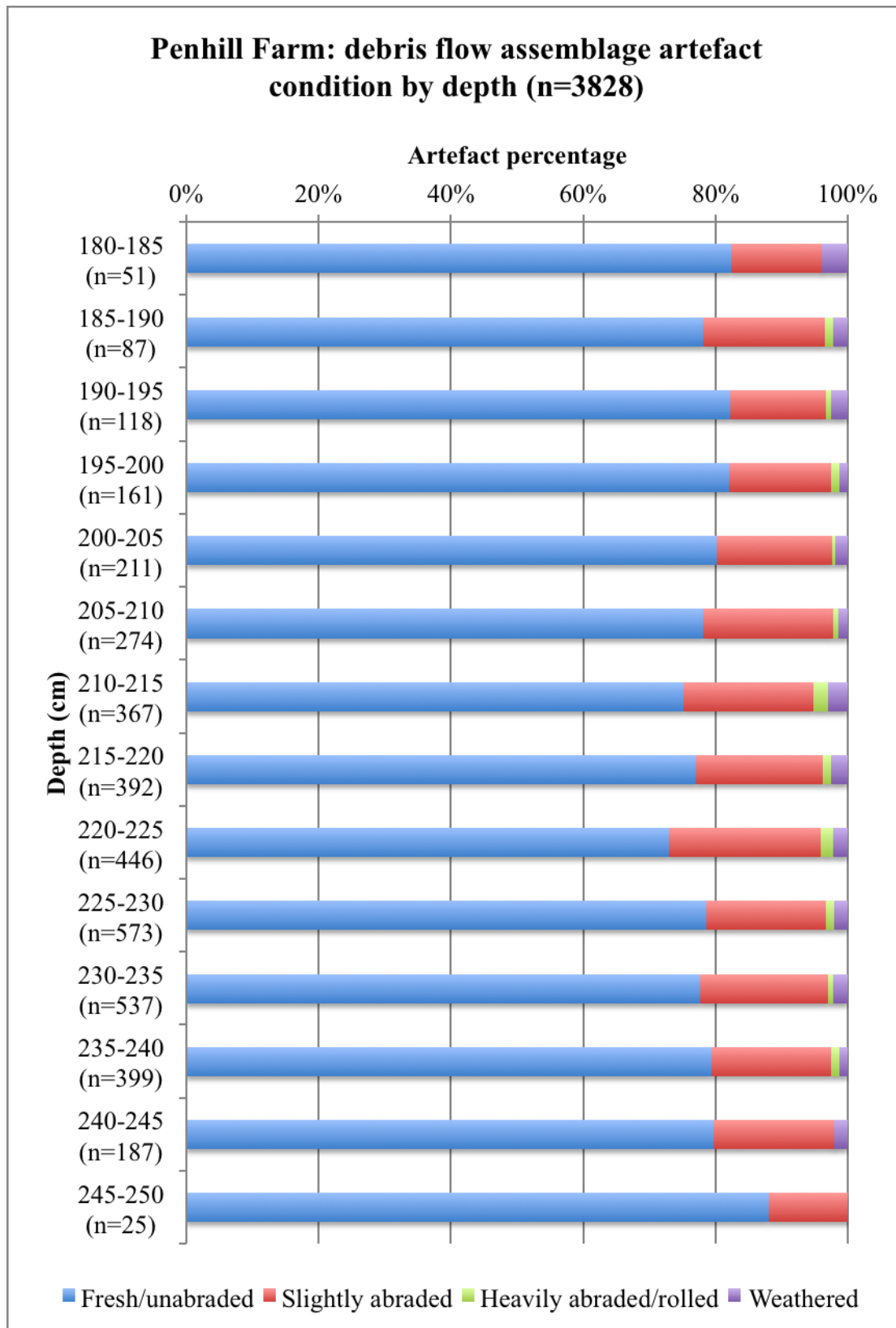


Figure 4.4.18. Artefact condition for the ≥ 20 mm debris flow sample, by depth.

4.4.2.4 Artefact spatial distributions

Spatial data is exclusively from the debris flow assemblage. The numbers of artefacts, by depth and square, are shown in Figures 4.4.19 and 4.4.20. By depth it is clear that artefact numbers increase, up until 230-235 cm, thereafter decreasing towards the final spit depth of 245-250 cm. The lowest numbers of artefacts are found between 180-185 and 245-250 cm ($n=69$ and 58, respectively). Artefacts are most concentrated towards the middle to basal part of the debris flow, between depths 225-235 cm (collectively 2582 pieces).

By square, however, the number of artefacts for C1, D1 and E1 are lowest for all the excavated squares, in contrast to those numbers in CC1, CC2, DD1, DD2, EE1 and EE2 (Fig. 4.4.20). This shows that there is an increase in artefact numbers from east to west across the debris flow.

From north to south, a notable trend in artefact numbers is also evident (Fig. 4.4.20). Squares E1, EE1 and EE2 consistently have a lower number of artefacts than those found within squares C1, CC1 and CC2. However, all of these squares have lower artefact numbers than those from squares D1, DD1 and DD2, showing that artefact density is highest towards the middle of the excavated portion of the debris flow. This shows that the northern portion of the debris flow (squares C1, CC1 and CC2) and the southern portion of the debris flow (squares E1, EE1 and EE2) have increasing numbers of artefacts as one move towards the center squares (D1, DD1 and DD2).

The vertical and horizontal distribution of plotted artefacts is presented in Figures 4.4.21-4.4.26 ($n=1541$). By size there is no specific spatial arrangement of pieces across the excavation, in accordance with the nature of a debris flow deposit; all of the artefact size groups are well represented, randomly, across the entire excavation (Fig. 4.4.21). However, it is clear in squares E1 and C1 that a lower number of artefacts was plotted due to the discontinuous nature of the debris flow (especially clear in E1). This is evident in all the plan view plots (Figs. 4.4.21-4.4.23).

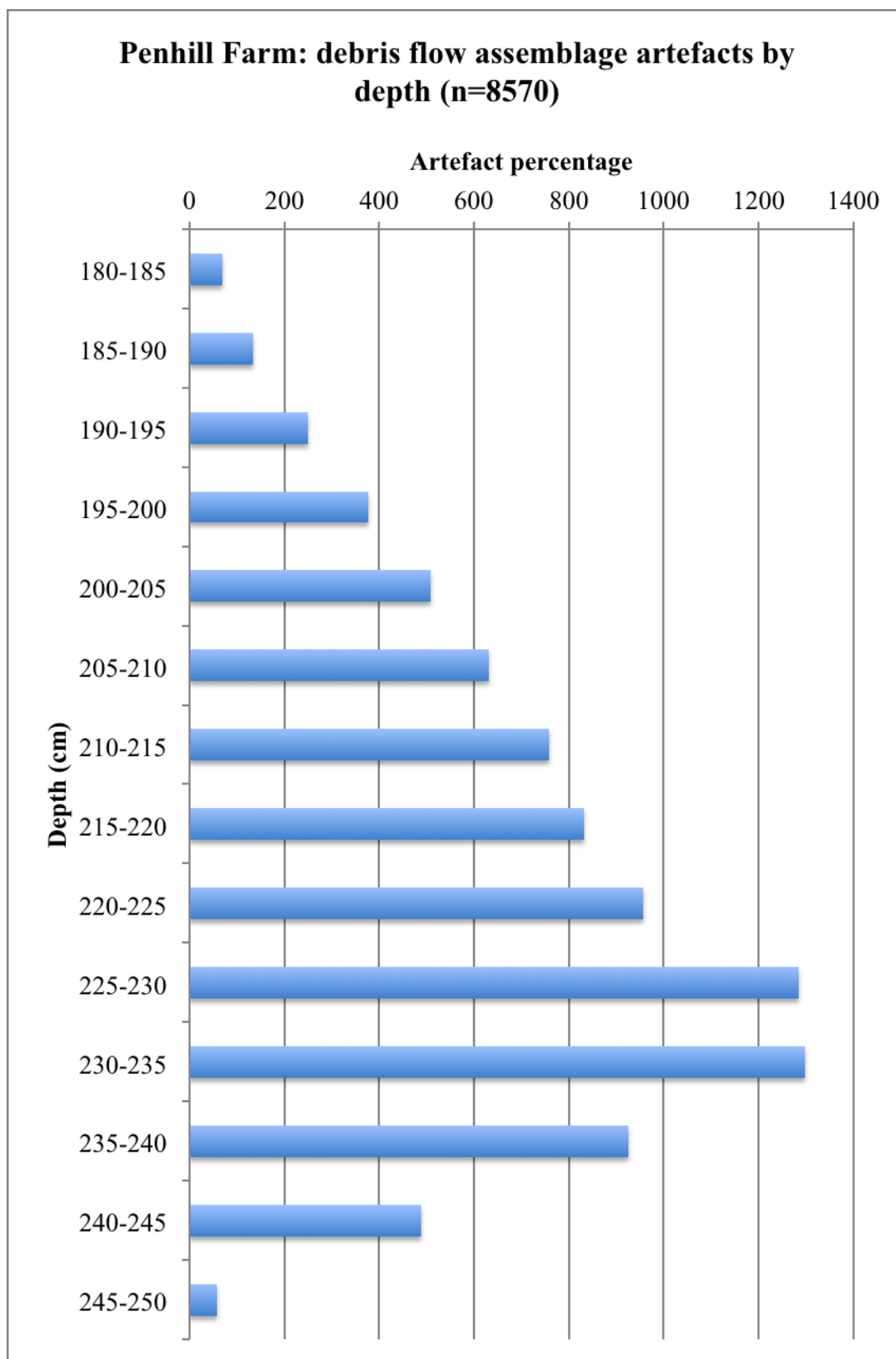


Figure 4.4.19. Number of artefacts by depth at Penhill Farm.

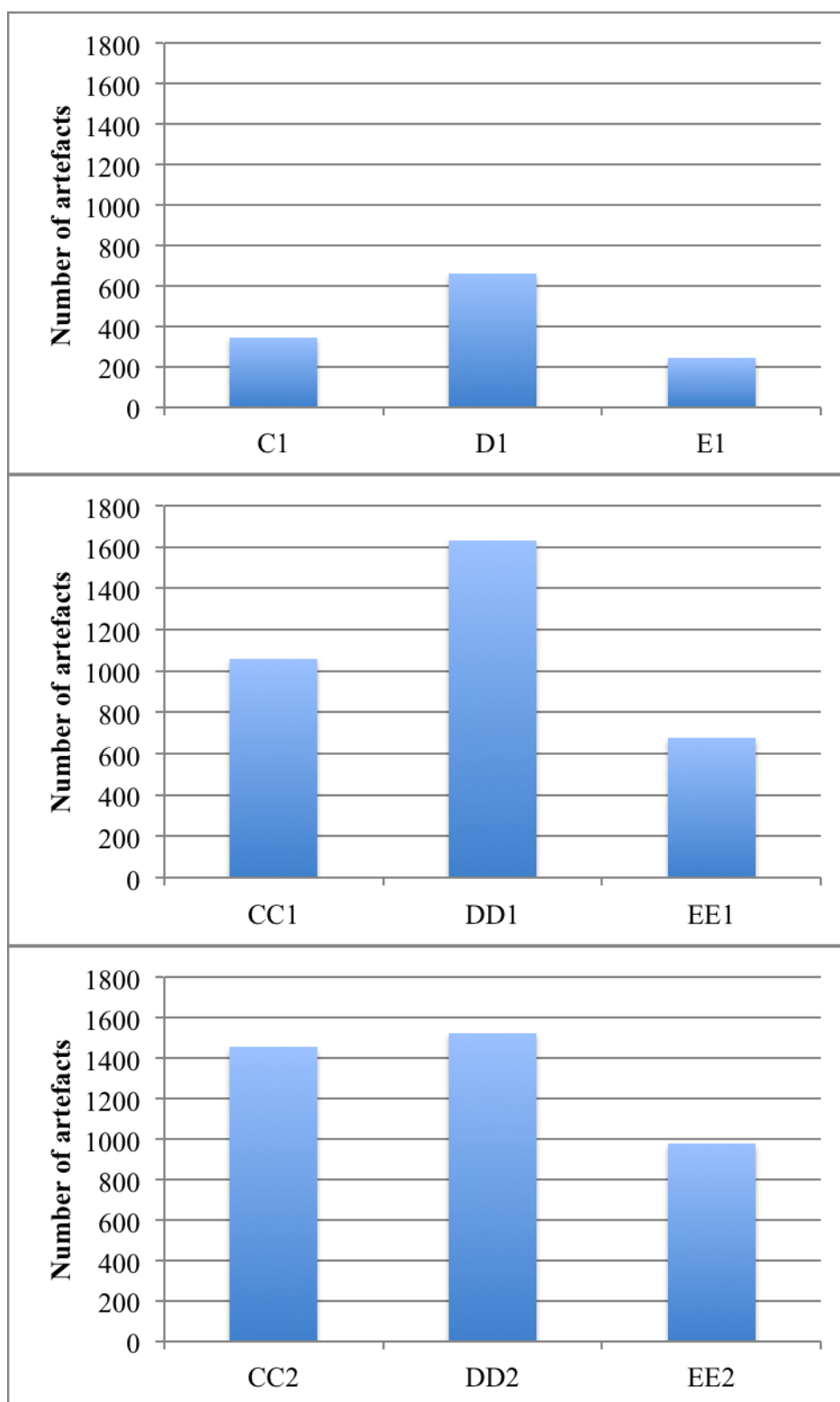


Figure 4.4.20. Artefact number by square for the debris flow assemblage (n=8570). Graphs arranged as if one were looking down on the excavation, with north to the left.

Figure 4.4.22 illustrates that the plotted artefacts retain no specific spatial arrangement, by condition. This plot also includes varnished pieces, even though this

was recorded as an additional (separate) category during analysis. Fresh/unabraded pieces clearly dominate the plot, as well as slightly abraded pieces. Weathered, varnished and heavily abraded/rolled pieces, although less abundant, are also found in all of the excavated squares (showing a completely random spatial distribution).

Artefact spatial arrangement, by type (Fig. 4.4.23), shows a similarly random distribution. This plot includes flaking debris, cores, complete flakes, formal tools (with the most abundant formal tools plotted separately, namely LCTs, denticulates, and scrapers) and others (including less abundant knives, choppers, flaked-flakes, burins, awls, composite pieces, retouched flakes, MRPs, and split and modified cobbles). Each of these types is well represented in all of the excavated squares and it is difficult to identify any specific spatial association between any items, especially cores and flakes.

Vertical artefact distributions (profile views), by size, condition and type, are presented in Figures 4.4.24-4.4.26, all of which show the random spatial arrangement of the Excavation 1 artefacts. By size there appears to be no specific size sorting or grading evident for any portion of the debris flow, and both large and small pieces are well represented across the excavation (Fig. 4.4.24). However, based on the frequency of readings towards the middle of the plot (what would be squares D1, DD1 and DD2), the number of plotted artefacts appears higher and more concentrated within the vertically thinnest portion of the debris flow. This is also evident in the plots by condition and type.

Artefacts by condition (Fig. 4.4.25) and by type (Fig. 4.4.26) show no specific vertical spatial arrangement. Artefacts of all condition types are well represented across the debris flow, including varnished pieces; heavily abraded/rolled pieces show no specific arrangement. All artefact types are well represented randomly throughout the debris flow.

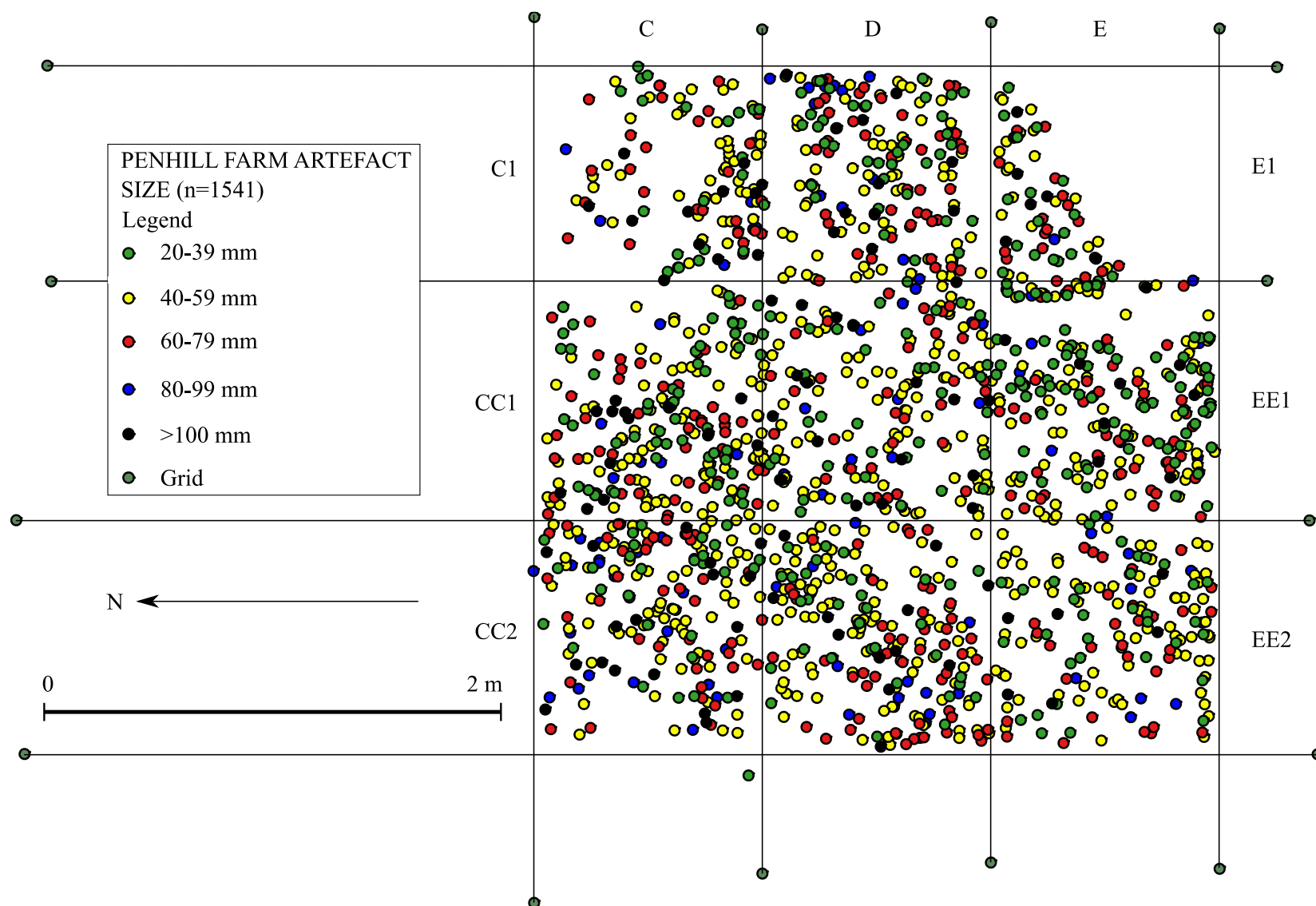


Figure 4.4.21. Horizontal spatial distribution of artefacts, by size.

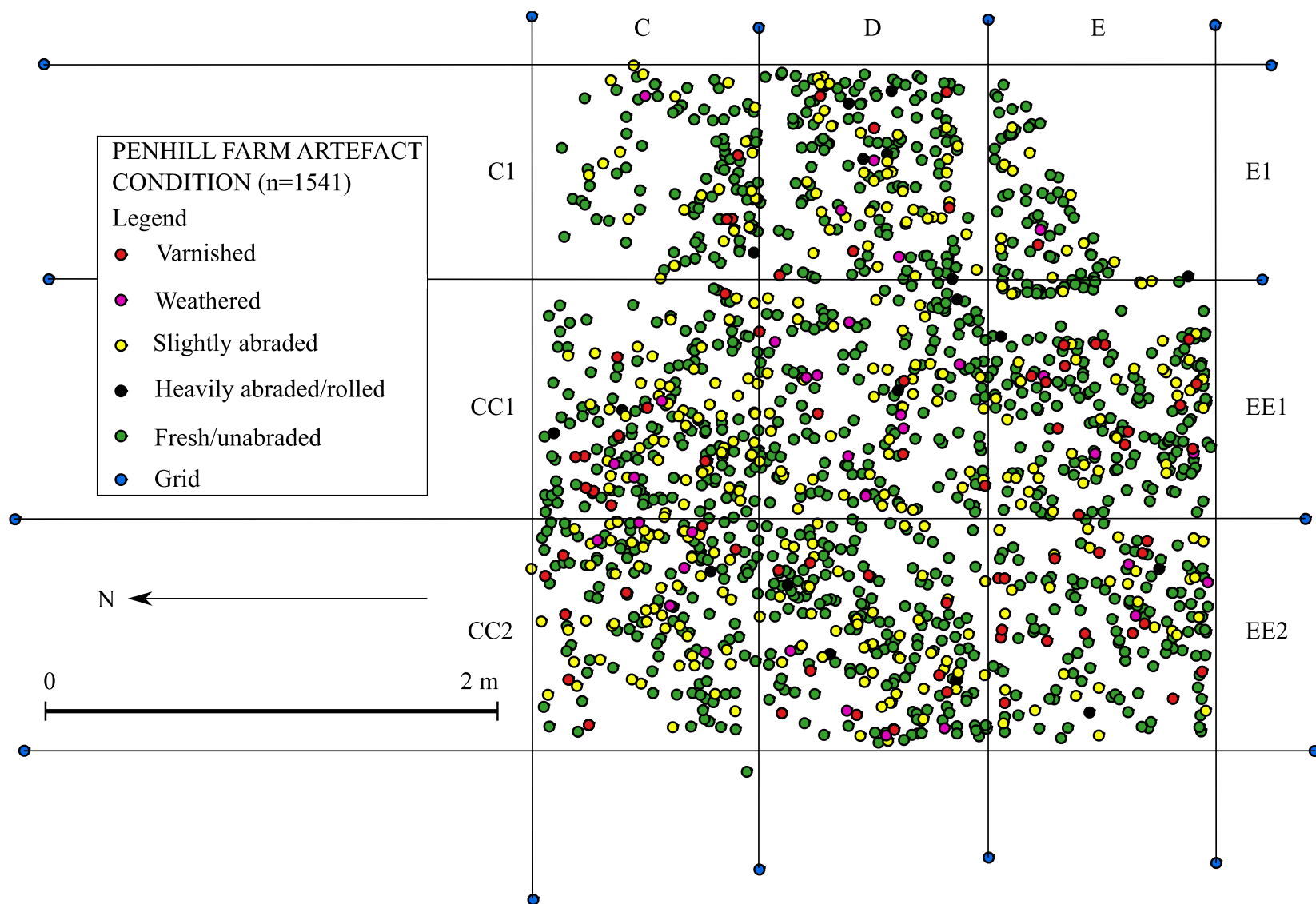


Figure 4.4.22. Horizontal spatial distribution of artefacts, by condition (including varnished pieces).

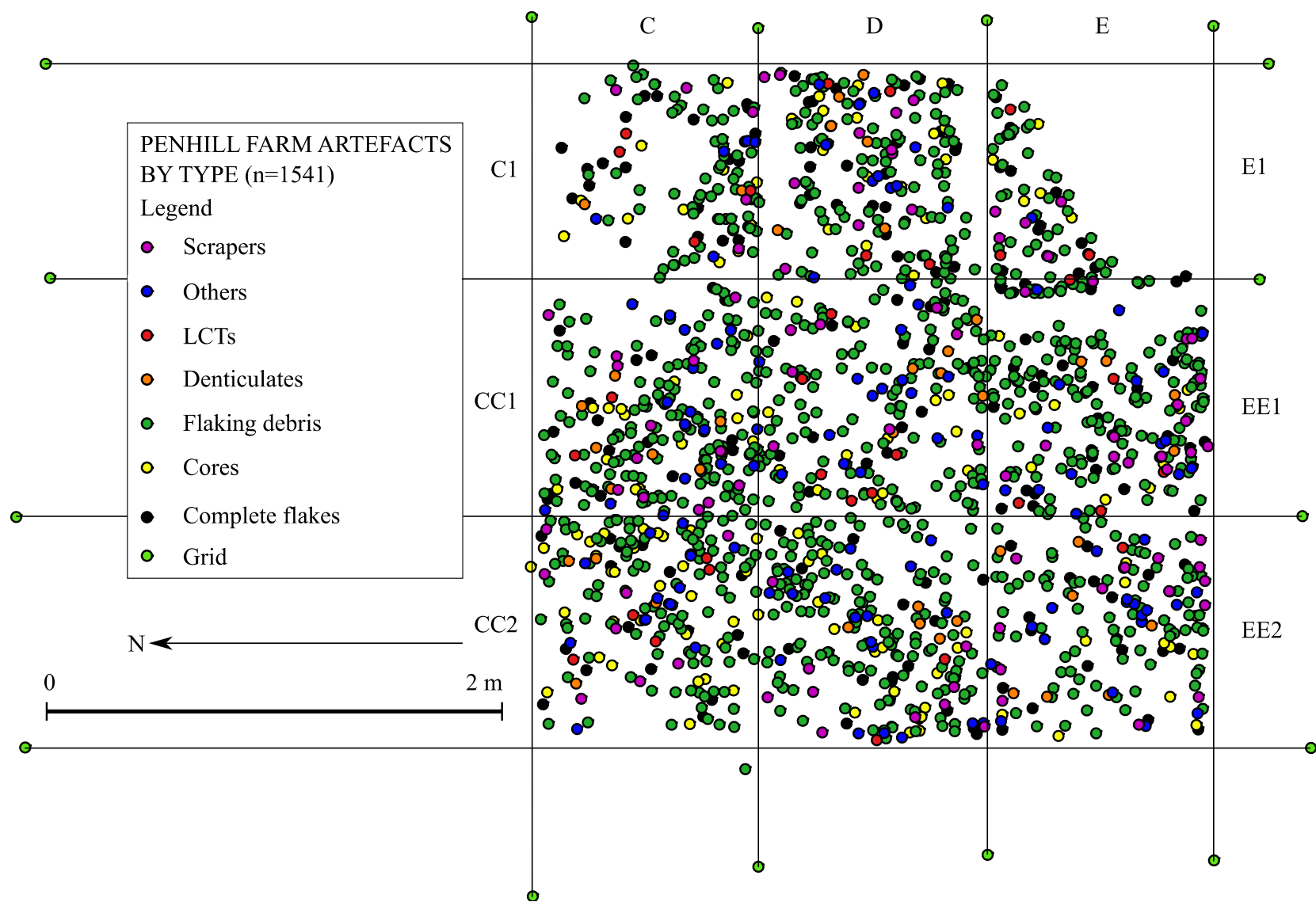


Figure 4.4.23. Horizontal spatial distribution of artefacts, by type.

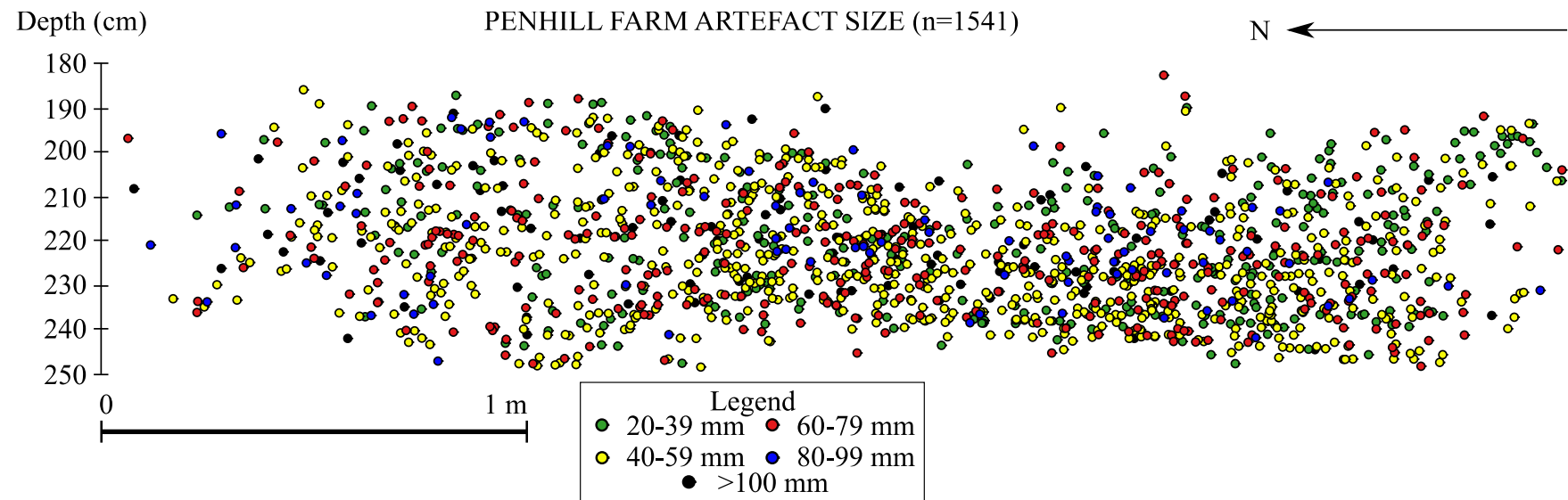


Figure 4.4.24. Vertical artefact distribution by size, looking east.

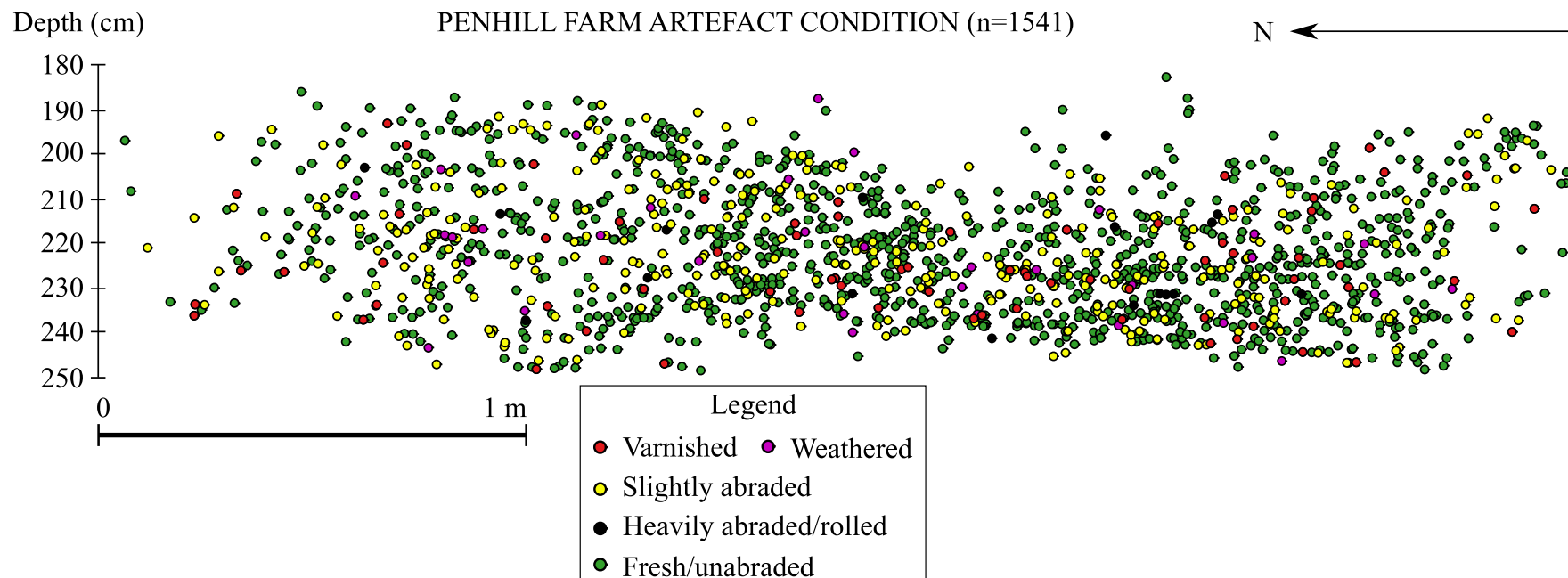


Figure 4.4.25. Vertical artefact distribution by condition, looking east.

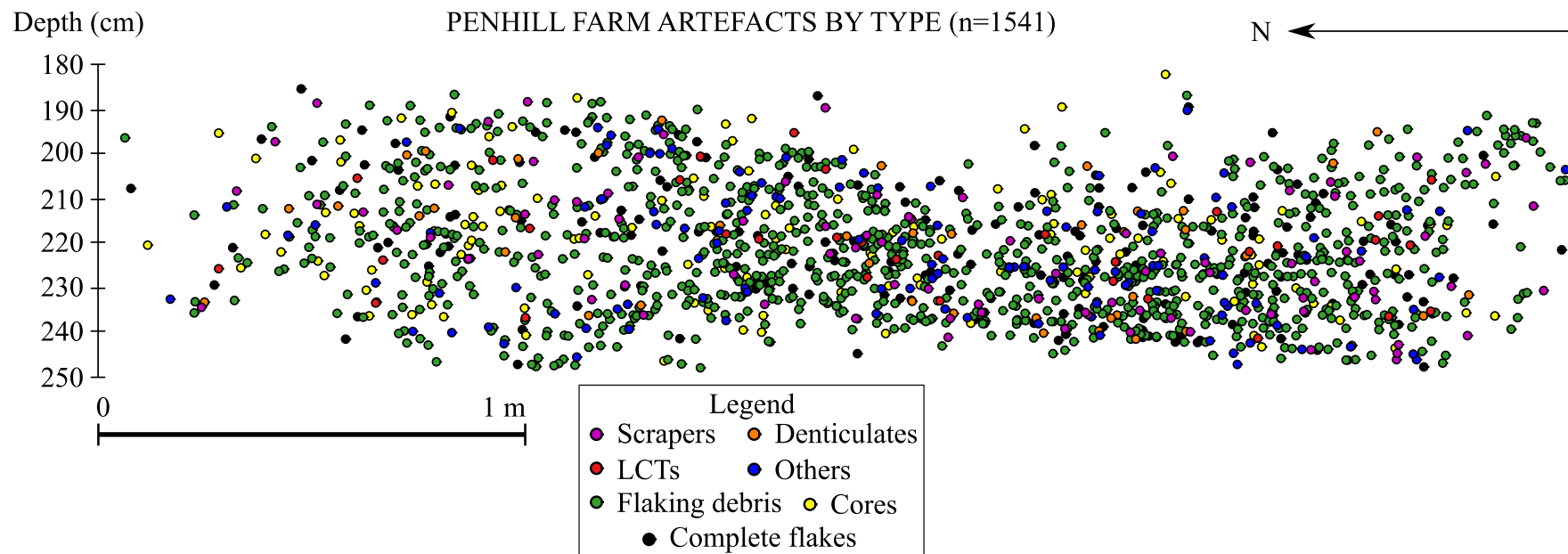


Figure 4.4.26. Vertical artefact distribution by type, looking east.

4.4.2.5 Artefact depositional (fabric) data

Depositional (dip angle and orientation) data obtained on artefacts within the debris flow assemblage are presented in Figures 4.4.27-4.4.28 and Table 4.4.6. These data are presented both collectively (combined totals) and for each individual excavated square; data by square are shown to assess the potential of depositional fabric within specific areas of the debris flow.

However, data shown in Figure 4.4.27 indicate that no single preferential artefact orientation occurs. The combined total (n=214) illustrates that artefacts are randomly aligned to any given direction, occupying almost all the available cardinal sectors. The highest percentage of orientations occurs between 90-95° (due east).

A similar pattern is evident when observing artefact orientation by square (Fig. 4.4.27). Although the sample size for some of these squares is not ideal, even where the samples are larger, artefacts seldom retain any specific orientation. The random alignment of artefacts is most evident in squares CC2, DD1, and E1. Possible alignment of artefacts occurs in squares D1 (NW to SE) and CC1 (N to S). Slight north and east components are evident in squares DD2, EE2 and EE1.

Table 4.4.6 indicates the results of a Rayleigh test of uniformity. This test is performed to assess whether a given dataset tends to cluster (to one or more specific orientations, therefore non-random), or, whether it is uniformly distributed (random). A p-value smaller than the chosen significance level (0.05) indicates the preferential orientation of the data in one or more directions. The Z-value is used to indicate the amount of clustering around the mean vector (a smaller value would therefore suggest low data clustering and a uniform distribution).

Artefact orientations for the combined total (n=214) indicate a uniformly random distribution (p=0.5; Table 4.4.6). In addition to this the clustering of data around the mean vector (37.159°) is low (0.693) and the circular standard deviation is high (137.176°).

Table 4.4.6. Rayleigh test statistical data (total combined sample).

Sample n=214	Orientation			
	Mean Vector (°)	Circular SD (°)	Rayleigh Z	Rayleigh <i>p</i>
	37.159°	137.176°	0.693	0.5
	Dip			
	Mean Vector (°)	Circular SD (°)	Rayleigh Z	Rayleigh <i>p</i>
	26.359°	15.952°	198.039	<0.0001

Artefact dip angle data is presented in Figure 4.4.28. The total combined sample (n=214) indicates that dips are most common between 10-20°. A large portion of the remaining readings occurs from 5-10° and 20-35°. Overall, dip angles are most frequent between 5-55°.

Artefact dip by square shows high variability; however, the majority of readings for all squares occurs between 5-55° (Fig. 4.4.28). Readings exceeding 60° occur in squares C1, D1, E1, CC1, DD1 and DD2. In addition to this pieces that were close to vertical (85-90°) are found only in square E1. Artefacts with small dip angles (0-5°) were recorded in squares E1, D1 and CC1. The highest percentage of readings for all the squares occurs between 10-35° (with the exception of squares E1 and DD1).

Rayleigh test results in Table 4.4.6 indicate a strong clustering of dip angle data (Z=198.039), with a small standard deviation (15.952°). This suggests a non-uniform arrangement of the debris flow dip angle data (non-random).

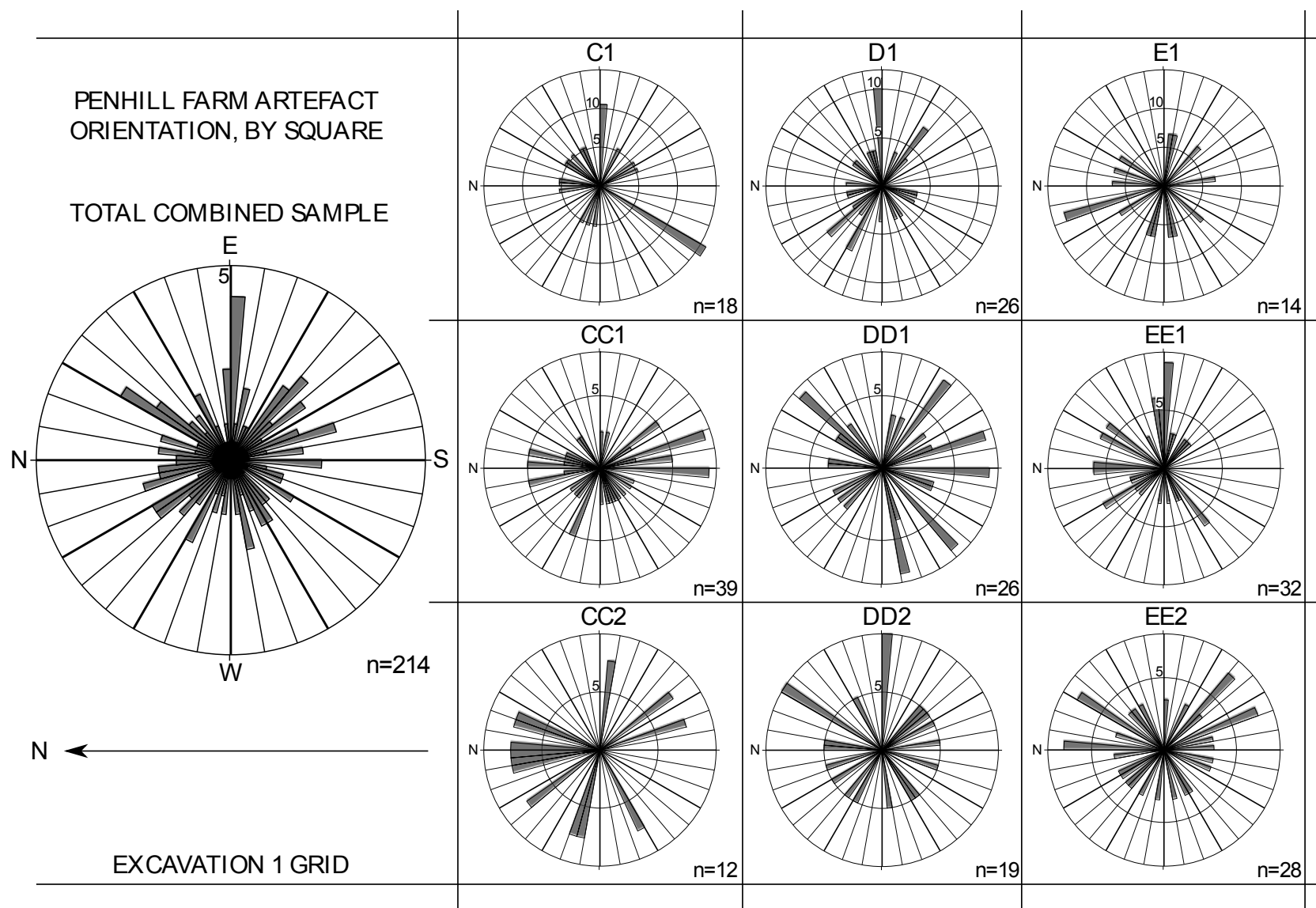


Figure 4.4.27. Excavation 1 artefact orientation.

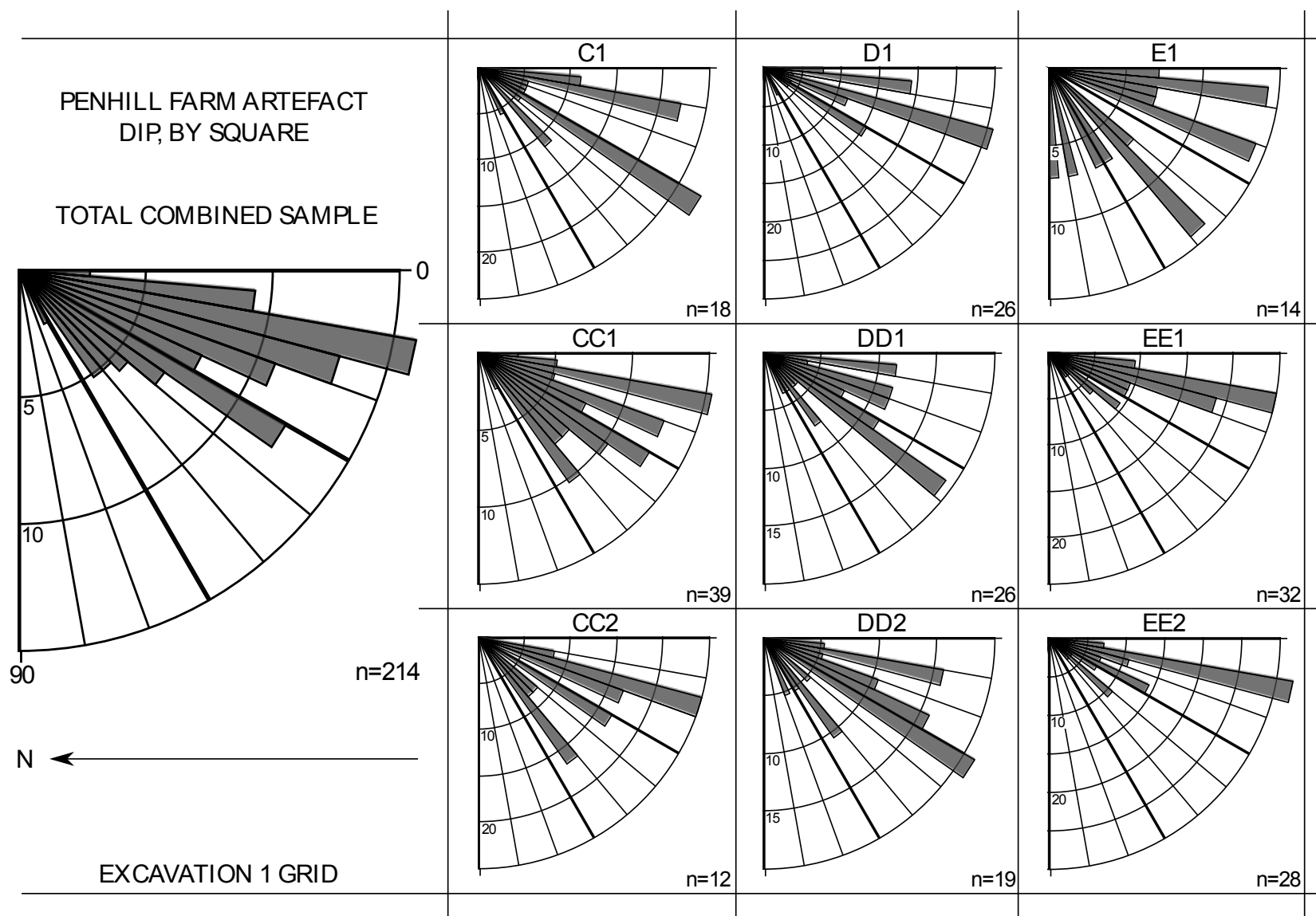


Figure 4.4.28. Excavation 1 dip angle data.

4.4.2.6 Debris flow dating results

Cosmogenic nuclide burial dating results on samples obtained from Excavation 1 square DD1 (natural pebbles and cobbles, n=9) are illustrated in Figures 4.4.29 and 4.4.30. A total of seven clasts was included in this analysis – one clast was re-worked and another did not clean up well for analysis, hence they were excluded.

The unrefined age presented in Figure 4.4.29 is 0.513 ± 0.050 Ma for the debris flow samples. This fit includes all seven clasts irrespective of how they cluster together on the plot.

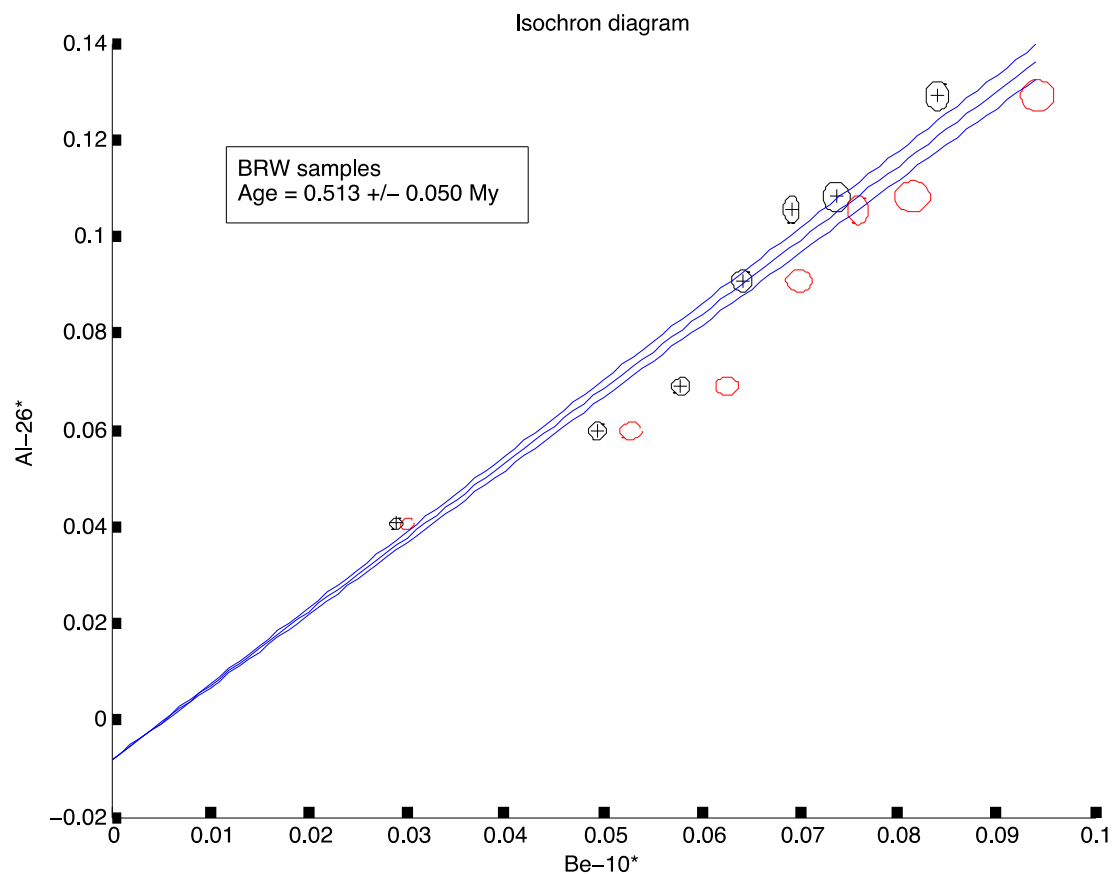


Figure 4.4.29. Unrefined dating results for the Excavation 1 debris flow (graph courtesy of D.E. Granger).

However, the refined age is 0.485 ± 0.051 Ma, obtained when including only the five 'best fit' samples (Fig. 4.4.30). These results provide an age for when the debris flow event took place.

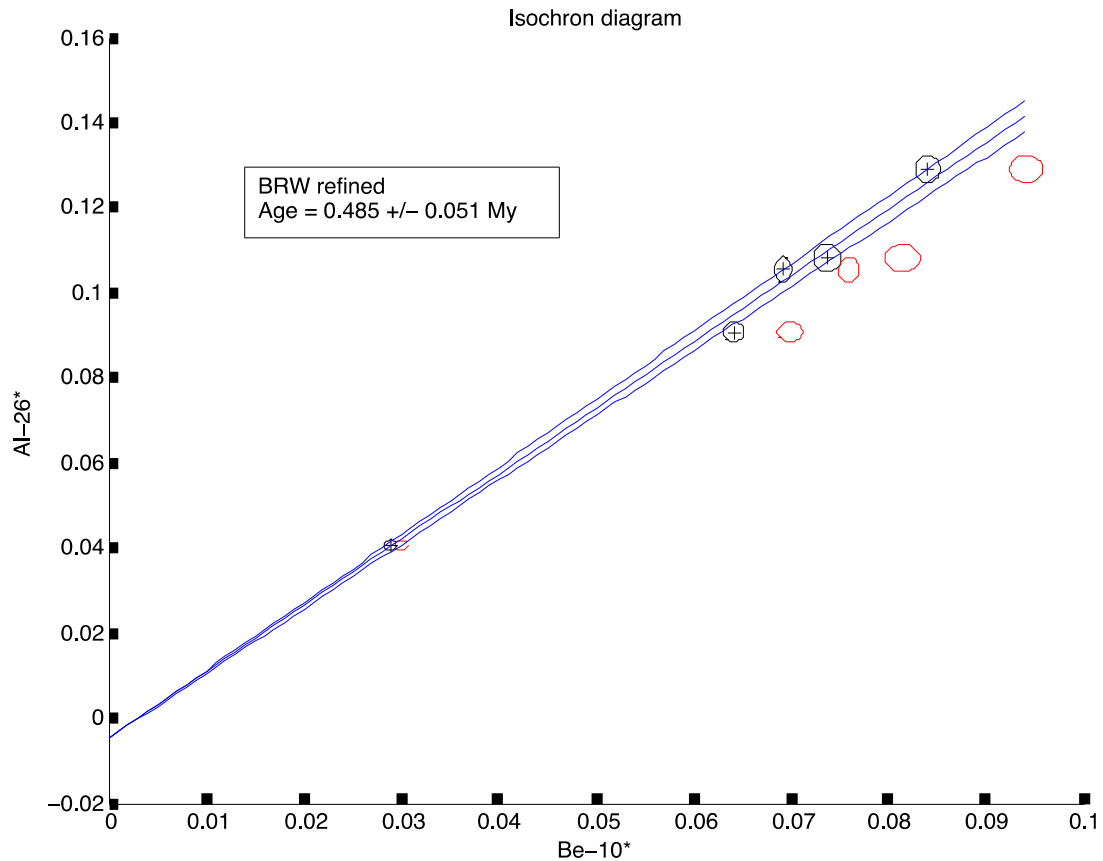


Figure 4.4.30. Refined dating results for the debris flow (graph courtesy of D.E. Granger).

The original date provided by Granger *et al.* (2013) of 1.37 ± 0.16 Ma therefore provides a maximum age for the Penhill Farm debris flow assemblage as this dates the deposition of the fine alluvium, within which the erosion channel formed and later filled with the debris flow and colluvial assemblages; using the refined result of 0.485 ± 0.051 Ma this provides a minimum age for the debris flow assemblage.

The deposition of the colluvial assemblage took place after (and on top of) the debris flow assemblage. As a result a maximum age for the accumulation of this assemblage is 0.485 ± 0.051 Ma (Fig. 4.4.30).

4.4.2.7 Summary

Particle size distribution data from Penhill Farm illustrate differences in grain size between the sediment samples. By grouping the samples into five main categories (alluvium, debris flow, colluvium, channel flow and bedrock) these differences relate

primarily to the level of grain sorting and the distribution of fine and coarse sediment fractions. Bedrock, alluvium and channel flow sediments all account for the most well-sorted samples. In addition to this the alluvium has the highest percentage of fines (clays to fine silts), whereas this fine component is missing in the channel flow sediment and in the upslope bedrock samples 42 and 44. The colluvium and debris flow sediments show remarkably similar distribution curves with a poor level of grain sorting. Both of these samples also retain a lower percentage of fine material (clays to fine silts) when compared to the alluvium. The alluvium and colluvium overlap in the coarser fractions showing that their peaks are similarly distributed; what differs between these samples is the percentage of fines.

An assessment of artefact size shows that both the colluvial and debris flow assemblages contain a full range, excluding only one size category for each assemblage. The major difference between these assemblages though is the percentage of SFD, which accounts for 22% of the colluvial assemblage and 55% for the debris flow. Thereafter, the majority of the remaining artefacts for the colluvial assemblage are larger than 30 mm and smaller than 100 mm, whereas for the debris flow the remaining majority occupies a smaller size range (larger than 30 mm and smaller than 80 mm). Both assemblages have a limited quantity of material that exceeds 100 mm. Artefact size by depth for the debris flow assemblage shows that no size sorting or grading occurs across the excavated levels. Only minor variation in artefact size occurs by depth.

Raw material data for both assemblages show a clear preference for fine-grained quartzites; little difference in raw material use occurs between the assemblages. Fine quartzite accounts for 84.4% of the colluvial assemblage and 79.6% for the debris flow. Although coarser-grained quartzites are also used in artefact production in both assemblages, they only account for small percentages. Following quartzite, siltstone and hornfels are the two most abundant remaining raw materials in both assemblages, followed by small samples of lava, silcrete, claystone and quartz. Where silt-quartzite is absent from the colluvial assemblage this material does occur in the debris flow, and crypto-crystalline materials do not occur in either assemblage.

Artefact condition data shows that the majority of artefacts in the colluvial assemblage retains a fresh/unabraded state (69.1%), followed by 26.7% that are slightly abraded; small percentages are heavily abraded/rolled and weathered. These patterns are largely similar for the debris flow, yet the overall percentage of fresh pieces is greater (77.9%) followed by a smaller percentage of slightly abraded pieces (19%). For both assemblages the most abundant raw materials (quartzite, siltstone and hornfels) show a range of preservation states, most likely due to the larger sample sizes for these materials. This is in contrast to the limited preservation states of the remaining raw material samples. Hornfels, however, shows a greater tendency to weather than any other raw material. Artefact varnishing is infrequent in both assemblages but is marginally more frequent in the debris flow (at 4.2%) than in the colluvial assemblage (2%). Artefact condition and raw material changes, by depth, shows that only minor variation occurs within the debris flow. Quartzite, siltstone and hornfels are the most abundant raw materials across all the excavated depths and only minor variation occurs in the remaining raw materials across these levels. By condition this trend is largely similar where fresh/unabraded and slightly abraded pieces are the most abundant for each level; variation in the remaining types is minimal.

Artefact numbers (frequency) by depth and square show some interesting trends for the debris flow assemblage. By depth the number of artefacts increases, up until 230-235 cm, thereafter decreasing towards the final spit depth of 245-250 cm; artefacts are least frequent between 180-185 and 245-250 cm. Artefacts are therefore most concentrated towards the middle to basal part of the debris flow. Graphing artefact numbers by square across the excavation shows that there is an increase in artefacts from east to west across the debris flow. In addition to this artefact frequency is greatest towards the middle portion (center squares) of the debris flow when looking north to south across the excavation. The debris flow is discontinuous in squares C1 and E1.

The vertical and horizontal distribution of plotted artefacts shows that there is no specific spatial arrangement of artefacts by size, condition or type; artefacts occur randomly throughout the excavated levels. However, these plots confirm some of the patterns noted above for artefact frequency by depth and square, namely: artefact

numbers increase as one moves from east to west across the excavation, artefacts are most concentrated in the center squares of the excavation (D1, DD1 and DD2), artefact numbers by depth are greatest towards the middle to basal part of the debris flow, and the flow is discontinuous (especially in square E1).

Depositional data obtained on artefacts within the debris flow assemblage indicates that no single preferential orientation occurs. The combined total (n=214) illustrates that artefacts are randomly aligned to any given direction, occupying almost all the available cardinal sectors. This pattern is largely similar for artefact orientation by square. Dip angles are most common between 5-55° and although the results of a Rayleigh test of uniformity show a non-random distribution of these data they occupy a wide range. This does not suggest any specific trends in dip angles.

Cosmogenic nuclide burial dating results from Excavation 1 provide a refined age 0.485 ± 0.051 Ma. The original date of 1.37 ± 0.16 Ma (Granger *et al.* 2013) therefore provides a maximum age for the Penhill Farm debris flow assemblage, whereas this new refined age provides a minimum. However, this refined result provides a maximum age for the accumulation of the colluvial assemblage as it occurs after and on top of the debris flow.

4.4.3 Typology

Penhill Farm artefact classification is summarised in Tables 4.4.7 and 4.4.8.

Table 4.4.7. Colluvial assemblage artefact classification (n=1258).

Flaking debris:	N	%	Complete flakes:	N	%
SFD	279	22.2	End-struck	44	3.5
Chunk	96	7.6	Side-struck	49	3.9
Incomplete flake	265	21.1	Corner-struck	21	1.7
Flake fragment	301	23.9	Kombewa	1	0.1
Split flake	7	0.6	Core trimming	1	0.1
Bipolar	24	1.9	Bipolar	9	0.7
Total	972	77.3	Handaxe trimming	4	0.3
Formal tools:			Bi-bulb	1	0.1
Handaxe	4	0.3	Core rejuvenation	4	0.3
Broken handaxe/LCT	0	0	Total	134	10.7
Cleaver	3	0.2	Cores:		
Pick	2	0.2	Core fragment	5	0.4
Biface	2	0.2	Casual	11	0.9
Knife	0	0	Bipolar	0	0
Chopper	1	0.1	Chopper-core	17	1.4
Side chopper	1	0.1	Discoidal	11	0.9
End chopper	0	0	Discoidal w/removal	1	0.1
Flaked-flake	3	0.2	Irregular	6	0.5
Retouched flake	7	0.6	Polyhedral	1	0.1
Scraper~			Single platform	5	0.4
<i>Composite</i>	4	0.3	Boulder-core	0	0
<i>Concave</i>	2	0.2	Total	57	4.5
<i>Convex</i>	1	0.1	Other:		
<i>End</i>	1	0.1	Modified cobble	0	0
<i>Side</i>	6	0.5	Split cobble	1	0.1
<i>Double side and end</i>	0	0	Total:	1	0.1
<i>Notched</i>	14	1.1			
<i>Convergent</i>	0	0			
<i>Denticulated</i>	19	1.5			
<i>Heavy-duty/core</i>	1	0.1			
MRP	11	0.9			
Burin	1	0.1			
Awl	0	0			
Denticulate	8	0.6			
Composite piece	3	0.2			
Total	94	7.5			

Assemblage total	1258	100
-------------------------	-------------	------------

Table 4.4.8. Debris flow assemblage artefact classification (n=8646).

Flaking debris:	N	%
SFD	4767	55.1
Chunk	202	2.3
Incomplete flake	1508	17.4
Flake fragment	1252	14.5
Split flake	3	0.03
Bipolar	11	0.1
Total	7743	89.6
Formal tools:		
Handaxe	12	0.1
Broken handaxe/LCT	6	0.1
Cleaver	12	0.1
Pick	5	0.1
Biface	3	0.03
Knife	4	0.05
Chopper	1	0.01
Side chopper	0	0
End chopper	0	0
Flaked-flake	12	0.1
Retouched flake	41	0.5
Scraper~		
<i>Composite</i>	11	0.1
<i>Concave</i>	6	0.1
<i>Convex</i>	9	0.1
<i>End</i>	4	0.05
<i>Side</i>	12	0.1
<i>Double side and end</i>	1	0.01
<i>Notched</i>	35	0.4
<i>Convergent</i>	1	0.01
<i>Denticulated</i>	47	0.5
<i>Heavy-duty/core</i>	1	0.01
MRP	106	1.2
Burin	1	0.01
Awl	1	0.01
Denticulate	74	0.9
Composite piece	11	0.1
Total	416	4.8
Complete flakes:	N	%
End-struck	121	1.4
Side-struck	117	1.4
Corner-struck	80	0.9
Kombewa	0	0
Core trimming	3	0.03
Bipolar	4	0.05
Handaxe trimming	6	0.1
Bi-bulb	1	0.01
Core rejuvenation	3	0.03
Total	335	3.9
Cores:		
Core fragment	8	0.1
Casual	43	0.5
Bipolar	1	0.01
Chopper-core	31	0.4
Discoidal	44	0.5
Irregular	12	0.1
Polyhedral	3	0.03
Single platform	7	0.1
Boulder-core	0	0
Total	149	1.7
Other:		
Modified cobble	1	0.01
Split cobble	2	0.02
Total:	3	0.03
Assemblage total	8646	100

The Penhill Farm colluvial assemblage provides a large sample of formal tools (n=94, 7.5%), complete flakes (n=134, 10.7%) and cores (n=57, 4.5%; Fig. 4.4.31). The majority of material, however, is comprised of flaking debris (n=972, 77.3%). A single split cobble makes up the remaining portion of the assemblage (0.1%).

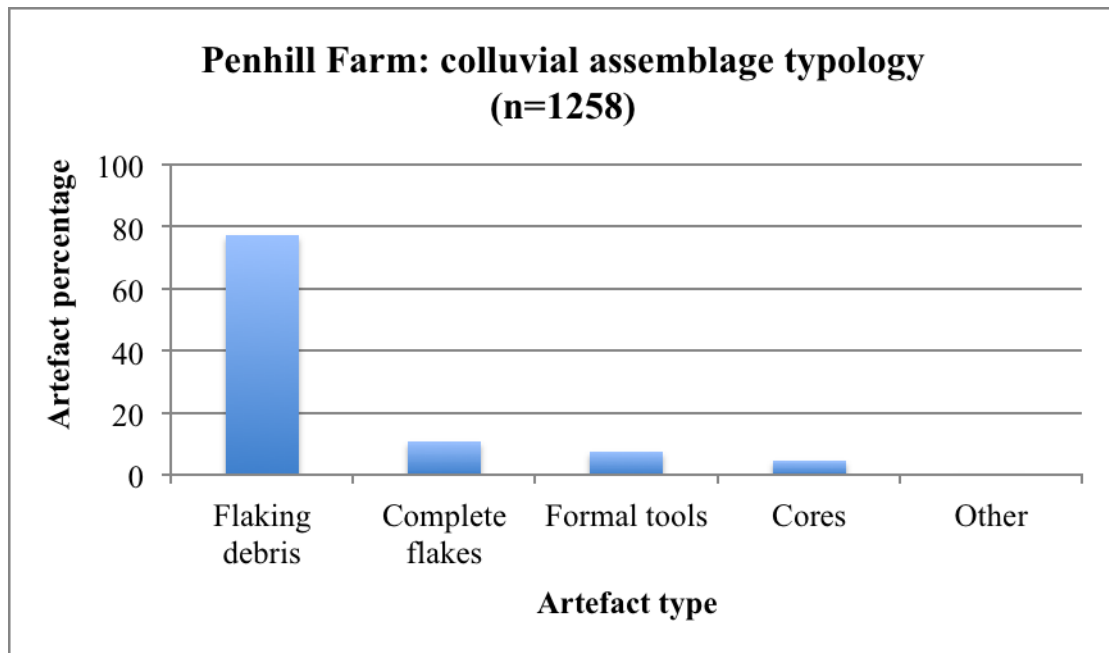


Figure 4.4.31. Colluvial assemblage artefact types.

Artefact classification for the lower lying debris flow assemblage shows an even higher abundance of flaking debris (n=7743, 89.6%; Fig. 4.4.32). Here however the number of formal tools (n=416, 4.8%) exceeds the number of complete flakes (n=335, 3.9%). The total core sample comprises of 149 pieces (1.7%), and the remaining artefacts comprise of a single modified cobble and two split cobbles.

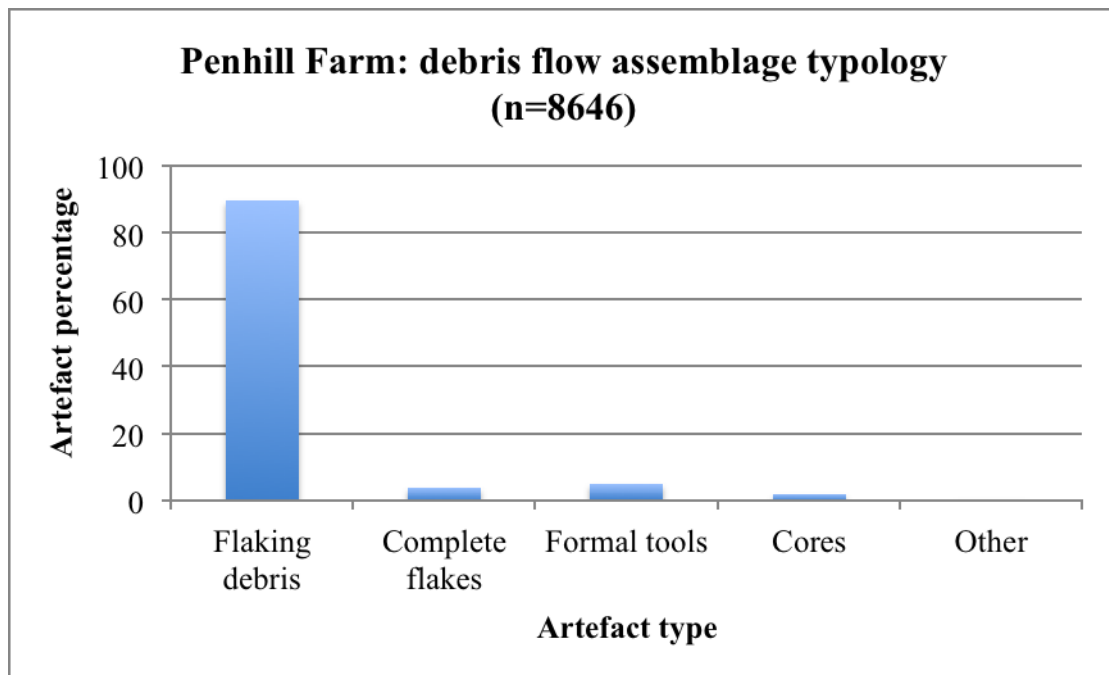


Figure 4.4.32. Debris flow assemblage artefact types.

4.4.3.1 Flaking debris

Flaking debris for both assemblages is broken down by type in Figures 4.4.33 and 4.4.34, and a small sample of bipolar debris is presented in Figures 4.4.35 and 4.4.36. By type, flake fragments, incomplete flakes and SFD are the most abundant for both assemblages. For the colluvial assemblage flaking debris sample (n=972), flake fragments account for 31% and incomplete flakes account for 27.3%; these types account for 16.2% and 19.5% for the debris flow sample (n=7743), respectively. However, SFD is far less abundant for the colluvial assemblage (n=279, 22.2%) in comparison to the lower lying debris flow assemblage (n=4767, 55.1%). The remaining types for the colluvial flaking debris sample comprise of chunks (9.9%), split flakes (0.7%) and bipolar elements (2.5%). These three types are proportionally less abundant for the debris flow assemblage (2.6%, 0.04% and 0.14%, respectively).

The colluvial assemblage flaking debris sample shows high variability in raw material use (all types represented; see Table 4.4.9 at the end of this section). This is most evident for SFD, the only debris to include quartz (0.2%) and lava (0.3%) pieces. However, for the total flaking debris sample (n=972) quartzite is clearly the dominant raw material (90.1%), followed thereafter by siltstone (5.5%) and hornfels (3%); lava, silcrete and claystone make up only a small percentage of the total sample (collectively 1.2%). Interestingly, split flakes (n=7) and bipolar pieces (n=24; Fig. 4.4.35) are produced exclusively on quartzite. The largest percentages of siltstone, hornfels, silcrete and claystone are from SFD, incomplete flake, and flake fragment debris types.

Raw material use in the debris flow assemblage also shows high variability for the SFD sample (and includes all raw material types); however, incomplete flakes and flake fragments also show this variability (all raw materials present, except for quartz; see Table 4.4.10 at the end of this section). The total flaking debris sample (n=7743) is again dominated by quartzite (86%), followed thereafter by 8% siltstone and 3.5% hornfels; silcrete use is highest (1%) for the SFD sample (n=81), with a total use of 1.1% (n=88). Split flakes (n=3) and bipolar pieces (n=11; Fig. 4.4.36) illustrate the use of both quartzite (n=12, 85.7%) and siltstone (n=2, 14.3%).

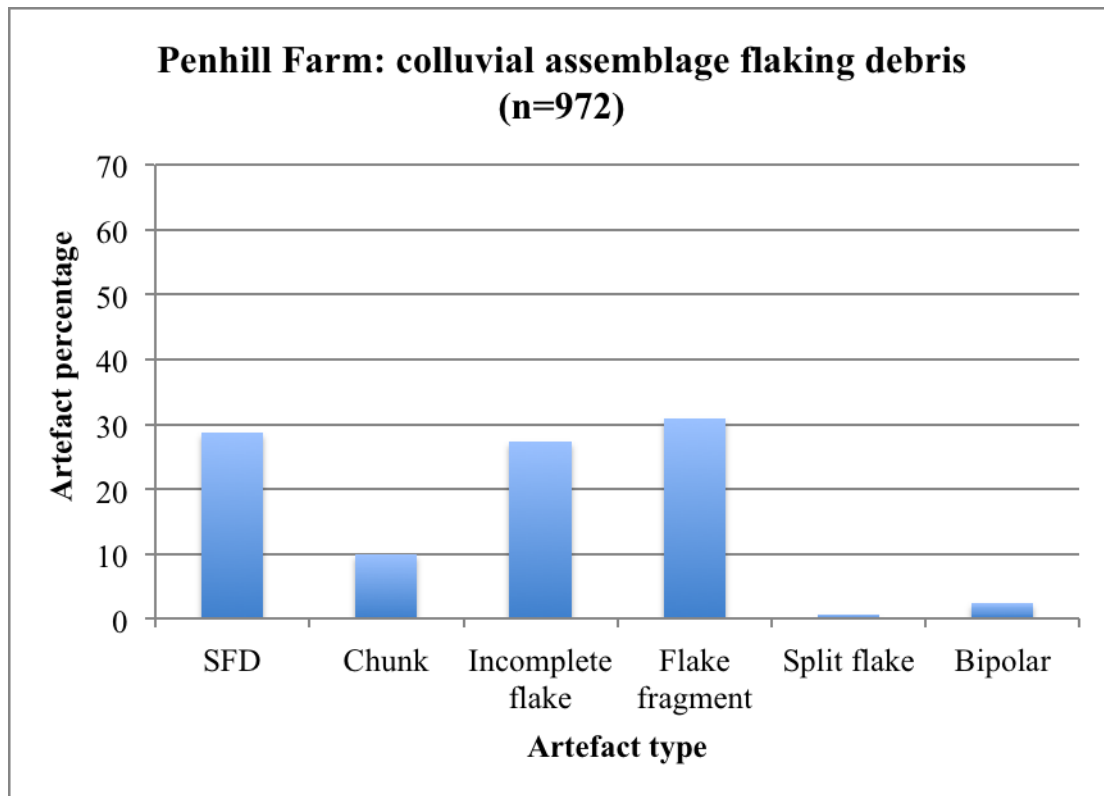


Figure 4.4.33. Flaking debris by type for the colluvial assemblage.

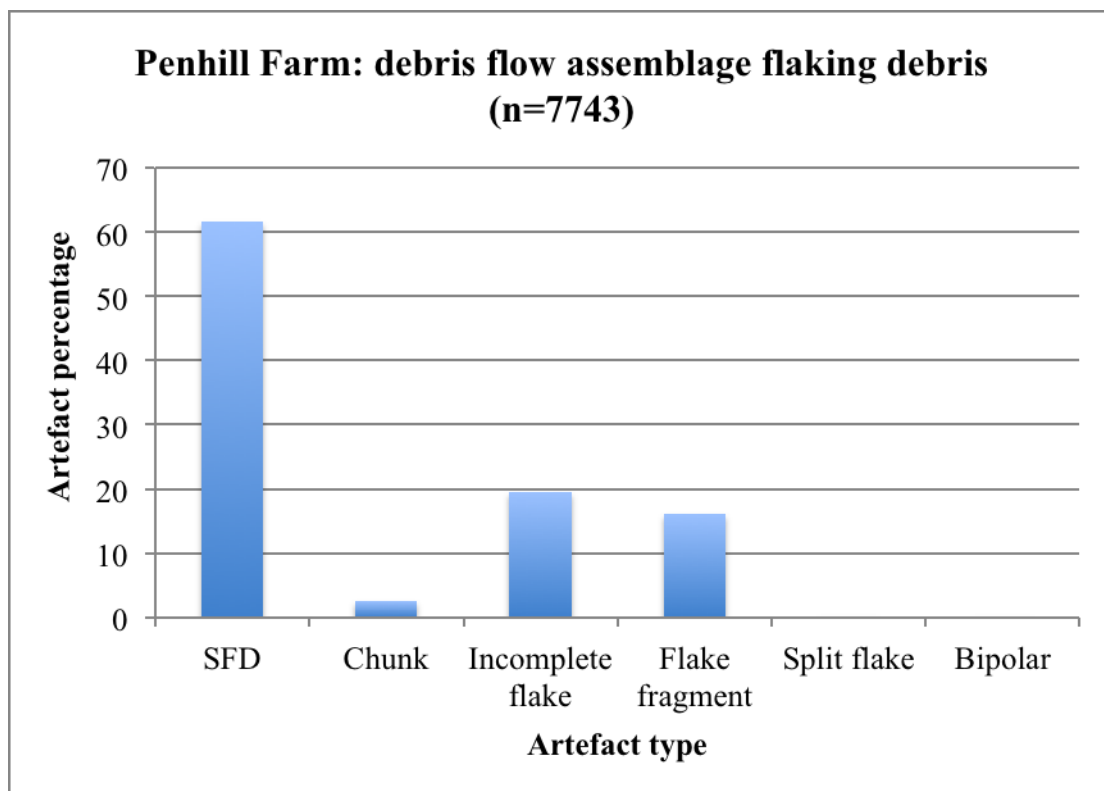


Figure 4.4.34. Flaking debris by type for the debris flow assemblage.

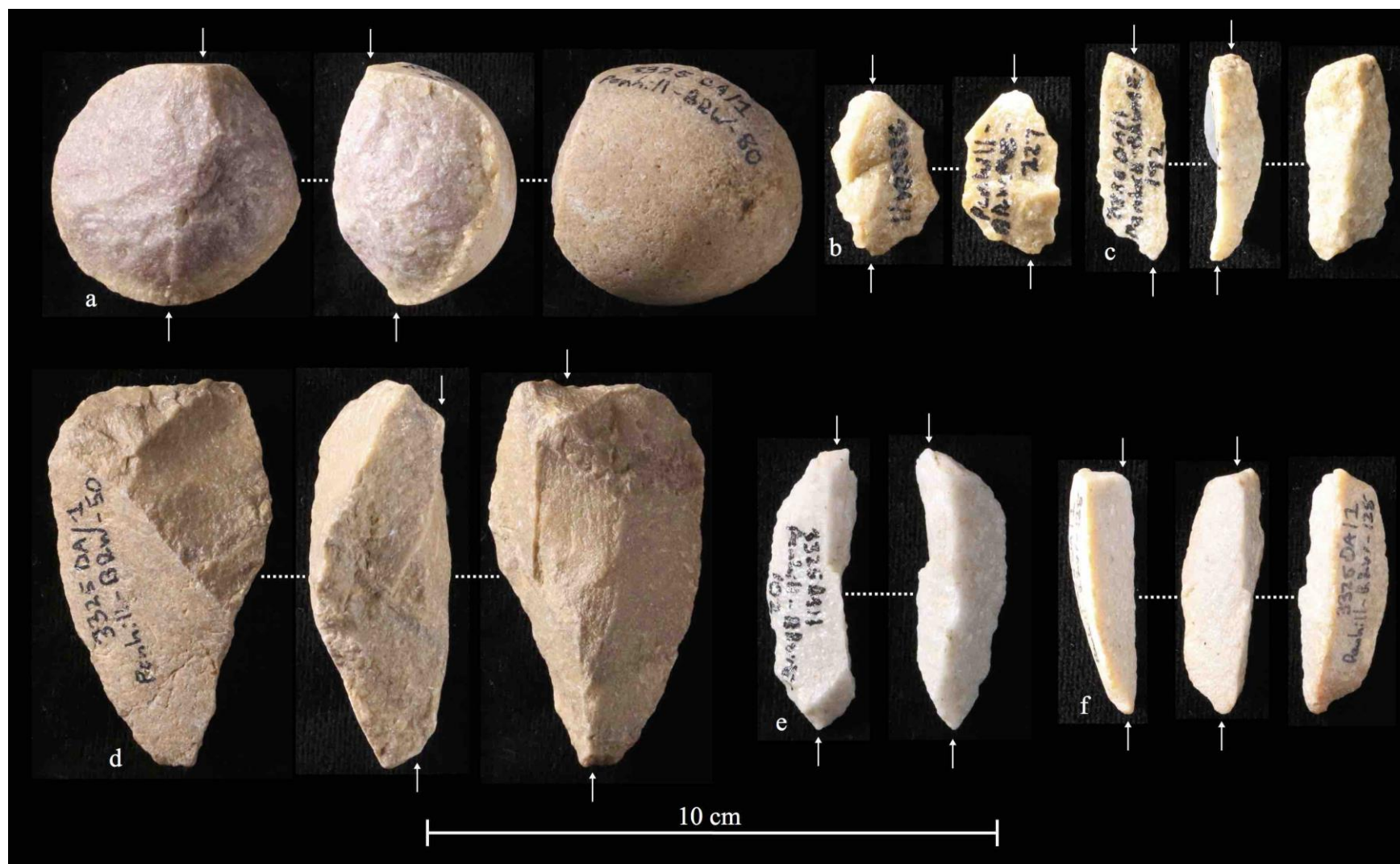


Figure 4.4.35. Quartzite bipolar flaking debris from the colluvial assemblage. Arrows indicate percussion points.

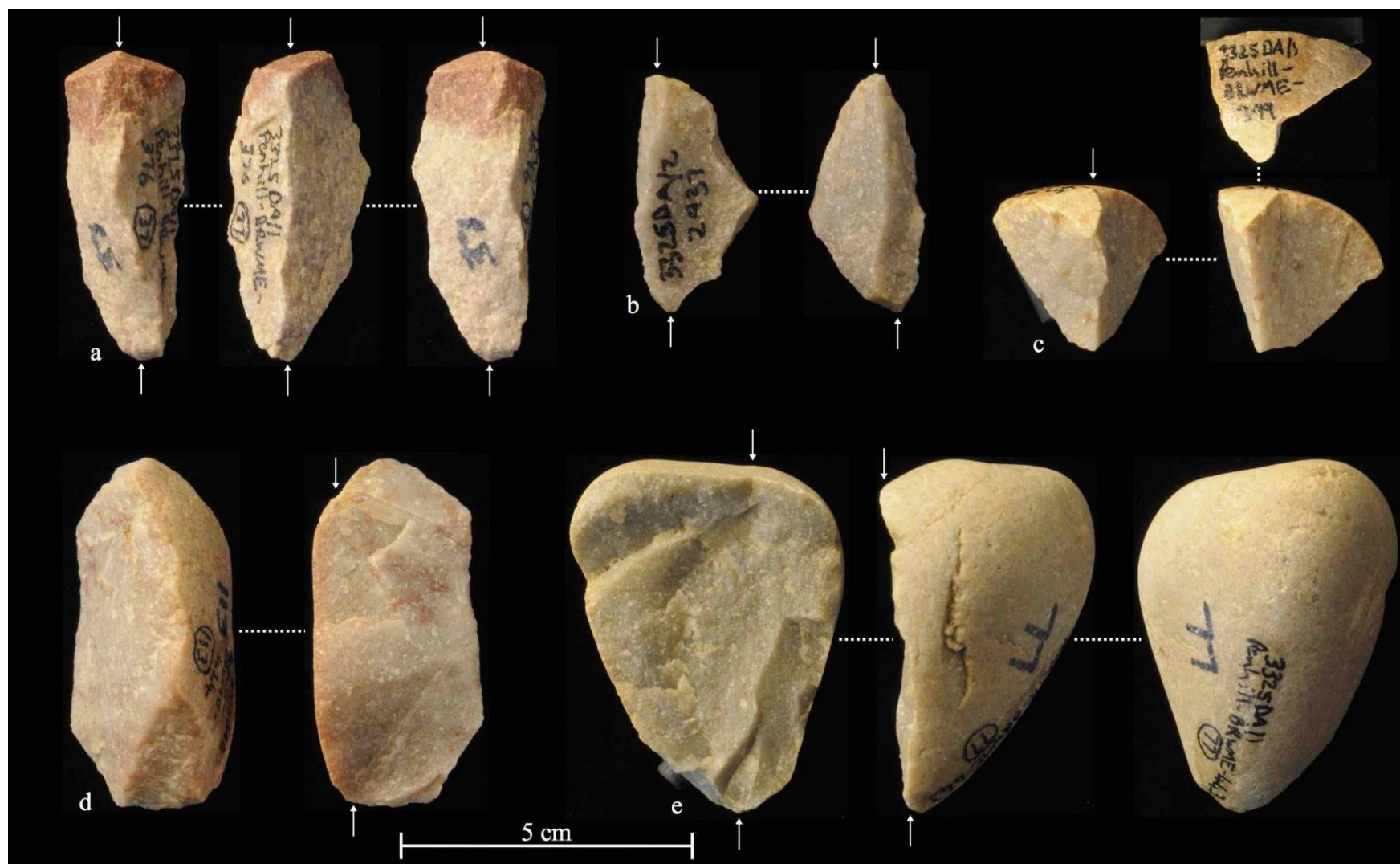


Figure 4.4.36. Quartzite bipolar flaking debris from the debris flow. Arrows indicate percussion points.

4.4.3.2 Complete flakes

The colluvial assemblage complete flake types are broken down in Figure 4.4.37 and a sample of flakes is presented in Figure 4.4.39. Side- (36.6%) and end-struck (32.8%) flakes are the most abundant types, followed thereafter by corner-struck (15.7%) and bipolar pieces (6.7%). Flakes that appear to have been struck from an LCT, for shaping purposes, are equally as frequent as core rejuvenation elements (n=4 each). The remaining sample is comprised of one Kombewa flake (Fig. 4.4.39b), one core trimming flake, and one flake that preserved two bulbs on its ventral surface (bi-bulb; Fig. 4.4.39f).

The colluvial assemblage complete flakes illustrate that quartzite is the favoured raw material (76.9%) followed thereafter by siltstone (11.2%) and hornfels (10.4%; Table 4.4.9). Lava and silcrete account for the remaining 1.5% (n=1 each) and no claystone or quartz complete flakes were found. Interestingly, end- and side-struck flakes (n=13) account for 92.9% of the total hornfels sample, and corner-struck types are the only flakes that show both lava and silcrete use (n=2). Types made exclusively on quartzite include: bipolar complete flakes (n=9), core rejuvenation (n=4) and trimming flakes (n=1), and the single Kombewa flake. Siltstone use is evident on a handaxe trimming flake (n=1) and the bi-bulb flake (n=1). Overall, end-, side- and corner-struck flakes account for the greatest use of quartzite, siltstone and hornfels.

Complete flakes for the debris flow assemblage show a similar distribution, by type (Fig. 4.4.38); a sample of flakes is presented in Figures 4.4.40-4.4.43. The three most abundant types include end- (36.1%), side- (34.9%) and corner-struck (23.9%) flakes, collectively accounting for 94.9% (n=318) of the total sample (n=335). However, end- and corner-struck flakes are proportionally more abundant in relation to side-struck pieces when compared to the overlying colluvial assemblage (Figs. 4.4.37 & 4.4.38). The remaining debris flow complete flakes (core trimming, bipolar, handaxe trimming, core rejuvenation and bi-bulb) make up only a small percentage of the total sample (n=17, 5.1%) and no Kombewa flakes were recovered. Bipolar flakes only account for 1.2% of the complete flake sample (n=4); core trimming and rejuvenation flakes account for 1.8% collectively.

The debris flow assemblage complete flakes show a reduced use of quartzite (69.6%), and here the percentage of hornfels (19.7%) exceeds that of siltstone (9.3%; Table 4.4.10). Quartz and silt-quartzite is completely absent and only small percentages of claystone (0.9%), lava and silcrete (0.3% each) occur. The most common flake type includes quartzite side-struck pieces (26.3%). The highest percentages for all the raw materials occur in the side-, end- and corner-struck flake types. Those flakes that are made exclusively on quartzite include: core trimming (n=3), bipolar (n=4), handaxe trimming (n=6), bi-bulb (n=1) and core rejuvenation types (n=3).

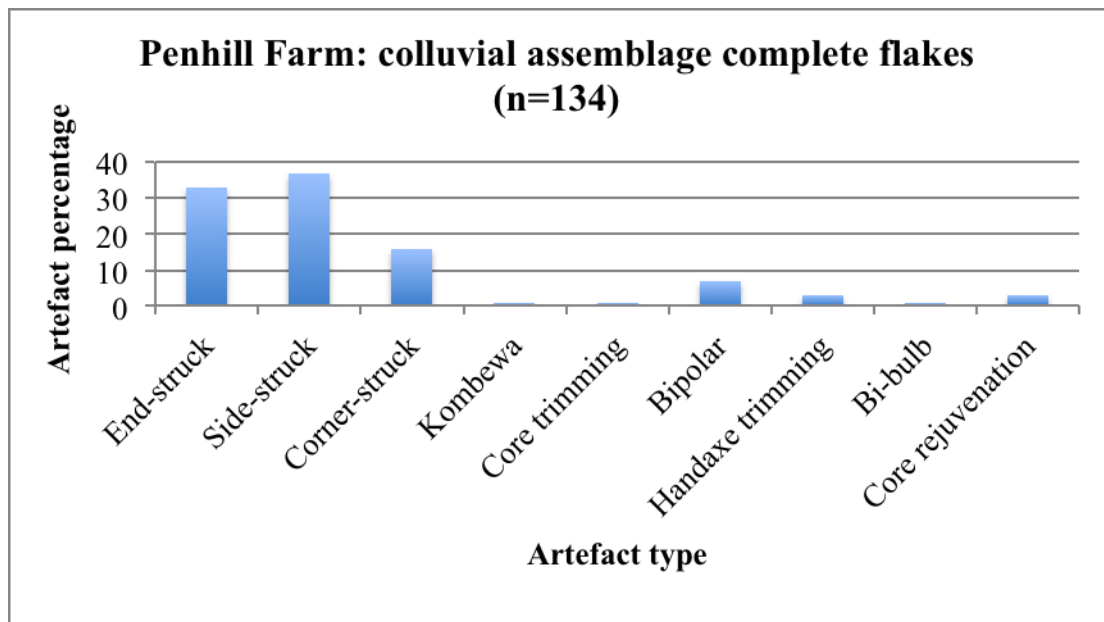


Figure 4.4.37. Colluvial assemblage complete flake types.

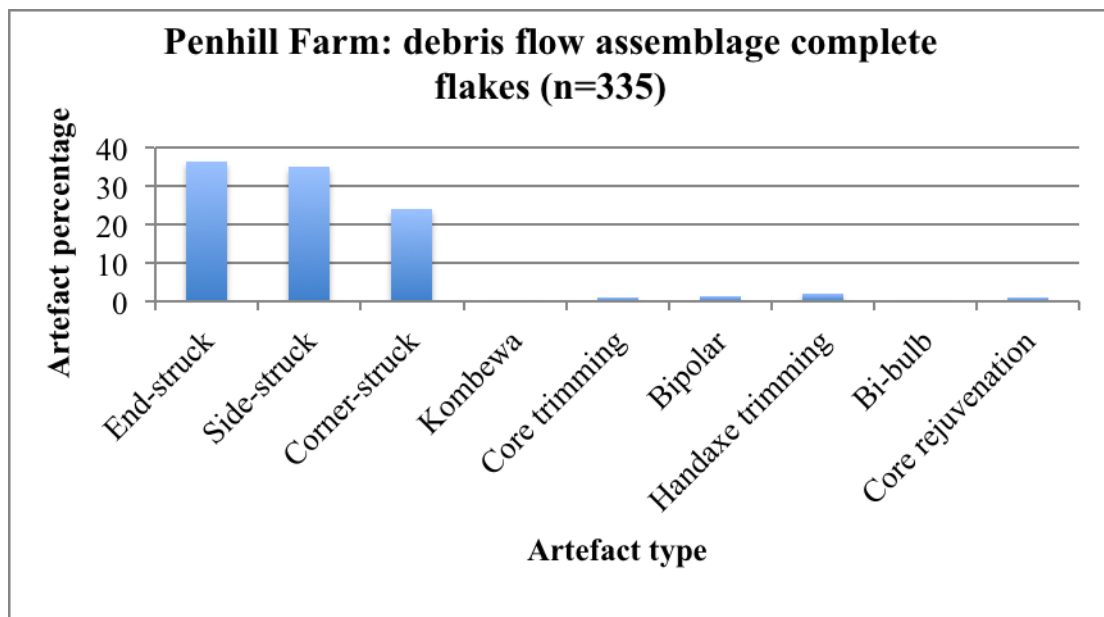


Figure 4.4.38. Debris flow assemblage complete flake types.

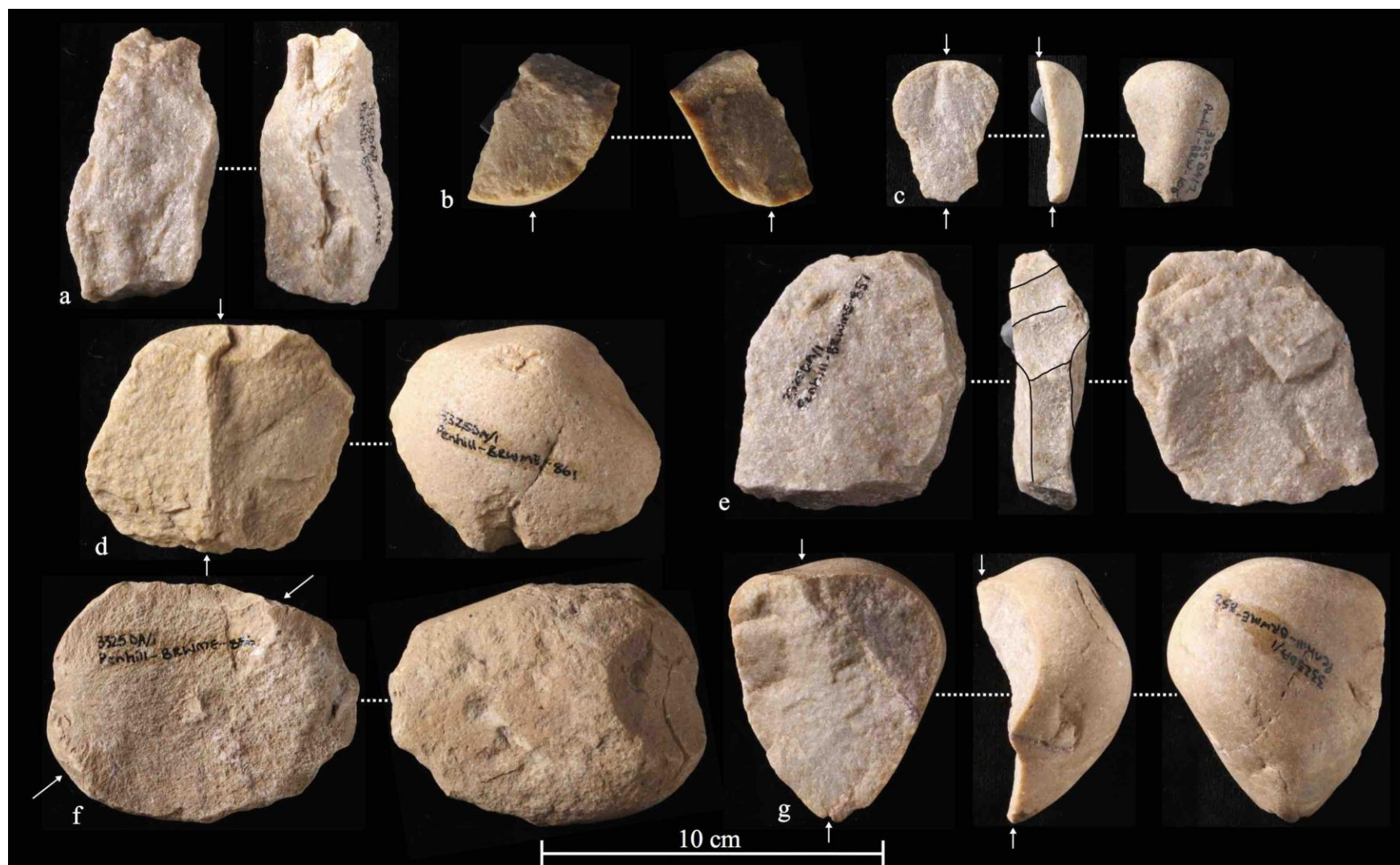


Figure 4.4.39. Colluvial assemblage complete flakes. Flakes are made on quartzite (a-e, g) and siltstone (f), and by type there are core rejuvenation (a, e), Kombewa (b), bipolar (c, d, g), and bi-bulb (f) flakes shown. Arrows indicate points of percussion.

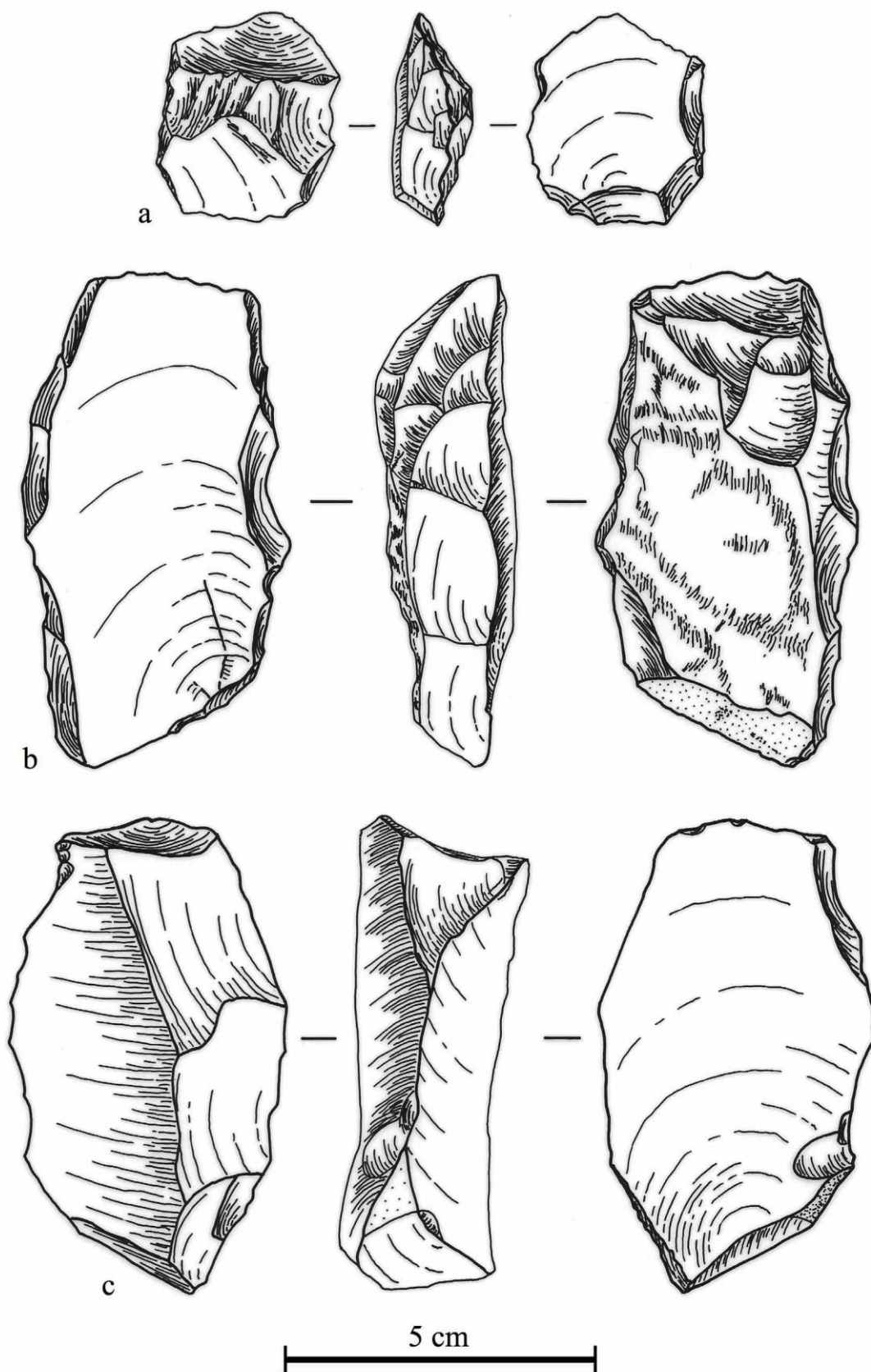


Figure 4.4.40. Debris flow assemblage end-struck quartzite complete flakes. Flakes illustrated include core trimming (a, c) and rejuvenation (b) types. Drawn by Wendy Voorvelt.

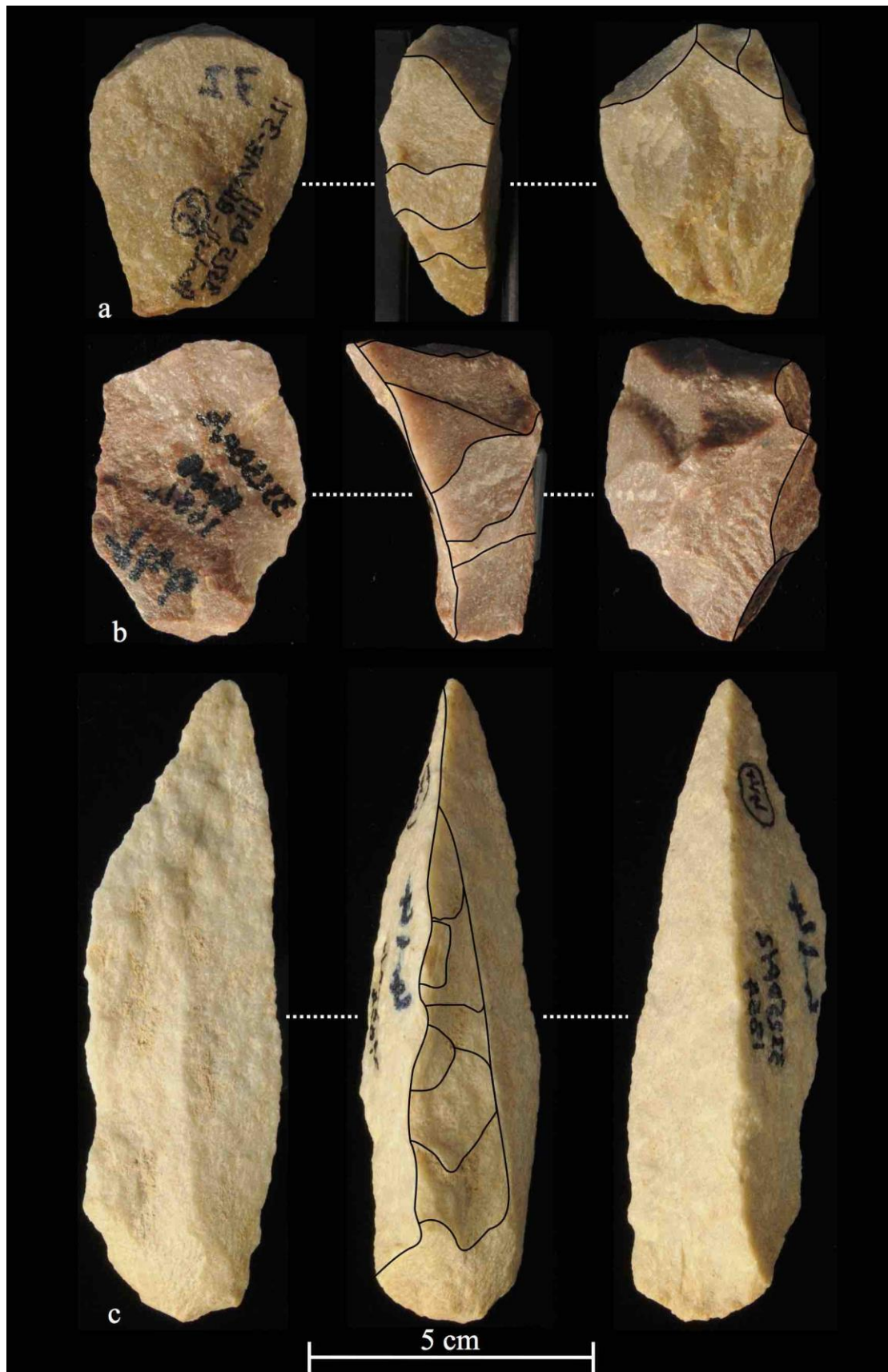


Figure 4.4.41. Debris flow assemblage end-struck quartzite complete flakes. Flakes include core rejuvenation (a, b) and trimming (c) types.

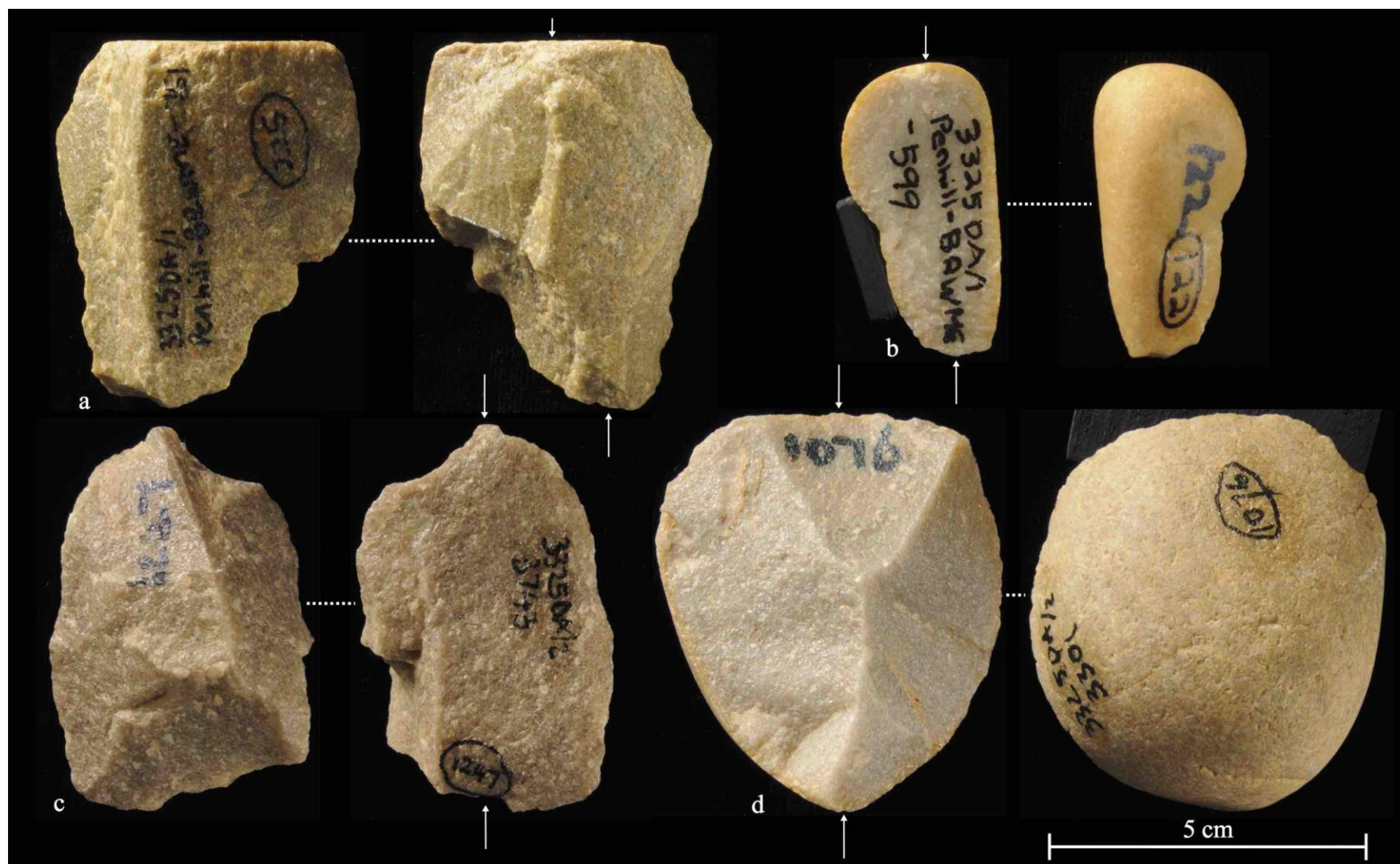


Figure 4.4.42. Debris flow bipolar complete flakes made on quartzite. Arrows indicate points of percussion.

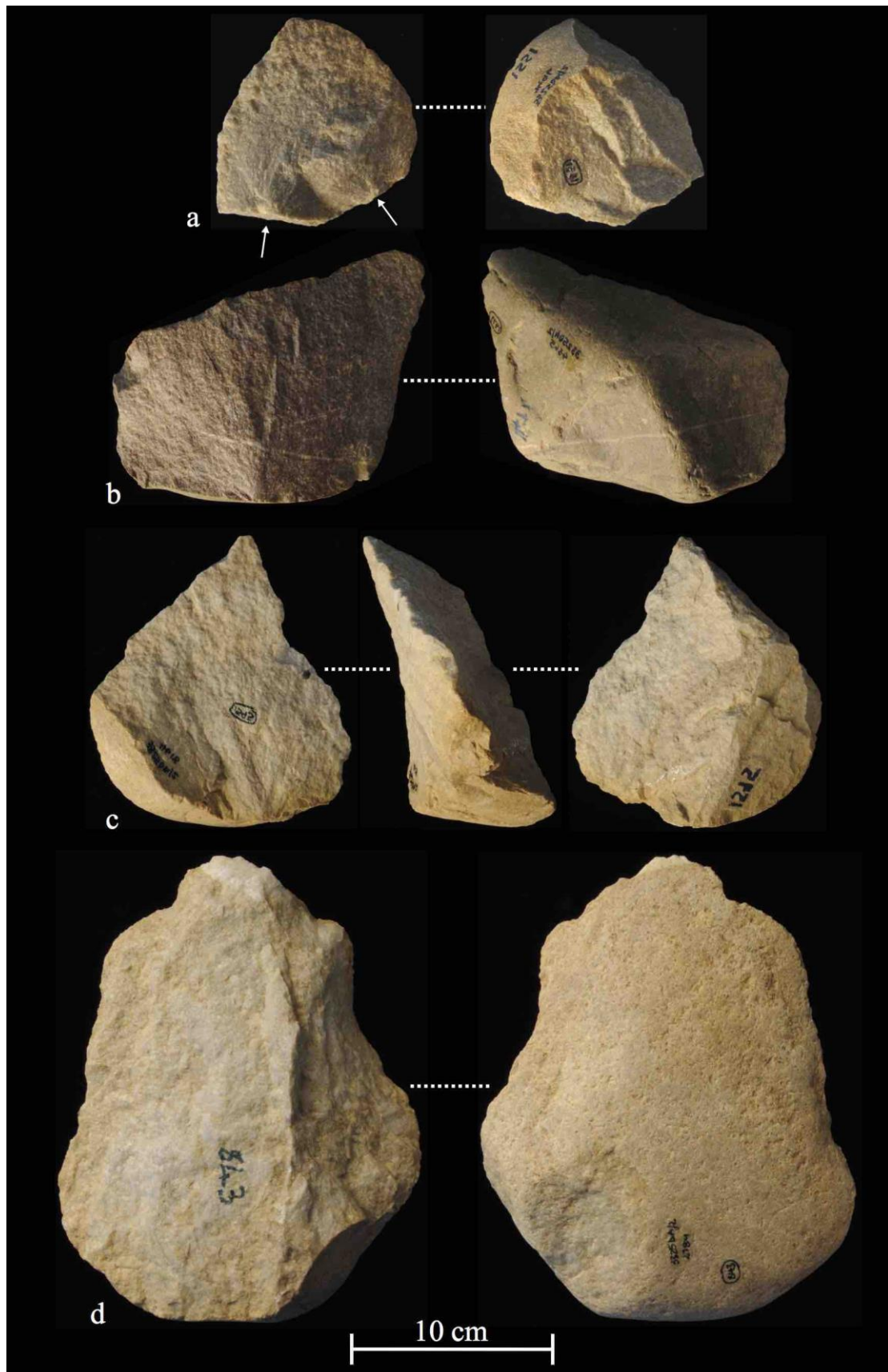


Figure 4.4.43. Debris flow assemblage large quartzite complete flakes (a-d). A large bi-bulb flake (a) and a flaked-flake (d) are also shown. Arrows indicate points of percussion.

4.4.3.3 Cores

Interestingly, core classification for the colluvial assemblage shows a complete absence of bipolar cores (Table 4.4.7; Fig. 4.4.44), although both bipolar flaking debris and bipolar complete flakes are found within the assemblage. A sample of cores for this assemblage is presented in Figures 4.4.46 and 4.4.47, and Table 4.4.7 shows that chopper-cores (n=17), casual and discoidal cores (n=11 each) are the most abundant types, collectively accounting for 68.4% of the total core sample. Irregular (n=6), single platform and core fragments (n=5 each) make up notably small portions of the total sample (ranging from 10.5-8.8%). Only a single core from the colluvial assemblage appeared to show a multiple platform exploitation pattern (polyhedral), and one 'more structured' discoid (with a single large removal) was also recovered (Fig. 4.4.47a).

The colluvial core assemblage (n=57) is dominated by quartzite pieces (75.4%; Table 4.4.9). Four of the core types are produced exclusively on this material, including: core fragments, discoid with large removal, polyhedrons and single platforms. Siltstone (14%), hornfels (8.8%) and claystone (1.8%) make up the remaining raw material types, and quartz, lava and silcrete are absent from the sample, even though flaking debris and complete flakes occur in these latter three materials. Chopper-cores provide the greatest raw material variability and are made on quartzite, siltstone, hornfels and claystone.

A sample of cores from the debris flow assemblage is shown in Figures 4.4.48-4.4.53, and Table 4.4.8 and Figure 4.4.45 highlight that the debris flow assemblage is also dominated by discoidal, casual, and chopper-cores (n=44, 43 and 31, respectively). Collectively these types account for 79.2% of the total core sample. However, for this assemblage the percentage of casual and discoidal cores exceeds the percentage of chopper-cores (in contrast to the colluvial assemblage; Figs. 4.4.44 & 4.4.45). Another notable difference for this assemblage is the presence of a single bipolar core (Fig. 4.4.51a). The remaining core sample is made up of small percentages of irregular cores (8.1%), damaged/broken cores (fragments, 5.4%), single platform cores (4.7%) and polyhedrons (2%). Boulder-cores were not recovered from the debris flow.

Raw material use for this core sample highlights that chopper-cores also retain the greatest raw material variability (four materials, including a single claystone piece; Table 4.4.10). Quartzite (81.2%) is the most favoured material, followed by hornfels (9.4%), siltstone (8.7%) and claystone (0.7%). Quartzite discoids are the most abundant type and the single bipolar core (Fig. 4.4.51a) is also comprised of quartzite. Siltstone use is highest for the casual cores (38.5% of the total siltstone sample) and hornfels use is greatest for the chopper-cores (42.9% of the total hornfels sample). No cores are made of quartz, silt-quartzite, lava or silcrete, even though both flaking debris and complete flakes occur on this material within the assemblage.

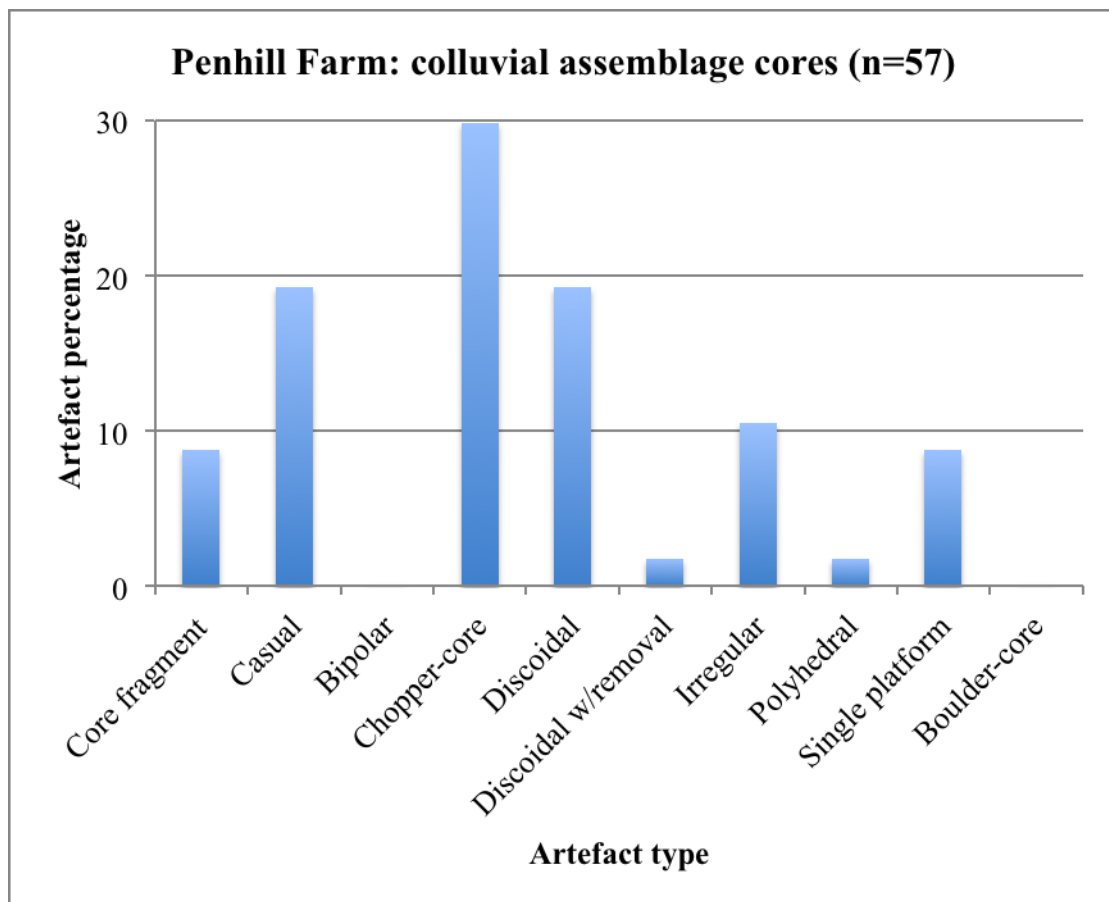


Figure 4.4.44. Core type classification for the colluvial assemblage.

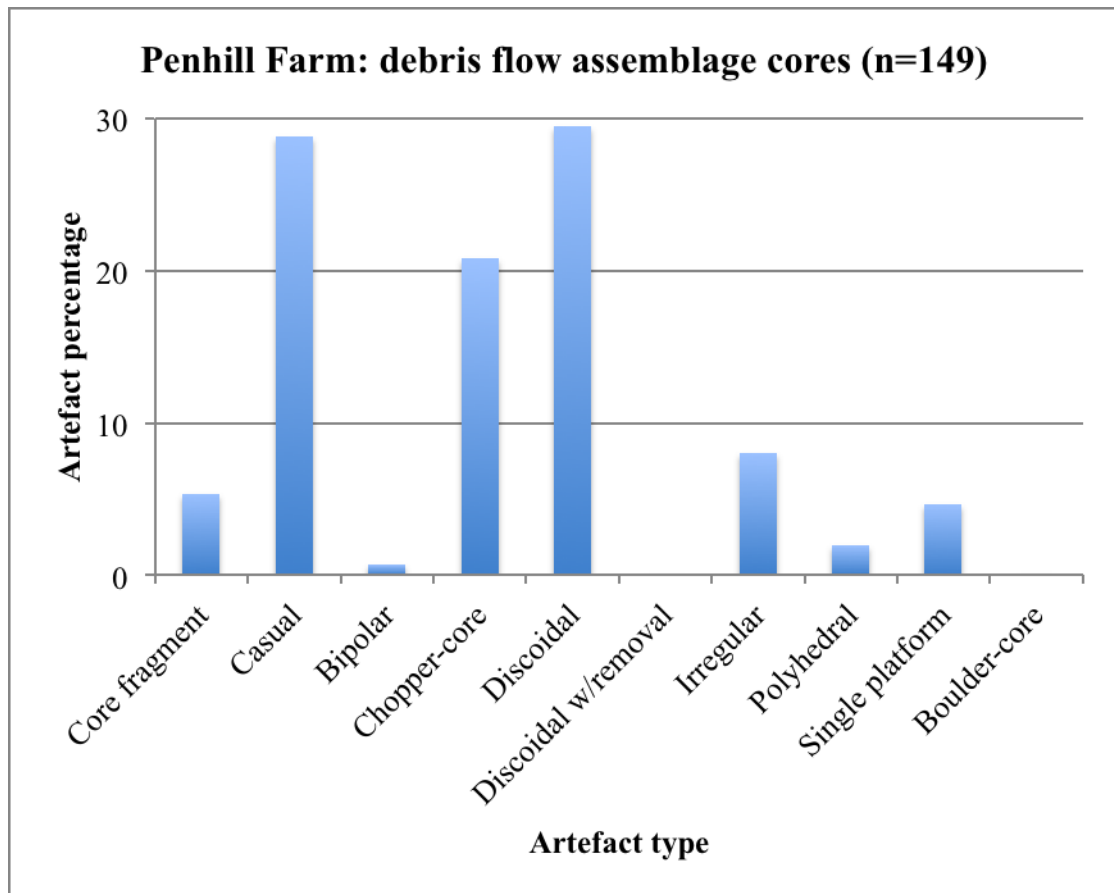


Figure 4.4.45. Debris flow assemblage core types.

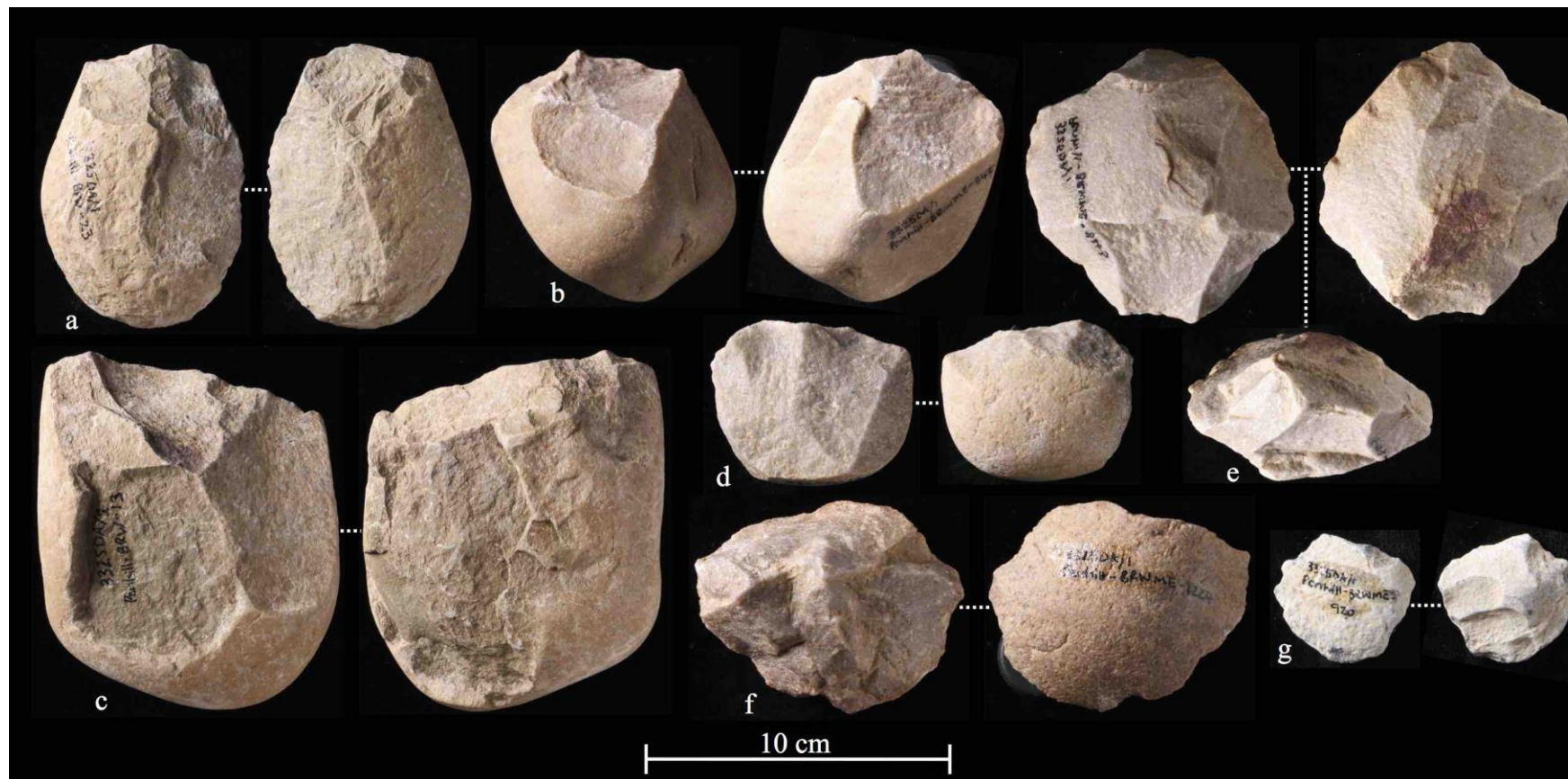


Figure 4.4.46. Colluvial assemblage cores. Blanks include cobbles (a-c), split cobbles (d), flakes (e) and indeterminate blanks (f & g), with those produced on quartzite (b, d-f), siltstone (a, c) and hornfels (g). Bifacial chopper-cores (a-d) and discoidal cores (e-g, f=unifacial) are shown.

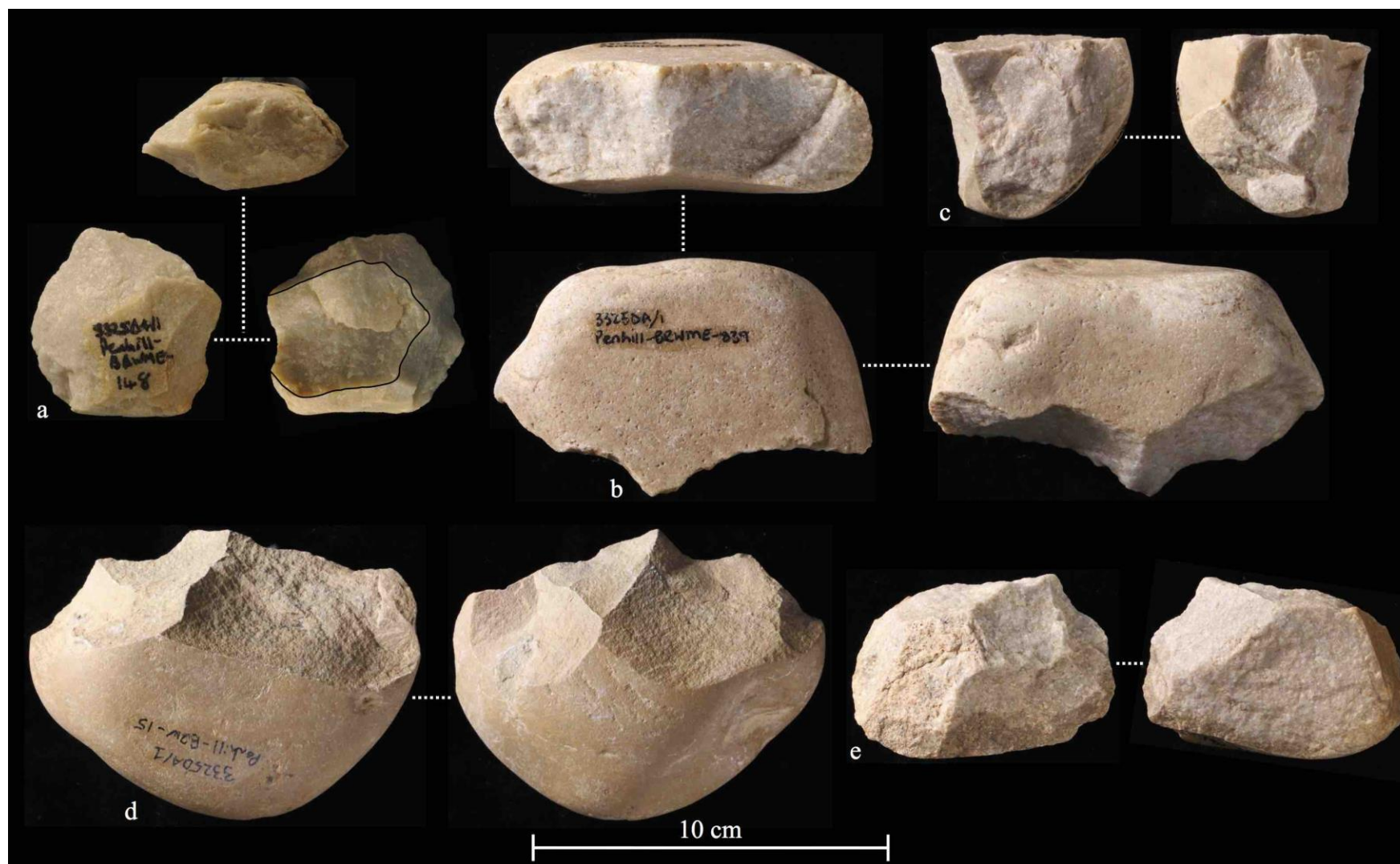


Figure 4.4.47. Colluvial assemblage cores (made on quartzite: a-c, e, and siltstone: d). Discoidal core on cobble showing a single large removal (a). Single platform core on cobble (b) and split cobble (c). Bifacial chopper-core on cobble (d). Irregular core on split cobble (e).

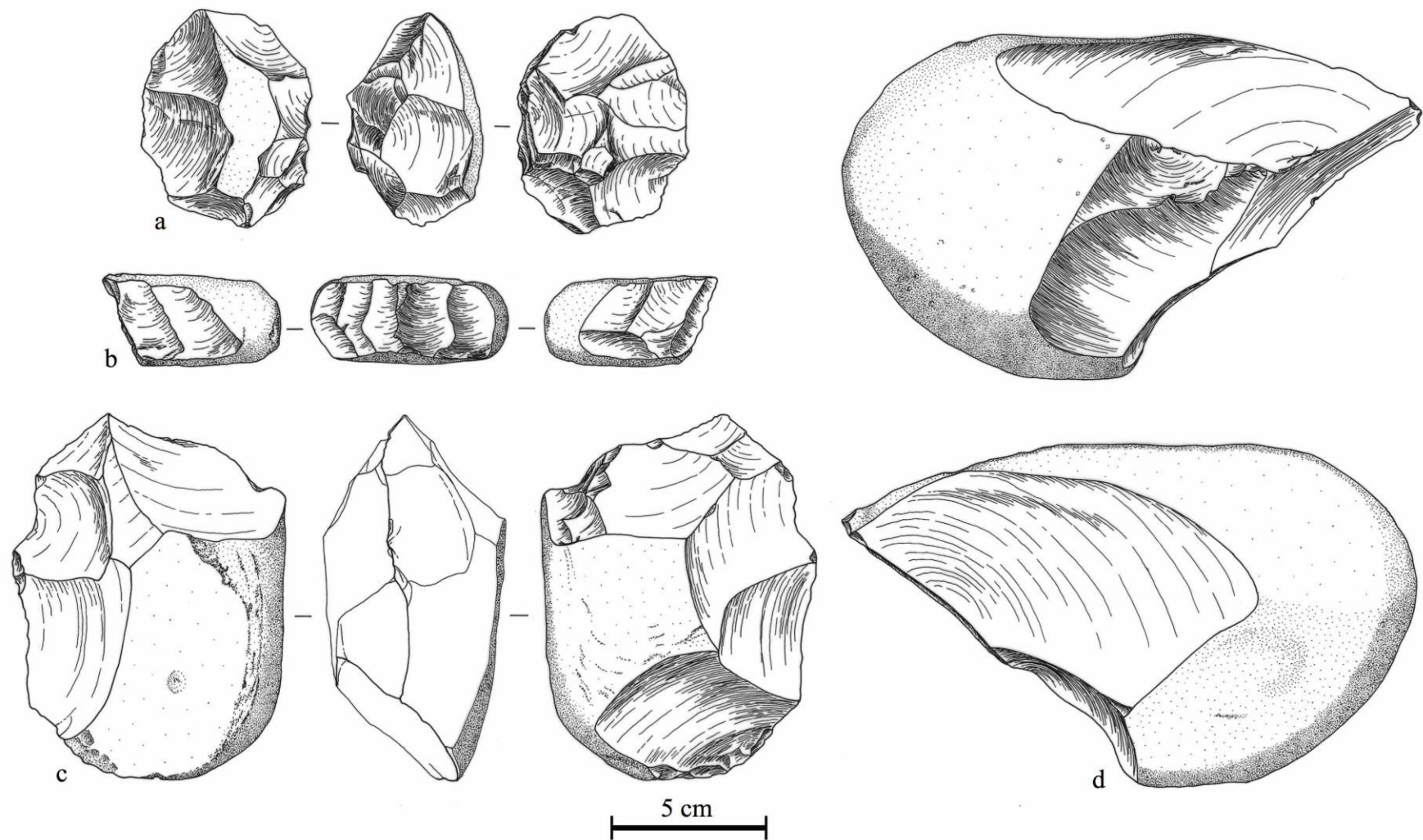


Figure 4.4.48. Debris flow assemblage cores on cobbles. Disoidal (a: quartzite), single platform (b: quartzite), chopper-core (c: siltstone), and irregular (d: siltstone) types are shown. Drawn by Wendy Voorvelt.

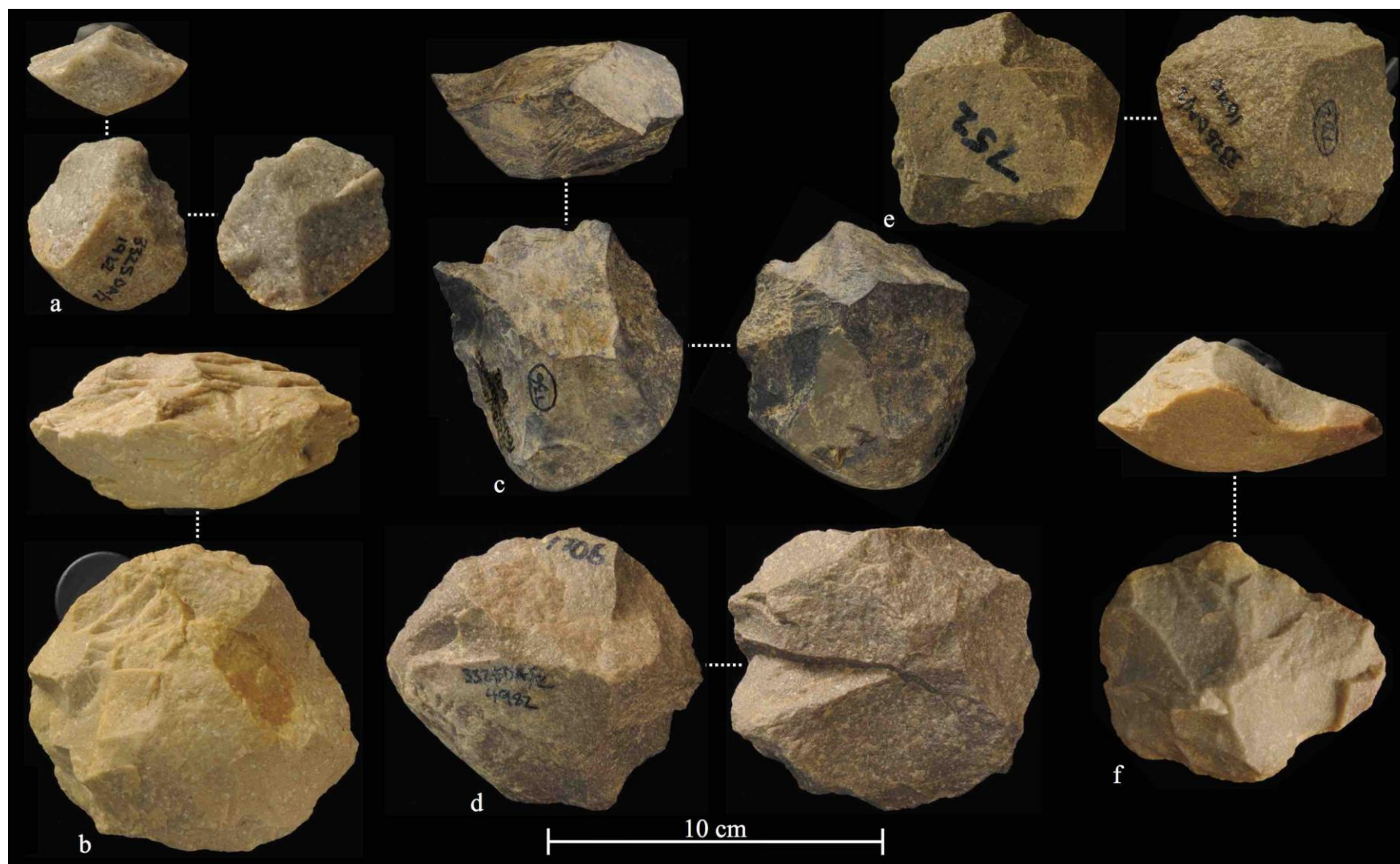


Figure 4.4.49. Debris flow assemblage discoidal cores. All are on flake blanks, except for 'a' with an indeterminate blank. Bifacial (a-e), on quartzite (a, b, d, e) and hornfels (c), and unifacial, on quartzite (f), cores are shown.

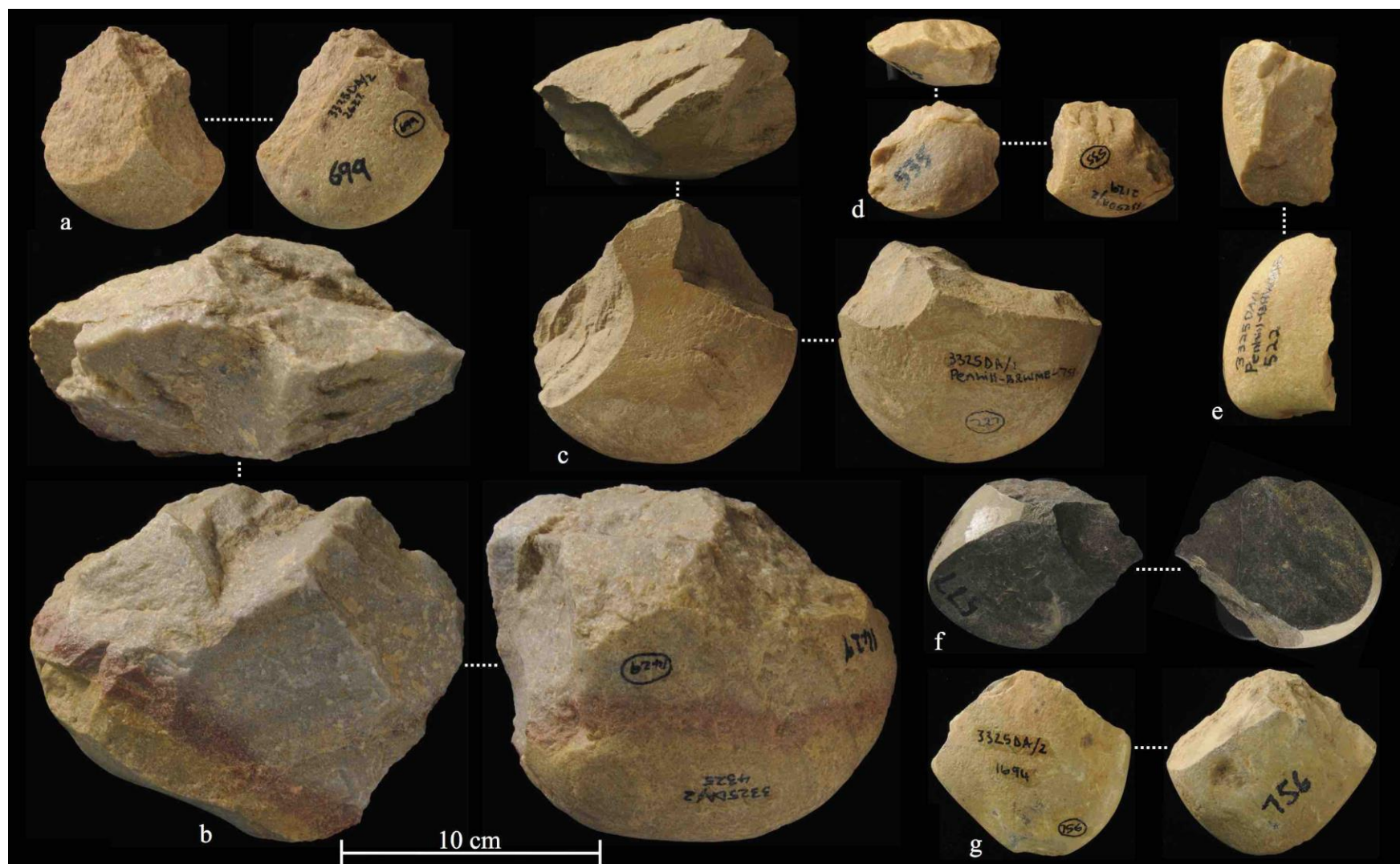


Figure 4.4.50. Debris flow assemblage chopper-cores. Blanks include cobbles (a, f, g), split cobbles (b, c, e) and a flake (d); a-d, f: bifacial on quartzite (a, b, d), siltstone (c) and hornfels (f); e, g: unifacial on quartzite (e) and hornfels (g).

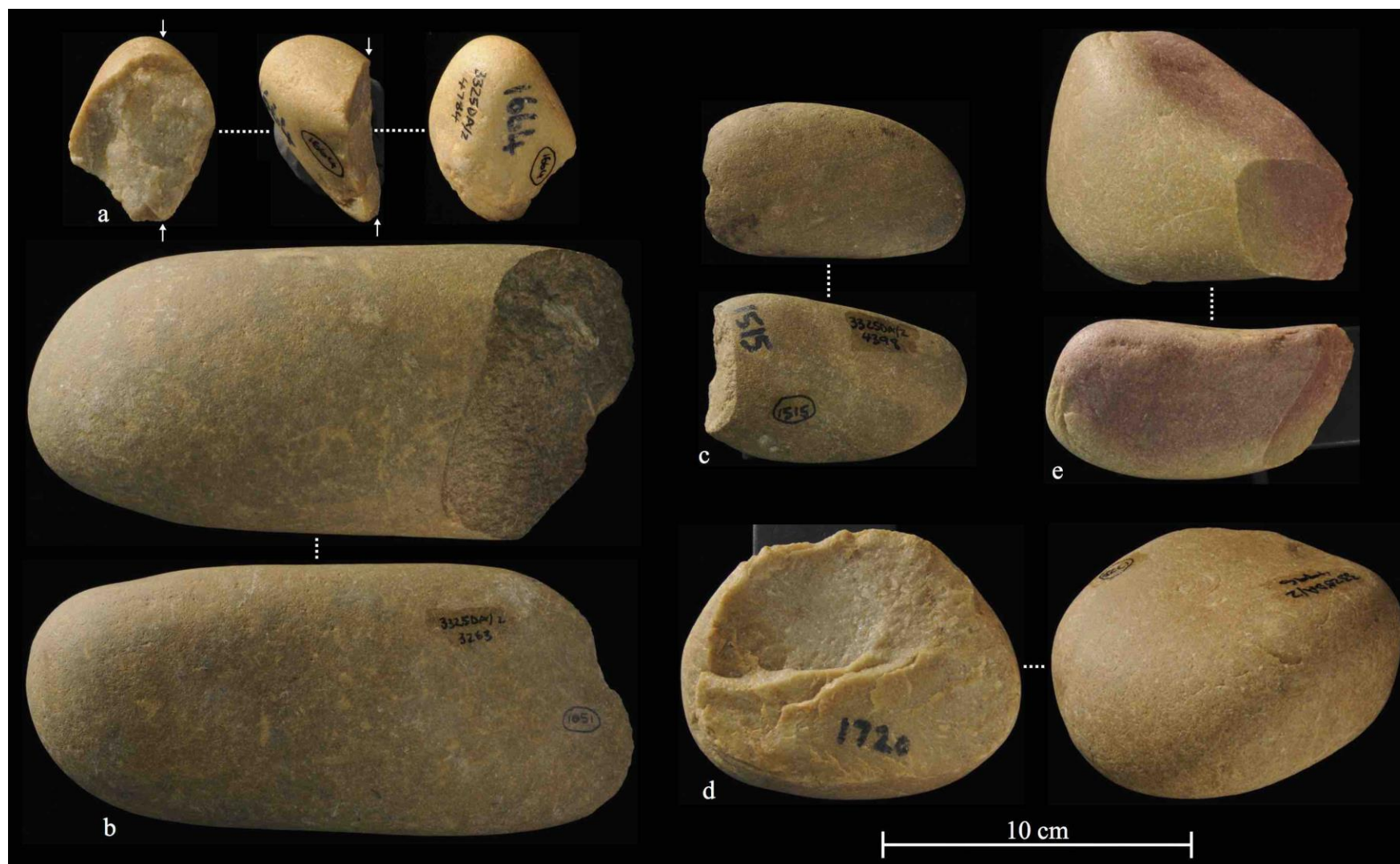


Figure 4.4.51. Debris flow assemblage cores; a: quartzite bipolar on split pebble/cobble, b-e: casual on quartzite split cobble (d) and cobble (e) and siltstone cobble (b, c). Arrows indicate points of percussion.

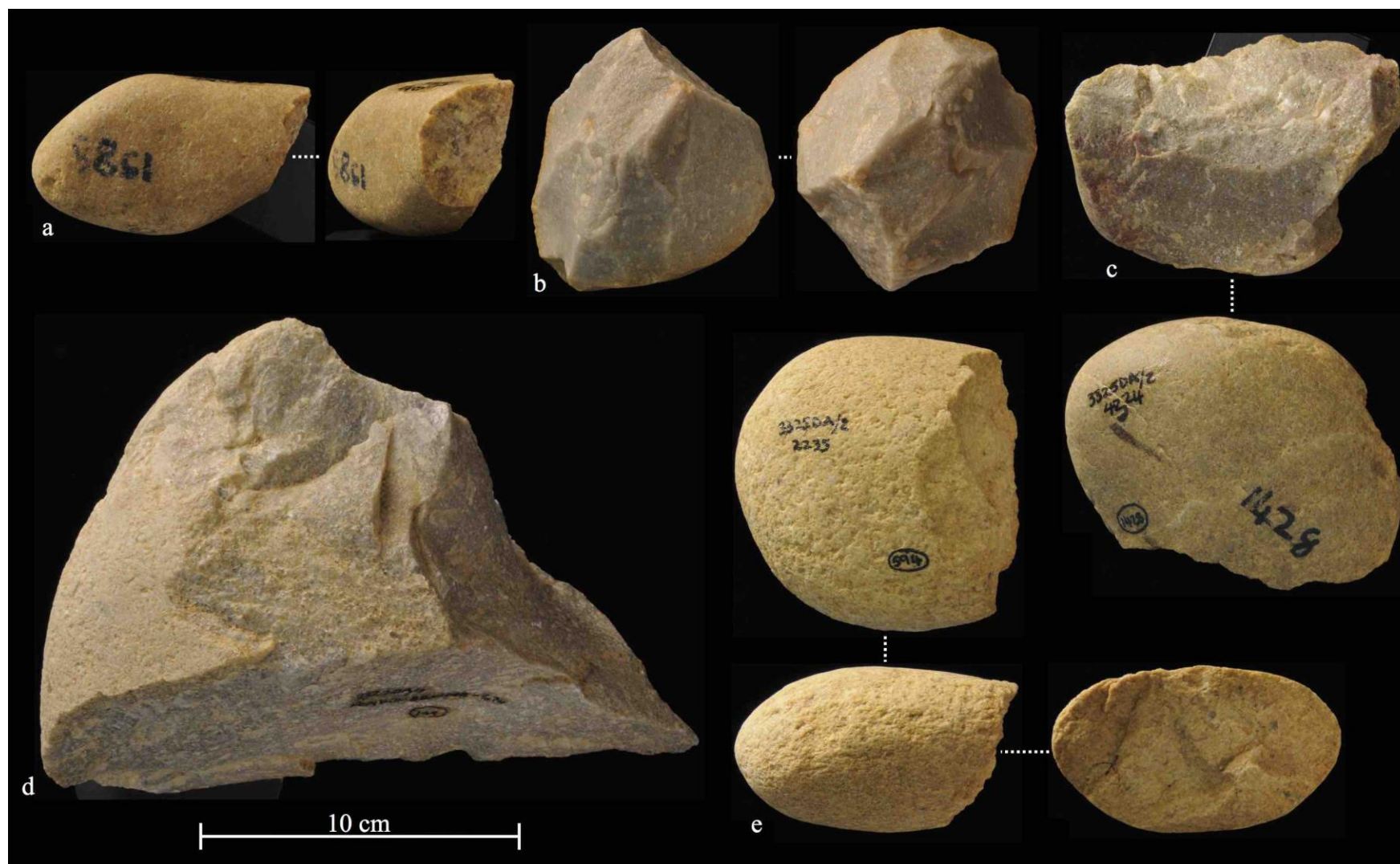


Figure 4.4.52. Debris flow assemblage quartzite cores. Blanks include cobbles (a, e) and split cobbles ('b' is bipolar, c, d); a: single platform, b: polyhedron, c: single platform, d: irregular, e: single platform.



Figure 4.4.53. Debris flow cores on cobbles with large scars (>10 cm); a: bifacial chopper-core, b, c: casual.

4.4.3.4 Formal tools

The percentage of each of the formal tool types for the colluvial assemblage is shown in Figure 4.4.54, and a sample of these formal tools is shown in Figure 4.4.56. From this there is a clear abundance of scrapers (51.1%), which account for 3.8% of the total assemblage (Table 4.4.7). Thereafter, equal quantities of miscellaneous retouched pieces and LCTs occur (n=11), each making up 11.7% of the formal tools sample. Denticulates and retouched flakes (combined total of 15 pieces) are less frequent and collectively contribute 16% of the total formal tool sample. Three composite pieces, three flaked-flakes, two choppers and a single burin make up the remaining parts of the formal tools sample. No awls or knives were recovered.

Raw material use is almost exclusively quartzite for this colluvial formal tool sample (n=85, 90.4%) and only nine pieces show different raw material use, namely: two handaxes, a cleaver, scraper and denticulate (n=5, 5.3%, siltstone), and one MRP and three scrapers (n=4, 4.3%, hornfels; Table 4.4.9). No formal tools were produced on quartz, lava, silcrete or claystone.

The debris flow formal assemblage (n=416; a sample of artefacts is presented in Figures 4.4.57-4.4.60) shows that scrapers are once again the dominant tool type (30.5%; Fig. 4.4.55; Table 4.4.8). In contrast to the overlying colluvial assemblage, MRPs and denticulates make up the largest remaining tool type percentages (25.5 and 17.8%, respectively). Although the LCT sample (n=38) from this assemblage is larger than that of the colluvial assemblage (n=11), the percentage contribution of these tools is lower (at 9.1%). Retouched flakes provide 9.9% of the total sample. In contrast to the colluvial assemblage, Figure 4.4.55 shows that both knives (1%) and a single awl (0.2%; Fig. 4.4.57b) form part of the debris flow (collectively 5 pieces). Flaked-flakes (n=12), composite pieces (n=11), and a single chopper (Fig. 4.4.58b) and burin make up the remaining tool types.

Raw material use in the debris flow formal tool assemblage shows far greater variability, in contrast to the colluvial assemblage (Table 4.4.10); six types of raw material are utilised in artefact production, namely: quartzite (83.4%), siltstone (10.1%), hornfels (3.4%), claystone (1.9%), silt-quartzite (0.7%), and lava (0.5%). No

formal tools are made on silcrete. Quartzite scrapers and MRPs are the most common types (n=201), accounting for 48.3% of the total formal tool sample. LCTs are only produced on quartzite (n=29, 76.3%) and siltstone (n=9, 23.7%), and the total silt-quartzite sample (n=3) comprises of two MRPs and one denticulate. Although the use of hornfels is marginally less frequent than for the colluvial assemblage (at 3.4%), its highest use (n=6, 1.4%) is in the scrapers category. Lava, comprising of only two pieces, included a flaked-flake and composite piece (0.5%). The use of claystone is evident only in the ‘smaller retouched pieces’, including: scrapers (n=3), MRPs (n=2), and a burin, denticulate and retouched flake (collectively n=8, 1.9%).

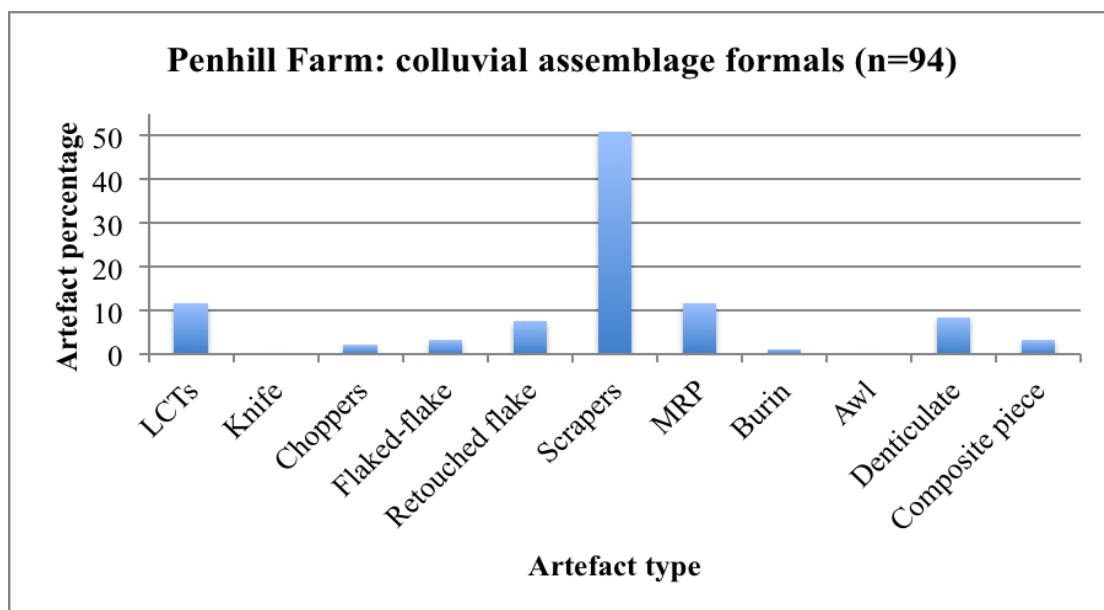


Figure 4.4.54. Formal tool types for the colluvial assemblage.

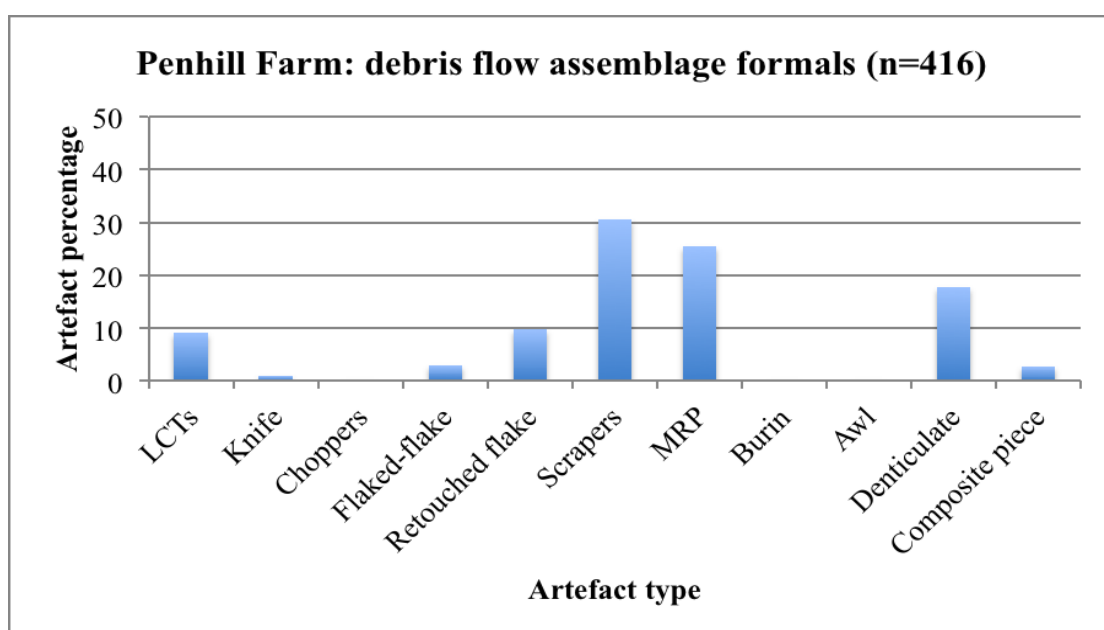


Figure 4.4.55. Debris flow assemblage formal tool types.

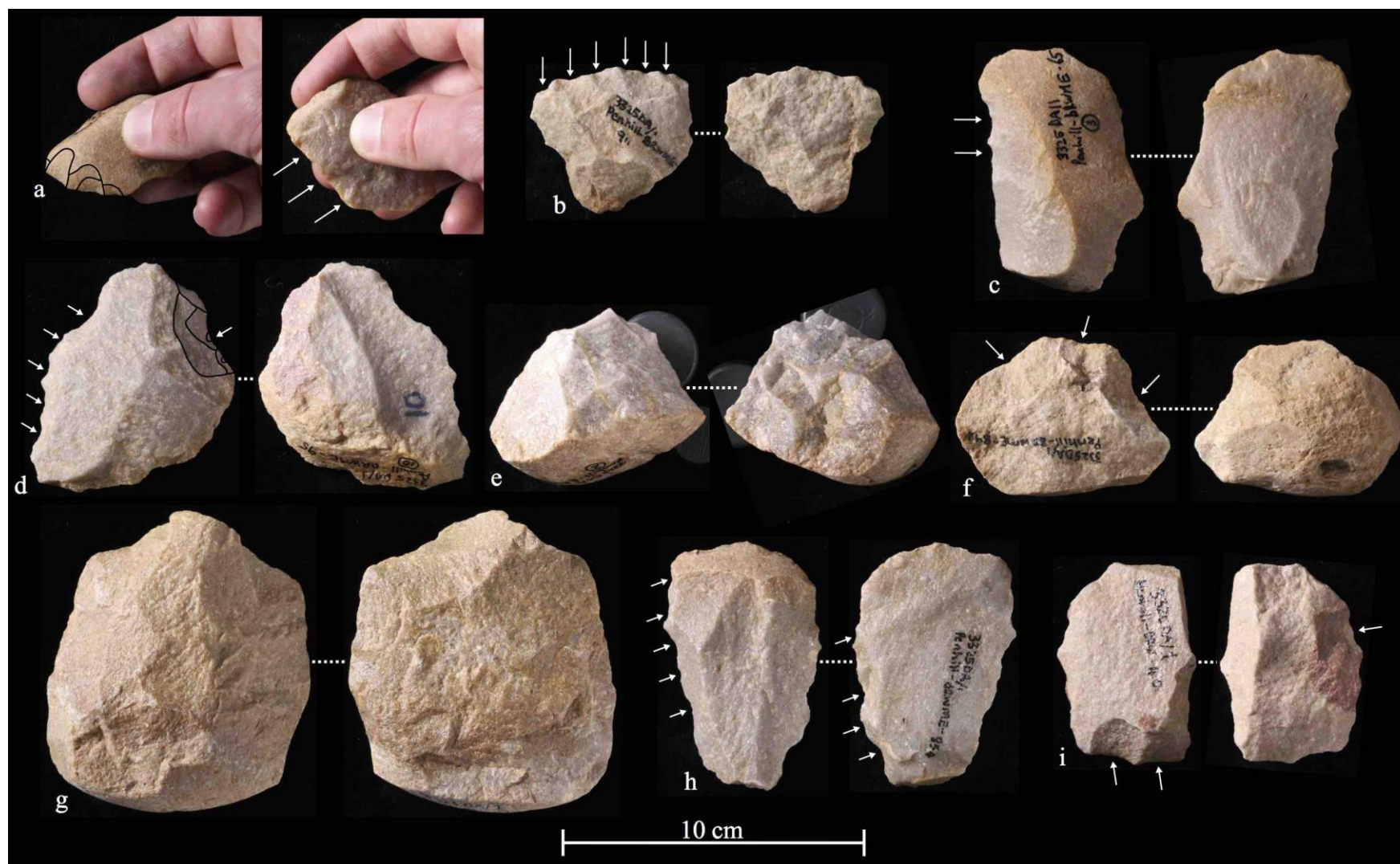


Figure 4.4.56. Colluvial assemblage quartzite formal tools; a: composite piece on flake with scraper (left) and denticulate (right), b: denticulate, c: retouched flake, d: composite piece on flake with denticulated edge and concave scraper, e, g: bifacial choppers on split cobble, f, i: flaked-flakes (arrows indicate points of percussion), h: denticulate on flake. Arrows indicate retouch.

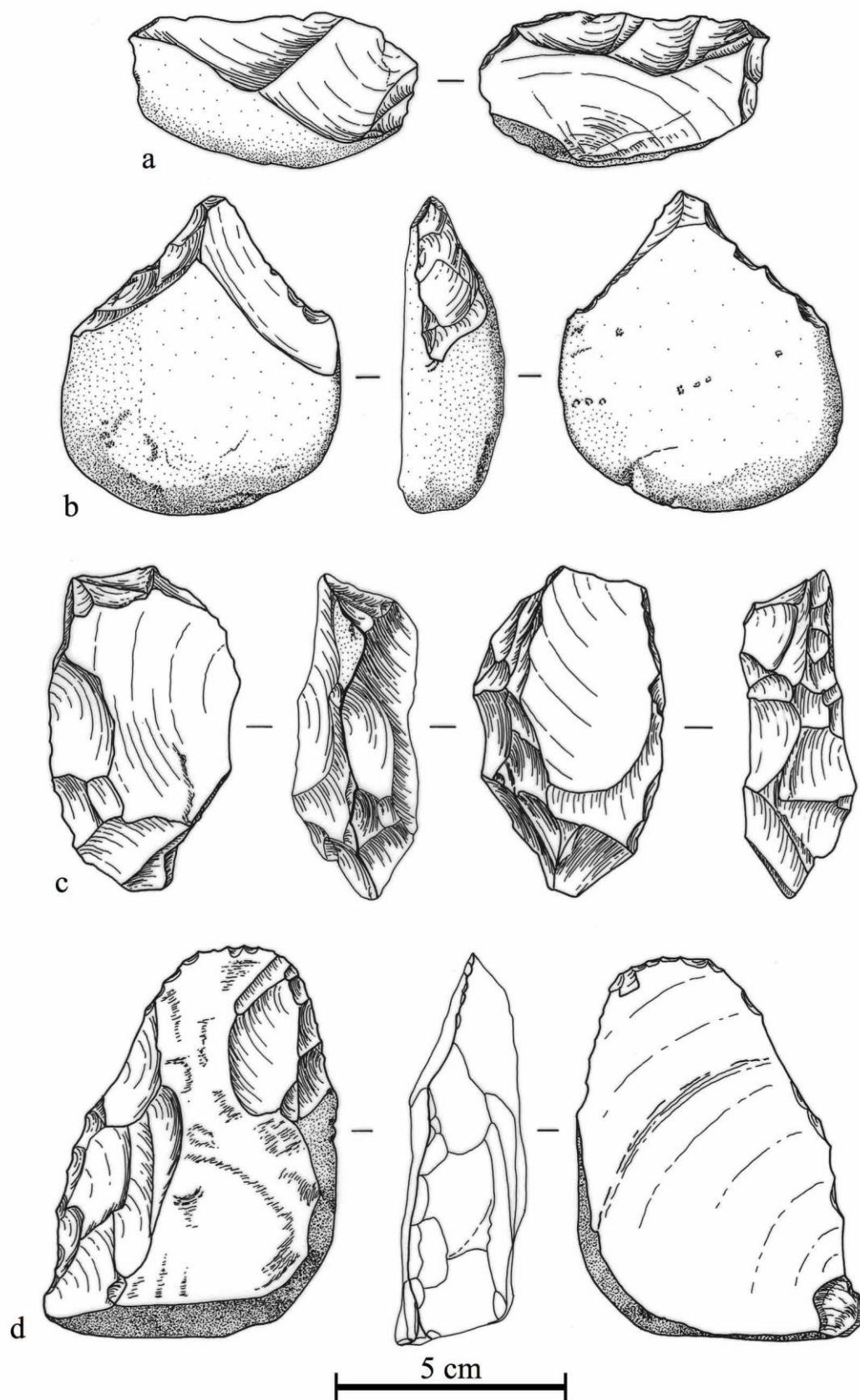


Figure 4.4.57. Debris flow formal tools; a: denticulate on quartzite flake, b: awl on quartzite cobble, c: quartzite composite piece (scraper and knife), d: siltstone knife. Drawn by Wendy Voorvelt.

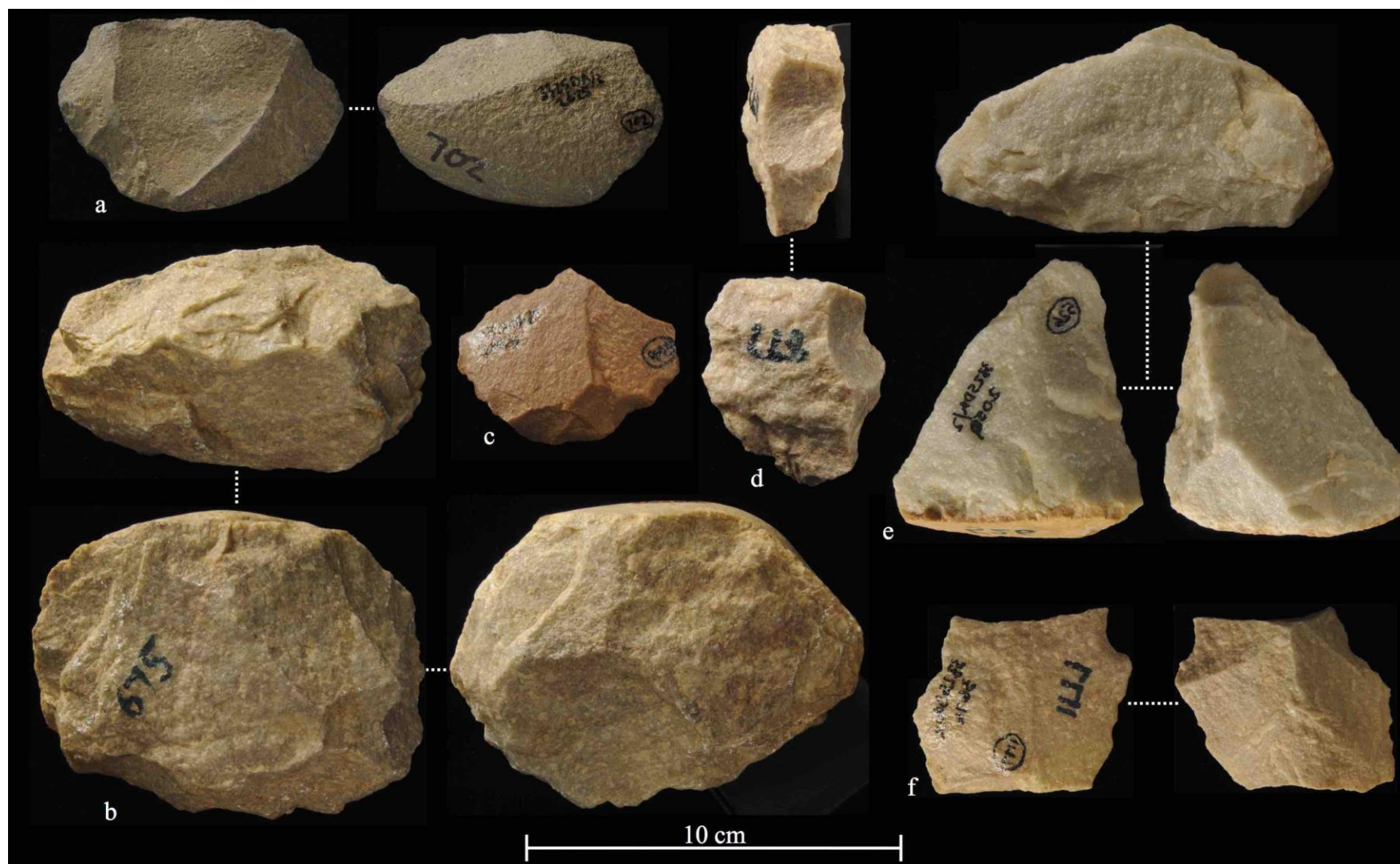


Figure 4.4.58. Debris flow assemblage formal tools. Raw materials include hornfels (a: flaked-flake) and quartzite (b: chopper on split cobble, c: retouched flake, d: flaked-flake, e: knife on a flake, f: retouched flake).



Figure 4.4.59. Debris flow assemblage denticulates. These are made on siltstone (a, c) and quartzite flakes (b, d, e). Arrows indicate retouch along flake edges.

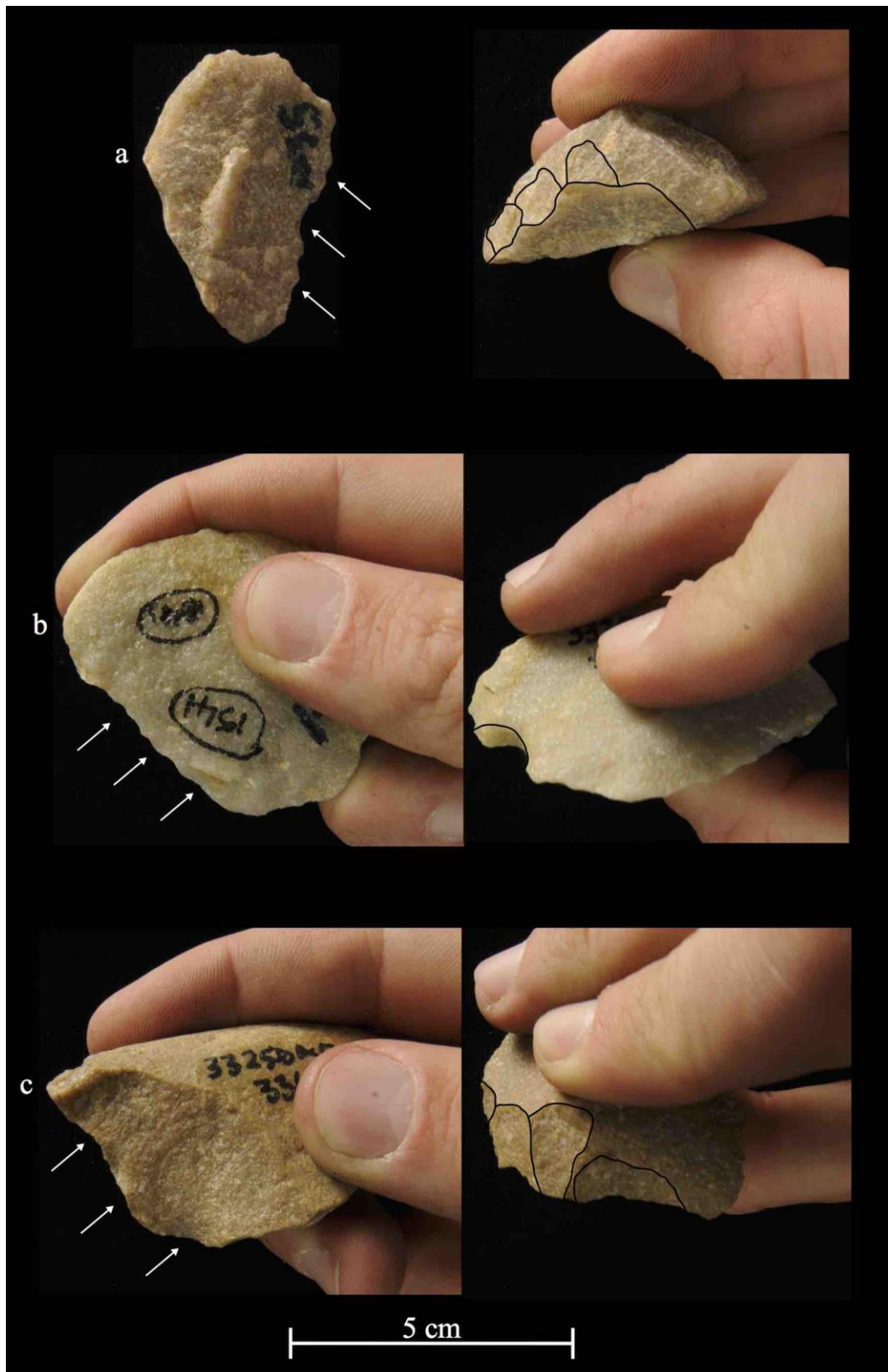


Figure 4.4.60. Debris flow quartzite flake composite pieces; a: denticulate (left) and scraper (right), b: knife (left) and notched scraper (right), c: denticulate (left) and scraper (right). Arrows indicate retouch (a, c) and utilisation damage (b).

Scrapers:

Tables 4.4.7 and 4.4.8 and Figures 4.4.61 and 4.4.62 illustrate the percentages of the different scraper types for both assemblages. For the colluvial assemblage (n=1258) scrapers account for 3.8% of the total sample (Table 4.4.7; see Figure 4.4.63 for a sample of these tools). The most abundant type is denticulated (n=19), making up 39.6% of the total scraper sample (Fig. 4.4.61). Notched scrapers and side scrapers make up the two largest remaining percentages by type (29.2 and 12.5%, respectively). Thereafter, percentages range from a maximum of 8.3% (composite scrapers) to a minimum of 2.1% (convex, end and heavy-duty/core scrapers) for the remaining types; double side and end and convergent scrapers were not recovered.

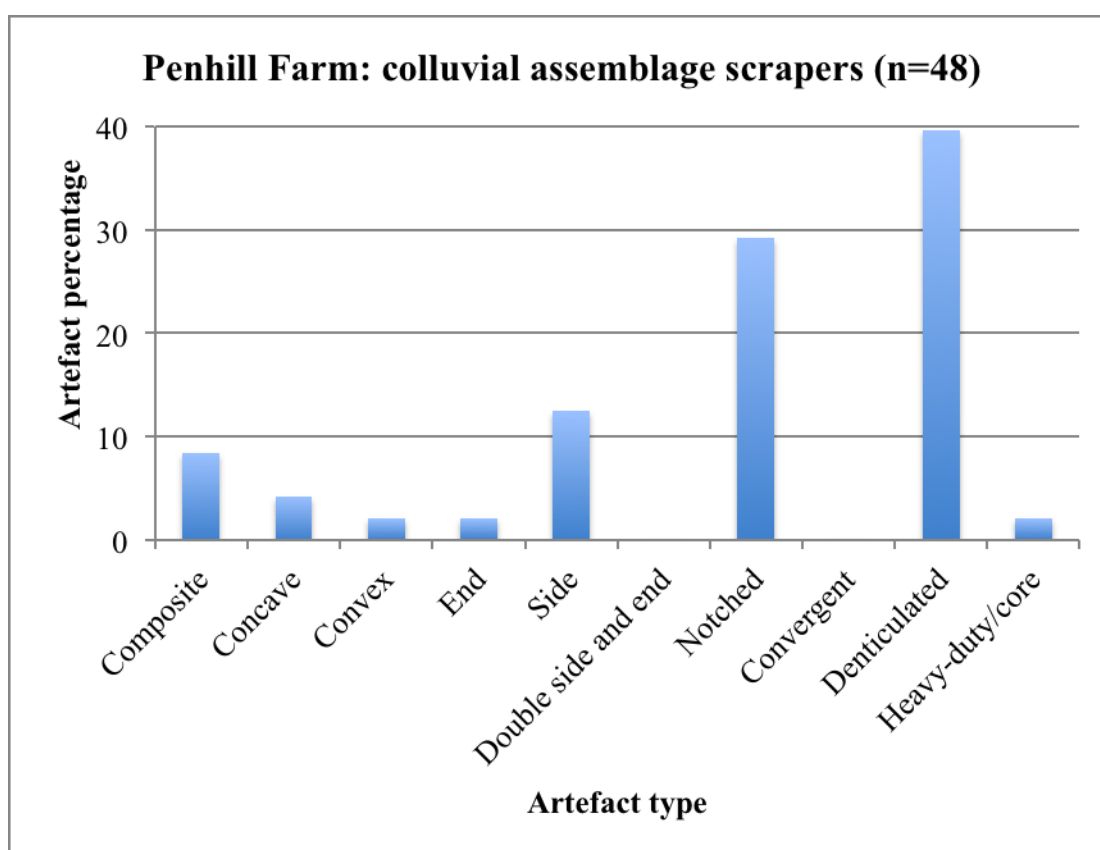


Figure 4.4.61. Scraper types for the colluvial assemblage.

Scraper distribution for the debris flow sample (n=127) shows that denticulated, notched and side types are also the most abundant (37, 27.6 and 9.4%, respectively; Fig. 4.4.62); a sample of scrapers is illustrated in Figures 4.4.64-4.4.66. Collectively these three types account for 74% of the total scraper sample (in contrast to 81.3% for the colluvial assemblage), highlighting the greater variation in scraper types for the lower lying debris flow assemblage. As a result there are higher percentages of

concave, convex and end type scrapers (between 7.1-3.1%), along with samples of double side and end (n=1; Fig. 4.4.64a), convergent (n=1; Fig. 4.4.66a) and heavy-duty/core scrapers (n=1; Fig. 4.4.64d).

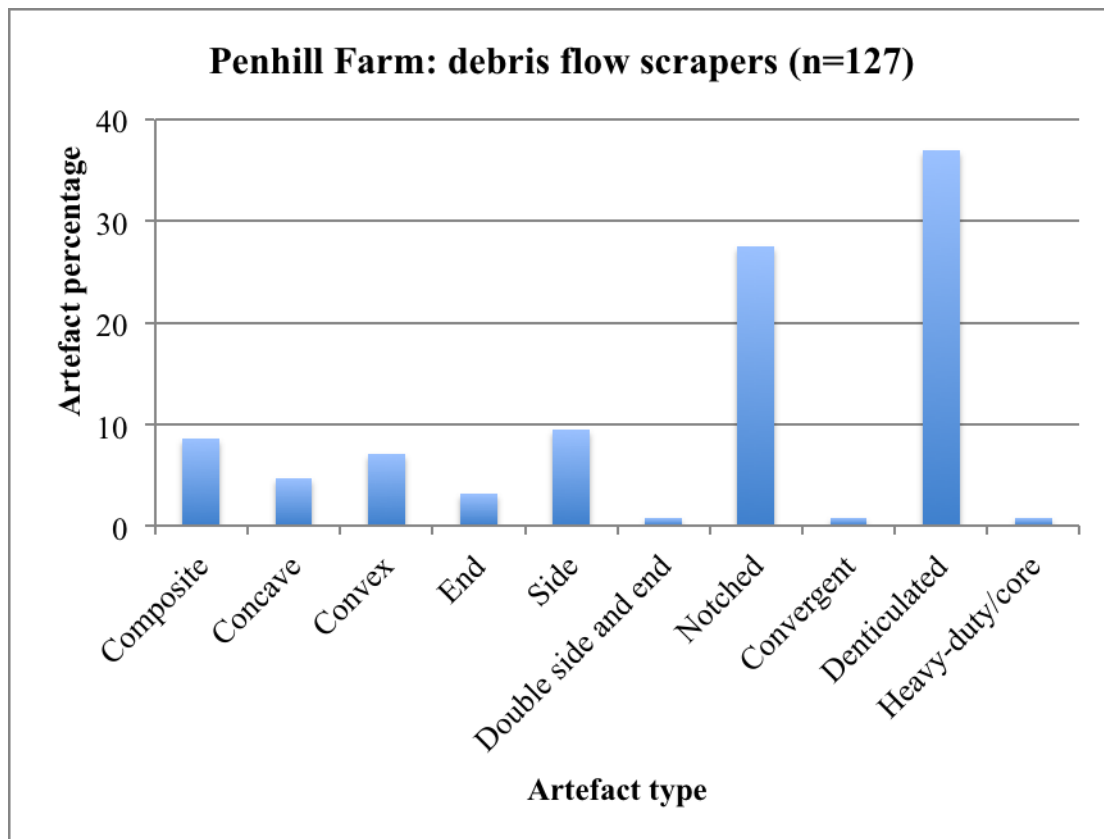


Figure 4.4.62. Scraper types for the debris flow assemblage.

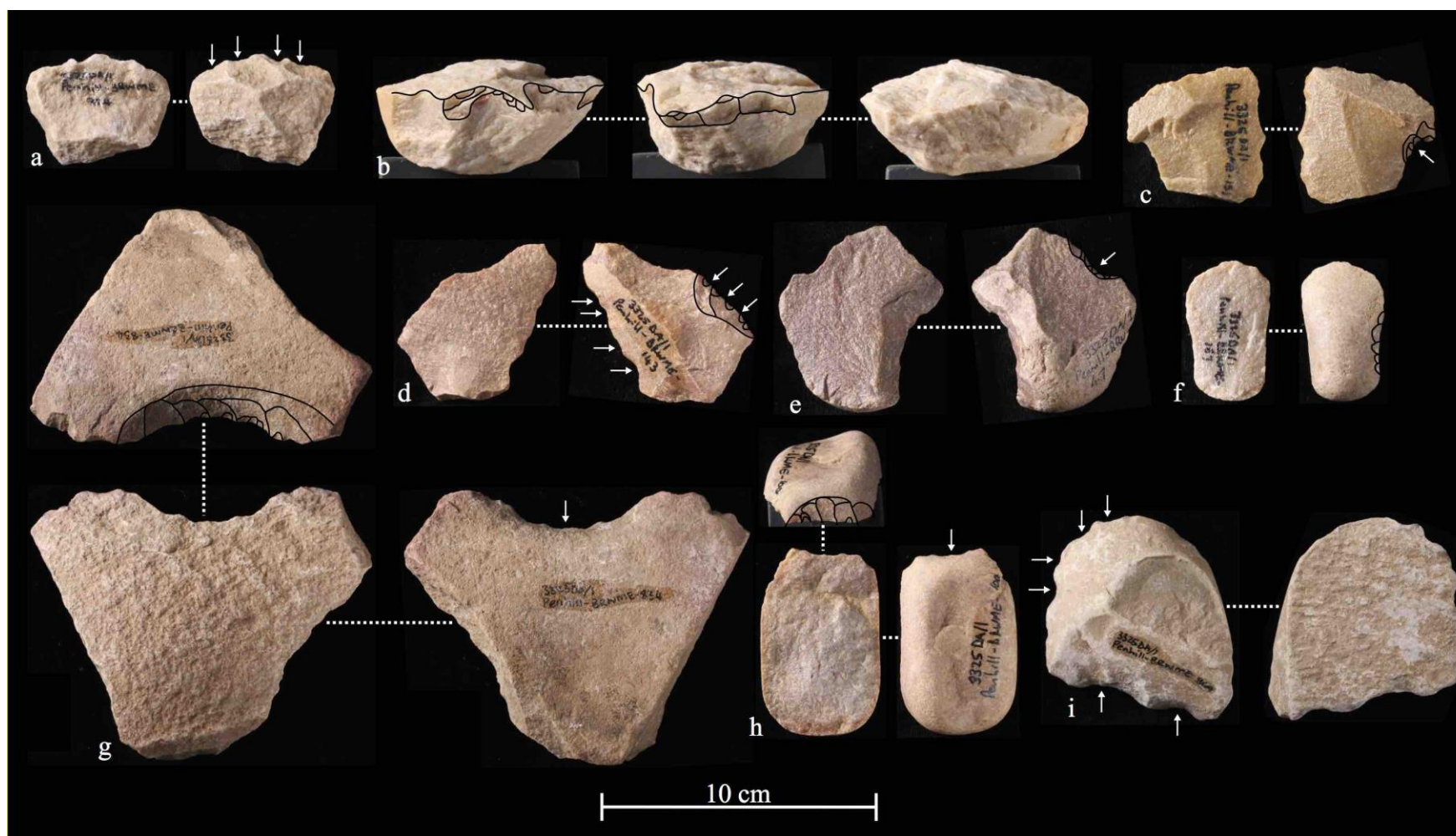


Figure 4.4.63. Colluvial assemblage scrapers. Raw materials include quartzite (a-f, h), siltstone (g) and hornfels (i); a: denticulated on flake, b: heavy-duty/core on split cobble, c, e: notched on flake, d: composite (denticulated and side) on flake, f: side on flake, g: concave on flake, h: end on flake, i: denticulated on split cobble. Arrows indicate retouch.

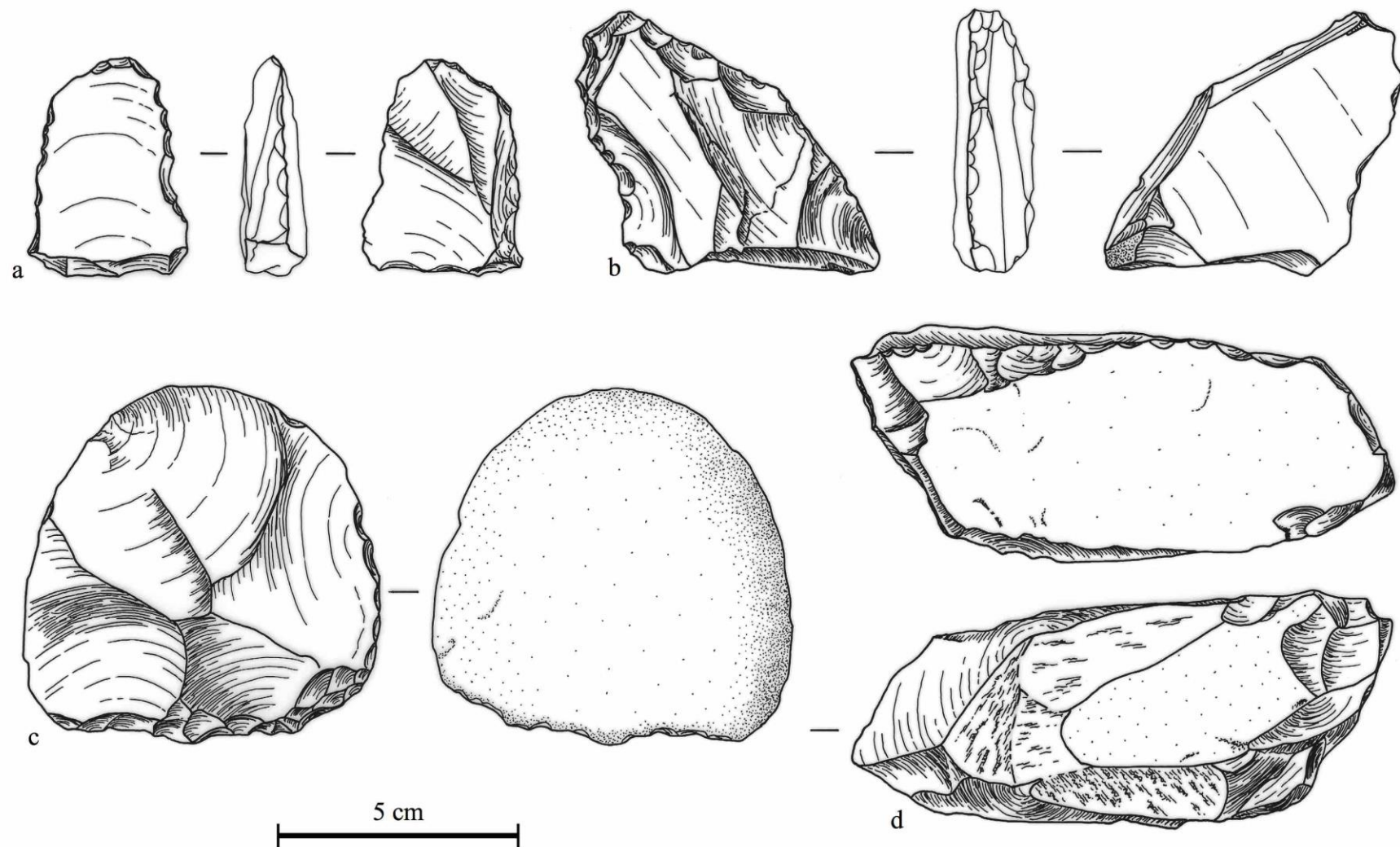


Figure 4.4.64. Debris flow assemblage quartzite scrapers; a: double side and end on flake, b: composite (notched and denticulated) on flake fragment, c: denticulated on unifacial discoidal core, d: heavy-duty on split cobble. Drawn by Wendy Voorvelt.



Figure 4.4.65. Debris flow scrapers. Raw materials include siltstone (a, b, e) and quartzite flakes (d, f-j), and a hornfels split cobble (c); a, f: denticulated, b, c: notched, d: convex, e, g, h: side, i: end, j: concave. Arrows indicate retouch.



Figure 4.4.66. Debris flow scrapers. These include those on quartzite (a, c, d, f) and siltstone flakes (e), and on a hornfels chunk (b); a: convergent, b, c: notched, d: convex, e: composite (concave and denticulated, on a recycled flake), f: denticulated. Arrows indicate retouch.

LCTs:

The LCT sample for the colluvial and debris flow assemblages is broken down, by type, in Figures 4.4.67 and 4.4.68; all LCTs are illustrated in Figures 4.4.69-4.4.71 (colluvial assemblage) and Figures 4.4.72-4.4.81 (debris flow assemblage).

The colluvial LCT sample makes up 0.9% of the total assemblage (Table 4.4.7). For this sample handaxes (n=4) and cleavers (n=3) dominate and by percentage these types account for 63.6% of the total LCT sample (Fig. 4.4.67). Picks and bifaces are equally frequent (n=2 each) and collectively make up the remaining 36.4% of the sample. For this assemblage the number of handaxes exceeds the number of cleavers, and no broken (damaged) handaxes/LCTs were recovered.

LCTs by percentage are less abundant in the debris flow assemblage, comprising only 0.4% of the total assemblage (Table 4.4.8). Figure 4.4.68 illustrates that handaxes and cleavers are equally frequent; these types account for 63.1% of the total LCT sample. The quantity of broken handaxes/LCTs is far higher for this assemblage at 15.8% in comparison to 0% for the overlying colluvial assemblage. Picks (n=5) and bifaces (n=3) are less abundant by percentage (13.2 and 7.9%, respectively) than those from the colluvial LCT sample (Figs. 4.4.67 and 4.4.68).

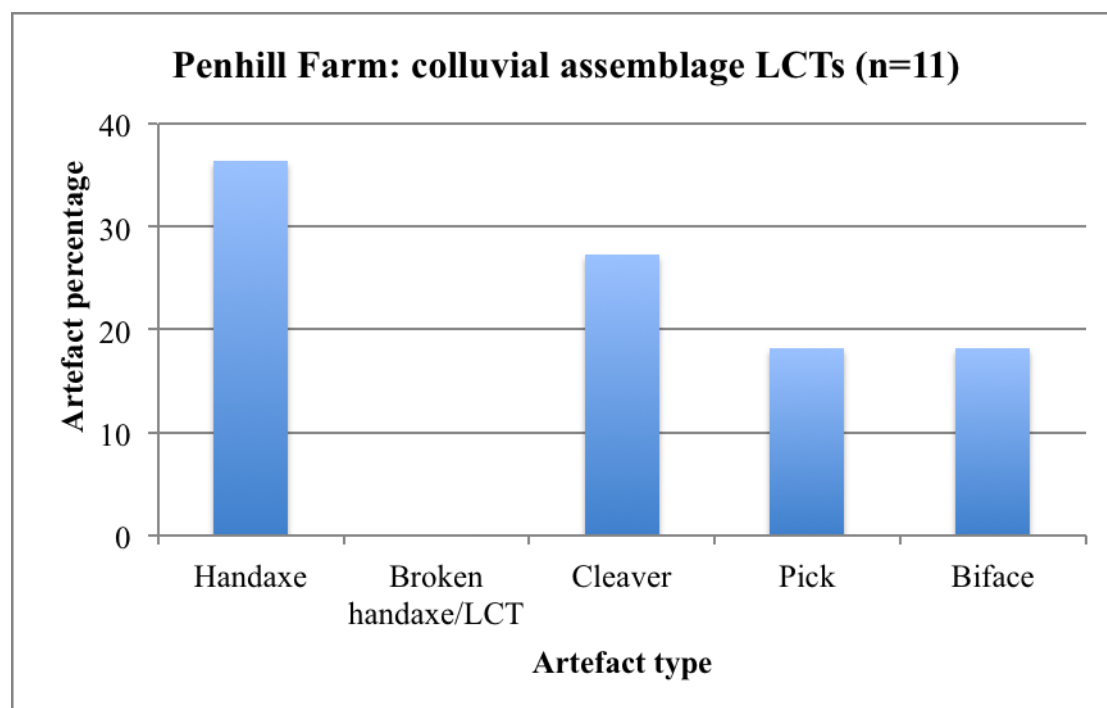


Figure 4.4.67. LCT type distribution for the colluvial assemblage.

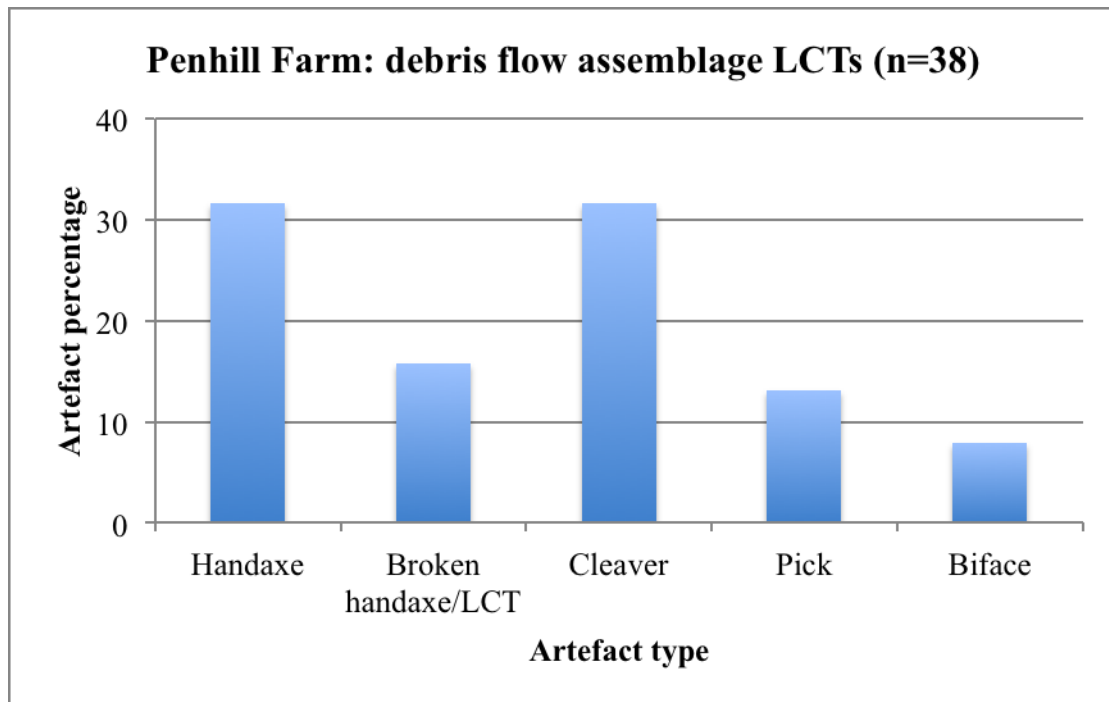


Figure 4.4.68. Debris flow assemblage LCT types.

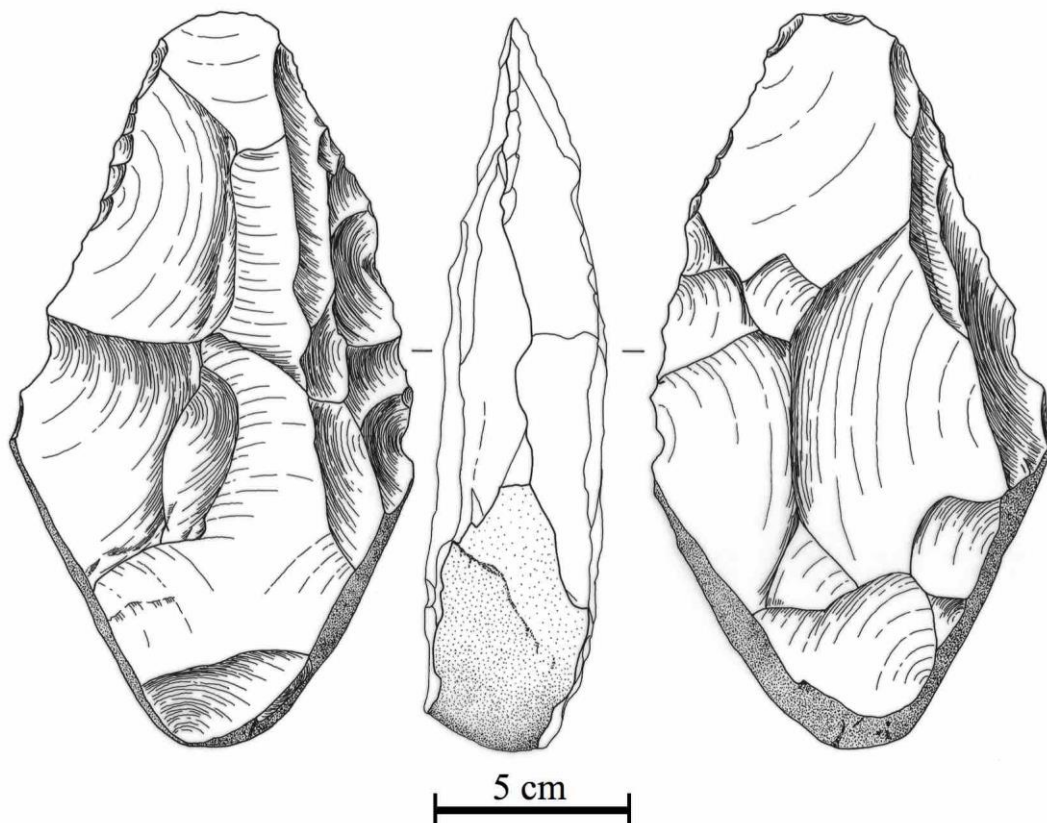


Figure 4.4.69. Colluvial assemblage handaxe (convergent rounded distal and made on a large corner-struck quartzite flake). Drawn by Wendy Voorvelt.

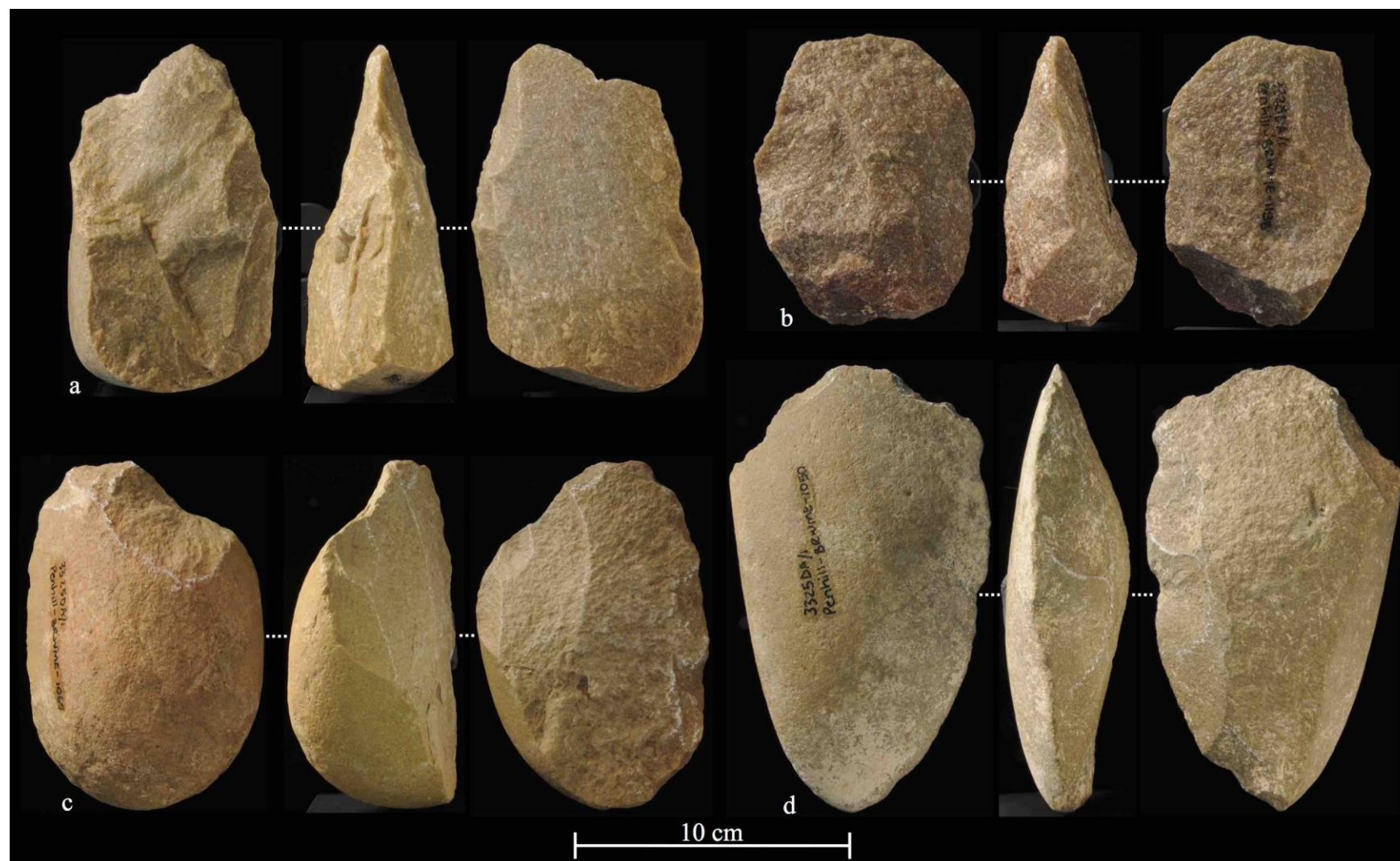


Figure 4.4.70. Colluvial assemblage LCTs. Types include cleavers (a, b, d) and a handaxe (c), all made on flake blanks; a, b: quartzite, c, d: siltstone.

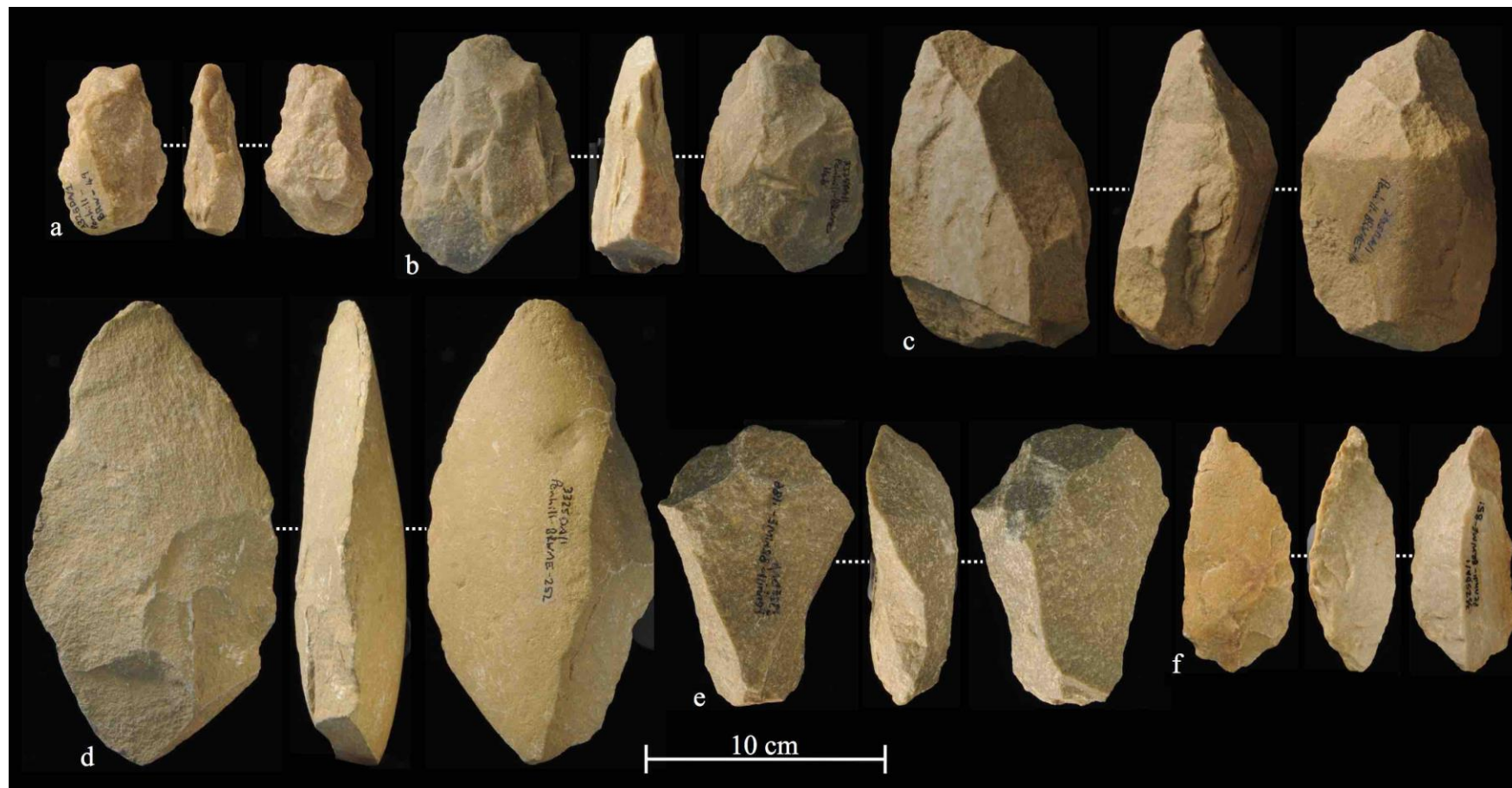


Figure 4.4.71. Colluvial assemblage LCTs; biface on quartzite flake (a, e), handaxe (b, d) on quartzite flake (b) and siltstone flake (d), picks (c, f) on quartzite (c: split cobble, f: flake).

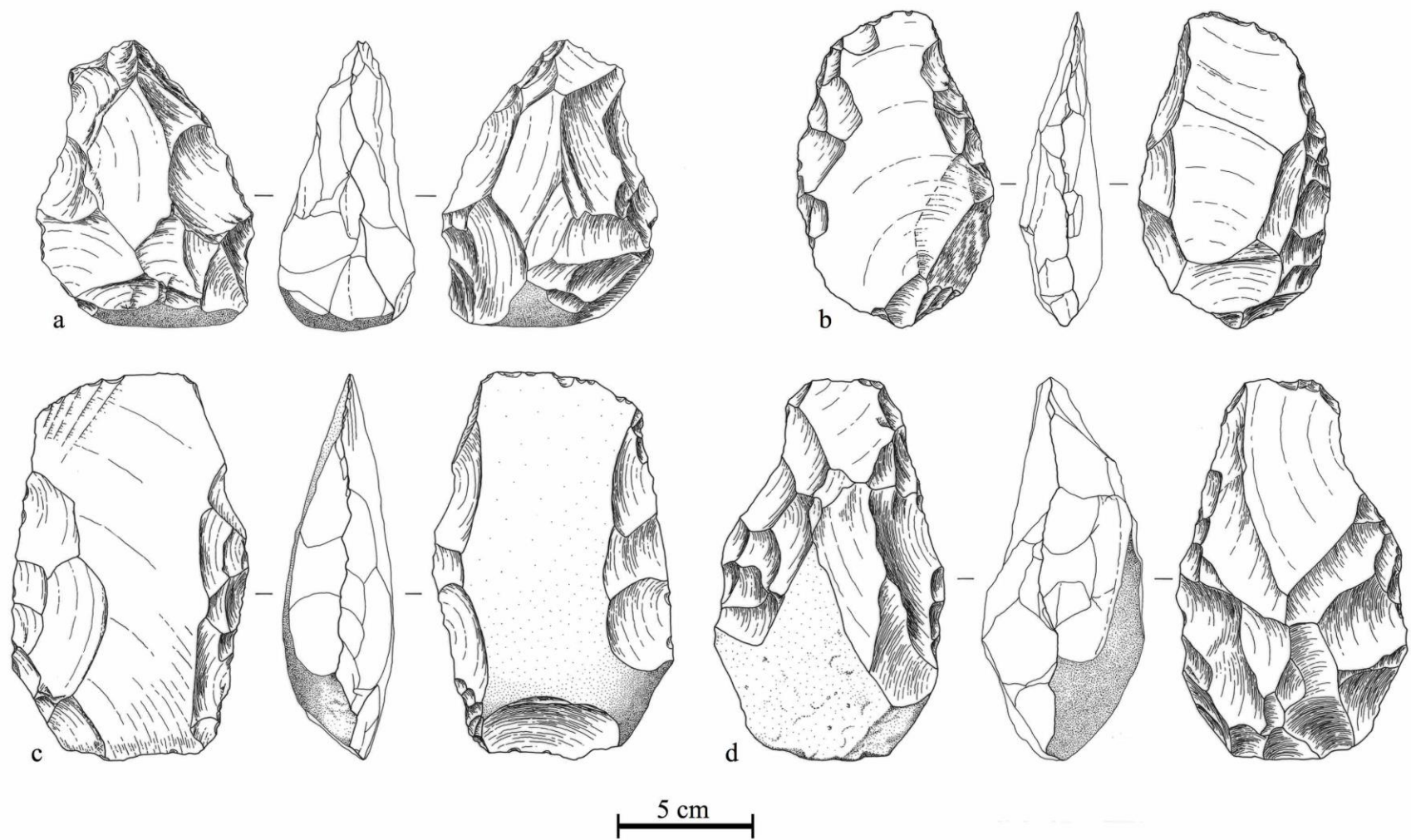


Figure 4.4.72. Debris flow assemblage cleavers. These are made on quartzite flakes (a, b) and siltstone flakes (c), and on a quartzite cobble (d). Drawn by Wendy Voorvelt.

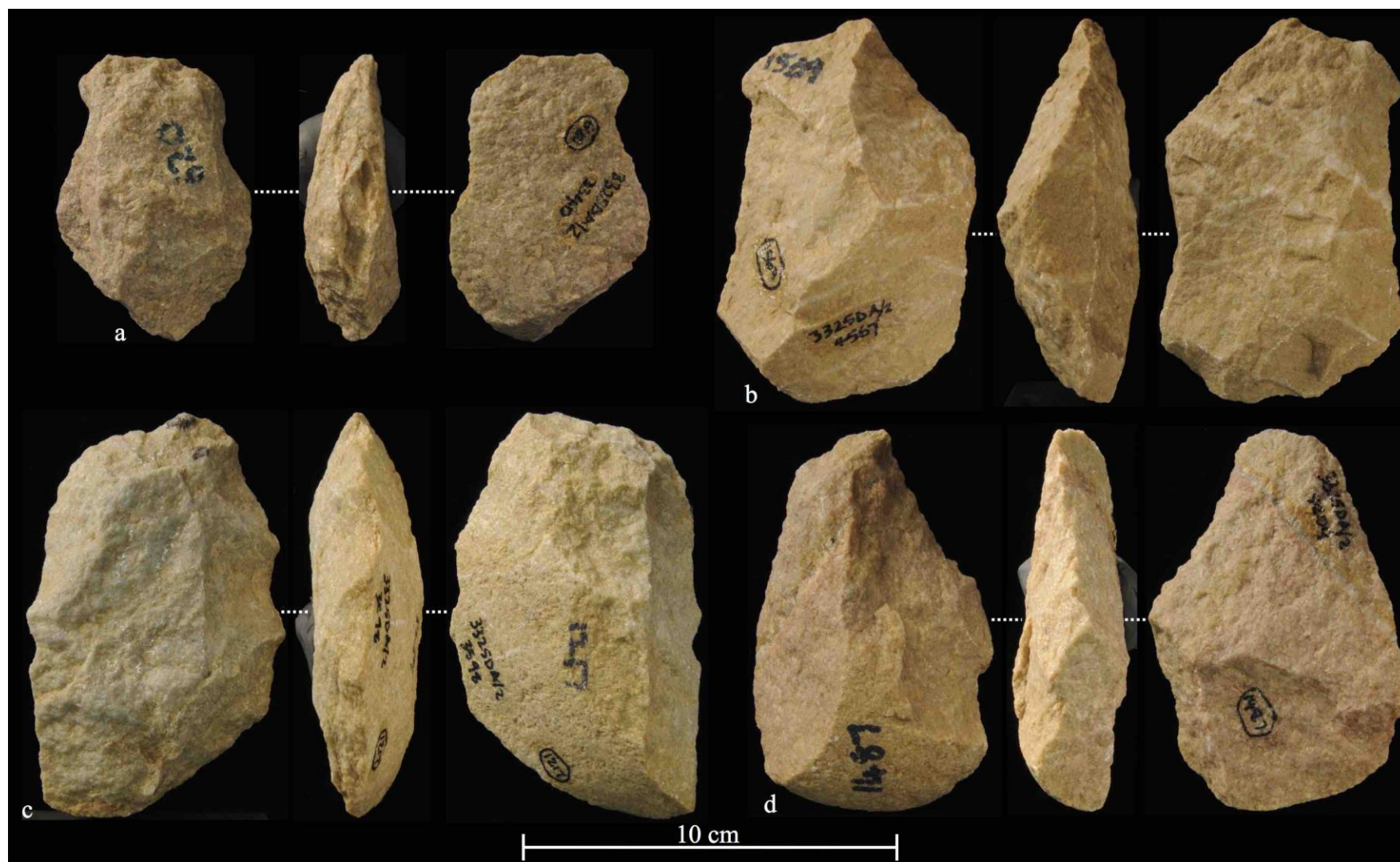


Figure 4.4.73. Debris flow assemblage cleavers (quartzite flake blanks).

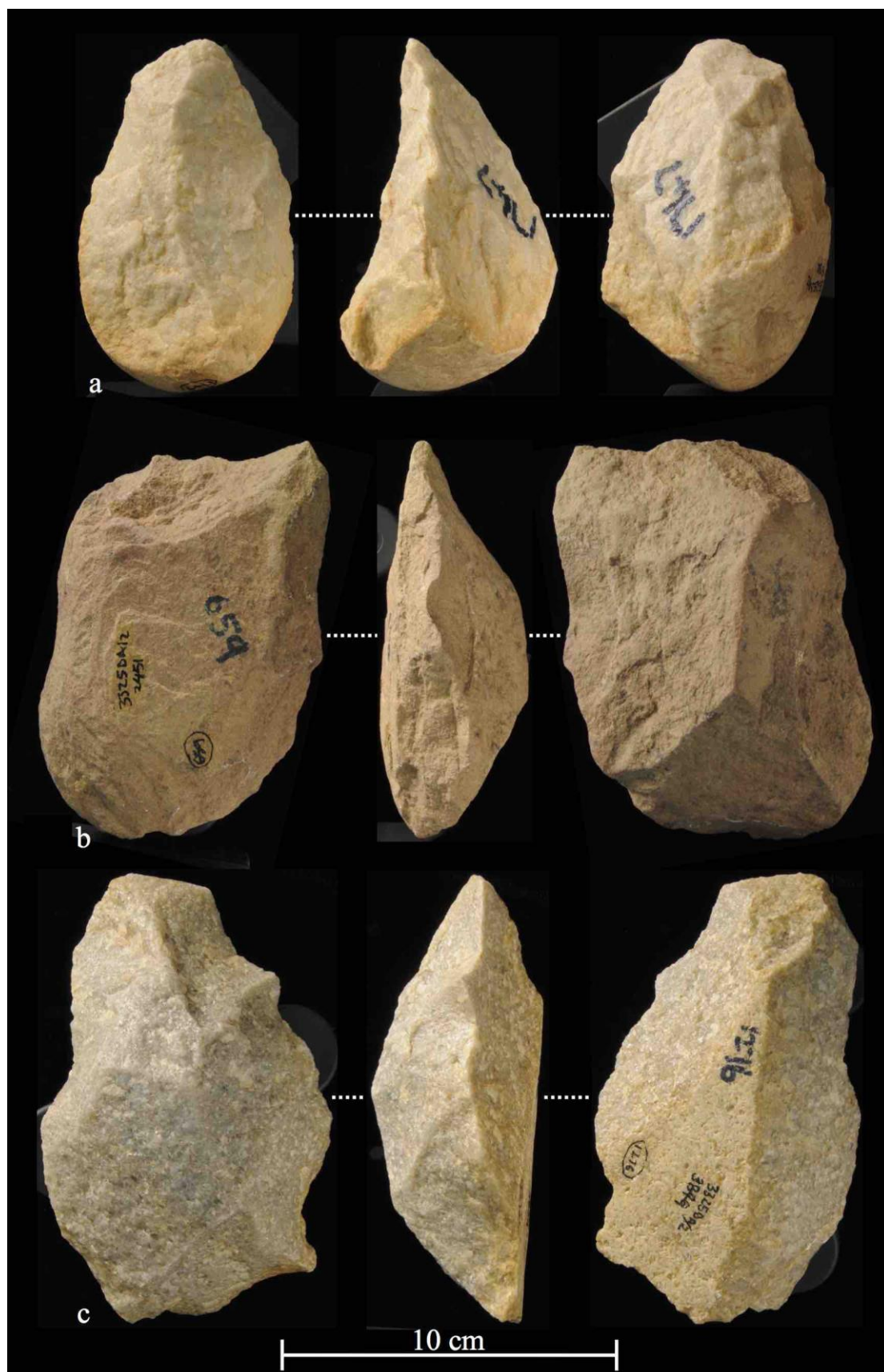


Figure 4.4.74. Debris flow assemblage cleavers. These are made on a quartzite split cobble (a) and flakes (b: siltstone, c: quartzite).

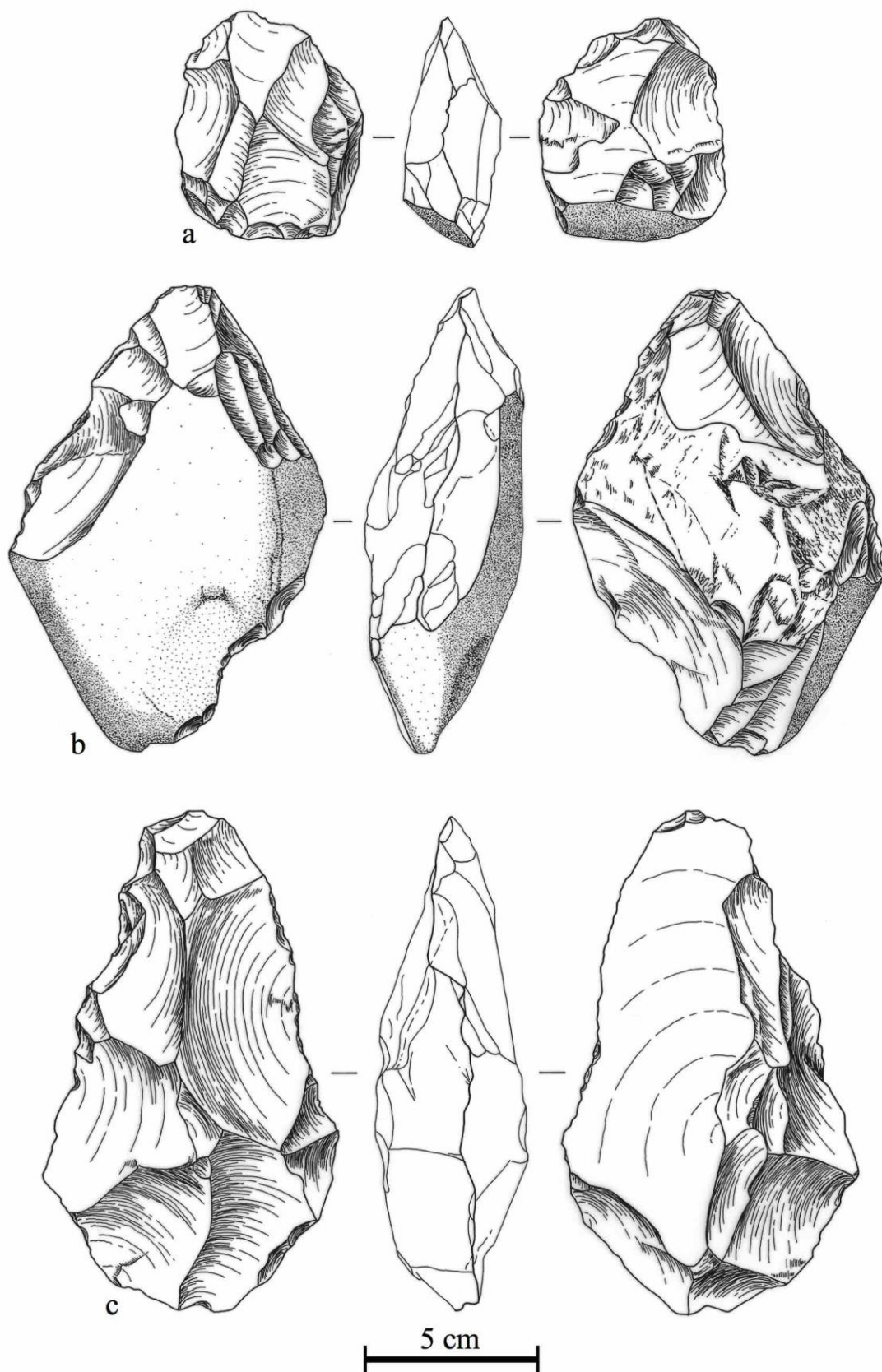


Figure 4.4.75. Debris flow assemblage LCTs; biface on quartzite flake (a) and handaxes on siltstone (b) and quartzite (c) flakes. Drawn by Wendy Voorvelt.

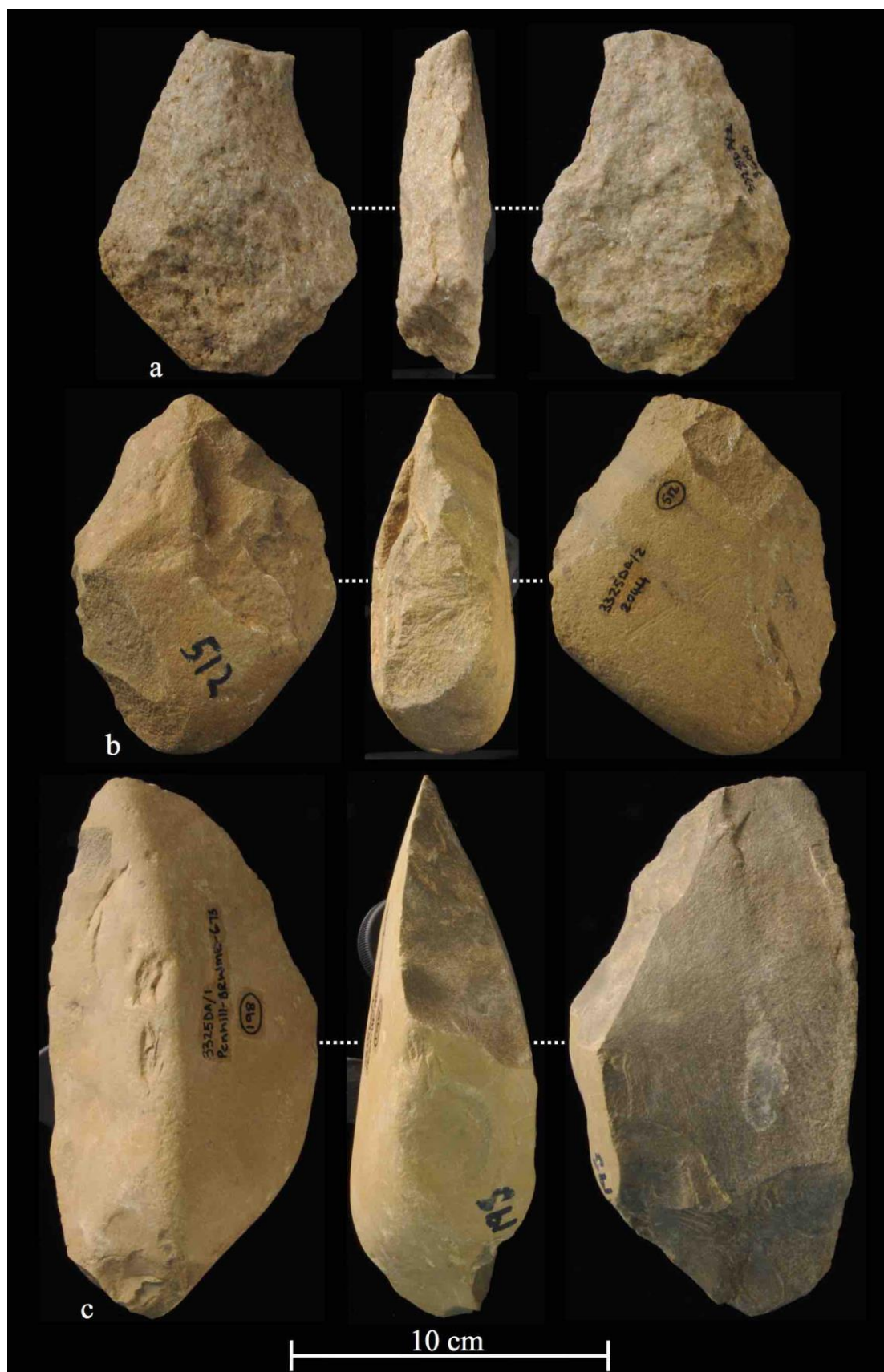


Figure 4.4.76. Debris flow assemblage handaxes. These are made on a quartzite flake (a: showing broken distal), siltstone cobble (b) and siltstone flake (c).

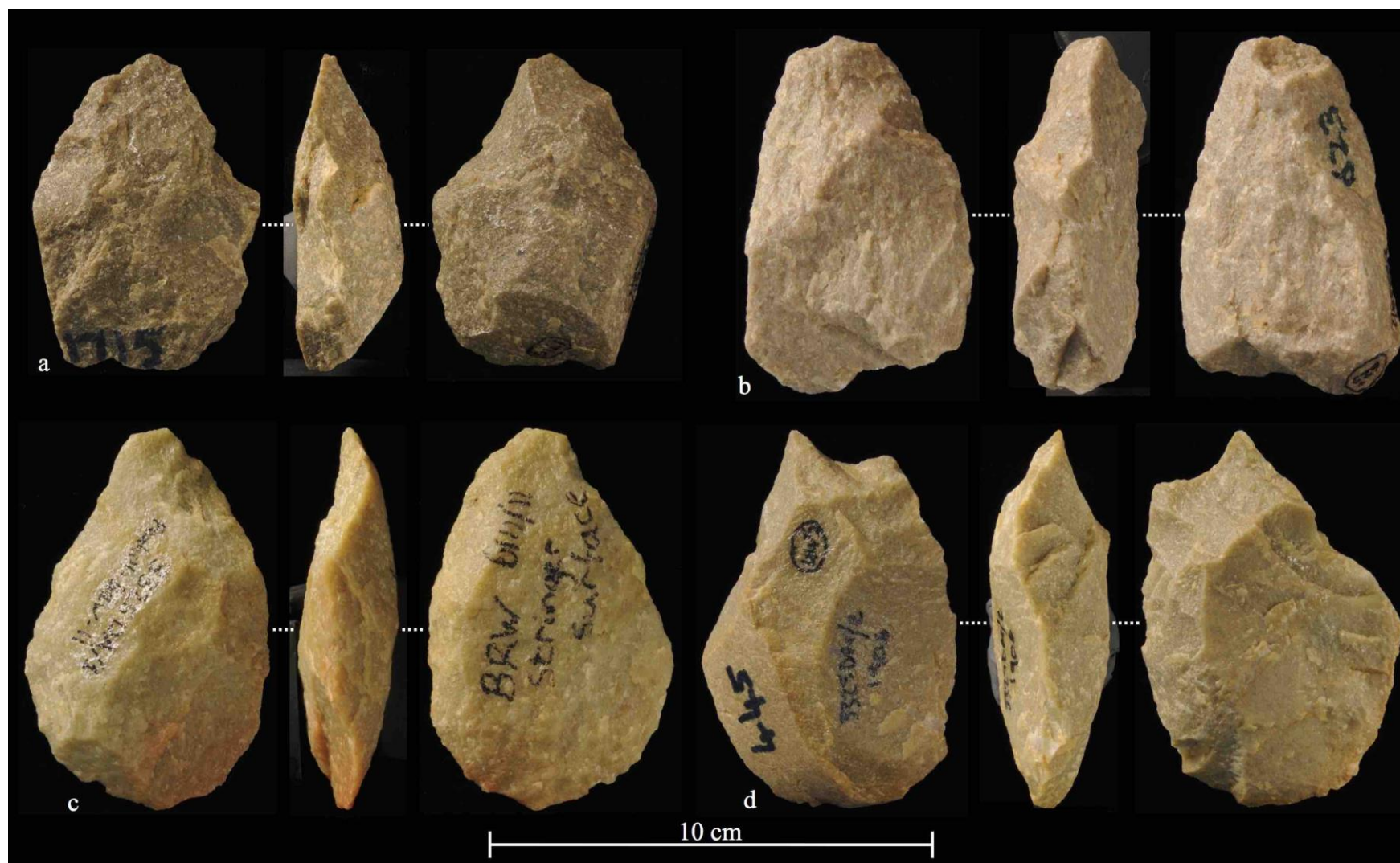


Figure 4.4.77. Debris flow assemblage quartzite handaxes on flakes (except for 'b', which has an indeterminate blank type).

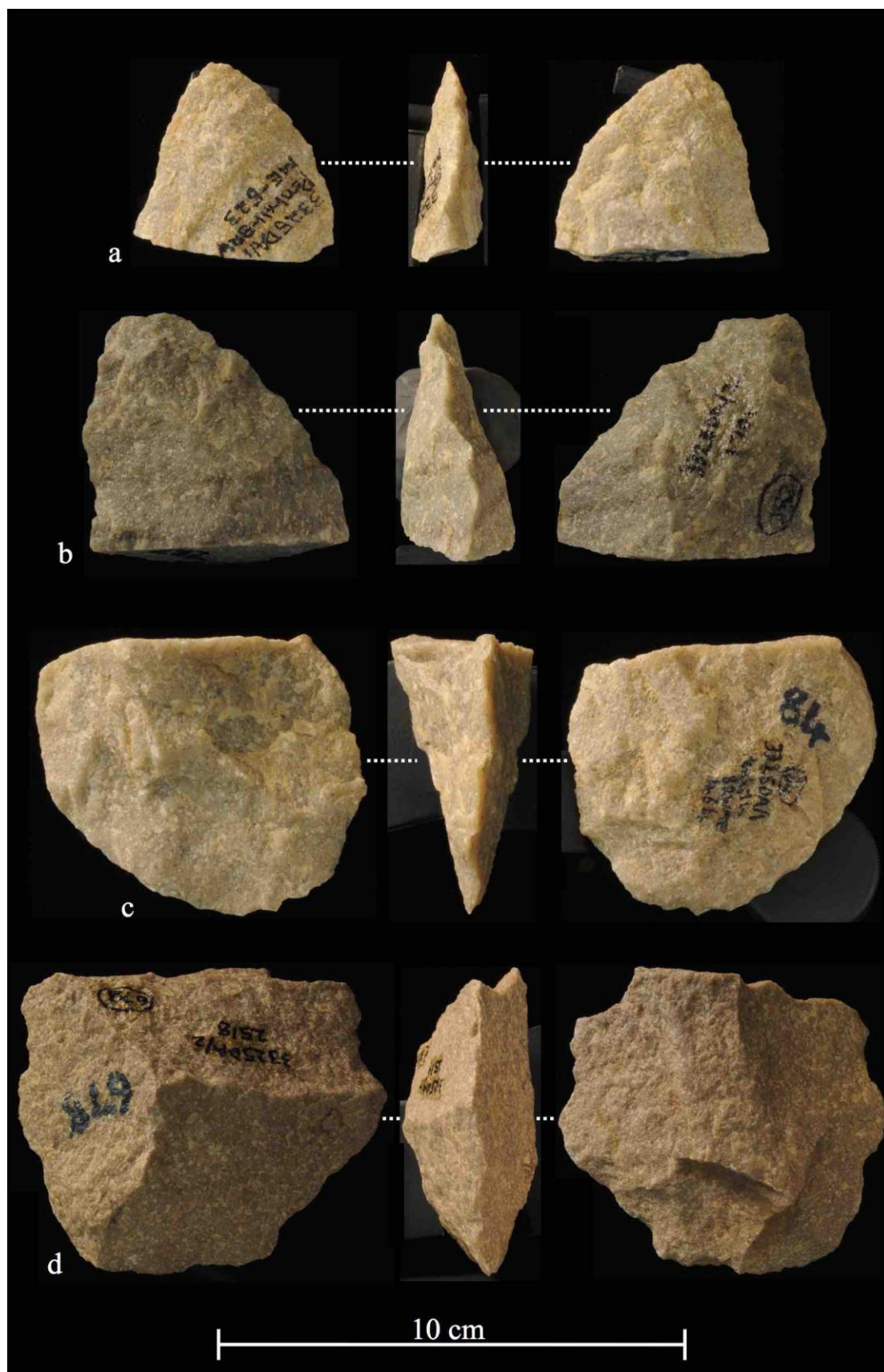


Figure 4.4.78. Debris flow quartzite broken handaxes/LCTs; a, b: butt break, c, d: tip break.

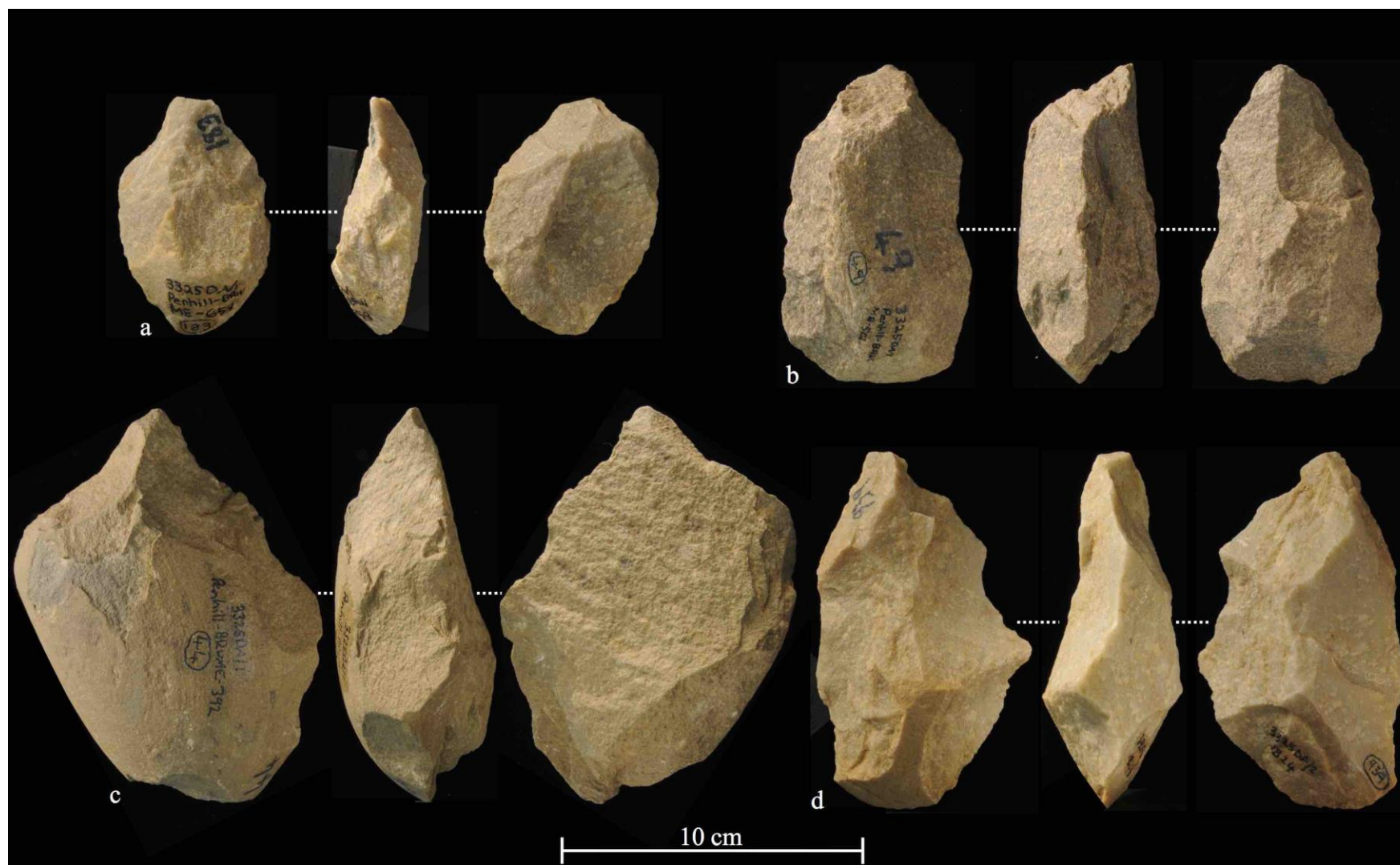


Figure 4.4.79. Picks from the debris flow assemblage; a: quartzite flake, b: quartzite cobble, c: siltstone flake, d: indeterminate quartzite blank.

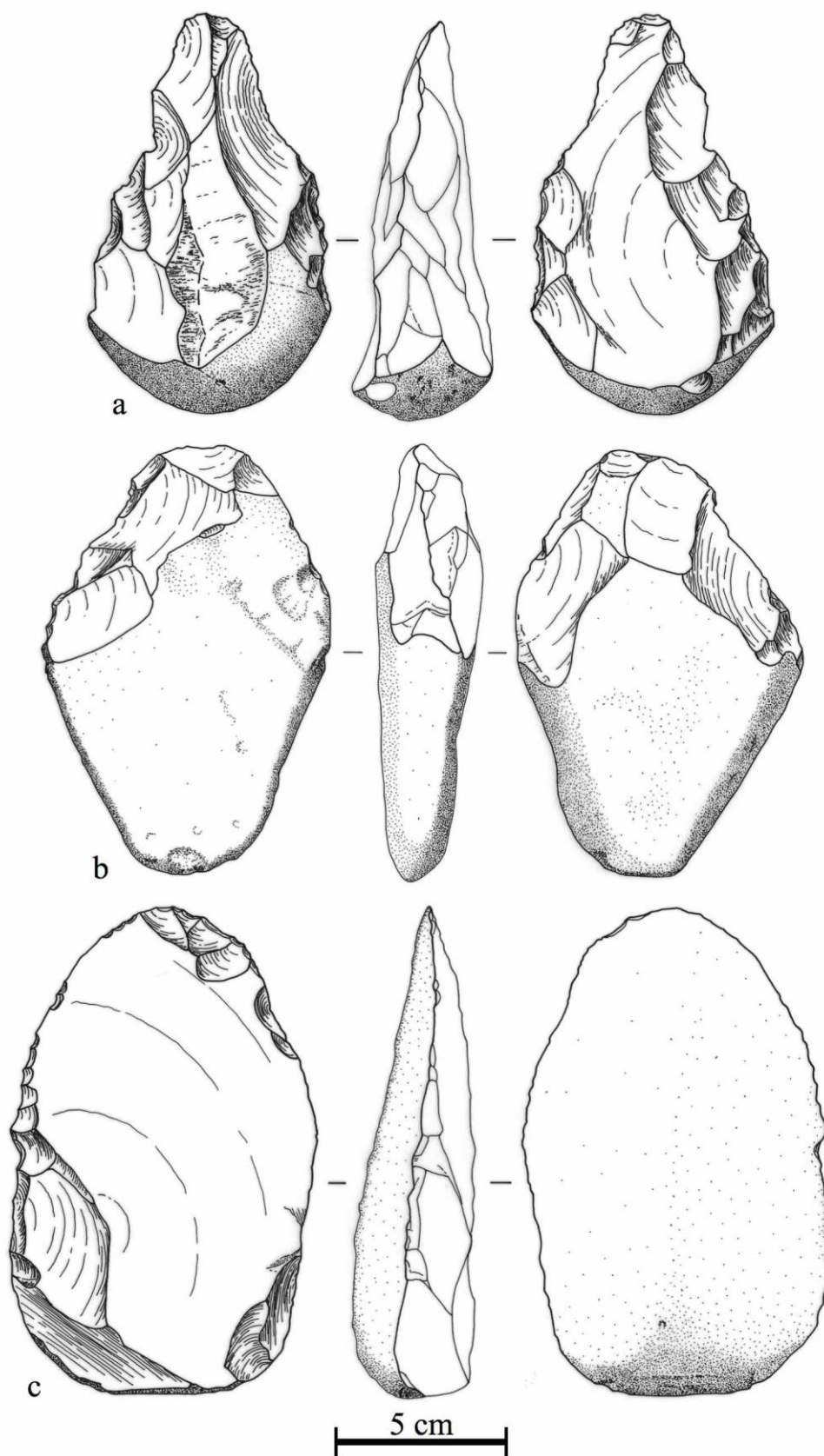


Figure 4.4.80. Debris flow LCTs. Pick on siltstone flake (a), siltstone biface on cobble (b) and quartzite handaxe on flake (c). Drawn by Wendy Voorvelt.



Figure 4.4.81. Debris flow assemblage LCTs. Handaxes on quartzite flakes (a, b), cleaver on siltstone cobble (c) and biface on quartzite flake (d).

4.4.3.5 Other

The sample of modified and split cobbles from both assemblages is extremely limited. The colluvial assemblage comprises a single quartzite split cobble (0.1% of the total assemblage), whereas the debris flow assemblage contains two split cobbles (one quartzite and one siltstone; Fig. 4.4.82a) and a single modified siltstone cobble (Fig. 4.4.82b).

4.4.3.6 Additional features

Evidence to suggest the recycling of lithics, for the colluvial assemblage, is found on a single flake fragment and a casual core (n=2), the latter of which is shown in Figure 4.4.83c. Utilisation damage is found on ten pieces, which includes: two side-struck flakes (Fig. 4.4.83a & b), two end-struck flakes, two flake fragments, one MRP, one casual core, one composite scraper and one handaxe.

Tool recycling (n=9) was most prevalent on cores from the debris flow assemblage (n=5), including three casual (with one shown in Figure 4.4.84b), one chopper, and one irregular core. The remaining recycled pieces include three scrapers (composite, side and notched) and one handaxe.

Tool utilisation damage is more prevalent for the debris flow assemblage (n=34) and includes a range of pieces: flaking debris (five incomplete flakes, one flake fragment and one bipolar incomplete), complete flakes (two end-struck – Figure 4.4.84a – four side-struck and two corner-struck) and three cores (one irregular, casual – Figure 4.4.84c – and discoidal). Formal tools with utilisation damage include: one MRP, two handaxes, one composite piece, two knives, three cleavers (Fig. 4.4.84d), one convex scraper, one flaked-flake, two denticulates, two denticulated scrapers, and one side scraper.

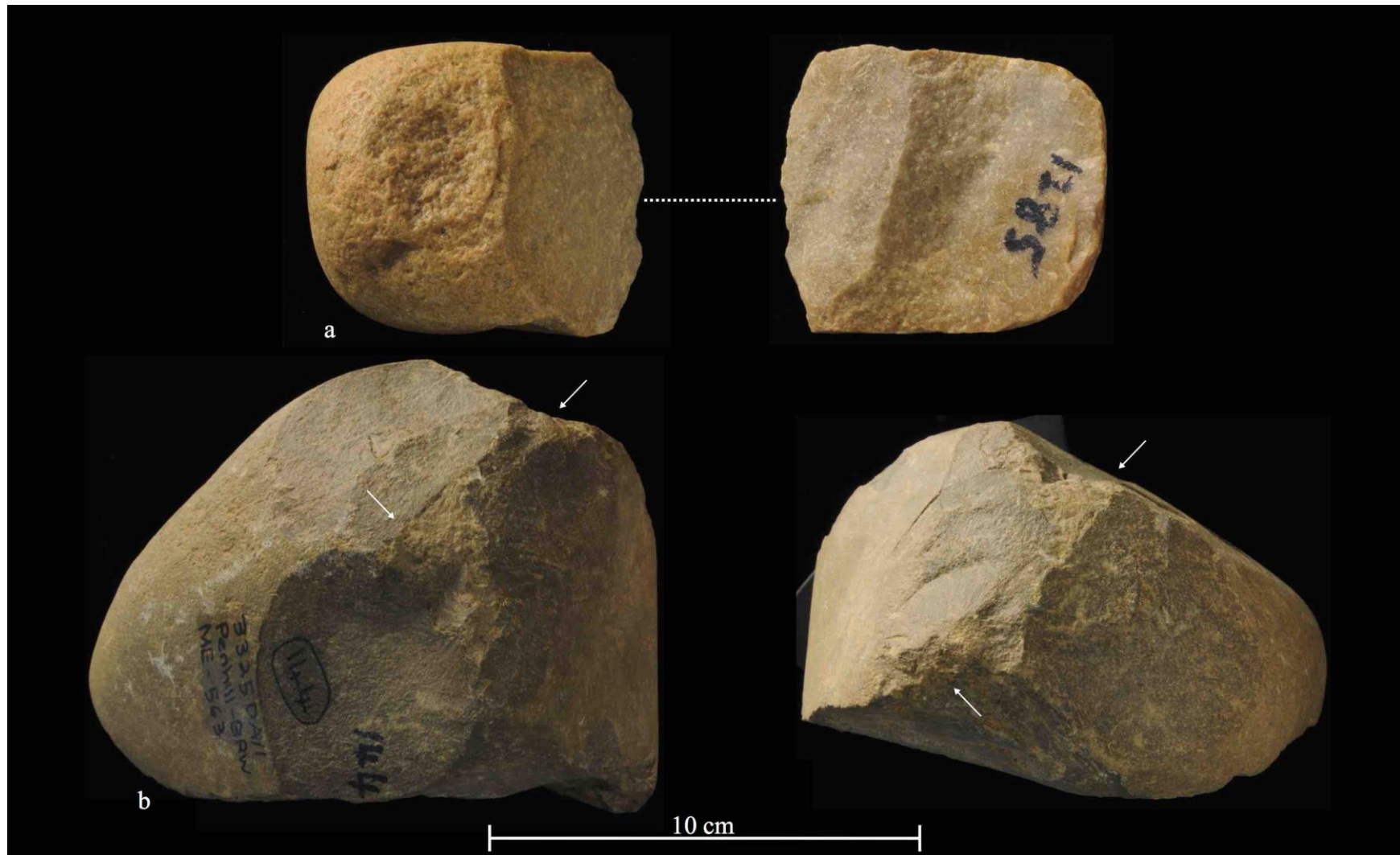


Figure 4.4.82. Debris flow cobbles; split cobble (a) and modified cobble (b). Arrows highlight areas with progressive impact damage.

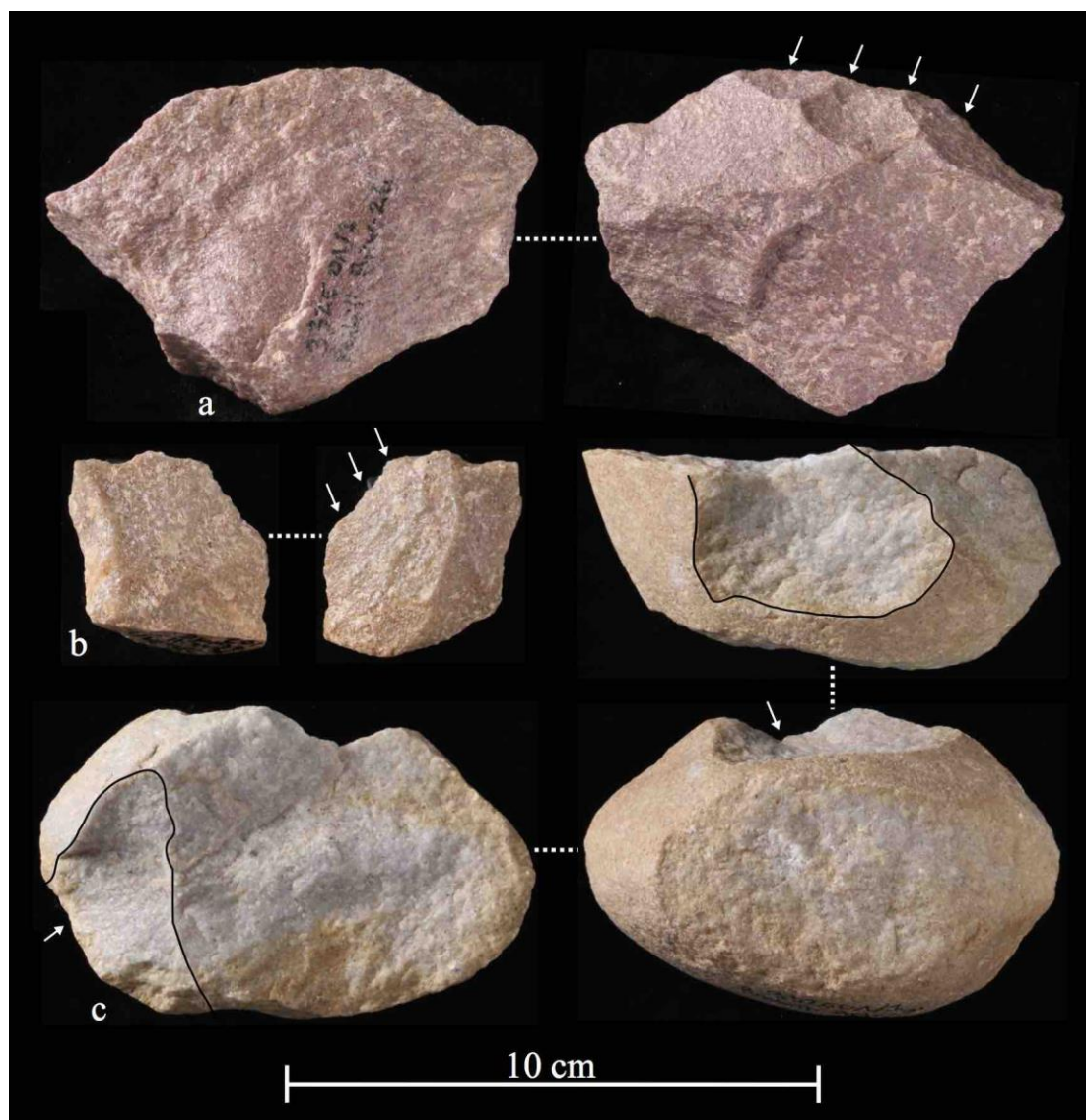


Figure 4.4.83. Colluvial assemblage utilised (a, b) and recycled (c) pieces. Quartzite complete flakes showing edge damage at distal ends (a, b), and quartzite casual core on slightly abraded split cobble with fresh removals (c).

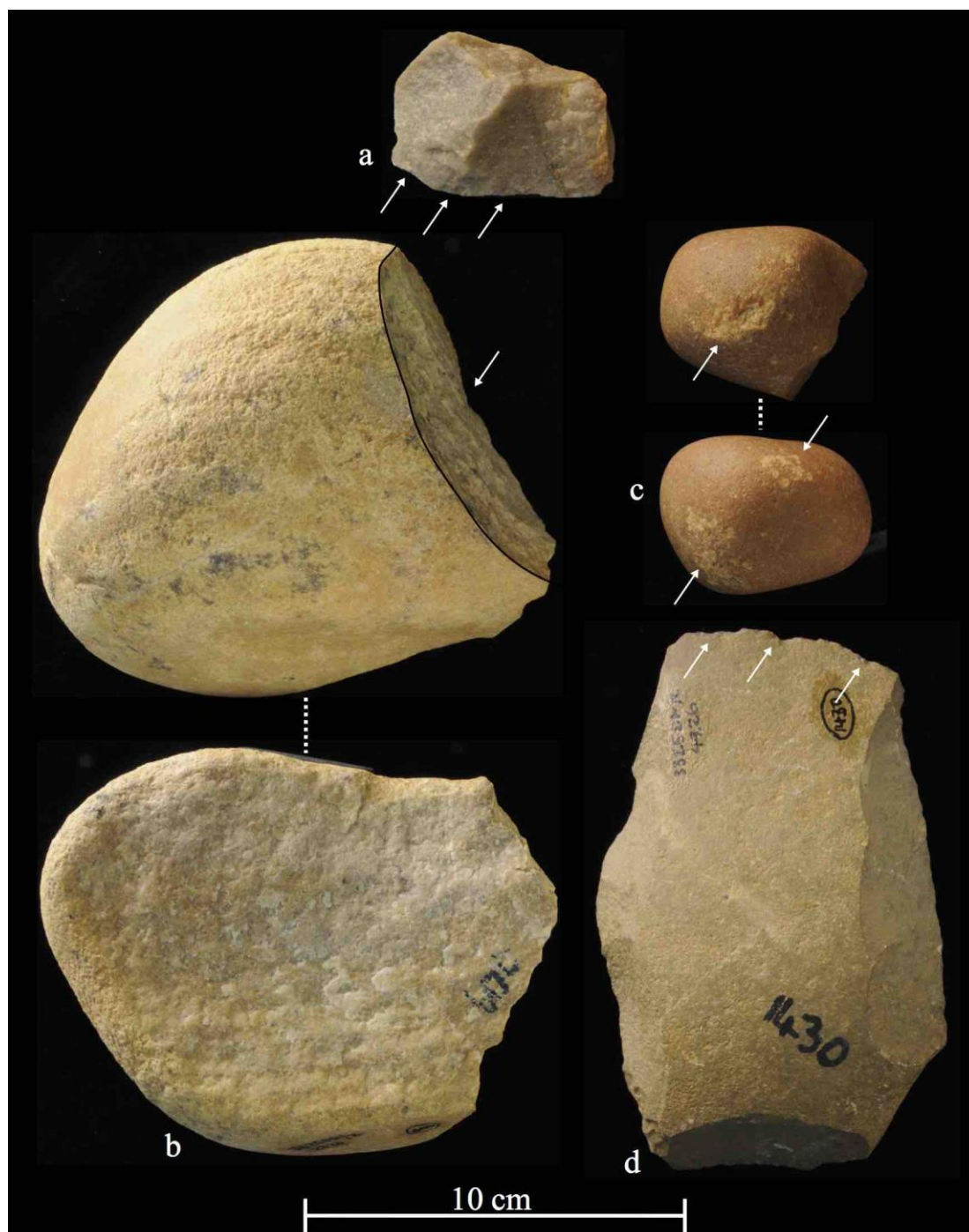


Figure 4.4.84. Debris flow assemblage utilised (a, c, d) and recycled (b) pieces. Cutting damage on end-struck quartzite complete flake (a), quartzite casual core (fresh removal on upper image) on large flake (heavily abraded/rolled, bottom image; b), quartzite casual core on cobble with possible percussion damage (bipolar?; c), siltstone cleaver with utilisation damage (d).

Table 4.4.9. Raw material use, by artefact type, for the colluvial assemblage. No pieces were made on CCS, silt-quartzite or indeterminate raw materials.

Flaking debris:	Total	Raw material type													
		Quartz		Quartzite		Siltstone		Hornfels		Lava		Silcrete		Claystone	
		N	%	N	%	N	%	N	%	N	%	N	%	N	%
SFD	279	2	0.2	249	25.6	17	1.7	6	0.6	3	0.3	1	0.1	1	0.1
Chunk	96	0	0	91	9.4	2	0.2	2	0.2	0	0	0	0	1	0.1
Incomplete flake	265	0	0	226	23.3	23	2.4	13	1.3	0	0	2	0.2	1	0.1
Flake fragment	301	0	0	279	28.7	11	1.1	8	0.8	0	0	0	0	3	0.3
Split flake	7	0	0	7	0.7	0	0	0	0	0	0	0	0	0	0
Bipolar	24	0	0	24	2.5	0	0	0	0	0	0	0	0	0	0
Total	972	2	0.2	876	90.1	53	5.5	29	3.0	3	0.3	3	0.3	6	0.6

Complete flakes:	Total	Quartz		Quartzite		Siltstone		Hornfels		Lava		Silcrete		Claystone	
		N	%	N	%	N	%	N	%	N	%	N	%	N	%
End-struck	44	0	0	33	24.6	4	3.0	7	5.2	0	0	0	0	0	0
Side-struck	49	0	0	40	29.9	3	2.2	6	4.5	0	0	0	0	0	0
Corner-struck	21	0	0	12	9.0	6	4.5	1	0.7	1	0.7	1	0.7	0	0
Kombewa	1	0	0	1	0.7	0	0	0	0	0	0	0	0	0	0
Core trimming	1	0	0	1	0.7	0	0	0	0	0	0	0	0	0	0
Bipolar	9	0	0	9	6.7	0	0	0	0	0	0	0	0	0	0
Handaxe trimming	4	0	0	3	2.2	1	0.7	0	0	0	0	0	0	0	0
Bi-bulb	1	0	0	0	0	1	0.7	0	0	0	0	0	0	0	0
Core rejuvenation	4	0	0	4	3.0	0	0	0	0	0	0	0	0	0	0
Total	134	0	0	103	76.9	15	11.2	14	10.4	1	0.7	1	0.7	0	0

Table 4.4.9 continued...

Cores:	Total	Raw material type													
		Quartz		Quartzite		Siltstone		Hornfels		Lava		Silcrete		Claystone	
		N	%	N	%	N	%	N	%	N	%	N	%	N	%
Core fragment	5	0	0	5	8.8	0	0	0	0	0	0	0	0	0	0
Casual	11	0	0	9	15.8	2	3.5	0	0	0	0	0	0	0	0
Chopper-core	17	0	0	9	15.8	5	8.8	2	3.5	0	0	0	0	1	1.8
Discoidal	11	0	0	8	14.0	1	1.8	2	3.5	0	0	0	0	0	0
Discoidal w/rem.	1	0	0	1	1.8	0	0	0	0	0	0	0	0	0	0
Irregular	6	0	0	5	8.8	0	0	1	1.8	0	0	0	0	0	0
Polyhedral	1	0	0	1	1.8	0	0	0	0	0	0	0	0	0	0
Single platform	5	0	0	5	8.8	0	0	0	0	0	0	0	0	0	0
Total	57	0	0	43	75.4	8	14.0	5	8.8	0	0	0	0	1	1.8

Formal tools:	Total	Quartz		Quartzite		Siltstone		Hornfels		Lava		Silcrete		Claystone	
		N	%	N	%	N	%	N	%	N	%	N	%	N	%
Handaxe	4	0	0	2	2.1	2	2.1	0	0	0	0	0	0	0	0
Cleaver	3	0	0	2	2.1	1	1.1	0	0	0	0	0	0	0	0
Pick	2	0	0	2	2.1	0	0	0	0	0	0	0	0	0	0
Biface	2	0	0	2	2.1	0	0	0	0	0	0	0	0	0	0
Choppers	2	0	0	2	2.1	0	0	0	0	0	0	0	0	0	0
Flaked-flake	3	0	0	3	3.2	0	0	0	0	0	0	0	0	0	0
Retouched flake	7	0	0	7	7.4	0	0	0	0	0	0	0	0	0	0
Scrapers	48	0	0	44	46.8	1	1.1	3	3.2	0	0	0	0	0	0
MRP	11	0	0	10	10.6	0	0	1	1.1	0	0	0	0	0	0
Burin	1	0	0	1	1.1	0	0	0	0	0	0	0	0	0	0
Denticulate	8	0	0	7	7.4	1	1.1	0	0	0	0	0	0	0	0
Composite piece	3	0	0	3	3.2	0	0	0	0	0	0	0	0	0	0
Total	94	0	0	85	90.4	5	5.3	4	4.3	0	0	0	0	0	0

Table 4.4.9 continued...

Other:	Total	Raw material type													
		Quartz		Quartzite		Siltstone		Hornfels		Lava		Silcrete		Claystone	
		N	%	N	%	N	%	N	%	N	%	N	%	N	%
Split cobble	1	0	0	1	100	0	0	0	0	0	0	0	0	0	0
Total	1	0	0	1	100	0	0	0	0	0	0	0	0	0	0

Table 4.4.10. Raw material use, by artefact type, for the debris flow assemblage. No pieces were made on CCS or indeterminate raw materials.

Flaking debris:	Total	Raw material type															
		Quartz		Quartzite		Siltstone		Silt-quartzite		Hornfels		Lava		Silcrete		Claystone	
		N	%	N	%	N	%	N	%	N	%	N	%	N	%	N	%
SFD	4767	9	0.1	4050	52.3	408	5.3	12	0.2	158	2.0	12	0.2	81	1.0	37	0.5
Chunk	202	0	0	177	2.3	13	0.2	0	0	8	0.1	0	0	1	0.01	3	0.04
Incomplete flake	1508	0	0	1288	16.6	123	1.6	4	0.1	72	0.9	3	0.04	4	0.1	14	0.2
Flake fragment	1252	0	0	1129	14.6	73	0.9	1	0.01	35	0.5	3	0.04	2	0.03	9	0.1
Split flake	3	0	0	2	0.03	1	0.01	0	0	0	0	0	0	0	0	0	0
Bipolar	11	0	0	10	0.1	1	0.01	0	0	0	0	0	0	0	0	0	0
Total	7743	9	0.1	6656	86.0	619	8.0	17	0.2	273	3.5	18	0.2	88	1.1	63	0.8

Table 4.4.10 continued...

Complete flakes:	Total	Raw material type															
		Quartz		Quartzite		Siltstone		Silt-quartzite		Hornfels		Lava		Silcrete		Claystone	
		N	%	N	%	N	%	N	%	N	%	N	%	N	%	N	%
End-struck	121	0	0	77	23.0	16	4.8	0	0	26	7.8	0	0	1	0.3	1	0.3
Side-struck	117	0	0	88	26.3	8	2.4	0	0	19	5.7	1	0.3	0	0	1	0.3
Corner-struck	80	0	0	51	15.2	7	2.1	0	0	21	6.3	0	0	0	0	1	0.3
Core trimming	3	0	0	3	0.9	0	0	0	0	0	0	0	0	0	0	0	0
Bipolar	4	0	0	4	1.2	0	0	0	0	0	0	0	0	0	0	0	0
Handaxe trimming	6	0	0	6	1.8	0	0	0	0	0	0	0	0	0	0	0	0
Bi-bulb	1	0	0	1	0.3	0	0	0	0	0	0	0	0	0	0	0	0
Core rejuvenation	3	0	0	3	0.9	0	0	0	0	0	0	0	0	0	0	0	0
Total	335	0	0	233	69.6	31	9.3	0	0	66	19.7	1	0.3	1	0.3	3	0.9

Cores:	Total	Quartz		Quartzite		Siltstone		Silt-quartzite		Hornfels		Lava		Silcrete		Claystone	
		N	%	N	%	N	%	N	%	N	%	N	%	N	%	N	%
Core fragment	8	0	0	8	5.4	0	0	0	0	0	0	0	0	0	0	0	0
Casual	43	0	0	34	22.8	5	3.4	0	0	4	2.7	0	0	0	0	0	0
Bipolar	1	0	0	1	0.7	0	0	0	0	0	0	0	0	0	0	0	0
Chopper-core	31	0	0	21	14.1	3	2.0	0	0	6	4.0	0	0	0	0	1	0.7
Discoidal	44	0	0	40	26.8	2	1.3	0	0	2	1.3	0	0	0	0	0	0
Irregular	12	0	0	8	5.4	3	2.0	0	0	1	0.7	0	0	0	0	0	0
Polyhedral	3	0	0	3	2.0	0	0	0	0	0	0	0	0	0	0	0	0
Single platform	7	0	0	6	4.0	0	0	0	0	1	0.7	0	0	0	0	0	0
Total	149	0	0	121	81.2	13	8.7	0	0	14	9.4	0	0	0	0	1	0.7

Table 4.4.10 continued...

Formal tools:	Total	Raw material type															
		Quartz		Quartzite		Siltstone		Silt-quartzite		Hornfels		Lava		Silcrete		Claystone	
		N	%	N	%	N	%	N	%	N	%	N	%	N	%	N	%
Handaxe	12	0	0	9	2.2	3	0.7	0	0	0	0	0	0	0	0	0	0
Broken LCT	6	0	0	6	1.4	0	0	0	0	0	0	0	0	0	0	0	0
Cleaver	12	0	0	9	2.2	3	0.7	0	0	0	0	0	0	0	0	0	0
Pick	5	0	0	3	0.7	2	0.5	0	0	0	0	0	0	0	0	0	0
Biface	3	0	0	2	0.5	1	0.2	0	0	0	0	0	0	0	0	0	0
Knife	4	0	0	3	0.7	1	0.2	0	0	0	0	0	0	0	0	0	0
Choppers	1	0	0	1	0.2	0	0	0	0	0	0	0	0	0	0	0	0
Flaked-flake	12	0	0	10	2.4	0	0	0	0	1	0.2	1	0.2	0	0	0	0
Retouched flake	41	0	0	33	7.9	5	1.2	0	0	2	0.5	0	0	0	0	1	0.2
Scrapers	127	0	0	104	25.0	14	3.4	0	0	6	1.4	0	0	0	0	3	0.7
MRP	106	0	0	97	23.3	2	0.5	2	0.5	3	0.7	0	0	0	0	2	0.5
Burin	1	0	0	0	0	0	0	0	0	0	0	0	0	0	0	1	0.2
Awl	1	0	0	1	0.2	0	0	0	0	0	0	0	0	0	0	0	0
Denticulate	74	0	0	59	14.2	11	2.6	1	0.2	2	0.5	0	0	0	0	1	0.2
Composite piece	11	0	0	10	2.4	0	0	0	0	0	0	1	0.2	0	0	0	0
Total	416	0	0	347	83.4	42	10.1	3	0.7	14	3.4	2	0.5	0	0	8	1.9

Other:	Total	Quartz		Quartzite		Siltstone		Silt-quartzite		Hornfels		Lava		Silcrete		Claystone	
		N	%	N	%	N	%	N	%	N	%	N	%	N	%	N	%
Modified cobble	1	0	0	0	0	1	33.3	0	0	0	0	0	0	0	0	0	0
Split cobble	2	0	0	1	33.3	1	33.3	0	0	0	0	0	0	0	0	0	0
Total	3	0	0	0	33.3	1	66.7	0	0	0	0	0	0	0	0	0	0

4.4.3.7 Summary

A typological assessment of the Penhill Farm assemblages provides important information on both the character and composition of the excavated artefacts. The total colluvial assemblage consists of 1258 artefacts and although it is dominated by flaking debris (77.3%) it provides good samples of cores (n=57), complete flakes (n=134) and formal tools (n=94). The lower lying debris flow assemblage is also dominated by flaking debris, here accounting for 89.6% of the total assemblage, and larger samples of cores (n=149), complete flakes (n=335) and formal tools (n=416) are found.

Flake fragments, incomplete flakes and SFD account for the most frequent flaking debris types, for both assemblages. A major difference between the assemblages though is the lower percentage (22.2%) of SFD in the colluvial assemblage, versus the higher percentage (55.1%) in the debris flow. In addition to this bipolar debris is marginally more frequent in the colluvial assemblage (1.9%) than in the debris flow (0.1%). Raw material use for this flaking debris shows large variability for both assemblages and all raw material types are represented (except for CCS). Although this is the case quartzite is most abundant, followed thereafter by siltstone and hornfels; all other raw materials are rare.

The classification of complete flakes from Penhill Farm illustrates that side- and end-struck flakes are the most frequent types in both assemblages, followed thereafter by corner-struck pieces. All of the other remaining flake types are rare, but a notably higher percentage (6.7%) of bipolar flakes occurs in the colluvial assemblage than in the debris flow (1.2%). Raw material use here follows the same trend above where quartzite is the most favoured, yet where the use of siltstone exceeds that of hornfels in the colluvial flaking debris sample this pattern is reversed in the debris flow.

Core classification illustrates that casual, discoidal and chopper-cores are the most frequent types in both assemblages. For the colluvial core sample chopper-cores are the most abundant (n=17), followed thereafter by equal quantities of casual and discoidal cores (n=11); discoidal (n=44) and casual cores (n=43) exceed the number of chopper-cores (n=31) in the debris flow. Interestingly, no bipolar cores are found in

the colluvial core sample even though both bipolar flaking debris and complete flakes occur. Only a single bipolar core occurs in the debris flow sample. The remaining core types are uncommon in both assemblages and no boulder-cores occur in either. Raw material use is dominated by quartzites, yet where siltstone exceeds the use of hornfels for the colluvial cores, hornfels exceeds siltstone in the debris flow cores. Interestingly, no cores occur on quartz, lava and silcrete (for both assemblages) or on silt-quartzite (debris flow assemblage), even though both flaking debris and complete flakes occur on these materials.

Formal tool classification shows an abundance of scrapers accounting for 51.1% of the colluvial formal tools and 30.5% for the debris flow. MRPs and LCTs each account for 11.7% of the colluvial formal tool sample and the remaining tool types are uncommon (e.g., denticulates, retouched flakes, flaked-flakes, composite pieces, choppers and burins); no awls or knives occur. In contrast, the debris flow formal tools show a much higher percentage of MRPs (25.5%) and denticulates (17.8%), and the remaining types individually account for less than ten percent (awls and knives do occur). By percentage, the debris flow LCTs are less frequent at 9.1% than in the colluvial assemblage. Raw material use for both assemblages shows that LCTs are only made on quartzite and siltstone, the former being the most favoured material. For formal tools, siltstone and hornfels use follows thereafter for both assemblages, yet raw material use is more variable in the debris flow sample where six types are represented. No formal tools are made on quartz, lava, silcrete or claystone in the colluvial assemblage, whereas only quartz and silcrete pieces are absent from the debris flow sample (excluding CCS).

A closer look at the Penhill Farm scrapers shows a high frequency of denticulated types, followed thereafter by notched and side types. Collectively, these three types account for 81.3% of the colluvial scrapers and 74% for the debris flow scrapers. The remaining types are less frequent and no double side and end or convergent scrapers occur in the colluvial sample; these latter two types do occur in the debris flow (n=1 each), and concave, convex and end scrapers are marginally more frequent in this assemblage.

LCT classification shows that handaxes (n=4) are marginally more frequent than cleavers (n=3) in the colluvial assemblage; these types are equally as abundant in the debris flow (n=12 each). Picks and bifaces account for the remaining LCT sample in the colluvial assemblage and no broken handaxes/LCTs occur. Picks (n=5) exceed bifaces (n=3) in the debris flow and a notable sample (n=6) of broken handaxes/LCTs also occurs.

Other artefacts include a single split cobble in the colluvial assemblage and two spilt cobbles and a single modified cobble in the debris flow. This modified cobble illustrates what looks like some interesting percussive damage.

A final mention of tool recycling and utilisation damage shows these features to be largely uncommon in both assemblages, especially the former. The colluvial assemblage has 10 pieces that show some form of utilisation damage, including one handaxe. A larger sample (n=34) with utilisation damage occurs in the debris flow, including a range of pieces of all types.

4.4.4 Technology

Technological data for the Penhill Farm assemblages is presented in the following order:

1. Flaking debris and complete flakes
2. Cores
3. Formal tools: retouched pieces first, then LCTs
4. Other artefacts (split and modified cobbles)

This will be followed by the residue and use-wear analysis on a single complete flake with utilisation damage.

4.4.4.1 Flaking debris and complete flakes

All data obtained on incomplete flakes and complete flakes are combined within this section (see explanation in Chapter 3.4). As a result the following maximum sample sizes apply:

Colluvial assemblage (n=446)~

- Incomplete flakes: n=265
- Formal tools on incomplete flakes: n=20
- Complete flakes: n=134
- Formal tools on complete flakes: n=27

Debris flow assemblage (n=2008)~

- Incomplete flakes: n=1508
- Formal tools on incomplete flakes: n=84
- Complete flakes: n=335
- Formal tools on complete flakes: n=81

Any data that was not clear were excluded from the respective samples.

Data in this section will focus on the complexity of flaking and the level of reduction for the respective samples.

Flaking debris and complete flake dimensions/size:

Combined flaking debris mass data for the Penhill Farm assemblages is presented in Table 4.4.11. The colluvial assemblage shows a limited quantity of SFD<10 mm (n=51), which accounts for only 4.03 g of the total assemblage weight. Although the quantity of SFD<20 mm is higher, the majority of flaking debris by both quantity and weight is larger than >20 mm (n=693, 12801.14 g). The debris flow has notably high quantities of SFD<10 and <20 mm, yet the weight contribution of these samples is minimal in comparison to the >20 mm debris sample (45996.31 g).

Table 4.4.11. SFD and flaking debris >20 mm sample weights.

Assemblage	Mass data					
	SFD <10 mm		SFD <20 mm		Flaking debris >20 mm	
	N	Weight (g)	N	Weight (g)	N	Weight (g)
Colluvial	51	4.03	228	218.34	693	12801.14
Debris flow	1952	210.52	2815	2170.87	2976	45996.31
Total	2003	214.55	3043	2389.21	3669	58797.45

Flake measurement data is presented in Tables 4.4.12-4.4.15 and because only minor differences occur in these measurements, by method, measurements recorded using alternative methods are not discussed here but are presented in Appendix B Tables 1-4.

Flake measurement data for the colluvial assemblage, by raw material, is presented in Table 4.4.12. The sample sizes for lava, silcrete and claystone are extremely small so little mention will be made of these materials. From Table 4.4.12 it is clear that siltstone flakes provide the largest mean values for all of the flake measurements, including weight; these pieces also provide most of the largest SD values. However, if one observes the mean measurements for the two most abundant remaining materials (quartzite and hornfels), a clear pattern in flake measurements becomes evident. Siltstone pieces provide the largest values, followed by quartzite and then by hornfels. This size trend is also evident for flake measurements in Appendix B Table 1, following different recording methods. Interestingly, for the quartzite and siltstone samples the mean technological flake width exceeds the mean technological flake length.

The debris flow assemblage flake measurements, by raw material, are presented in Table 4.4.13. Although samples of silt-quartzite, lava, silcrete and claystone are limited, worth noting is that where values were obtained on silcrete these flake measurements exceed those on all of the other raw materials.

Table 4.4.12. Colluvial assemblage flake measurements, by raw material (n=446). Grey blocks indicate where sample is <15 pieces. Weight data and artefact maximum length data only includes complete flakes (as these are unmodified pieces). See Appendix B Table 1 for additional measurements.

Flake measurement data (mm)		Raw materials					
		Quartzite	Siltstone	Hornfels	Lava	Silcrete	Claystone
*Max. length	Mean	50.3	58.4	45.4	50	53	-
	SD	20.7	20.7	17.1	-	-	-
Length	Mean	38	41.3	35.3	27.9	30.9	-
	SD	16.9	21.1	17.3	-	16.1	-
Width	Mean	39.5	43.6	34.7	45.4	27.7	-
	SD	15.4	16.3	16.3	-	16.2	-
Thickness	Mean	16.3	16.6	12.1	12.7	15	-
	SD	7.4	5.8	5.9	-	-	-
Platform thickness	Mean	11.3	11.7	7.7	11.5	10.7	13.7
	SD	5.6	6.2	4.7	-	6.3	-
Platform width	Mean	26.5	36.6	16.7	38.9	21.6	14.3
	SD	12.6	19.9	8.2	-	-	-
*Weight (g)	Mean	44.5	52.9	24.3	27.4	38.3	-
	SD	78.9	54.9	31	-	-	-
Length & width	Technological flake length and width following Braun <i>et al.</i> 2008						
Thickness	Flake maximum thickness following Andrefsky 2005						
Platform thickness	Platform maximum thickness following Andrefsky 2005						
*Maximum length data only includes complete flakes (no incompletes or formal tools)							
*Weight data only includes complete flakes (no incompletes or formal tools)							

For the debris flow sample siltstone flakes also account for the majority of the largest mean values, except for platform thickness and width, and weight (larger for quartzite flakes). This is also evident in data from Appendix B Table 2. Thereafter, quartzite pieces follow in size, followed then by hornfels pieces. As seen in the colluvial flakes,

here the quartzite and siltstone mean technological flake widths also exceed the mean technological lengths.

Table 4.4.13. Debris flow flake measurements, by raw material (n=2208; qzte=quartzite). Grey blocks indicate where sample is <15 pieces. Weight data and artefact maximum length data only includes complete flakes (as these are unmodified pieces). See Appendix B Table 2 for additional measurements.

Access). See Appendix B Table 2 for additional measurements.

Flake measurement data (mm)		Raw materials						
		Qzte	Siltstone	Silt-qzte	Hornfels	Lava	Silcrete	Claystone
*Max. length	Mean	52.3	57.3	-	43.5	40.9	70.2	51.3
	SD	23.4	22.7	-	15.7	-	-	18.9
Length	Mean	38.4	41.9	33	31.4	34.1	47.6	39.4
	SD	18	18.3	-	13.5	5	16.6	11.8
Width	Mean	41.9	45.2	34.2	31.4	22.1	63.8	43.9
	SD	21.7	22.5	9.4	11.1	-	-	10.2
Thickness	Mean	16.4	16.8	-	12.6	10.3	27.6	15.7
	SD	8.7	9.4	-	5.5	-	-	4.9
Platform thickness	Mean	11.4	11	10.4	9.2	2.1	14.1	12
	SD	6.4	6.9	1.8	4.5	1.3	9.3	7.9
Platform width	Mean	26.5	24.6	20.3	22.5	4.9	30.5	24.3
	SD	14.1	12.3	4.2	8.8	2.2	12.1	11.2
*Weight (g)	Mean	49.6	42.8	-	22.3	8.9	125.4	17.5
	SD	97.3	51.5	-	29.6	-	-	10.1
Length & width	Technological flake length and width following Braun <i>et al.</i> 2008							
Thickness	Flake maximum thickness following Andrefsky 2005							
Platform thickness	Platform maximum thickness following Andrefsky 2005							
*Maximum length data only includes complete flakes (no incompletes or formal tools)								
*Weight data only includes complete flakes (no incompletes or formal tools)								

An assessment of complete flake measurements, by flaking axis, is presented in Tables 4.4.14 and 4.4.15 (see Appendix B Tables 3 and 4 for additional data).

For the colluvial assemblage Table 4.4.14 illustrates that the largest complete flakes (mean artefact maximum length) are corner- and end-struck (ranging from 53.7-53.8 mm). To be expected the largest mean technological lengths are greatest for the end-struck flakes (ranging from 44.5-51.6 mm), and technological widths are greatest for

the side-struck flakes (ranging from 40.1-45.3 mm). Mean flake maximum thickness is greatest for corner- and end-struck pieces (16-16.5 mm).

Platform measurements show little variation in mean maximum platform thickness, which range from 10.7-11 mm, and platform width follows a predictable trend in size (greatest for side-struck flakes, smallest for end-struck flakes). Mean flake weight is greatest for corner-struck types (56.6 g).

Table 4.4.14. Colluvial complete flake measurements, by flaking axis (n=134). See Appendix B Table 3 for additional measurements.

Complete flake measurement data (mm)		Flaking axis		
		Corner	End	Side
Maximum length	Mean	53.8	53.7	44.6
	SD	22.5	20.9	15.5
Length	Mean	41.6	46.4	26.7
	SD	19.9	19.2	9.7
Width	Mean	39.9	33.6	40.1
	SD	17.1	14.4	14.3
Thickness	Mean	16.5	16	13.2
	SD	8.3	7.8	5.1
Platform thickness	Mean	11	10.7	10.9
	SD	5.4	5.5	5.2
Platform width	Mean	26.2	22.5	30.5
	SD	11.6	10.5	13.5
Weight (g)	Mean	56.6	46.7	22.9
	SD	97.1	55.9	28.1
Length & width	Technological flake length and width following Braun <i>et al.</i> 2008			
Thickness	Flake maximum thickness following Andrefsky 2005			
Platform thickness	Platform maximum thickness following Andrefsky 2005			
Flaking axis	Technological flaking axis following Mason 1965			

For the debris flow assemblage Table 4.4.15 illustrates that mean artefact maximum length is greatest for corner-struck complete flakes (53 mm). End-struck types account for the heaviest mean weight (48.4 g) and also account for the greatest flake thickness (15.5 mm).

Table 4.4.15. Debris flow complete flake measurements, by flaking axis (n=335). See Appendix B Table 4 for additional measurements.

Complete flake measurement data (mm)		Flaking axis		
		Corner	End	Side
Maximum length	Mean	53	49.5	50.2
	SD	22.7	22.8	21.3
Length	Mean	38.3	43	30.6
	SD	16.5	20.9	14.5
Width	Mean	37.1	32	44.4
	SD	18.4	18	19.8
Thickness	Mean	15.1	15.5	15.1
	SD	7.3	8.9	8.7
Platform thickness	Mean	11.7	10.2	12.2
	SD	5.9	6.1	8.1
Platform width	Mean	27.7	20.8	33.1
	SD	13.7	10	16.6
Weight (g)	Mean	45	48.4	38.1
	SD	89.8	108.7	52.5
Length & width	Technological flake length following Braun <i>et al.</i> 2008			
Thickness	Flake maximum thickness following Andrefsky 2005			
Platform thickness	Platform maximum thickness following Andrefsky 2005			
Flaking axis	Technological flaking axis following Mason 1965			

Maximum lengths for complete flakes by technological flaking axis are shown in Figures 4.4.85-4.4.86. For the colluvial flakes (n=134; Fig. 4.4.85) the majority is in the 30-50 mm size categories, with the remaining pieces reaching the 90 mm size category. A small percentage (0.8) occurs in the 130 mm size category, and by axis these are corner-struck types. End-struck types account for the highest percentages in the 80 and 90 mm size categories. The debris flow (n=335; Fig. 4.4.86) shows a similar distribution for flakes in the 30-50 mm size categories, however, for this assemblage the size range of flakes is greater. A higher percentage of flakes occur up until 120 mm, with small percentages in the 140 and 170 mm size categories. By axis, end-struck types account for the highest percentages of larger flakes (thus showing the greatest size range), and those flakes in the 170 mm size category are corner-struck.

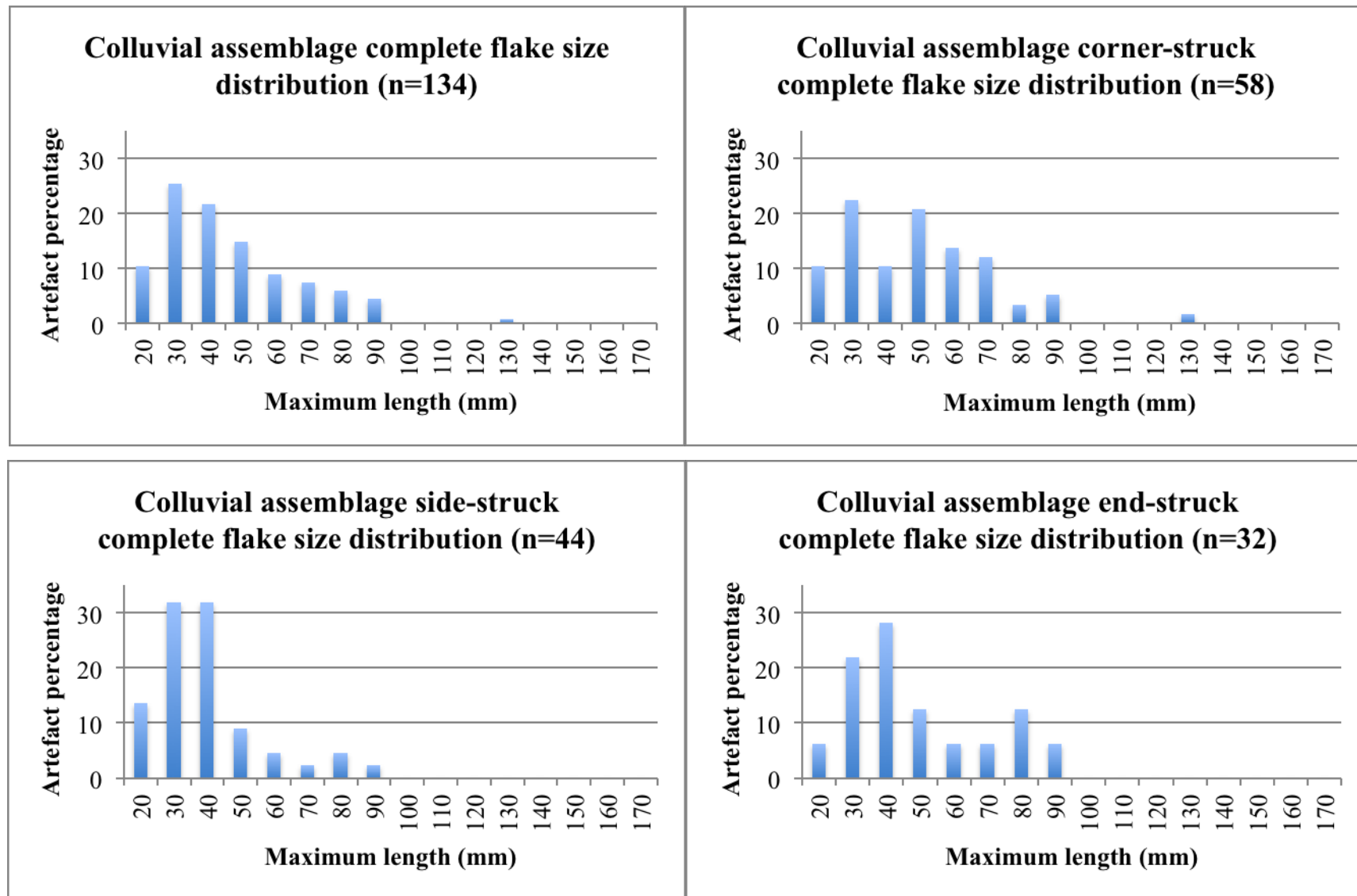


Figure 4.4.85. Colluvial assemblage flake size distribution, by flaking axis (following Mason 1965).

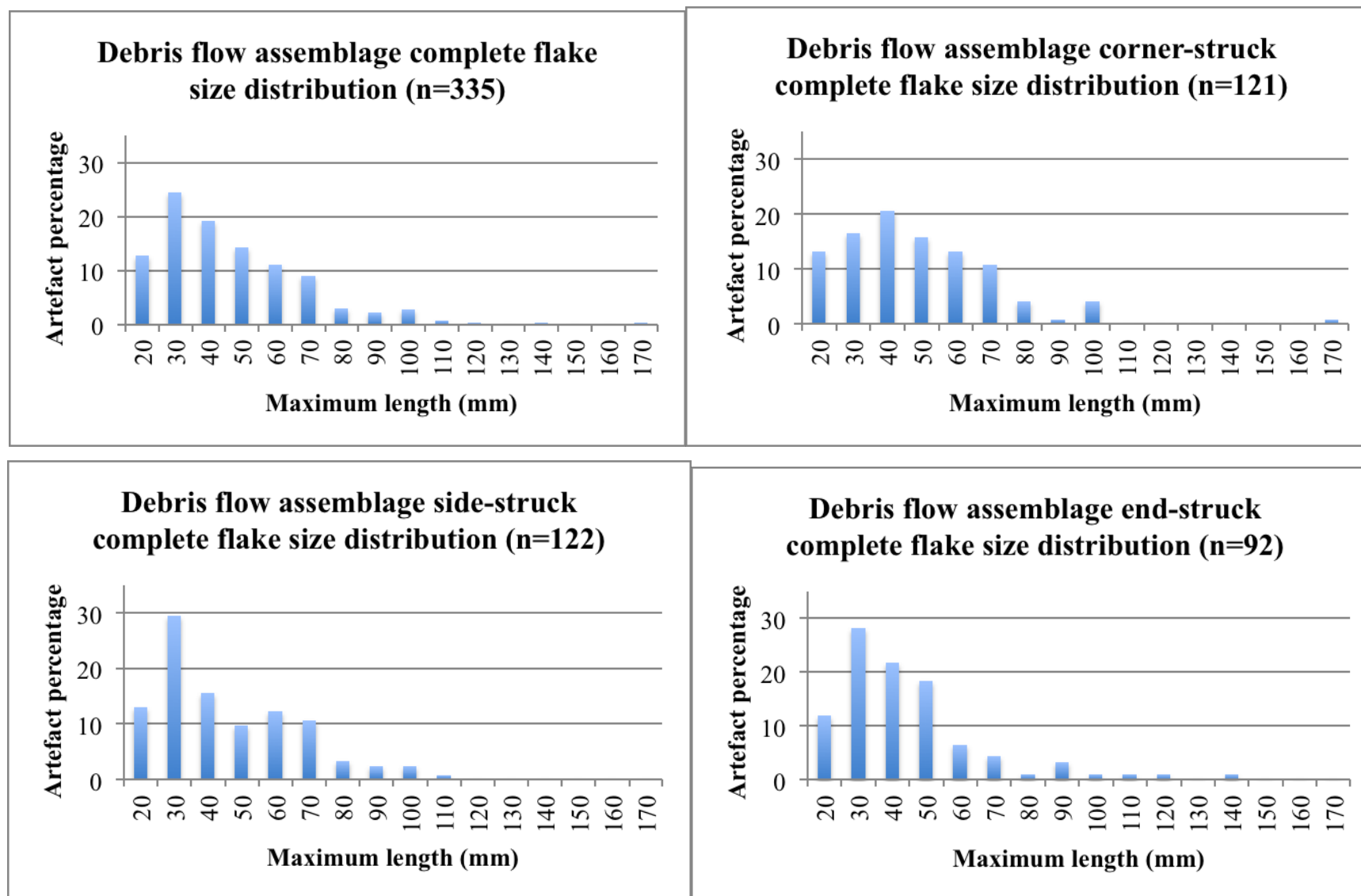


Figure 4.4.86. Debris flow assemblage flake size distribution, by flaking axis (following Mason 1965).

Flaking strategy:

An assessment of flaking axis distribution, for both assemblages, is presented in Figures 4.4.87 and 4.4.88, and in Appendix B Figures 1 and 2. It is clear from these figures that flake axis distribution is different when applying the two approaches (Mason 1965; Isaac & Keller 1968).

For the colluvial assemblage complete flake sample (n=134; Fig. 4.4.87) corner-struck types are the most frequent (43.3%), with end-struck types being the least (23.9%). Although higher percentages are to be expected for flake axis distribution following Isaac and Keller (1968; see Appendix B Figure 1) due to only two axes for comparison (versus three), a contrasting pattern shows that end-struck types are more frequent (53%), followed by marginally less-frequent side-struck types (47%). This is due to the majority of the corner-struck types being included in the end-struck category. Interestingly, irrespective of measurement method, side-struck types are the most favoured for formal tool production (40.7% following Mason 1965 and 55.6% following Isaac & Keller 1968).

For the debris flow assemblage Figure 4.4.88 shows a largely similar pattern in flaking axis distribution. For the complete flake sample (n=335) side-struck flakes are the most frequent (at 36.4%), however, corner-struck types are only marginally less common (36.1%). From this it is clear that the complete flake samples for both assemblages are dominated by corner- and side-struck complete flakes (Figs. 4.4.87 & 4.4.88). Following Isaac and Keller (1968; see Appendix B Figure 2) however, the complete flake sample shows a very similar pattern in axis distribution when compared to the colluvial assemblage, with end-struck flakes the most frequent at 53.7% followed by side-struck types at 46.3%. Following this approach both assemblages have end-struck flakes as the most frequent types. Formal tool production on complete flakes in the debris flow (n=81) shows a similar preference for side-struck types, irrespective of measurement method.

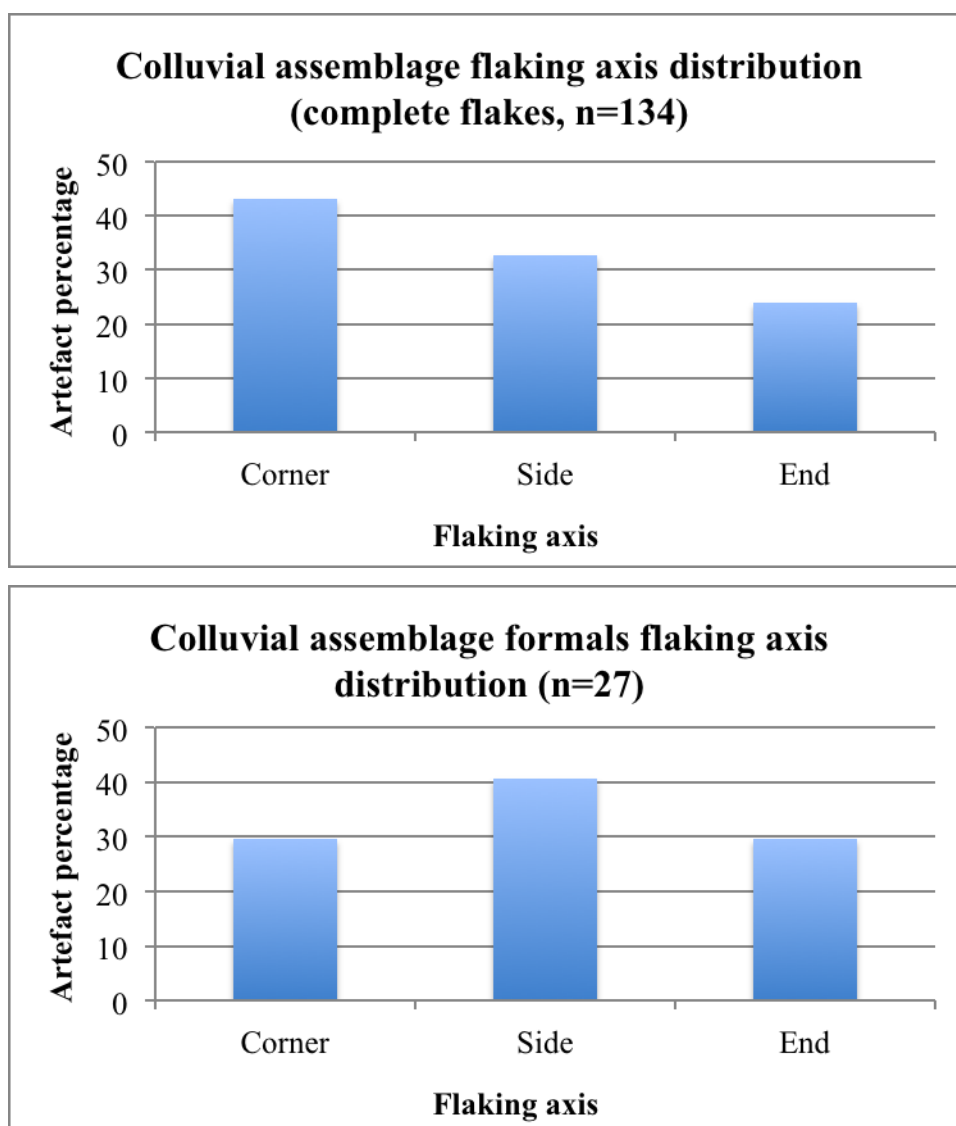


Figure 4.4.87. Colluvial assemblage flaking axis distribution (following Mason 1965) for complete flakes and formal tools on complete flakes. See Appendix B Figure 1 for the Isaac and Keller (1968) method.

An assessment of flaking axis (following Mason 1965) by raw material is presented in Tables 4.4.16 and 4.4.17; samples here include the combined complete flake samples for both assemblages (complete flakes and formal tools on complete flakes). See Appendix B Tables 5 and 6 for this data following the Isaac and Keller (1968) method.

The colluvial assemblage quartzite and hornfels samples show that corner-struck types are the most frequent for these materials (41.4 and 40%, respectively), when excluding the small lava and silcrete samples (Table 4.4.16). Similarly, for both quartzite and hornfels, the least frequent flake axis type is end-struck (22.7 and

26.7%, respectively). However, siltstone shows a contrasting pattern where end-struck flakes are notably the most abundant type (at 43.8%), followed thereafter by corner-struck pieces (31.3%). Following Isaac and Keller (1968) most of this variation is absent when comparing flake axis by the different raw materials (see Appendix B Table 5).

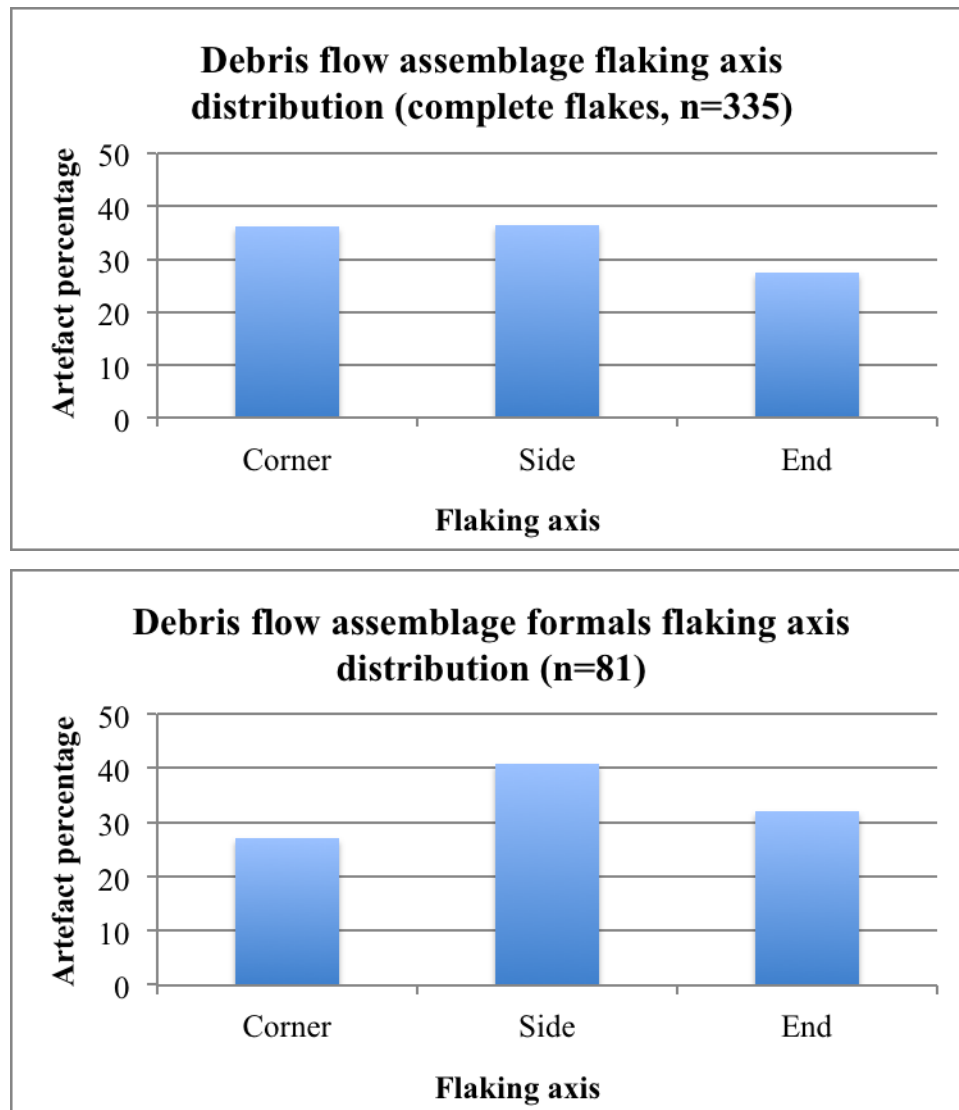


Figure 4.4.88. Debris flow assemblage flaking axis distribution (following Mason 1965) for complete flakes and formal tools on complete flakes. See Appendix B Figure 2 for the Isaac and Keller (1968) method.

Table 4.4.17 shows a different pattern in flake axis distribution for the debris flow assemblage. In contrast to the colluvial assemblage, both quartzite and siltstone show that side-struck flakes are the most common types for these materials (38.7 and 45%, respectively); end-struck types are the least frequent (albeit marginally). Where siltstone showed a different flake axis distribution in the colluvial assemblage, for the

debris flow hornfels shows a notably higher percentage of corner-struck types (at 49.3%, excluding lava and claystone), followed thereafter by side-struck pieces. The small samples of lava, silcrete and claystone (collectively n=7) show that corner-struck types are the most frequent (n=4). Appendix B Table 6 shows little variability in flaking axis by raw material; however, hornfels shows a high percentage of end-struck types (62.3%).

Table 4.4.16. Colluvial assemblage flaking axis, by raw material. See Appendix B Table 5 for the Isaac and Keller (1968) method.

Raw material	Flaking axis n=161 (Mason 1965)							
	Corner (n=66)		Side (n=55)		End (n=40)		Total	
	N	%	N	%	N	%	N	%
Quartzite	53	41.4	46	35.9	29	22.7	128	100
Siltstone	5	31.3	4	25	7	43.8	16	100
Hornfels	6	40	5	33.3	4	26.7	15	100
Lava	1	100	0	0	0	0	1	100
Silcrete	1	100	0	0	0	0	1	100

Table 4.4.17. Debris flow assemblage flaking axis, by raw material. See Appendix B Table 6 for the Isaac and Keller (1968) method.

Raw material	Flaking axis n=416 (Mason 1965)							
	Corner (n=143)		Side (n=155)		End (n=118)		Total	
	N	%	N	%	N	%	N	%
Quartzite	93	31	116	38.7	91	30.3	300	100
Siltstone	12	30	18	45	10	25	40	100
Hornfels	34	49.3	19	27.5	16	23.2	69	100
Lava	1	100	0	0	0	0	1	100
Silcrete	0	0	1	100	0	0	1	100
Claystone	3	60	1	20	1	20	5	100

The number of flaking directions preserved on the dorsal surfaces of complete flakes is presented in Figures 4.4.89 and 4.4.90. For both assemblages there is a notable abundance of flakes with only a single dorsal scar direction (49% for the colluvial sample and 47.6% for the debris flow sample). In addition to this, both assemblages have a maximum number of five directions, although this is less than 1% in each sample. The number of flakes with one and two directions accounts for 69.8% of the colluvial sample and 73.4% for the debris flow assemblage. In addition to this the debris flow sample has a lower percentage of flakes with four directions (3.7%)

versus 8.7% in the colluvial assemblage. Flakes with no directions (cortical flakes and/or indeterminate directions) have a similar distribution for both assemblages.

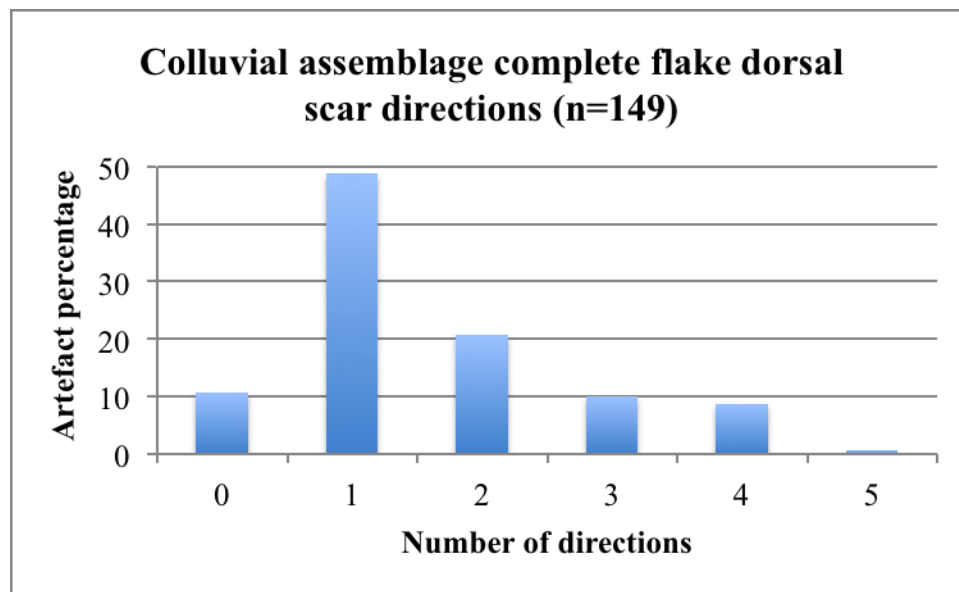


Figure 4.4.89. Colluvial assemblage dorsal scar directions (including formal tools on complete flakes).

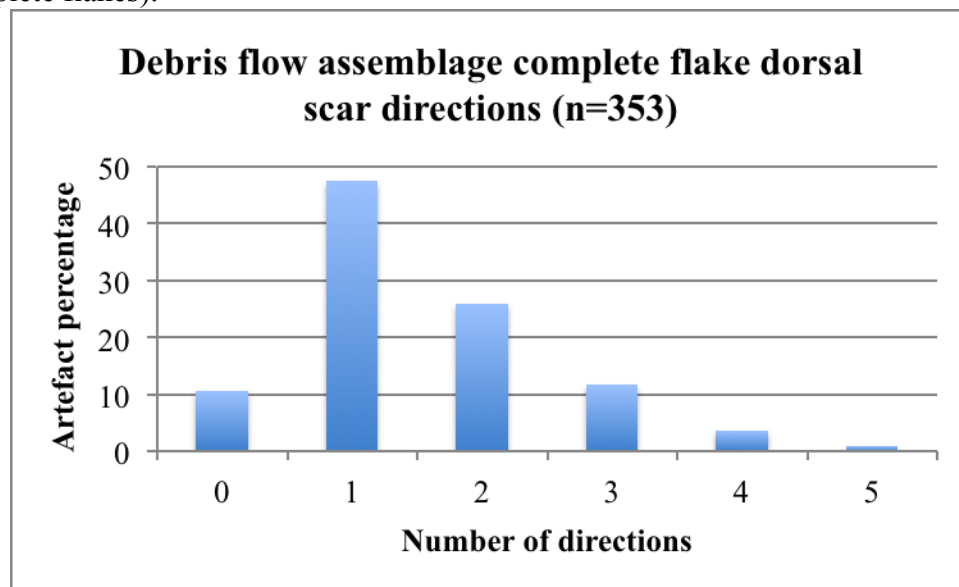
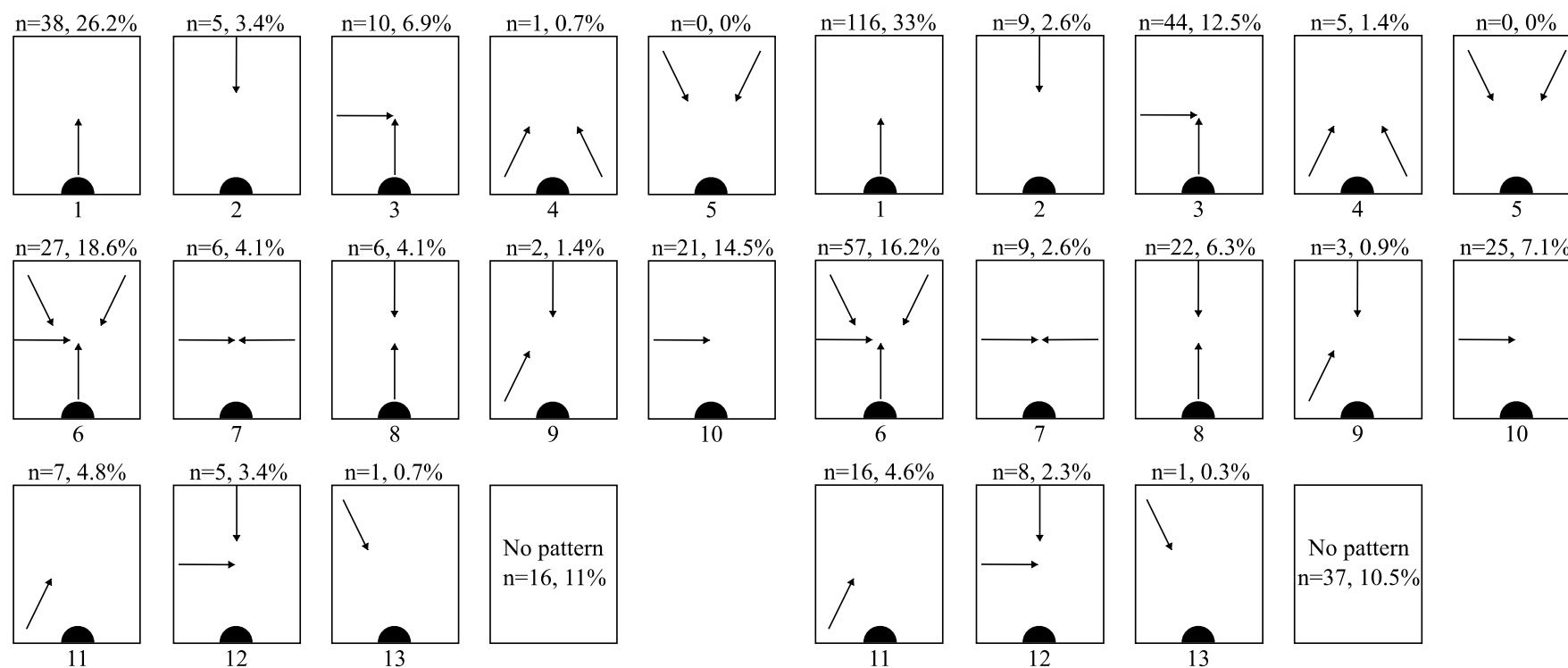


Figure 4.4.90. Debris flow assemblage dorsal scar directions (including formal tools on complete flakes).

The pattern of dorsal flake scar directions (Fig. 4.4.91) shows that both assemblages have a high frequency of unidirectional-proximal types (26.2% for the colluvial sample and 33% for the debris flow, making them the most common). However, the second most abundant pattern includes radial types (with three or more directions), accounting for 18.6% of the colluvial complete flake patterns and 16.2% for the debris flow sample.



0	None	7	Transverse-opposed
1	Unidirectional-proximal	8	Parallel-opposed
2	Unidirectional-distal	9	Complex
3	Unidirectional-transverse-proximal	10	Transverse
4	Convergent-proximal	11	Intermediate-proximal
5	Convergent-distal	12	Unidirectional-transverse-distal
6	Radial	13	Intermediate-distal

Figure 4.4.91. Complete flake dorsal scar patterns. Colluvial assemblage (including formal tools on complete flakes, n=145; left); debris flow assemblage (including formal tools on complete flakes, n=352; right).

Interestingly, variation does occur between the two assemblages in the percentage of transverse and unidirectional-transverse-proximal patterns (Fig. 4.4.91). Transverse types provide the third most frequent dorsal scar pattern for the colluvial assemblage (at 14.5%), whereas unidirectional-transverse-proximal types are the third most frequent in the debris flow (at 12.5%). Both assemblages have no convergent-distal patterns preserved, and only small percentages of the remaining dorsal scar patterns occur.

Assessing these dorsal scar patterns by raw material (Tables 4.4.18 & 4.4.19) reveals an interesting trend in the radial pattern sample for the colluvial assemblage. Here quartzite flakes account for 96.3% (n=26) of the total radial sample (n=27). For the most abundant raw materials (quartzite, siltstone and hornfels) the unidirectional-proximal pattern is the most common (ranging from 24.3-38.5%), and the quartzite sample retains the greatest range of dorsal scar patterns (most likely due to the larger sample size). Siltstone flakes account for the highest unidirectional-distal percentage (12.5%) and hornfels has the largest percentage of transverse types (15.4%).

Table 4.4.18. Colluvial assemblage dorsal scar pattern, by raw material (including formal tools on complete flakes, n=145).

Dorsal scar pattern	Raw material										
	Quartzite		Siltstone		Hornfels		Lava		Silcrete		Total
	N	%	N	%	N	%	N	%	N	%	
0	12	10.4	1	6.3	3	23.1	0	0	0	0	16
1	28	24.3	5	31.3	5	38.5	0	0	0	0	38
2	3	2.6	2	12.5	0	0	0	0	0	0	5
3	7	6.1	1	6.3	1	7.7	0	0	1	100	10
4	1	0.9	0	0	0	0	0	0	0	0	1
5	0	0	0	0	0	0	0	0	0	0	0
6	26	22.6	1	6.3	0	0	0	0	0	0	27
7	5	4.3	1	6.3	0	0	0	0	0	0	6
8	6	5.2	0	0	0	0	0	0	0	0	6
9	1	0.9	1	6.3	0	0	0	0	0	0	2
10	17	14.8	2	12.5	2	15.4	0	0	0	0	21
11	5	4.3	1	6.3	1	7.7	0	0	0	0	7
12	3	2.6	1	6.3	1	7.7	0	0	0	0	5
13	1	0.9	0	0	0	0	0	0	0	0	1
Total	115	100	16	100	13	100	0	0	1	100	145

For the debris flow, Table 4.4.19 also shows that unidirectional-proximal types are the most common (ranging from 25-34.9%). As with the colluvial assemblage, hornfels accounts for the largest percentage (16.1%) of complete flakes with zero dorsal scar patterns (excluding silcrete). A contrasting pattern is evident in the percentage of radial patterns, now highest for the siltstone sample (20%, albeit only marginally higher than the quartzite sample). Hornfels patterns are dominated by simple transverse (17.7%) and unidirectional-transverse-proximal patterns (11.3%); siltstone provides the largest percentage (17.1%) for the latter pattern (excluding lava).

Table 4.4.19. Debris flow assemblage dorsal scar pattern, by raw material (including formal tools on complete flakes, n=352).

Dorsal scar pattern	Raw material												
	Quartzite		Siltstone		Hornfels		Lava		Silcrete		Claystone		Total
	N	%	N	%	N	%	N	%	N	%	N	%	
0	24	9.6	2	5.7	10	16.1	0	0	1	100	0	0	37
1	87	34.9	9	25.7	19	30.6	0	0	0	0	1	25	116
2	6	2.4	2	5.7	1	1.6	0	0	0	0	0	0	9
3	30	12	6	17.1	7	11.3	1	100	0	0	0	0	44
4	3	1.2	2	5.7	0	0	0	0	0	0	0	0	5
5	0	0	0	0	0	0	0	0	0	0	0	0	0
6	48	19.3	7	20	2	3.2	0	0	0	0	0	0	57
7	8	3.2	0	0	1	1.6	0	0	0	0	0	0	9
8	15	6	3	8.6	3	4.8	0	0	0	0	1	25	22
9	1	0.4	1	2.9	1	1.6	0	0	0	0	0	0	3
10	12	4.8	0	0	11	17.7	0	0	0	0	2	50	25
11	8	3.2	3	8.6	5	8.1	0	0	0	0	0	0	16
12	6	2.4	0	0	2	3.2	0	0	0	0	0	0	8
13	1	0.4	0	0	0	0	0	0	0	0	0	0	1
Total	249	100	35	100	62	100	1	100	1	100	4	100	352

The last data to be presented in this section concerns flake termination type, by raw material (Tables 4.4.20 & 4.4.21). The manner in which a flake terminates is not a ‘strategy’ employed by the knapper, but rather, a result of the knapping process. However, this data is included here as termination type can be indicative of the forces used to detach flakes (Andrefsky 2005) and may thus potentially involve some kind of basic strategy.

Flake termination by raw material shows largely similar distributions for the two assemblages for quartzite, siltstone and hornfels. Feather terminations are the most

abundant type for all the raw materials (ranging from 68.8-100% for the colluvial assemblage and 57.5-100% for the debris flow). However, both siltstone and hornfels have notably smaller percentages for these termination types in the debris flow assemblage (excluding silcrete).

Siltstone accounts for the lowest percentages of feathered flake terminations (57.5 and 68.8%) and the highest percentages of hinged terminations (31.3 and 35%) for both assemblages (excluding silcrete).

In the colluvial assemblage step and overshoot terminations only occur on quartzite (perhaps due to the larger sample size); these types are represented across a wider range of materials within the debris flow. In general though these types account for only small percentages of the assemblages (Tables 4.4.20 & 4.4.21).

Table 4.4.20. Colluvial complete flake termination types, by raw material (including formal tools on complete flakes, n=161).

Raw material	Termination type									
	Feather		Step		Hinge		Overshoot		Total	
	N	%	N	%	N	%	N	%	N	%
Quartzite	99	77.3	12	9.4	16	12.5	1	0.8	128	100
Siltstone	11	68.8	0	0	5	31.3	0	0	16	100
Hornfels	12	80	0	0	3	20	0	0	15	100
Lava	1	100	0	0	0	0	0	0	1	100
Silcrete	1	100	0	0	0	0	0	0	1	100

Table 4.4.21. Debris flow complete flake termination types, by raw material (including formal tools on complete flakes, n=416).

Raw material	Termination type									
	Feather		Step		Hinge		Overshoot		Total	
	N	%	N	%	N	%	N	%	N	%
Quartzite	218	72.7	20	6.7	61	20.3	1	0.3	300	100
Siltstone	23	57.5	2	5	14	35	1	2.5	40	100
Hornfels	44	63.8	4	5.8	21	30.4	0	0	69	100
Lava	1	100	0	0	0	0	0	0	1	100
Silcrete	0	0	0	0	1	100	0	0	1	100
Claystone	5	100	0	0	0	0	0	0	5	100

Level of reduction:

Assessing the retention of cortex on the dorsal surfaces of flakes and on flake platforms is shown by the technological flake type analysis in Figures 4.4.92 and 4.4.93.

The colluvial assemblage (Fig. 4.4.92) has the highest percentage (30.4%) of flakes in the type VI category (non-cortical dorsal surface and platform), and the second most abundant type (23%) is type V (non-cortical platform and partially cortical dorsal surface). Those flakes that preserve the greatest amounts of cortex (types I and IV) only account for 10.6 and 5.6% (collectively 16.2%) of the entire assemblage, respectively. Flakes with cortical platforms (types I to III) account for 41.1% of the total colluvial sample.

A similar pattern is evident in the debris flow assemblage, with subtle differences (Fig. 4.4.93). Here the combined percentage of flakes with cortical platforms is notably lower (at 33%) and those flakes with the greatest amounts of cortex are marginally less abundant (collectively accounting for 15.4% of the total sample). A similar abundance for types V and VI occurs in the debris flow assemblage, with type VI accounting for 39.4% of the total sample.

Technological flake type by raw material is presented in Tables 4.4.22 and 4.4.23, both of which highlight that for the most abundant raw materials (quartzite and siltstone), from either assemblage, types V and VI dominate. However, the colluvial assemblage shows that hornfels types I and II are the most abundant across the different raw materials (Table 4.4.22). Little can be said for the small lava and silcrete samples.

By raw material the debris flow assemblage also shows an interesting technological flake type distribution for the hornfels sample (Table 4.4.23). For this raw material the percentage of type V flakes is the second smallest (at 20.3%) and for type VI flakes it is the lowest (at 27.5%, excluding lava and claystone). Hornfels accounts for the highest percentages of type I (13%), II (21.7%) and IV (11.6%) flakes (excluding silcrete). Lava, silcrete and claystone flakes (n=7) show a high percentage of types V and VI (n=5, 71.4% of the total sample).

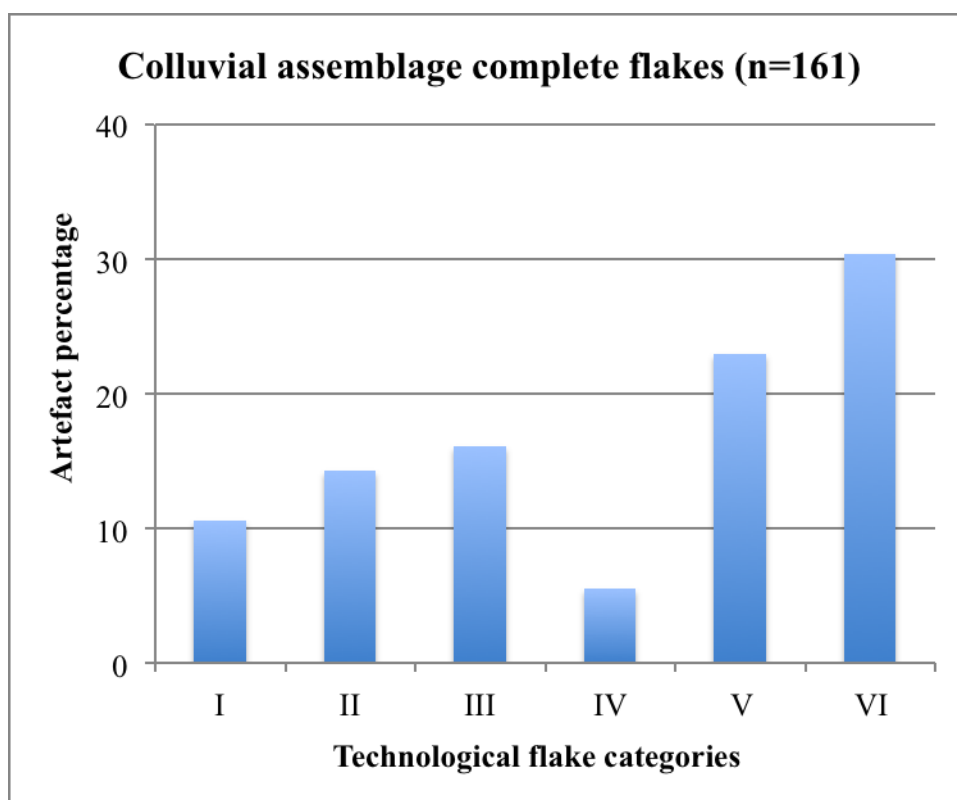


Figure 4.4.92. Technological flake types for the colluvial assemblage (including formal tools on complete flakes).

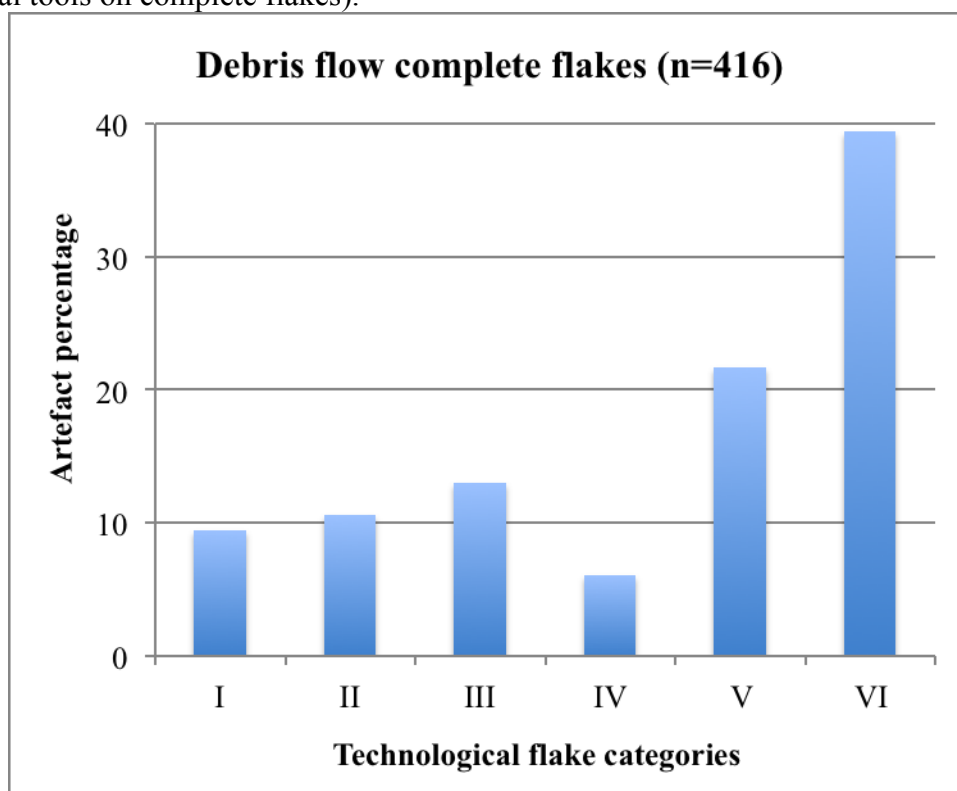


Figure 4.4.93. Technological flake types for the debris flow assemblage (including formal tools on complete flakes).

Table 4.4.22. Colluvial technological flake type, by raw material (including formal tools on complete flakes, n=161).

Raw material	Technological flake category													
	I		II		III		IV		V		VI		Total	
	N	%	N	%	N	%	N	%	N	%	N	%	N	%
Quartzite	11	8.6	16	12.5	23	18.0	7	5.5	29	23	42	32.8	128	100
Siltstone	1	6.3	2	12.5	2	12.5	2	12.5	5	31	4	25.0	16	100
Hornfels	5	33.3	4	26.7	1	6.7	0	0.0	2	13	3	20.0	15	100
Lava	0	0	0	0	0	0.0	0	0.0	1	100	0	0.0	1	100
Silcrete	0	0	1	100	0	0.0	0	0.0	0	0	0	0.0	1	100

Table 4.4.23. Debris flow technological flake type, by raw material (including formal tools on complete flakes, n=416).

Type	Technological flake category													
	I		II		III		IV		V		VI		Total	
	N	%	N	%	N	%	N	%	N	%	N	%	N	%
Quartzite	25	8.3	24	8	48	16	14	4.7	60	20	129	43	300	100
Siltstone	4	10	4	10	2	5	3	7.5	13	32.5	14	35	40	100
Hornfels	9	13	15	21.7	4	5.8	8	11.6	14	20.3	19	27.5	69	100
Lava	0	0	0	0	0	0	0	0	0	0	1	100	1	100
Silcrete	1	100	0	0	0	0	0	0	0	0	0	0	1	100
Claystone	0	0	1	20	0	0	0	0	3	60	1	20	5	100

An expanded sample for both assemblages is presented here when assessing flake platform facets; these samples also include platform information that was recorded on incomplete flakes and formal tools made on incomplete flakes (Figs. 4.4.94 & 4.4.95).

The distribution of platform facets is largely similar for both of the assemblages. Both have plain platforms as the most common types, accounting for 47.7% of the colluvial sample and 45.6% for the debris flow. Similarly, cortical and partly cortical platform percentages are largely the same for the assemblages (39.5 and 40.2% for the former, and 3 and 3.8% for the latter). A notable difference between the assemblages is in the marginally higher percentage of flakes with two or more facets in the colluvial assemblage. Collectively, these types account for 11.8% of the total colluvial sample, whereas these types account for 10.4% of the debris flow sample. Most notable, however, is the absence of multi-faceted platforms in the debris flow, despite the large sample size. A single flake (n=1, 0.3%) retains a multi-faceted platform in the colluvial assemblage.

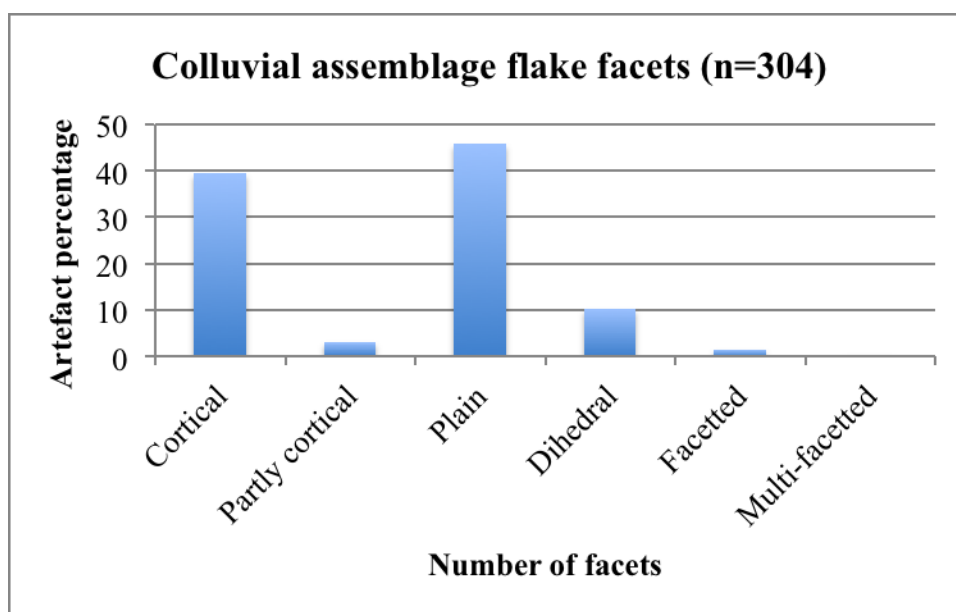


Figure 4.4.94. Colluvial assemblage flake platform facets (includes complete flakes, incomplete flakes, and formal tools made on either).

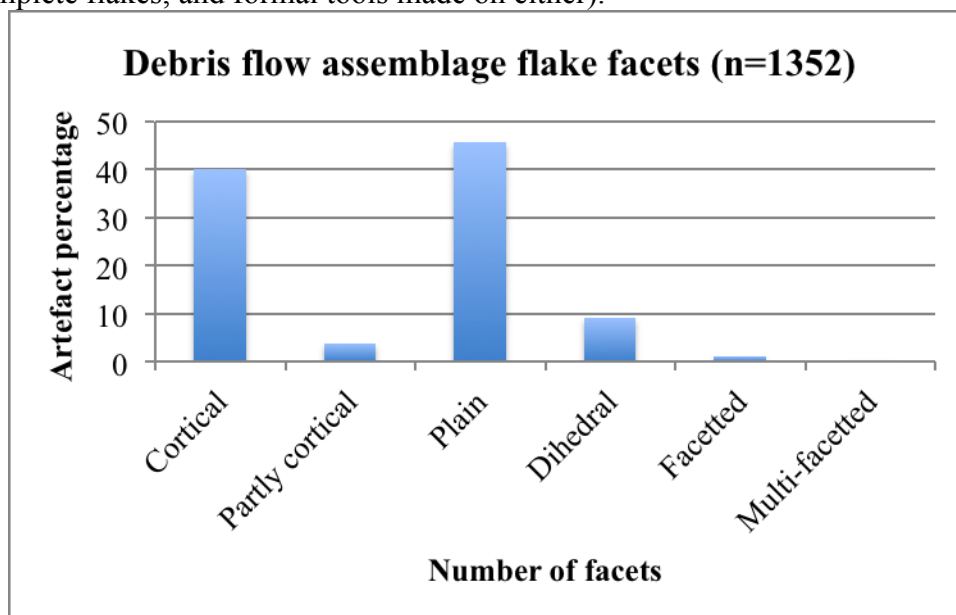


Figure 4.4.95. Debris flow assemblage flake platform facets (includes complete flakes, incomplete flakes, and formal tools made on either).

Tables 4.4.24 and 4.4.25 show that, for both assemblages, quartzite flakes account for those platforms with the highest facet numbers (facetted and multi-facetted types). Interestingly, the highest percentage (23.1%) of dihedral platforms occurs on siltstone flakes (for the colluvial assemblage; Table 4.4.24). The remaining raw materials show that platforms are primarily plain, and hornfels accounts for the highest percentage of cortical platforms (excluding silcrete and claystone; Table 4.4.24).

Table 4.4.25 shows that quartzite flakes in the debris flow account for the highest percentage (10%) of dihedral platforms. Although the majority of all raw materials retains plain platforms (including the small silt-quartzite and lava samples), hornfels flakes once again provide the highest percentage (42.7%) of cortical platforms (excluding silcrete). Silcrete platforms are exclusively cortical.

Table 4.4.24. Colluvial assemblage flake facets, by raw material (includes complete flakes, incomplete flakes, and formal tools made on either, n=304).

Raw material	Platform facets													
	Cortical		Partly cortical		Plain		Dihedral		Facetted		Multi-facetted		Total	
	N	%	N	%	N	%	N	%	N	%	N	%	N	%
Quartzite	95	38	8	3.2	118	47.2	24	9.6	4	1.6	1	0.4	250	100
Siltstone	10	38.5	1	3.8	9	34.6	6	23.1	0	0	0	0	26	100
Hornfels	12	50	0	0	11	45.8	1	4.2	0	0	0	0	24	100
Lava	0	0	0	0	1	100	0	0	0	0	0	0	1	100
Silcrete	2	100	0	0	0	0	0	0	0	0	0	0	2	100
Claystone	1	100	0	0	0	0	0	0	0	0	0	0	1	100

Table 4.4.25. Debris flow assemblage flake facets, by raw material (qzte=quartzite; includes complete flakes, incomplete flakes, and formal tools made on either, n=1352).

Raw material	Platform facets													
	Cortical		Partly cortical		Plain		Dihedral		Facetted		Multi-facetted		Total	
	N	%	N	%	N	%	N	%	N	%	N	%	N	%
Quartzite	442	40.4	40	3.7	487	44.5	110	10	16	1.5	0	0	1095	100
Siltstone	40	36	6	5.4	58	52.3	7	6.3	0	0	0	0	111	100
Silt-qzte	2	40	0	0	3	60	0	0	0	0	0	0	5	100
Hornfels	50	42.7	5	4.3	56	47.9	6	5.1	0	0	0	0	117	100
Lava	1	33.3	0	0	2	66.7	0	0	0	0	0	0	3	100
Silcrete	4	100	0	0	0	0	0	0	0	0	0	0	4	100
Claystone	4	23.5	1	5.9	11	64.7	1	5.9	0	0	0	0	17	100

The number of flake scars recorded on the dorsal surface of complete flakes is shown in Figures 4.4.96 and 4.4.97. For both assemblages the majority of flakes have one to four scars, collectively accounting for 80.4% of the colluvial assemblage and 80.8% of the debris flow assemblage. Notable differences for the debris flow sample include the lower percentage (17.8%) of flakes with a single dorsal scar (versus 28% in the colluvial assemblage), and, the higher percentages (15.1 and 9.7%) of flakes with four

and five scars, respectively (versus 9.8 and 6.3%, respectively, in the colluvial sample). Thereafter, both assemblages have only small samples of flakes with scars that exceed five in number, yet these percentages are marginally lower for the debris flow. However, the debris flow is the only assemblage to have a flake with 10 dorsal scars.

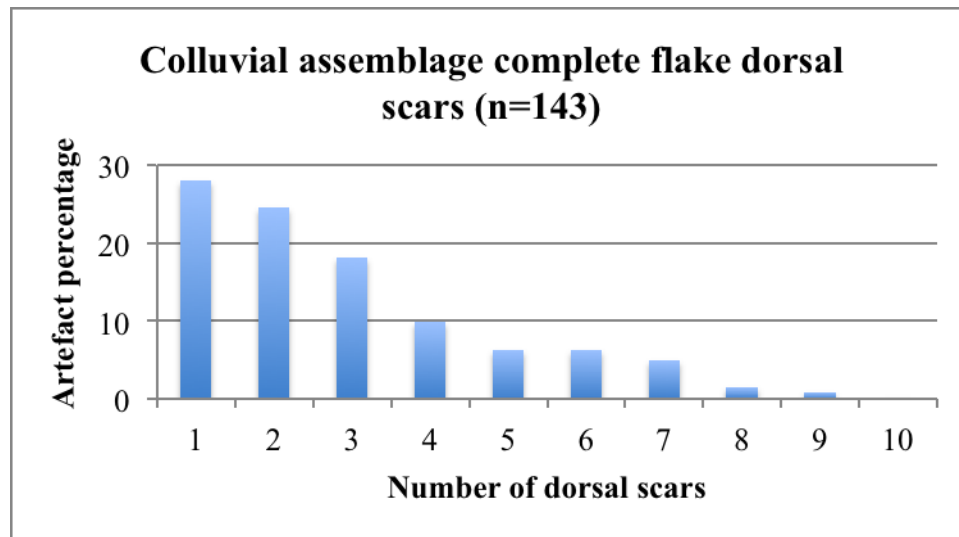


Figure 4.4.96. Colluvial assemblage dorsal scar number (including formal tools on complete flakes).

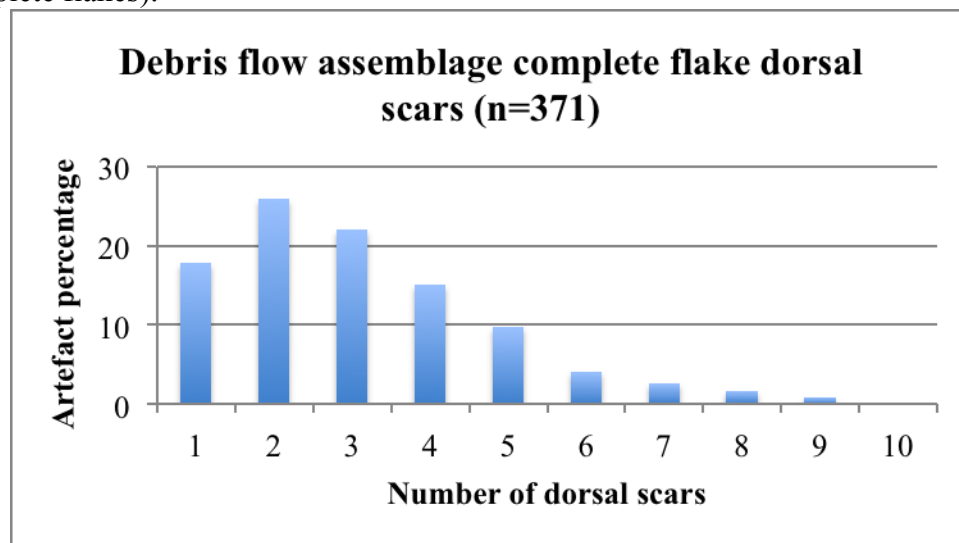


Figure 4.4.97. Debris flow assemblage dorsal scar number (including formal tools on complete flakes). A single flake has 10 dorsal scars.

An assessment of these dorsal scar numbers by raw material (Tables 4.4.26 & 4.4.27) shows that, for both assemblages, hornfels accounts for the highest percentage of flakes with only a single scar (54.5% for the colluvial assemblage, excluding lava, and 35.1% for the debris flow). Quartzite and hornfels flake scars are the most frequent from one to four, and these materials also provide the highest percentages for

scars exceeding five (albeit small samples for both of the assemblages). The lava, silcrete and claystone samples are limited, but where these materials do occur they account for flake scar numbers ranging from one to five (when looking at both assemblages).

Table 4.4.26. Colluvial assemblage complete flake scars, by raw material (including formal tools on complete flakes, n=143).

Number	Dorsal flake scars									
	Quartzite		Siltstone		Hornfels		Lava		Silcrete	
	N	%	N	%	N	%	N	%	N	%
1	28	24.3	5	33.3	6	54.5	1	100	0	0
2	31	27	1	6.7	3	27.3	0	0	0	0
3	19	16.5	5	33.3	1	9.1	0	0	1	100
4	12	10.4	2	13.3	0	0	0	0	0	0
5	7	6.1	1	6.7	1	9.1	0	0	0	0
6	9	7.8	0	0	0	0	0	0	0	0
7	7	6.1	0	0	0	0	0	0	0	0
8	1	0.9	1	6.7	0	0	0	0	0	0
9	1	0.9	0	0	0	0	0	0	0	0
10	0	0	0	0	0	0	0	0	0	0
Total	115	100	15	100	11	100	1	100	1	100

Table 4.4.27. Debris flow assemblage complete flake scars, by raw material (including formal tools on complete flakes, n=371).

Number	Dorsal flake scars											
	Quartzite		Siltstone		Hornfels		Lava		Silcrete		Claystone	
	N	%	N	%	N	%	N	%	N	%	N	%
1	37	13.6	8	22.2	20	35.1	0	0	0	0	1	20
2	63	23.2	9	25	22	38.6	0	0	0	0	2	40
3	69	25.4	5	13.9	7	12.3	0	0	0	0	1	20
4	44	16.2	6	16.7	5	8.8	1	100	0	0	0	0
5	30	11	4	11.1	1	1.8	0	0	0	0	1	20
6	14	5.1	1	2.8	0	0	0	0	0	0	0	0
7	7	2.6	2	5.6	1	1.8	0	0	0	0	0	0
8	5	1.8	1	2.8	0	0	0	0	0	0	0	0
9	2	0.7	0	0	1	1.8	0	0	0	0	0	0
10	1	0.4	0	0	0	0	0	0	0	0	0	0
Total	272	100	36	100	57	100	1	100	0	0	5	100

For the amount of cortex preservation on the dorsal surfaces of complete flakes, both assemblages show a clear abundance for types with no (0%) cortex (42.9% of the colluvial assemblage and 47.8% of the debris flow; Figs. 4.4.98 & 4.4.99). In addition

to this only minor variation can be seen across the remaining dorsal cortex categories. For the colluvial assemblage, percentages peak in the 31-50 and 71-90% categories (10.6%) and the least frequent types retain 1-10% cortex (3.1%). The debris flow shows a similar peak in the 31-50% category (10.1%) and a minimum value for flakes with 1-10% cortex preservation (5.8%; Figs. 4.4.98 & 4.4.99).

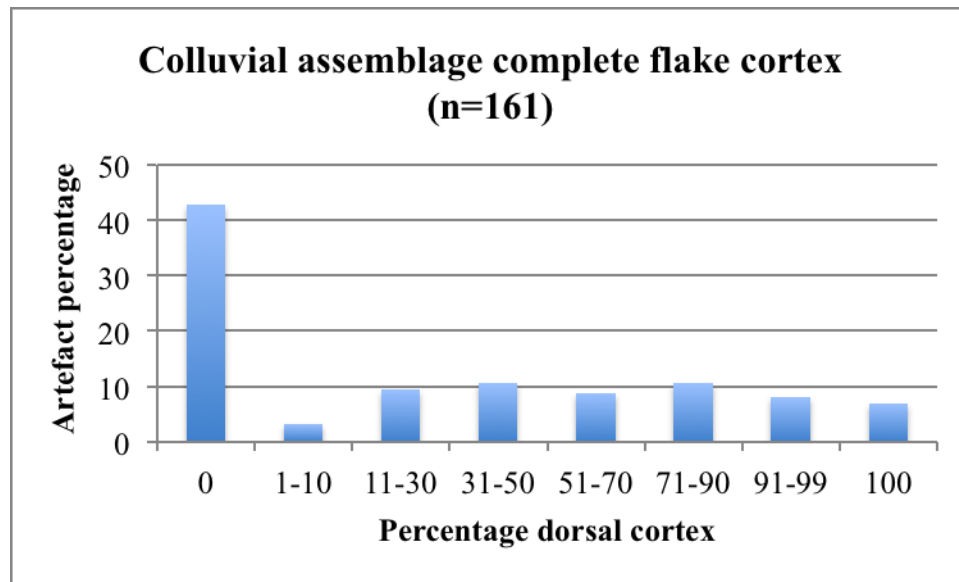


Figure 4.4.98. Colluvial complete flake dorsal cortex (including formal tools on complete flakes).

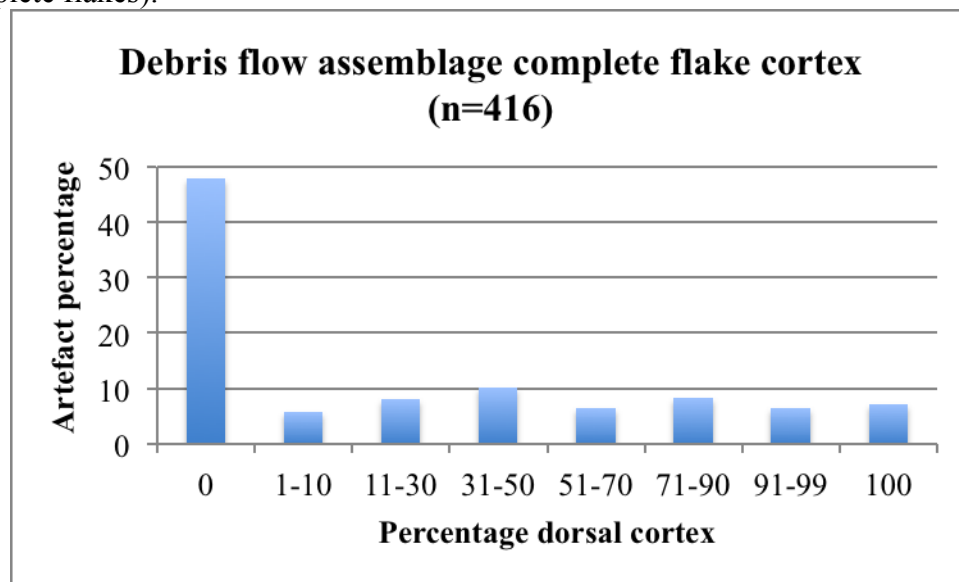


Figure 4.4.99. Debris flow complete flake dorsal cortex (including formal tools on complete flakes).

Cortex by raw material shows that hornfels accounts for the highest percentages of flakes with 91-99 and 100% cortex (for both assemblages; Tables 4.4.28 & 4.4.29). In addition to this both assemblages show the following trends: quartzite flakes retain

the least (0%) cortex (46.1% for the colluvial sample and 55%, excluding lava, for the debris flow); in most cases siltstone and hornfels account for the highest percentages of flakes with cortex exceeding 10%.

Table 4.4.28. Colluvial complete flake dorsal cortex, by raw material (including formal tools on complete flakes, n=161).

%	Dorsal cortex									
	Quartzite		Siltstone		Hornfels		Lava		Silcrete	
	N	%	N	%	N	%	N	%	N	%
0	59	46.1	6	37.5	4	26.7	0	0	0	0
1-10	4	3.1	0	0	1	6.7	0	0	0	0
11-30	12	9.4	2	12.5	1	6.7	0	0	0	0
31-50	13	10.2	1	6.3	2	13.3	0	0	1	100
51-70	12	9.4	2	12.5	0	0	0	0	0	0
71-90	13	10.2	2	12.5	2	13.3	0	0	0	0
91-99	7	5.5	2	12.5	3	20	1	100	0	0
100	8	6.3	1	6.3	2	13.3	0	0	0	0
Total	128	100	16	100	15	100	1	100	1	100

Table 4.4.29. Debris flow complete flake dorsal cortex, by raw material (including formal tools on complete flakes, n=416).

%	Dorsal cortex											
	Quartzite		Siltstone		Hornfels		Lava		Silcrete		Claystone	
	N	%	N	%	N	%	N	%	N	%	N	%
0	165	55	12	30	21	30.4	1	100	0	0	0	0
1-10	16	5.3	4	10	3	4.3	0	0	0	0	1	20
11-30	17	5.7	5	12.5	10	14.5	0	0	0	0	1	20
31-50	27	9	5	12.5	8	11.6	0	0	0	0	2	40
51-70	19	6.3	2	5	6	8.7	0	0	0	0	0	0
71-90	23	7.7	5	12.5	5	7.2	0	0	0	0	1	20
91-99	13	4.3	5	12.5	9	13	0	0	0	0	0	0
100	20	6.7	2	5	7	10.1	0	0	1	100	0	0
Total	300	100	40	100	69	100	1	100	1	100	5	100

Although similar to the technological flake types presented in Figures 4.4.92 and 4.4.93, the dorsal cortex location data in Figures 4.4.100 and 4.4.101 only address the location of cortex on the flake dorsal surface (excluding the platform). As such this approach provides more detail on the flake dorsal surface, to provide further information on the stages of core reduction. With this approach, both assemblages show an abundance of flakes with no dorsal cortex (type four, tertiary). These types account for 42.9% of the colluvial sample and 47.1% of the debris flow. The

distribution of the remaining types is largely similar between the assemblages (small samples and percentages for each), and both have types two (crescent shaped) and one (primary) as the most abundant remaining types (after type four). However, a notable difference between the two assemblages is the lower percentage for these two types in the debris flow assemblage (collectively 38.7% for this assemblage, versus 46% for the colluvial assemblage).

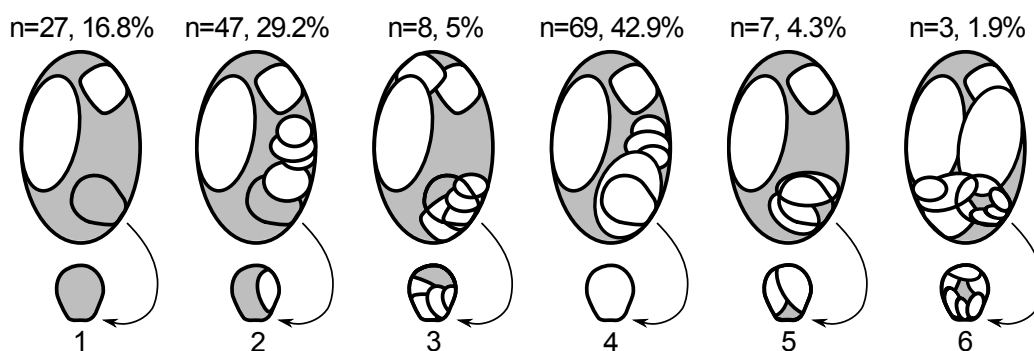


Figure 4.4.100. Dorsal cortex location for the colluvial complete flakes (including formal tools on complete flakes, n=161).

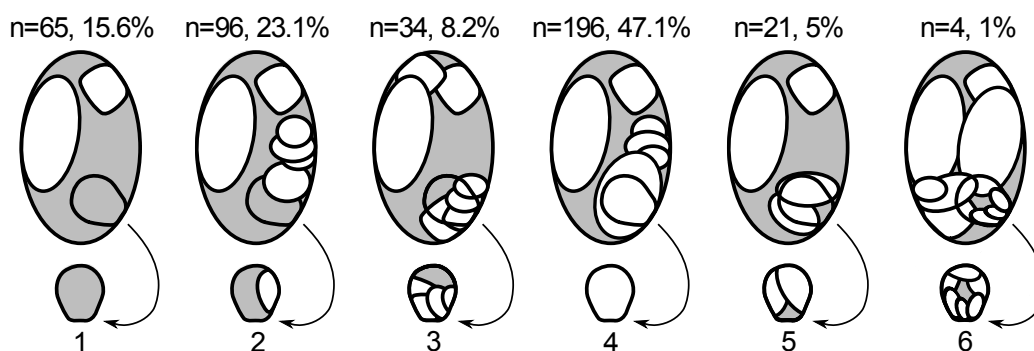


Figure 4.4.101. Dorsal cortex location for the debris flow complete flakes (including formal tools on complete flakes, n=416).

Interior and exterior platform angles that were recorded on complete flakes are presented in Table 4.4.30. From this only minor variation can be seen between the two assemblages. Interior angles for both assemblages have similar or the same minimums, maximums and standard deviations, with a mean interior angle of 111.6° for the colluvial assemblage and a slightly more obtuse mean of 113.8° for the debris flow sample.

A similar trend in the platform readings is observed when viewing the exterior angles. These range from 25-90° for the colluvial sample and 26-96° for the debris flow. The former has a mean of 69.4° and the latter a mean of 64.8°.

Table 4.4.30. Complete flake interior and exterior platform angles (including formal tools on complete flakes).

Assemblage	Platform angles (°)									
	Interior					Exterior				
	Min	Max	Mean	SD	N	Min	Max	Mean	SD	N
Colluvial	90	155	111.6	11.9	158	25	90	69.4	14.2	108
Debris flow	90	154	113.8	12.2	390	26	96	64.8	14	283

Summary:

Excavations at Penhill Farm have provided large samples of flaking debris and complete flakes. SFD is clearly infrequent in the colluvial assemblage when compared to the debris flow, where this material accounts for 55.1% of the total assemblage (by number). By weight, however, the majority of debris is >20 mm for both assemblages.

Measurements obtained on flakes illustrate an interesting size trend for the three most abundant raw materials, namely quartzite, siltstone and hornfels; there is little that can be said about the remaining raw materials due to their rarity. For both assemblages siltstone flakes account for the majority of the largest mean values, thereafter followed by quartzite and hornfels, as sizes decrease. This pattern is evident regardless of the methods used to measure flake length, width and thickness.

Both assemblages have an abundance of flakes that are 30-50 mm in maximum length. Although the overall number of flakes >100 mm in length is rare, these larger types are more frequent in the debris flow assemblage, where the largest reaches 170 mm in length (n=1).

Two methods were used to study technological flaking axis and these provide largely different results. Mason's (1965) approach is favoured as it takes into account corner-struck types.

Flake size by flaking axis illustrates that corner- and end-struck types are the largest flakes in the colluvial assemblage. Corner-struck flakes are also the most common type in the colluvial assemblage complete flake sample (n=134), with end-struck

flakes being the least frequent. Formal tools are made primarily on side-struck flakes in this assemblage.

The debris flow corner-struck flakes are also the largest types for this assemblage, however here end-struck flakes are the heaviest and thickest. For the debris flow complete flake sample (n=335) side- and corner-struck flakes are the most frequent. Formal tools also show a preference for side-struck types.

Flaking axis by raw material in the colluvial assemblage shows that for quartzite and hornfels, corner-struck flakes are the most common type. For siltstone, end-struck flakes are the most abundant. These patterns are largely different in the debris flow where side-struck flakes are most common in quartzite and siltstone. Hornfels here accounts for a high percentage of corner-struck types.

The number of dorsal scar directions illustrates that flakes with a single direction are the most common for both assemblages (49% of the colluvial assemblage and 47.6% of the debris flow). In addition to this flakes from both assemblages have a maximum number of five dorsal scar directions, although flakes with three or more directions are infrequent. Flakes with no pattern (either indeterminate directions or cortical dorsal surfaces) show almost equal percentages for both assemblages (10.5 and 10.7%).

Dorsal flake scar patterns show that the unidirectional-proximal pattern is the most frequent in both assemblages, for quartzite, siltstone and hornfels; this is followed by the radial flaking pattern. The majority of the remaining patterns are infrequent in both assemblages. By raw material some interesting patterns occur. In the colluvial assemblage, quartzite flakes account for the highest percentage of the radial flaking pattern, whereas siltstone flakes account for the highest percentage of the unidirectional-distal pattern. Hornfels flakes provide the largest percentage for no flaking pattern, also seen in the debris flow sample. In the debris flow the radial pattern is most frequent on siltstone flakes.

Flake termination types are largely similar for both assemblages and for the three most abundant raw materials. Feather terminations are the most frequent, yet in the

debris flow these termination types are marginally less common on siltstone and hornfels flakes. In both assemblages, siltstone flakes have the lowest percentage of feather terminations and the highest percentage of hinge terminations. Step and overshoot terminations are largely infrequent.

Technological flake types V and VI are the most common for the Penhill Farm assemblages. In addition to these types, however, flakes with cortical platforms (namely types I to III) collectively account for 41.1% of the colluvial sample and 33% of the debris flow sample. By raw material the quartzite and siltstone samples from both assemblages show an abundance of flake types V and VI, whereas hornfels accounts for the highest percentages of flake types I and II.

Flake platform facets are predominantly plain (47.7% of the colluvial assemblage and 45.6% of the debris flow) and cortical; both assemblages show a similar distribution for the remaining flake facet categories. A notable difference between the two assemblages is the presence of a single multi-facetted flake in the colluvial assemblage, versus none in the debris flow. Also, flakes with two or more facets are generally more common in the colluvial assemblage. In both assemblages by raw material, quartzite and siltstone flakes generally have higher facet counts (2 or more) when compared to the remaining raw materials. Hornfels flakes have the highest percentage of cortical platforms in either assemblage.

Dorsal scar counts show a high percentage of flakes with one to four, which collectively account for 80.4% of the colluvial sample and 80.8% of the debris flow. There is only minor difference in the number of flake scars between the assemblages, and those flakes with five or more scars are few. A single flake in the debris flow sample has 10 scars. By raw material, hornfels accounts for the highest percentage of flakes with only a single scar (for both assemblages) and quartzite and siltstone flakes illustrate both a greater range of flake scar numbers and greater percentages for those with one to four scars.

The percentage of dorsal cortex on flakes shows that those with 0% cortex are the most abundant in both assemblages; the remaining types provide only small

percentages (each less than 10.6%). Once again hornfels flakes are the most cortical (91-99 and 100% cortex), whereas quartzite flakes are the least.

A detailed look at the location of this dorsal cortex shows that tertiary flakes (no cortex) are the most common in either assemblage. However, types two (crescent) and one (primary) are the second and third most frequent, respectively.

Interior and exterior platform angle measurements show very similar values for both assemblages. Mean interior angles range from 111.6-113.8° and mean exterior angles range from 64.8-69.4°.

4.4.4.2 Cores

All data obtained on cores from the colluvial and debris flow assemblages are presented here. As a result the following maximum sample sizes apply:

- Colluvial core assemblage (n=51). This sample excludes core fragments (n=5), and a single polyhedral core that could not be relocated after performing the initial typological analysis.
- Debris flow assemblage (n=143). This sample excludes core fragments (n=8), but it includes two formal tools (chopper and denticulated scraper) that were made on cores (chopper-core and unifacial discoid, respectively, both on quartzite).

As with the flaking debris and complete flake section, data here will focus on the complexity of flaking and the level of reduction for the cores.

Core dimensions/size:

An assessment of core dimensions and weight, by both raw material and core type, is presented in Tables 4.4.31-4.4.34. For the colluvial assemblage Table 4.4.31 shows that siltstone cores provide the majority of the largest measurements, including most of the largest SD; the small claystone sample also provides notably large core measurements and accounts for the largest flake scar length (74.7 mm). The siltstone cores also have the greatest mean core size (114132.3).

A clear difference between the siltstone cores and the remaining materials is evident in the core measurements. Hornfels cores account for the smallest mean readings for all of the measurements, and quartzite cores appear to be intermediate between both hornfels and siltstone types. In addition to this hornfels cores have the smallest mean length for the longest flake scar (44.3 mm). Although this size trend occurs, the small sample sizes for siltstone and hornfels must be considered.

Core measurements are largely similar for the debris flow sample (Table 4.4.32), and the trends present in the colluvial sample are also evident here, with slightly larger samples for both siltstone and hornfels. However, here the difference between the

larger siltstone cores and smaller quartzite types is far greater (the former having a mean length of 128.6 mm, and the latter of 88.1 mm).

Table 4.4.31. Colluvial assemblage core measurements, by raw material (n=51). Where n=1, values are single measurements and not mean values.

Core measurements (mm)		Raw materials			
		Quartzite (n=37)	Siltstone (n=8)	Hornfels (n=5)	Claystone (n=1)
Artefact maximum length	Mean	92.3	109.3	67.9	126
	SD	31.4	38.5	23.2	-
Length	Mean	88.6	107.4	63.6	115
	SD	30	37.9	23.3	-
Width	Mean	69.4	79.4	54.6	94
	SD	24.2	19.3	15.6	-
Thickness	Mean	48.1	51.3	30.2	47
	SD	18	22.4	16.2	-
Weight (g)	Mean	485.1	734.8	165.7	680.4
	SD	656.3	1031.1	167.6	-
Largest scar length	Mean	51.9	64.5	44.3	74.7
	SD	17.9	18.3	24.9	-
Size	Mean	62827.1	114132.3	14151.8	85725.4
	SD	124067.4	218462.1	16388.7	-

Table 4.4.32. Debris flow assemblage core measurements, by raw material (n=143). Where n=1, values are single measurements and not mean values.

Core measurements (mm)		Raw materials			
		Quartzite (n=115)	Siltstone (n=13)	Hornfels (n=14)	Claystone (n=1)
Artefact maximum length	Mean	92.6	133.5	67.5	118.2
	SD	36.3	53.7	9	-
Length	Mean	88.1	128.6	64.9	118
	SD	32.4	51	9.7	-
Width	Mean	72.1	83.9	53	92
	SD	25.4	25	7.3	-
Thickness	Mean	44.5	56.8	28.1	58
	SD	19	22.1	9.7	-
Weight (g)	Mean	478.1	943.1	129	738.9
	SD	752.4	767.3	62.2	-
Largest scar length	Mean	53.4	73.8	42.1	71
	SD	19.6	29.5	9.5	-
Size	Mean	68721.9	161572.4	9176.4	87336.8
	SD	176187.3	162137.5	5395.4	-

Overall, when comparing the core measurements between the two assemblages, the debris flow has smaller quartzite and hornfels cores and larger siltstone and claystone cores. Siltstone and claystone cores account for the largest flake scar lengths in both assemblages (ranging from 64.5-74.7 mm).

A comparison of these core measurements, by core type, shows that chopper-cores and casual cores provide the majority of the largest mean values within the colluvial sample (Table 4.4.33). For most of these measurements the two core types are largely comparable, and irregular and single platform types are next in rank order. Discoids are the smallest and lightest cores (with a mean weight of 247.9 g). The largest mean flake scar lengths are found in the chopper-core sample (58.9 mm), along with the greatest SD (22.7). Interestingly, the discoid with a single 'large' removal accounts for the smallest flake scar length (42.1 mm).

Table 4.4.33. Colluvial assemblage core measurements, by core type (n=51). Where n=1, values are single measurements and not mean values.

Core measurements (mm)		Core type					
		Chopper-core (n=17)	Irregular (n=6)	Discoidal (n=11)	Discoidal w/removal (n=1)	Single platform (n=5)	Casual (n=11)
Max. length	Mean	100.6	86.9	80.6	57	94.1	101
	SD	40.1	38.4	16.4	-	20.7	34.7
Length	Mean	97.4	84	77.6	52	87.8	97.1
	SD	38.9	37.6	17	-	22.6	31.6
Width	Mean	76.2	66.3	65.2	50	66.2	70.8
	SD	27.1	28.7	16.4	-	12.8	25.3
Thickness	Mean	49.8	46.8	41.2	26	48.8	48.9
	SD	18.6	27.2	14.8	-	10.8	22.1
Weight (g)	Mean	625.6	522.4	247.9	70.5	410.8	610.6
	SD	809.3	712.4	145.2	-	247.2	964.4
Scar length	Mean	58.9	45.4	50.3	42.1	53.2	54.3
	SD	22.7	20.9	17.3	-	10.9	17.9
Size	Mean	90997.6	66589.9	21936	4020.2	42385.6	90036.7
	SD	162914.9	108155.4	14968.3	-	32181.8	196857.6

As with the colluvial assemblage, Table 4.4.34 shows that chopper-cores and casual cores also account for the majority of the largest mean core measurements, although for the debris flow this also includes large irregular cores (mean lengths for these three types ranges from 93-98.2 mm). A comparison of the overall measurements for

the chopper-cores and casual cores between the two assemblages shows that chopper-cores are marginally smaller and lighter in the debris flow, whereas the casual cores are larger and heavier. Single platform core measurements are largely comparable to those for the discoids and polyhedrons. In the debris flow the smallest and lightest cores are the discoids, with a mean length of 78.7 mm and a mean weight of 250.3 g (excluding the single bipolar core, which is the smallest and lightest for all of the debris flow types). Although the polyhedral core sample is small (n=3), these types account for the largest mean flake scar length (58.4 mm). Casual, irregular and chopper-core mean scar length measurements follow thereafter as this measurement decreases.

Table 4.4.34. Debris flow assemblage core measurements, by core type (n=143). Where n=1, values are single measurements and not mean values.

Core measurements (mm)		Core type						
		Chopper-core (n=32)	Irregular (n=12)	Discoidal (n=45)	Polyhedral (n=3)	Single platform (n=7)	Bipolar (n=1)	Casual (n=43)
Max. length	Mean	96.6	103.2	81.8	88.9	86.6	56.9	104.3
	SD	35.2	49.4	24.2	19	21	-	50
Length	Mean	93	98.2	78.7	88.7	82.9	56	98
	SD	33.7	48.5	23.3	19.5	20.7	-	43.6
Width	Mean	75.2	70.5	67.1	70	65.1	42	75.1
	SD	25	30.2	18.3	16.6	20.8	-	30.1
Thickness	Mean	44.1	52.8	36.9	56	40.9	33	49
	SD	15	24.5	12.7	2.6	8.9	-	25.5
Weight (g)	Mean	491.3	603.2	250.3	458.6	324.3	78.4	723.9
	SD	502.6	708.2	230.5	227.8	221.1	-	1118
Scar length	Mean	55.3	55.4	52.3	58.4	43.9	42.2	56.8
	SD	18.7	27.6	16.3	10.4	7.8	-	26.2
Size	Mean	63950.6	93613	25631.3	43674.8	31822.4	4459.3	125053.9
	SD	96274.5	139731.7	33644.7	31433	27744.6	-	270538.1

Flaking strategy:

Although each of the cores from Penhill Farm was typologically classified according to the types listed in Chapter 3.4, a more detailed analysis of the flaking strategies employed in core reduction is shown in Figures 4.4.102 and 4.4.103 and Tables 4.4.35 and 4.4.36.

The colluvial assemblage (Fig. 4.4.102) has 10 types of flaking strategy represented. The most common pattern is the bifacial simple partial exploitation (BSP, 29.4%). Casual cores account for 21.6%, and had this been combined with the unifacial simple partial (USP) and the BSP exploitation patterns, collectively these types would represent 54.9% of the total colluvial core sample. Other strategies include discoidal (15.7%) and multifacial (11.8%) types.

Collectively, only 17.5% of the colluvial core sample is made up of the remaining patterns, and these include: unidirectional abrupt unifacial exploitation on one knapping surface (UAU1, 5.9%); unifacial abrupt unidirectional total (UAUT) and unifacial centripetal (UC) exploitation (both 3.9%); and unifacial peripheral (UP) and bifacial hierarchical centripetal (BHC) exploitation (both 1.9%). No cores represent a bipolar strategy in core reduction.

The debris flow core sample (Fig. 4.4.103) shows similar variability in core flaking strategies, also with 10 types represented, although here UP and BHC types are absent and polyhedral and bipolar types occur. The flaking of simple casual cores is the most common strategy (29.4%), followed thereafter by discoids at 23.8%.

A notable difference between the debris flow and colluvial assemblage is the lower percentage of BSP exploitation types (accounting for 17.5% here, versus 29.4%), but combining the casual types with both USP and BSP exploitation patterns collectively accounts for 51.7% (only marginally less frequent than for the colluvial assemblage, at 54.9%). In addition to this UAU1 and UAUT exploitations are less common in the debris flow (both 2.8%) than those in the colluvial sample (5.9 and 3.9%, respectively), yet UC types here are more frequent (7%). A single bipolar core accounts for 1.4% of the debris flow core sample.

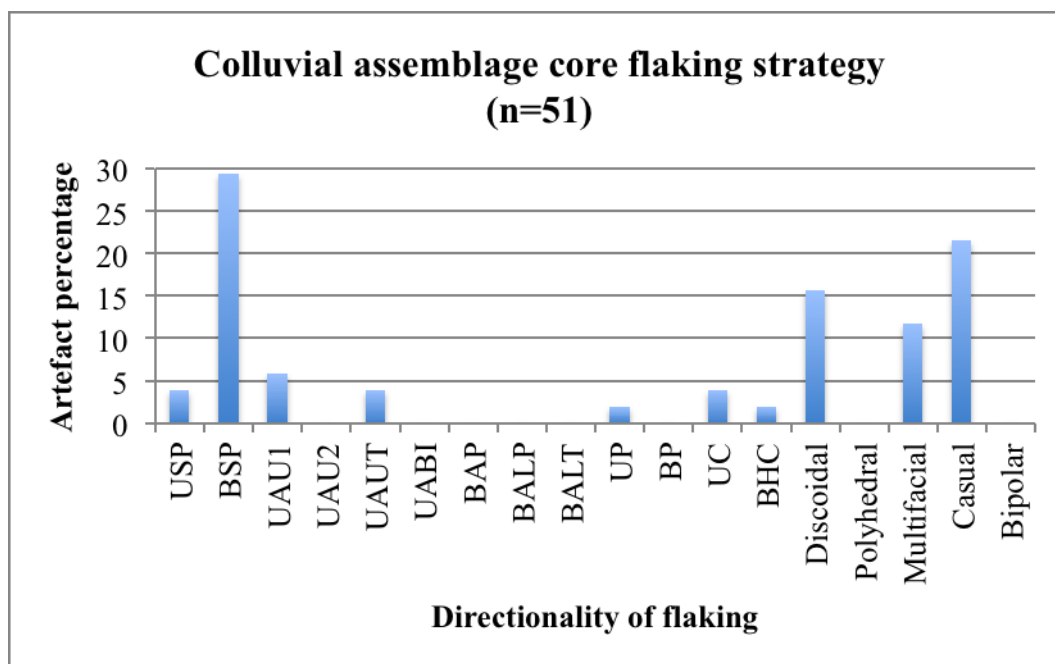


Figure 4.4.102. Directionality of core flaking for the colluvial assemblage.

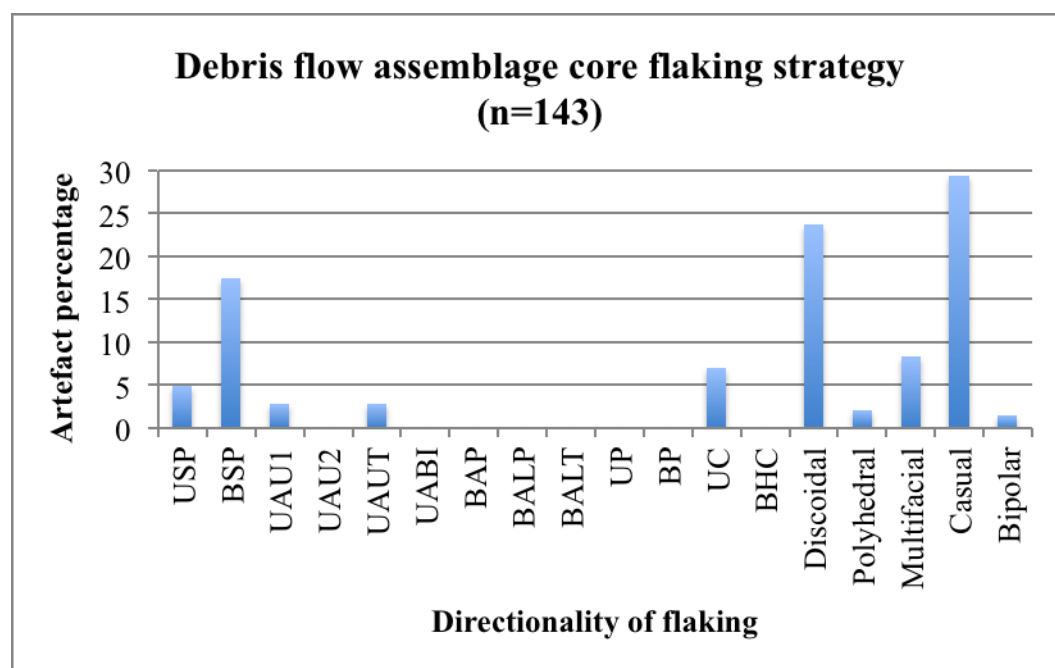


Figure 4.4.103. Directionality of core flaking for the debris flow assemblage.

Table 4.4.35 shows the distribution of core flaking patterns by raw material for the colluvial assemblage. Here the range of flaking patterns is greatest for the quartzite sample, due mainly to it being a larger sample. BSP and discoidal flaking strategies are the most frequent for all the raw material types. Casual core flaking is also common, however, this only occurs on siltstone (25%) and quartzite (24.3%). Several flaking strategies occur exclusively on quartzite and these include: UAU1 (8.1%);

UAUT (5.4%); UP (2.7%) and BHC (2.7%) types. All the other flaking strategies that occur on siltstone, hornfels and claystone, also occur on quartzite.

Table 4.4.35. Core flaking pattern, by raw material, for the colluvial assemblage.

Flaking strategy	Raw materials								Total
	Quartzite		Siltstone		Hornfels		Claystone		
	N	%	N	%	N	%	N	%	
USP	1	2.7	1	12.5	0	0	0	0	2
BSP	8	21.6	4	50	2	40	1	100	15
UAU1	3	8.1	0	0	0	0	0	0	3
UAU2	0	0	0	0	0	0	0	0	0
UAUT	2	5.4	0	0	0	0	0	0	2
UABI	0	0	0	0	0	0	0	0	0
BAP	0	0	0	0	0	0	0	0	0
BALP	0	0	0	0	0	0	0	0	0
BALT	0	0	0	0	0	0	0	0	0
UP	1	2.7	0	0	0	0	0	0	1
BP	0	0	0	0	0	0	0	0	0
UC	1	2.7	0	0	1	20	0	0	2
BHC	1	2.7	0	0	0	0	0	0	1
Discoidal	6	16.2	1	12.5	1	20	0	0	8
Polyhedral	0	0	0	0	0	0	0	0	0
Multifacial	5	13.5	0	0	1	20	0	0	6
Casual	9	24.3	2	25	0	0	0	0	11
Bipolar	0	0	0	0	0	0	0	0	0
Total	37	100	8	100	5	100	1	100	51

For the debris flow Table 4.4.36 also shows that quartzite cores retain the greatest range of flaking patterns, although the siltstone and hornfels core samples in this assemblage are larger. In addition to this the core reduction patterns for these latter two materials are largely the same (excluding UAU1, which is absent in siltstone).

As with the colluvial sample the most frequent core flaking strategies, across the raw materials, include BSP, discoidal and casual patterns. Interestingly, USP and BSP types have the highest percentages in the hornfels sample (21.4% for both). Casuals are most common on siltstone (38.5% of the total sample), as are discoids on quartzite (26.1% of the total sample). Other types that occur exclusively on quartzite include UAUT (3.5%) and UC (8.7%) flaking patterns.

Table 4.4.36. Core flaking pattern, by raw material, for the debris flow assemblage.

Flaking strategy	Raw materials								Total
	Quartzite		Siltstone		Hornfels		Claystone		
	N	%	N	%	N	%	N	%	
USP	3	2.6	1	7.7	3	21.4	0	0	7
BSP	19	16.5	2	15.4	3	21.4	1	100	25
UAU1	3	2.6	0	0	1	7.1	0	0	4
UAU2	0	0	0	0	0	0	0	0	0
UAUT	4	3.5	0	0	0	0	0	0	4
UABI	0	0	0	0	0	0	0	0	0
BAP	0	0	0	0	0	0	0	0	0
BALP	0	0	0	0	0	0	0	0	0
BALT	0	0	0	0	0	0	0	0	0
UP	0	0	0	0	0	0	0	0	0
BP	0	0	0	0	0	0	0	0	0
UC	10	8.7	0	0	0	0	0	0	10
BHC	0	0	0	0	0	0	0	0	0
Discoidal	30	26.1	2	15.4	2	14.3	0	0	34
Polyhedral	3	2.6	0	0	0	0	0	0	3
Multifacial	8	7	3	23.1	1	7.1	0	0	12
Casual	33	28.7	5	38.5	4	28.6	0	0	42
Bipolar	2	1.7	0	0	0	0	0	0	2
Total	115	100	13	100	14	100	1	100	143

The blanks most commonly utilised in core reduction are presented in Figures 4.4.104 and 4.4.105. From this it is clear for both assemblages that cobbles and split cobbles (predominantly round to oval in shape) are the most frequent blank types, collectively accounting for 76.5% of the colluvial core sample and 60.1% for the debris flow. Both assemblages also show that smaller pebbles are seldom used in core reduction.

However, there are notable differences in the distribution of flakes and indeterminate blank types. For the colluvial assemblage flake blanks are less frequent at 9.8%, also equal to the percentage of indeterminates. The slightly lower abundance of cobbles and split cobbles in the debris flow sample gives rise to higher percentages of flake blanks (at 18.9%) and indeterminate blanks (at 15.4%). Another notable difference is the presence of a bipolar split cobble/pebble in the debris flow core sample (accounting for 3.5%).

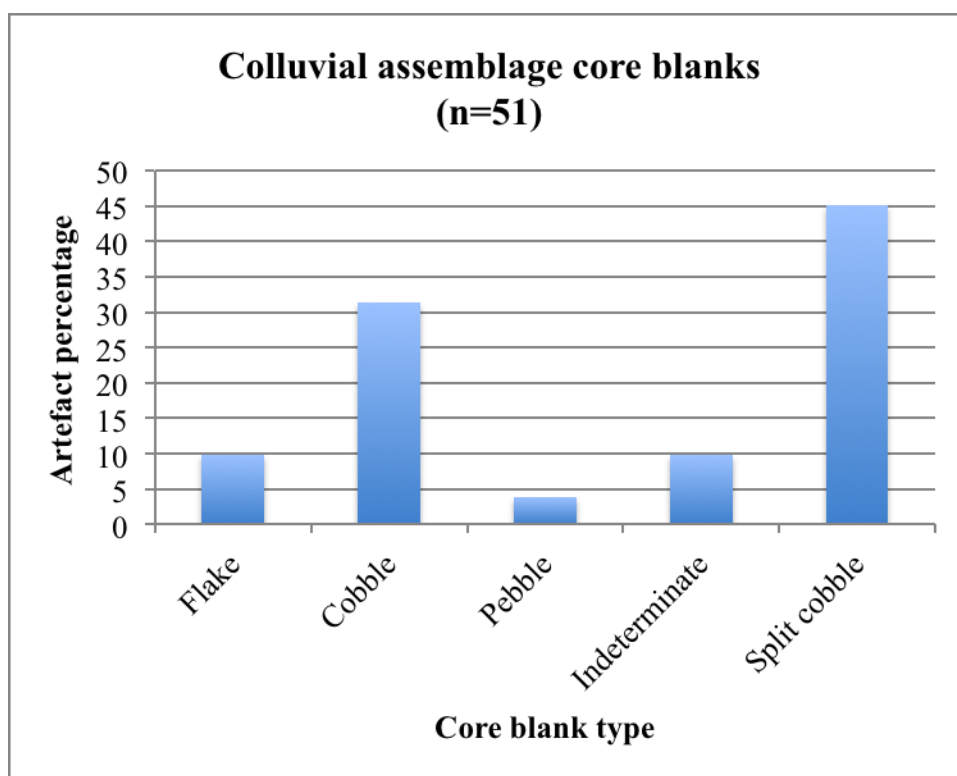


Figure 4.4.104. Blank type distribution for the colluvial assemblage cores.

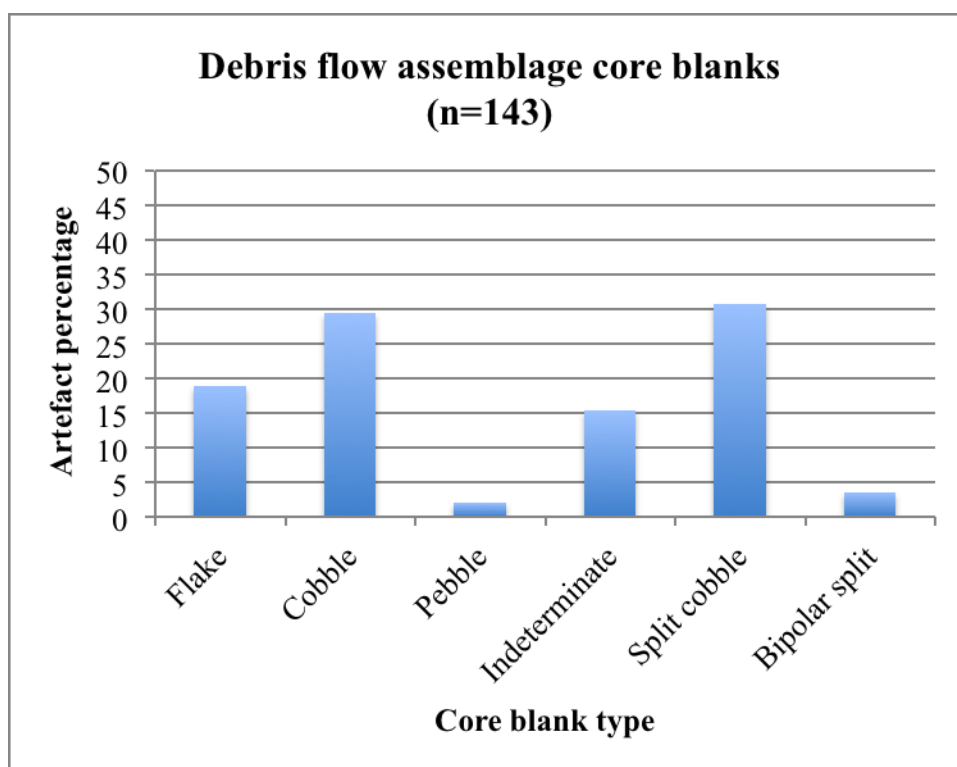


Figure 4.4.105. Blank type distribution for the debris flow assemblage cores.

Table 4.4.37 illustrates core blank type, by both raw material and core type, for the colluvial assemblage. The majority of all cores, for all raw materials, has the greatest

percentages in the cobble and split cobble blank categories. By sample size quartzite and siltstone chopper-cores are the most abundant on cobble blanks (n=3 each), as are quartzite casual (n=6) and irregular (n=5) cores on split cobbles. The only cores to occur on flake blanks include two quartzite chopper-cores and three quartzite discoids. Those cores produced on pebbles, although limited, include one quartzite casual core and one quartzite chopper-core.

For the debris flow cores (Table 4.4.38), the blank type distributions are largely similar to the colluvial assemblage, where the majority of all core types, and materials, have their highest percentages in the cobble and split cobble blank categories. By sample size, quartzite chopper-cores and casual cores are the most abundant types on these blanks. However, in contrast to the colluvial assemblage the debris flow cores on flake blanks show greater variability (5 types represented, ranging from 12.5-50% for the relevant samples). Those cores produced on pebbles show a more restricted distribution here, and only casual cores are represented (n=2 quartzite and n=1 hornfels). A notable inclusion within the debris flow are bipolar split cobble/pebble types, which account for quartzite chopper-cores (n=1), polyhedrons (n=1), bipolar (n=1), and casual cores (n=2).

Table 4.4.37. Colluvial core blank type, by raw material and core type (n=51).

Core type	Raw material	Blank type											
		Flake		Cobble		Pebble		Indet.		Split cobble		Total	
		N	%	N	%	N	%	N	%	N	%	N	%
Chopper-core n=17, 33.3%	Quartzite	2	22.2	3	33.3	1	11.1	0	0	3	33.3	9	100
	Siltstone	0	0	3	60	0	0	0	0	2	40	5	100
	Hornfels	0	0	1	50	0	0	0	0	1	50	2	100
	Claystone	0	0	1	100	0	0	0	0	0	0	1	100
Irregular n=6, 11.8%	Quartzite	0	0	0	0	0	0	0	0	5	100	5	100
	Siltstone	0	0	0	0	0	0	1	100	0	0	1	100
Discoidal n=11, 21.6%	Quartzite	3	37.5	1	12.5	0	0	2	25	2	25	8	100
	Siltstone	0	0	1	100	0	0	0	0	0	0	1	100
	Hornfels	0	0	0	0	0	0	2	100	0	0	2	100
Discoidal w/rem. n=1, 1.9%	Quartzite	0	0	1	100	0	0	0	0	0	0	1	100
Single platform n=5, 9.8%	Quartzite	0	0	2	40	0	0	0	0	3	60	5	100
Casual n=11, 21.6%	Quartzite	0	0	2	22.2	1	11.1	0	0	6	66.7	9	100
	Siltstone	0	0	1	50	0	0	0	0	1	50	2	100

Table 4.4.38. Debris flow core blank type, by raw material and core type (n=143).

Core type	Raw material	Blank type													
		Flake		Cobble		Pebble		Indet.		Split cobble		Bipolar split		Total	
		N	%	N	%	N	%	N	%	N	%	N	%	N	%
Chopper-core n=32, 22.4%	Quartzite	3	13.6	8	36.4	0	0	0	0	10	45.5	1	4.5	22	100
	Siltstone	0	0	2	66.7	0	0	0	0	1	33.3	0	0	3	100
	Hornfels	0	0	6	100	0	0	0	0	0	0	0	0	6	100
	Claystone	0	0	1	100	0	0	0	0	0	0	0	0	1	100
Irregular n=12, 8.4%	Quartzite	1	12.5	2	25	0	0	3	37.5	2	25	0	0	8	100
	Siltstone	0	0	1	33.3	0	0	0	0	2	66.7	0	0	3	100
	Hornfels	0	0	0	0	0	0	1	100	0	0	0	0	1	100
Discoidal n=45, 31.5%	Quartzite	17	41.5	1	2.4	0	0	14	34.1	9	22	0	0	41	100
	Siltstone	0	0	1	50	0	0	0	0	1	50	0	0	2	100
	Hornfels	1	50	1	50	0	0	0	0	0	0	0	0	2	100
Polyhedral n=3, 2.1%	Quartzite	0	0	1	33.3	0	0	0	0	1	33.3	1	33.3	3	100
Single platform n=7, 4.9%	Quartzite	0	0	3	50	0	0	1	16.7	2	33.3	0	0	6	100
	Siltstone	0	0	1	100	0	0	0	0	0	0	0	0	1	100
Bipolar n=1, 0.7%	Quartzite	0	0	0	0	0	0	0	0	0	0	1	100	1	100
Casual n=43, 30.1%	Quartzite	5	14.7	9	26.5	2	5.9	2	5.9	14	41.2	2	5.9	34	100
	Siltstone	0	0	4	80	0	0	0	0	1	20	0	0	5	100
	Hornfels	0	0	1	25	1	25	1	25	1	25	0	0	4	100

Figures 4.4.106 and 4.4.107 provide a comparison between the largest flake scar lengths recorded on cores and the complete flake maximum lengths (excluding formal tools made on these blanks). Although these data may also relate to the level of core reduction, it is purposefully presented here in an attempt to investigate core reduction strategies and large flake blank production, on- and off-site.

Figure 4.4.106 shows that most of the longest scars on colluvial cores are smaller than 80 mm, but some are greater than 100 mm. The size of the largest flakes exceed 120 mm.

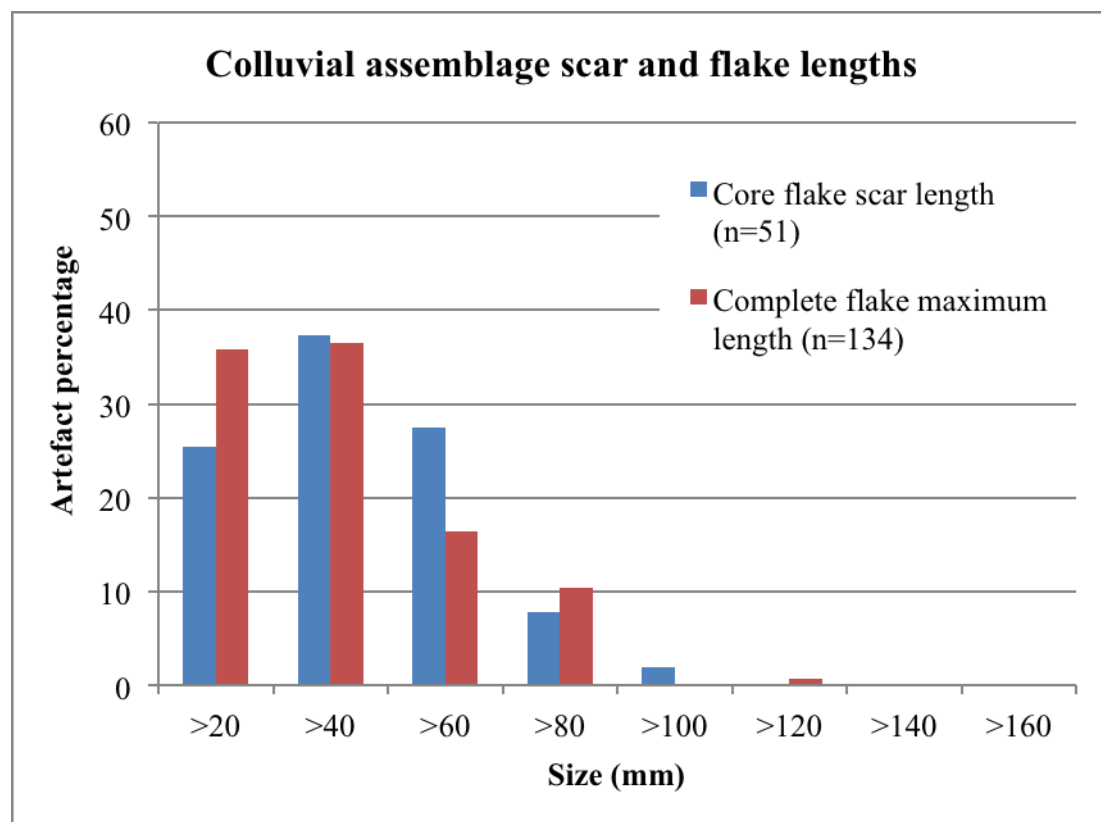


Figure 4.4.106. Scar length comparison for the colluvial assemblage (largest flake scar lengths recorded on cores and complete flake maximum lengths).

A similar pattern is observed for the debris flow sample (Fig. 4.4.107). Core scar maximum lengths show several exceeding 100 mm, with the largest scars exceeding 120 mm. As with the colluvial sample the debris flow complete flake lengths show even greater sizes, here exceeding 100 mm and continuing up to >160 mm.

Both assemblages appear to show an absence of cores with large flake removals that are comparable to the largest complete flake lengths.

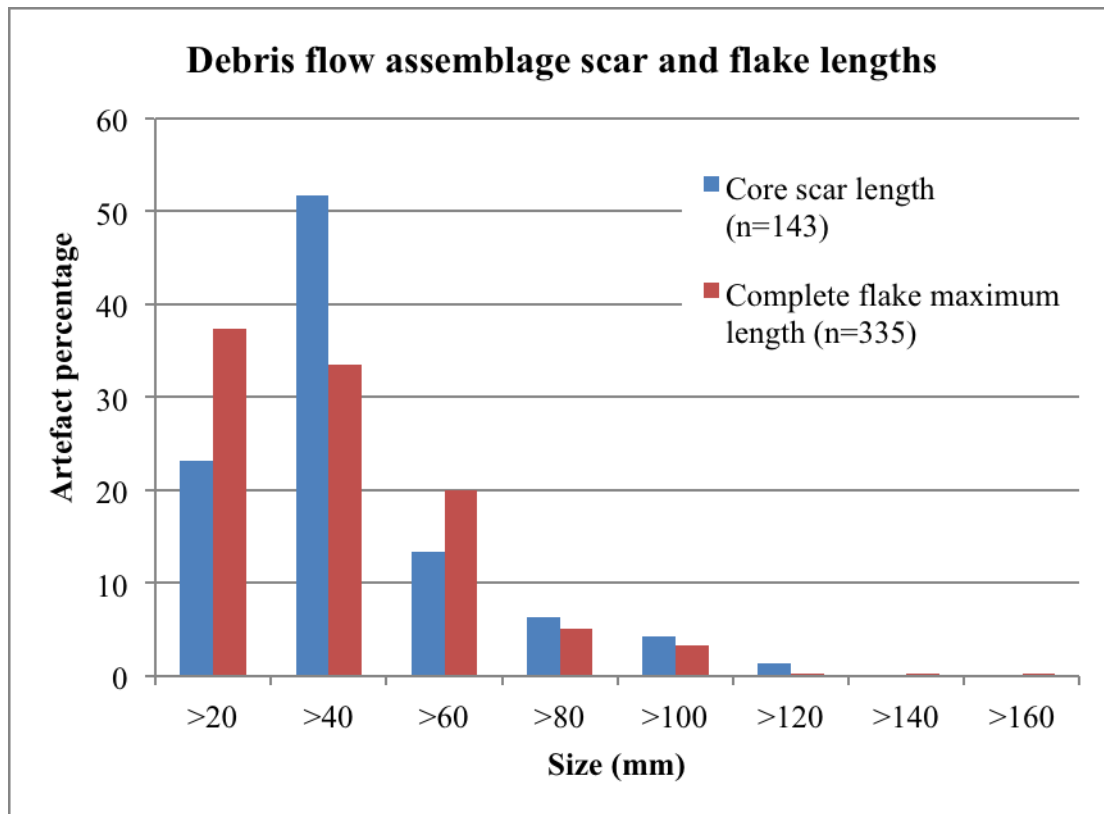


Figure 4.4.107. Scar length comparison for the debris flow assemblage (the largest flake scar lengths recorded on cores and complete flake maximum lengths).

The negative flake scar terminations on the Penhill Farm cores were quantified, which may be informative of raw material differences or problems during core reduction.

The colluvial core assemblage shows that feather terminations are equally as common on quartzite, siltstone and hornfels (ranging from 39-41%; Fig. 4.4.108). Although quartzite has the highest percentage of step terminations (at 25.2%, excluding the claystone sample), the percentage of hinge terminations is the lowest for all the raw materials (at 31.7%). Quartzite is also the only material to have overshoot terminations (2.2%). Negative flake terminations are largely comparable for the hornfels and siltstone samples, with step terminations ranging from 8.7-15% and hinge terminations ranging from 45-52.2%. Claystone terminations are only comprised of step (40%) and hinge (60%) types.

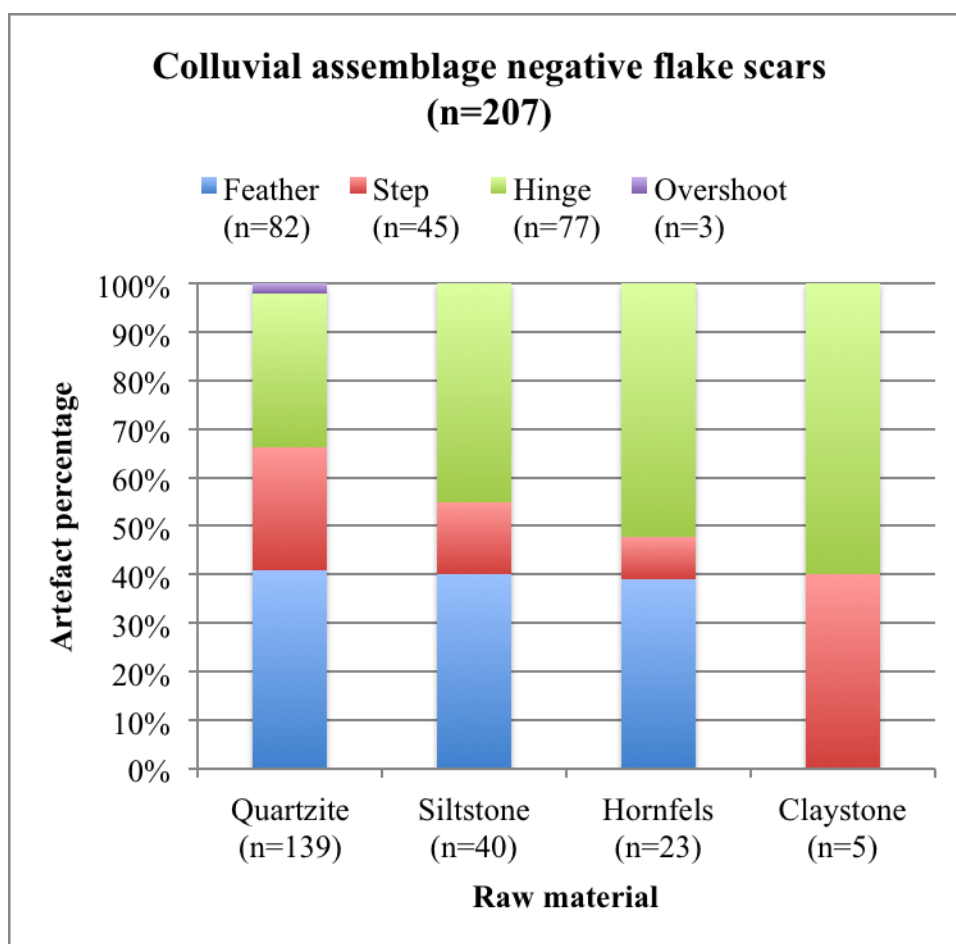


Figure 4.4.108. Flake scar negatives for the colluvial assemblage cores.

The debris flow siltstone cores illustrate that negative feather terminations are largely lower in number (28.1%) when compared to the colluvial sample (Fig. 4.4.109). However, the remaining raw materials have largely comparable termination type distributions, especially for quartzite, once again the only material to have overshoot terminations. Hornfels has a higher percentage of feather terminations (46.3%), followed by less step and hinge types as a result. As with the colluvial sample, siltstone and hornfels cores also account for the highest percentages of hinge terminations, excluding the claystone sample. Claystone in the debris flow is comprised of only hinge terminations.

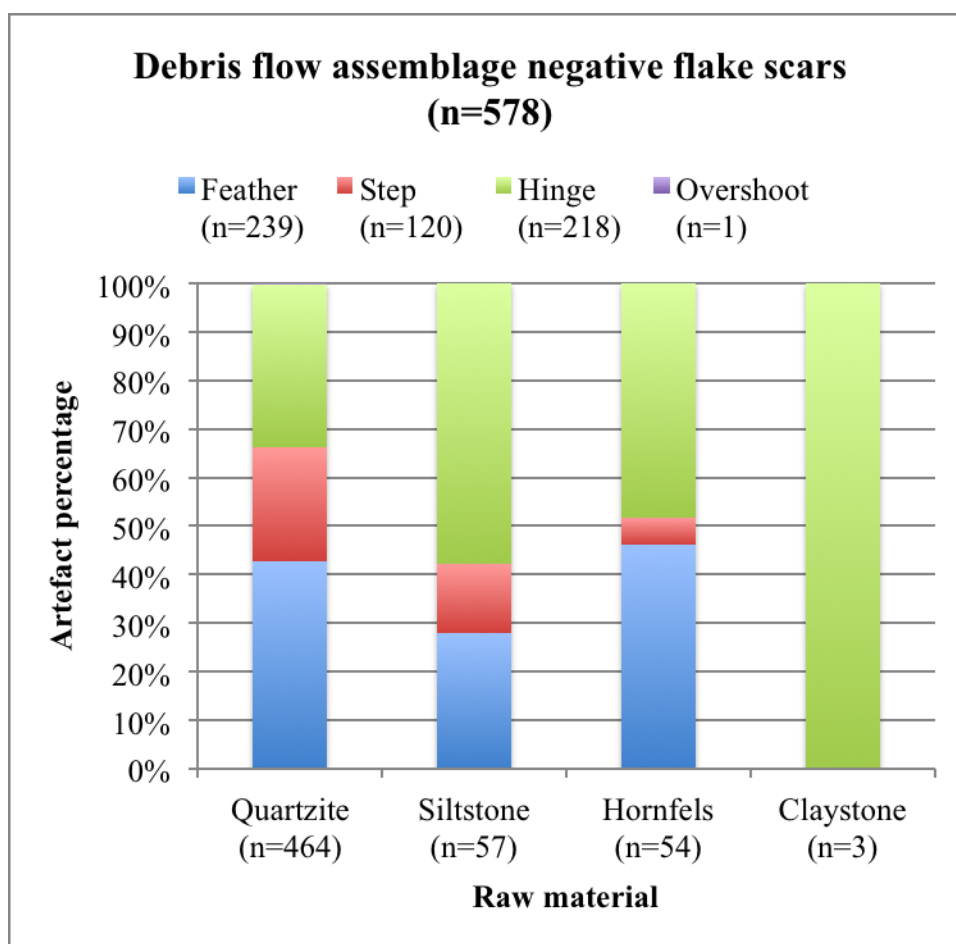


Figure 4.4.109. Flake scar negatives for the debris flow cores.

Level of reduction:

All cores from the colluvial assemblage (n=51) have a combined mean flake scar count of 4.1 and a standard deviation of 2.5, with the majority having between one and four removals (Fig. 4.4.110). Collectively, 68.6% of the colluvial cores have four or fewer removals. Those cores with five or more removals do not exceed 10% (individually). No cores occur that have more than 10 removals.

The debris flow cores (n=143) have an average of 4 scars and a standard deviation of 2.9 scars. Figure 4.4.111 shows a different pattern in core flake scar numbers. Here the percentage of cores with one removal is the most common type (28%) and those with two are very few (4.2%). If one combines the percentages for cores with between one and four scars, collectively this accounts for 58.7% of the total sample (marginally lower than when compared to the colluvial sample). As a result a higher percentage of cores within the debris flow have five or more removals, ranging from 13.3% (5 scars) to 0.7% (>10 scars).

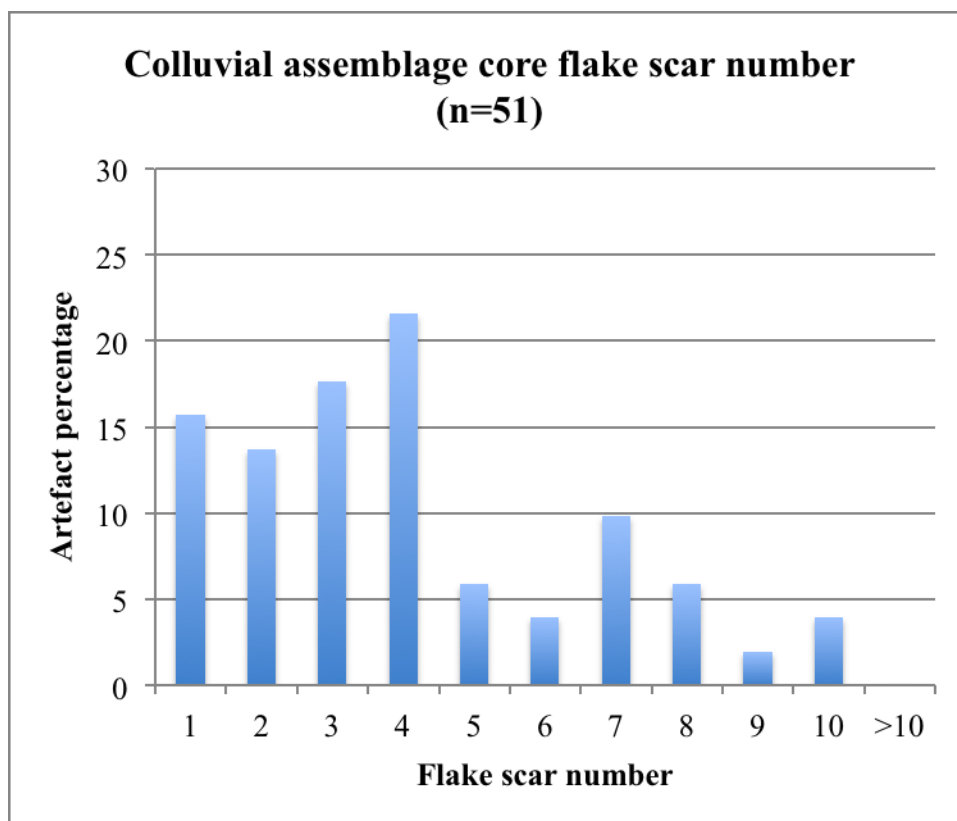


Figure 4.4.110. Number of flake scars on the colluvial cores.

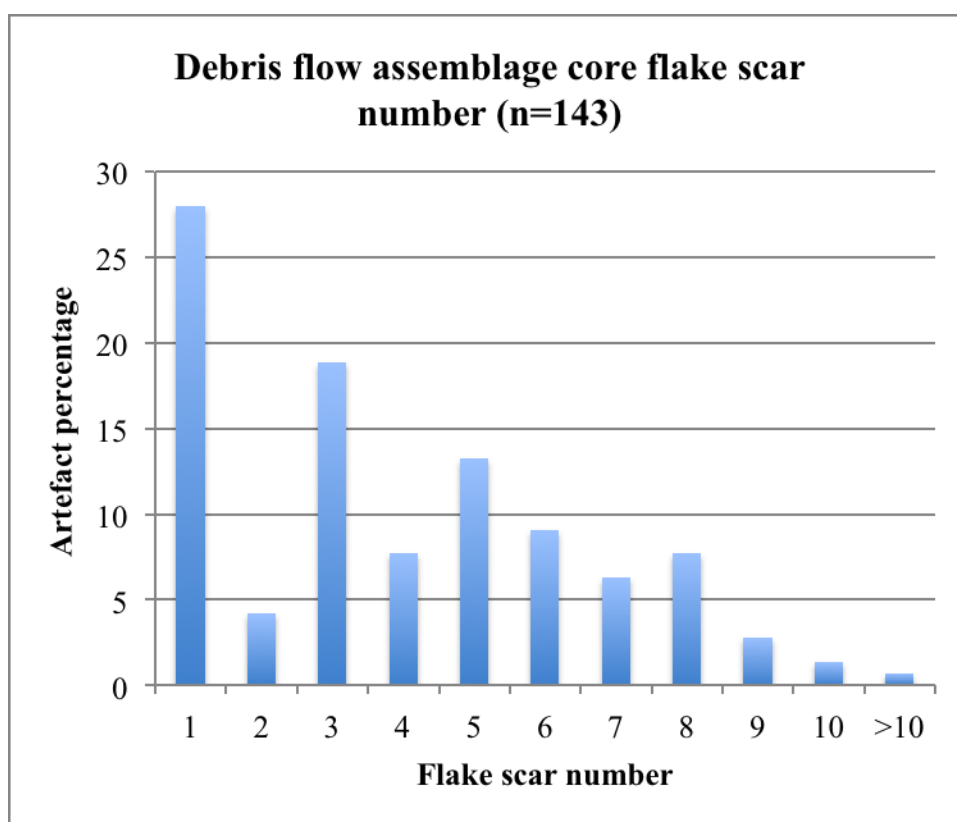


Figure 4.4.111. Number of flake scars on the debris flow cores.

For raw material and core type, Table 4.4.39 shows that colluvial core mean scar numbers are lowest for the casual cores (to be expected, at 1.3, also with the lowest SD at 0.5). Single platform and irregular cores follow thereafter, with slightly higher mean scar numbers. Discoidal cores have the highest mean flake scar number (6.5 scars), ranging from six for quartzite to 10 for siltstone; the discoid with a single large removal has eight scars. Chopper-cores have a minimum mean flake scar number of 3.5 (for hornfels) and a maximum of 4.4 (for quartzite).

The debris flow assemblage has a large sample of casual cores (n=43) and the majority has only a single removal (Table 4.4.39). This most likely accounts for the peak evident in Figure 4.4.111 (1 scar). Single platform, irregular, polyhedral cores and the single bipolar core account for notably low mean flake scar numbers, especially for quartzite irregular cores (4 scars) and hornfels single platform cores (3 scars). Here, discoids also account for the highest mean flake scar numbers (6 scars), and again siltstone types have the highest mean (at 9.5 scars). Chopper-cores have a mean scar number ranging from 3 (claystone) to 5.6 (quartzite).

The final data to be presented in this section concerns the amount of remaining cortex on the core samples. This data is presented in Figures 4.4.112 and 4.4.113 and Tables 4.4.40 and 4.4.41.

Figure 4.4.112 shows that the majority of colluvial cores has a cortex range of 25-49%, followed by a high percentage (25.5%) of cores that have 75-100% cortex; the latter are most likely the casual cores with only one or two removals. Only a very small percentage of cores is completely non-cortical (2%).

This pattern is largely the same for the debris flow assemblage, which also has over 30% of cores with 25-49% cortex (Fig. 4.4.113). Here, however, those types with 50-74% cortex are the second most abundant type (at 23.8%). Only 3.5% of all debris flow cores are non-cortical.

Table 4.4.39. Core flake scar number, by raw material and core type. Where n=1 scar counts are not mean values.

Colluvial assemblage (n=51)				Debris flow assemblage (n=143)				
Core type and scars	Raw material	Flake scars		Core type and scars	Raw material	Flake scars		
		Mean	SD			Mean	SD	
Chopper-core (n=17) Mean: 4.6 SD: 1.8	Quartzite	4.4	2.1	Chopper-core (n=32) Mean: 5.3 SD: 3.5	Quartzite	5.6	4	
	Siltstone	5.6	1.5		Siltstone	6	3.6	
	Hornfels	3.5	0.7		Hornfels	4.2	1.5	
	Claystone	4	-		Claystone	3	-	
Irregular (n=6) Mean: 3.5 SD: 0.8	Quartzite	3.6	0.9	Irregular (n=12) Mean: 4.6 SD: 2	Quartzite	4	1.8	
	Siltstone	-	-		Siltstone	5	2	
	Hornfels	3	-		Hornfels	8	-	
	Claystone	-	-		Claystone	-	-	
Discoidal (n=11) Mean: 6.5 SD: 2.6	Quartzite	6	2.4	Discoidal (n=45) Mean: 6 SD: 2	Quartzite	5.8	1.9	
	Siltstone	10	-		Siltstone	9.5	0.7	
	Hornfels	6.5	3.5		Hornfels	7	1.4	
	Claystone	-	-		Claystone	-	-	
Discoidal w/removal (n=1) Mean: 8	Quartzite	8	-	Polyhedral (n=3) Mean: 5 SD: 2.6	Quartzite	5	2.6	
	Siltstone	-	-		Siltstone	-	-	
	Hornfels	-	-		Hornfels	-	-	
	Claystone	-	-		Claystone	-	-	
Single platform (n=5) Mean: 3 SD: 1.2	Quartzite	3	1.2	Single platform (n=7) Mean: 3.3 SD: 0.8	Quartzite	3.3	0.8	
	Siltstone	-	-		Siltstone	-	-	
	Hornfels	-	-		Hornfels	3	-	
	Claystone	-	-		Claystone	-	-	
Casual (n=11) Mean: 1.3 SD: 0.5	Quartzite	1.3	0.5	Bipolar (n=1) Mean: 1	Quartzite	1	-	
	Siltstone	1	0		Siltstone	-	-	
	Hornfels	-	-		Hornfels	-	-	
	Claystone	-	-		Claystone	-	-	
				Casual (n=43) Mean: 1.1 SD: 0.3	Quartzite	1.1	0.3	
					Siltstone	1	0	
					Hornfels	1	0	
					Claystone	-	-	

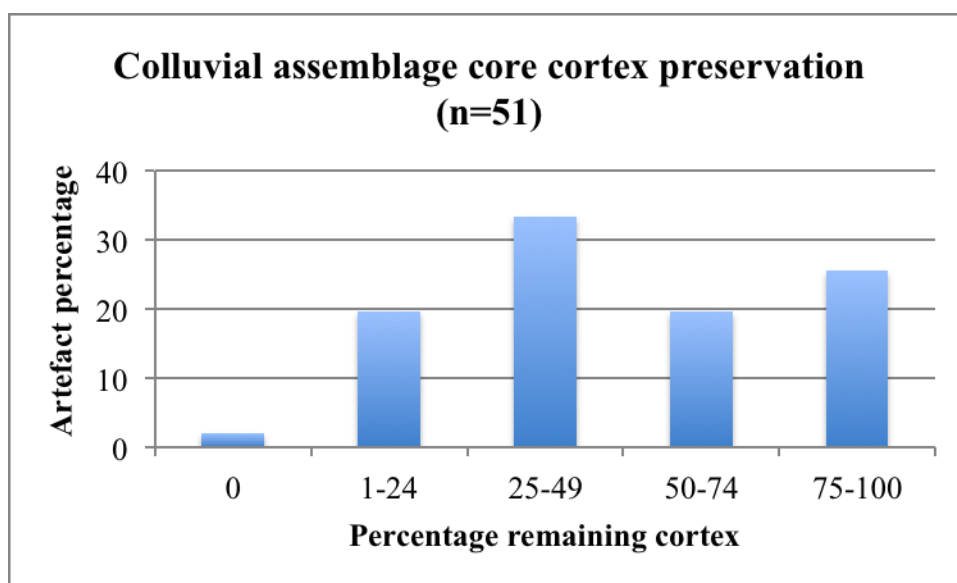


Figure 4.4.112. Remaining cortex on the colluvial cores.

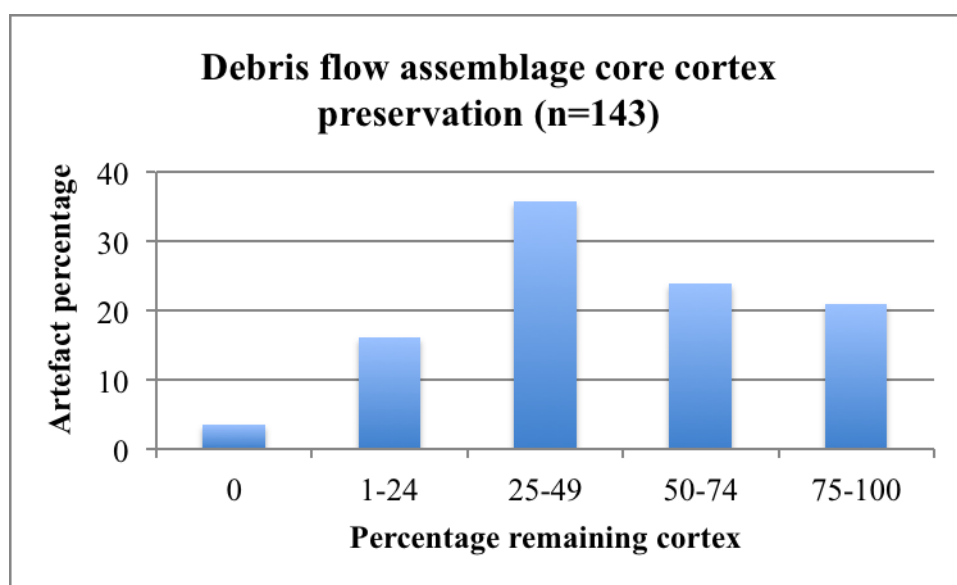


Figure 4.4.113. Remaining cortex on the debris flow cores.

A correlation of cortex preservation with raw material for the colluvial assemblage shows that quartzite and siltstone cores generally preserve the most cortex (Table 4.4.40). Interestingly, the only core to be completely non-cortical is also made on quartzite (n=1, 2.7%).

Table 4.4.41 shows that the most cortical (75-100%) cores in the debris flow are made on siltstone and hornfels. Once again quartzite cores are the only type to show 0% cortex (4.3% of the total quartzite sample). Hornfels cores show a high percentage of cortex preservation (92.9% are 25-100% cortical).

Table 4.4.40. Remaining cortex, by raw material, for the colluvial cores (n=51).

Raw materials	Percentage remaining cortex											
	0		1-24		25-49		50-74		75-100		Total	
	N	%	N	%	N	%	N	%	N	%	N	%
Quartzite	1	2.7	7	18.9	13	35.1	6	16.2	10	27	37	100
Siltstone	0	0	1	12.5	0	0	4	50	3	37.5	8	100
Hornfels	0	0	2	40	3	60	0	0	0	0	5	100
Claystone	0	0	0	0	1	100	0	0	0	0	1	100

Table 4.4.41. Remaining cortex, by raw material, for the debris flow cores (n=143).

Raw materials	Percentage remaining cortex											
	0		1-24		25-49		50-74		75-100		Total	
	N	%	N	%	N	%	N	%	N	%	N	%
Quartzite	5	4.3	20	17.4	44	38.3	28	24.3	18	15.7	115	100
Siltstone	0	0	2	15.4	3	23.1	2	15.4	6	46.2	13	100
Hornfels	0	0	1	7.1	4	28.6	4	28.6	5	35.7	14	100
Claystone	0	0	0	0	0	0	0	0	1	100	1	100

Summary:

Excavations at Penhill Farm have provided adequate core samples for both the colluvial assemblage (n=51) and for the lower lying debris flow (n=143); however, cores on materials other than quartzite are generally infrequent and trends discussed here must be treated with caution.

Overall core dimensions in the colluvial assemblage show that siltstone cores are the largest, whereas hornfels cores are the smallest. The more abundant quartzite cores are intermediate in size between these materials, although with a larger sample for the less frequent materials this pattern may change. However, this trend is also evident in the debris flow cores where these rare raw material samples are larger. When comparing core size between the assemblages, in the debris flow quartzite and hornfels cores are smaller and siltstone and claystone cores are larger.

By type chopper-cores and casual cores account for the majority of the largest mean values, in both assemblages, yet in the debris flow irregular cores are also large in size. Both assemblages are characterised by a high percentage of small, light discoidal cores. Interestingly, the largest core flake scar lengths occur on chopper-cores in the colluvial sample, versus on polyhedral cores in the debris flow. Overall, chopper-

cores are slightly smaller and lighter in the debris flow, whereas casual cores are larger and heavier.

The flaking strategies employed to reduce cores at Penhill Farm are largely comparable for the assemblages, the most frequent of which are simple USP, BSP and casual types. In the colluvial assemblage BSP types are the most frequent and these, combined with USP and casual types, account for 54.9% of the total core sample; discoidal reduction strategies account for 15.7% and no bipolar cores occur. In the debris flow this pattern is largely the same and the three simple core reduction strategies discussed above account for 51.7% of the cores. However, here casual core reduction strategies are the most frequent, and a single bipolar core occurs. Reduction strategies by raw material show that quartzite cores have the greatest range of reduction patterns, most likely due to the larger sample size. Discoidal and BSP flaking strategies account for the highest percentages on all raw material types, in both assemblages, yet in the colluvial assemblage casual cores are only found on quartzite and siltstone. In the debris flow these three core types (BSP, discoidal and casual) account for all of the highest percentages on all of the raw materials.

The reduction of cores takes place primarily on cobble and split cobble blanks, for both assemblages. These blanks occur locally and are round to oval in shape. Although other blanks are utilised they are infrequent. However, the debris flow cores show a greater use of flakes as blanks.

A comparison of core maximum scar lengths and the length of complete flakes shows that in both assemblages there is an absence of cores with removals that are comparable to the largest flake lengths. Had formal tool flakes been incorporated into this sample (e.g., LCTs on large flakes), this would be even more apparent.

Flake scar negative termination types reveal that feather terminations are the most frequent type in both assemblages, although these are relatively less frequent in the debris flow cores. Interestingly, both assemblages show that siltstone and hornfels cores have the highest percentage of hinge terminations. Overall though these data are largely uninformative.

Core scar counts show that only 4.1 removals, on average, are present on the colluvial cores, and four scars in the debris flow. In both assemblages, the largest proportion of cores have one to four removals (68.6% for the colluvial cores and 58.7% for the debris flow). Core scar counts exceeding 10 only occur in the debris flow (0.7% of the sample). By type casual cores understandably have the lowest scar counts, whereas discoids have the highest, followed thereafter by chopper-cores; single platform and irregular cores also have low scar counts. For chopper-cores and discoids, siltstone types have higher mean flake scar counts than those on quartzite, in both assemblages.

The percentages of remaining cortex on cores is largely comparable between the two assemblages, where cores retaining 25-49% cortex are the most frequent. Very few cores retain 0% cortex, but where they do these are made on quartzite, even though quartzite cores account for some of the most cortical pieces. In the colluvial assemblage, quartzite and siltstone cores are the most cortical, whereas in the debris flow hornfels and siltstone cores are the most cortical.

4.4.4.3 Formal tools

Retouched pieces:

All data obtained on the Penhill Farm retouched pieces are presented here. The following maximum sample sizes apply:

- Colluvial assemblage (n=78). This excludes two choppers and three flaked-flakes, which were included in the preceding data sections – complete flakes and cores – where possible.
- Debris flow (n=365). This excludes one chopper and 12 flaked-flakes, which were included in the preceding data sections – complete flakes and cores – where possible.

Differing sample sizes from those presented above are either due to indeterminate readings obtained during analysis, or, more than one reading/measurement obtained per artefact (especially relevant for retouch analysis, where composite pieces and composite scrapers retain more than one kind of retouch).

Data will be presented following the same methods used for flaking debris and complete flakes, and cores (dimensions, flaking strategy, and level of reduction).

Retouched piece dimensions/size:

A summary of the mean measurements obtained on all the Penhill Farm retouched pieces is presented in Tables 4.4.42 and 4.4.43. By raw material, siltstone artefacts are the largest and heaviest in the colluvial assemblage (Table 4.4.42). Thereafter, hornfels and quartzite pieces follow as mean size measurements decrease. The sample sizes for both siltstone and hornfels are limited so this trend in artefact size and weight must be viewed with caution.

However, the debris flow assemblage (Table 4.4.43) has larger samples of siltstone and hornfels, and a similar pattern is evident. Siltstone artefacts here also account for the largest and heaviest artefacts, and by mean weight, hornfels pieces follow thereafter. The remaining small samples of lava, silt-quartzite and claystone provide notably small mean measurements, especially for weight.

Table 4.4.42. Formal tool measurements for the colluvial assemblage (n=78).

Measurement data (mm)		Raw materials		
		Quartzite (n=72)	Siltstone (n=2)	Hornfels (n=4)
Max. length	Mean	57.9	83.7	68.3
	SD	20.7	7.5	11
Length	Mean	51.7	70	63
	SD	22.7	-	7
Width	Mean	42.8	58	53.3
	SD	18.5	-	18
Thickness	Mean	19.8	26	21.8
	SD	11.1	-	0.8
Weight (g)	Mean	67.5	118.1	94.3
	SD	109.1	10.2	32.8

Table 4.4.43. Formal tool measurements for the debris flow assemblage (n=365; qzte=quartzite).

Measurement data (mm)		Raw materials					
		Quartzite (n=307)	Siltstone (n=33)	Hornfels (n=13)	Lava (n=1)	Silt-qzte (n=3)	Claystone (n=8)
Max. length	Mean	51.4	63	50.9	53.4	37.4	44.1
	SD	19.1	26.5	19.8	-	6.3	19.7
Length	Mean	44.4	53.3	49.5	52	32.7	33.3
	SD	16.8	22.9	22.5	-	5.9	12.6
Width	Mean	37.1	46	31.5	43	30.7	27.5
	SD	14.7	20.6	12.6	-	10.6	14.5
Thickness	Mean	15.5	17.5	22	15	10.3	10.4
	SD	6.8	8.6	12.4	-	2.1	5.5
Weight (g)	Mean	40.2	73.2	50.4	34.4	11.7	23.9
	SD	55.9	84.3	55.5	-	5.2	21.9

Flaking strategy:

The blank types most favoured for retouching are presented in Figures 4.4.114 and 4.4.115, and by raw material in Tables 4.4.44 and 4.4.45. Both assemblages show a strong preference (exceeding 75%) for flake blanks. The remaining blank types make up only small percentages of the colluvial assemblage, notably 9% on split cobbles, 7.7% on fragments, and 3.9% on chunks; these types account for 2.2%, 8.5%, and 10.4%, respectively, in the debris flow sample (Figs. 4.4.114 & 4.4.115). Blank type variability is greater in the debris flow with the addition of two types (a retouched cobble and discoidal core), most likely due to the larger sample size.

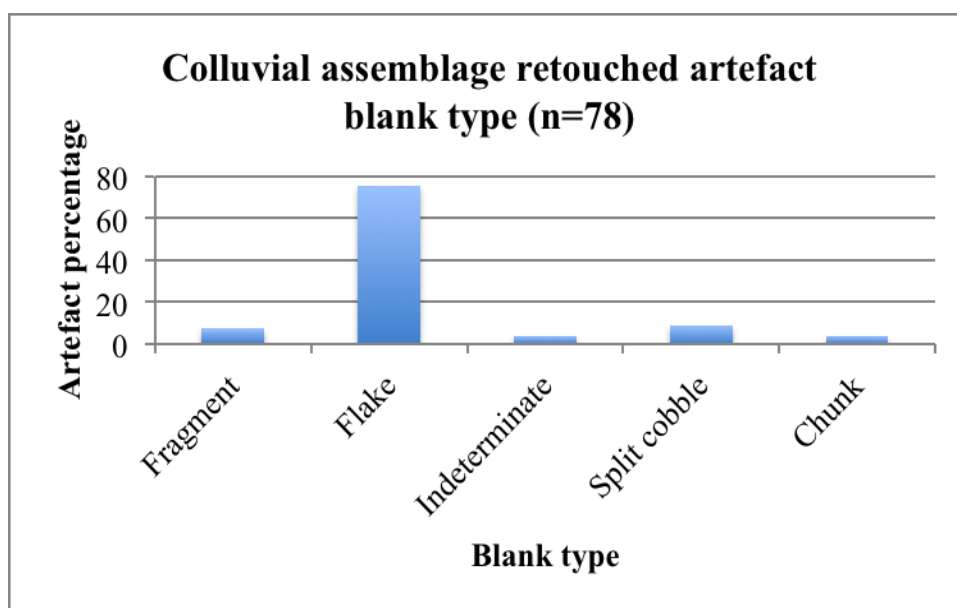


Figure 4.4.114. Blank type distribution for the colluvial assemblage.

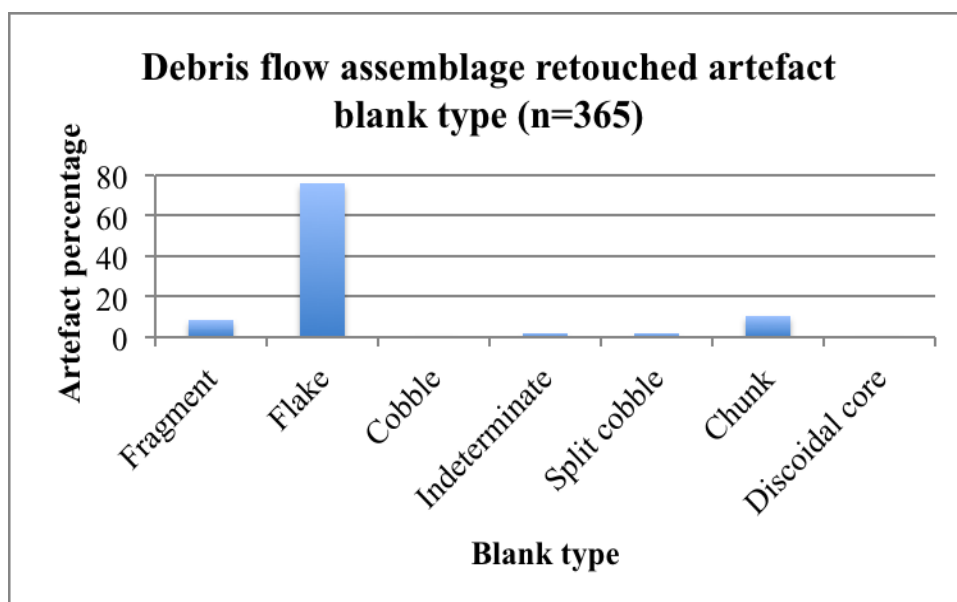


Figure 4.4.115. Blank type distribution for the debris flow assemblage.

By raw material the colluvial assemblage shows that flakes and split cobbles are the most common blanks for the less frequent raw materials (siltstone and hornfels; Table 4.4.44). Quartzite artefacts account for the widest range of the remaining blank types, most likely due to the large sample size, and flakes are clearly favoured (n=56, 77.8%).

The debris flow sample (Table 4.4.45) shows that quartzite chunks are marginally more frequent (11.1%) when compared to the colluvial assemblage, and although

flakes are also the most frequent for most of the raw materials, hornfels shows notably high percentages for split cobble (23.1%) and chunk (30.8%) use. However, the small sample size of this material must be considered. The retouched cobble and discoidal core are made on quartzite.

Table 4.4.44. Blank type by raw material for the colluvial sample (n=78).

Blank type	Raw materials					
	Quartzite		Siltstone		Hornfels	
	N	%	N	%	N	%
Fragment	6	8.3	0	0	0	0
Flake	56	77.8	1	50	2	50
Indeterminate	3	4.2	0	0	0	0
Split cobble	4	5.6	1	50	2	50
Chunk	3	4.2	0	0	0	0
Total	72	100	2	100	4	100

Table 4.4.45. Debris flow sample blank type, by raw material (n=365).

Blank type	Raw materials											
	Quartzite		Siltstone		Hornfels		Lava		Silt-qzite		Claystone	
	N	%	N	%	N	%	N	%	N	%	N	%
Fragment	28	9.1	3	9.1	0	0	0	0	0	0	0	0
Flake	234	76.2	28	84.8	6	46.2	0	0	3	100	7	87.5
Cobble	1	0.3	0	0	0	0	0	0	0	0	0	0
Indet.	5	1.6	1	3	0	0	1	100	0	0	1	12.5
Split cobble	4	1.3	1	3	3	23.1	0	0	0	0	0	0
Chunk	34	11.1	0	0	4	30.8	0	0	0	0	0	0
Discoid	1	0.3	0	0	0	0	0	0	0	0	0	0
Total	307	100	33	100	13	100	1	100	3	100	8	100

The location of retouch on the Penhill Farm artefacts is shown in Figures 4.4.116 and 4.4.117. Both assemblages show that the majority of retouch is found on dorsal surfaces and originates from the ventral surface of flakes (direct retouch), accounting for 68.7% of the colluvial sample and 49.2% in the debris flow; retouch that originates from the ventral surface along one edge and from the dorsal surface on another (alternate retouch) is the second most abundant type for both assemblages (>16% for both). The slightly lower percentage of direct retouch in the debris flow means that the remaining types here (inverse, alternate and alternating) are marginally more frequent, collectively accounting for the remaining 50.8% of the total sample

(versus 29.8% in the colluvial assemblage). Bifacial retouch only occurs in the colluvial sample and crossed retouch is absent in both assemblages.

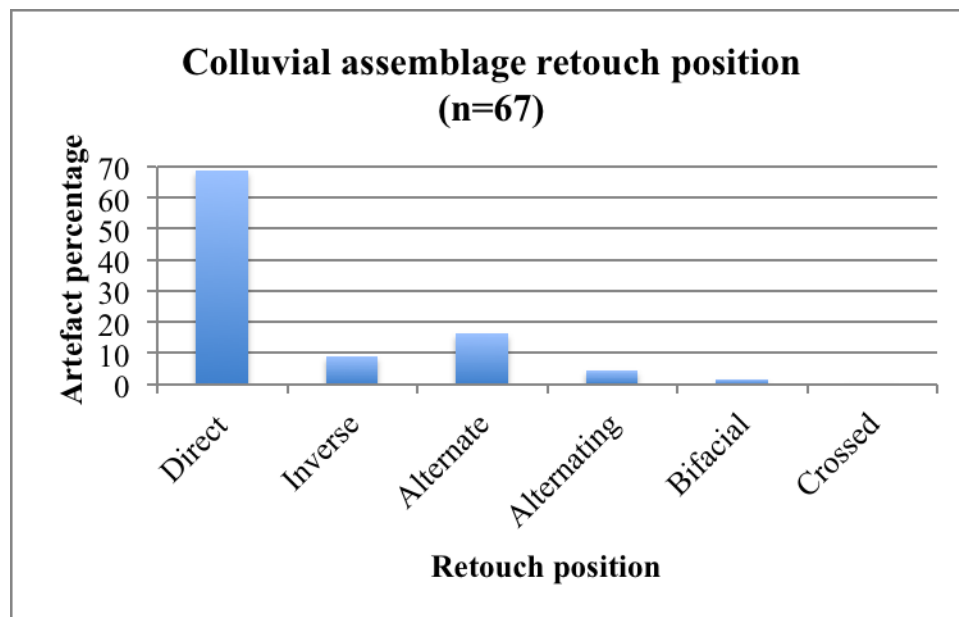


Figure 4.4.116. Retouch position for the colluvial assemblage formal tools.

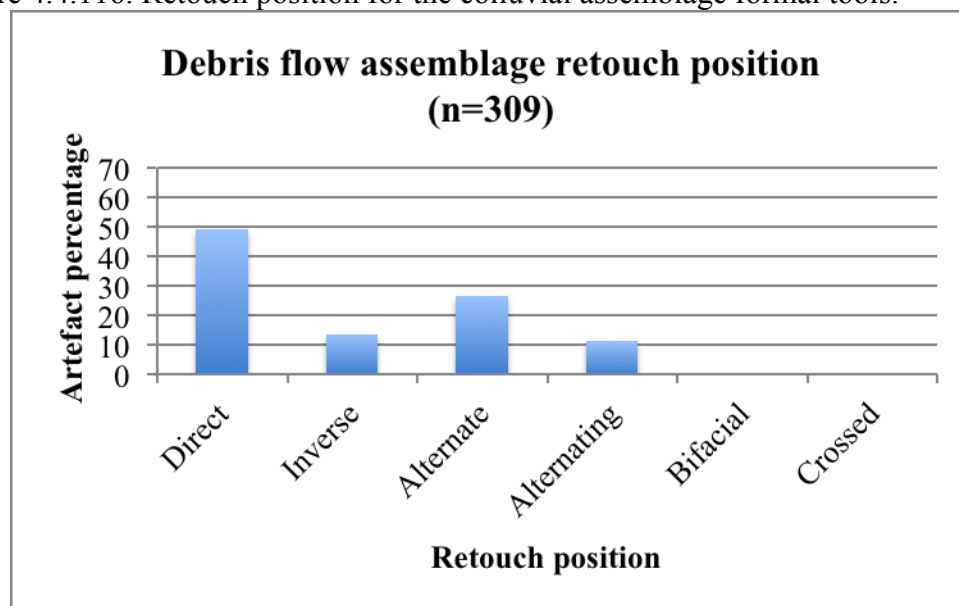


Figure 4.4.117. Debris flow formal tool retouch position.

For those artefacts that could be correctly orientated, the place where retouch is most abundant is shown in Figures 4.4.118 and 4.4.119. Both assemblages show a similar distribution, each having a complete absence of pieces with basal retouch. In addition to this the percentage of proximal retouch on formal tools is largely comparable for the two assemblages (19.9% for the colluvial sample and 21.4% for the debris flow).

Only minor variation occurs between the assemblages when looking at the percentage of mesial and distal retouch. Where the colluvial assemblage has a marginally higher percentage of artefacts with distal retouch (41.4%; Fig. 4.4.118), the debris flow sample has the same amount with mesial retouch (Fig. 4.4.119). However, for both assemblages it is these two types that account for the greatest percentage of artefacts.

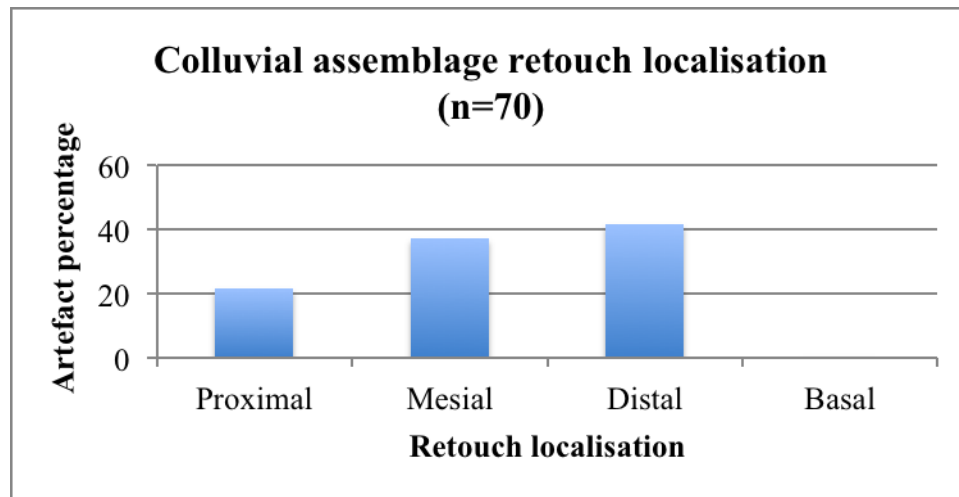


Figure 4.4.118. Colluvial assemblage retouch classification, by localisation.

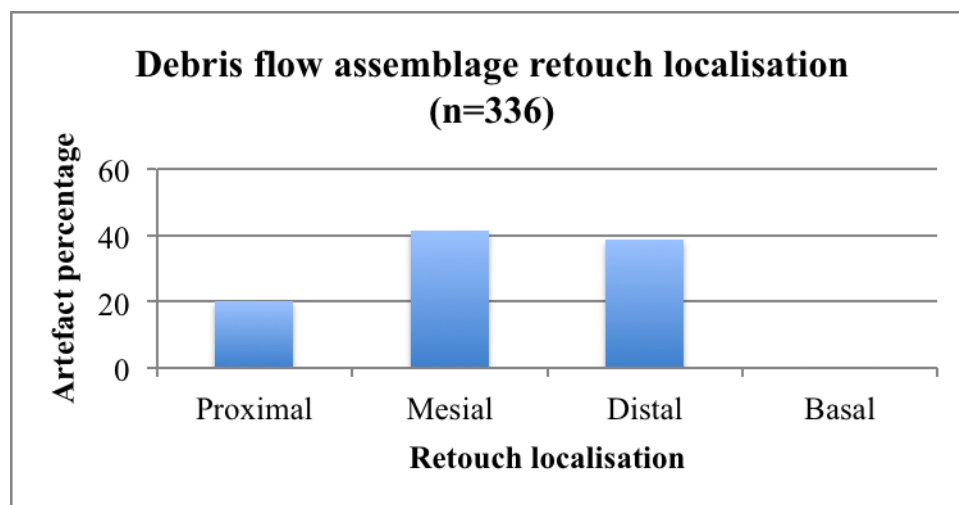


Figure 4.4.119. Debris flow assemblage retouch classification, by localisation.

Retouched edge shape classification shows that only a limited number of types occur in both assemblages (Figs. 4.4.120 & 4.4.121). The most frequent shapes include notched and denticulated edges, collectively accounting for 68.2% of the colluvial sample and 82.5% of the debris flow sample. Irregular edge shapes are notably more abundant in the colluvial assemblage (23.5%).

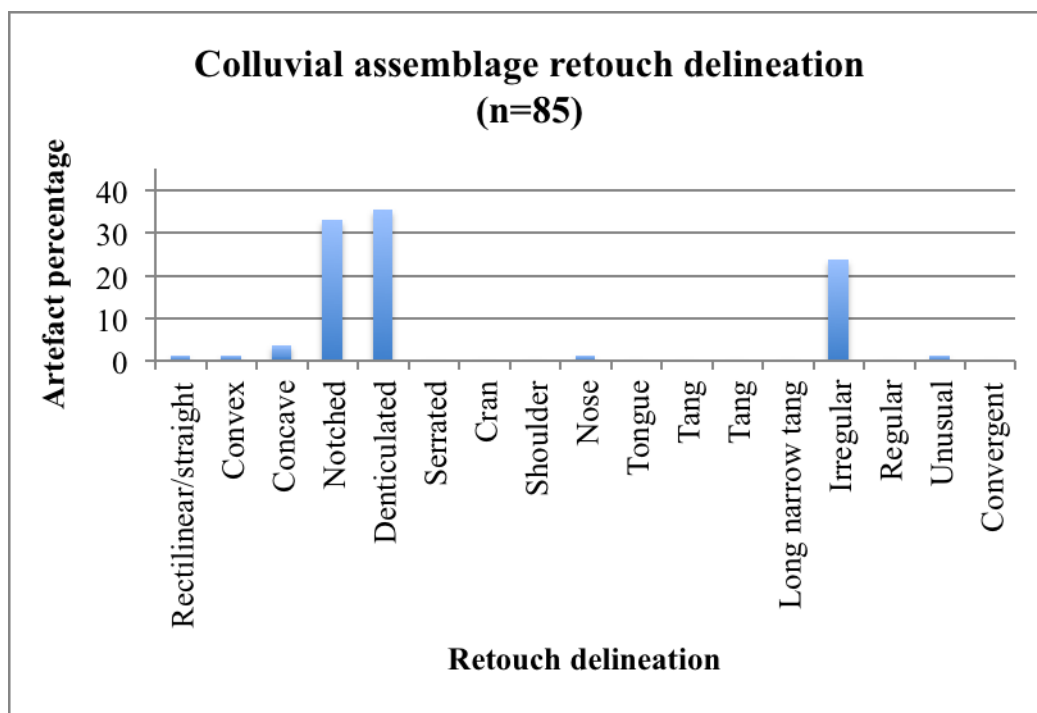


Figure 4.4.120. Retouched edge shape classification for the colluvial sample.

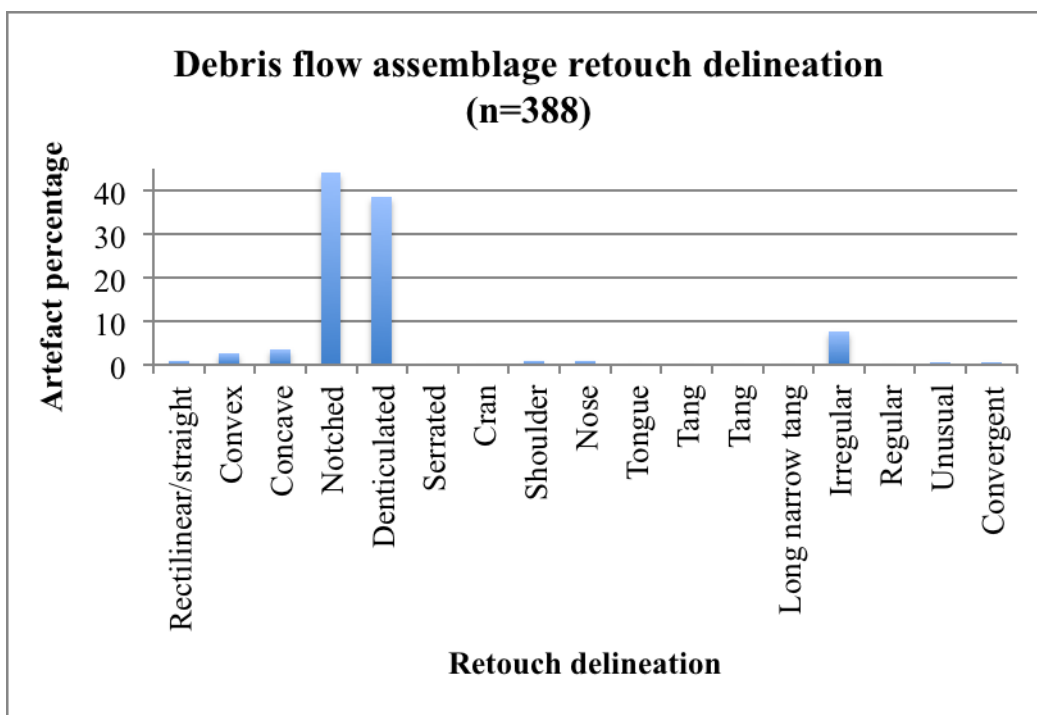


Figure 4.4.121. Retouched edge shape classification for the debris flow sample.

Although the debris flow formal tools show a greater number of edge shapes (10), the contribution of the remaining types to the overall sample is minimal (all <5%, excluding irregular edges at 7.7%). A similar pattern is seen in the colluvial sample, and arguably the more ‘complex’ edge shapes (e.g., cran, tongue and tangs) are

completely absent from both assemblages. A notable inclusion in the debris flow is artefacts with shoulder shaped edges (0.8%) and those with convergent edges (0.5%).

The angle of the removals, or steepness of the edge created by retouch shows that abrupt types (edges that are approximately 90°) are the most common in the colluvial sample (62.7%; Fig. 4.4.122). Semi-abrupt edge angles (those closer to 45°) account for the remaining artefact sample (37.3%).

A contrasting edge angle pattern is evident in the debris flow assemblage, where intermediate (45°) edges are more common (49.5%; Fig. 4.4.123). Although crossed abrupt and low edge angles are absent in the colluvial assemblage, low angled pieces occur in the debris flow (accounting for 4.2% of the total sample).

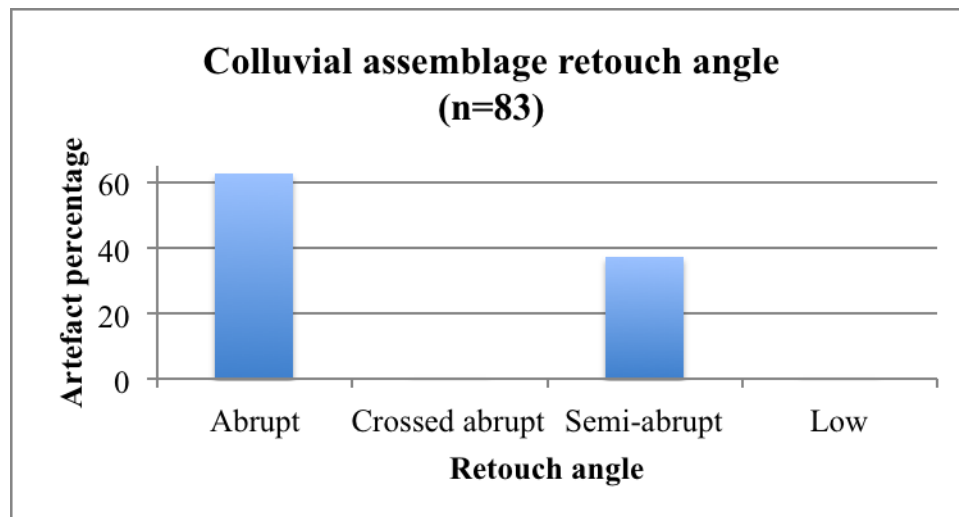


Figure 4.4.122. Edge angle classification for the colluvial assemblage.

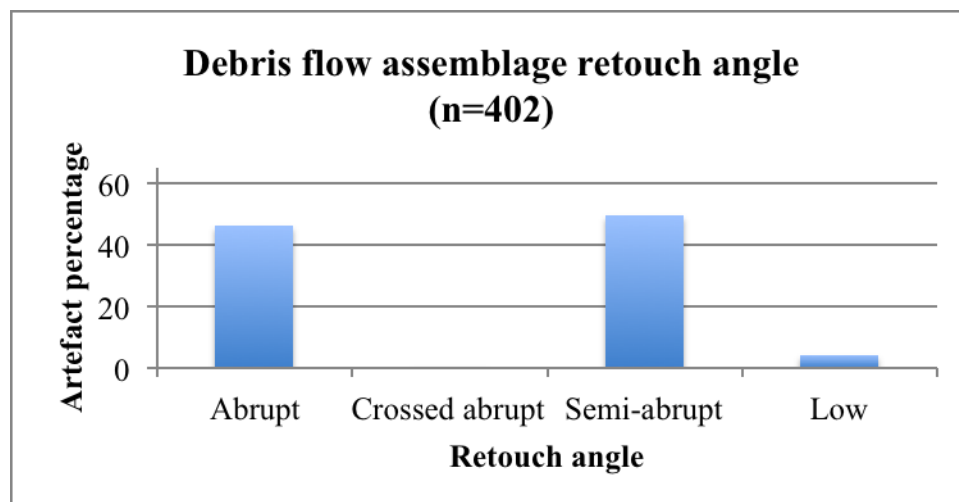


Figure 4.4.123. Edge angle classification for the debris flow assemblage.

Level of reduction:

The continuity of retouch along the edge of the Penhill Farm formal tools is shown in Figures 4.4.124 and 4.4.125. For both assemblages it is clear that discontinuous retouch is the most frequent, and it is more prevalent on artefacts in the debris flow (82%) than on those in the colluvial sample (62.8%). Those types of retouch that suggest a greater continuity along edges (total and continuous) account for only a small percentage of artefacts (with total retouch completely absent in both assemblages). Partial retouch is more common in the colluvial sample (33.3%) than in the debris flow (15.3%).

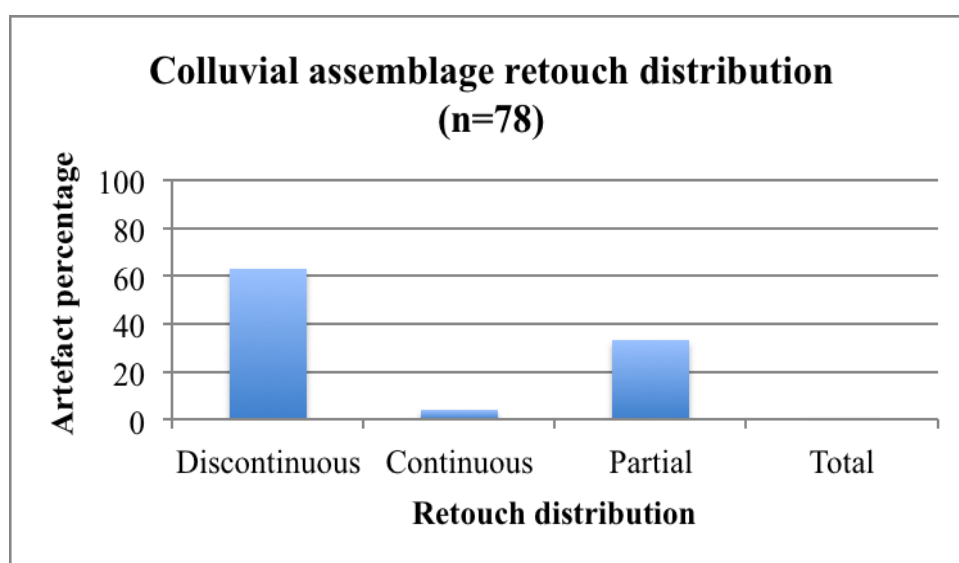


Figure 4.4.124. Retouch continuity for the colluvial formal tools.

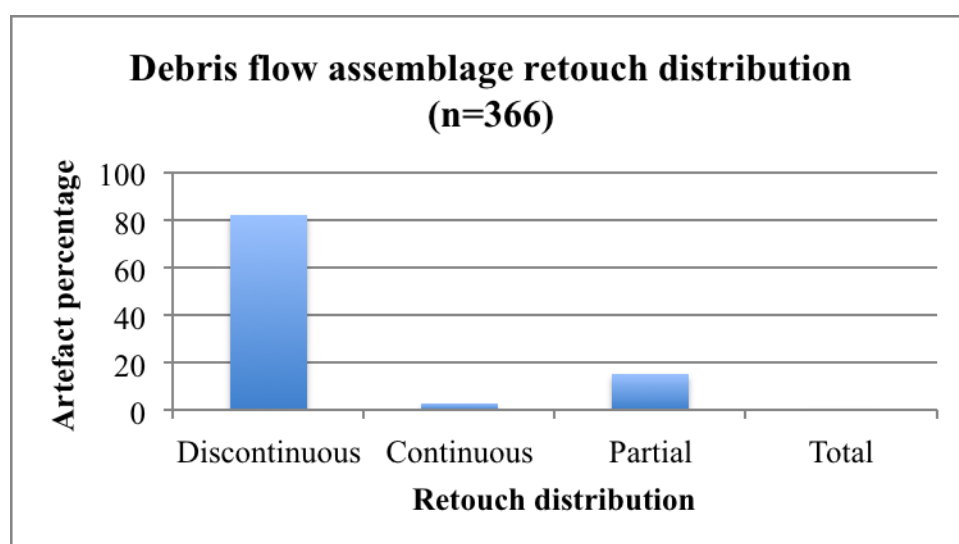


Figure 4.4.125. Debris flow formal tool retouch continuity.

An assessment of the extent (invasiveness) of this retouch shows that short removals characterise the majority of all artefact retouch at Penhill Farm, accounting for 65.8% of the colluvial and 85.6% of the debris flow samples (Figs. 4.4.126 & 4.4.127). A notable difference between the assemblages is the higher percentage of long removals in the colluvial sample (31.6%, versus 13.6% in the debris flow), coupled with more invasive retouch (2.5%, versus 0.8% in the debris flow).

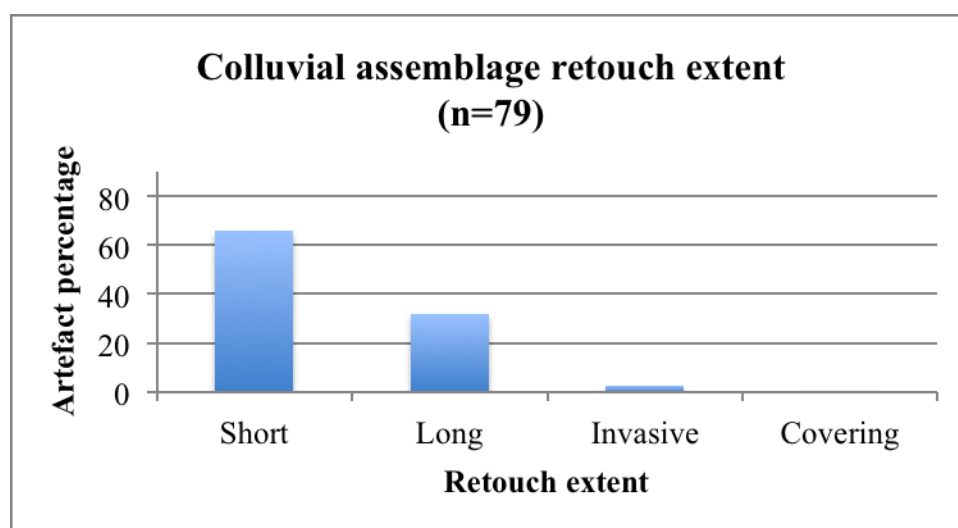


Figure 4.4.126. Invasiveness of edge retouch for the colluvial assemblage.

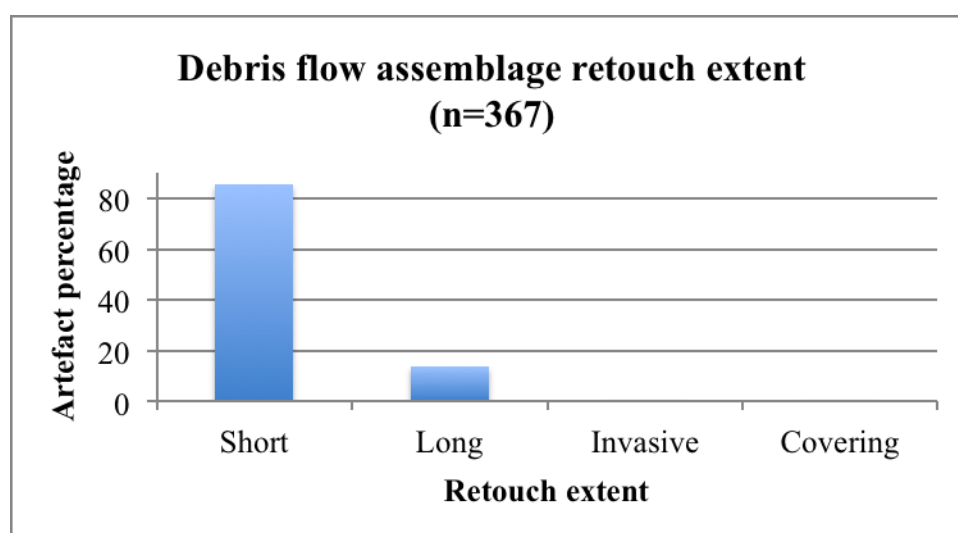


Figure 4.4.127. The extent of artefact retouch for the debris flow assemblage.

The final data to be presented on the Penhill Farm retouched pieces concerns the amount of preserved cortex (Figs. 4.4.128 & 4.4.129; Tables 4.4.46 & 4.4.47). Both assemblages illustrate an abundance of artefacts with none (0%) or only minimal (1-24%) cortex, collectively 69.8% of the colluvial and 75.6% of the debris flow

samples. Formal tools that are near or completely cortical (75-100%) only occur in the debris flow (0.6%; Fig. 4.4.129).

By raw material the colluvial quartzite sample has the majority of artefacts in the two least cortical categories (0 and 1-24%, each at 36.1%; Table 4.4.46). Although the samples of siltstone and hornfels are small, interestingly the hornfels artefacts account for the highest percentage (50%) of pieces with the most cortex (50-74%).

The debris flow shows a largely similar trend in cortex preservation, by raw material (Table 4.4.47). Collectively 77.9% of the total quartzite sample is only minimally cortical (0-24%). Siltstone and hornfels artefacts are predominantly more cortical (1-49%), and with quartzite, these three types account for the most cortical artefacts (cortex >50%).

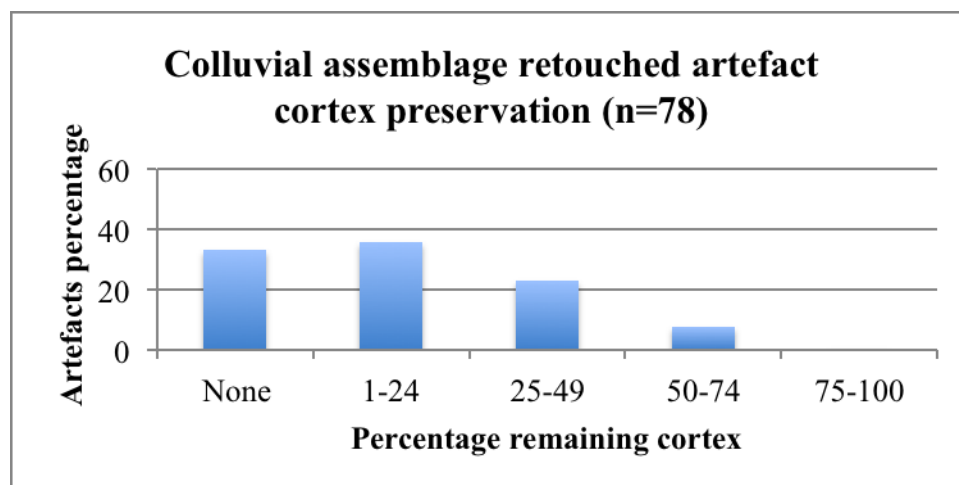


Figure 4.4.128. Cortex preservation on the colluvial retouched pieces.

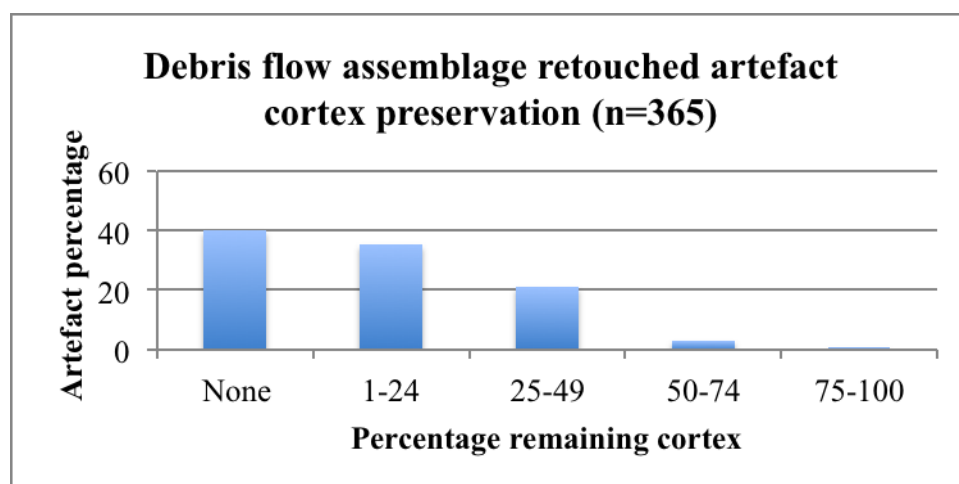


Figure 4.4.129. Debris flow assemblage cortex preservation.

Table 4.4.46. Colluvial assemblage remaining cortex, by raw material (n=78).

Raw materials	Percentage cortex										Total	
	0		1-24		25-49		50-74		75-100			
	N	%	N	%	N	%	N	%	N	%	N	%
Quartzite	26	36.1	26	36.1	16	22.2	4	5.6	0	0	72	100
Siltstone	0	0	1	50	1	50	0	0	0	0	2	100
Hornfels	0	0	1	25	1	25	2	50	0	0	4	100

Table 4.4.47. Debris flow assemblage remaining cortex, by raw material (n=365; qzte=quartzite).

Raw materials	Percentage cortex										Total	
	0		1-24		25-49		50-74		75-100			
	N	%	N	%	N	%	N	%	N	%	N	%
Quartzite	135	44	104	33.9	58	18.9	9	2.9	1	0.3	307	100
Siltstone	7	21.2	16	48.5	9	27.3	1	3	0	0	33	100
Hornfels	2	15.4	5	38.5	5	38.5	0	0	1	7.7	13	100
Lava	0	0	0	0	1	100	0	0	0	0	1	100
Silt-qzte	3	100	0	0	0	0	0	0	0	0	3	100
Claystone	0	0	4	50	4	50	0	0	0	0	8	100

Summary:

There is little difference in the retouched tools for the colluvial and debris flow assemblages. Both samples have a high number of quartzite artefacts, and all other raw materials are uncommon. However, siltstone and hornfels are the second and third most abundant remaining materials in both assemblages, and although samples of these materials are larger in the debris flow, overall trends discussed for these materials must be treated with caution.

Formal tool size illustrates that siltstone artefacts are the largest for both assemblages. Hornfels and quartzite artefacts follow thereafter as size and weight decreases. This trend is evident in both the colluvial formal tool sample (with limited siltstone and hornfels pieces) and in the debris flow where samples are larger. The remaining raw materials in the debris flow indicate small artefact weight and size.

The blanks most favoured for retouching are flakes, which account for >75% in both assemblages. Blank types in the debris flow show more variability, most likely due to the larger sample size. All other remaining blanks types are infrequent.

Retouch classification data concerning location illustrates an abundance of artefacts with direct retouch (that which originates from the flake ventral surface) in both assemblages (68.7% of the colluvial sample and 49.2% in the debris flow). Alternate retouch is the second most frequent type in both assemblage samples, and no crossed retouch occurs in either. The colluvial formal tools are the only ones to have bifacial retouch.

Retouch localization indicates that basal retouch is absent in both assemblages. Mesial and distal retouch is the most frequent, followed lastly by proximal retouch. However, the percentage difference between these three types is minimal.

Retouch edge shape classification shows a clear abundance for denticulated and notched shapes. These types account for 68.2% of the colluvial formal tools and 82.5% in the debris flow; all other shapes are uncommon.

The steepness of edge created by retouch shows an abundance of abrupt and semi-abrupt angles. Crossed-abrupt edges are absent in both assemblages and low angled edges only occur in the debris flow formal tools.

The continuity of retouch along artefact edges is mostly discontinuous in both assemblages (62.8% in the colluvial assemblage and 82% in the debris flow). Retouch that appears to show any greater edge continuity is very uncommon. Partial retouch is more frequent in the colluvial formal tools.

The invasiveness of retouch for both assemblages is dominated by short removals. Long and invasive removals are marginally more frequent in the colluvial formal tools.

The final data concerning the amount of preserved cortex shows that most formal tools at Penhill Farm are either not cortical (0%) or only minimally (1-24%) cortical. By raw material, quartzite artefacts show a tendency to be less cortical, whereas the limited samples of hornfels and siltstone indicate more cortex preservation.

LCTs:

All data that were recorded on the Penhill Farm LCTs are presented in this section. As with the previous sections these data are presented together, for both of the assemblages. The following sample sizes apply:

- Colluvial assemblage (n=11).
- Debris flow assemblage (n=38). This sample includes all broken LCT fragments (n=6). However, for the majority of the analysis these pieces are excluded.

LCT data will first address size and shape (through technological measurements, including weight) and then reduction. It must be emphasised here that sample size is important to consider when interpreting any of the data presented below (especially for the colluvial assemblage).

LCT size and shape:

Size and weight measurements for the Penhill Farm LCTs are presented in Tables 4.4.48 (colluvial assemblage) and 4.4.49 (debris flow assemblage). See Appendix B Tables 7-10 for individual LCT measurements and ratios.

Table 4.4.48 for the colluvial assemblage shows that handaxes account for the majority of the largest measurements, including weight (but excluding thickness). In addition to this, those made on siltstone are marginally larger and heavier than those on quartzite. By minimum weight there is a notably light pick (113.91 g) and a biface (98.39 g), and by mean weight these two LCT types account for the lightest pieces overall. The greatest variation (SD=495.88) in weight occurs in the quartzite handaxe sample (n=2).

Although some of the colluvial LCTs show minimum lengths that are less than 100 mm (a pick, biface handaxe and cleaver), by mean length all of these types (excluding bifaces) exceed 100 mm. For the remaining width and thickness measurements there is a great deal of variability amongst the LCTs, with mean measurements for the former ranging from 58.5-85.5 mm, and for the latter ranging from 29.5-60.15 mm.

Table 4.4.48. Colluvial LCT data, by type and raw material. See Appendix B Table 11 for additional measurement data.

Colluvial assemblage (n=11)		Pick (n=2)	Biface (n=2)	Handaxe (n=4)		Cleaver (n=3)	
		Quartzite	Quartzite	Quartzite	Siltstone	Quartzite	Siltstone
Weight (g)	Min	113.91	98.39	188.65	556.37	274.42	596.94
	Median	382.45	180.52	539.29	613.70	397.90	-
	Max	650.99	262.64	889.93	671.03	521.37	596.94
	Mean	382.45	180.52	539.29	613.70	397.90	-
	SD	379.77	116.14	495.88	81.08	174.62	-
Length (mm)	Min	97.00	73.00	99.00	116.00	95.00	154.00
	Median	114.50	90.50	142.00	148.00	106.50	-
	Max	132.00	108.00	185.00	180.00	118.00	154.00
	Mean	114.50	90.50	142.00	148.00	106.50	-
	SD	24.75	24.75	60.81	45.25	16.26	-
Width (mm)	Min	45.20	44.00	67.00	78.00	72.00	89.00
	Median	63.10	58.50	84.50	85.50	78.00	-
	Max	81.00	73.00	102.00	93.00	84.00	89.00
	Mean	63.10	58.50	84.50	85.50	78.00	-
	SD	25.31	20.51	24.75	10.61	8.49	-
Thickness (mm)	Min	31.00	27.00	32.00	41.00	50.00	40.00
	Median	55.00	29.50	37.50	49.00	60.15	-
	Max	79.00	32.00	43.00	57.00	70.30	40.00
	Mean	55.00	29.50	37.50	49.00	60.15	-
	SD	33.94	3.54	7.78	11.31	14.35	-
L/W ratio	Min	1.63	1.48	1.48	1.49	1.32	1.73
	Median	1.89	1.57	1.65	1.72	1.36	-
	Max	2.15	1.66	1.81	1.94	1.40	1.73
	Mean	1.89	1.57	1.65	1.72	1.36	-
	SD	0.37	0.13	0.23	0.32	0.06	-
T/W ratio	Min	0.69	0.44	0.42	0.44	0.60	0.45
	Median	0.83	0.53	0.45	0.59	0.79	-
	Max	0.98	0.61	0.48	0.73	0.98	0.45
	Mean	0.83	0.53	0.45	0.59	0.79	-
	SD	0.20	0.12	0.04	0.21	0.27	-

LCT elongation (L/W ratio) data show that the quartzite picks and the handaxes account for the most elongated specimens (with mean ratios ranging from 1.65-1.89); the cleavers and bifaces account for the shortest pieces. LCT refinement (T/W ratio) data shows, predictably, that the small pick sample retains the thickest pieces (mean=0.83); however, this is followed closely by the quartzite cleaver sample (mean=0.79). Both of these samples have the same maximum refinement ratio (0.98).

Conversely, the thinnest types include the quartzite handaxes (mean=0.45) and the bifaces (mean=0.53).

The larger LCT sample in the debris flow assemblage (Table 4.4.49) shows an interesting size trend between siltstone and quartzite tools. For those pieces produced on both materials, the weight, length, width and thickness measurements for siltstone pieces are consistently greater than those for quartzite pieces. This is most apparent when looking at mean weight, where the quartzite means are close to half of the siltstone means for some samples. The heaviest LCT types include all those that are made on siltstone (picks, handaxes and cleavers). Quartzite picks, bifaces and handaxes account for notably light mean weights (ranging from 82.57-208.17 g).

By mean length, the only quartzite LCTs to exceed 100 mm in length include the cleavers. Thereafter, all quartzite LCTs (picks, bifaces, and handaxes) are smaller, although most do have individual pieces that exceed 100 mm in maximum length. As with the colluvial assemblage, quartzite bifaces account for the smallest mean length (63.75 mm). The larger siltstone LCTs have mean lengths ranging from 118.5 mm (siltstone picks) to 133.33 mm (siltstone handaxe).

As with the weight and length measurements, the siltstone types account for the largest mean width measurements (picks, handaxes and cleavers); however, quartzite types account for the smallest mean thicknesses, most notably the bifaces (at 25.20 mm).

LCTs that are notably elongated include the quartzite picks (as seen in the colluvial assemblage) and the siltstone handaxes (means ranging from 1.6-1.66). The shortest pieces include the quartzite bifaces and siltstone cleavers (with mean ratios ranging from 1.29-1.46). However, these two types, including quartzite handaxes, account for the most refined pieces (with mean ratios ranging from 0.44-0.51); refinement is better on the siltstone picks and cleavers, versus those produced on quartzite. As with the colluvial assemblage tool refinement is poorest on the quartzite picks.

Table 4.4.49. Debris flow LCT data, by type and raw material. See Appendix B Table 12 for additional measurement data.

Debris flow assemblage (n=32)		Pick (n=5)		Biface (n=3)		Handaxe (n=12)		Cleaver (n=12)	
		Quartzite	Siltstone	Quartzite	Siltstone	Quartzite	Siltstone	Quartzite	Siltstone
Weight (g)	Min	94.58	279.16	67.86	381.57	72.42	448.50	104.82	497.36
	Median	226.57	404.51	82.57	-	150.05	533.71	236.20	550.67
	Max	303.35	529.86	97.28	381.57	483.06	642.98	703.02	578.98
	Mean	208.17	404.51	82.57	-	206.61	541.73	328.34	542.34
	SD	105.59	177.27	20.80	-	146.06	97.49	181.19	41.44
Length (mm)	Min	77.00	113.00	63.00	123.00	73.00	112.00	77.00	120.00
	Median	102.00	118.50	63.75	-	83.00	133.00	106.00	127.00
	Max	116.00	124.00	64.50	123.00	143.00	155.00	141.00	140.00
	Mean	98.33	118.50	63.75	-	96.89	133.33	109.39	129.00
	SD	19.76	7.79	1.06	-	27.19	21.50	18.78	10.15
Width (mm)	Min	51.00	67.00	47.50	81.50	50.00	80.00	50.00	80.00
	Median	59.00	78.50	49.75	-	68.00	83.00	72.00	89.00
	Max	67.00	90.00	52.00	81.50	86.50	88.50	89.00	97.00
	Mean	59.00	78.50	49.75	-	65.72	83.83	72.00	88.67
	SD	8.00	16.26	3.18	-	14.21	4.31	11.00	8.50
Thickness (mm)	Min	25.10	37.00	23.40	34.00	16.00	41.00	24.00	42.00
	Median	41.00	43.00	25.20	-	28.00	44.80	35.00	45.00
	Max	46.00	49.00	27.00	34.00	46.50	50.00	61.00	49.00
	Mean	37.37	43.00	25.20	-	29.12	45.27	39.94	45.33
	SD	10.91	8.49	2.55	-	8.49	4.52	13.42	3.51

Table 4.4.49 continued...

Debris flow assemblage (n=32)		Pick (n=5)		Biface (n=3)		Handaxe (n=12)		Cleaver (n=12)	
		Quartzite	Siltstone	Quartzite	Siltstone	Quartzite	Siltstone	Quartzite	Siltstone
L/W ratio	Min	1.51	1.38	1.21	1.51	1.04	1.35	1.37	1.31
	Median	1.73	1.53	1.29	-	1.46	1.50	1.54	1.50
	Max	1.73	1.69	1.36	1.51	1.73	1.94	1.65	1.57
	Mean	1.66	1.53	1.29	-	1.47	1.60	1.52	1.46
	SD	0.13	0.22	0.11	-	0.20	0.31	0.09	0.13
T/W ratio	Min	0.49	0.54	0.49	0.42	0.32	0.49	0.39	0.47
	Median	0.61	0.55	0.51	-	0.43	0.51	0.48	0.51
	Max	0.78	0.55	0.52	0.42	0.61	0.63	0.82	0.56
	Mean	0.63	0.55	0.51	-	0.44	0.54	0.55	0.51
	SD	0.14	0.01	0.02	-	0.10	0.08	0.14	0.05

Additional data that relates to the overall shape of the LCTs and to tool breakage are presented in Tables 4.4.50-4.4.55 and Figures 4.4.130 and 4.4.131. Tables 4.4.50 and 4.4.51 show that LCT damage is more frequent in the debris flow assemblage, and that only a single colluvial cleaver retained a partial edge break (with the remaining LCTs being complete and undamaged). In contrast to this the debris flow assemblage shows that 11 LCTs retain some kind of damage, which includes seven partial tip breaks (n=2 handaxes, n=2 broken handaxes/LCTs, n=1 biface and n=2 picks) and four partial butt breaks (seen on four broken handaxe/LCT fragments).

Table 4.4.50. Colluvial assemblage LCT damage, by type.

Colluvial assemblage (n=11)	Damage/break		
	Partial tip/cleaver edge	Partial lateral edge	Partial butt
Pick (n=2)	0	0	N/A
Biface (n=2)	0	0	N/A
Handaxe (n=4)	0	0	0
Cleaver (n=3)	1	0	N/A

Table 4.4.51. Debris flow assemblage LCT damage, by type.

Debris flow assemblage (n=38)	Damage/break		
	Partial tip/cleaver edge	Partial lateral edge	Partial butt
Pick (n=5)	2	0	N/A
Biface (n=3)	1	0	N/A
Broken LCT (n=6)	2	0	4
Handaxe (n=12)	2	0	0
Cleaver (n=12)	0	0	N/A

Table 4.4.52 and Figure 4.4.130 illustrate the abundance of generalised convergent tip shapes in the colluvial LCTs (n=6), accounting for 54.6% of the total sample. This tip shape accounts for all the bifaces (n=2), most of the handaxes (n=3) and a single pick. Markedly convergent tips occur on a pick and handaxe, collectively accounting for 18.2% of the LCT sample. Cleaver tip shapes are unique in the sense that no other LCTs retain the same tip shapes (n=1 convergent square, n=1 convergent oblique and n=1 oblique tip with divergent/parallel sided edges). Square and wide tip LCTs are not represented.

Table 4.4.52. Colluvial assemblage LCT tip shape, by type (n=11).

Tip shape	Type			
	Pick (n=2)	Biface (n=2)	Handaxe (n=4)	Cleaver (n=3)
1) Markedly convergent	1 (50%)	0	1 (25%)	0
2) Convergent square	0	0	0	1 (33.3%)
3) Convergent oblique	0	0	0	1 (33.3%)
4) Generalised convergent	1 (50%)	2 (100%)	3 (75%)	0
5) Square tip: divergent/parallel	0	0	0	0
6) Oblique tip: divergent/parallel	0	0	0	1 (33.3%)
7) Wide with convex tip	0	0	0	0
Total	2 (100%)	2 (100%)	4 (100%)	3 (100%)

A similar pattern in LCT tip shape is evident for the debris flow, with a preference for generalised convergent types (n=12, 37.5% of the LCT sample; Table 4.4.53; Fig. 4.4.131). Another notable similarity in these assemblages is the complete absence of tip types five and seven. Convergent oblique (n=8) tip shapes account for 66.7% of the cleaver sample. Picks account for the highest percentage (80%) of markedly convergent tip shapes (n=4). Handaxes are dominated by generalised convergent tip shapes (n=8, 66.7% of the total sample), as are bifaces (n=2, 66.7%).

Table 4.4.53. Debris flow assemblage LCT tip shape, by type (n=32).

Tip shape	Type			
	Pick (n=5)	Biface (n=3)	Handaxe (n=12)	Cleaver (n=12)
1) Markedly convergent	4 (80%)	1 (33.3%)	3 (25%)	0
2) Convergent square	0		1 (8.3%)	3 (25%)
3) Convergent oblique	0	0	0	8 (66.7%)
4) Generalised convergent	1 (20%)	2 (66.7%)	8 (66.7%)	1 (8.3%)
5) Square tip: divergent/parallel	0	0	0	0
6) Oblique tip: divergent/parallel	0	0	0	0
7) Wide with convex tip	0	0	0	0
Total	5 (100%)	3 (100%)	12 (100%)	12 (100%)

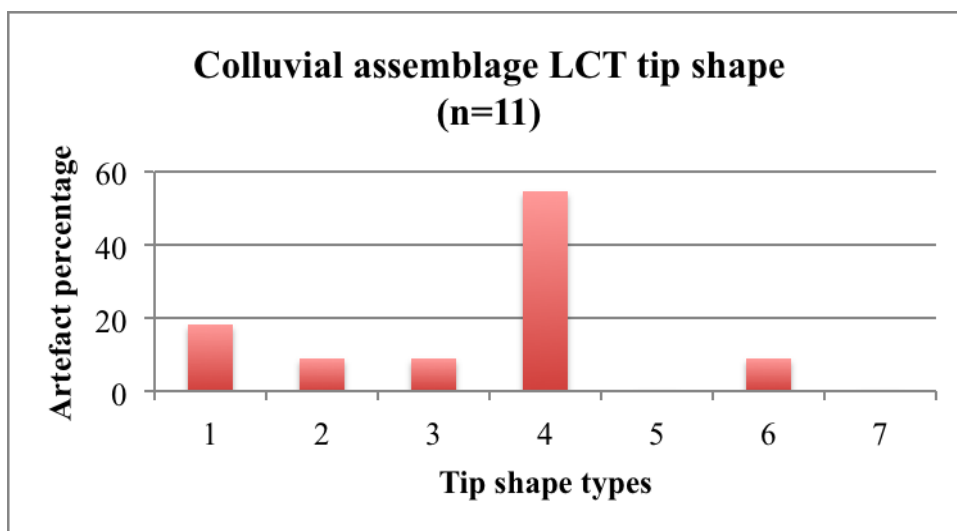


Figure 4.4.130. Colluvial assemblage LCT tip shape. Numbers 1-7 as per those listed in Table 4.4.52.

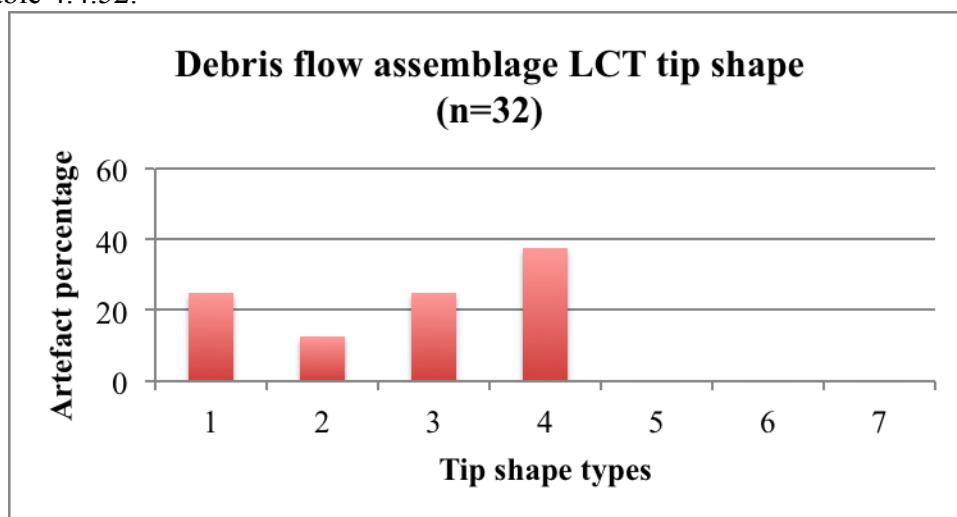


Figure 4.4.131. Debris flow assemblage LCT tip shape. Numbers 1-7 as per those listed in Table 4.4.53.

The final LCT morphological data to be presented concerns the cleaver butt plan profiles for the colluvial assemblage sample (n=3; Table 4.4.54) and the debris flow sample (n=12; Table 4.4.55). No cleaver butts in the colluvial assemblage are intentionally shaped to any of the three types described here; however, two rounded and a single square butt occur in the debris flow that are intentionally shaped. Both samples show that rounded butts are more frequent on cleavers, thereafter followed by pointed types. Square butts are only seen in the debris flow sample (n=3, 25%; Table 4.4.55).

Table 4.4.54. Colluvial assemblage cleaver butt plan shape.

Type	Butt plan			Total
	Rounded	Squared	Pointed	
Cleaver (n=3)	2 (66.6%)	0	1 (33.3%)	3 (100%)

Table 4.4.55. Debris flow assemblage cleaver butt plan shape.

Type	Butt plan			Total
	Rounded	Squared	Pointed	
Cleaver (n=12)	6 (50%)	3 (25%)	3 (25%)	12 (100%)

LCT reduction:

Tables 4.4.56 and 4.4.57 illustrate that flake blanks are favoured for LCT production, for both assemblages. This is most obvious in the colluvial sample (n=11), where only a single quartzite pick was made on another blank type (split cobble).

Although the debris flow sample (n=32) shows a similar flake blank preference (n=24, 75%) a wider range of blanks occurs, including: cobbles (n=5) and a split cobble (n=1). By type and raw material the cobble sample comprises one quartzite pick, one siltstone biface, one siltstone handaxe and two cleavers; the single split cobble comprises a quartzite cleaver. Combining this cobble and split cobble sample (n=6), siltstone and quartzite show equal numbers for these blanks (n=3 LCTs each). Both assemblages have no blocks, fragments, pebbles or bipolar split cobbles/pebbles utilised in LCT production (Tables 4.4.56 & 4.4.57).

Flake scar numbers are indicative of the level of LCT reduction and these results, by raw material and tool type, are shown in Tables 4.4.58 and 4.4.59, with a summary presented in Figures 4.4.132 and 4.4.133.

A clear trend is evident for the colluvial LCTs where those made on siltstone have a lower combined mean number of flake scars than those on quartzite (Table 4.4.58). Notably high combined flake scar means occur for the quartzite handaxes, picks, and cleavers, the highest of which occurs on the handaxe sample (with a combined mean of 20.5 scars). It is these quartzite handaxes that also retain the greatest means for primary and secondary flake scars. The siltstone handaxes and cleaver account for the lowest number of combined mean flake scars.

Table 4.4.56. Colluvial LCT blank type, by raw material and type.

Blank type	Type						Total
	Pick (n=2)	Biface (n=2)	Handaxe (n=4)		Cleaver (n=3)		
	Quartzite	Quartzite	Quartzite	Siltstone	Quartzite	Siltstone	
Block	0	0	0	0	0	0	0
Fragment	0	0	0	0	0	0	0
Flake	1	2	2	2	2	1	10 (90.9%)
Cobble	0	0	0	0	0	0	0
Pebble	0	0	0	0	0	0	0
Indeterminate	0	0	0	0	0	0	0
Split cobble	1	0	0	0	0	0	1 (9.1%)
Bipolar split	0	0	0	0	0	0	0
Total	2 (18.2%)	2 (18.2%)	2 (18.2%)	2 (18.2%)	2 (18.2%)	1 (9.1%)	11 (100%)

Table 4.4.57. Debris flow LCT blank type, by raw material and type.

Blank type	Type								Total
	Pick (n=5)		Biface (n=3)		Handaxe (n=12)		Cleaver (n=12)		
	Quartzite	Siltstone	Quartzite	Siltstone	Quartzite	Siltstone	Quartzite	Siltstone	
Block	0	0	0	0	0	0	0	0	0
Fragment	0	0	0	0	0	0	0	0	0
Flake	1	2	2	0	8	2	7	2	24 (75%)
Cobble	1	0	0	1	0	1	1	1	5 (15.6%)
Pebble	0	0	0	0	0	0	0	0	0
Indeterminate	1	0	0	0	1	0	0	0	2 (6.3%)
Split cobble	0	0	0	0	0	0	1	0	1 (3.1%)
Bipolar split	0	0	0	0	0	0	0	0	0
Total	3 (9.4%)	2 (6.2%)	2 (6.2%)	1 (3.1%)	9 (28.1%)	3 (9.4%)	9 (28.1%)	3 (9.4%)	32 (100%)

For all the colluvial LCTs the mean number of secondary flake scars exceeds the mean number of primary scars, although for siltstone the difference between these means is greater.

Table 4.4.58. Average number of flake scars (≥ 10 mm) for the colluvial LCTs (n=11). Where n=1 (siltstone cleaver) these values are not means.

Type	Raw material	Scar counts					
		Combined mean	SD	Mean primary	SD	Mean secondary	SD
Pick (n=2)	Quartzite	14.00	2.83	6.50	3.54	7.50	0.71
Biface (n=2)	Quartzite	12.00	2.83	5.50	2.12	6.50	4.95
Handaxe (n=4)	Quartzite	20.50	3.54	10.00	1.41	10.50	2.12
	Siltstone	9.50	0.71	2.50	0.71	7.00	0.00
Cleaver (n=3)	Quartzite	13.50	0.71	4.50	0.71	9.00	0.00
	Siltstone	7.00	-	2.00	-	5.00	-

Interestingly, in contrast to the colluvial LCT sample, for all the debris flow LCTs that are made on both quartzite and siltstone the combined mean number of flake scars on siltstone LCTs is higher (Table 4.4.59). As a result the flake scars are greatest for the siltstone handaxes and cleavers (combined means of 16.67 and 17 scars, respectively). Bifaces show the least scars.

Table 4.4.59. Average number of flake scars (≥ 10 mm) for the debris flow LCTs (n=32). Where n=1 (siltstone biface) these values are not means.

Type	Raw material	Scar counts					
		Combined mean	SD	Mean primary	SD	Mean secondary	SD
Pick (n=5)	Quartzite	14.67	7.23	7.67	3.06	7.00	4.58
	Siltstone	15.00	0.00	6.00	0.00	9.00	0.00
Biface (n=3)	Quartzite	9.50	2.12	4.50	0.71	5.00	1.41
	Siltstone	11.00	-	6.00	-	5.00	-
Handaxe (n=12)	Quartzite	12.22	4.55	4.00	2.40	8.22	3.70
	Siltstone	16.67	8.08	6.67	2.52	10.00	6.56
Cleaver (n=12)	Quartzite	16.00	7.52	7.44	3.57	8.56	5.00
	Siltstone	17.00	7.81	8.00	4.58	9.00	5.57

Mean primary flake scar counts are greatest for the siltstone cleaver sample (8), which is followed closely thereafter by the quartzite picks. Mean secondary flake scar counts are notably higher on the siltstone picks, handaxes and cleavers, and following the

trend observed in the colluvial LCT sample, the difference between the mean primary and secondary flake scar counts is greater for the siltstone LCTs.

Irrespective of raw material type Figure 4.4.132 shows that the colluvial picks and handaxes have the greatest total mean scar numbers (14 and 15 scars, respectively); cleavers show the least amount of scars. However, handaxes and cleavers show the greatest numerical difference between mean primary and secondary scar counts.

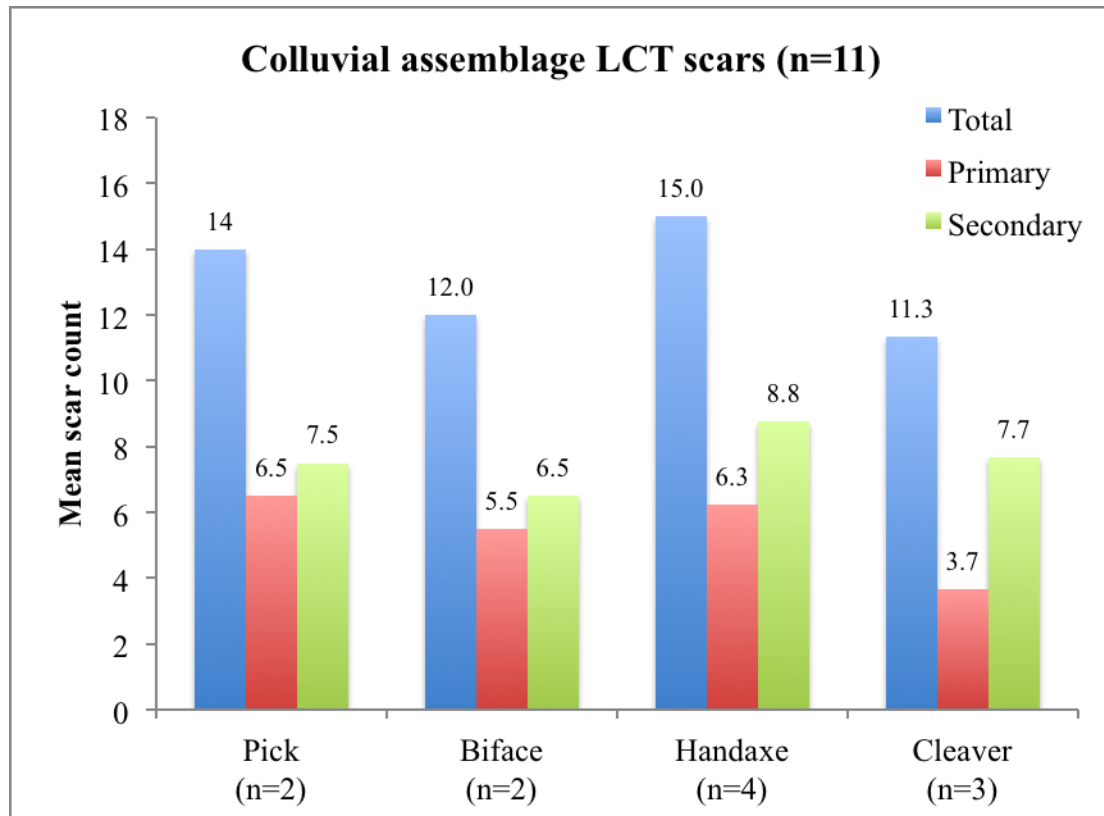


Figure 4.4.132. Average number of flake scars, by colluvial LCT type.

Figure 4.4.133 illustrates that the debris flow cleavers have the greatest quantity of flake scars (16.3), having both the highest mean primary (7.6) and secondary (8.7, equal to that of handaxes) scar numbers. Handaxes, although having the lowest mean primary scar count (4.7), retain just as much secondary shaping as the cleavers. Interestingly, scar counts for the picks are largely comparable to those in the colluvial assemblage.

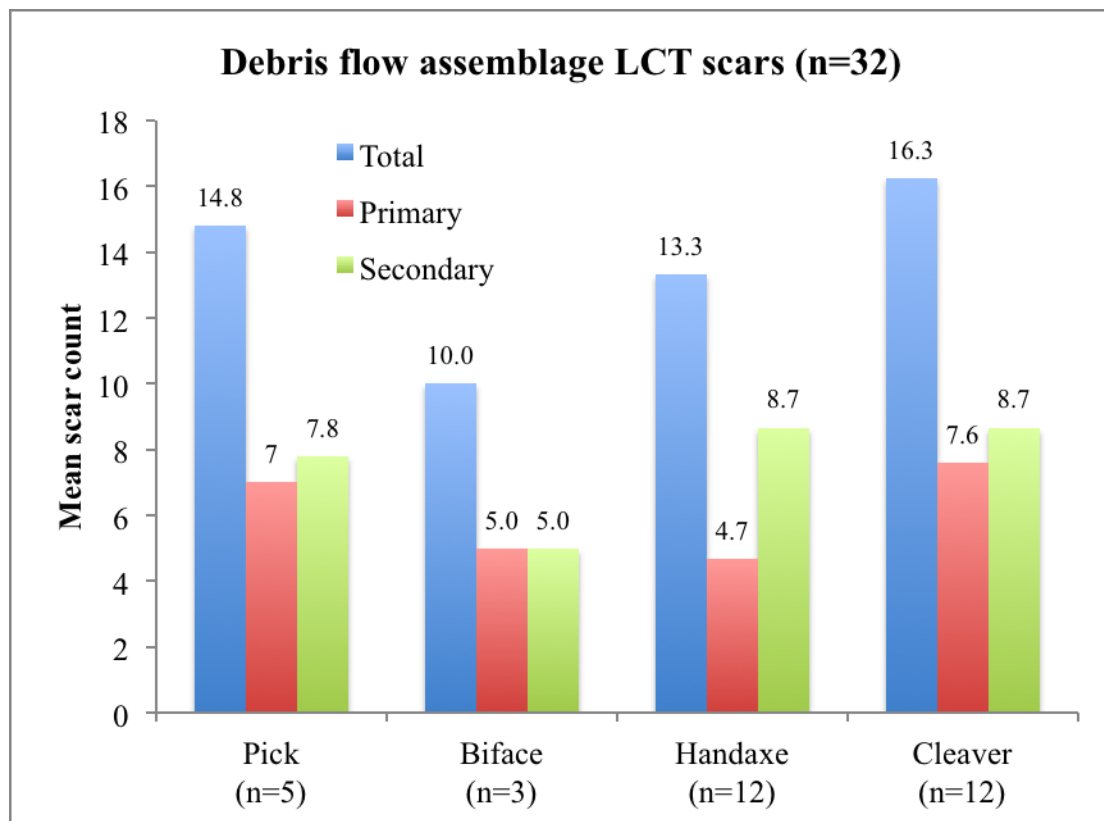


Figure 4.4.133. Average number of flake scars, by debris flow LCT type.

Flake scar negatives are depicted in Figures 4.4.134 and 4.4.135. From this it is clear that feather, step and hinge terminations are similarly frequent in both assemblages. Overshoot terminations do not occur in any assemblage. The colluvial assemblage shows marginally greater percentages for feather and step terminations (the two most frequent), whereas the debris flow shows an increase in the percentage of hinge terminations relative to step terminations. However, the percentage differences between these terminations, and between the assemblages, are minor.

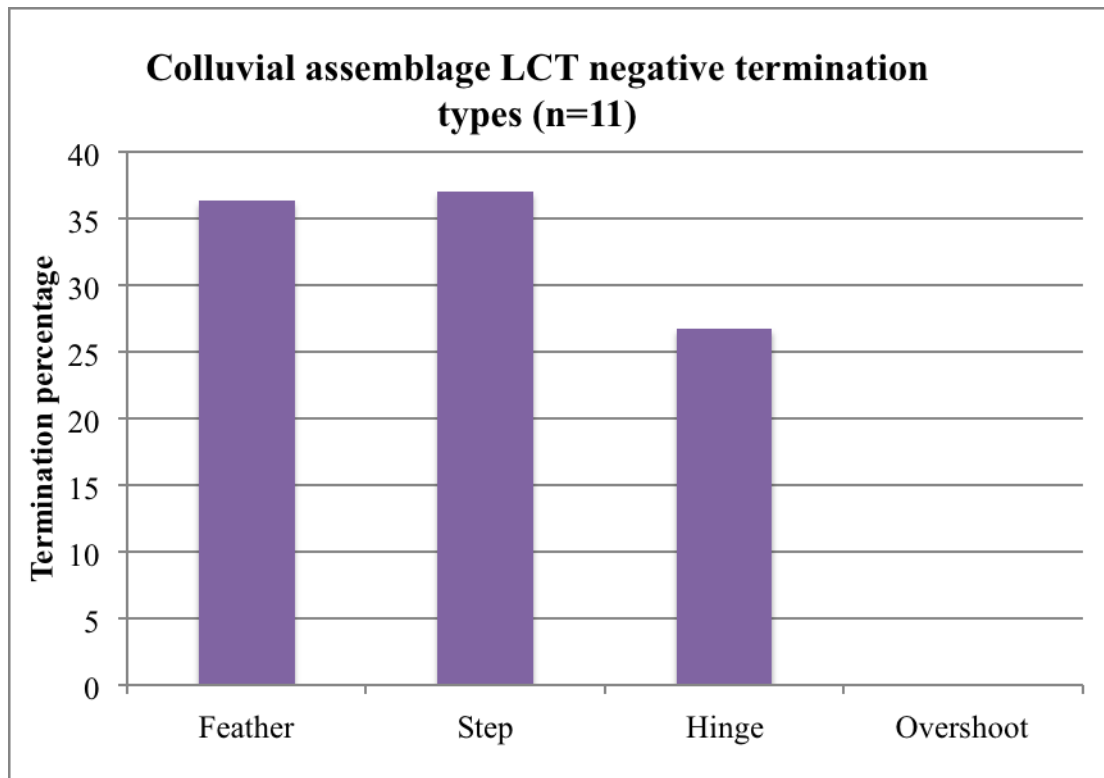


Figure 4.4.134. Negative termination types on the colluvial LCTs.

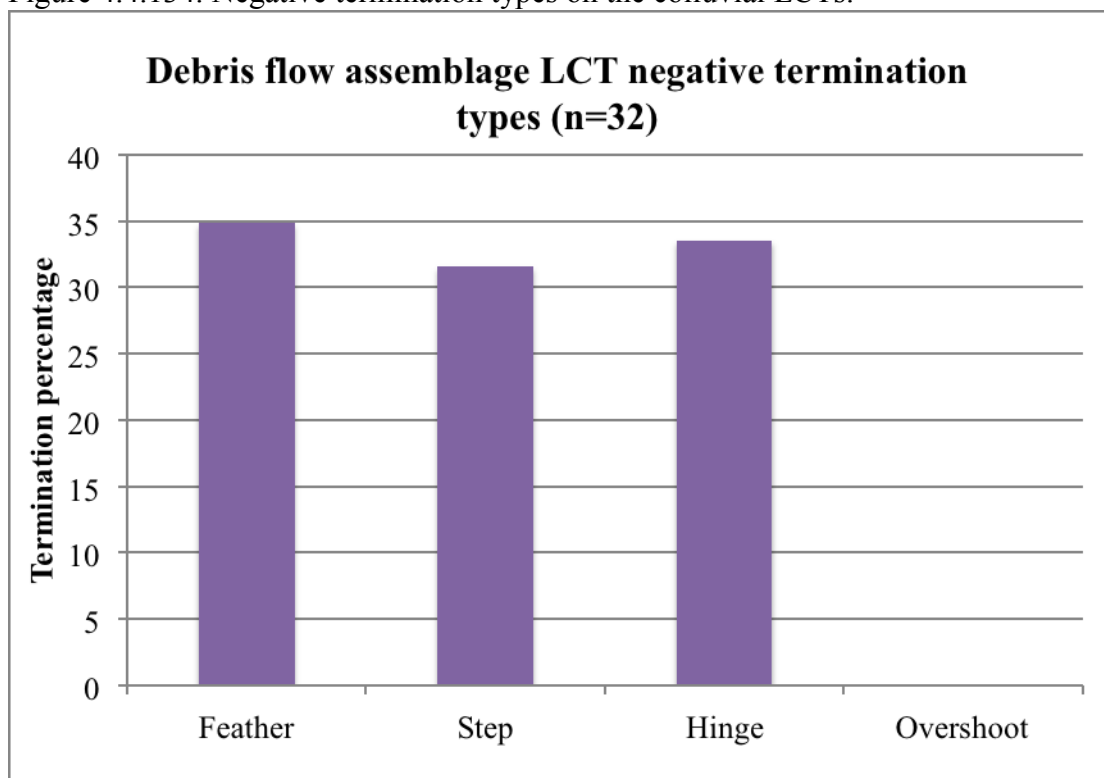


Figure 4.4.135. Negative termination types on the debris flow LCTs.

An assessment of LCT flaking extent and location is presented in Tables 4.4.60-4.4.63, with an illustration provided by Figures 4.4.136 and 4.4.137. The colluvial

LCT sample is dominated by bifacial pieces (n=7), including: two picks, one biface, two handaxes and two cleavers (Table 4.4.60). Partly bifacial pieces include two handaxes and a biface, collectively accounting for 27.3% of the LCT sample, and only a single unifacial cleaver was recovered.

Table 4.4.60. Shaping data for the colluvial LCT sample.

Type	Bifacial	Partly bifacial	Unifacial	Sample
Pick	2	0	0	2 (18.2%)
Biface	1	1	0	2 (18.2%)
Handaxe	2	2	0	4 (36.4%)
Cleaver	2	0	1	3 (27.3%)
Total	7 (63.6%)	3 (27.3%)	1 (9.1%)	11 (100%)

LCT shaping in the debris flow shows a largely similar trend where bifacial pieces dominate (n=23, 71.9%; Table 4.4.61). This includes all of the picks (n=5), two bifaces, seven handaxes and nine cleavers. However, here the percentage of partly bifacial LCTs (12.5%) is lower than in the colluvial sample, and unifacial pieces are more frequent (15.6% versus 9.1% in the colluvial sample). Unifacial pieces include three handaxes and two cleavers.

Table 4.4.61. Shaping data for the debris flow LCT sample.

Type	Bifacial	Partly bifacial	Unifacial	Sample
Pick	5	0	0	5 (15.6%)
Biface	2	1	0	3 (9.4%)
Handaxe	7	2	3	12 (37.5%)
Cleaver	9	1	2	12 (37.5%)
Total	23 (71.9%)	4 (12.5%)	5 (15.6%)	32 (100%)

An illustration of this shaping, by sector, shows that the colluvial LCTs have primary removals in all sectors across both faces, yet these are marginally more abundant in sectors 2, 4 and 6 on face 1 and sectors 7, 9, and 11 on face 2 (Fig. 4.4.136).

Secondary shaping is proportionally more abundant towards the distal and medial portions of the LCTs, on both faces, with little towards the proximal ends. To be expected, cortex preservation is greatest towards the proximal (basal) portion of the LCTs; however, it is worth noting that it is also found towards the distal and medial portions on face 1 as well. Flake ventral surfaces are preserved throughout face 2, yet they are most frequent in sectors 8, 10 and 12.

The debris flow LCTs show that there is little variation in the distribution of primary removals, across the faces and sectors (Fig. 4.4.137). However, there are notably higher percentages of secondary working on both faces towards the medial and distal portions, especially in the distal (tip) sectors (1, 2, 7 and 8). As with the colluvial sample cortex is common towards the base of the LCTs, yet in this sample cortex occurs in almost all sectors (excluding 7) on both faces.

A summary of the data presented in Figures 4.4.136 and 4.4.137 is shown in Tables 4.4.62 and 4.4.63. The total colluvial LCT sector sample (n=132) shows that 60% of the sectors retain primary and secondary flaking (combined), and secondary 'edge refinement' occurs in 19% of these sectors (Table 4.4.62). This flaking coverage, by LCT type, shows that the picks and bifaces retain the greatest percentages (71% and 75%, respectively) of primary and secondary working; handaxes and cleavers show only 54% and 50%, respectively, for this flaking. Secondary flaking is most common in the bifaces (25%) and handaxes (21%).

Table 4.4.63 shows that the total debris flow LCT sector sample (n=384) has a largely comparable percentage (20%) of secondary working to the colluvial sample (19%), yet here the combined percentage of primary and secondary flaking is more abundant across the sectors (68%). By type, primary and secondary flaking is greatest on the picks (75%, as seen in the colluvial sample) and cleavers (72%). Handaxes and bifaces show the lowest percentages of primary and secondary flaking (63% and 61%, respectively). Secondary flaking is most frequent in the cleaver sectors, at 22%, and least common on the bifaces (17%).

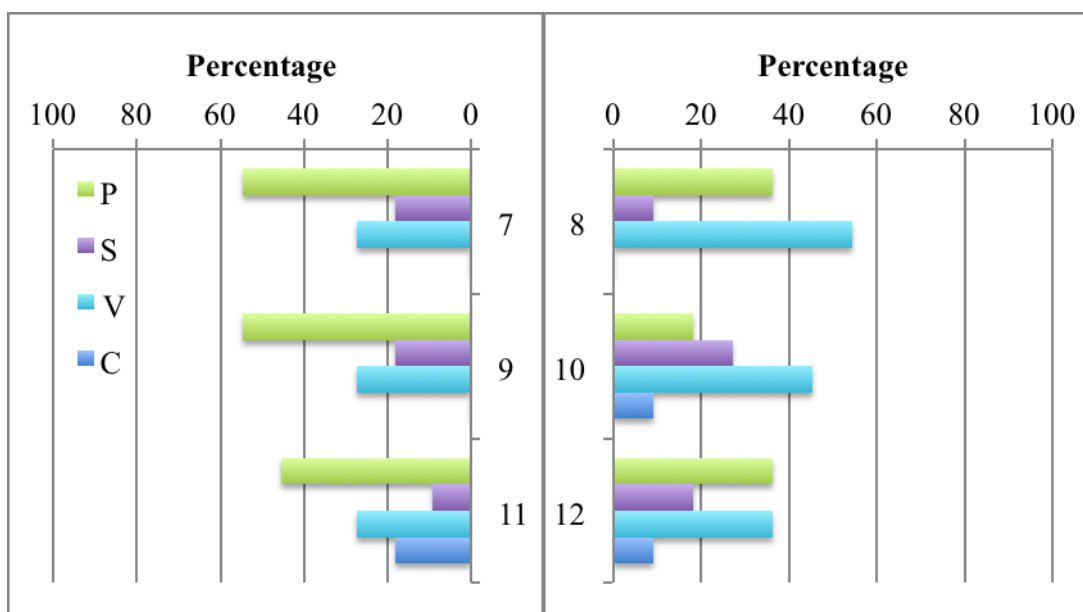
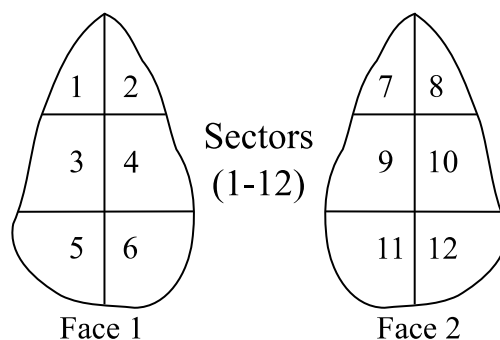
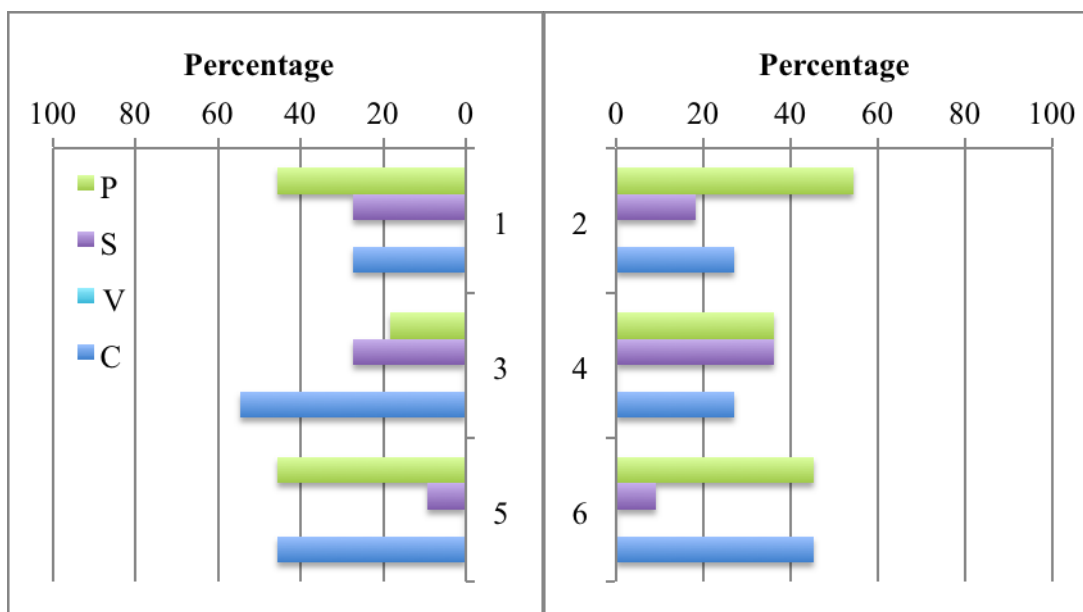


Figure 4.4.136. Flaking location for the colluvial LCT sample (n=11). P: primary; S: secondary; V: ventral/no working; C: cortical. For flake blanks the dorsal surface is recorded first (face 1, upper graphs) and the ventral second (face 2, lower graphs).

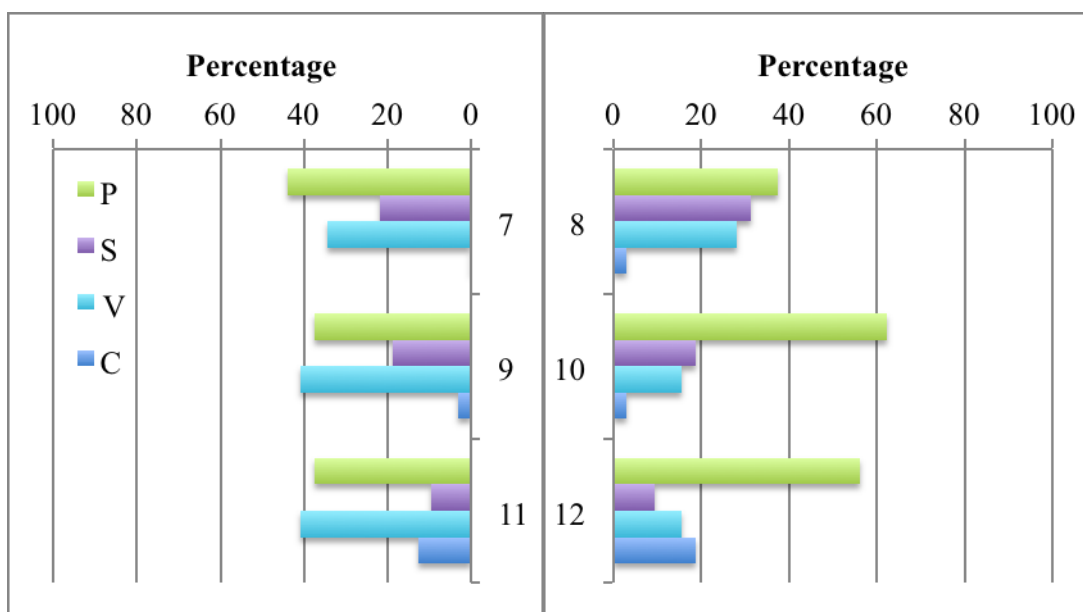
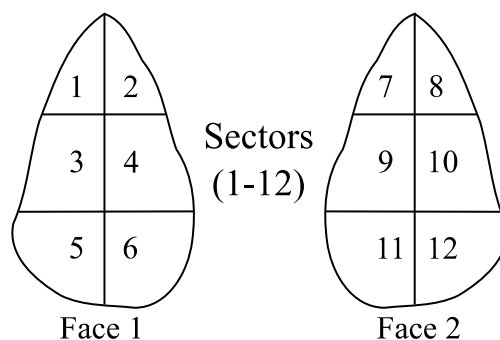
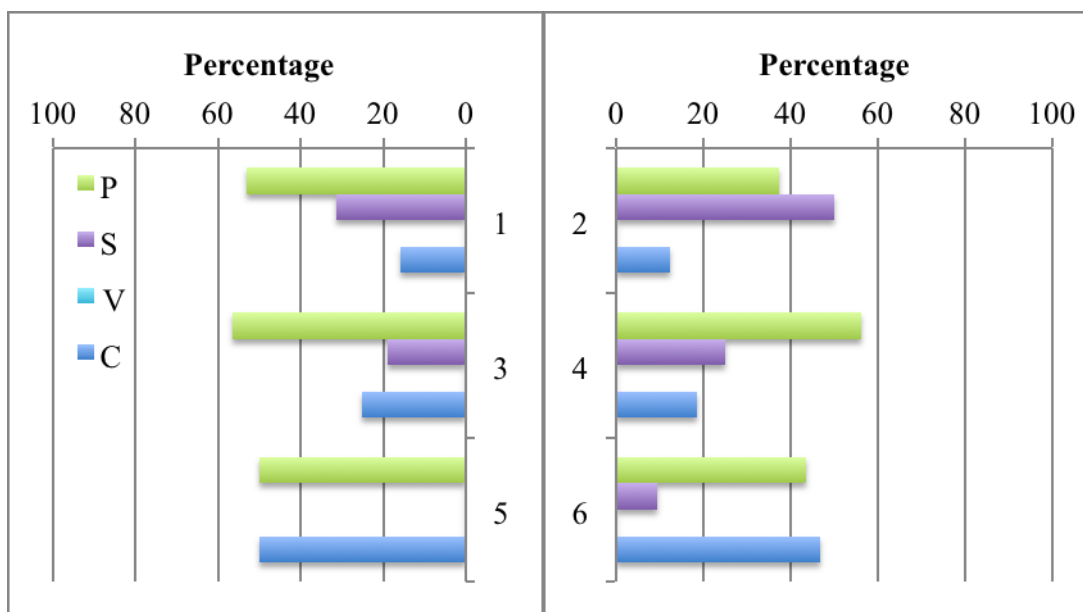


Figure 4.4.137. Flaking location for the debris flow LCT sample (n=32). P: primary; S: secondary; V: ventral/no working; C: cortical. For flake blanks the dorsal surface is recorded first (face 1, upper graphs) and the ventral second (face 2, lower graphs).

Table 4.4.62. Mean flaking coverage in the 12 sectors for the colluvial LCTs. Values below are discussed as percentages.

LCT sample	Sector sample	Mean flaking coverage		
		Type	Primary and secondary	Secondary
n=11	n=132	All	0.60	0.19
n=2	n=24	Pick	0.71	0.13
n=2	n=24	Biface	0.75	0.25
n=4	n=48	Handaxe	0.54	0.21
n=3	n=36	Cleaver	0.50	0.17

Table 4.4.63. Mean flaking coverage in the 12 sectors for the debris flow LCTs. Values below are discussed as percentages.

LCT sample	Sector sample	Mean flaking coverage		
		Type	Primary and secondary	Secondary
n=32	n=384	All	0.68	0.20
n=5	n=60	Pick	0.75	0.20
n=3	n=36	Biface	0.61	0.17
n=12	n=144	Handaxe	0.63	0.19
n=12	n=144	Cleaver	0.72	0.22

The percentage of remaining cortex on the colluvial LCTs shows that the majority has between 1-24% cortex (n=6, 54.6%; Fig. 4.4.138). By type this includes two quartzite bifaces, handaxes and cleavers (Table 4.4.64). No LCTs retain 0% cortex, or 75-100%, and those with the greatest percentage (50-74%) include a siltstone handaxe and cleaver, collectively accounting for 18.2% of the colluvial LCT sample.

Table 4.4.64. Remaining cortex on the colluvial LCTs.

Type	Raw material	Remaining cortex (%)					Total
		0	1-24	25-49	50-74	75-100	
Pick (n=2)	Quartzite	0	0	2 (100%)	0	0	2 (100%)
Biface (n=2)	Quartzite	0	2 (100%)	0	0	0	2 (100%)
Handaxe (n=4)	Quartzite	0	2 (100%)	0	0	0	2 (100%)
	Siltstone	0	0	1 (50%)	1 (50%)	0	2 (100%)
Cleaver (n=3)	Quartzite	0	2 (100%)	0	0	0	2 (100%)
	Siltstone	0	0	0	1 (100%)	0	1 (100%)

In contrast to the colluvial sample several debris flow LCTs retain no cortex at all (n=7, 21.9%; Fig. 4.4.139), all of which are comprised of quartzite (Table 4.4.65). Interestingly, those LCTs with 1-24% cortex are also comprised primarily of quartzite (n=11, 91.7% of this category). For those LCTs where the percentage cortex exceeds

25% (n=13), 61.5% are comprised of siltstone (n=8). A siltstone biface accounts for the most cortical (75-100%) LCT.

Table 4.4.65. Remaining cortex on the debris flow LCTs.

Type	Raw material	Remaining cortex (%)					Total
		0	1-24	25-49	50-74	75-100	
Pick (n=5)	Quartzite	0	3 (100%)	0	0	0	3 (100%)
	Siltstone	0	0	2 (100%)	0	0	2 (100%)
Biface (n=3)	Quartzite	0	2 (100%)	0	0	0	2 (100%)
	Siltstone	0	0	0	0	1 (100%)	1 (100%)
Handaxe (n=12)	Quartzite	4 (44%)	3 (33%)	0	2 (22%)	0	9 (100%)
	Siltstone	0	0	2 (67%)	1 (33%)	0	3 (100%)
Cleaver (n=12)	Quartzite	3 (33%)	3 (33%)	3 (33%)	0	0	9 (100%)
	Siltstone	0	1 (33%)	2 (67%)	0	0	3 (100%)

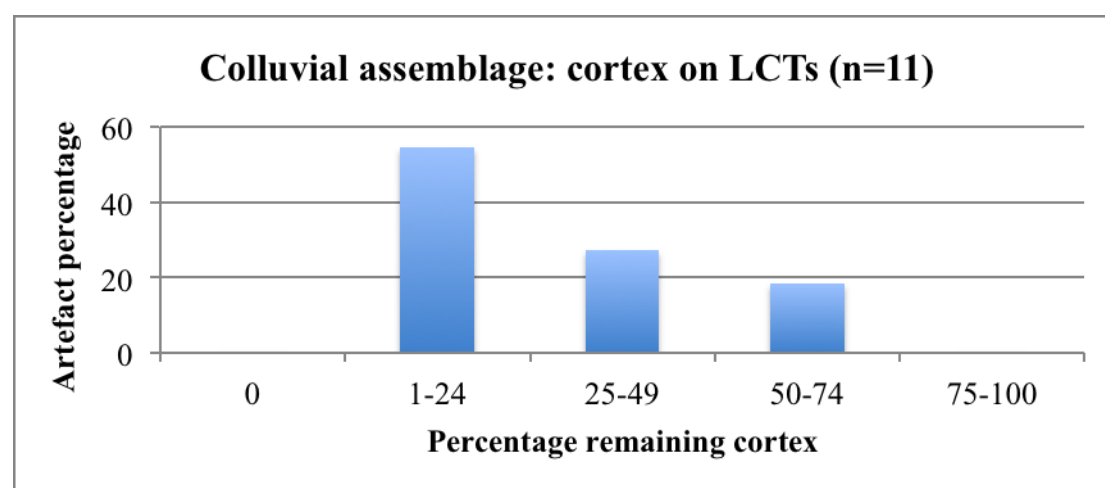


Figure 4.4.138. Percentage remaining cortex on the colluvial LCT sample.

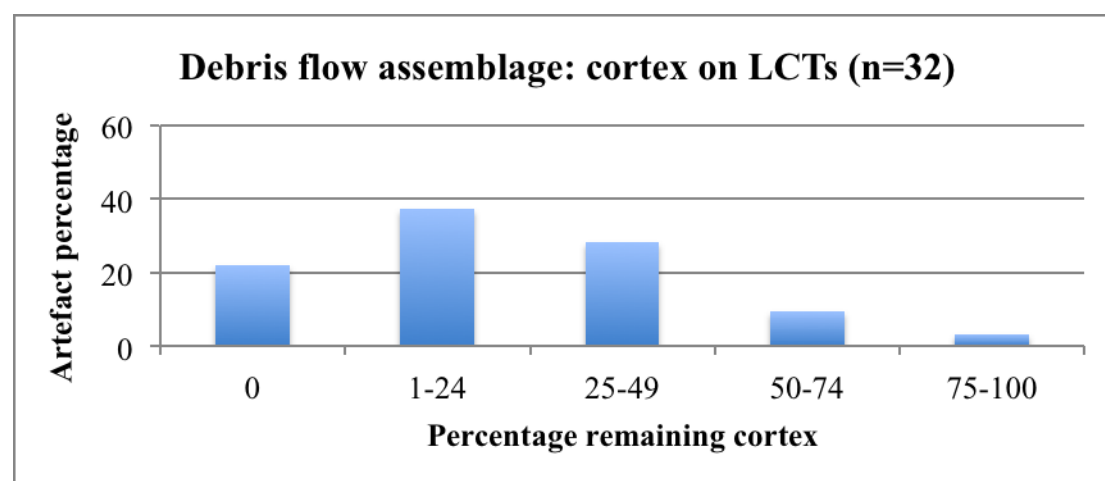


Figure 4.4.139. Percentage remaining cortex on the debris flow LCT sample.

Summary:

A detailed technological analysis of the Penhill Farm LCTs shows some interesting trends, by both type and raw material.

Handaxes are the largest and heaviest LCT type for the colluvial assemblage, and those made on siltstone are marginally heavier and larger than those on quartzite, even though quartzite types show the greatest variation in weight. The lightest pieces include quartzite picks and bifaces. Overall variation in length, width and thickness measurements is high in the colluvial LCTs, and by mean length all LCTs exceed 100 mm, except for quartzite bifaces which are notably small in length, width and thickness. Tool elongation (L/W ratio) is greatest for the quartzite picks and the handaxes (most elongated), and lowest for the cleavers and bifaces (least elongated). LCT refinement (T/W ratio) shows that quartzite handaxes and bifaces are the most refined, whereas quartzite picks and cleavers show high T/W ratios and thus poor refinement.

The debris flow LCTs show a clear trend in size for those made on both siltstone and quartzite, where those made on the former are heavier, larger, wider and thicker than those made on the latter. As a result siltstone picks, handaxes and cleavers account for the heaviest LCTs, whereas those lightest types include quartzite picks, bifaces and handaxes. Interestingly, mean lengths for all the siltstone LCTs exceed 100 mm, whereas none do for those on quartzite (except for the quartzite cleavers); quartzite LCTs also account for the smallest mean thicknesses. LCT elongation is greatest for the quartzite picks and siltstone handaxes and lowest for the quartzite bifaces and siltstone cleavers (as seen in the colluvial assemblage). However, LCT refinement is greatest on these quartzite bifaces and siltstone cleavers, and on the quartzite handaxes (also seen in the colluvial assemblage). Quartzite picks are also the least refined LCT type for this assemblage.

Only a single colluvial cleaver retained any kind of damage (partial edge break). This is in contrast to the debris flow where a higher number of LCTs (n=11) is damaged, including seven partial tip and four butt breaks. As a result LCT damage is more frequent in the debris flow.

LCT tip shapes show that generalised convergent types are the most common in both assemblages, accounting for 54.6% of the colluvial LCTs and 37.5% for the debris flow. In the colluvial assemblage this tip shape accounts for the majority of the handaxes and bifaces. Thereafter, by percentage, markedly convergent tips follow (18.2%), including one handaxe and one pick. The colluvial cleaver tip shapes are variable and those that do occur are unique to these tools. In the debris flow markedly convergent (mostly picks) and convergent oblique (mostly cleavers) tip shapes follow after generalised convergent shapes, and they each account for 25% of the LCT sample. As with the colluvial sample, both handaxes and bifaces are dominated by generalised convergent tip shapes.

A final note on cleaver morphology shows that rounded butt shapes are the most frequent for both assemblages at Penhill Farm. No cleaver butts are purposefully shaped though in the colluvial assemblage, and rather, these butt plans represent the naturally occurring shape of the utilised blanks. In the debris flow, however, two rounded and one squared butt were purposefully shaped this way, with the remaining shapes occurring naturally on the selected blanks.

Flake blanks are most favoured for LCT reduction, in both assemblages, yet the debris flow illustrates a greater range of blank types overall. This is likely due to the larger sample of LCTs in this assemblage. By raw material there is little data to suggest specific blank selection.

The number of scars on the Penhill Farm LCTs illustrates some interesting trends by both LCT and raw material type. In the colluvial assemblage siltstone LCTs have lower combined mean flake scar counts than those on quartzite. As a result quartzite handaxes account for the highest combined mean scar count (20.5 scars), also having the highest mean primary and secondary scar counts. For all the colluvial LCTs the mean quantity of secondary flake scars exceeds the quantity of primary flake scars, and for siltstone the differences between these mean counts is larger than those counts on quartzite. By type, picks and handaxes have the greatest total mean scar counts, and cleavers the least.

In the debris flow a contrasting pattern is seen in the LCTs where those on siltstone have higher combined mean scar counts than those on quartzite. As a result siltstone handaxes and cleavers account for the highest combined mean flake scar counts, and quartzite bifaces the least. Mean secondary flake scar counts are greatest for the siltstone picks, handaxes and cleavers, and once again the difference between this count and the mean primary scar count is larger on the siltstone pieces. By type, cleavers have the greatest total mean scar count, plus the greatest mean primary and secondary scar counts. Handaxes have the same quantity of secondary flake scars when compared to these cleavers, and bifaces show the least scars overall.

An assessment of the negative terminations of these flake scars shows little difference between the colluvial and debris flow LCTs. Both assemblages have similar proportions of feather, step and hinge negative termination types. This analysis is largely uninformative.

A detailed look at the location and extent of flaking on the Penhill Farm LCTs shows that bifacial pieces are most frequent in both assemblages. These types account for 63.6% of the colluvial assemblage (n=7) and 71.9% of the debris flow (n=23). Partly bifacial and unifacial LCTs are less frequent, although the latter are relatively more frequent in the debris flow, including three handaxes and two cleavers.

The location of primary and secondary flake scars, by sector, shows that secondary flaking is more common towards the medial and distal sectors of all the Penhill Farm LCTs, with little in the proximal (basal) sectors. Primary flaking occurs throughout almost all sectors for the LCTs in both assemblages. Predictably, proximal sectors have the greatest cortex preservation; however, in the debris flow LCTs this cortex occurs in a greater number of sectors on both faces. By percentage only 60% of all the colluvial LCT sectors show both primary and secondary flaking, with only 19% showing secondary flaking. The combined debris flow LCT sectors show a largely comparable percentage of secondary working yet here the combined percentage of primary and secondary flaking is higher at 68%.

By type the colluvial assemblage shows that picks and bifaces have the greatest percentages of primary and secondary flaking, across the sectors, whereas handaxes

and cleavers have the lowest. Secondary shaping is greatest in the biface (25%) and handaxe (21%) sectors. For the debris flow, picks and cleavers have the most primary and secondary working, across the sectors; handaxes and bifaces have the least. Secondary flaking is greatest on the cleavers, at 22% of all sectors, and lowest in the bifaces.

The final data to be summarised here concerns the amount of preserved cortex on the Penhill Farm LCTs. Both assemblages show an abundance of LCTs with 1-24% cortex. In the colluvial assemblage no LCTs show 0% or 75-100% cortex, and siltstone LCTs are generally more cortical than quartzite LCTs. This pattern is also seen in the debris flow, where 61.5% of those LCTs with >25% cortex are made on siltstone. Those produced on quartzite show less cortex preservation, especially evident for those LCTs with 0% cortex (n=7, all exclusively made on quartzite).

4.4.4.4 Modified and split cobbles (Other)

A limited number of other artefacts was recovered from Penhill Farm (Table 4.4.66). The colluvial assemblage has only a single quartzite split cobble and the remaining pieces are all from the debris flow (two split cobbles and a single large modified cobble).

However, the significance of this data is limited due to the small sample of artefacts.

Table 4.4.66. Split and modified cobble data from Penhill Farm.

Type	Assemblage	Weight (g)	Raw material	Length (mm)	Width (mm)	Thickness (mm)
Split cobble	Colluvial	264.36	Quartzite	93	60	46
Split cobble	Debris flow	99.58	Siltstone	59	38	34
Split cobble		123.23	Quartzite	52	45	37
Modified cobble		1436.29	Siltstone	149	110	70

4.4.5 Residue and use-wear analysis

A single debris flow utilised complete flake was analysed by G. Langejans for use-wear and residue preservation (Fig. 4.4.140).

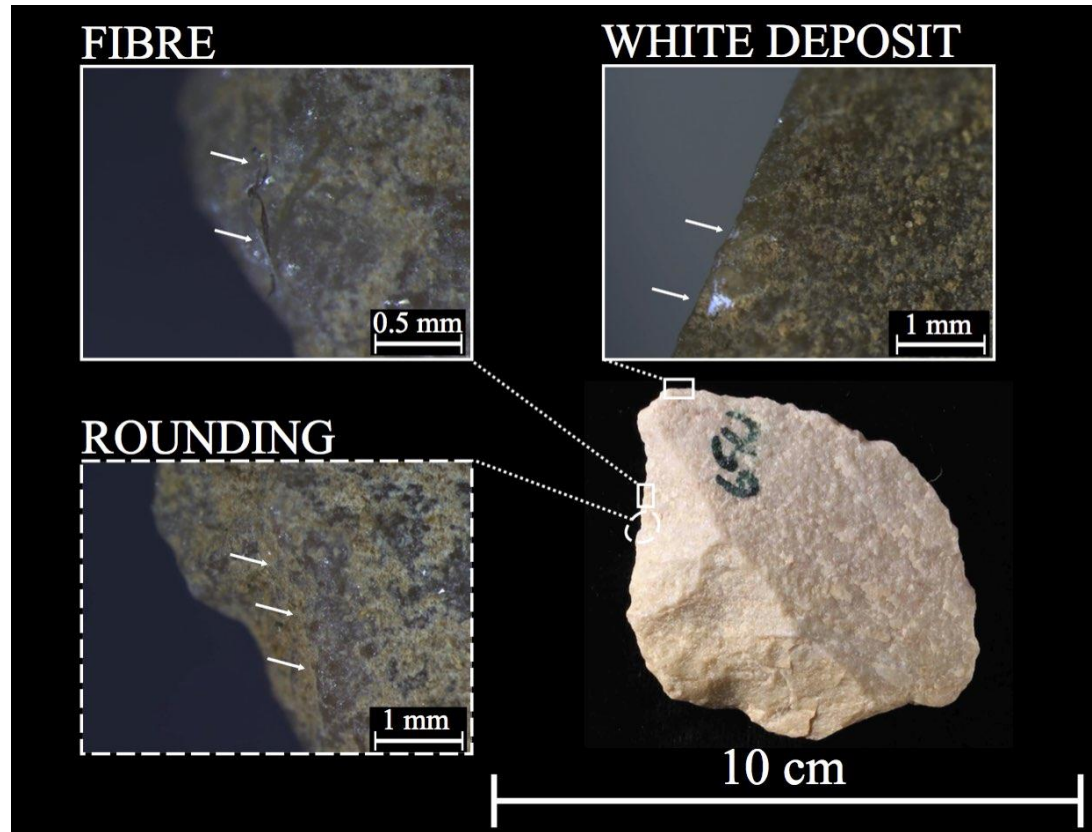


Figure 4.4.140. Use-wear and residue analysis on a complete flake (magnified images courtesy of G. Langejans).

By examining the edges of the flake (those shown in Figure 4.4.140) the following features were identified: fibres, most likely cotton due to their flat shape and colour; a white surface deposit that is ‘fluffy’ in appearance, most likely some form of fat deposit introduced onto the artefact surface post-depositionally or during analysis and handling; and edge rounding that is discontinuous and occurs on ridges close to the edge of the artefact, potentially indicating use-wear. The analysis of a larger sample of artefacts is needed to confirm the prevalence of these features.

4.4.6 Non-lithic material

Non-lithic data, for the Penhill Farm assemblages, is presented in Tables 4.4.67 and 4.4.68. A sample of bone and shell fragments is presented in Figure 4.4.141.

From these data it is clear that the preservation of organic remains is extremely limited, especially in the debris flow assemblage where the total combined weight for organic material is 4.72 g; this assemblage also preserved no charcoal and eggshell. Although by weight the colluvial assemblage has more material, a single large bone fragment (28.09 g) makes up the majority of the total sample weight (30.23 g). Overall, snail shell fragments are most frequent in the colluvial assemblage (n=19) whereas bone is most common in the debris flow (n=40).

Table 4.4.67. Colluvial assemblage non-lithic material.

Type	Number of fragments	Weight (g)
Bone	4	*28.40
Charcoal	5	0.36
Eggshell	1	0.27
Snail shell	19	1.20

*Heaviest bone fragment weighed 28.09 g

Table 4.4.68. Debris flow assemblage non-lithic material.

Type	Number of fragments	Weight (g)
Bone	40	*4.70
Charcoal	0	0
Eggshell	0	0
Snail shell	2	0.02

*Heaviest bone fragment weighed 0.85 g

The extremely fragmented nature (and small size) of these non-lithic remains meant faunal identification on bone was impossible. Performing a chemical analysis on these fragments (e.g., on tooth fragments specifically; <40% of the total bone sample) was also not possible due to the poor preservation of these pieces and their likely contamination by water.



Figure 4.4.141. Non-lithic material obtained from Penhill Farm. Small snail shell (a) and bone fragments (b) are shown.

Chapter 5

Discussion

5.1 Introduction

This discussion will be presented in three sections. The first will summarise and discuss the significance of all findings, by site, relating to context, artefact typology and technology. Where relevant, all data obtained on non-lithic material will also be discussed here. Thereafter, the second and third sections will provide an inter-site comparison between the Sundays River assemblages, followed by a comparison with other local and international Acheulean sites, respectively.

It must be emphasised here that research at Atmar Farm is very limited due to poor preservation and at Bernol Farm it is preliminary because the majority of excavation time was spent at Penhill Farm. The overall significance of these two sites is therefore limited and the conclusions presented herein must be considered in light of the small samples. As a result the majority of this discussion will address the larger and well-preserved assemblages at Penhill Farm.

5.2 Atmar Farm

5.2.1 Site context

Only basic contextual data are provided for Atmar Farm. That which is presented confirms what is to be expected for a secondary context alluvial gravel deposit. Artefact size distribution data show that the majority of the smallest assemblage components is absent as only 13% is <20 mm in size. The range of artefact sizes, although nearly complete, clearly illustrates a heavy bias towards pieces larger than 20 mm and smaller than 80 mm; those that are larger are present but infrequent.

Studies investigating the size distribution of artefacts (Schick 1987, 1991, 1997; Kuman & Field 2009) show that a high percentage of SFD (60-87%), coupled with a full size range of artefacts (thus refuting lithic re-concentration) and the presence of flakes and cores, characterises a site of primary knapping activity. Low SFD percentages are likely due to the removal of these components by some kind of natural site modification process, and/or, the possibility that knapping did not take place on-site (Schick 1987, 1991, 1997; Kuman & Field 2009).

A basic typological analysis at Atmar Farm indicates that both cores and flakes occur within the discontinuous gravels, and the majority of these is cortical. This overall pattern suggests that knapping did occur on or within the catchment of Terrace 10 (Kuman & Field 2009), and the reason for SFD removal is due to site formation processes. As a result the representation of this knapping appears distorted. It is likely that the smallest assemblage components were winnowed away and re-distributed downstream due to fluvial action (Schick 1991). It is also likely that this small material became re-concentrated somewhere downstream where flow velocity was reduced, somewhere beyond the boundaries of our excavations (Schick 1991).

This fluvial action may also account for the general 'low density' of artefacts within the gravels at Atmar Farm. It would appear that the original site/s where lithic reduction took place were located further upstream. Lithic material then became

incorporated into the Sundays River, through time, and this material was then re-distributed downstream across a larger area, mixing with natural gravels and cobbles as it was transported. This would give rise to the diffuse distribution of artefacts that occurs on-site today (Schick 1991).

Artefact condition and raw material data further illustrate the influence of these fluvial forces, clearly seen in the modified condition of the Atmar Farm artefacts. The condition of an artefact is dependent upon the type of raw material used (as each will weather in a specific way), and on the rate and type of weathering/abrasion, which will reflect the type and intensity of the erosive process involved (Shackley 1974; Pappu 1996; Shea 1999; Holmes *et al.* 2008; Thompson 2009). The vast majority (78%) of the artefacts at Atmar Farm has slightly to heavily abraded/rolled exterior surfaces, which would suggest that the artefacts were re-worked within the fluvial system for a considerable period of time (Shea 1999). Fresh artefacts are less common and this suggests their inclusion into this system took place at a later point in time, or, that their transport downstream took place over a shorter distance prior to deposition (Shea 1999). Conversely, the opposite could be said for those more abraded pieces.

Although the influence of raw material on artefact condition is important, quartzites are the most common material and all other types are rare. There is only a minor difference in the condition of artefacts by material type. This is most relevant for the small hornfels sample, which indicates a susceptibility to *in-situ* weathering (likely linked to the moisture content of the deposit; see Chapter 2.3 discussion on Ubeidiya by Shea 1999).

The absence of non-lithic material is also mainly linked to the contextual nature of the Atmar Farm alluvial deposit. Based on the largely abraded condition of the lithic material, it appears unlikely that bone or any other organic material would be adequately preserved. Another contributing factor may have been the moisture content of the deposit both during and after deposition, which may have aided in the breakdown of non-lithic material that was potentially incorporated in the deposit.

5.2.2 Typology

The small and poorly preserved lithic assemblage from Atmar Farm comprises 345 pieces, the vast majority of which are produced on quartzite. The limited size of this assemblage, coupled with the general poor condition of the artefacts, meant that detailed analysis could not be conducted. As a result our understanding of this site is extremely limited.

A basic typological classification of the lithic assemblage shows that flaking debris is most common. Unfortunately this is the least informative group of artefacts and little can be said regarding the assorted sample of SFD, incomplete flakes, flake fragments, and chunks. This does, however, suggest that some lithic reduction was occurring within the catchment of the site, and this material subsequently became incorporated into the gravels. The SFD was predominantly re-distributed elsewhere.

The small complete flake sample shows a slight preference for side- and corner-struck flake production. In addition to this a single core trimming flake suggests an understanding of core management, where a platform has been adjusted to assist in flake removal.

The small core sample illustrates that the knapping of quartzite cobbles was most favoured. These were worked through simple reduction strategies, with casual cores and unifacial and bifacial chopper-cores most common; discoids are uncommon and there is no evidence for bipolar reduction. Core scar counts also indicate that the quantity of flakes removed is minimal, and overall cortex preservation is high. This would suggest a non-intensive use of raw materials, most likely due to the abundance of quartzite cobbles that were readily available nearby.

Although an assessment of the largest flake scar length was not conducted on the Atmar Farm cores, there is a lack of large (>10 cm) flake removals. It would appear that the emphasis was on small flake production, versus large flakes that could have served as blanks for LCTs. Either the fluvial forces were not strong enough to

incorporate the larger cores, or large flake production may have been conducted on boulders, and LCT blanks were transported to the area.

The formal tool sample at Atmar Farm is extremely limited (n=7) but some interesting observations can be made, the most significant of which is that for a very limited formal tool sample the quantity of retouched flakes (n=2, a denticulate and denticulated scraper) is marginally less than for the LCT sample (n=3). Although this assemblage is of secondary context and contains mixed contents, either way this suggests the importance of small retouched tools and LCTs in the local landscape (within the catchment of the site).

Quartzite flakes are favoured for the six formal tools, although a single unifacial handaxe is produced on a hornfels flake. Interestingly, there is almost a complete absence of hornfels in the complete flake and flaking debris samples (only one hornfels flake and two SFD), and no cores are made on hornfels. The mixing of assemblage components from multiple sites, and subsequent deposition in the gravels, may account for the presence of this hornfels LCT and the general absence of material that would indicate its production and/or reduction.

Retouched artefacts (a denticulate and a denticulated scraper) at Atmar Farm are informal. Flake blanks are favoured for tool production and the overall character of edge refinement shows little standardisation. This is clearly seen in the sporadic, discontinuous, nature of tool retouch and the noninvasive extent of the removals. In addition to this the majority of retouch is unifacial and geared towards creating a denticulated scraper or cutting edge. In contrast, the single bifacial chopper illustrates slightly more extensive edge shaping, yet overall, the small formal tool assemblage shows simplicity in its production.

The three LCTs (handaxe, biface and cleaver) are produced on large corner-struck flakes, and the unifacial handaxe and cleaver show a high level of cross-sectional symmetry. This appears to be the result of the blanks utilised in production, which overall are thin and well-suited as LCT blanks. Both of these LCTs also retain a significant amount of dorsal cortex, yet the need to remove this and thin the biface further appears unnecessary. There has also been only minor shaping of the flake

ventral surfaces (as there appears no need), and small removals are most frequent towards the edges of these two LCTs, to provide some basic edge refinement, plus some tip shaping is present in the handaxe. In contrast to the unifacial handaxe and cleaver, the quartzite biface shows that a much larger flake blank has been utilised, one that is great in cross-sectional thickness and one that bears little symmetry overall. In addition this biface is characterised by a series of large, invasive, primary removals that shape the tool, likely an attempt to thin the biface. Although the condition of this piece is poor, secondary edge refinement appears absent.

Is it possible that this biface represents LCT reduction from a different time period? We know that the Atmar Farm gravels are of secondary context and that the assemblage contains mixed contents, potentially from one or more sites further upstream. It is also likely that lithic material from this/these site/s was incorporated into the river at different periods, and it would not be impossible for older artefacts to become mixed in with younger ones, and then be deposited together. The overall condition of this LCT is far poorer (significantly heavily abraded/rolled), which suggests that it has either been transported further or, that it has been within the river for a longer period of time. Either way there is a limit to what can be concluded for such a small LCT sample, and without the detailed analysis of a larger sample this must remain purely speculative. From a contextual perspective this piece is interesting though, but these differences in LCT production should, at present, rather be taken to represent the variability in reduction strategies.

5.2.3 Final comments

Overall, Atmar Farm is a low quality site that provides a small poorly preserved, minimally informative, later Acheulean assemblage from Terrace 10; overbank fine deposition here is dated to 0.65 ± 0.06 Ma (Erlanger *et al.* 2012). It is unfortunate that the density of artefacts in the gravels is so sparse. It is also unfortunate that the preservation of artefacts is so poor, and that organic material is almost completely absent (including phytolith and pollen remains). It is clear that the Atmar Farm assemblages are a product of their context and as a result further excavations at Atmar Farm would not be required or be worthwhile.

However, with more surveying on the property it may be possible to find denser concentrations of artefacts elsewhere, both in the gravels and potentially also in the fine sediment overburden. A preliminary investigation into these fine sediments suggests that typologically younger artefacts occur towards the upper portions of this deposit, and even if these are derived from the surface there is the potential that a dense concentration may occur somewhere. Finding such a site though that is not disturbed by local farming (orchard) activities is unlikely. Terrace 10 exposures are not only limited to Atmar Farm and others occur in the lower Sundays River Valley. For future work it may be possible to locate these exposures and conduct excavations in more favourable deposits.

5.3 Bernol Farm

5.3.1 Site context

Only basic contextual data is provided for Bernol Farm and this primarily relates to the condition of the artefacts. This data confirms that although the artefacts are from secondary context gravels and fine sediments at the dated location, or from the four survey sites that are either colluvial and/or alluvial in origin, overall artefact damage is minor. This is shown by the fresh appearance of the majority (74%) of the artefacts; none is heavily abraded/rolled.

This finding confirms that the re-working of artefacts was minor, and perhaps this also indicates that whatever transport there was of these artefacts, that this took place over only a short distance (Shea 1999; Thompson 2009). In addition to this the presence of bone and shell at Bernol Farm attests to favourable preservation conditions for both lithic and non-lithic material. Unfortunately more research is needed to fully understand the contextual nature of the four survey sites. This is of vital importance considering that the majority of the sampled artefacts is from these areas, and thus the artefact condition data above relates more to these sites than to those gravel stringers at and near the dated location. At the current stage of analysis, artefact condition data can therefore only be used to show that artefact damage is minor, but the reasons for this (for e.g., moderate fluvial action or colluvial wash) cannot be confirmed at present.

5.3.2 Typology

Bernol Farm has provided a small (n=19) sample of quartzite artefacts comprised primarily of formal tools (n=11 LCTs). Little can be said regarding these assemblage components, but what is apparent from the core and flake sample is the production of large flakes occurred locally as there are large flake scars on the cores. This is also seen in the LCTs as the majority is on large flake blanks. In general for those cores sampled at Bernol Farm reduction strategies are simple, seen in the basic chopper-

cores and discoidal cores. It also appears that boulder-cores were reduced locally (as shown in Chapter 4.3; Fig. 4.3.4) to provide large flakes, possibly serving as LCT blanks.

As handaxes and cleavers dominate this selected collection, little can be said regarding the percentage frequency of these formal tool types, but the sample includes both a pick and biface. This illustrates the varied production of LCTs at Bernol Farm following multiple approaches, which will be discussed in more detail below.

5.3.3 Technology

Technological data at Bernol Farm was obtained only on the small sample of LCTs.

5.3.3.1 LCT size and shape

The limited sample of quartzite LCTs makes it difficult to assess differences in overall size and shape between the LCTs, especially as some only have a single piece (e.g., one pick), but what is clear is the high level of variability in these measurements. Illustrating this most clearly would be the Bernol Farm cleavers (n=6), which by weight alone range from approximately 120 g for the lightest piece up to 1000 g for the heaviest. Tool elongation and refinement ratio data, which is regarded as being useful to distinguish between different assemblages (Shipton & Petraglia 2010), also illustrates variability between the LCT types. Irrespective of this variability the sampled LCTs illustrate a size and shape difference between the handaxe and cleaver samples, where the former are smaller, lighter, and more refined, versus the latter that are heavier and larger, and more elongated. The limited samples for these pieces must be considered though, and these trends must be treated with caution.

Another important aspect of the Bernol Farm LCTs is the variability in tool tip shape, an aspect of LCT morphology that has been discussed by McNabb *et al.* (2004). These authors originally discussed the classification of tip shape (along with other aspects of LCTs) in an attempt to question the role of social traditions and what

impact these may have had in the standardisation of tool morphology. There are several factors that influence tool morphology, some of which may include: skill of the knapper, time constraints, raw material constraints, social factors and controls, and blank type and size (McNabb *et al.* 2004). These are clearly important issues, yet for the Sundays River assemblages I will talk more broadly about tool use (function) than what role these pieces played within a social setting.

These authors note that different tip shapes indicate that tools would have been conceived of very differently and would then have been reduced differently to produce the desired result (McNabb *et al.* 2004). Another important point they discuss is that cores may have been systematically worked to produce large flake blanks for LCTs, but that the blanks themselves may not have been standardised in overall shape and size and this may account for some of the variability in LCT sizes and shapes (McNabb *et al.* 2004). At Bernol Farm perhaps these two points are relevant. The variability in tool tip shapes, although showing a preference for generalised convergent types, may indicate a clear differentiation in tools based purely on a functional response to a given task at hand. Tool reduction would then have followed a specific strategy to create the desired tip shape for a given activity. In addition to this the overall variability evident in tool measurements may have been influenced by tool blank shape and size, as this process may have been poorly controlled when cores were reduced. Once again without a larger sample of LCTs and without more detailed analysis this must remain speculative. What can be said of the Bernol Farm LCTs though is that sizes and shapes are variable, as are tip shapes, and that these tip shapes would have been uniquely and carefully shaped (possibly for a range of different activities).

5.3.3.2 LCT reduction

The production of LCTs at Bernol Farm takes place primarily on large flake blanks. This is a clear indication that the production of large flakes was important at the time. The presence of a single large boulder-core near the dated location at Bernol Farm suggests that these flake blanks may have been obtained from generally large, possibly immovable boulders. These may have been located close to the original river at the time, or they may have been sourced away from the river higher upslope, where

older river terraces contained suitably large material. A larger sample of cores from the Bernol Farm property would be needed to assess this idea.

Scar counts on the Bernol Farm LCTs are important to assess the level of artefact reduction, the simple premise being that a higher flake scar count indicates a greater level of reduction/shaping (Li *et al.* 2015). In addition addressing the emphasis on tool shaping (primary flaking) versus edge refinement (secondary flaking) can be performed by quantifying each of these flake scars by type, the premise here being that a higher secondary scar count will indicate an emphasis on tool edge refinement (Kuman *et al.* 2014; Li *et al.* 2015). An assessment of negative flake scar termination types proved to be uninformative.

LCT scar counts show that the biface and handaxes retain the highest combined primary and secondary scar counts, followed by the picks and cleavers. This indicates a higher level of reduction/shaping for the biface and handaxes. However, this count must be considered in relation to overall tool size to make it more informative (Li *et al.* 2015), and doing so shows that the handaxes and biface, the smallest LCTs, are in fact the most reduced. The larger cleavers and pick are less reduced based on the lower flake scar counts.

An assessment of which LCTs have an emphasis on shaping versus edge refinement shows that for the majority secondary flake scar counts exceed primary. Overall this suggests an emphasis on edge refinement; however, for the pick this clearly relates to the careful shaping of the markedly convergent distal tip. Interestingly, the small handaxes have a higher number of primary removals than secondary removals, which may indicate an attempt to reduce tool thickness effectively prior to regularising the edges.

Another important way of assessing LCT reduction, in conjunction with the simple scar counts above, is to assess the overall location and coverage of these scars across LCT surfaces. The 12-sector method recently developed by Kuman *et al.* (2014) was utilised in this research, and it is suggested here that such a method should always be implemented in conjunction with the simple scar counts above. The reason for this is that secondary scars are generally smaller and less invasive than primary scars. Using

the 12-sector method alone, which will classify a sector as having 'secondary flaking,' based only on whether this flaking covers 50% or more of a given sector, does not take into account that secondary flake scars by nature are smaller and are generally concentrated along smaller areas of the tool edge. As a result many sectors that contain secondary retouch may be classified as primary, as these scars cover a greater portion of any given sector. By having an individual count of these secondary scars, coupled with an assessment of the location of where they occur, a more accurate understanding of LCT reduction can be achieved.

The location of these flake scars shows that the majority of the LCT sample (n=8) has been reduced and shaped bifacially, so although the scar counts may be low for some LCTs the overall distribution/location of these scars shows an emphasis on reduction across both faces of the tools in all sectors. The variability in flaking is minimal based on this pattern. However, cleavers are the only type to show a range of reduction patterns, including partly bifacial and unifacial types. Cortex is predominantly found on the proximal (butt) sectors of the LCTs on both faces, but primary and secondary shaping/edge refinement of these butts also occurs.

An assessment of the overall percentage of secondary flaking (edge refinement), by sector, illustrated a general lack thereof (only 13% of all sectors); primary and secondary flaking when combined is extensive (70%). Once again this relates back to the inability of the 12-sector method to quantify the less extensive secondary retouch by sector. Referring back to the total scar counts, the quantity of secondary scars generally exceeded the quantity of primary, and based on this it would appear that secondary edge refinement (or tip shaping for the pick) was important in the Bernol Farm LCTs.

A final indication of the level of reduction can clearly be seen in the percentage of remaining cortex. Overall, the majority of LCTs (n=7, 64%) is either 0% or 1-24% cortical. In addition none has cortex that exceeds 50%. This pattern confirms what has been discussed above, that LCT reduction has generally been substantial across the majority of all sectors on both faces; bifacial flaking including both primary and secondary removals covers the majority of these sectors.

5.3.4 Use-wear and residue analysis

The single handaxe from Bernol Farm studied by G. Langejans was shown to have three different organic residues, as well as discontinuous edge rounding that suggested tool use. However, one must interpret these observations conservatively. Although there are preserved organic residues these may rather be some kind of contaminant that was introduced onto the artefact surface during analysis, or whilst the artefact remained *in situ* (possibly through root growth). The same explanation is most likely applicable for the fibres found covering the artefact surface; these may be derived from some kind of cloth or fabric that artefacts were placed upon during analysis. The remaining green deposit is most likely the result of bacterial/algal growth in the sample bag of the artefact (due to condensation).

With reference to the use-wear damage, if an artefact is re-worked within a deposit one would assume natural edge damage to be more extensive and continuous across the piece. In this case the handaxe shows distinct rounded edges that are discontinuous and concentrated only on the distal edges of the tool. This may possibly indicate use-wear damage, but without a more detailed analysis of a larger sample of artefacts from Bernol Farm these ‘edge-wear’ results are purely speculative.

5.3.5 Final comments

Bernol Farm provides a complex and interesting exposure of Terrace 9 deposits, which at the dated location yields an age of 1.14 ± 0.2 Ma (Granger *et al.* 2013). A major issue though is understanding the contextual nature of the survey sites and how these relate to the dated alluvium for Terrace 9. Irrespective of this, Bernol Farm does preserve Early Acheulean artefacts in fine alluvium, along with partially fossilised bone and other shell fragments (but no phytolith and pollen remains) and the potential of this site is therefore high. With careful survey and excavations in the future this site may provide some very well-preserved Acheulean assemblages from which we can further enhance our understanding of the local Acheulean Tradition. This work may also provide a sample of faunal material from which we can begin to understand more clearly the local habitat during the time of occupation.

5.4 Penhill Farm

5.4.1 Site context

5.4.1.1 Sediment PSD analysis

These results are in accordance with what we currently understand about the site and surrounding landscape (discussed in Chapter 3.2), and based on the subdivision of five deposit types, important differences are evident both in the level of grain sorting and in the percentage of fine and coarse material between these samples.

The alluvium at Penhill Farm is well-sorted and has the highest percentage of fines (clays to fine silts). This illustrates the influence of water in promoting grain sorting and provides an indication for the low energy floodplain deposition that gave rise to the Terrace 9 alluvium. Schick (1984) notes that if clays and silts are the only material available in the local landscape, then flow velocities can still be high, as this is the only material available that can be transported, but this seems unlikely at Penhill Farm for the fine alluvium.

Upslope from the excavation there are several bedrock outcrops. The analysis of these crushed bedrock sediments shows a high level of grain sorting and, for two of the four samples, a high percentage of fines. Still upslope of the excavation, but lower than the bedrock outcrops, the sampled colluvial sediments show a drop in the level of fines and indicate a much lower level of grain sorting. This is to be expected for colluvial sediments where there is a winnowing of the finest components and the re-distribution and mixing of material in the local area, downslope, both of which are likely the result of some kind of surface wash/flow.

These alluvium, bedrock and colluvium samples characterise the local sediments within which the erosion channel developed. This is further supported by the sampled alluvium that occurs beneath the erosion channel (under the debris flow), which also shows a high level of grain sorting and higher percentages of fine material.

Accordingly, this channel formed by eroding into the fine, well-sorted host alluvium. Thereafter, this channel was filled with colluvial sediments that would have been washing in from upslope. Understandably, these should be poorly sorted and be devoid of most of the finer material (clays and fine silts), and based on the analysis of these samples this is what we find. At the base of the erosion channel occurs the debris flow sediment. This sediment is remarkably similar to the upslope colluvial sediment, which is to be expected considering that this deposit is comprised of similar sediments from upslope.

During the infilling of the erosion channel with colluvium, a number of smaller channels developed where sediment and water flow became channelised. These channels contain a range of materials, all of which is sorted, imbricated and, in places, clast-supported. The sediments from within these features also illustrate a high level of sorting and an absence of fines. This is to be expected due to the likely influence of hydrological processes (e.g., sheetwash/flow).

5.4.1.2 Artefact size distributions

Size profiles for both assemblages at Penhill Farm indicate some interesting differences and similarities; these data talk to the contextual integrity of the assemblages.

Both assemblages contain a near complete size range of artefacts coupled with the presence of cores and flakes. This would suggest that the removal of assemblage components has been minor, and that knapping is likely to have occurred within the catchment of the site (Schick 1991, 1997; Kuman & Field 2009). The only major difference between these assemblages is in the percentage of material <20 mm, which is far less abundant in the overlying colluvial assemblage when compared to the lower lying debris flow. Although both of the assemblages at Penhill Farm are ‘colluvial’ in origin, this difference in the smallest assemblage components is clearly important.

Perhaps this can be linked primarily to the way in which the two assemblages formed through time. The debris flow assemblage represents a single debris flow event, or multiple smaller debris flows difficult to distinguish between, that collected most if

not all of the artefacts upslope of the site. These were then rapidly deposited into the base of the erosion channel. Debris flows can be slow or rapid events (Charlton 2008). The fact that there is a high percentage of SFD supports rapid deposition, as the majority of the upslope contents would have been transported downslope and buried quickly, thus preserving the contents of the assemblage and reducing the potential for assemblage winnowing (Schick 1991, 1997; Kuman & Field 2009). Artefact condition data further supports rapid burial as the vast majority of artefacts is extremely fresh and indicates favourable preservation conditions (versus long term surface exposure; Shea 1999; Thompson 2009).

The high percentage of SFD in the debris flow assemblage does not appear to be the result of some kind of fluvial re-concentration. This is due to two important features. First, artefact spatial arrangements are completely random and do not indicate the preferential re-distribution of assemblage components based on size, either vertically or horizontally, and thus all forms of sorting and grading are absent (Schick 1991). Second, artefact depositional (fabric) data show very poor preferential orientations and trends in dip angles, which would again suggest a lack of fluvial influence (Petraglia & Potts 1994). Although there is the possibility that some of the smallest assemblage components were winnowed away, this appears to have been minor and the overall integrity of the debris flow assemblage is high.

In contrast, the upper colluvial assemblage appears to represent somewhat slower, more punctuated deposition of the upslope colluvium, after and on top of the debris flow. As a result, this deposition may have left artefacts exposed at the surface for longer periods, thus making them more susceptible to winnowing through natural processes. Slower deposition also appears likely based on artefact condition data for this assemblage, which shows that fewer artefacts retained a fresh exterior condition (when compared to the debris flow). Exposed artefacts could then have been winnowed through rain splash or sheetwash/flow erosion (Goldberg & Macphail 2006; Charlton 2008; Anderson & Anderson 2010), or even some form of rill and gully erosion (Boardman *et al.* 2012) that channeled away these assemblage components. Channel features do occur within the colluvium overlying the debris flow, and these features clearly show the imbrication of clasts and sorting of material; this supports the modification of these features, and the smallest assemblage

components within these would definitely have been susceptible to removal and redistribution elsewhere. Overall, it appears that the potential for artefact winnowing in the colluvial assemblage is far greater due to possibly slower deposition and longer surface exposure, and most likely, the greater influence of hydrological forces that would cause winnowing. It is also possible that the colluvium was affected to some degree by bioturbative processes, which may account for the general lack of stratigraphy in this deposit (Stein 1983; Erlandson 1984; McBrearty 1990; Morton 2004; Anderson & Anderson 2010; Lotter *et al.* 2016).

A cautionary note must be made here regarding these differences in burial for the two assemblages. Overall, the deposition of the colluvial assemblage need not have taken place that much more slowly than that of the debris flow assemblage. To be more conservative, perhaps this lower percentage of SFD in the colluvial assemblage could simply be the result of more winnowing than a result of slower deposition. It may also be more related to the catchment of the site, as a significantly smaller portion of the assemblage may have remained upslope after the debris flow had swept the majority of it away. Those artefacts that occur above the debris flow in the colluvium may therefore be the last remnants of a single assemblage that was sporadically deposited later in time above the debris flow. This will be addressed again in greater detail towards the end of this section and in the following typology and technology sections.

A concluding note must be made that concerns the techniques used during excavation. The colluvium (upper 1.8 m of deposit) was excavated rapidly in order to reach the debris flow deposit. Even though this was the case, every effort was made to carefully sieve the deposits and retrieve all artefactual material. It therefore appears that the large reduction in SFD for the colluvial assemblage cannot be the result of different excavation techniques, when compared to the excavation of the debris flow.

For the debris flow assemblage the rainfall damage that occurred in certain squares (see Chapter 3.3 discussion) may also account for a slightly reduced SFD percentage of 55% versus potentially >60% (as shown in experiments by Schick 1997 and Kuman & Field 2009). This is due to the removal of the wet eroded sediments, from the excavation, and an inability to sieve them. In addition to this, several smaller rainfall events thereafter limited the use of the 2 mm sieve at times. A combination of

this poor weather and an inability to use the 2 mm sieve is likely to have lowered the overall percentage of SFD for the debris flow assemblage.

5.4.1.3 Artefact condition and raw material data

Focus here will be placed upon artefact condition in relation to raw material type, versus placing an emphasis solely on which raw materials were more abundant. The latter has little to do with site context and is influenced more by cultural preferences (to be discussed in the following typology and technology sections).

Artefact condition studies emphasise that artefacts will frequently weather in a way that relates to the material upon which they are made, and artefact condition will reflect the type and intensity of the process/es that have affected the assemblage (Shackley 1974; Pappu 1996; Shea 1999; Holmes *et al.* 2008; Thompson 2009).

Artefact condition data show that the majority of artefacts in both assemblages at Penhill Farm is fresh in condition, and this data by depth in the debris flow shows no specific trends. Overall, this percentage of fresh artefacts indicates that assemblage integrity is high and that the modification of artefacts through natural processes is minimal.

Referring back to the artefact size distribution discussion above, this would suggest that predominantly low energy conditions gave rise to the deposition of these artefacts, and that the rate of artefact burial between the assemblages is largely comparable. However, the marginally higher percentage of artefacts with modified surfaces in the colluvial assemblage does suggest that artefacts were exposed for a longer period during the colluvial assemblage accumulation (also supported by the lower SFD percentage for this sample; Schick 1991; Thompson 2009). Colluvial assemblage artefacts specifically from the channel features, however, may account for these marginally poorer artefact conditions. Yet, without having recorded these features individually during the excavation of the upper 1.8 m of colluvium, this cannot be confirmed.

By raw material type, the three most abundant (quartzite, siltstone and hornfels) show a range of preservation states and there is little to suggest that any of these materials weathers/erodes in a unique way. Hornfels, however, has a greater susceptibility to weathering, in both assemblages. This may be due to exposure of these artefacts at the surface or, most likely, *in situ* breakdown of the material due to sediment moisture content (as discussed by Shea 1999 at Ubeidiya).

A final mention will concern the prevalence of varnished artefacts. This type of surface abrasion/smoothing is largely uncommon and accounting for why it occurs is difficult. As such this form of sporadic artefact modification, at present, should be treated as anomalous and is most likely the result of some kind of basic natural abrasion/smoothing (Thompson 2009).

5.4.1.4 Artefact spatial distributions

Initially the emphasis of research work at Penhill Farm was to understand the contextual nature of the artefact-rich debris flow deposit. Although now it is clearly understood to be a colluvial deposit, originally the possibility of this assemblage representing some kind of living surface or primary context accumulation was not ruled out. For this reason a careful investigation of artefact spatial arrangements was conducted. Subsequently, through continued excavation and exposure of the debris flow it became clear that a colluvial origin was more appropriate, and that the accumulation was clearly of secondary context. Spatial data obtained on artefacts from the debris flow support this interpretation.

A basic assessment of artefact numbers by depth and square clearly illustrate that the majority of artefacts occurs towards the middle to basal part of the excavated debris flow, in vertical space. Horizontally, two trends are clear. The first is that artefacts are more abundant in the west squares of the excavation (CC2, DD2 and EE2), and the second is that artefacts are more common in the center squares (D1, DD1 and DD2), when compared to the remaining squares.

These patterns in artefact distribution are likely due to the way in which the debris flow swept into the erosion channel and how it spread out into a depositional cone. It

is most likely that the debris flow entered the erosion channel from the upslope east direction. Most erosion channels are narrow and have steep sidewalls (Charlton 2008), but it appears that the erosion channel at Penhill Farm was wide, thus allowing the flow to spread out over a considerable area as it moved downslope through the channel. The majority of the material appears to have become concentrated towards the middle part of the excavated channel (the center squares, even though vertically the distribution of pieces here is more restricted). This material moved downslope with the majority coming to rest at the most distal point in the base of the channel (the west squares). As was highlighted in Chapter 3.2 the debris flow is therefore ‘wedged out’ and is thickest in the east and thinnest in the west.

The vertical and horizontal distribution of point-plotted artefacts in the debris flow shows that there is no specific spatial arrangement of artefacts by size, condition or type; artefacts occur randomly throughout the excavated levels. As such it can be concluded that there are no patterns that would indicate knapping locales, site stretching and a displacement of assemblage components horizontally across the site, or a vertical sorting of artefacts (as discussed in Chapter 2.3). This is to be expected for a colluvial debris flow deposit. In addition to this, these plots confirm the patterns noted above for artefact frequency by depth and square. In addition to this these plots show the discontinuous nature of the debris flow in squares C1 and E1.

Is it possible for other processes to have affected the spatial arrangement of the debris flow artefacts at Penhill Farm, after deposition? This is an important point that needs to be explored.

Trampling disturbance to the assemblage appears unlikely as the damage (e.g., breakage, micro-flaking and abrasion) that would result appears absent (Kuman 1989; Nielsen 1991; McBrearty *et al.* 1998). Furthermore, this damage would be restricted to artefacts in the uppermost levels of the debris flow, which only accounts for a small percentage of the overall sample. Its significance is therefore limited.

Bioturbation is a common process that affects many archaeological deposits and it is primarily caused by four main agents (termites, earthworms, plant roots and burrowing animals; Stein 1983; Erlandson 1984; McBrearty 1990; Morton 2004;

Lotter *et al.* 2016). Although each of these ‘pattern’ a deposit in a specific way (see Chapter 2.3) it would be difficult to assess the impact of these processes in the past at Penhill Farm as the contents of the assemblage are already displaced due to the colluvial nature of the debris flow. It is entirely plausible that bioturbation may have had some influence on the debris flow artefacts that were deposited, and perhaps the most plausible agent would be root growth from plants and vegetation at the surface of the deposit. Based on a recent study by Lotter *et al.* (2016) this can cause sediment mixing and the vertical displacement of artefacts. However, one must consider the surrounding local landscape at the time and remember the fact that even though the erosion channel became filled in with debris flow artefacts and sediment, the channel itself was still an erosional feature on the landscape. As such, conditions for plant growth were likely poor due to the constant removal of sediments through surface wash/flow (as can be seen in many erosional channels today). At present, roots do occur in the colluvium found above the debris flow and some of these extend down towards and into the debris flow. From this it is clear that root action is playing a role in site modification today, but this influence at depth appears only to be minor.

Is it possible that some of the smallest assemblage components at the surface of the debris flow were winnowed away, either through aeolian or hydrological processes? It is entirely plausible that the latter would have played some role in the modification of the assemblage at the debris flow surface. Although the debris flow appears to have been deposited rapidly, thus filling the base of the erosion channel, once deposited the upper surface would have been exposed. This may have winnowed away some of the assemblage (most likely the smallest components of the assemblage). This could have been caused by rain splash, sheetwash/flow, and potentially some form of rill and gully erosion. However, clear evidence for the latter was not found. In accordance with the artefact condition data, perhaps the presence of ‘varnished’ artefacts is an indication of this abrasion/smoothing due to surface wash. Aeolian influence is not entirely impossible, but this may have been far less common and sporadic.

5.4.1.5 Artefact depositional (fabric) data

This analysis was conducted primarily for two reasons, both of which relate to our initial poor understanding of the site. First, previous research (Erlanger *et al.* 2012)

had classified the artefact-bearing deposits at Penhill Farm as gravel stringers, thus fluvial features. It was therefore our understanding that these artefacts remained preserved within low energy fine alluvium. The second reason was therefore to determine the level of disturbance for these artefact accumulations.

With more detailed work it later became clear that the artefact accumulations were the result of colluvial deposition. However, debris flows can preserve depositional fabric, especially in the lateral margins of the flow (Bertran & Texier 1999), so an investigation is therefore still informative. However, the results of this analysis show that no single preferential orientation occurs. Although by square there appears to be some very weakly preferred orientations, the combined sample indicates no such pattern (confirmed by the uniform random distribution of the data). This trend is also seen in the artefact dip data, which occupies a large range and shows no preferred dip angle. Overall, this allows us to conclude that the excavated portion of the debris flow deposit retains no trends in artefact dips or orientations.

5.4.1.6 Debris flow dating results

The final contextual data to be discussed for Penhill Farm concerns the age of the assemblages. The original date of 1.37 ± 0.16 Ma (Granger *et al.* 2013) provides a maximum age for the Penhill Farm assemblages. Our understanding of the significance of this date though has changed with a better interpretation of the context of the site. An explanation follows.

As has already been discussed, we originally thought that the artefact-bearing deposits at Penhill Farm were alluvial and were contained within fine, low energy floodplain sediments (Erlanger 2010; Erlanger *et al.* 2012). Gravels obtained from the southern exposure of the borrow pit (Granger *et al.* 2013) and dated using the cosmogenic nuclide burial dating method provided an age for the deposition of this fine alluvium on top of the gravels, and hence its burial age. Because the artefacts were retained within this fine alluvium we therefore assumed that this date of 1.37 ± 0.16 Ma related directly to the artefacts within these ‘gravel stringers.’

With continued excavations and our realisation that the artefacts were in fact preserved within a distinct erosion channel that had cut into this fine alluvium, it became clear that a new date was needed for two key reasons. First, although the fine alluvium was deposited at 1.37 ± 0.16 Ma, the time that it would have taken for the erosion channel to develop within these sediments would have been considerable. Second, this erosion channel then needed to be filled in with colluvium. Although the deposit at the base of the channel (the debris flow assemblage) came in rapidly, it appears that the remaining colluvium came in thereafter possibly over a longer period. Either way, from these two points it was clear that a new date was needed.

The new cosmogenic nuclide dating results from Excavation 1 provide a refined age 0.485 ± 0.051 Ma for clasts sampled directly from the debris flow deposit. By nature, this age does not directly date when the debris flow took place, but rather it dates when the colluvium was deposited after and on top of the debris flow. This has important implications.

From the contextual data presented in this section, it appears that the conditions for deposit accumulation for the debris flow and the overlying colluvium are different. The debris flow assemblage appears to have been deposited in a rapid event. In contrast, the overlying colluvium has several contextual features that indicate a possibly slower period of accumulation and a greater potential for assemblage modification.

In addition to this, the features present within the colluvium (discussed in detail in Chapter 3.2) may provide some important insight into how long this deposit took to accumulate on top of the debris flow. It is, after all, 1.8 m worth of deposit, versus the <20 to >50 cm thick debris flow found at the base of the erosion channel. Chapter 3.2 highlights that five distinct channel flow features occur within a single larger cut and fill deposit, within the overlying colluvium. From this it appears that the colluvium took time to infill, as it would have taken time, first, for the channel to be cut through erosion, and second, for the five channels to develop within the cut and fill.

Initially we had anticipated that the Penhill Farm debris flow assemblage was not so young as the later Acheulean, but the new burial age of 0.485 ± 0.051 Ma suggests

this young date must be considered. The typological and technological analysis presented by this research shows that the differences between the colluvial assemblage and the underlying debris flow assemblage are not extreme (discussed in more detail in the following sections). In fact, the nature and characteristics of these two assemblages appear to be largely comparable. Perhaps these two assemblages are indeed part of the same original site that existed upslope of the erosion channel, with the contents working their way down at different rates – the majority coming down initially and rapidly as the debris flow, followed by a lengthy period of slower deposition of the remaining material in the overlying colluvial assemblage. Perhaps then the difference in time between the deposition of these two assemblages is considerable, but the actual difference in time for the production of the artefacts is not. Conversely, perhaps the difference in time for both production and accumulation of the two assemblages is minimal.

It is our opinion that the new age of 0.485 ± 0.051 Ma does not directly date the debris flow assemblage. It provides a maximum age for the accumulation of the colluvium overlying the debris flow (i.e., for the burial of the debris flow), but it does not necessarily date the technology of these artefacts nor pin them to the later Acheulean. The two dates currently available for the site are thus >0.485 and <1.37 Ma. However, if we argue that the younger date does not relate to the technology of these assemblages, we would then have to provide a model that would account for how and why the artefacts remained preserved upslope, prior to being incorporated into the erosion channel downslope.

Compounding the problem is the overall condition of the artefacts, especially in the debris flow, which indicates minimal abrasion and damage due to some kind of long-term surface exposure. This artefact condition data does not suggest that any of the Penhill Farm artefacts were exposed at the surface for hundreds of thousands of years earlier, prior to deposition. This is most relevant for the debris flow assemblage, as the high retention of the smallest assemblage components clearly suggests otherwise.

There is a small possibility that the artefacts were produced closer to 1.37 Ma and lay in a sealed deposit upslope, preserved and protected from a number of natural processes that would otherwise cause considerable artefact modification. However,

providing a model that could account for such a situation is beyond the limits of the existing data. Accordingly, the most likely explanation is that the assemblages are younger than 1.37 Ma, and because the two are largely comparable in typology and technology, the difference in age between the two does not appear to be considerable.

For now we must accept what the data indicate:

1. All assemblages at Penhill Farm are younger than 1.37 ± 0.16 Ma.
2. The maximum age for the accumulation of the upper 1.8 m of colluvium is 0.485 ± 0.051 Ma.
3. The debris flow assemblage has a minimum age of 0.485 ± 0.051 Ma. But, based on similarities with the colluvial assemblage above, it is most likely that these two assemblages are comparable in age. Furthermore, based on these similarities, these two assemblages could be regarded as a single assemblage with differential re-deposition downslope, through time.

In order to test the feasibility of whether the debris flow artefacts at Penhill Farm could be considerably older, artefacts will be directly dated with the cosmogenic nuclide burial dating method (versus the dating of non-artefactual gravels that have already been used in this study). Our hope with this dating is that we can establish the age of the technology of the artefacts more accurately, versus when the artefacts were deposited. We will be looking for some older inherited ^{26}Al and ^{10}Be concentrations in the artefacts that could indicate they are not dated by the debris flow event.

5.4.1.7 Final comments

Although we have a better understanding of the Penhill Farm site today, we are now walking away with even more unanswered questions. This means that there is still a great deal of work to be done on the property, and the importance of these questions is paramount if we are to one day provide a complete explanation for why the site occurs where it does and what this may tell us about the past landscape.

A selection of contextual questions below provides an illustration of what will form the basis for future work at the site; most of these questions refer back to points raised in Chapter 3.2. At present we are unable to answer these questions, but it is nevertheless important that these issues are raised.

1. How much more of the debris flow deposit is left to uncover, and how extensive is the erosion channel? How much more of the assemblages may be present?
2. Do the edges, or the upper limits, of the erosion channel reach the ancient land surface, and if so, where does this occur?
3. Does another similarly infilled erosion channel nearby (visible in the southeast face of the borrow pit) bear artefacts? Is the formation of the excavated debris flow completely unique or have similar conditions in the past caused replicable deposit formation?
4. Where is the source of the re-worked calcrete and silcrete nodules that are abundant in the debris flow deposit, which occur less frequently in the overlying colluvium?. Are they from a very localised source upslope that the erosion channel tapped into as it extended upslope?
5. Are some of the natural pebbles and cobbles in the erosion channel from the upslope colluvial wedge coming from the older higher terrace preserved upslope? Was the erosion channel tapping into a portion of this colluvial wedge?
6. Alternatively, if the erosion channel was not tapping into this upslope source of gravels, were these natural pebbles and cobbles then sourced locally by hominids and carried into the original site, thereafter being deposited downslope during the debris flow?
7. Where exactly was the original site upslope and was this a primary context accumulation? Was this site located further upslope within the erosion channel (as hominids came to utilise raw materials and produce artefacts), or did it occur outside along the channel edges?

Although we have investigated these questions, unfortunately our ideas remain speculative at this point. Overall, Penhill Farm is an important site that contains a large quantity of well-preserved artefacts. An investigation into site context illustrates that overall assemblage integrity is high, but there are important differences in the formation and accumulation history of the colluvial and debris flow assemblages. With continued survey and excavation on the property we may likely locate similar deposits, if not on the property then perhaps in the rest of the lower valley. However, there is still work to be done at Penhill Farm.

5.4.2 Typology

A typological assessment of the Penhill Farm assemblages provides important information on the character and composition of the excavated artefacts. From this analysis there appears only to be some minor percentage differences in the types of artefacts between the assemblages. A more detailed discussion of these artefacts will be presented in the following technology section.

Both assemblages provide a large sample of lithic material, although it is clearer that the debris flow assemblage (which ranges in thickness from <20 to >50 cm) has a far denser concentration of artefacts than the overlying 1.8 m of colluvium. A comparison of the five main artefact types (flaking debris, complete flakes, cores, formal tools and other cobbles) highlights the abundance of flaking debris in both assemblages. The remaining samples of complete flakes, cores, formal tools and other cobbles contribute far smaller percentages to the overall assemblages.

5.4.2.1 Flaking debris

The majority of both assemblages is comprised of flaking debris. These components are clearly important if we are to assess the prevalence of knapping, within the original site or within the catchment of the site, and the abundance of this material clearly confirms that this sort of activity has occurred in the past.

Overall, flake fragments, incomplete flakes and SFD (22.2% for the colluvial assemblage and 55.1% for the debris flow) account for the most frequent flaking debris types, for both assemblages. Small percentages of bipolar flaking debris occur in both assemblages. However, the overall significance of this debris is low due to the extremely small samples.

An interesting trend for both assemblages is the high variability in raw materials for the flaking debris and complete flake samples, versus fewer raw materials represented in the core and formal tool samples. In other words, a wider range of raw materials is

represented in the flaking debris and complete flake samples. In fact, flaking debris is the only artefact type to account for every raw material (excluding CCS).

How is it that these represent a wider range of materials but the cores, from which this material would have been removed, do not occur? If one looks at the overall quantity of pieces on materials other than quartzite, siltstone and hornfels, these pieces are infrequent or at best rare. This would suggest that a very limited number of cores was reduced that were not comprised of the three most abundant materials. If this is the case then the absence of these cores may be attributed purely to the catchment of the site, and their limited number may be due to sampling error. This may explain their absence. As a result, the excavations at Penhill Farm appear not to have recovered the complete assemblage from the site upslope and these cores may likely occur in unexcavated portions of the deposits. It may also be that these cores were reduced but then carried off-site, but confirming this without having excavated the entire portion of the debris flow and colluvial assemblages is not possible.

5.4.2.2 Complete flakes

The classification of complete flakes from Penhill Farm illustrates that side- and end-struck flakes are the most frequent in both assemblages, followed thereafter by corner-struck pieces. All of the other remaining flakes are rare, but a notably higher percentage (6.7%) of bipolar flakes on quartzite occur in the colluvial assemblage than in the debris flow (1.2%); nevertheless, this does indicate the bipolar reduction of cores in both assemblages. Raw materials are predominantly quartzite, siltstone and hornfels, but lava and silcrete complete flakes also occur infrequently in both assemblages, as well as claystone types in the debris flow assemblage.

A brief discussion concerning the prevalence of side-, end- and corner-struck flakes, in relation to raw material shapes, must be presented here. Raw materials in the lower Sundays River Valley are primarily in the form of round to oval river pebbles, cobbles and boulders; core blanks are therefore consistent in shape (quartzite and siltstone). The percentage difference between side- and end-struck types, in both assemblages, is minimal and the frequency of corner-struck types is less. Research by Isaac and Keller (1968) on the proportional abundance of these flakes suggests that Acheulean

assemblages are characterised by a sub-equal proportion of end- and side-struck flakes, as most flakes are equidimensional (as long as is wide, as shown in Chapter 4.4 and to be discussed in greater detail in the following technology discussion); later ‘post-Acheulean’ assemblages have a higher proportion of elongated end-struck types. Perhaps the latter can be attributed to improvements in core reduction and a greater control over flake dimensions prior to detachment. As the Penhill Farm assemblages are made on consistent core blank shapes, the high proportion of side- and end-struck types is the result of simple core reduction strategies where flake shapes and dimensions are poorly controlled.

An interesting feature in both assemblages is the infrequent number of flakes (core trimming and rejuvenation types) geared towards core management and maintenance. It is clear based on their frequency that these flakes are more the exception than the norm, and based on the predominance of simple core reduction strategies, these flakes could be regarded as being anomalous. Nonetheless, their presence indicates that even though raw materials were abundant in the valley, careful attention was given to some cores such that platform angles and edges could be adjusted, or in more extreme cases removed, to facilitate the removal of flakes. Perhaps these flakes provide a good indication of the ‘upper technological limits’ of the Penhill Farm assemblages.

A final mention must be given to the more atypical flakes recovered from Penhill Farm, specifically: handaxe (or LCT) trimming flakes, Kombewa flakes, and bi-bulb flakes, all of which are infrequent. Those few LCT trimming flakes that do occur, however, indicate that some LCT reduction was occurring within the catchment of the site. This is clearly important considering that large flakes (e.g., LCT blanks) do not appear to have been removed from many of the cores at Penhill Farm (to be discussed in the following core section). It would appear that large blanks were predominantly carried into the site and then reduced to shape LCTs. A more detailed investigation into the presence of these trimming flakes may support this idea, but at present, we must accept that only minimal LCT shaping was happening on-site, and that blanks for this shaping are most likely to have been brought in.

Flakes that represent the Kombewa technique possess two ventral surfaces. These pieces are linked to the reduction of large raw material blanks and they can be

common in sites where large flakes are used as cores (Kuman 2001). Only a single Kombewa flake was recovered from the colluvial assemblage and the significance of this piece is therefore minor. Another interesting atypical flake type is the bi-bulb, of which one occurred in each assemblage. Once again the significance of these flakes is minimal due to their infrequency, but a possible reason for why they occur may be related to core reduction. Both bi-bulb flakes show two clear bulbs of percussion, which would suggest two points of impact. It is suggested here that perhaps one bulb represents an initial partial, failed attempt, to remove the flake, and the second represents the final blow that managed to detach the flake from the core. This indicates the manipulation and rotation of the core so that the flake could be struck off from an edge nearby.

5.4.2.3 Cores

Cores at Penhill Farm are not unlike those that would occur in any other Acheulean assemblage; simple casual, discoidal and chopper-cores dominate both assemblages, and polyhedral, single platform and irregular cores are also found infrequently. Interestingly, no cores occur on quartz, lava and silcrete (for both assemblages) or on silt-quartzite (debris flow assemblage), even though both flaking debris and complete flakes occur on these materials. The significance of this has already been discussed.

The high frequency of casual cores at Penhill Farm is interesting, especially since raw materials are so readily available. This is likely the reason for why these cores are so common. Hominids could afford to be more selective in the materials they chose to reduce, and testing them beforehand was thus important. This suggests that hominids in the area were conscious of raw material variability, and testing cobbles was necessary to ensure success in core reduction. Alternatively, perhaps many of these casual cores illustrate the detachment of a single or a maximum of two flakes to serve a specific purpose at a given point in time. This would suggest expedient core reduction.

Irrespective of these casual cores, there is some variability in core reduction. Irregular core reduction is less frequent, as seen in the limited irregular and polyhedral cores. Some discoids are better shaped and small in size, approaching the appearance of

those from MSA assemblages. Perhaps these neat discoids represent the upper limits of core technology at Penhill Farm. In addition to this, a single discoid in the colluvial assemblage shows what appears to be a single large 'preferential' removal. Although this core is not prepared, it does suggest that there was some consideration for the overall dimension/shape of the final removal. This could also have happened purely by chance.

A notable difference between the assemblages though is the absence of bipolar cores in the colluvial assemblage, even though there is the presence of bipolar flaking debris and complete flakes. Only a single bipolar core occurs in the debris flow sample. Overall, the significance of bipolar reduction is therefore minimal and the use of this technique was therefore more an exception than the norm.

5.4.2.4 Formal tools

Formal tool production at Penhill Farm takes place primarily on quartzite, siltstone and hornfels. For the debris flow assemblage, claystone, silt-quartzite and lava artefacts are also represented, albeit infrequently. This increase in raw material variability in the debris flow may be attributed to the larger number of formal tools for this assemblage.

The classification of formal tools indicates that small retouched pieces were produced most frequently, especially scrapers, and these account for 51.1% of the colluvial formal tools and 30.5% for the debris flow. Thereafter, MRPs, denticulates and retouched flakes represent the remaining most common retouched types. A notable difference between the assemblages though is in the lower percentage of scrapers and the higher percentage of MRPs and denticulates that occurs in the debris flow.

Why is it that small retouched tools are more numerous in the lower Sundays River Valley than LCTs? Perhaps this can be answered purely from a functional perspective. Subsistence activities at the time may have required the production of these tools to satisfy basic scraping or cutting tasks. Extending the speculation, perhaps the environment at the time dictated the need for these tools in processing wood and other items. Irrespective of what the reason is, the production of these small

retouched items occurred more frequently than the production of larger LCTs, and perhaps this relates to their efficiency in the tasks at hand.

The remaining formal tools are less frequent (e.g., LCTs, knives, flaked-flakes, composite pieces, choppers, burins and awls) in both assemblages. Specific mention must be made, however, of the composite pieces. These are pieces that show more than one kind of retouch and that illustrate potentially different uses (e.g., denticulate for cutting and notched scraper for scraping). This retouch need not have been made all in one episode, and these pieces may therefore indicate tool recycling. Furthermore, perhaps these pieces illustrate the economisation of raw materials, but based on their abundance in the lower Sundays River Valley this appears unlikely. A more detailed classification of the scrapers and LCTs follows below.

Scrapers:

The types of scrapers represented in both assemblages are largely consistent, and the only difference between the assemblages is in the presence of a single double side and end scraper and a single convergent scraper in the debris flow. Both assemblages show a distinct preference for denticulated, notched and side scrapers. Collectively, these three types account for 81.3% of the colluvial scrapers and 74% for the debris flow scrapers.

The remaining types are less frequent and there is little to suggest the preferential production of one type over the other. It seems most likely that the more favoured denticulated, notched and side scrapers were more capable of handling the required tasks at hand, and the production of the remaining types was needed only infrequently. Mention must be made of the composite scrapers. These are tools that possess more than one kind of scraper retouch, and this may indicate their use in more than a single task.

LCTs:

The variability in the production of the Penhill Farm LCTs is clear when looking at the overall form of these tools, and this will be discussed in greater detail in the following technology section.

By type, both assemblages illustrate that handaxes and cleavers are most common, followed thereafter by less frequent picks and bifaces. LCT production occurs only on quartzite and siltstone. The numbers of cleavers and handaxes are largely equal within the two assemblages.

Overall, the greater quantity of handaxes and cleavers suggests these were the most favoured LCTs. This may be due to some functional reason, and perhaps the small pick sample would best illustrate this point. These are pieces with very narrow, robust, convergent tips, and it would appear their uses were quite specific. The low frequency of these pieces at Penhill Farm suggests that handaxes and cleavers were functionally better suited, and the need to produce such ‘task specific’ LCTs was not required as frequently.

The greatest distinction between the assemblages is in the quantity of broken LCTs. These pieces are absent in the colluvial assemblage but in the debris flow they account for 16% of the total LCT sample. Why are these pieces more abundant in the debris flow? Perhaps this relates to the flow and the way in which artefacts were transported downslope, but the low frequency of damage on the rest of the debris flow artefacts suggests otherwise. Perhaps it is more related to breaks during manufacture or re-sharpening. At present it is difficult to account for why they occur.

5.4.2.5 Other

There is little that can be said regarding the small sample of cobbles (n=4) recovered from Penhill Farm, and very little detailed analysis could be conducted on these pieces. These cobbles were divided into two types, namely split cobbles and modified cobbles.

Split cobbles show some kind of damage that may pertain to bipolar core reduction/splitting, or potentially damage to a hammerstone, but clear evidence to suggest the latter was not identified. Perhaps these split cobbles illustrate an important step in the core reduction process. Suitable cobbles may have been sourced locally and were then split on-site to provide angular edges from which to work. Core blank types will be discussed in the following section, but the use of split cobbles is clearly

favoured. It would be difficult to confirm what specific method was used to split these cobbles, but perhaps some form of anvil technique was employed.

A single modified cobble in the debris flow assemblage showed some interesting bashing/pounding damage. This does not appear to be the result of damage incurred during deposition, as it is restricted to only two areas on the artefact. This concentrated damage suggests that either this cobble was used as a large hammerstone and this represents repeated percussive damage, or perhaps this is a cobble that could not be split and the surface damage represents these attempts to break it.

5.4.2.6 Additional features

Tool recycling and utilisation damage are largely uncommon in both assemblages. The purpose of identifying these features though was not to provide a high level of detail on how and where these features occur. Rather, it was to assess whether these features could be identified on any particular kinds of artefacts. As a result, what follows below is more a summary of which artefacts retained these features.

The colluvial assemblage contained only two clear recycled pieces, including a flake fragment and a casual core. These pieces are abraded and evidence to suggest recycling is in the form of fresher removals (ones that suggest more recent flaking; double patina; Barkai *et al.* 2015; Vaquero *et al.* 2015). This pattern is largely similar with the debris flow recycled artefacts, the majority of which is cores. This would imply that cores were re-used later in time, even though raw materials were readily available in the local landscape. The flaking of cores with angles was likely easier than flaking a round cobble. A single handaxe in the debris flow assemblage was also recycled, which would have been faster than producing a new handaxe.

Tool utilisation damage was found on artefacts from both assemblages, and overall this was more prevalent in the debris flow assemblage (likely due to the larger sample). Both assemblages have utilisation damage that occurs on complete flakes, cores, and several formal tools. In the debris flow, some flaking debris also appeared to show some damage.

It is interesting that such a range of pieces retains this damage, and perhaps this talks to the potential for conducting use-wear analysis on artefacts from Penhill Farm. Although only a single utilised complete flake was analysed for use-wear and residue traces, having showed potential, it would appear from the great number of utilised pieces that there is potential to perform this analysis on a wider range of artefacts.

5.4.3 Technology

A more detailed discussion of the Penhill Farm assemblages will be presented in this section. This will look more carefully at the strategies employed in artefact production. Accordingly, this section will provide a discussion that pertains to three key themes, namely the size/dimensions of the artefacts, the flaking strategy employed to produce these pieces, and lastly, to what degree these pieces have been reduced. Flaking debris and complete flake data will be discussed first, followed thereafter by core, formal tool, and lastly, modified and split cobble data.

5.4.3.1 Flaking debris and complete flakes

Trends discussed here will concern the three most abundant materials, namely quartzite, siltstone and hornfels. Unfortunately all the other raw materials are rare and the sample sizes on which we can base any conclusions are inadequate. It must also be stated that the samples of siltstone and hornfels artefacts within the colluvial assemblage are extremely limited, so any trends discussed herein must be treated with caution.

Flaking debris and complete flake dimensions/size:

A series of measurements was obtained on the incomplete and complete flakes from Penhill Farm, and in certain instances multiple methods were used to provide these measurements.

Most important is that irrespective of the methods employed, the three most abundant raw materials showed a consistent size trend for both assemblages, with siltstone flakes accounting for the majority of the largest measurements, followed by quartzite

and hornfels flakes. Another important finding is that both assemblages have largely comparable flake dimension/size measurements, especially evident in the large quartzite samples, and it is likely that the minor variation that does occur between the assemblages (and in the remaining raw materials) is due to differences in sample sizes. The last important finding shows that the majority of flakes is equidimensional, which according to Isaac and Keller (1968) is a characteristic of Acheulean assemblages.

Flake dimension/size data has been shown to provide important information that can relate to the level of reduction in an assemblage. Accordingly, a decrease in flake size (be it lengths, widths, thicknesses and weights) is shown to correlate negatively with the level of reduction (Andrefsky 2005; Braun *et al.* 2008). However, there are several factors that can influence this trend in size and these can relate to raw material blank properties and quality, and artefact discard behaviours and production strategies, to name a few. Regardless of these factors, perhaps it is possible then to discuss differences in the level of reduction between quartzite, siltstone and hornfels at Penhill Farm.

Siltstone flakes are the largest and heaviest flakes whereas hornfels flakes are the smallest and lightest. Quartzite flakes are intermediate between the two. The character and shape of raw material blanks at Penhill Farm has already been mentioned (predominantly round to oval river cobbles), but this pertains primarily to quartzite and siltstone. No hornfels was found in the local landscape and we are uncertain whether blanks are in the form of pebbles/cobbles (most likely) or outcrops. We are therefore uncertain what influence raw material blank properties would have had on the smaller hornfels samples.

Overall, the size distribution of flakes from both assemblages shows those that are 30-50 mm in maximum length are most frequent, and the overall number >100 mm in length is rare. The general absence of flakes >100 mm, considering the majority of the LCT sample is made on these larger flakes, suggests the transporting of these items on-site, versus their production from cores on-site.

An assessment of these flake dimensions by flaking axis provided largely different results. Following Isaac and Keller (1968), the percentages of side- and end-struck flakes were largely similar in both assemblages, and there appeared only to be minor variation between them, perhaps best explained by the dominance of equi-dimensional flakes in early assemblages (Isaac & Keller 1968). For this reason the Mason (1965) method was favoured.

Following this approach some interesting patterns occur in the assemblages. First, corner-struck flakes account for the majority of the largest flake measurements in both assemblages. Second, corner- and side-struck flakes are most frequently produced, in both assemblages, and end-struck types are less common. Perhaps this second point relates to the simple techniques employed during core reduction that seldom gave rise to elongated, narrow, flakes. Third, both assemblages show that side-struck flakes were favoured for formal tool production. From this analysis of flaking axis distribution, there appears only to be minor variation between the two assemblages.

Flaking strategy:

Three primary analyses were employed to assess flaking strategies at Penhill Farm. These analyses concerned the number of flake dorsal scar directions, the patterns represented by these scars, and lastly, the way in which flakes terminated. However, before discussing this data a final mention must be made of flaking axis distribution by raw material.

The colluvial assemblage shows that for quartzite and hornfels, corner-struck flakes are the most common type. For siltstone, end-struck flakes are the most abundant. These patterns are largely different in the debris flow where side-struck flakes are most common in quartzite and siltstone. Hornfels here accounts for a high percentage of corner-struck types. Accordingly, although there are differences, quartzite corner- and side-struck flakes are most readily produced, in both assemblages. In addition to this, hornfels shows that corner-struck types are most favoured, followed thereafter by side- and end-struck types, in both assemblages. However, the significance of these differences though may relate purely to variation within and between the assemblage/s.

The number of dorsal scar directions on flakes is used as a proxy that indicates the number of flaking series removed from a given edge, prior to the flake in question; a series of flakes is struck from a single direction, and thus multiple directions suggest multiple series (Braun *et al.* 2008). At Penhill Farm the number of dorsal scar directions is largely comparable between both assemblages, and they illustrate the abundance of flakes with only a single dorsal scar direction (49% of the colluvial assemblage and 47.6% of the debris flow), thereafter followed by flakes with two directions. Both assemblages also show that flakes with three or more directions are infrequent. Flakes with no pattern (either indeterminate directions or cortical dorsal surfaces) show almost equal percentages for both assemblages (10.5 and 10.7%). These data indicate that the number of dorsal scar directions is low, as is the number of flaking series. Although this also pertains to core reduction, and that will be dealt with in the next section, these data suggest that primarily simple core reduction strategies were used.

The patterns represented by these dorsal scar directions can further illustrate this point. Kuman (2001) states that although cores provide valuable information on the pattern of flake removals, these patterns only represent the final stages of knapping. As a result, the dorsal scar patterns on flakes provide more detailed information that pertains to the flaking techniques (Kuman 2001). For both assemblages the unidirectional-proximal pattern is the most frequent (one direction running from the proximal to the distal end of the flake), for quartzite, siltstone and hornfels; this is followed by the radial flaking pattern (three or more directions). Other notable samples include unidirectional-transverse-proximal (two directions), transverse (one direction) and no patterns (cortical or indeterminate), in both assemblages. The other remaining patterns are infrequent.

These data indicate that flakes are primarily removed following the same direction of the previous removal. This also indicates limited rotation of the cores as a single edge is worked multiple times to provide a series of flakes. Although this may be the case for a large percentage of the flakes at Penhill Farm, radial flaking patterns indicate more complex flaking of cores and the reduction of edges from multiple directions, giving rise to a series of removals from each direction. It is also important to note that

largely comparable percentages of flakes in both assemblages were either cortical or retained indeterminate patterns.

A comparison of these flake scar patterns by raw material shows some interesting patterns. In the colluvial assemblage, quartzite flakes account for the highest percentage of the radial flaking pattern, whereas siltstone flakes account for the highest percentage of the unidirectional-distal pattern. Hornfels flakes provide the largest percentage for no flaking pattern (predominantly cortical), also seen in the debris flow sample. In the debris flow the radial pattern is most frequent on siltstone flakes (albeit only marginally more than for quartzite). Perhaps these data illustrate the more extensive reduction of quartzite and siltstone, versus hornfels.

The final flaking strategy data to be discussed concerns flake termination types, and it is these data that can provide information on the forces used to detach flakes from cores (Andrefsky 2005). These data illustrate that feather terminations are the most frequent on all the raw materials, and that results are largely similar for both assemblages and for the three most abundant raw materials. In both assemblages, siltstone flakes have the lowest percentage of feather terminations and the highest percentage of hinge terminations. However, in the debris flow these feathered types are marginally less common on siltstone and hornfels flakes. Step and overshoot terminations are largely infrequent. The only raw materials to have overshoot terminations include quartzite and siltstone.

There is little evidence at Penhill Farm to suggest that any technique other than hard hammer percussion was used to detach flakes. It must also be noted that these flake terminations are heavily influenced by the raw materials and their respective qualities, and perhaps questioning the prevalence of these termination types in relation to the different raw materials is more worthwhile. These data show that quartzite has the highest percentage of feathered flake terminations, and perhaps this would explain why it was so readily used over the other two remaining materials, although, this may also relate to its availability within the landscape.

Level of reduction:

Assessing the level of reduction in any assemblage is an important undertaking. Toth (1985) developed a technological flake classification system that assesses the distribution of cortical and non-cortical flakes in a complete assemblage, with the simple premise being that an assemblage with earlier stages of knapping will have more flakes with cortical platforms (types I-III), and those assemblages in their final stages of reduction will have higher percentages of flakes with non-cortical platforms (types IV-VI). Although this classification is based on the experimental replication of Oldowan cores, it is still a useful approach. Many of the cores in Acheulean assemblages are largely comparable to those from earlier Oldowan assemblages.

Accordingly, Toth (1985) provides a series of percentage values that should characterise a site where primary knapping has occurred and these are as follows:

- Type I: 1-9%
- Type II: 2-32%
- Type III: 4-11%
- Type IV: 3-9%
- Type V: 25-49%
- Type VI: 20-69%

Any deviation in the above percentages talks to variability in site use and the potential modification of an assemblage through lithic transport. For example, higher percentages of non-cortical platform flakes IV-VI would suggest that later stages of knapping are represented, and that potentially decorticated pieces were brought on-site to be reduced further. Conversely, higher percentages of cortical platform flakes I-III would illustrate earlier stages of knapping, and they may suggest the site served as a factory location where the initial stages of core reduction took place.

At Penhill Farm both assemblages show remarkably similar technological flake type distributions, with only minor variation. Where variation does occur in relation to those percentages presented above (Toth 1985), this occurs for the same technological flake types, namely: type I (both assemblages have marginally higher percentages ranging from 0.3-1.6%), type III (both assemblages have higher percentages ranging from 2-5.1%), and type V (both assemblages have lower percentages ranging from 2-3.4%). However, types V and VI still dominate both assemblages, yet flakes with cortical platforms (namely types I to III) collectively account for 41.1% of the colluvial sample and 33% of the debris flow sample. By raw material the quartzite

and siltstone samples from both assemblages show an abundance of flake types V and VI, whereas hornfels accounts for the highest percentages of flake types I and II.

This indicates that there is only minor variation in the experimental values above proposed by Toth (1985), and that there is only marginally greater representation of early stages of knapping at Penhill Farm in both assemblages. Overall, it would appear that there has been some transporting of artefacts at Penhill Farm. This may likely explain why there is a slight under-representation of non-cortical flakes. Although by raw material there appears to be earlier stages of core knapping represented in the small hornfels samples, and later stages in the larger quartzite and siltstone samples, these trends must be treated with caution based on their limited samples. In addition to this it must be stated that the assemblages at Penhill Farm have not been fully excavated. These trends in flake distributions can currently only serve as estimates of the bigger picture. At present we can conclude that the technological flake type distributions at Penhill Farm are largely comparable to the experimental values proposed by Toth (1985) for complete assemblages in which the early stages of knapping are marginally better represented, but there has potentially been some transporting of decorticated lithics off-site.

A more detailed look at the location of this flake dorsal cortex following Nishimura (2005) and Marwick (2008) illustrates the abundance of tertiary flakes (no cortex) in both assemblages. However, types two (crescent shaped cortex) and one (primary, completely cortical) are the second and third most frequent, respectively. The problem with this approach to dorsal cortex location is that predictable flake type percentages are not provided. The only explanation offered as to which types should characterise an assemblage with early knapping is an abundance of types one and two (primary and crescent, respectively; Nishimura 2005). Conversely, assemblages with later stages of knapping and/or re-sharpening of artefacts should be characterised by high quantities of flake types three and four (distal and tertiary, respectively, which are largely non-cortical). The problem here is that once a core has been decorticated, generally through the removal of only a limited number of cortical flakes, the non-cortical flakes removed from the core generally always exceed the quantity of these initial cortical removals. Using this approach then, any assemblage with a low number of cortical flakes and a higher number of non-cortical flakes could be interpreted to

represent later stages of knapping. As a result, Toth's (1985) method above provides a more reliable assessment.

Nonetheless, it is notable that flakes with distally located cortex (type three) and centrally located cortex (type six) provide important information on the later stages of core reduction. Following Marwick (2008), type three flakes are produced through the rotation of the core, as invasive flakes begin to overlap previous removals. A similar situation would give rise to type six flakes. However, both of these flake types only account for minor percentages in the assemblages and their significance is therefore limited.

Another important assessment of assemblage reduction concerns the quantity of facets on flake platforms. This analysis is provided here to question the overall level of flaking intensity at Penhill Farm, and not to infer any kind of platform preparation prior to flaking. Following Delagnes and Roche (2005), facets on flake platforms preserve previous flake removals that then serve as a platform from which more flakes can be struck. Conversely, cortical platforms illustrate flakes removed during the early stages of core reduction. At Penhill Farm both assemblages have a comparable distribution of flake facet counts, with the majority in either assemblage being plain (one facet; 47.7% of the colluvial assemblage and 45.6% of the debris flow) and cortical (no facets; 39.5% of the colluvial assemblage and 40.2% of the debris flow). Facet counts that exceed one are therefore infrequent (12.8% of the colluvial assemblage and 14.2% of the debris flow), and the only assemblage to have multi-faceted flake platforms is the colluvial assemblage (n=1), but these are rare. By raw material both assemblages illustrate that quartzite and siltstone flakes generally have higher facet counts (two or more) when compared to the remaining raw materials, and hornfels flakes have the highest percentage of cortical platforms in either assemblage.

This limited platform faceting in flakes at Penhill Farm indicates that the assemblages are in the early stages of reduction. In addition to this the rotation of cores during flaking, and the re-use of platforms with previous flake scars, accounts for only a few flakes in each assemblage. For the three most abundant materials, these facet counts suggest a greater level of reduction in the quartzite and siltstone flakes, versus the

hornfels flakes that show earlier stages of reduction. Once again perhaps this is linked to the specific blank properties of hornfels.

The number of dorsal scars on complete flakes is an indication of the level of core reduction (Kuman 2001). The simple premise with this variable is that the greater the flake scar count, the greater the level of core reduction (Braun *et al.* 2008). However, as cores are reduced more extensively the smaller flakes that are produced are likely to have fewer scars, as their surface area is limited (Braun *et al.* 2008). It is therefore important to assess this variable in relation to flake size, specifically flake surface area. For the purposes of this study though, and the fact that intense core reduction does not occur at Penhill Farm, a simple assessment of these scar counts will be provided that does not consider flake size.

The vast majority of flakes at Penhill Farm has one to four scars (collectively accounting for 80.4% of the colluvial sample and 80.8% of the debris flow), and those with five or more scars are infrequent. There is only a minor difference in the number of flake scars between the assemblages. Interestingly, these counts by raw material suggest a greater level of reduction in the quartzite and siltstone cores (producing flakes with higher dorsal scar counts) versus hornfels cores, as these flakes have the highest percentages of one or two scars, in both assemblages. These data suggest that the level of core reduction at Penhill Farm is not extensive. Although there are flakes that preserve a greater number of scars, these are the minority in either assemblage.

Perhaps one of the most obvious indicators of reduction would be the quantity of preserved cortex on the dorsal surface of flakes. This cortex is said to decrease as the level of reduction increases (Braun *et al.* 2008). Once again these data are largely consistent between the assemblages, and a large percentage of the flakes preserves no cortex at all (42.9% in the colluvial assemblage and 47.8% in the debris flow). However, if one looks at the remaining flakes in either assemblage, this would indicate that the majority retains cortex (57.1% in the colluvial assemblage and 52.2% in the debris flow). Hornfels flakes are the most cortical (91-99 and 100% cortex), whereas quartzite flakes are the least. These data suggest that a large portion of the flakes at Penhill Farm document the early stages of core reduction. Although a considerable proportion of flakes indicate later stages of knapping decorticated cores,

it is clear that early stages of knapping are represented in both assemblages at Penhill Farm.

The final data to be presented concerns interior and exterior platform angles. Marwick (2008) explains that the interior platform angles for early reduction flakes normally cluster around 90°, whereas flakes in later stages of reduction cluster between 90-100°. The problem with this measurement is in obtaining reliable measurements, and although Marwick (2008) discusses this issue, its application is supported in his research. During the analysis of artefacts for this study though it became clearly evident that obtaining measurements on non-cortical platforms was easier. Obtaining measurements on the frequently 'rounded' cortical flake platforms was generally impossible, and inaccurate, so these were mostly excluded. As such, the mean interior angles provided for both assemblages are heavily biased towards those that could be reliably measured, in other words, flakes that would indicate later stages of knapping. Platform angles range from 111.6-113.8° for both assemblages. This is only just beyond the range expected for flakes in the later stages of reduction. However, with the exclusion of a large portion of the cortical platform flakes (up to 40% of flakes in either assemblage), these measurements do not accurately represent the level of reduction in flakes at Penhill Farm.

A similar problem exists with the exterior platform angle measurements. Studies have linked changes in exterior platform angles to changes in flake weight, size, and platform area and depth (Dibble 1997; Dibble & Rezek 2009). Accordingly, high exterior platform angles give rise to larger flakes, whereas lower exterior platform angles and a low core size give rise to smaller flakes (Dibble 1997; Dibble & Rezek 2009). The mean exterior platform angles at Penhill Farm range from 64.8-69.4° for both assemblages.

No study provides an expected range of platform angles that could be used to assess an assemblage with either high or low levels of reduction, and it appears that this variable is more valuable when compared to other flake measurements (mentioned above). By observing the heavy bias towards non-cortical flakes above, the validity of this data also needs to be questioned due to difficulties experienced during analysis (inability to measure curved cortical flakes). As such, little can be said about what

these angles mean and what relevance they would have even when compared to flake size, weight and platform measurements. For this reason these data will not be discussed any further.

5.4.3.2 Cores

Cores on materials other than quartzite are generally infrequent (especially claystone cores) and trends discussed here must be treated with caution. Furthermore, some core analysis is broken down by core type, of which there are only a few examples in certain cases. As such, trends discussed for cores other than the more abundant chopper-cores, discoids and casual cores must be treated with caution.

Core dimensions/size:

Perhaps the most compelling trend at Penhill Farm is in the size difference between quartzite, siltstone and hornfels cores. This is a clear trend that occurs in both assemblages, even though in the colluvial assemblage the sample sizes for these latter two materials are notably smaller. Overall, core dimensions in the assemblages show that siltstone cores are the largest, whereas hornfels cores are the smallest; quartzite cores are thus intermediate between the two. When comparing core size between the assemblages, in the debris flow quartzite and hornfels cores are smaller (albeit only marginally) and siltstone and claystone cores are larger. Perhaps this minor size variability between the assemblages is linked to differences in sample sizes.

The size difference between quartzite, siltstone and hornfels cores is likely linked to raw material blank properties. It has already been highlighted that blank size and shape for siltstone and quartzite is largely the same, whereas hornfels blanks are poorly understood at the current stage of analysis. To be more cautious then these size differences should be taken to represent variability in these blanks.

An assessment of core size by type shows that chopper-cores and casual cores account for the majority of the largest mean values, in both assemblages, and there is only minor size variation in these cores between the assemblages; irregular cores in the debris flow assemblage are also large in size. Thereafter the remaining core types are all smaller in size, and both assemblages are characterised by a high percentage of

small, light discoidal cores. If one contrasts the sizes of these cores it would appear that the small, light discoidal cores show a greater level of reduction when compared to the larger chopper- and irregular cores. This will be readdressed in the following sections.

Flaking strategy:

Core flaking patterns at Penhill Farm show the abundance of simple, unstructured, reduction strategies. In addition to this, both assemblages show remarkably similar distributions for each of the different strategies, and only minor variations occur for unifacial peripheral (unifacial discoidal core with removals that do not meet in the middle of the upper surface) and bifacial hierarchical exploitations (discoidal core with single large removal), which are present in the colluvial assemblage and absent in the debris flow, and for polyhedral and bipolar exploitations (present in the debris flow and absent in the colluvial assemblage). However, samples for these cores are extremely small and thus their significance is limited.

Perhaps what best illustrates this simplicity in core reduction is in the distribution of unifacial simple partial, bifacial simple partial and casual exploitation patterns, which account for 54.9% of the total colluvial core sample and 51.7% of the debris flow cores. These patterns indicate that short, unstructured, reduction strategies characterise the majority of all cores at Penhill Farm, and this also suggests a high level of expediency in reduction (de la Torre 2011). These simple types also show that there is little relationship between the upper and lower surfaces (planes) of the core as reduction takes place (i.e., in bifacial working), but where this does occur the removals are only partial along a given edge. It therefore appears that flakes were removed quickly and rapidly from serviceable core edges. Multifacial/irregular cores could also be included in this discussion as these types illustrate a clear lack of organised knapping and the irregular use of available flaking angles.

Slightly more structured knapping can be seen in the discoidal cores, and these types account for 15.7% of the colluvial core sample and 23.8% of the debris flow sample. This pattern indicates a more careful reduction of edges and the rotation of the core to correctly manage the central volume (de la Torre 2011). These cores therefore illustrate a planned relationship between the upper and lower surface of the core as

reduction occurs (de la Torre 2011). It would appear that these discoidal cores reflect the upper technological limits of core reduction at Penhill Farm, and as has been mentioned in the typological discussion, several of these were small in size (approaching MSA-like dimensions). This is most likely linked to their greater level of reduction. A single discoidal core from the colluvial assemblage also retained a level of asymmetry (bifacial hierarchical exploitation) and had what appeared to be a single large 'preferential' removal. However, this was more likely an accident than a desired outcome, which is evident in the general lack of shaping of the core.

By raw material there is little to suggest that cores are reduced differently, although the small sample sizes in both assemblages may limit this kind of comparison. Overall, quartzite cores have the greatest range of reduction strategies represented, likely due to the large samples in both assemblages. Thereafter, all raw materials illustrate that USP, BSP, casual and more structured discoidal cores account for the majority of all the reduction strategies.

The core blanks for these reduction strategies are predominantly cobbles and split cobbles (>60% of cores in both assemblages), and although the use of large flakes is infrequent this is more common in the debris flow. Interestingly, a comparison of core blank type by raw material and core type shows that where flakes are utilised in either assemblage, these are generally made on quartzite and are used in discoidal and chopper-core (USP or BSP) reduction.

Overall, core blanks at Penhill Farm indicate the expedient use of cobbles and split cobbles. Although some cobbles are split to provide serviceable edges, a large percentage of cobbles is unmodified prior to the start of reduction. This suggests there was little attention given to what blanks were best suited for what core, but rather, blanks were chosen out of the surrounding landscape at random and reduced in an expedient fashion to provide a series of flakes.

This is further supported by the general absence of large flake removals on these cores. By comparing the maximum length of complete flakes (excluding LCTs on large complete flakes) and the largest flake scars preserved on these cores, it is clear that some large flakes are likely to have been obtained from cores elsewhere. If these

large flakes were predominantly cortical, perhaps this may account for the slight over-representation of cortical flakes at Penhill Farm (based on the technological flake types presented earlier, following Toth 1985).

Level of reduction:

The cores at Penhill Farm are in the early stages of reduction. This is clearly seen in the low number of scars and, the high percentages of cortex that remain on their surfaces.

Core scar counts are a simple way to assess reduction intensity, as cores with a high number of flake scars are more reduced than those with lower scar counts. Although there are several factors that can influence this (e.g., core size, blank properties, reduction strategies), this is the simple premise being explored here.

The average number of scars on the colluvial cores is 4.1, versus 4 in the debris flow. The majority in both assemblages also has only one to four removals.

Understandably, certain core types illustrate greater levels of reduction, and this is seen in the discoids (highest flake scar counts in both assemblages), versus the less reduced casual cores. For chopper-cores and discoids, siltstone types have higher mean flake scar counts than those on quartzite, in both assemblages, suggesting a greater level of reduction in these types. However, the percentage of remaining cortex in cores by raw material shows that siltstone has higher levels of cortex preservation than those quartzite (as do the hornfels cores in the debris flow). This suggests greater reduction in the quartzite cores, which are also the only ones to be completely decorticated. However, this could also be related to the shape and size of the original blanks, but these are largely the same for both quartzite and siltstone. Overall, the percentage of remaining cortex on cores is largely comparable between the two assemblages and is generally high (>25%); reduction intensity is therefore low.

5.4.3.3 Formal tools

Retouched pieces:

Retouched formal tools at Penhill Farm are largely comparable between the two assemblages, and there are only minor differences in the character of these artefacts. Following the raw material trends seen in previous sections, quartzite is favoured for retouching, along with less frequent siltstone and hornfels. All the other raw materials are rare, and the range of materials represented in the debris flow assemblage is greater, likely due to the larger sample excavated.

Retouched piece dimensions/size:

Interestingly, variations in the size and weight of retouched pieces are high, between the assemblages and between the different raw materials. As has already been shown in the previous core and flake discussions, siltstone artefacts are generally the largest, followed as sizes decrease by quartzite and hornfels artefacts. For retouched formal tools, both assemblages show a similar trend and retouched siltstone tools are the largest and heaviest in either.

Perhaps this should be expected in light of the core and flake data. However, for the remaining retouched tools on quartzite and hornfels, quartzite pieces are the smallest and lightest, versus hornfels artefacts (as seen in the core and flake data). This is an interesting contrast and it is difficult to explain. Could this be related to the level of reduction for quartzite artefacts? A greater level of reduction in these pieces would lead to an overall decrease in artefact weight and size. The amount of remaining cortex on these artefacts may be able to shed light on this question, and these data do show that quartzite artefacts account for the highest percentages of completely non-cortical pieces, in both assemblages.

One important difference between the assemblages is in the dimensions/size of these retouched quartzite artefacts. As quartzite pieces are the most abundant in either assemblage, comparison of these samples is more feasible and shows that quartzite artefacts in the debris flow are smaller and lighter. The following sections will illustrate that the production of these artefacts is largely consistent between the assemblages, so this size difference is likely related to sample variability.

Flaking strategy:

There is little data to suggest that there are significant differences between the assemblages in the strategies employed in retouched formal tool production. In fact the majority of these strategies illustrates the simplicity and expediency in the production of these tools, and they also illustrate a lack of emphasis on careful artefact modification.

The vast majority of retouched artefacts is made on flake blanks (>75% in each assemblage), and by raw material there is little data to suggest the differential use of raw materials blanks for specific purposes. The debris flow assemblage does, however, have a wider range of blank types, and perhaps the most atypical is a single unifacial discoidal core. Although this accounts for only one blank out of the majority of flakes, this retouched piece does illustrate a willingness to recycle and re-use a pre-existing artefact (a core). The remaining blank types are infrequent in both assemblages. Retouch is generally applied to the mesial and distal portions of the blanks.

For retouched pieces made on flake blanks, the location of retouch shows a preference for simple direct retouch that originates from the ventral surface of the flake and gives rise to dorsal retouch. This unifacial retouch accounts for the vast majority of artefacts in both assemblages, followed by alternate retouch. This is retouch that occurs on two flake edges opposite each other, with one on the dorsal and one on the ventral. Both of these retouch locations illustrate the simple trimming of artefact edges, and perhaps this is best illustrated by alternate retouch. To achieve this retouch an artefact is held and retouched along one edge, then the piece is flipped horizontally and the opposite edge is worked from another face in the exact same fashion. As such the knapper does not need to make any kind of adjustment to the knapping method or strategy at hand. This also illustrates limited artefact manipulation and rotation during the reduction process.

Overall, retouched formal tool production at Penhill Farm documents very little interaction between the upper and lower planes of an artefact, during retouch. As such, alternating, crossed and bifacial retouch is infrequent, but where this does occur perhaps this is an illustration of the upper technological limits in each assemblage. It

would appear that there has been minor consideration for creating more complex retouched edges, and this may relate to tool function or raw material properties.

Perhaps the best illustration of tool simplicity is in the shapes of the edges created during tool retouch. These shapes are predominantly denticulated and notched, along with less frequent irregular edges. The remaining edge shapes are largely uncommon. These edges are either characterised by isolated, discontinuous and localised removals (notched), interspaced and continuous removals along a portion of an edge (denticulated), or a completely irregular pattern of removals.

The shape of these edges is important as it may relate to the intention of the knapper, from both a functional and possibly a behavioural perspective. The fact that the majority of these retouched edges is simple may illustrate the expediency in tool production at Penhill Farm. Then again, perhaps this is more linked to tool function and the fact that there may have been no need to create more refined edges. This edge simplicity may also relate to high raw material availability, and the fact that there was no need to economise the use of material. Slightly more complex edge shapes do occur (e.g., convergent) in the debris flow assemblage and perhaps these illustrate the upper technological limits of the assemblage as well.

A final mention must be made of the steepness of the retouched edges. This is important as perhaps this can provide information that relates to the function of these tools. It would appear that steep retouched edges would be better suited for scraping tasks, whereas more gradual (sharper) edges would be better for cutting tasks. Both assemblages show the majority of retouched edges are steep (90°), with the remaining majority having angles closer to 45° (semi-abrupt). Low angled edges ($\pm 10^\circ$) only occur in the debris flow formal tool sample. From this, perhaps the major function of retouched tools at Penhill Farm was to perform basic scraping tasks, followed by less frequent cutting tasks using robust semi-abrupt edges.

Level of reduction:

The level of reduction in the retouched tools at Penhill Farm is low, and this would be in agreement with the previously discussed core and flake data. Three distinct data sets are used to assess this level of reduction.

First, the continuity of retouch along a given edge can be taken to represent the time given to shape an edge or re-sharpen it, and thus the level to which it has been altered/reduced. The simple idea being explored here is that more continuous edge retouch illustrates higher levels of reduction. In contrast, discontinuous retouch would suggest a lower level of re-sharpening or of shaping. Accordingly, both assemblages show an abundance of discontinuous retouch (>60% in each assemblage). This suggests that the attention paid to edge modification is low, as well as the level of reduction. However, perhaps the need to provide more continuous retouch was unnecessary, either due to functional reasons or perhaps this relates to raw material quality. Although both assemblages do have small samples with more extensive edge reduction (slightly more common in the colluvial assemblage), this appears to have been more the exception than the norm. These retouch continuity data indicate the expediency of retouched tool production at Penhill Farm.

Second, the invasiveness of edge retouch is a good indicator of reduction intensity. From this it is clear that the majority of artefact edges have been only minimally affected by retouch (short removals, >65% in both assemblages), with removals that are more invasive in the minority. Although this might be due to functional reasons, the near-complete absence of invasive and covering retouch is important.

Third and last, the percentage of remaining cortex on retouched tools shows that the majority is cortical (66.7% of the colluvial sample and 59.7% of the debris flow sample). Interestingly, by raw material both hornfels and siltstone tend to be more cortical and although some quartzite pieces are largely cortical, they account for the highest percentages of those that are non-cortical. Overall this suggests a lower level of reduction in the siltstone and hornfels formal tools, and a higher level of reduction in the quartzite tools, in both assemblages.

LCTs:

Excavation 1 at Penhill Farm has provided a total sample of 49 LCTs, of which the majority comes from the lower lying debris flow assemblage (n=38). Raw material use in both assemblages is dominated by quartzite, thereafter followed by siltstone. All trends discussed below must be considered in light of the limited sample sizes

within the assemblages, especially for siltstone LCTs, but also when LCTs are broken down by type (limited picks and bifaces).

Typologically there appears to be little that distinguishes the two assemblages and this technological data discussion will further illustrate this point; differences between the assemblages are most likely the result of a larger sample of LCTs in the debris flow assemblage, showing increased variability.

LCT size and shape:

Overall variability in LCT dimension/size is high at Penhill Farm, and this is evident in the range of LCT types, as well in the different raw materials.

Both assemblages illustrate that when LCTs are made on siltstone and quartzite, those on siltstone tend to be larger and heavier. As such in the colluvial assemblage siltstone handaxes account for the largest and heaviest LCTs, as do siltstone picks, handaxes and cleavers in the debris flow assemblage. If we refer back to the siltstone flake and core data in the preceding sections, the larger size of these siltstone LCTs should be expected (even though the samples here are limited). However, the variation (SD) in dimensions/sizes is generally higher for the quartzite artefacts, perhaps due to the larger samples in either assemblage. In addition to this, both assemblages are characterised by small and light quartzite picks and bifaces.

Overall, an assessment of LCT mean length by raw material shows that all exceed 100 mm in the colluvial assemblage, except for quartzite bifaces, which are notably small in length, width and thickness. A similar trend is observed in the debris flow, except here the majority of quartzite LCTs is smaller than 100 mm, whereas those on siltstone are larger. This could be linked to a greater level of reduction in those smaller quartzite LCTs, or more likely, to the smaller size of the quartzite blanks.

Tool elongation (L/W ratio) and refinement (T/W ratio) data provides largely similar results for both assemblages by LCT type, yet these ratios vary between the assemblages. Accordingly, in both assemblages those LCTs that are the most elongated include handaxes and picks, whereas cleavers and bifaces are the least; handaxes are also the most refined LCTs, along with bifaces. Cleavers overall show low elongation and poor levels of refinement, in both assemblages. A comparison of

these ratios, by assemblage, shows that LCT elongation is higher in the colluvial assemblage, but the level of refinement is lower. Conversely, LCT elongation is lower in the debris flow assemblage yet LCT refinement is greater.

Why is there this difference between the assemblages in LCT elongation and refinement? Could it be related to differences in reduction intensity? At present it is difficult to answer this question, but a conservative view is that these trends are due to the limited sample size for the colluvial assemblage. Furthermore, the following sections will show that largely similar techniques were used in both assemblages during LCT reduction. This variability may also therefore relate purely to blank size differences.

Another important aspect of the LCTs at Penhill Farm is the high variability in tool tip shape within both assemblages, also by LCT type. McNabb *et al.* (2004) discuss the significance of different tip shapes, and a brief summary of this work has already been presented in the Bernol Farm LCT section. For this reason another summary will not be repeated here, but two key concepts will be mentioned: first, different tip shapes indicate that tools would have been conceived of very differently and would then have been reduced differently to produce the desired result; second, there was likely a poor level of standardisation in LCT flake blank size and shape due to a lack of emphasis on controlled core reduction (McNabb *et al.* 2004).

Tip shape variability at Penhill Farm may also relate to these two points, and perhaps to a range of other factors that would have influenced LCT production (e.g., time, skill of the knapper, raw material constraints). Although both assemblages show a preference for generalised convergent tip shapes, from a functional perspective these more generalised tips may have been better suited to the specific tasks at hand. It is also possible that LCTs were used in more than a single task, and thus having a more generalised tip would have made re-use far easier.

Conversely, tips that are markedly convergent illustrate an intention to produce specific tips for specific purposes (e.g., more robust and pointed), and it would appear from a functional perspective then that the use of these LCTs (e.g., picks) would differ from the more generalised types. Furthermore, cleavers are dominated by

convergent square and oblique edges, and again, if these tools were each conceived of in a unique way, in relation to a given function, they would then have been shaped a specific way to perform this given task.

Overall, the large degree of variability that occurs in the LCT measurements at Penhill Farm may be linked to variability in LCT blank size and shape. Core reduction at Penhill Farm has already been shown to follow simple and generally expedient reduction methods, so it is unlikely that blank size and shape was controlled/managed at the time. We can therefore conclude that overall LCT size and shape at Penhill Farm is highly variable, as are tip shapes.

In addition to this, cleaver morphology shows that pre-existing blank shapes have influenced butt plans. The majority of cleavers at Penhill Farm has unshaped butts that are round in shape, and thus these represent the naturally occurring shape of the blank. Only three cleavers in the debris flow assemblage showed intentional shaping of the butts to produce rounded and squared shapes, but the significance of this shaping is minimal due to the limited sample; this shaping is more the exception than the norm. This suggests that hominids at the time were content to accept the pre-existing shape of the blank, and there was little emphasis on modifying the butts of these pieces to a specific shape and/or for a specific purpose.

LCT reduction:

LCTs at Penhill Farm are produced primarily on large flake blanks, and as this has already been discussed in the flake and core data sections, it would appear that at least some of these larger flake blanks were struck from cores elsewhere and were transported into the site. Irrespective of where some of these blanks were obtained, the fact that the majority of all Penhill Farm LCTs occurs on these large blanks highlights the significance of their production. A more detailed survey in the local area is needed to investigate this further.

Importantly, by raw material and blank type, there is little to suggest that specific blanks were utilised for specific LCTs. The range of blanks represented is greater in the debris flow assemblage, showing a marginally more frequent use of cobbles and split cobbles, but again this cannot be linked to a specific raw material or use in

specific LCT types. Overall, this pattern illustrates that the production strategy was to make large flake blanks in either siltstone or quartzite, upon which a range of LCTs could be made. The use of cobbles and split cobbles is infrequent and its significance is therefore limited. When these pieces do occur, perhaps this relates to the need to expediently produce a tool, as was seen in many of the expediently produced and reduced cores and retouched pieces.

The quantity of primary and secondary scars provides some interesting results for the Penhill Farm LCTs, by tool type and by raw material. These counts provide important information that allows one to question the level of artefact reduction, and question whether tool shaping (primary removals) or edge refinement (secondary shaping) was more important based on their quantitative differences (Kuman *et al.* 2014; Li *et al.* 2015).

In the colluvial assemblage, siltstone LCTs have lower combined mean flake scar counts than those on quartzite. Overall this would suggest a lower level of reduction/shaping for these siltstone LCTs. This is especially relevant considering that tool size is an important factor in analysis of scar count and reduction intensity, and these siltstone pieces are larger than those on quartzite. Quartzite handaxes account for the highest combined mean scar count (20.5 scars), and they also have the highest mean primary and secondary scar counts. By type, these handaxes show the greatest level of reduction/shaping in the colluvial assemblage (15 scars), followed thereafter as scar counts decrease by picks, bifaces and cleavers.

Conversely, the debris flow siltstone LCTs have higher combined mean scar counts than those on quartzite. As a result siltstone handaxes and cleavers account for the highest combined mean flake scar counts, and quartzite bifaces the least. However, by type, cleavers illustrate the highest level of reduction/shaping in the debris flow (16.3 scars), followed thereafter as scar counts decrease by picks, handaxes and bifaces.

Overall though, these differences in scar counts between siltstone and quartzite LCTs and between the different LCT types must be viewed in light of their respective sample sizes; siltstone LCTs are limited, as are picks and bifaces.

More informative though is assessing the location of primary versus secondary LCT scars. For the majority of the Penhill Farm LCTs, the latter exceeds the former in number. However, the quantity of secondary scars can easily exceed that of primary scars due to their small size, and thus it is also important to consider the distribution and coverage of these scars using the 12-sector method (Kuman *et al.* 2014). This shows that the majority of LCTs in both assemblages has been reduced and shaped bifacially. These bifacial types account for 63.6% of the colluvial assemblage (n=7) and 71.9% of the debris flow (n=23). This shows that the primary strategy in LCT shaping/reduction is to work both faces and the majority of sectors, and this would suggest that variability in LCT flaking/reduction is minimal. Partly bifacial and unifacial LCTs do occur in both assemblages, but they are less frequent (although the latter are more common in the debris flow).

However, by LCT type there is an important difference in reduction patterns. In both assemblages handaxes and cleavers account for a wider range of reduction patterns (including partly bifacial and unifacial pieces). This increased variability though is most likely due to the fact that handaxes and cleavers are the most abundant LCTs at Penhill Farm, thus they are likely to document higher levels of variability in reduction.

The location of primary and secondary flake scars shows that secondary flaking is more common towards the medial and distal sectors of all the Penhill Farm LCTs, with little in the proximal (basal) sectors. Primary flaking occurs throughout almost all sectors for the LCTs in both assemblages, but again this flaking is more common in the medial and distal sectors. Predictably, proximal sectors have the greatest cortex preservation, but in the debris flow LCTs cortex occurs in more sectors overall on both faces.

Primary and secondary flaking by sector shows that 60% of all the colluvial LCT sectors show both primary and secondary flaking, with 19% of sectors showing only secondary flaking. This pattern is largely similar in the debris flow, where 68% of all LCT sectors contain primary and secondary flaking, with secondary flaking alone occupying 20% of all sectors. Based on this analysis it would seem as if the importance of secondary edge refinement is low, but the numerical scar counts above

suggest otherwise (as secondary scars exceed primary scars). In addition to this it would appear that the overall number of sectors that shows that both primary and secondary flaking is limited, in both assemblages. This suggests that the overall amount of LCT reduction/shaping at Penhill Farm is limited. To provide some comparison a recent study by Li *et al.* (submitted) on later Acheulean LCTs from Cave of Hearths shows that 92% of all sectors contain both primary and secondary flaking (following the same 12-sector method). Furthermore, an earlier Acheulean sample obtained from the Rietputs Formation (dated to 1.3 Ma) showed flaking in 77% of all sectors.

An analysis of primary and secondary flaking by LCT type shows that for the colluvial assemblage, picks and bifaces have the greatest percentages of primary and secondary flaking by sector, whereas handaxes and cleavers have the lowest. Secondary shaping is greatest in the biface (25%) and handaxe (21%) sectors. This is in contrast to the scar count data that suggested handaxes and picks had the highest level of reduction/shaping, followed by less flaking in the bifaces and cleavers. However, flaking by sector is an area measurement, whereas scar data are based on counts.

For the debris flow, picks and cleavers have the most primary and secondary working by sector; handaxes and bifaces have the least. Secondary flaking is greatest on the cleavers, at 22% of all sectors, and lowest in the bifaces. This data is in agreement with the scar count data and illustrates that reduction/shaping is more extensive in the debris flow picks and cleavers and less extensive in the handaxes and bifaces.

The final data to be presented concerns the amount of cortex remaining on the LCTs. This is a good indication of the level of reduction as higher amounts of cortex are associated with less extensive reduction/shaping. Both assemblages show the majority of LCTs retain 1-24% cortex, and the remaining pieces are cortical (1-100%), whereas in the colluvial assemblage no LCTs show 0% or 75-100% cortex; siltstone LCTs are generally more cortical than quartzite LCTs. These patterns by raw material also occur in the debris flow LCTs. Overall, this cortex preservation data confirms that Penhill Farm LCT reduction is limited and only a small number of artefacts from the debris flow assemblage show that all cortex has been removed.

5.4.4 Residue and use-wear analysis

The single utilised complete flake analysed by G. Langejans was shown to have three features: a white fat deposit across its surface, fibres, and discontinuous edge rounding.

The white deposit, likely fat, and fibres are contaminants that were most likely introduced to the artefact surface during analysis. This is clearly the case for the fibre, as its shape and colour suggests it is cotton. This was likely introduced onto the artefact when it was placed on a cloth during analysis. The fat deposit is likely due to artefact handling.

More significant though is the discontinuous edge rounding along certain edges of the flake, and it is this feature that may indicate use-wear traces on the periphery of the flake. This artefact is from the debris flow, and hence it was deposited rapidly. The possibility that this may be some form of artefact edge damage due to natural processes is not strong, as we would expect this edge damage to be more continuous across the edges of the artefact had it been re-worked and damaged during deposition. However, without a more detailed analysis of a larger sample of artefacts this 'possible' use-wear damage must remain speculative.

It has already been discussed in the typological section that a number of artefacts from Penhill Farm retains what appears to be utilisation damage. This suggests that there is potential for this kind of analysis in the future.

5.4.5 Non-lithic

The preservation of non-lithic material at Penhill Farm is poor. The rapid burial that occurred in the debris flow did not provide favourable conditions. This is likely due to the fragmentation of bone and other materials as they were transported downslope, or perhaps due to the high moisture content of the sediments (aiding in the break-down of organic material *in situ*). Thereafter, the colluvial assemblage illustrates slightly

slower deposition, during which time exposed bone and other organic material was likely removed from the site by a host of natural processes.

5.4.6 Final comments

Penhill Farm provides a large quantity of well-preserved artefacts found within an erosion channel that has cut into Terrace 9 fine alluvium. The typological and technological analysis presented here shows that the differences between the two assemblages are minor, and it is likely that both assemblages are in fact part of a single assemblage that was located upslope. Having also attained a better contextual understanding of the site we can now account for the unfortunate lack of non-lithic materials.

However, there is a great deal of work that still remains to be done at Penhill Farm and as a result we now have new questions that can be asked in light of what has been presented by this research. A selection of these questions is provided below:

1. Why is it that Penhill Farm was a favoured location for stone tool production?
Wherever the site was located, did the local area provide some degree of protection, shade, and/or resources (such as water and raw materials)? Were there other similar areas nearby?
2. How much more of the assemblages are we missing and is it possible that certain assemblage components are under-represented?
3. Were the blanks for core reduction sourced from upslope in the erosion channel or from the colluvial wedge coming off the older terrace higher upslope; were they carried in as manuports and then reduced?

We are now leaving Penhill Farm with more unanswered questions; this is an illustration of the high research potential of this property. We will continue our work at this site to investigate these issues, and furthermore we will continue with our efforts to correctly date the technology represented in this assemblage.

5.5 Atmar, Bernol and Penhill Farm inter-site comparison

This section will provide only basic comparisons between the three sites where there are comparable data. Penhill Farm will therefore serve as the core site against which comparisons will be made; these will be done in relation to a single large assemblage (due to only minor differences between the two assemblages). We start with a typological comparison between the Atmar and Penhill Farm cores and formal tools (retouched pieces and LCTs). Thereafter, an LCT technological data comparison will be done only between Bernol and Penhill Farm, focusing on LCT size/shape and reduction, because Bernol Farm typological data is based on a biased collection and is therefore not suitable for comparison. In addition to this, this comparison needs to be treated with caution as the Bernol Farm LCTs represent a biased collection.

5.5.1 Atmar and Penhill Farm artefact typology

The typological classification of artefacts from these two sites shows that both are largely comparable.

Although the sample of cores from Atmar Farm is small, these cores show the following trends:

- Casual and chopper-cores are the most frequent core types
- Knapping involves the simple reduction of quartzite cobbles
- Cores illustrate a low number of scars, showing that core reduction is limited
- There is limited core knapping that shows the interaction between the upper and lower surfaces of the core (bifacial)
- Cores show an absence of large scars, which suggests that large blanks for LCT production were struck from cores elsewhere
- No bipolar cores occur, along with no bipolar complete flakes or flaking debris

These trends also occur in the Penhill Farm cores, and perhaps the only notable differences between these sites, by core type, is in the higher frequency of discoidal cores at Penhill Farm and the presence of a single bipolar core in the debris flow

assemblage (coupled with bipolar complete flakes and flaking debris). There is a greater range of reduction patterns and raw materials evident at Penhill Farm, but this is likely due to the far larger core sample. Overall, there is very little that distinguishes the two sites in the cores.

The formal tool sample at Atmar Farm comprises only seven pieces. However, some basic trends are apparent in the retouched pieces and LCTs. Retouched pieces, namely the denticulated scraper and denticulate show (n=2):

- Flake blanks are favoured for tool production
- Simple and informal production of tools
- Retouch is predominantly sporadic, discontinuous and/or partial, and the extent of the removals is short and noninvasive
- Direct retouch is favoured
- Edge delineation shows that denticulated edges are produced

Once again these are all trends that could quite easily describe the retouched tools from Penhill Farm. Although the use of different raw materials and the production of a wider range of retouched artefacts do occur at Penhill Farm, this is likely due to the larger excavated sample. Overall, artefact production at Penhill Farm is expedient and the careful modification of edges does not occur. This comparison suggests that there is little that distinguishes these sites when assessing retouched artefact types and their methods of production.

Regarding the LCTs, the Atmar types are limited – only three LCTs, a handaxe, a biface and a cleaver. Characteristics are as follows:

- Large, cortical flake blanks are favoured for LCT production
- Flake blanks appear to be well-suited for LCT production and are thin
- The number of scars on the LCTs is low
- LCT tip shapes show a preference for generalised convergent types for the handaxe and the biface
- Hornfels is used in LCT production (unifacial handaxe)

LCT types at Penhill Farm also illustrate the production of handaxes, cleavers and bifaces, but with the addition of picks in both assemblages. Handaxes and cleavers occur in nearly similar proportions.

LCT production at Penhill Farm follows very similar trends to those noted above, yet a few important differences occur. First, hornfels is not used in LCT production and the only material utilised other than quartzite is siltstone. Second, the flake blanks used at Atmar Farm (although limited) show they are thin, and perhaps this accounts for the limited flake scars on these artefacts (as further reduction of the blank was not required). Some of the flake blanks used at Penhill Farm were definitely larger and required more reduction to assist in the shaping of the LCTs, yet thin blanks are also not uncommon. Nonetheless, LCTs at Penhill Farm also show limited flaking and only 60-68% of all sectors on LCTs show some form of primary and secondary working; large remaining portions of these tools are therefore cortical and/or unworked.

An assessment of LCT tips also shows largely comparable shapes for both sites. The small Atmar Farm sample matches the Penhill Farm sample where handaxes and bifaces are dominated by generalised convergent types and cleavers are dominated by convergent oblique types. Beyond this, the range of tip shapes is greater at Penhill Farm due to the larger sample excavated.

Overall, what is the significance of this inter-site comparison and what does this tell us about the assemblages from Atmar and Penhill Farm? What can we deduce from the comparison of these limited (especially Atmar Farm) samples? Most important is that the two sites show a remarkable similarity in the types of artefacts made and how they were produced. Atmar Farm is a later Acheulean site from Terrace 10. Essentially, this site therefore characterises the Later Acheulean in the valley, at least at a site where raw material is abundant. The much larger assemblages from Penhill Farm, both older than 0.485 ± 0.051 Ma but younger than 1.37 Ma, likely belong to the later Acheulean based on these distinct assemblage similarities. As such it is suggested here that the assemblages from both sites are largely comparable in time. Comparison with the Bernol LCTs will further test this hypothesis. However, the thinner LCT blanks from Atmar Farm may indicate a younger age for this site when compared to Penhill Farm.

5.5.2 Bernol and Penhill Farm LCT technology

There are several important differences that occur in the production of LCTs between these two sites. None of the LCTs recovered from Bernol Farm comes from the dated location though, and thus it is difficult to determine the age of these LCTs (see Chapter 4.3). We cannot be certain that the date provided by Granger *et al.* (2013) of 1.14 ± 0.2 Ma for overbank fine deposition provides any indication as to what could be the age of these artefacts, locally.

Some similarities, however, do occur in the production of LCTs at both sites and these will be highlighted first. Accordingly:

- By length, width, thickness and weight, both assemblages illustrate the presence of large, heavy cleavers and picks, and small bifaces
- Tip shapes show a similar preference for generalised convergent types
- Cleaver butt plans show a preference for rounded and squared shapes
- Shaping data shows that bifacial reduction on large flake blanks is most common
- Secondary scar counts generally always exceed primary scar counts

More informative though are the differences that occur between the sites and these relate to all aspects of LCT size and shape, as well as reduction. These are summarised below:

- LCT size and shape data:
 - Length/width/thickness/weight: Bernol Farm picks and cleavers are the largest and heaviest artefacts, with smaller handaxes and bifaces. In contrast, Penhill Farm shows that handaxes, by type, are frequently amongst the largest and heaviest artefacts at the site, especially those on siltstone.
 - Elongation (L/W ratios): Bernol Farm LCT ratios range from 1.49-1.62. Cleavers account for the most elongated LCTs. At Penhill Farm, these ratios range from 1.29-1.89, and picks and handaxes are the most elongated. The highest ratios at both sites provide an illustration of the upper technological limits of the assemblages. As such, tool elongation

is higher in the Penhill Farm LCTs. Comparing handaxe and cleaver ratios between the sites, handaxes show greater elongation at Penhill Farm whereas cleavers are more elongated at Bernol Farm.

- Refinement (T/W ratios): Bernol Farm LCT ratios range from 0.55-0.75, with handaxes being the most refined. At Penhill Farm, these ratios range from 0.44-0.83, with bifaces being the most refined. Considering the smallest ratios (thus technological limits), tool refinement is greater at Penhill Farm. Comparing handaxe and cleaver ratios between the sites, both handaxes and cleavers show greater refinement at Penhill Farm.
- Tip shapes: Bernol Farm cleavers are dominated by generalised convergent tip shapes, yet at Penhill Farm these LCTs have mostly convergent oblique shapes. This illustrates different flaking/shaping strategies in cleaver production between the sites.
- LCT reduction:
 - Scar counts: Bernol Farm LCTs have an average scar count range of 12.2-19 scars, and excluding the single biface, handaxes show the greatest number of scars (18.7). Penhill Farm LCTs have an average scar count range of 10-16.3 scars, and picks and cleavers show the greatest number of scars (14.8 and 16.3, respectively); handaxe average scar counts range from 13.3-15. These ranges illustrate that the average number of flakes removed from the Penhill Farm LCTs is lower.
 - Flaking coverage: the total Bernol Farm LCT sample shows that 70% of all sectors show primary and secondary working, with only 13% showing secondary flaking. The total Penhill Farm LCT sample shows that 66% of all sectors show primary and secondary working, with 20% showing secondary working. This illustrates that flaking coverage and thus reduction intensity appears less extensive in the Penhill Farm LCTs, yet secondary edge refinement is more common. By type, this is most evident in the Penhill Farm handaxe LCT sectors, which show only 61% have both primary and secondary working, compared with the Bernol Farm handaxes, which show 72%.

- Percentage cortex: Bernol Farm LCTs are predominantly cortical, yet a large percentage (27.3%) shows 0% cortex and none has cortex exceeding 50%. All of the Penhill Farm colluvial LCTs are cortical (ranging from either 1-74%), as are the majority in the debris flow assemblage (78% of all LCTs, with cortex ranging from 1-100%); 22% show no cortex. Overall, this is in agreement with the scar count and flaking coverage data above, and further suggests that LCTs are less reduced at Penhill Farm.

What is the importance of these differences in LCT production between Bernol and Penhill Farm, and can these differences really be treated as ‘differences’ when sample sizes are so limited? Is the Bernol Farm LCT sample even representative? Either way the points listed above provide an important indication of the technological strategies employed in LCT production at the two sites.

As such, large flake production has clearly played an important role in providing LCT blanks. However, it appears that the quality of these blanks may have changed through time (a concept discussed by Sharon 2010) based on the more elongated and refined LCTs at Penhill Farm that show less reduction/shaping was needed to shape the tools. Without assessing a suitable core and flake sample from Bernol Farm though this cannot be confirmed.

Another important finding between these assemblages is the preference for generalised convergent LCT tip shapes. Although it remains to be proven whether a generalised tip would be better suited for a wider range of activities, from a purely morphological perspective it would appear so, versus more specialised shapes (e.g., markedly convergent shapes – namely picks – suggesting more specific uses). Overall, this suggests that the shaping of LCTs in the lower Sundays River Valley favoured more generalised tip production.

Overall, this comparison has noted some important differences and similarities between the LCT samples from each site. But, without a more detailed assessment of a larger, unbiased sample from Bernol Farm (preferably from the dated location), these findings are only preliminary.

5.6 Comparison between the lower Sundays River sites and other local and international sites

The purpose of this section is to provide some basic comparisons between the lower Sundays River archaeological sites and other local and international Acheulean sites, highlighted in Chapter 2.2, that are within the general time range of the Sundays River sites. These include:

- Olduvai Gorge (Beds III, IV and Masek; Leakey & Roe 1994); 1.15-0.5 Ma
- Peninj (Moinik Formation sites; ST-69: Diez-Martín *et al.* 2009b; PEES2: Domínguez-Rodrigo *et al.* 2009d); 1.3-1.2 Ma
- Olorgesailie (Members 1, 6/7 and 10/11; Isaac 1977); 0.99-0.6 Ma
- Canteen Kopje (Pit 6 Victoria West levels; Leader 2014); >1 Ma
- Wonderwerk Cave (Strata 5-10; Chazan 2015); 1.07 to <1 Ma
- Amanzi Springs (Deacon 1970); undated
- Cave of Hearths (Beds 1-3; McNabb 2009); <0.78 Ma
- Montagu Cave (Layers 3 and 5; Keller 1973); <0.6 Ma

The emphasis here will be to draw upon those notes summarised in Chapter 2.2 that highlighted basic typological and technological information relating to three of the most informative assemblage components in each site, namely cores, retouched pieces and LCTs. Only the beds, sites, layers and members above are noted in the following comparison.

At the outset it must be stated here that providing such comparisons, from a purely descriptive and qualitative standpoint, is difficult. Variability at the assemblage level is present in all of the sites discussed in Chapter 2.2, and the summaries here make every effort to synthesise basic trends that are most prevalent, along with other notable variations. Differences in artefact analysis through time, namely in typological and technological approaches, must also be factored in. This section will therefore attempt to provide both similarities and differences between all of these assemblages such that broad comparisons can be made. Although this section is largely speculative because of the variability in published data, it is informative

nonetheless as it provides a rough indication for site-level similarities between the assemblages.

5.6.1 Core reduction

Interestingly, there is a great deal of similarity in the way cores are reduced at each of the highlighted sites. As such:

- Discoidal cores with radial/centripetal reduction strategies account for the majority of all cores in most of the sites, especially for Olduvai Gorge (all beds), Peninj ST-69, Olorgesailie (all members), Amanzi Springs, Montagu Cave (all layers) and Cave of Hearths (all beds)

However, some sites do illustrate greater variability in core reduction and retain notable samples with differing strategies, namely:

- Cores that show a multidirectional reduction strategy are most frequent at Peninj PEES2
- The Victoria West levels at Canteen Kopje show that simple casual cores are the most frequent core type
- Although not the most abundant core type at Amanzi Springs, casual cores are notably frequent

From this it would appear then that the high frequency of radial core reduction at Penhill Farm is largely comparable with the majority of the highlighted sites.

Although Chapter 2.2 does not provide information that relates to the reduction intensity of cores, or what blanks were favoured, the fact that radial core reduction has played an important role in the majority of these sites is significant. One interesting point though is a lack of bipolar cores at all of the highlighted sites, yet at Penhill Farm these elements do occur. This indicates some variety in the reduction of cores at Penhill Farm, but the fact that these pieces are so infrequent suggests such activity was rather the exception than the norm.

Perhaps more interesting is the high frequency of casual cores at both Canteen Kopje and Amanzi Springs, which should relate to the high abundance of raw materials in the local landscape at both sites (Deacon 1970; Leader 2014). A similar trend is

evident at both Atmar and Penhill Farm, where raw materials are readily available in the local landscape, coupled with a high frequency of these simple casual cores. It would appear at all these sites then that there was no need to economise raw materials and extensively reduce cores. This would be further supported by the low scar counts on the remaining cores from Atmar and Penhill Farm.

5.6.2 Retouched piece frequency and reduction

Once again there are remarkable similarities in the types of retouched artefacts that are common in most of the highlighted sites. Accordingly:

- Scrapers, although variable between all of the sites, are common and account for notable percentages of retouched formal tools in most of the sites, including: Amanzi Springs, Montagu Cave (all layers), Olorgesailie (all members), Olduvai Gorge (all beds), Cave of Hearths (all beds) and Canteen Kopje (Victoria West levels)
- Side scrapers are generally more common, especially at Olduvai Gorge (all beds) and Amanzi Springs

Conversely, there are some important differences that occur in the frequency of retouched pieces at certain sites, and these are as follows:

- Peninj (all sites) and Wonderwerk Cave (all strata) generally have a lack of information on small retouched tools
- Cave of Hearths (all beds) retouched artefacts show a greater range of types, including: denticulates and composite pieces
- Montagu Cave (all layers) has a high frequency of minimally trimmed flakes, chips and chunks

To be conservative, only Penhill Farm is useful for comparison here as the Atmar Farm formal tool sample is so limited (n=7, of which only one is a scraper). Overall, scrapers are the most frequent retouched formal tools at Penhill Farm. Although denticulated and notched scrapers are most common, side scrapers account for notable samples in both assemblages. This suggests that Penhill Farm compares well with the majority of the highlighted sites, yet proportions of simpler denticulated and notched types at Penhill Farm are higher.

Perhaps there is also good comparability to sites like Cave of Hearths and Montagu Cave. These sites show a wider range of retouched items, and most significantly they also include composite pieces (Cave of Hearths; McNabb 2009) and minimally trimmed pieces (Montagu Cave; Keller 1973). As composite pieces are absent from the rest of the highlighted sites, this type may therefore form an important component in certain Later Acheulean assemblages. Composite pieces, although infrequent at Penhill Farm, have clearly played an important role in subsistence activities. In addition to this, the high percentage of MRPs may be largely comparable to those ‘minimally trimmed items’ from Montagu Cave. Both of these sites are cave sites, and although the Cave of Hearth assemblages do not appear to represent a long-term occupation or one by a large group of hominids (McNabb 2009), Montagu Cave illustrates repeated site visits and occupations over multiple periods (Keller 1973). Clearly Penhill Farm was never a cave site, but perhaps then the presence of these tools here, and in the two cave sites, may purely then relate to similarities in site-based activities.

Available data that highlight the way in which these retouched artefacts are produced show the following similarities between the sites:

- Retouch, although highly variable, is generally irregular, noninvasive (short removals), marginal to blank edges, and the edge shapes created show little standardisation (exceptions do occur)
- Where data are available, flake blanks are favoured for retouching (e.g., at Amanzi Springs, all members at Olorgesailie, and all beds at Cave of Hearths)

By site, however, there are some notable differences that characterise these retouched pieces:

- Olduvai Gorge: discontinuous retouch and the range of edge shapes is high (all beds); notched retouch is common (Bed III)
- Olorgesailie (all members): denticulated retouch is uncommon although edges are irregular
- Canteen Kopje (Victoria West levels): notched and denticulated retouch occurs infrequently
- Amanzi Springs: denticulated retouch is common but notching is uncommon

- Peninj (all sites): continuous and more complex (i.e., bifacial) retouch is common

Penhill Farm retouched artefacts clearly share some of the traits listed above.

However, there is a clear preference for simpler notched and denticulated edges at this site and these types may compare well with those at Olduvai Gorge (especially Bed III), Olorgesailie (all members), Canteen Kopje (Victoria West levels), and Amanzi Springs.

It is interesting that Amanzi Springs also retains a high prevalence of denticulated edges, as does Penhill Farm, and with this site occurring in the same region, perhaps these edges were best suited to subsistence activities in the local landscape at the time. However, these types also occur in the majority of sites, which only illustrates their importance in providing a solution to specific subsistence activities.

5.6.3 LCT frequency and reduction

The most difficult artefacts to compare between the sites are most definitely the LCTs. This is mainly due to the high level of variability that occurs in their production, between sites and even within single assemblages. Furthermore, we need to consider that our understanding of LCT production has changed through time, as have the methods we use to quantify and describe this technology. Perhaps this high variability should be expected when discussing the artefacts. Nonetheless, a basic assessment of which LCTs are most frequent at the highlighted sites and a discussion of the general strategies employed in their reduction will help shed light on how exactly the Sundays River LCTs compare.

Accordingly, the frequency of LCT types shows the following similarities between the sites:

- Handaxes are the most common LCTs at Olduvai Gorge (all beds), Peninj (all sites), Olorgesailie (all members), Amanzi Springs (with other large bifaces), Montagu Cave (all layers; marginally more than cleavers) and Wonderwerk Cave (all strata)

- Cleavers are most frequent at Canteen Kopje (Victoria West levels) and Cave of Hearths (all beds)
- Overall, handaxes and cleavers are most common in the majority of sites; where picks and bifaces do occur they are generally less frequent; this is a typical feature for the Acheulean in general, with the exception of some very early Acheulean sites that are dominated by pick-like handaxes

Conversely, there are some notable differences between these sites and they are as follows:

- Olorgesailie (Member 6/7) has a high prevalence of robust pick-like forms
- Amanzi Springs has a high prevalence of handaxes with other large (variable) bifaces
- Montagu Cave (all layers) shows a large sample of variable bifaces (which appears to be related to its context as a factory site)

Only Atmar and Penhill Farm are suitable for comparison here as the Bernol Farm LCTs represent a biased collection. Accordingly, Penhill Farm shows that handaxes are the most frequent LCTs, followed closely by cleavers; picks are infrequent and bifaces are rare. The small LCT sample (n=3) from Atmar Farm shows that handaxes, bifaces and cleavers are all equally represented.

These Sundays River LCT samples would compare well then with the majority of sites above, where handaxes and cleavers are the most frequent types. However, there is a clear difference between the Sundays River sites versus Canteen Kopje and Cave of Hearths, where these latter two sites show an abundance of cleavers. In addition to this, the low frequency of more robust forms (e.g., picks) in the Sundays River samples suggests largely different subsistence conditions to those experienced during Member 6/7 times at Olorgesailie. Furthermore, the large samples of variable bifaces that occur at Amanzi Springs and Montagu Cave are clearly a component that is missing in the Sundays River assemblages. Perhaps this is more related to the methods used in LCT classification though.

One must remember that LCTs were functional items (Kuman 2014b), and that these pieces would have been created to perform specific tasks in the local environment.

Perhaps then the Sundays River sites indicate what could arguably be similar functional responses to a given environment, and therefore basic subsistence activities, in relation to the majority of the highlighted sites.

Data that highlight the way in which LCTs are produced are broken down here into seven sections, namely: blank type, thinning, shaping, edge refinement and retouching, symmetry, standardisation and tip shapes. To make comparisons between the relevant sites easier, data that relates to thinning, shaping and edge refinement will be grouped together. The following similarities and differences occur between the assemblages.

Blanks:

- Flake blanks are favoured for LCT production in the large majority of the highlighted sites, regardless of raw material, including: Montagu Cave (all layers), Olorgesailie (all members), Olduvai Gorge (all beds), Peninj (all sites), Cave of Hearths (all beds) and Canteen Kopje (Victoria West levels)
- Cobble blanks are favoured for LCT production at Amanzi Springs
- Flat slabs are favoured at Wonderwerk Cave

Thinning, shaping and edge refinement/retouching:

- Collectively, this tends to be more extensive at the following sites: Olduvai Gorge (Masek Beds), Peninj ST-69, Olorgesailie (Members 10/11), Montagu Cave (all layers), and Wonderwerk Cave (Strata 5-8); Cave of Hearths LCTs show high variability with sporadic elegantly shaped pieces (all beds), as do the Olduvai Gorge Bed IV LCTs
- Collectively, this tends to be less extensive (minimal) at the following sites: Olduvai Gorge (Beds III), Peninj PEES2, Olorgesailie (Members 1 and 6/7), Amanzi Springs, and Wonderwerk Cave (Strata 8-10)

Symmetry:

- Where data are available, LCT symmetry tends to be absent or very low at the majority of sites, including: Olorgesailie (Member 6/7), Canteen Kopje (Victoria West levels), Amanzi Springs, Montagu Cave (all layers) and Cave of Hearths (all beds)
- LCT symmetry tends to be high at the following sites: Olduvai Gorge (Masek Beds) and Peninj ST-69

Standardisation:

- Where data are available, LCT standardisation is high at the following sites: Olduvai Gorge (Beds IV and Masek) and Peninj ST-69
- It is low at the following sites: Canteen Kopje (McNabb & Beaumont 2011b) and Cave of Hearths (all beds)

Tip shapes (McNabb *et al.* 2004):

- Where data are available, tip shapes are predominantly generalised convergent at: Amanzi Springs, Montagu Cave (all layers) and Cave of Hearths (all beds)
- Wide or divergent tips are also frequent at Cave of Hearths (all beds) and Montagu Cave (all layers)

The manner in which the Sundays River LCTs are produced shows some important similarities to, and some differences from, several of the trends noted above. First, in all three sites (Atmar, Bernol and Penhill Farm), flake blanks are favoured for LCT production; blank use is comparable with the majority of the highlighted sites. However, Amanzi Springs shows that cobble blanks are more favoured (Deacon 1970).

This is interesting considering that cobble blanks are also readily available in the lower Sundays River Valley, yet hominids here preferred to work cores first to obtain large LCT flake blanks. Even more interesting is that raw material use between these sites is largely consistent (quartzites are favoured). Overall, this clearly shows that the strategies employed in LCT reduction between Amanzi Springs and the Sundays River sites differ. The flaking strategies required by cobble blank reduction, versus flake blank reduction, will vary.

Continuing with LCT reduction, although the vast majority of the Sundays River LCTs shows bifacial working, the quantity of flake scars and the coverage of these scars is generally low. This is especially evident at Penhill Farm, and slightly less so at Bernol Farm, although variability does occur. More refined and elegant LCTs are found in all three of the sites, but these are in the minority. This suggests that the Sundays River LCTs tend to compare better with those from older sites and/or

assemblages, i.e., those above that show less extensive LCT thinning, shaping and edge refinement. This is significant considering the age range for these sites/assemblages is 1.3-0.78 Ma, including: Olduvai Gorge Bed III, Peninj PEES2, Olorgesailie Members 1 and 6/7, and Wonderwerk Cave Strata 8-10 (excluding the undated Amanzi Springs).

In addition to this, the level of standardisation (e.g., in shape, size and finishing) in the Sundays River LCTs, along with symmetry, is low. Once again, although there are exceptions to this in the three sites, the vast majority of LCTs shows very little to suggest either of the above. Low levels of LCT symmetry have been noted at Olorgesailie (Member 6/7), Canteen Kopje (Victoria West levels), Amanzi Springs and Montagu Cave (all layers). Furthermore, also low at Canteen Kopje is LCT standardisation, a pattern also evident at Cave of Hearths (all beds). It would appear then that there are similarities in the overall appearance of LCTs between these highlighted sites and those in the lower Sundays River Valley. All these observations though illustrate the large degree of variability in the Acheulean LCTs through time.

The final comparison to be made concerns LCT tip shapes. Although these data are not available at all of the highlighted sites, where it is present the majority of the sites have generalised convergent tipped LCTs. Although this occurs at Montagu Cave (all layers) and Cave of Hearths (all beds), most relevant is that these types also occur at Amanzi Springs. Occupying the same region, both Amanzi Springs and the Sundays River sites may illustrate a uniform and consistent approach in LCT tip shaping, which best suited the local environment at the time. LCT tips play a crucial role in tool function, and the fact that these generalised types are common at both sites is an important feature that may speak to the similarities in tool use between these sites.

In summary, a speculative chronological placement of the Sundays River sites would be as follows based on the assemblage similarities and differences highlighted above:

- Core reduction: 1.2 Ma to younger than 0.6 Ma, with core reduction at the oldest site in the Moinik Formation at Peninj (PEES2; 1.3-1.2 Ma) being largely different

- Retouched pieces: 1.15 Ma to younger than 0.6 Ma, but based on the wider range of retouched tools at sites like Cave of Hearths and Montagu Cave, ages of <0.78 Ma and <0.6 Ma would seem more appropriate
- LCTs: more important to look at here is the way LCTs are produced, versus which types are more abundant; an age of between 1.3-0.78 Ma would seem appropriate based on similarities in thinning, shaping and edge refinement

Chapter 6

Final summary and conclusion

Research efforts in the lower Sundays River Valley have been focused on the careful survey and excavation of three dated sites, all of which occur in alluvial terrace deposits. Based on our investigations we have shown that largely different contextual conditions occur at each site, and the assemblages at each are also highly variable. It is now time to look back at the original research questions presented in Chapter 1 and to both summarise and conclude the main findings of this research.

6.1 Research question 1

What specific site formation conditions can be established for the artefact-bearing horizons within these deposits, and how have these affected site integrity and context?

The Sundays River has a very long and complex evolutionary history; the unique underlying geology of this region has enabled the lower Sundays River Valley to record changes in drainage evolution in the form of preserved alluvial terrace deposits (Hattingh & Rust 1999). These deposits have been the focus of research since the 1920s (beginning with Haughton in 1928), and from the 1990s up until more recently our understanding of these terraces and their formation has been greatly improved. These terraces are divided into both upper older (1-9) and lower younger (10-13) terraces, and based on recent dating work by Erlanger *et al.* (2012), these upper terraces are now seen to span the Early Miocene to Middle Pleistocene, with the lower terraces now spanning the Late Pleistocene to Holocene. These terrace deposits therefore span a large period of the southern African Stone Age.

Our research has focused on the survey and excavation of three properties with terrace deposits bearing Stone Age artefacts that span the Early to the Later Acheulean.

Conditions for site formation and transformation are highly variable between them, and thus each site is summarised separately below.

6.1.1 Atmar Farm

This site is characterised by a simple west facing exposure of gravels and fine sediment alluvium from Terrace 10. The upper fine sediments indicate low energy floodplain deposition, whereas the underlying gravels indicate high energy deposition. A low-density scatter of poorly preserved Later Acheulean artefacts is found within these gravels. Based on work conducted by Erlanger (2010), Erlanger *et al.* (2012) and Granger *et al.* (2013) on clasts sampled from these lower lying gravels, overbank fine deposition and burial of the gravels is dated to 0.65 ± 0.06 Ma using the cosmogenic burial dating method.

Although only basic data are provided for Atmar Farm, they confirm what is to be expected for a poor secondary context alluvial gravel deposit. Accordingly, the smallest assemblage components have been winnowed away and re-distributed downstream due to fluvial action. As a result the Atmar Farm assemblage is heavily biased towards material that is larger than 20 mm. Artefact condition and raw material data illustrate that the vast majority of artefacts is poorly preserved (78% heavily abraded/rolled). This indicates that the artefacts were re-worked within the alluvial gravels either for a considerable period of time or over a prolonged distance, prior to deposition. The scarcity of non-lithic material at Atmar Farm is also likely linked to the poor context of these gravels. Overall, these findings clearly highlight the poor-integrity of the deposit.

6.1.2 Bernol Farm

This site is comprised of a complex southwest exposure of Terrace 9 alluvium consisting of bedded overbank fine sediments (silts and sands) overlying gravels sitting atop sandstone bedrock. Research here was conducted at five locations, namely at the dated location and the four survey sites.

The dated location preserves a thick (>3 m) deposit comprised of silts and sands, and discontinuous imbricated gravels (with upper thin stringers and a thicker basal unit). The upper portion of this deposit indicates floodplain deposition with minor re-working and sorting by river flow (Granger *et al.* 2013). Early Acheulean artefacts and bone occur in both the upper gravel stringers and in the lower lying gravels. Based on the age provided by Granger *et al.* (2013) using the cosmogenic burial dating method on clasts sampled from the lower gravels, overbank fine deposition occurred here at 1.14 ± 0.2 Ma.

Unfortunately our contextual understanding of the four remaining survey sites is poor and presently we are uncertain as to how these sites relate to the dated location. They appear to be colluvial and/or possibly alluvial in origin, and they contain a range of shell, bone, gravels and Earlier and Middle Stone Age artefacts. Although the majority of the survey sites is largely comparable in height to the dated gravels, a more detailed investigation is needed to fully understand these deposits.

Irrespective of these contextual uncertainties, the condition of the recovered artefacts is good. Although all of the sites are of secondary context, this suggests overall assemblage integrity is high.

6.1.3 Penhill Farm

Contextually, Penhill Farm provides a complex exposure of deposits that are visible in profile within a borrow pit quarry. As a result, these deposits are exposed in a circular (amphitheater-like) fashion with vertical walls comprised of Terrace 9 alluvium. The subsequent transformation of these deposits towards the east of the borrow pit has been extensive.

This Terrace 9 exposure is dominated by several meters of fine alluvium, which are massive and structureless. These are well-sorted and contain a high percentage of fines (clays and silts), and they document extensive low energy floodplain deposition. In the southern most portion of the borrow pit underlying these fine sediments occurs a gravel horizon, from which clasts were sampled for dating using the cosmogenic

nuclide burial method. As a result, an age of 1.37 ± 0.16 Ma is provided for overbank fine deposition that buried the gravel (Granger *et al.* 2013). No artefacts occur within the fine alluvium or in the lower lying gravels here.

In contrast, however, the east portion of the borrow pit shows that a roughly 2.5 m deep erosion channel has been cut into the fine host alluvium. This erosion channel has subsequently been filled with poorly sorted colluvium from upslope that includes poorly sorted fine sediments (devoid of fines), gravels, calcrete, silcrete, preserved root casts, and ESA artefacts. This colluvium has been divided into two deposits, one that extends from the surface down to 1.8 m (colluvial assemblage), and underlying this a distinct debris flow (containing the debris flow assemblage). ESA artefacts occur in both deposits, yet artefact frequency is far greater in the debris flow when compared to the overlying 1.8 m of colluvium. Overall the frequency of non-lithic material is scarce in both deposits and this can be linked to their open-site colluvial origin.

The upper 1.8 m of colluvium has several important features that illustrate its formation, modification and accumulation. The upper 1 m is heavily bioturbated and this activity continues down towards and within the debris flow. This activity likely accounts for the general lack of stratigraphy in this deposit. In addition to this, several smaller erosion channels occur within a cut and fill deposit in this colluvium. These features indicate the downslope (east to west) erosion of this deposit. The general absence of SFD coupled with a higher percentage of abraded artefacts supports the winnowing of material, likely by rainsplash or sheetwash/flow erosion. As a result the colluvial assemblage indicates somewhat slower, more punctuated deposition during which time artefacts were likely exposed at the surface for longer periods. The potential for assemblage modification was therefore high; assemblage integrity is poor.

Conversely, very different conditions occur for the accumulation of the lower lying debris flow deposit. Here, artefact preservation is better and there is a high percentage of SFD. This high concentration of SFD is not the result of a fluvial re-concentration, an interpretation supported by the completely random spatial arrangement of artefacts and very poor preferential orientations and trends in dip angles. In addition to this our

spatial analysis shows that the flow entered the erosion channel from the upslope east direction, and the majority of the material appears to have become concentrated towards the middle part of the excavated channel (the center squares). This material moved downslope with the majority coming to rest at the most distal point in the base of the channel (the west squares). Artefact spatial data thus confirms that the debris flow is 'wedged out' and is thickest in the east and thinnest in the west.

The debris flow assemblage therefore represents the rapid downslope deposition and burial of the majority of a site that likely occurred only several meters upslope. It represents the downslope deposition of an upslope lag of re-worked calcrete and silcrete nodules, gravels and artefacts, into a cone (Granger *et al.* 2013). The overall integrity of the debris flow assemblage is high. Any influence by natural processes post-depositionally on the exposed debris flow was likely restricted to only the upper levels of the deposit.

Irrespective of the difference in the rate of downslope deposition between the two assemblages, the colluvial assemblage deposit indicates poorer conditions for preservation and illustrates a greater potential for assemblage winnowing through natural processes. Our interpretation is that a smaller portion of the original upslope site remained after the deposition of the debris flow, and less material (potentially minimal SFD) was left behind to be transported downslope at a later stage. Poorer artefact condition data and the presence of distinct erosion channels within the colluvium highlights the low integrity of this assemblage.

Most significant now is our revised understanding of the age of the Penhill Farm assemblages. The original date of 1.37 ± 0.16 Ma (Granger *et al.* 2013) provides a maximum age for the Penhill Farm assemblages. The new cosmogenic nuclide dating results from Excavation 1 provide a refined age of 0.485 ± 0.051 Ma on cobbles within the debris flow. This age does not directly date when the debris flow took place, but rather it dates when the colluvium was deposited after and on top of the debris flow.

Contextually it is thus clear that conditions for deposit accumulation differ greatly between the two assemblages. However, the typological and technological analysis of

the Penhill Farm assemblages shows that the differences between them are minor, and it is most likely that these assemblages are indeed part of the same site that existed upslope, with the contents working their way down at different rates – the majority came down initially and rapidly within the debris flow, followed by a lengthy period of slower deposition of the remaining material in the overlying colluvial assemblage. This suggests that the difference in time between the deposition of these two assemblages is considerable, but the actual difference in time for the production of the artefacts is not. Conversely, perhaps the difference in time for both the production and accumulation of the two assemblages is minimal, but assemblage modification has just been more extensive in the upper 1.8 m of colluvium.

It is our opinion now that the new age of 0.485 ± 0.051 Ma does not directly date the debris flow assemblage, and neither does it date the technology of these artefacts. As a result the two dates currently available for the site are thus $>0.485 \pm 0.051$ and $<1.37 \pm 0.16$ Ma, and both of the assemblages fall within this period. Although it is possible that the assemblages may be closer to 1.37 Ma, providing a model that can account for this is beyond the limits of the existing data. Future work will, however, focus on the dating of artefacts to investigate the possibility that they may have remained buried and sealed upslope prior to moving downslope.

Having investigated the context for the formation and transformation of the three Sundays River sites, we must now turn to the second research question.

6.2 Research question 2

What is the typological and technological nature of the lower Sundays River valley ESA archaeology?

This question has been investigated though both the survey and excavation of the three research sites, which together are able to characterise the lower Sundays River ESA archaeology. An important factor that has influenced the assemblages is the surrounding geology. The upstream Klein Winterhoek Mountains account for more

than 95% of the clasts that occur downstream (Ruddock 1948; Hattingh 1994; Hattingh & Rust 1999). These clasts are comprised of quartzite, so the general rarity in all other raw materials should be expected. While our best understanding of the archaeology comes from Penhill Farm, the key characteristics of each site are summarised below.

6.2.1 Atmar Farm

Our understanding of this site is limited due to the small, poorly preserved lithic assemblage recovered. Detailed analysis could not be conducted. However, some basic trends can be highlighted. Overall, quartzite is most favoured for artefact production. A typological classification shows that flaking debris is most common, followed thereafter by small samples of complete flakes, cores and formal tools. The reduction of quartzite cobbles is favoured, giving rise to simple casual and chopper-cores. These are minimally reduced (low scar count) and the overall percentage of remaining cortex is high. Flake scars are also small suggesting that larger blanks for LCTs were struck from cores elsewhere, or that the cores from which they were struck were not incorporated into the deposit. A single core trimming flake suggests an appreciation for core management, yet overall the need for such activity was unnecessary most likely due to the high local abundance of raw materials.

Most informative is the extremely limited formal tool sample, which shows that flake blanks, predominantly in quartzite, are favoured for tool production. Two retouched artefacts show that there is little standardisation in edge refinement, and retouch is generally sporadic, discontinuous, and noninvasive. Overall these illustrate simplicity in their production.

The three LCTs at Atmar Farm on large flake blanks show minimal shaping and edge refinement. It appears that the flake blanks utilised for LCT production were well-suited and thin to begin with, reducing the need for intense reduction. Conversely, a single quartzite biface shows more invasive shaping and minimal edge refinement. The reduction of LCTs at Atmar Farm is thus variable in this small sample.

6.2.2 Bernol Farm

Only limited data have been recorded on artefacts other than that from LCTs, but what is clear is that quartzite is prominent in artefact production. The small core and flake sample illustrates the production of large flakes locally, also seen in the presence of boulder-cores on-site. Overall though, core reduction is generally simple, seen in the basic chopper- and discoidal cores.

The major focus of analysis here though was on the 11 LCTs, comprising of six cleavers, three handaxes, and a single pick and biface. The detailed technological analysis on these LCTs shows some interesting trends in size, shape and reduction, although the limited sample makes it difficult to assess differences between them. These LCTs represent a biased collection.

Nevertheless, there is a great deal of variability in the LCT measurements and shapes between the types, also seen in the tool elongation and refinement ratio data. When comparing these measurements and indices for handaxes and cleavers, the former are smaller, lighter, and more refined, versus the latter that are heavier and larger, and more elongated. LCT tip shapes are also highly variable, but they do show a preference for generalised convergent types. It is likely that each of these variable tip shapes would have been uniquely and carefully shaped, possibly for a range of different activities.

The strategies employed at Bernol Farm indicate that flake blanks were favoured in LCT production. The extent to which these blanks are reduced varies by LCT type, but overall the handaxes and biface, the smallest LCTs, are the most reduced, whereas the larger cleavers and pick are less reduced, based on the lower flake scar counts. However, the majority of the LCT sample shows that bifacial reduction is most common, across 70% of the LCT sectors, and it is the cleavers that show the greatest range of reduction strategies (including partly bifacial and unifacial types). There is a lack of preserved cortex on these LCTs, which confirms that LCT reduction has been substantial across the majority of all sectors on both faces. In addition, the number of

secondary removals generally always exceeds the number of primary removals, and this suggests that secondary edge refinement is important in the Bernol Farm LCTs.

6.2.3 Penhill Farm

The typological and technological classification of the two Penhill Farm assemblages provides the most detailed information on what characterises the ESA of the lower Sundays River Valley.

Both assemblages are dominated by flaking debris, and the remaining samples of complete flakes, cores, formal tools and other cobbles contribute far smaller percentages to the overall assemblages. Raw material use here is dominated by quartzite, followed thereafter by infrequent siltstone and hornfels. All other raw materials are rare.

Flaking debris provides some interesting features:

- It confirms that knapping activity has occurred in the past within the catchment of the site. However, the reduced quantity of SFD in the colluvial assemblage is clearly important, contextually, and the significance of this has already been discussed under *question 1*.
- There are more raw materials represented, when compared to the remaining core and formal tool samples; this feature is also evident in the complete flake samples. The cores from which this material would have been struck were not recovered, either due to their exclusion from the deposits during accumulation, or perhaps to their preservation in unexcavated portions of the deposit.

Complete flakes illustrate two important features, by type:

1. Those flakes that represent core management and maintenance are found in both assemblages. While these pieces are largely infrequent, it is clear that careful attention was given to some cores during reduction; however, this sort of strategy is more the exception than the norm, likely due to the high abundance of raw materials in the local landscape.

2. Bipolar pieces, although infrequent, occur in both assemblages, and bipolar flaking debris also occurs in both assemblages.

A combined technological analysis of flaking debris and complete flakes illustrates some interesting trends in dimensions/sizes, flaking strategies and the level of reduction, all of which confirm that the Penhill Farm assemblages represent early stages of core reduction; there are also important differences between the three most abundant materials. Accordingly:

- By raw material, siltstone artefacts account for the majority of the largest measurements, followed by quartzite and hornfels pieces as sizes decrease. Overall though, flakes tend to be equidimensional, which is a characteristic feature of Acheulean assemblages (Isaac & Keller 1968).
- By size, flakes 30-50 mm in length are abundant, whereas those >100 mm are infrequent. Considering that almost all of the LCTs are made on large flake blanks and that core reduction is not intensive, this suggests that LCT blanks were transported to the site.
- The strategies employed in flaking illustrate several important features:
 1. Corner- and side-struck flakes are most commonly produced in both assemblages; end-struck flakes are infrequent. In addition to this formal tool production favours side-struck flakes.
 2. The number of dorsal scar directions on these flakes is low and this highlights the general simplicity in core reduction. This is further supported by the dorsal scar pattern data, which illustrates the majority of flakes is removed following the same direction as the previous removal. When comparing this by the different raw materials though, quartzite and siltstone flakes generally retain more complex flaking patterns, whereas hornfels pieces are mostly cortical and indeterminate.

This last point relates to the difference in reduction intensity between the three most abundant raw materials, and the remaining analyses here will further illustrate this point:

- An analysis of technological flake types following Toth's (1985) simulations shows that the Penhill Farm assemblages provide largely comparable

percentages of types I-VI, but there is a minor over-representation of the early stages of core reduction (types I-III). This suggests that there has potentially been some transporting of decorticated lithics off-site. In addition to this, by raw material, quartzite and siltstone flakes have high percentages of types V and VI (later stages of reduction), whereas hornfels flakes have high percentages of types I and II (early stages).

- Platform faceting is limited in the flake samples (mostly plain or cortical) and this is in agreement with the technological flake type data above (Toth types). This supports that the assemblages represent early stages of core reduction. Quartzite and siltstone flakes generally have a higher facet count (two or more) than those on hornfels (mostly cortical).
- Dorsal scar counts show that the majority of flakes has one to four scars, with few having more than five scars. In addition to this those quartzite and siltstone flakes have higher scar counts than those on hornfels. Overall though the low number of scars confirms the limited core reduction at Penhill Farm.
- The quantity of preserved cortex on flakes illustrates that the majority is in the early stages of reduction (having preserved cortex), and by raw material quartzite and siltstone flakes are the least cortical, whereas hornfels flakes are the most.

An assessment of the various core types at Penhill Farm shows that simple cores are most frequent. These are not unlike the simple cores found in most Acheulean assemblages – casual, discoidal and chopper-cores dominate. Polyhedral, single platform and irregular cores are also found infrequently at Penhill Farm. Some interesting features of the cores are as follows:

- There is a high frequency of casual cores, undoubtedly related to the fact that raw materials are readily available. This illustrates either the testing of raw material suitability or the expedient production of one or two flakes for immediate use.
- Some discoids are better shaped, approaching the appearance of those from MSA assemblages. Perhaps these represent the upper limits of core technology.

- Only a single bipolar core occurs in the debris flow sample. It is clear that this kind of core reduction is more the exception than the norm.

The assessment of these cores for dimensions/sizes, flaking strategies and levels of reduction indicates several important features. Overall, core dimensions/sizes show:

1. Siltstone cores are the largest, whereas hornfels cores are the smallest. Quartzite cores are intermediate between the two. This is most likely related to size differences in core blanks.
2. By type, chopper-cores and casual cores are the largest, whereas discoidal cores tend to be small and light, which reflects the degree of reduction typical of these types.

The strategies employed in core reduction, overall, show some interesting trends. Accordingly:

- There is an abundance of simple, unstructured, knapping strategies on predominantly cobble and split cobble blanks. This is clearly seen in the high percentage of unifacial and bifacial simple partial and casual core exploitation patterns. These illustrate short reduction strategies and suggest a high level of expediency. By raw material there is little to suggest that cores are reduced differently.
- A notable sample of discoidal cores occurs in both assemblages and these illustrate more structured and controlled knapping.
- There is a general absence of large flake scars on the cores, or those scars that would otherwise be comparable in size to those used in LCT production. From this it appears that at least some large flakes were struck from cores off-site.

Data that investigate the level of reduction indicates that the Penhill Farm cores are in the early stages of reduction. Accordingly:

- Core scar counts are low, with the majority having one to four removals. By type, discoids show greater levels of reduction versus those less reduced casual cores.

- The percentage of remaining cortex is high, generally exceeding 25% on all the cores. By raw material the only cores to be completely decorticated are made on quartzite; hornfels cores are generally more cortical.

Although the sample sizes for siltstone and hornfels cores are limited, perhaps this is in agreement with the flaking debris and complete flake data that shows greater reduction in the quartzite artefacts and lower reduction in the hornfels pieces.

The formal tool assemblage at Penhill Farm is large and extremely informative. The following features in tool types are notable:

- Tool production takes place primarily on quartzite, siltstone and hornfels.
- Small retouched tools were most readily produced, especially scrapers, followed thereafter by MRPs, denticulates and retouched flakes. It would appear that these small retouched tools were functionally better suited to perform the specific tasks at hand.
- A small sample of composite pieces illustrates the use of artefacts in more than a single task, and this may be a Later Acheulean trait. Perhaps these represent a form of recycling.
- Scrapers are dominated by denticulated, notched and side types.
- LCTs, produced only on quartzite and siltstone, are dominated by handaxes and cleavers; picks and bifaces are less frequent. Broken LCTs are common in the debris flow assemblage, yet the reason for this is uncertain.

The analysis of retouched artefacts shows several important features in their production, and these are as follows:

- Those retouched tools produced on siltstone are the largest, which should be expected considering the preceding flake and core discussions.
- Flake blanks are favoured for tool production.
- The majority of tools illustrates simplicity and expediency in their production, with little emphasis on careful edge modification. This is seen in the following features:
 - Direct and alternate retouch illustrates the simple trimming of artefact edges, and retouch that documents the interaction between the upper and lower planes of an artefact is infrequent.

- Edge shapes are simple and dominated by denticulated and notched types.
- Retouch is predominantly discontinuous and noninvasive.
- The majority of retouched artefacts have cortex, yet by raw material quartzite pieces show greater levels of reduction (less cortical) than those on siltstone and hornfels (more cortical).
- Edge angles are predominantly steep and may illustrate the more frequent use of these tools in scraping tasks.

The analysis of the LCTs also provides important information that relates to their size and shape, and reduction. Accordingly:

- LCT size and shape is highly variable by both tool type and raw material, and although those on siltstone tend to be larger and heavier, size variation is greater on the quartzite LCTs (likely the result of the larger samples).
- Tool elongation (L/W ratio) is greatest in the handaxes and picks, whereas tool refinement (T/W ratio) is greatest in the handaxes and bifaces. Cleavers overall show low elongation and poor refinement.
- Tool tip shapes are highly variable. There is a preference for generalised convergent types, which may have some functional significance (greater range of applications and easier re-use).
- The primary strategy in LCT production is to use large flake blanks upon which a range of LCTs could be made.
- Subsequent reduction of these large flakes shows that there is little difference in the level of reduction (scar counts) between quartzite and siltstone blanks. By LCT type there is also little difference, with the greatest level of reduction/shaping in the colluvial assemblage being on the handaxes (15 scars), whereas cleavers show the greatest scar count (16.3) in the debris flow assemblage.
- Blanks are shaped/reduced bifacially, and both handaxes and cleavers illustrate greater variability in reduction patterns (including partly bifacial and unifacial types) when compared to the less frequent picks and bifaces.

- The overall coverage of this reduction is limited though, covering only 60% of the LCT sectors in the colluvial assemblage and 68% in the debris flow. Furthermore, secondary flaking is limited.
- The majority of all LCTs show remaining cortex, which confirms their reduction/shaping is limited. Those LCTs on siltstone tend to retain more cortex than those on quartzite.

6.2.4 Key features

Overall, to summarise four key points, the lower Sundays River ESA archaeology is best described by the following:

1. Simple strategies are employed in the reduction of cores, which occur on cobble blanks.
2. Low levels of reduction occur on all cores and formal tools, along with differential reduction by raw material (especially evident in the core and flake samples at Penhill Farm).
3. Retouched formal tools are made on flake blanks and they show simplicity and expediency in their production, with little emphasis on careful edge modification.
4. LCTs are variable in size and shape and are also made on flake blanks. The primary strategy in shaping is bifacial reduction across large portions of the LCTs, although the majority retains some cortex and thus reduction/shaping is still limited. Generalised convergent shaped tips are most favoured.

The typological and technological analysis of these Sundays River assemblages has provided important detail on what characterises the regional ESA archaeology. However, we must now turn to the third research question to address the importance of these findings.

6.3 Research question 3

What significance do these ESA sites have with regard to the wider archaeological record of the Eastern Cape?

The significance of this question lies in the fact that the Eastern Cape ESA archaeological record is both poorly represented and poorly understood. This can be attributed primarily to the low frequency of sites in this region (Sampson 1974; Klein 2000a; Mitchell 2002; Phillipson 2005; Herries 2011; Lombard *et al.* 2012). In addition to this, only a single ESA site has been extensively excavated for this entire province (Amanzi Springs; Deacon 1970). Although there is a significant number of surface sites within the region (Laidler 1947; Sampson 1974; Binneman 2010, 2011), the majority of these is unnamed and of minimal value. Furthermore, although the typological and technological information from Amanzi Springs provides crucial data that help to characterise this region's ESA archaeology, this information is marred by one key point – our inability to date the site.

Overall, well-dated Acheulean sites in southern Africa are few, but in the Eastern Cape then these are completely absent. There has thus been a need to provide more ESA sites in this region so that we can understand crucial aspects of hominid behaviour within these sorts of ecological, climatological, and environmental contexts; our interpretations of the southern African Acheulean are heavily biased towards a few keyhole sites and those located in the interior of the country. In addition to this, there has been an important need to provide adequate typological and technological descriptions of the recovered artefacts, and to account for the conditions that led to deposit formation and transformation. This project has sought to address these issues.

Early work in the lower Sundays River Valley noted the presence of ESA artefacts within alluvial terraces bordering the river; artefacts were also found within the neighboring Coega River Valley (Ruddock 1957). It is interesting that until now, no research had investigated these occurrences in relation to the alluvial terraces.

For the first time in half a century, and for the first time in the entire Eastern Cape Province, with the dating results provided by Erlanger *et al.* (2012) and Granger *et al.* (2013), we have now been able to investigate ESA artefact occurrences within a general chronological framework. This study thus provides the first comprehensively described ESA sites for this region, from which we can now begin to construct our

understanding of the local Acheulean Tradition. In addition to this the following three points are pertinent.

First, a fundamental problem with many sites is our inability to compare them chronologically. The fact that all of the Sundays River sites have been constrained to specific periods means that their suitability for such comparison is high. Furthermore, the detailed analysis performed on these artefacts provides comparable ESA artefact data not only for the region but also for the continent.

Second, the lower Sundays River Valley has an extremely complex distribution of alluvial terrace deposits, and based on what has been recovered from only two of these terraces (and three sites), the research potential in this valley is high. With more surveys it is entirely possible that more sites will be located, and although the contextual nature of these will likely vary, there is great potential to expand research efforts. The Vaal River Basin has in the past provided a large number of sites, which contextually have not been ideal. Irrespective of this though, these alluvial sites have contributed significantly to our understanding of the Acheulean Tradition. From this research, it is now possible for the lower Sundays River Valley to contribute equally to these understandings, and to provide important comparative data from largely different ecological and environmental contexts.

Third and last, although the conditions for terrace formation have been unique for the Sundays River, it would be hard to think that the neighboring valleys do not provide informative assemblages (e.g., Coega, already reported by Ruddock 1957), possibly within datable contexts. The potential for exploration in this region is thus great.

Perhaps most significant is that for the first time since Amanzi Springs was excavated, analysed, and published, there are now another three ESA sites against which the Amanzi Springs material can be compared. Although this study provides a basic comparison, future work will focus on more detailed investigations.

Nonetheless, important similarities and differences occur between all of the regional assemblages.

First, simple core reduction is favoured, along with minimal reduction (e.g., frequent casual cores). This illustrates there was no need to economise raw materials and reduce cores extensively. This is likely due to the high local abundance of quartzite cobbles. Second, scrapers are the most common retouched tools, and the retouching of edges is variable, irregular, and noninvasive, but denticulated edges are common. This suggests the high functional suitability of these tools within the local landscape, and thus their presence within the sites may indicate similarities in site-based activities. Notched retouch is more abundant in the Sundays River assemblages, but this is largely absent at Amanzi Springs. Third, LCT types vary between the sites, with handaxes and cleavers common in the Sundays River sites, whereas handaxes and bifaces are most frequent at Amanzi Springs, and cleavers are rare. The way LCTs are reduced is generally consistent though, showing minimal thinning, shaping and edge refinement. However, a notable difference is in the use of cobble blanks at Amanzi Springs. This suggests different strategies were employed in LCT production here. LCT tip shapes are largely comparable and may once again indicate similarities in functional responses to the local environment and site-based subsistence activities.

It is now time to turn to the final research question posed by this research, the most challenging of the four.

6.4 Research question 4

Where does the Eastern Cape archaeological sequence 'fit in' with regard to the wider ESA sequence of southern Africa and beyond, and what basic comparisons can be made between these assemblages and those elsewhere?

Our answer to this question must remain speculative at this point. Although a basic comparison between relevant sites is provided by this research, these are purely descriptive. However, it is still possible for us to 'contextualise' the Sundays River ESA sites by assessing similarities and differences according to three important points, namely chronology, typology and technology. The focus here will be on similarities between the sites.

Chronologically speaking we are confident that the Sundays River ESA sites fall between <1.37 Ma and >0.485 Ma. As a result this places them within the Early to Later Acheulean, within southern Africa. Although Amanzi Springs remains undated, this site clearly fits into this period as well.

Typologically and technologically speaking then, the Eastern Cape assemblages share numerous similarities with those sites elsewhere from a similar period. On aspects of core classification and reduction, the high prevalence of radial reduction strategies in the Eastern Cape is largely comparable with that which occurs elsewhere, especially evident at sites like Olduvai Gorge, Peninj ST-69, Olorgesailie, Montagu Cave and Cave of Hearths. In addition to this, the simpler reduction of casual cores is a feature that is shared by Canteen Kopje and the Eastern Cape sites, and this can be linked to the high local abundance of raw materials. From the reduction of cores then there is little to suggest that the Eastern Cape sites are atypical.

Continuing with these similarities, scrapers are the most common retouched tools at the majority of the highlighted sites (e.g., Montagu Cave, Olorgesailie, Olduvai Gorge, Cave of Hearths and Canteen Kopje); the Eastern Cape sites share this feature. Although there is great variability in retouched tools between the sites, this trend overall suggests great comparability. There thus appears to be similarities in site-based subsistence activities. This is further illustrated by the way in which these tools are made, the majority of which show little standardisation in edge forms, and variable, irregular, noninvasive and marginal retouch. From this it appears that the strategies employed in formal tool production are largely consistent, and simple.

The Eastern Cape LCT samples compare well with the majority of sites elsewhere, where handaxes and cleavers are the most frequent types. However, Amanzi Springs has few cleavers and a high percentage of large bifaces. Where there are significant differences between the sites in the LCTs produced, these are likely the result of specific functional responses (e.g., high prevalence of cleavers at Canteen Kopje). The way in which LCTs are made shows that minimal thinning, shaping and edge refinement characterises most assemblages. Where more elegant LCTs do occur these are generally found in later assemblages. As a result the Sundays River LCTs appear to compare better with those from sites that are >0.78 Ma.

6.5 Future work

A great deal of work still needs to be done in the lower Sundays River Valley, and the series of questions posed in Chapter 5 attest to this. Although we have attained some understanding of the complex distribution of these sites, how they have been formed and transformed, along with what assemblages they contain, there are still numerous questions that need to be addressed in the future. To not repeat what has been raised in Chapter 5, some new issues are highlighted below.

Future research at Atmar Farm should focus on additional site surveys, with the emphasis being on finding well-preserved artefacts in the fine overbank sediments. Terrace 10 exposures are not limited to this property though, so there is great potential to expand our work into other areas of the valley.

Bernol Farm is perhaps the most promising of all the sites, but it will be the most challenging to excavate. This property contains well-preserved Early Acheulean artefacts within fine alluvium, a general rarity by any standards, and it is therefore paramount that excavations are conducted here in order to obtain a representative sample. Furthermore, based on only a preliminary investigation into artefact use-wear, Bernol Farm has a high potential for this kind of analysis.

Although a great deal of work has occurred at Penhill Farm, there are several important issues that need to be resolved (highlighted in Chapter 5). More excavations are clearly needed if we are to resolve some of these issues, and most important would be the controlled excavation of the upper 1.8 m of colluvium above the debris flow. The emphasis here would be to carefully map in the cut and fill deposit and associated erosion channels. In addition to this, what appears to be another debris flow deposit occurs at Penhill Farm towards the south of the borrow pit. Although from a preliminary investigation the density of artefacts here is low, it would be worthwhile to conduct basic test pit excavations into this deposit. This may provide comparable material.

Another vital form of analysis that could not be conducted during this study is artefact refitting. Conjoining artefacts provide extremely important information that not only relates to the context of a site but also to the strategies employed in artefact reduction. From the detailed analysis of artefacts at Penhill Farm, and taking into account our site formation model that proposes downslope transport of the artefacts from a nearby site upslope, there is a very high possibility that some artefacts will refit. Sufficient attention must be given to this analysis in the future. Furthermore, based on the preliminary study of artefact use-wear patterns, this analysis should also be performed on a larger sample of artefacts in the future.

Lastly, we will continue with our efforts to date the technology of the assemblages at Penhill Farm. At present we are selecting artefacts upon which we can apply the cosmogenic nuclide burial dating method. We hope to uncover evidence from these samples that suggests the possible upslope burial of these artefacts prior to downslope deposition, which could be revealed by some older inherited ^{26}Al and ^{10}Be concentrations.

References

- Abbate, E., Albanelli, A., Azzaroli, A., Benvenuti, M., Tesfamariam, B., Bruni, P., Cipriani, N., Clarke, R.J., Ficarelli, G., Macchiarelli, R., Napoleone, G., Papini, M., Rook, L., Sagri, M., Tecle, T.M., Torre, D. & Villa, I. 1998. A one-million-year old *Homo* cranium from the Danakil (Afar) Depression of Eritrea. *Nature* 393: 458-460.
- Abrahams, A.D., Parsons, A.J. & Hirsh, P.J. 1985. Hillslope gradient-particle size relations: evidence for the formation of debris slopes by hydraulic processes in the Mojave Desert. *The Journal of Geology* 93: 347-357.
- Abrahams, A.D., Soltyka, N., Parsons, A.J. & Hirsh, P.J. 1990. Fabric analysis of a desert debris slope: Bell Mountain, California. *The Journal of Geology* 98: 264-272.
- Akerman, H.J. 1984. Notes on talus morphology and processes in Spitsbergen. *Geografiska Annaler Series A, Physical Geography* 66: 267-284.
- Albjar, G., Rehn, J. & Stromquist, L. 1979. Notes on talus formation in different climates. *Geografiska Annaler Series A, Physical Geography* 61: 179-185.
- Almond, J., De Klerk, B. & Gess, R. 2009. Palaeontological heritage of the Eastern Cape (consulted June 2015): <http://www.sahra.org.za/wp-content/uploads/2014/08/EC-FOSSIL-HERITAGE-full-version.pdf>
- Alperson-Afil, N. & Goren-Inbar, N. 2010. *The Acheulian Site of Gesher Benot Ya'aqov Volume II: Ancient Flames and Controlled Use of Fire*. London: Springer.
- Alperson-Afil, N., Richter, D. & Goren-Inbar, N. 2007. Phantom hearths and the use of fire at Gesher Benot Ya'aqov, Israel. *PaleoAnthropology* 2007: 1-15.
- Anderson, R.S. & Anderson, S.P. 2010. *Geomorphology: The Mechanics and Chemistry of Landscapes*. Cambridge: Cambridge University Press.
- Andrefsky, W. 2005. *Lithics: Macroscopic Approaches to Analysis. Second Edition*. Cambridge: Cambridge University Press.
- Andrews, J.T. & Smithson, B.B. 1966. Island, Northwest Territories, Canada Till Fabrics of the Cross-Valley Moraines of North-Central Baffin. *Geological Society of America Bulletin* 77: 271-290.

- Antón, S.C. & Snodgrass, J.J. 2012. Origins and evolution of the genus *Homo* new perspectives. *Current Anthropology* 53: S479-S496.
- Archer, W. & Braun, D.R. 2010. Variability in bifacial technology at Elandsfontein, Western Cape, South Africa: a geometric morphometric approach. *Journal of Archaeological Science* 37: 201-209.
- Armanini, A. & Michiue, M. 1997. *Recent Developments on Debris Flows*. New York: Springer.
- Asfaw, B., Beyene, Y., Suwa, G., Walter, R.C., White, T.D., WoldeGabriel, G. & Yemane, T. 1992. The earliest Acheulean from Konso-Gardula. *Nature* 360: 732-735.
- Asfaw, B., Gilbert, W.H., Beyene, Y., Hart, W.K., Renne, P.R., WoldeGabriel, G., Vrba, E.S. & White, T.D. 2002. Remains of *Homo erectus* from Bouri, Middle Awash, Ethiopia. *Nature* 416: 317-320.
- Ashley, G.M., Domínguez-Rodrigo, M., Bunn, H.T., Mabulla, A.Z.P. & Baquedano, E. 2010. Sedimentary geology and human origins: a fresh look at Olduvai Gorge, Tanzania. *Journal of Sedimentary Research* 80: 703-709.
- Assaf, E., Parush, Y., Gopher, A. & Barkai, R. 2015. Intra-site variability in lithic recycling at Qesem Cave, Israel. *Quaternary International* 361: 88-102.
- Avery, D.M. 2001. The Plio-Pleistocene vegetation and climate of Sterkfontein and Swartkrans, South Africa, based on micromammals. *Journal of Human Evolution* 41: 113-132.
- Avery, G. 1988. Some features distinguishing various types of occurrence at Elandsfontein, Cape Province, South Africa. *Palaeoecology of Africa* 19: 213-219.
- Backwell, L.R. & d'Errico, F. 2003. Additional evidence on the early hominid bone tools from Swartkrans with reference to spatial distribution of lithic and organic artefacts. *South African Journal of Science* 99: 259-266.
- Ballantyne, C.K. & Benn, D.I. 1994. Paraglacial slope adjustment and resedimentation following recent glacial retreat, Fåbergstølsdalen, Norway. *Arctic and Alpine Research* 26: 255-269.
- Bamford, M.K. 1986. Aspects of the palaeoflora of the Kirkwood and Sundays River Formations, Algoa Basin, South Africa. Unpublished MSc dissertation. Johannesburg: University of the Witwatersrand.

- Bar-Yosef, O. & Belfer-Cohen, A. 2001. From Africa to Eurasia – early dispersals. *Quaternary International* 75: 19-28.
- Bar-Yosef, O. & Goren-Inbar, N. 1993. *The Lithic Assemblage of 'Ubeidiya': A Lower Palaeolithic Site in the Jordan Valley. Volume 34. Qedem – Monographs of the Institute of Technology*. Jerusalem: Hebrew University of Jerusalem.
- Barkai, R., Lemorini, C. & Vaquero, M. 2015. The origins of recycling: a Palaeolithic perspective. *Quaternary International* 361: 1-3.
- Beaumont, P.B. 1990. Doornlaagte 1. In: Beaumont, P.B. & Morris, D. (eds) *Guide to Archaeological Sites in the Northern Cape*: 17-18. Kimberley: McGregor Museum.
- Beaumont, P.B. 2004. Canteen Kopje. In Morris, D. & Beaumont, P.B. (eds) *Archaeology in the Northern Cape: Some Key Sites*: 26-30. Kimberley: McGregor Museum.
- Beaumont, P. 2011. The edge: more on fire-making by about 1.7 million years ago at Wonderwerk Cave in South Africa. *Current Anthropology* 52: 585-595.
- Beaumont, P.B. & McNabb, J. 2000. Canteen Kopje: the recent excavations. *The Digging Stick* 17: 3-6.
- Beaumont, P.B. & Vogel, J.C. 2006. On a timescale for the past million years of human history in central South Africa. *South African Journal of Science* 102: 217-228.
- Bell, P. & Wright, D. 1985. *Rocks and Minerals*. Italy: Hamlyn Publishing.
- Benito-Calvo, A. & de la Torre, I. 2011. Analysis of orientation patterns in Olduvai Bed I assemblages using GIS techniques: implications for site formation processes. *Journal of Human Evolution* 61: 50-60.
- Berger, L.R., de Ruiter, D.J., Steininger, C.M. & Hancox, J. 2003. Preliminary results of excavations at the newly discovered Coopers D deposit, Gauteng, South Africa. *South African Journal of Science* 99: 276-278.
- Berna, F., Goldberg, P., Horwitz, L.K., Brink, J., Holt, S., Bamford, M. & Chazan, M. 2012. Microstratigraphic evidence of *in situ* fire in the Acheulean strata of Wonderwerk Cave, Northern Cape Province, South Africa. *Proceedings of the National Academy of Sciences* 109: 1-6.
- Bertran, P., Hetu, B., Texier, J-P. & van Steijn, H. 1997. Fabric characteristics of subaerial slope deposits. *Sedimentology* 44: 1-16.

- Bertran, P. & Texier, J-P. 1995. Fabric analysis: application to palaeolithic sites. *Journal of Archaeological Science* 22: 521-535.
- Bertran, P. & Texier, J-P. 1999. Facies and microfacies of slope deposits. *Catena* 35: 99-121.
- Beyene, Y. 2003. The emergence and development of the Early Acheulean at Konso, Ethiopia. *Anthropological Science* 111: 58.
- Beyene, Y., Katoh, S., WoldeGabriel, G., Hart, W.K., Uto, K., Sudo, M., Kondo, M., Hyodo, M., Renne, P.R., Suwa, G. & Asfaw, B. 2013. The characteristics and chronology of the earliest Acheulean at Konso, Ethiopia. *Proceedings of the National Academy of Sciences* 110: 1584-1591.
- Biberson, P. 1961. *Le Paléolithique Inférieur du Maroc Atlantique* 17. Rabat: Publications du Service des Antiquités du Maroc.
- Binneman, J. 2010. A phase 1 archaeological Heritage Impact Assessment for the proposed Deep River Wind Energy Project, Kouga Municipality, District of Humansdorp, Eastern Cape Province (consulted September 2011): <http://www.savannahsa.com/documents/1444/Deep%20River%20DEIR%20Appendix%20K%20-%20HIA.pdf>
- Binneman, J. 2011. A phase 1 archaeological Heritage Impact Assessment for the proposed Happy Valley Wind Energy Facility near Humansdorp, Kouga Local Municipality, District of Humansdorp, Eastern Cape Province (consulted September 2011): [http://www.savannahsa.com/documents/1840/HV%20DEIR%20-%20Appendix%20J%20\(HIA\).pdf](http://www.savannahsa.com/documents/1840/HV%20DEIR%20-%20Appendix%20J%20(HIA).pdf)
- Binneman, J. & Beaumont, P. 1992. Use-wear analysis of two Acheulean handaxes from Wonderwerk Cave, Northern Cape. *Southern African Field Archaeology* 1: 92-97.
- Bishop, W.W. 1978. Geological framework of the Kilombe Acheulian archaeological site, Kenya. In: Bishop, W.W. (ed) *Geological Background to Fossil Man*: 329-336. Edinburgh: Scottish Academic Press.
- Blair, T.C. & McPherson, J.G. 1999. Grain-size and textural classification of coarse sedimentary particles. *Journal of Sedimentary Research* 69: 6-19.
- Blott, S.J. & Pye, K. 2001. Gradistat: a grain size distribution and statistics package for the analysis of unconsolidated sediments. *Earth Surface Processes and Landforms* 26: 1237-1248.

- Blott, S.J. & Pye, K. 2012. Particle size scales and classification of sediment types based on particle size distributions: review and recommended procedures. *Sedimentology* 59: 2071-2096.
- Bluck, B.J. 1987. Bed forms and clast size changes in gravel-bed rivers. In Richards, K. (ed) *River Channels: Environment and Process*: 159-178. Norwich: Basil Blackwell.
- Blumenschine, R.J. 1991. Breakfast at Olorgesailie: the natural history approach to Early Stone Age archaeology. *Journal of Human Evolution* 21: 307-327.
- Boardman, J., Hoffman, M.T., Holmes, P.J. & Wiggs, G.F.S. 2012. Soil erosion and land degradation. In: Holmes, P. & Meadows, M. (eds) *Southern African Geomorphology: Recent Trends and New Directions*: 307-328. Bloemfontein: Sun Press.
- Boëda, E. 1988. Le concept laminaire: rupture et filiation avec le concept Levallois. In: Kowzowski, J. (ed) *L'Homme de Neandertal, La Mutation. Volume 8*: 41-59. Liège: ERAUL.
- Boëda, E. 1993. Le débitage discoïde et le débitage levallois récurrent centripète. *Bulletin de la Société Pré historique Française* 90: 392-404.
- Boëda, E. 1994. *Le concept Levallois: variabilité des méthodes*. Paris: CNRS.
- Boëda, E. 1995. Levallois: a volumetric construction, methods, a technique. In: Dibble, H.L. & Bar-Yosef, O. (eds) *The Definition and Interpretation of Levallois Technology*: 41-68. Madison: Prehistoric Press.
- Botha, G.A., Wintle, A.G. & Vogel, J.C. 1994. Episodic late Quaternary palaeogully erosion in northern KwaZulu Natal, South Africa. *Catena* 23: 327-340.
- Brain, C.K. 1993a. Structure and stratigraphy of the Swartkrans Cave in the light of the new excavations. In Brain, C.K. (ed) *Swartkrans: A Cave's Chronicle of Early Man*: 23-33. Pretoria: Transvaal Museum.
- Brain, C.K. 1993b. The occurrence of burnt bones at Swartkrans and their implications for the control of fire by early hominids. In Brain, C.K. (ed) *Swartkrans: A Cave's Chronicle of Early Man*: 229-242. Pretoria: Transvaal Museum.
- Brain, C.K. & Sillen, A. 1988. Evidence from the Swartkrans Cave for the earliest use of fire. *Nature* 336: 464-466.
- Brain, C.K. & Watson, V. 1992. A guide to the Swartkrans early hominid cave site. *Annals of the Transvaal Museum* 35: 343-365.

- Brantingham, P.J. & Kuhn, S.L. 2001. Constraints on Levallois core technology: a mathematical model. *Journal of Archaeological Science* 28: 747-761.
- Braun, D.R., Harris, J.W.K. & Maina, D.N. 2009. Oldowan raw material procurement and use: evidence from the Koobi Fora Formation. *Archaeometry* 51: 26-42.
- Braun, D.R., Levin, N.E., Stynder, D., Herries, A.I.R., Archer, W., Forrest, F., Roberts, D.L., Bishop, L.C., Matthews, T., Lehmann, S.B., Pickering, R. & Fitzsimmons, K.E. 2013. Mid-Pleistocene hominin occupation at Elandsfontein, Western Cape, South Africa. *Quaternary Science Reviews* 82: 145-166.
- Braun, D.R., Tactikos, J.C., Ferraro, J.V., Arnow, S.L. & Harris, J.W.K. 2008. Oldowan reduction sequences: methodological considerations. *Journal of Archaeological Science* 35: 2153-2163.
- Brenner, P. & Oertli, H.J. 1976. Lower Cretaceous ostracodes (Valanginian to Hauterivian) from the Sundays River Formation, Algoa Basin, South Africa. *Centre Recherches Pau, Société Nationale des Pétroles d'Aquitaine, Bulletin* 10: 471-533.
- Bridge, J.S. 2003. *Rivers and Floodplains: Forms, Processes and Sedimentary Record*. Cornwall: Blackwell Science Ltd.
- Bridgland, D. & Westaway, R. 2008. Climatically controlled river terrace staircases: a worldwide Quaternary phenomenon. *Geomorphology* 98: 285-315.
- Brink, J.S., Herries, A.I.R., Moggi-Cecchi, J., Gowlett, J.A.J., Bousman, C.B., Hancox, J.P., Grün, R., Eisenmann, V., Adams, J.W. & Rossouw, L. 2012. First hominine remains from a ~1.0 million year old bone bed at Cornelia-Uitzoek, Free State Province, South Africa. *Journal of Human Evolution* 63: 527-535.
- Brown, A.G. 1997. *Alluvial Geoarchaeology: Floodplain Archaeology and Environmental Change*. Cambridge: Cambridge University Press.
- Brown, J.T. 1977. On *Araucarites rogersii* seaward from the Lower Cretaceous Kirkwood Formation of the Algoa Basin, Cape Province, South Africa. *Palaeontologia Africana* 20: 47-51.
- Brown, J.T. & Gow, C.E. 1976. Plant fossils as indicators of the rate of deposition of the Kirkwood Formation in the Algoa basin. *South African Journal of Science* 72: 278-279.
- Bunn, H.T. 1994. Early Pleistocene hominid foraging strategies along the ancestral Omo River at Koobi Fora, Kenya. *Journal of Human Evolution* 27: 247-266.

- Bunn, H.T., Harris, J.W.K., Isaac, G., Kaufulu, Z., Kroll, E., Schick, K., Toth, N. & Behrensmeyer, A.K. 1980. An Early Pleistocene site in northern Kenya. *World Archaeology* 12: 109-136.
- Butler, R.W.H. 1982. A structural analysis of the Moine Thrust Zone between Loch Eriboll and Foinaven, NW Scotland. *Journal of Structural Geology* 4: 19-29.
- Butzer, K.W. 1974. Geo-archaeological interpretation of Acheulean calc-pan sites at Doornlaagte and Rooidam (Kimberley, South Africa). *Journal of Archaeological Science* 1: 1-25.
- Bye, B.A., Brown, F., Cerling, T. & McDougall, I. 1987. Increased age estimate for the Lower Paleolithic hominid site at Olorgesailie, Kenya. *Nature* 329: 237-239.
- Cahen, D. & Moeyersons, J. 1977. Subsurface movements of stone artefacts and their implications for the prehistory of Central Africa. *Nature* 266: 812-815.
- Callow, P. 1994. The Olduvai bifaces: technology and raw materials. In: Leakey, M.D. & Roe, D.A. (eds) *Olduvai Gorge Volume 5: Excavations in Beds III, IV and the Masek Beds, 1968-1971*: 254-298. Cambridge: Cambridge University Press.
- Cerling, T.E. & Hay, R.L. 1986. An isotopic study of palaeosol carbonates from Olduvai Gorge. *Quaternary Research* 25: 63-78.
- Charlton, R. 2008. *Fundamentals of Fluvial Geomorphology*. London: Routledge.
- Chavaillon, J. & Berthelet, A. 2004. The archaeological sites of Melka Kunture. In: Chavaillon, J. & Piperno, M. (eds) *Studies on the Early Palaeolithic Site of Melka Kunture, Ethiopia*: 25-80. Firenze: Origines, Istituto Italiano di Preistoria e Protostoria.
- Chavaillon, J., Chavaillon, N., Hours, F. & Piperno, M. 1979. From the Oldowan to the Middle Stone Age at Melka-Kunture (Ethiopia): understanding cultural changes. *Quaternaria* 21: 1-26.
- Chavaillon, J. & Piperno, M. 2004. *Studies on the Early Palaeolithic site of Melka Kunture, Ethiopia*. Firenze: Origines, Istituto Italiano di Preistoria e Protostoria.
- Chazan, M. 1997. Redefining Levallois. *Journal of Human Evolution* 33: 719-735.
- Chazan M. 2015. Technological trends in the Acheulean of Wonderwerk Cave, South Africa. *African Archaeological Review* 32: 701-728.
- Chazan, M., Avery, D.M., Bamford, M.K., Berna, F., Brink, J., Fernandez-Jalvo, Y., Goldberg, P., Holt, S., Matmon, A., Porat, N., Ron, H., Rossouw, L., Scott, L.

- & Horwitz, L.K. 2012. The Oldowan horizon in Wonderwerk Cave (South Africa): archaeological, geological, palaeontological, and palaeoclimatic evidence. *Journal of Human Evolution* 63: 859-866.
- Chazan, M., Ron, H., Matmon, A., Porat, N., Goldberg, P., Yates, R., Avery, M., Sumner, A. & Horwitz, L.K. 2008. Radiometric dating of the Earlier Stone Age sequence in excavation I at Wonderwerk Cave, South Africa: preliminary results. *Journal of Human Evolution* 55: 1-11.
- Choiniere, J.N., Forster, C.A. & De Klerk, W.J. 2012. New information on Nqwebasaurus thwazi, a coelurosaurian theropod from the Early Cretaceous Kirkwood Formation in South Africa. *Journal of African Earth Sciences* 71-72: 1-17.
- Clark, J.D. 1980. The Plio-Pleistocene environmental and cultural sequence at Gadeb, northern Bale, Ethiopia. In: Leakey, R.E.F. & Ogot, B.A. (eds) *Proceedings of the 8th Pan African Congress on Prehistory and Quaternary Studies*: 189-193. Nairobi: TILLMIAP.
- Clark, J.D. 1987. Transitions: *Homo erectus* and the Acheulean: the Ethiopian sites of Gadeb and the Middle Awash. *Journal of Human Evolution* 16: 809-826.
- Clark, J.D. 1990. The earliest cultural evidences of hominids in southern and south central Africa. In: Sperber, G.H. (ed) *From Apes to Angels: Essays in Anthropology in Honour of Phillip V. Tobias*: 1-15. New York: John Wiley & Sons.
- Clark, J.D. 1991. Stone artefact assemblages from Swartkrans, Transvaal, South Africa. In: Clark, J.D. (ed) *Cultural Beginnings: Approaches to Understanding Early Hominid Life-ways in the African Savanna*: 79-107. Bonn: Dr. Rudolf Habelt GMBH.
- Clark, J.D. 1992. The Earlier Stone Age/Lower Palaeolithic in North Africa and the Sahara. In: Klees, F. & Kuper, R. (eds) *New Light on the Northeast African Past*: 19-37 Koln: Heinrich-Barth-Institute.
- Clark, J.D. 1993. Stone artefact assemblages from Members 1-3, Swartkrans Cave. In: Brain, C.K. (ed) *Swartkrans: A Cave's Chronicle of Early Man*: 167-194. Pretoria: Transvaal Museum.
- Clark, J.D. 1998. The Early Palaeolithic of the eastern region of the Old World in comparison to the West. In: Petraglia, M. & Korisettar, R (eds) *Early Human*

Behaviour in Global Context: The Rise and Diversity of the Lower Palaeolithic Record: 425-438. London: Routledge.

- Clark J.D. 2001. Variability in primary and secondary technologies of the Later Acheulian in Africa. In: Milliken, S. & Cook, J. (eds) *A Very Remote Period Indeed*. Oxford: Oxbow Books.
- Clark, J.D., de Heinzelin, J., Schick, K.D., Hart, W.K., White, T.D., WoldeGabriel, G., Walter, R.C., Suwa, G., Asfaw, B., Vrba, E. & H.-Selassie, Y. 1994. African *Homo erectus*: old radiometric ages and young Oldowan assemblages in the Middle Awash Valley, Ethiopia. *Science* 264: 1907-1910.
- Clark, J.D. & Haynes, C.V. 1970. An elephant butchery site at Mwanganda's Village, Karonga, Malawi, and its relevance for palaeolithic archaeology. *World Archaeology* 1: 390-411.
- Clark, J.D. & Kleindienst, M. 1974. The Stone Age cultural sequence: terminology, typology and raw material. In: Clark, J.D. (ed) *Kalambo Falls Prehistoric Site Volume II*: 71-106. Cambridge: Cambridge University Press.
- Clark, J.D. & Kleindienst, M. 2001. The Stone Age cultural sequence: terminology, typology and raw material. In: Clark, J.D. (ed) *Kalambo Falls Prehistoric Site Volume III. The Earlier Cultures: Middle and Earlier Stone Age*: 34-65. Cambridge: Cambridge University Press.
- Clark, J.D. & Kurashina, H. 1979. An analysis of earlier Stone Age bifaces from Gadeb (Locality 8E), Northern Bale Highlands, Ethiopia. *The South African Archaeological Bulletin* 34: 93-109.
- Clark, J.D. & Schick, K.D. 2000. Acheulean archaeology of the Eastern Middle Awash. In: de Heinzelin, J., Clark, J.D., Schick, K.D. & Gilbert, W.H. (eds) *The Acheulean and the Plio-Pleistocene Deposits of the Middle Awash Valley, Ethiopia*: 51-121. Tervuren: Royal Museum of Central Africa.
- Clarke, R.J. 1990. The Ndutu cranium and the origin of *Homo sapiens*. *Journal of Human Evolution* 19: 699-736.
- Clarke, R.J. 1994a. On some new interpretations of Sterkfontein stratigraphy. *South African Journal of Science* 90: 211-214.
- Clarke, R.J. 1994b. The significance of the Swartkrans *Homo* to the *Homo erectus* problem. In: Franzen, J.L.(ed) *100 years of Pithecanthropus*: 185-193. Senckenberg: Coureir Forschungsinstitut.

- Clarke, R.J. 2012. A brief review of history and results of 40 years of Sterkfontein excavations. In: Reynolds, S.C. & Gallagher, A. (eds) *African Genesis: Perspectives on hominin evolution*: 120-141. Cambridge: Cambridge University Press.
- Clarke, R.J. 2014. Earliest African Hominids. In: Smith, C. (ed) *Encyclopedia of Global Archaeology*: 3446-3449. New York: Springer.
- Coolidge, F.L. & Wynn, T. 2009. *The Rise of Homo sapiens: The Evolution of Modern Thinking*. Oxford: John Wiley & Sons Ltd.
- Cooper, M.R. 1979. A new species of *Myophorella* (Bivalvia, Trigonidae) from the Sundays River Formation, South Africa. *Annals of the South African Museum* 78: 21-27.
- Cooper, M.R. 1981. Revision of the Late Valanginian Cephalopoda from the Sundays River Formation of South Africa, with special reference to the Genus *Olcostephanus*. *Annals of the South African Museum* 83: 147-366.
- Cooper, M.R. 1983. The ammonite genus *Umgazanicerias* in the Sundays River Formation. *Transactions of the Geological Society of South Africa* 86: 63-64.
- Cornelissen, E. 1992. *Site GnJh-17 and its implications for the archaeology of the Middle Kapthurin Formation, Baringo, Kenya*. *Annales, Sciences Humaines* 133. Tervuren: Musée Royale de l'Afrique Centrale.
- Cornelissen, E., Boven A., Dabi, A., Hus, J., Ju Yong, K., Keppens, E., Langohr, R., Moeyersons, J., Pasteels, P., Pieters, M., Uytterschaut, H., van Noten, F. & Workineh, H. 1990. The Kapthurin Formation revisited. *The African Archaeological Review* 8: 23-75.
- Couzens, R.A. 2012. An analysis of the symmetry of large cutting tools within the South African Acheulean. Unpublished MSc dissertation. Johannesburg: University of the Witwatersrand.
- Cowling, R.M. 1983. Phytochorology and vegetation history in the south-eastern Cape, South Africa. *Journal of Biogeography* 10: 393-419.
- Crompton, R.H. & Gowlett, J.A.J. 1993. Allometry and multidimensional form in Acheulean bifaces from Kilombe, Kenya. *Journal of Human Evolution* 25: 175-199.
- Culling, W.E.H. 1963. Soil creep and the development of hillside slopes. *The Journal of Geology* 71: 127-161.

- Curnoe, D. 2009. The mandible from Bed 3. In: McNabb, J. & Sinclair, A. (eds) *The Cave of Hearths Makapan Middle Pleistocene Research Project: Field Research by Anthony Sinclair and Patrick Quinney, 1996-2001*: 138-149. Oxford: Archeopress.
- Curry, A.M. & Ballantyne, C.K. 1999. Paraglacial modification of glacial sediment. *Geografiska Annaler. Series A, Physical Geography* 81: 409-419.
- D'Andrea, A., Gallotti, R. & Piperno, M. 2002. Taphonomic interpretation of the Developed Oldowan site of Garba IV (Melka Kunture, Ethiopia) through a GIS application. *Antiquity* 76: 991-1001.
- de Jong, S.M., Paracchini, M.L., Bertolo, F., Folving, S., Megier, J., de Roo, A.P.J. 1999. Regional assessment of soil erosion using the distributed model SEMMED and remotely sensed data. *Catena* 37: 291-308.
- De Klerk, W.J., Forster, C.A., Ross, C.F., Sampson, S.D. & Chinsamy, A. 1997. New maniraptoran and iguanodontian dinosaurs from the Early Cretaceous Kirkwood Formation, South Africa. *Journal of Vertebrate Palaeontology* 17: 42A.
- De Klerk, W.J., Forster, C.A., Ross, C.F., Sampson, S.D. & Chinsamy, A. 1998. A review of recent dinosaur and other vertebrate discoveries in the Early Cretaceous Kirkwood Formation in the Algoa Basin, Eastern Cape, South Africa. *Journal of African Earth Sciences* 27: 55.
- De Klerk, W.J., Forster, C.A., Sampson, S.D., Chinsamy, A. & Ross, C.F. 2000. A new coelurosaurian dinosaur from the Early Cretaceous of South Africa. *Journal of Vertebrate Palaeontology* 20: 324-332.
- de la Torre, I. 2009. Technological strategies in the Lower Pleistocene at Peninj (West of Lake Natron, Tanzania). In: Schick, K. & Toth, N. (eds) *The Cutting Edge: New Approaches to the Archaeology of Human Origins*: 94-113. Gosport: Stone Age Institute Press.
- de la Torre, I. 2011. The Early Stone Age lithic assemblages of Gadeb (Ethiopia) and the Developed Oldowan/early Acheulean in East Africa. *Journal of Human Evolution* 60: 768-812.
- de la Torre, I. & Mora, R. 2005. Technological Strategies in the Lower Pleistocene at Olduvai Beds I & II. Liege: ERAUL 112.
- de la Torre, I. & Mora, R. 2009. The technology of the ST Site Complex. In: Domínguez-Rodrigo, M., Alcalá, L. & Luque, L. (eds) *Peninj: A Research Project on Human Origins 1995-2005*: 145-189. New York: Oxbow Books.

- de la Torre, I. & Mora, R. 2014. The transition to the Acheulean in East Africa: an assessment of paradigms and evidence from Olduvai Gorge (Tanzania). *Journal of Archaeological Method and Theory* 21: 781-823.
- de la Torre, I., Mora, R., Domínguez-Rodrigo, M., de Luque, L. & Alcalá, L. 2003. The Oldowan industry of Peninj and its bearing on the reconstruction of the technological skills of Lower Pleistocene hominids. *Journal of Human Evolution* 44: 203-224.
- de la Torre, I., Mora, R. & Martínez-Moreno, J. 2008. The early Acheulean in Peninj (Lake Natron, Tanzania). *Journal of Anthropological Archaeology* 27: 244-264.
- de Ruiter, D.J., Pickering, R., Steininger, C.M., Kramers, J.D., Hancox, P.J., Churchill, S.E., Berger, L.R. & Backwell, L. 2009. New *Australopithecus robustus* fossils and associated U-Pb dates from Coopers Cave (Gauteng, South Africa). *Journal of Human Evolution* 56: 497-513.
- De Wit, M.C.J. 1996. The distribution and stratigraphy of inland alluvial diamond deposits in South Africa. *Africa Geoscience Review Special Edition* 3: 19-33.
- De Wit, M.C.J. 2008. Canteen Koppie at Barkly West: South Africa's first diamond mine. *South African Journal of Geology* 111: 53-66.
- Dasgupta, P. 2003. Sediment gravity flow – the conceptual problems. *Earth Science Reviews* 62: 265-281.
- Deacon, H.J. 1970. The Acheulean occupation at Amanzi Springs Uitenhage District, Cape Province. *Annals of the Cape Provincial Museums* 8: 89-189.
- Deacon, H.J. 1988. Geology at the Doornlaagte site. In: Mason, R. (ed) *Cave of Hearths, Makapansgat, Transvaal*: 643-647. Johannesburg: University of the Witwatersrand.
- Deacon, H.J. 1998. Elandsfontein and Klasies River revisited. In: Ashton, N.M., Healy, F. & Pettitt, P.B. (eds) *A Master of His Craft: Papers in Stone Age Archaeology Presented to John Wymer*: 23-28. Oxford: Oxbow Books.
- Deacon, H.J. & Deacon, J. 1999. *Human Beginnings in South Africa: Uncovering the Secrets of the Stone Age*. Cape Town: David Phillip.
- Deacon, H.J. & Geleijnse, V.B. 1988. The stratigraphy and sedimentology of the main site sequence, Klasies River, South Africa. *South African Archaeological Bulletin* 43: 5-14.

- Dean, M.C., Leakey, M.G., Reid, D., Schrenk, F., Schwartz, G.T., Stringer, C. & Walker, A. 2001. Growth processes in teeth distinguish modern humans from *Homo erectus* and earlier hominins. *Nature* 414: 628-631.
- Dean, M.C. & Smith, B.H. 2009. Growth and development of the Nariokotome youth, KNM-WT 15000. In: Grine, F.E., Fleagle, J.G. & Leakey, R.E. (eds) *The First Human: Origin and Early Evolution of the Genus Homo*: 101-120. New York: Springer.
- Deino, A.L. & McBrearty, S. 2002. $^{40}\text{Ar}/^{39}\text{Ar}$ dating of the Kapthurin Formation, Baringo, Kenya. *Journal of Human Evolution* 42: 185-210.
- Deino, A.L. & Potts, R. 1990. Single crystal $^{40}\text{Ar}/^{39}\text{Ar}$ dating of the Olorgesailie Formation, southern Kenya Rift. *Journal of Geophysical Research* 95: 8453-8470.
- Deino, A.L., Trauth, M.H., Bergner, A.G. & Potts, R. 2004. $^{40}\text{Ar}/^{39}\text{Ar}$ age calibration of the lacustrine sediments at Kariandusi, Central Kenya Rift. Conference paper presented at the American Geophysical Union, Fall Meeting 2004, San Francisco.
- Deitrich, W.E. 1987. Mechanics of flow and sediment transport in river beds. In: Richards, K. (ed) *River Channels: Environment and Process*: 179-227. UK: Basil Blackwell.
- Delagnes, A. & Roche, H. 2005. Late Pliocene hominid knapping skills: the case of Lokalalei 2C, West Turkana, Kenya. *Journal of Human Evolution* 48: 435-472.
- Dibble, H.L. 1997. Platform variability and flake morphology: a comparison of experimental and archaeological data and implications for interpreting prehistoric lithic technological strategies. *Lithic Technology* 22: 150-170.
- Dibble, H.L. & Rezek, Z. 2009. Introducing a new experimental design for controlled studies of flake formation: results for exterior platform angle, platform depth, angle of blow, velocity, and force. *Journal of Archaeological Science* 36: 1945-1954.
- Diez-Martín, F., Cuartero, F., Yustos, P.S., Baena, J., Rubio, D. & Domínguez-Rodrigo, M. 2012. Testing cognitive skills in Early Pleistocene hominins: an analysis of the concepts of hierarchisation and predetermination in the lithic assemblages of the Type Section (Peninj, Tanzania). In: Domínguez-Rodrigo, M. (ed) *Stone Tools and Fossil Bones: Debates in the Archaeology of Human Origins*: 245-309. Cambridge: Cambridge University Press.

- Diez-Martín, F. & Eren, M.I. 2012. The Early Acheulean in Africa: past paradigms, current ideas, and future directions. In: Domínguez-Rodrigo, M. (ed) *Stone Tools and Fossil Bones: Debates in the Archaeology of Human Origins*: 310-357. Cambridge: Cambridge University Press.
- Diez-Martín, F., Sánchez, P., Domínguez-Rodrigo, M., Mabulla, A. & Barba, R. 2009a. Were Olduvai hominins making butchering tools or battering tools? Analysis of a recently excavated lithic assemblage from BK (Bed II, Olduvai Gorge, Tanzania). *Journal of Anthropological Archaeology* 28: 274-289.
- Diez-Martín, F., Luque, L. & Domínguez-Rodrigo, M. 2009b. ST-69: an Acheulean assemblage in the Moinik Formation of Type Section. In: Domínguez-Rodrigo, M., Alcalá, L. & Luque, L. (eds) *Peninj: A Research Project on Human Origins 1995-2005*: 191-204. New York: Oxbow Books.
- Diez-Martín, F., Sánchez Yustos, P., Uribelarrea, D., Baquedano, E., Mark, D.F., Mabulla, A., Fraile, C., Duque, J., Díaz, I., Pérez-González, A., Yravedra, J., Egeland, C.P., Organista, E. & Domínguez-Rodrigo, M. 2015. The origin of the Acheulean: the 1.7 million-year-old site of FLK West, Olduvai Gorge (Tanzania). *Nature Scientific Reports* 5: 17839.
- Dingle, R.V. & Scrutton, R.A. 1974. Continental breakup and the development of post-Paleozoic sedimentary basins around Southern Africa. *Geological Society of America Bulletin* 85: 1467-1474.
- Dollar, E.S.J. 1998. Palaeofluvial geomorphology in southern Africa: a review. *Progress in Physical Geography* 22: 325-349.
- Domínguez-Rodrigo, M., Alcalá, L. & Luque, L. 2009a. Conclusions. In: Domínguez-Rodrigo, M., Alcalá, L. & Luque, L. (eds) *Peninj: A Research Project on Human Origins 1995-2005*: 257-258. New York: Oxbow Books.
- Domínguez-Rodrigo, M., Barba, R. & Egeland, C.P. 2007. *Deconstructing Olduvai: A Taphonomic Study of the Bed I Sites*. Dordrecht: Springer.
- Domínguez-Rodrigo, M., de la Torre, I., Luque, L., Alcalá, L., Mora, R., Serrallonga, J. & Medina, V. 2002. The ST Site Complex at Peninj, West Lake Natron, Tanzania: implications for early hominid behavioural models. *Journal of Archaeological Science* 29: 639-665.
- Domínguez-Rodrigo, M., Diez-Martín, F., Luque, L., Alcalá, L. & Bushozi, P. 2009b. The Acheulean sites from the North Escarpment. In: Domínguez-Rodrigo, M.,

- Alcalá, L. & Luque, L. (eds) *Peninj: A Research Project on Human Origins 1995-2005*: 227-255. New York: Oxbow Books.
- Domínguez-Rodrigo, M., Lopez-Saez, J.A., Vincens, A., Alcalá, L., Luque, L. & Serrallonga, J. 2001a. Fossil pollen from the Upper Humbu Formation of Peninj (Tanzania): hominid adaptation to a dry open Plio-Pleistocene savanna environment. *Journal of Human Evolution* 40: 151-157.
- Domínguez-Rodrigo, M., Mabulla, A., Bunn, H.T., Barba, R., Diez-Martín, F., Egeland, C.P., Espílez, E., Egeland, A., Yravedra, J. & Sánchez, P. 2009c. Unraveling hominin behaviour at another anthropogenic site from Olduvai Gorge (Tanzania): new archaeological and taphonomic research at BK, Upper Bed II. *Journal of Human Evolution* 57: 260-283.
- Domínguez-Rodrigo, M., Serrallonga, J., Juan-Tresserras, J., Alcalá, L. & Luque, L. 2001b. Woodworking activities by early humans: a plant residue analysis on acheulean stone tools from Peninj (Tanzania). *Journal of Human Evolution* 40: 289-299.
- Domínguez-Rodrigo, M., Serrallonga, J., Luque, L., Diez-Martín, F., Alcalá, L. & Bushozi, P. 2009d. The Acheulean sites from the South Escarpment. In: Domínguez-Rodrigo, M., Alcalá, L. & Luque, L. (eds) *Peninj: A Research Project on Human Origins 1995-2005*: 205-226. New York: Oxbow Books.
- Doucet, F. 2010. Effective CO₂-specific sequestration capacity of steel slags and variability in their leaching behaviour in view of industrial mineral carbonation. *Minerals Engineering* 23: 262-269.
- Drennan, M.R. 1953. The Saldanha skull and its associations. *Nature* 172: 191.
- Durkee, H. & Brown, F.H. 2014. Correlation of volcanic ash layers between the Early Pleistocene Acheulean sites of Isinya, Kariandusi, and Olorgesailie, Kenya. *Journal of Archaeological Science* 49: 510-517.
- Dusseldorp, G., Lombard, M. & Wurz, S. 2013. Pleistocene *Homo* and the updated Stone Age sequence of South Africa. *South African Journal of Science* 109: 1-7.
- Egeland, C.P. & Domínguez-Rodrigo, M. 2008. Taphonomic perspectives on hominid site use and foraging strategies during Bed II times at Olduvai Gorge, Tanzania. *Journal of Human Evolution* 55: 1031-1052.
- Egeland, C.P., Pickering, T.R., Domínguez-Rodrigo, M. & Brain, C.K. 2004. Disentangling Early Stone Age palimpsests: determining the functional

- independence of hominid- and carnivore-derived portions of archaeofaunas. *Journal of Human Evolution* 47: 343-357.
- El-Swaify, S.A., Dangler, E.W. & Armstrong, C.L. 1982. *Soil Erosion by Water in the Tropics*. Honolulu: University of Hawaii.
- Eren, M.I., Lycett, S.J., Roos, C.I. & Garth Sampson, C. 2011. Toolstone constraints on knapping skill: Levallois reduction with two different raw materials. *Journal of Archaeological Science* 38: 2731-2739.
- Erlandson, J. M. 1984. A case study in faunalurbation: delineating the effects of the burrowing pocket gopher on the distribution of archaeological materials. *American Antiquity* 49: 785-790.
- Erlanger, E.D. 2010. Rock uplift, erosion, and tectonic uplift of South Africa determined with cosmogenic ^{27}Al and ^9Be . Unpublished MSc dissertation. Indiana: Purdue University.
- Erlanger, E.D., Granger, D.E. & Gibbon, R.J. 2012. Rock uplift rates in South Africa from isochron burial dating of fluvial and marine terraces. *Geology* 40: 1019-1022.
- Evans, D.J.A. 2000. A gravel outwash/deformation till continuum, Skálafellsjökull, Iceland. *Geografiska Annaler, Series A, Physical Geography* 82: 499-512.
- Fannin, R.J. & Wise, M.P. 2001. An empirical-statistical model for debris flow travel distance. *Canadian Geotechnical Journal* 38: 982-994.
- Field, A.S. 1999. An analytical and comparative study of the Earlier Stone Age archaeology of the Sterkfontein Valley. Unpublished MSc dissertation. Johannesburg: University of the Witwatersrand.
- Fluck, H. 2002. The Victoria West: an investigation into the prepared core technology of South Africa. Unpublished MA dissertation. Southampton: University of Southampton.
- Forbes, A.T. & Allanson, B.R. 1970. Ecology of the Sundays River part I. Water chemistry. *Hydrobiologia* 36: 479-488.
- Forssman, T. & Pargeter, J. 2014. Assessing surface movement at Stone Age open-air sites: first impressions from a pilot experiment in northeastern Botswana. *Southern African Humanities* 26: 157-176.
- Forster, C.A., Frost, S. & Ross, C.F. 1995. New dinosaur material and paleoenvironment of the Early Cretaceous Kirkwood Formation, Algoa Basin, South Africa. *Journal of Vertebrate Palaeontology* 15: 28A.

- Frost, S. 1996. Early Cretaceous alluvial palaeosols (Kirkwood Formation, Algoa Basin, South Africa) and their palaeoenvironmental and palaeoclimatological significance. Unpublished MSc dissertation. Grahamstown: University of Rhodes.
- Gallotti, R. 2013. An older origin for the Acheulean at Melka Kunture (Upper Awash, Ethiopia): techno-economic behaviours at Garba IVD. *Journal of Human Evolution* 65: 594-620.
- Galton, P.M. & Molnar, R.E. 2012. An unusually large theropod dinosaur tooth from the Kirkwood Formation (Lower Cretaceous) of South Africa. *Neues Jahrbuch für Geologie und Paläontologie* 263: 17-23.
- Germaine, J.T. & Germaine, A.V. 2009. *Geotechnical Laboratory Measurements for Engineers*. New Jersey: John Wiley & Sons, Inc.
- Gibbon, R.J., Granger, D.E., Kuman, K., Leader, G.M., Lotter, M.G. & Forssman, T. 2013. Isochron burial dating of the Earlier Stone Age deposits at Canteen Kopje, South Africa. Conference paper presented at the Association of Southern African Professional Archaeologists Biennial Conference, University of Gaborone, Botswana.
- Gibbon, R.J., Granger, D.E., Kuman, K. & Partridge, T.C. 2009a. Early Acheulean technology in the Rietputs Formation, South Africa, dated with cosmogenic nuclides. *Journal of Human Evolution* 56: 152-160.
- Gibbon, R.J., Leader, G.M. & Kuman, K. 2008. Canteen Kopje-SAHRA report for 2007-2008. Unpublished manuscript. Johannesburg: University of the Witwatersrand Archaeology Department.
- Gibbon, R.J., Leader, G.M. & Kuman, K. 2009b. Canteen Kopje-SAHRA report for 2008-2009. Unpublished manuscript. Johannesburg: University of the Witwatersrand Archaeology Department.
- Gibbon, R.J., Pickering, T.R., Sutton, M.B., Heaton, J.L., Kuman, K., Clarke, R.J., Brain, C.K. & Granger, D.E. 2014. Cosmogenic nuclide burial dating of hominin-bearing Pleistocene cave deposits at Swartkrans, South Africa. *Quaternary Geochronology* 24: 10-15.
- Goldberg, P., Berna, F. & Chazan, M. 2015. Deposition and diagenesis in the Earlier Stone Age of Wonderwerk Cave, Excavation 1, South Africa. *African Archaeological Review* 32: 613-643.

- Goldberg, P. & Macphail, R.I. 2006. *Practical and Theoretical Geoarchaeology*. Oxford: Blackwell Publishing.
- Gomez, B., Bamford, M., Martinez-Delclos, X. 2002a. Lower Cretaceous plant cuticles and amber (Kirkwood Formation, South Africa). *Comptes Rendus Palevol* 1: 83-87.
- Gomez, B., Martínez-Delclòs, X., Bamford, M. & Philippe, M. 2002b. Taphonomy and palaeoecology of plant remains from the oldest African Early Cretaceous amber locality. *Lethaia* 35: 300-308.
- Gonzales, D.P.G., Damrosch, D.B., Damrosch, D.R., Pryor, J. & Thunen, R.L. 1985. The third dimension in site structure: an experiment in trampling and vertical dispersal. *American Antiquity* 50: 803-818.
- Goren-Inbar, N & Sharon, G. 2006. Invisible handaxes and visible Acheulean biface technology at Gesher Benot Ya aqov, Israel. In: Goren-Inbar, N. & Sharon, G. (eds) *Axe Age: Acheulian Tool-making from Quarry to Discard*: 111-136. London: Equinox Publishing Ltd.
- Gowlett, J.A.J. 1978. Kilombe – an Acheulean site complex in Kenya. In: Bishop, W.W. (ed) *Geological Background to Fossil Man*: 337-360. Edinburgh: Scottish Academic Press.
- Gowlett, J.A.J. 1979. A contribution to studies of the Acheulean in East Africa, with especial reference to Kilombe and Kariandusi. Unpublished PhD thesis. Cambridge: University of Cambridge.
- Gowlett, J.A.J. 1988. A case of Developed Oldowan in the Acheulean? *World Archaeology* 20: 13-26.
- Gowlett, J.A.J. 1991. Kilombe – review of an Acheulean site complex. In: Clark, J.D. (ed) *Cultural Beginnings: Approaches to Understanding Early Hominid Life-ways in the African Savanna*: 129-135. Bonn: Dr. Rudolf Habelt GMBH.
- Gowlett, J.A.J. 2006. The elements of design form in Acheulean bifaces: modes, modalities, rules and language. In: Goren-Inbar, N. & Sharon, G. (eds) *Axe Age: Acheulean Tool-making from Quarry to Discard*: 203-221. London: Equinox.
- Gowlett, J.A.J. 2011. The vital sense of proportion: transformation, Golden Section, and 1:2 preference in Acheulean bifaces. *PaleoAnthropology* 2011: 174-187.
- Gowlett, J.A.J. & Crompton, R.H. 1994. Kariandusi: Acheulean morphology and the question of allometry. *The African Archaeological Review* 12: 3-42.

- Grab, S.W. & Deschamps, C.L. 2004. Geomorphological and geoecological controls and processes following gully development in alpine mires, Lesotho. *Arctic, Antarctic, and Alpine Research* 36: 49-58.
- Granger, D.E. 2006. A review of burial dating methods using ^{26}Al and ^{10}Be . In: Siame, L.L., Bourlès, D.L. & Brown, E.T. (eds) *In Situ-produced Cosmogenic Nuclides and Quantification of Geological Processes*: 1-16. Colorado: Geological Society of America.
- Granger, D.E. 2014. Cosmogenic nuclide burial dating in archaeology and paleo-anthropology. In: Holland, H.D. & Turekian, K.K. (eds) *Treatise on Geochemistry, Second Edition, Volume 14*: 81-97. Oxford: Elsevier.
- Granger, D.E., Gibbon, R.J., Kuman, K., Clarke, R.J., Bruxelles, L. & Caffee, M.W. 2015. New cosmogenic burial ages for Sterkfontein Member 2 *Australopithecus* and Member 5 Oldowan. *Nature* 522: 85-88.
- Granger, D.E., Gibbon, R.J., Kuman, K., Lotter, M.G. & Erlanger, E. 2013. Isochron burial dating method and application to an Earlier Stone Age chronosequence on the Sundays River, South Africa. Poster presented at the Association of Southern African Professional Archaeologists Biennial Conference, Gaborone, Botswana.
- Granger, D.E. & Muzikar, P.F. 2001. Dating sediment burial with in situ-produced cosmogenic nuclides: theory, techniques, and limitations. *Earth and Planetary Science Letters* 188: 269–281.
- Graves, R.R., Lupo, A.C., McCarthy, R.C., Wescott, D.J. & Cunningham, D.L. 2010. Just how strapping was KNM-WT 15000? *Journal of Human Evolution* 59: 542-554.
- Grine, F.E., Fleagle, J.G. & Leakey, R.E. 2009. *The First Humans – Origin and Early Evolution of the Genus Homo*. New York: Springer.
- Hall, G. 2004. New archaeological material from the Plio-Pleistocene sites of Coopers Cave, Plovers Lake and Gladysvale. Conference paper presented at the annual conference of the Palaeontological Society of South Africa, University of the Witwatersrand, Johannesburg, South Africa.
- Hand, B.M. 1997. Inverse grading resulting from coarse-sediment transport lag. *Journal of Sedimentary Research* 67: 124-129.

- Harmand, S. 2007. Economic behaviors and cognitive capacities of early hominins between 2.34 Ma and 0.70 Ma in West Turkana, Kenya. *Mitteilungen der Gesellschaft für Urgeschichte* 16: 11-23.
- Harmand, S., Lewis, J.E., Feibel, C.S., Lepre, C.J., Prat, S., Lenoble, A., Boës, X., Quinn, R.L., Brenet, M., Arroyo, A., Taylor, N., Clément, S., Daver, G., Brugal, J-P., Leakey, L., Mortlock, R.A., Wright, J.D., Lokorodi, S., Kirwa, C., Kent, D.V. & Roche, H. 2015. 3.3-million-year-old stone tools from Lomekwi 3, West Turkana, Kenya. *Nature* 521: 310-315.
- Harris, J.W.K., Braun, D.R. & Pante, M. 2007. 2.7 MYR-300,000 years ago in Africa. In: Elias, S. (ed) *Encyclopedia of Quaternary Science, Volume 1*: 63-72. London: Elsevier.
- Hattingh, J. 1994. Depositional environment of some gravel terraces in the Sundays River Valley, Eastern Cape. *South African Journal of Geology* 97: 156-166.
- Hattingh, J. 1996. Fluvial response to allocyclic influences during the development of the lower Sundays River, Eastern Cape, South Africa. *Quaternary International* 33: 3-10.
- Hattingh, J. 2008. Fluvial systems and landscape evolution. In: Lewis C.A. (ed) *Geomorphology of the Eastern Cape*: 21-42. Grahamstown: NISC.
- Hattingh, J. & Goedhart, M.L. 1997. Neotectonic control on drainage evolution in the Algoa Basin, Southeastern Cape Province. *South African Journal of Geology* 100: 43-52.
- Hattingh, J. & Rust, I.C. 1999. Drainage evolution of the Sundays River, South Africa. In: Miller, A. & Gupta, A. (eds) *Varieties in Fluvial Form*: 145-166. Chichester: John Wiley and Sons.
- Haughton, S.H. 1928. The geology of the country between Grahamstown and Port Elizabeth: an explanation of Cape Sheet No. 9 (Port Elizabeth): Geological Survey of South Africa.
- Haughton, S.H. 1935. The geology portion of the country east of Steytleville, Explanation of Sheet No. 150 (Sundays River): Geological Survey of South Africa.
- Hay, R.L. 1976. *Geology of the Olduvai Gorge: A Study of Sedimentation in a Semiarid Basin*. Berkely: University of California Press.

- Hay, R.L. 1994. Geology and dating of Beds III, IV and the Masek Beds. In: Leakey, M.D. & Roe, D.A. (eds) *Olduvai Gorge Volume 5: Excavations in Beds III, IV and the Masek Beds, 1968-1971*: 8-14. Cambridge: Cambridge University Press.
- Herries, A.I.R. 2011. A chronological perspective on the Acheulian and its transition to the Middle Stone Age in southern Africa: the question of the Fauresmith. *International Journal of Evolutionary Biology* 2011: 1-25.
- Herries, A.I.R. & Latham, A.G. 2009. Archaeomagnetic studies at the Cave of Hearths. In: McNabb, J. & Sinclair, A. (eds) *The Cave of Hearths Makapan Middle Pleistocene Research Project: Field Research by Anthony Sinclair and Patrick Quinney, 1996-2001*: 59-64. Oxford: Archeopress.
- Hodge, R., Brasington, J. & Richards, K. 2009. Analysing laser-scanned digital terrain models of gravel bed surfaces: linking morphology to sediment transport processes and hydraulics. *Sedimentology* 56: 2024-2043.
- Hoffman, M.T. & Cowling, R.M. 1990. Desertification in the lower Sundays River Valley. *South African Journal of Arid Environments* 19: 105-17.
- Hoffman, M.T. & Cowling, R.M. 1991. Phytochorology and endemism along aridity and grazing gradients in the lower Sundays River Valley, South Africa: implications for vegetation history. *Journal of Biogeography* 18: 189-201.
- Hofman, J.L. 1986. Vertical movement of artifacts in alluvial and stratified deposits. *Current Anthropology* 27: 163-171.
- Holmes, C. E., Potter, B. A., Reuther, J. D., Mason, O. K., Thorson, R. M. & Bowers, P. M. 2008. Geological and cultural context of the Nogahabara 1 site. *American Antiquity* 73: 781-790.
- Hull, K.L. 1987. Identification of cultural site formation processes through microdebitage analysis. *American Antiquity* 52: 772-783.
- Inizan, M-L., Reduron-Ballinger, M., Roche, H. & Tixier, J. 1999. *Technology and Terminology of Knapped Stone*. Nanterre Cedex: CREP.
- Inskip, R.R. 1965. Earlier Stone Age occupation at Amanzi: a preliminary investigation. *South African Journal of Science* 61: 229-242.
- Isaac, G.L. 1977. *Olorgesailie: Archaeological Studies of a Middle Pleistocene Lake Basin in Kenya*. Chicago: The University of Chicago Press.
- Isaac, G.L. 1997. *Koobi Fora Research Project Volume 5: Plio-Pleistocene Archaeology*. Oxford: Clarendon Press.

- Isaac, G.L. & Behrensmeyer, A.K. 1997. Geological context and palaeoenvironments. In: Isaac, G. (ed) *Koobi Fora Research Project Volume 5: Plio-Pleistocene Archaeology*: 12-70. Oxford: Clarendon Press.
- Isaac, G.L. & Curtis, G.H. 1974. Age of early Acheulian industries from the Peninj Group, Tanzania. *Nature* 249: 624-627.
- Isaac, G.L. & Harris, J.W.K. 1978. Archaeology. In: Leakey, M.G. & Leakey, R.E. (eds) *Koobi Fora Research Project Volume 1: The Fossil Hominids and an Introduction to Their Context 1968-1974*: 64-85. Oxford: Clarendon Press.
- Isaac, G.L. & Harris, J.W.K. 1997. The stone artefact assemblages: a comparative study. In: Isaac, G. (ed) *Koobi Fora Research Project Volume 5, Plio-Pleistocene Archaeology*: 262-361. Oxford: Clarendon Press.
- Isaac, G.L. & Keller, C. 1968. Note on the proportional frequency of side- and end-struck flakes. *The South African Archaeological Bulletin* 23: 17-19.
- Jacoby, B., Phillips, N., Clarke, R.J. & Kuman, K. 2013. New research at the Goldsmith's Pleistocene site, Cradle of Humankind World Heritage Site (Gauteng Province, South Africa). Poster presented at the Association of Southern African Professional Archaeologists Biennial Conference University of Gaborone, Botswana.
- James, S.R. 1989. Hominid use of fire in the Lower and Middle Pleistocene. *Current Anthropology* 30: 1-26.
- Johnson, C.R., Ashley, G.M., de Wet, C.B., Dvoretzky, R., Parks, L., Hover, V.C., Owen, R.B. & McBrearty, S. 2009. Tufa as a record of perennial fresh water in a semi-arid rift basin, Kapthurin Formation, Kenya. *Sedimentology* 56: 1115-1137.
- Johnson, C.R. & McBrearty, S. 2010. 500,000 year old blades from the Kapthurin Formation, Kenya. *Journal of Human Evolution* 58: 193-200.
- Johnson, C.R. & McBrearty, S. 2012. Archaeology of middle Pleistocene lacustrine and spring palaeoenvironments in the Kapthurin Formation, Kenya. *Journal of Anthropological Archaeology* 31: 485-499.
- Jones, P.R. 1979. Effects of raw materials on biface manufacture. *Science* 204: 835-836.
- Jones, P.R. 1980. Experimental butchery with modern stone tools and its relevance for Palaeolithic archaeology. *World Archaeology* 12: 153-165.

- Jones, P.R. 1994. Results of experimental work in relation to the stone industries of Olduvai Gorge. In: Leakey, M.D. & Roe, D.A. (eds) *Olduvai Gorge Volume 5: Excavations in Beds III, IV and the Masek Beds, 1968-1971*: 254-298. Cambridge: Cambridge University Press.
- Kandel, A.W., Felix-Henningsen, P. & Conard, N.J. 2003. An overview of the spatial archaeology of the Geelbek Dunes, Western Cape, South Africa. In: Füleký, G. (ed) *Papers of the 1st International Conference on Archaeology and Soils*: 37-44. Hungary: BAR International Series.
- Karkanás, P., Bar-Yosef, O., Goldberg, P. & Weiner, S. 2000. Diagenesis in prehistoric caves: the use of minerals that form *in situ* to assess the completeness of the archaeological record. *Journal of Archaeological Science* 27: 915-929.
- Kaufulu, Z.M. & Stern, N. 1987. The first stone artefacts to be found *in situ* within the Plio-Pleistocene Chiwondo Beds in northern Malawi. *Journal of Human Evolution* 16: 729-740.
- Keller, C.M. 1973. *Montagu Cave in Prehistory: A Descriptive Analysis*. California: University of California.
- Kimura, Y. 2002. Examining time trends in the Oldowan technology at Beds I and II, Olduvai Gorge. *Journal of Human Evolution* 43: 291-321.
- Klein, R.G. 1978. The fauna and overall interpretation of the ‘‘Cutting 10’’ Acheulean site at Elandsfontein (Hopefield), Southwestern Cape Province, South Africa. *Quaternary Research* 10: 69-83.
- Klein, R.G. 1983. The Stone Age prehistory of southern Africa. *Annual Review of Anthropology* 12: 25-48.
- Klein, R.G. 2000a. The Earlier Stone Age of Southern Africa. *The South African Archaeological Bulletin* 55: 107-122.
- Klein, R.G. 2000b. Archaeology and the evolution of human behaviour. *Evolutionary Anthropology* 9: 17-36.
- Klein R.G., Avery G., Cruz-Urbe K. & Steele T.E. 2007. The mammalian fauna associated with an archaic hominin skullcap and later Acheulean artifacts at Elandsfontein, Western Cape Province, South Africa. *Journal of Human Evolution* 52: 164-186.

- Klein, R.G. & Cruz-Urbe, K. 1991. The bovids from Elandsfontein, South Africa, and their implications for the age, palaeoenvironment, and origins of the site. *The African Archaeological Review* 9: 21-79.
- Kleindienst, M.R. 1961. Variability within the Late Acheulean assemblage in Eastern Africa. *The South African Archaeological Bulletin* 16: 35-52.
- Kleindienst, M.R. 1962. Components of the East African Acheulean assemblage: an analytical approach. In: Mortelmans, G. & Nenguin, J. (eds) *Actes du IV^e Congrès Panafricain de Préhistoire et de l'étude du Quaternaire*: 81-104. Tervuren: Musée Royale de l'Afrique Centrale.
- Kostic, B. & Aigner, T. 2007. Sedimentary architecture and 3D ground-penetrating radar analysis of gravelly meandering river deposits (Neckar Valley, SW Germany). *Sedimentology* 54: 789-808.
- Krige, A.V. 1927. An examination of the Tertiary and Quaternary changes of sea level in South Africa, with special stress on the evidence in favour of a world wide sinking of ocean level. *Annals of the University of Stellenbosch* 5: 1-81.
- Krumbein, W.C. 1939. Preferred orientation of pebbles in sedimentary deposits. *The Journal of Geology* 47: 673-706.
- Kuman, K. 1989. Florisbad and ∓Gi: the contribution of open-air sites to study of the Middle Stone Age in southern Africa. Unpublished PhD thesis. Pennsylvania: University of Pennsylvania.
- Kuman, K. 1994. The archaeology of Sterkfontein-past and present. *Journal of Human Evolution* 27: 471-495.
- Kuman, K. 1998. The earliest South African industries. In: Petraglia, M.D. & Korisettar, R. (eds) *Early Human Behaviour in Global Context: The Rise and Diversity of the Lower Palaeolithic Record*: 151-186. London: Routledge.
- Kuman, K. 2001. An Acheulean factory site with prepared core technology near Taung, South Africa. *The South African Archaeological Bulletin* 56: 8-22.
- Kuman, K. 2003. Site formation on the early South African Stone Age sites and its influence on the archaeological record. *South African Journal of Science* 99: 251-254.
- Kuman, K. 2007. The Earlier Stone Age in South Africa, site context, and the influence of cave studies. In Pickering, T.R., Schick, K. & Toth, N. (eds) *African Taphonomy: A Tribute to C.K. "Bob" Brain*. Indiana: Stone Age Institute Press.

- Kuman, K. 2014a. Oldowan Industrial Complex. In: Smith, C. (ed) *Encyclopedia of Global Archaeology*: 5560-5569. New York: Springer.
- Kuman, K. 2014b. Acheulean Industrial Complex. In: Smith, C. (ed) *Encyclopedia of Global Archaeology*: 7-18. New York: Springer.
- Kuman, K. In press. Development of the archaeological record in southern Africa during the Earlier Stone Age. In: Knight, J. & Grab, S. (eds) *Quaternary Environmental Change in Southern Africa: Physical and Human Dimensions*. Cambridge: Cambridge University Press.
- Kuman, K. & Clarke, R.J. 2000. Stratigraphy, artefact industries and hominid associations for Sterkfontein, Member 5. *Journal of Human Evolution* 38: 827-847.
- Kuman, K. & Field, A.S. 2009. The Oldowan Industry from Sterkfontein Caves, South Africa. In: Schick, K. & Toth, N. (eds) *The Cutting Edge: New Approaches to the Archaeology of Human Origins*: 151-169. Indiana: Stone Age Institute Press.
- Kuman, K., Gibbon, R.J., Kempson, H., Langejans, G., Le Baron, J., Pollarolo, L. & Sutton, M. 2005. Stone Age signatures in northernmost South Africa: early archaeology in the Mapungubwe National Park and vicinity. In: d'Errico, F. & Backwell, L. (eds) *From Tools to Symbols, From Early Hominids to Modern Humans*: 163-182. Johannesburg: Witwatersrand University Press.
- Kuman, K., Field, A.S. & Thackeray, J.F. 1997. Discovery of new artefacts at Kromdraai. *South African Journal of Science* 93: 187-193.
- Kuman, K., Li, C. & Li, H. 2014. Large cutting tools in the Danjiangkou Reservoir Region, central China. *Journal of Human Evolution* 76: 129-153.
- Laidler, P.W. 1947. The evolution of Middle Palaeolithic technique at Geelhout, near Kareedouw, in the southern Cape. *Transactions of the Royal Society of South Africa* 31: 283-313.
- Lal, R. 2001. Soil degradation by erosion. *Land Degradation and Development* 12: 519-539.
- Latham, A.G. & Herries, A.I.R. 2004. The formation and sedimentary infilling of the Cave of Hearths and Historic Cave Complex, Makapansgat, South Africa. *Geoarchaeology: An International Journal* 19: 323-342.
- Latham, A.G. & Herries, A.I.R. 2009. The formation and sedimentary infilling of the Cave of Hearths and Gwaša/Historic Cave Complex, Makapan, South Africa.

- In: McNabb, J. & Sinclair, A. (eds) *The Cave of Hearths Makapan Middle Pleistocene Research Project: Field Research by Anthony Sinclair and Patrick Quinney, 1996-2001*: 49-58. Oxford: Archeopress.
- Leader, G.M. 2009. Early Acheulean in the Vaal River basin, Rietputs Formation, Northern Cape Province, South Africa. Unpublished MSc dissertation. Johannesburg: University of the Witwatersrand.
- Leader, G.M. 2014. New Excavations at Canteen Kopje, Northern Cape Province, South Africa: a techno-typological comparison of three earlier Acheulean assemblages with new interpretations on the Victoria West phenomenon. Unpublished PhD thesis. Johannesburg: University of the Witwatersrand.
- Leakey, M.D. 1970. Stone artefacts from Swartkrans. *Nature* 225: 1222-1225.
- Leakey, M.D. 1971. *Olduvai Gorge Volume 3: Excavations in Beds I and II, 1960-1963*. Cambridge: Cambridge University Press.
- Leakey, M.D. 1976. A summary and discussion of the archaeological evidence from Bed I and Bed II, Olduvai Gorge, Tanzania. In: Isaac, G. & McCown, E. (eds) *Human Origins: Louis Leakey and the East African Evidence*. California: W.A. Benjamin.
- Leakey, M.D. 1979. *Olduvai Gorge: My Search for Early Man*. London: William Collins Sons & Co. Limited.
- Leakey, M.D. 1994a. Bed III. Site JK (Juma's Korongo). In: Leakey, M.D. & Roe, D.A. (eds) *Olduvai Gorge Volume 5: Excavations in Beds III, IV and the Masek Beds, 1968-1971*: 15-35. Cambridge: Cambridge University Press.
- Leakey, M.D. 1994b. The base of Bed IV. WK Hippo Cliff, PDK Trench IV, WK Lower Channel. In: Leakey, M.D. & Roe, D.A. (eds) *Olduvai Gorge Volume 5: Excavations in Beds III, IV and the Masek Beds, 1968-1971*: 36-44. Cambridge: Cambridge University Press.
- Leakey, M.D. 1994c. Lower Bed IV. HEB East, HEB and HEB West, WK Intermediate Channel. In: Leakey, M.D. & Roe, D.A. (eds) *Olduvai Gorge Volume 5: Excavations in Beds III, IV and the Masek Beds, 1968-1971*: 45-74. Cambridge: Cambridge University Press.
- Leakey, M.D. 1994d. Upper Bed IV. WK Upper Channel, WK East A and C, PDK Trenches I-III, HEB West Level I. In: Leakey, M.D. & Roe, D.A. (eds) *Olduvai Gorge Volume 5: Excavations in Beds III, IV and the Masek Beds, 1968-1971*: 75-115. Cambridge: Cambridge University Press.

- Leakey, M.D. 1994e. The Masek Beds and sites in uncertain stratigraphic positions. In: Leakey, M.D. & Roe, D.A. (eds) *Olduvai Gorge Volume 5: Excavations in Beds III, IV and the Masek Beds, 1968-1971*: 116-129. Cambridge: Cambridge University Press.
- Leakey, M.D. 1994f. The fauna. In: Leakey, M.D. & Roe, D.A. (eds) *Olduvai Gorge Volume 5: Excavations in Beds III, IV and the Masek Beds, 1968-1971*: 130-145. Cambridge: Cambridge University Press.
- Leakey, M.D. & Roe, D.A. 1994. *Olduvai Gorge Volume 5: Excavations in Beds III, IV and the Masek Beds, 1968-1971*. Cambridge: Cambridge University Press.
- Lepre, C. J. & Kent, D.V. 2010. Newmagnetostratigraphy for the Olduvai Subchron in the Koobi Fora Formation, northwest Kenya, with implications for early Homo. *Earth and Planetary Science Letters* 290: 362–374.
- Lepre, C.J., Roche, H., Kent, D.V., Harmand, S., Quinn, R.L., Brugal, J.P., Texier, P.J., Lenoble, A. & Feibel, C.S. 2011. An earlier origin for the Acheulian. *Nature* 477: 82-85.
- Li, H., Kuman, K., Leader, G.M. & Couzens, R.A. Submitted. Quantitative analysis of technological and morphological change in handaxes from the earlier to later Acheulean: Rietputs 15 and the Cave of Hearths, South Africa. *Quaternary International*.
- Li, H., Kuman, K. & Li, C. 2015. Quantifying the reduction intensity of handaxes with 3D technology: A pilot study on handaxes in the Danjiangkou Reservoir Region, Central China. *PLoS ONE* 10: 1-17.
- Li, H., Li, C. & Kuman, K. 2014. Rethinking the “Acheulean” in East Asia: evidence from recent investigations in the Danjiangkou Reservoir Region, central China. *Quaternary International* 347: 163-175.
- Lombard, M., Wadley, L., Deacon, J., Wurz, S., Parsons, I., Mohapi, M., Swart, J. & Mitchell, P. 2012. South African and Lesotho Stone Age sequence updated (I). *The South African Archaeological Bulletin* 67: 120-144.
- Lotter, M.G., Gibbon, R.J., Kuman, K., Leader, G.M., Forssman, T. & Granger, D.E. 2016. A geoarchaeological study of the Middle and Upper Pleistocene levels at Canteen Kopje, Northern Cape Province, South Africa. *Geoarchaeology: An International Journal* 2016: 1-20.

- Lowe, D.R. 1982. Sediment gravity flows: II. Depositional models with special reference to the deposits of high density turbidity currents. *Journal of Sedimentary Petrology* 52: 279-297.
- Ludwig, B.V. & Harris, J.W.K. 1998. Towards a technological reassessment of East-African Plio-Pleistocene lithic assemblages. In: Petraglia, M.D. & Korisettar, R. (eds) *Early Human Behaviour in Global Context: The Rise and Diversity of the Lower Palaeolithic Record*: 84-107. London: Routledge.
- Luyt, C.J. & Lee-Thorp, J.A. 2003. Carbon isotope ratios of Sterkfontein fossils indicate a marked shift to open environments c. 1.7 Myr ago. *South African Journal of Science* 99: 271-273.
- Luyt, C.J., Lee-Thorp, J.A. & Avery, G. 2000. New light on Middle Pleistocene west coast environments from Elandsfontein, Western Cape Province, South Africa. *South African Journal of Science* 96: 399-403.
- Lycett, S.J. 2008. Acheulean variation and selection: does handaxe symmetry fit neutral expectations? *Journal of Archaeological Science* 35: 2640-2648.
- Lycett, S.J. 2009a. Quantifying transitions: morphometric approaches to Palaeolithic variability and technological change. In: Camps, M. & Chauhan, P (eds) *Sourcebook of Paleolithic Transitions: Methods, Theories, and Interpretations*: 79-92. New York: Springer.
- Lycett, S.J. 2009b. Are Victoria West cores "proto-Levallois"? A phylogenetic assessment. *Journal of Human Evolution* 56: 175-191.
- Lycett, S.J. & Eren, M.I. 2013. Levallois economics: an examination of 'waste' production in experimentally produced Levallois reduction sequences. *Journal of Archaeological Sciences* 40: 2384-2392.
- Lycett, S.J. & von Cramon-Taubadel, N. 2008. Acheulean variability and hominin dispersals: a model-bound approach. *Journal of Archaeological Science* 35: 553-562.
- Lycett, S.J., von Cramon-Taubadel, N. & Gowlett, J.A.J. 2010. A comparative 3D geometric morphometric analysis of Victoria West cores: implications for the origins of Levallois technology. *Journal of Archaeological Science* 37: 1110-1117.
- Machin, A.J., Hosfield, R.T. & Mithen, S.J. 2007. Why are some handaxes symmetrical? Testing the influence of handaxe morphology on butchery effectiveness. *Journal of Archaeological Science* 34: 883-893.

- Maguire, J. 2009. An overview of the physical setting of Makapan. In: McNabb, J. & Sinclair, A. (eds) *The Cave of Hearths Makapan Middle Pleistocene Research Project: Field Research by Anthony Sinclair and Patrick Quinney, 1996-2001*: 29-48. Oxford: Archeopress.
- Major, J.J. 1997. Depositional processes in large-scale debris-flow experiments. *The Journal of Geology* 105: 345-366.
- Major, J.J. 1998. Pebble orientations on large, experimental debris-flow deposits. *Sedimentary Geology* 117: 151-164.
- Major, J.J. 2000. Gravity-driven consolidation of granular slurries – implications for debris-flow deposition and deposit characteristics. *Journal of Sedimentary Research* 70: 64-83.
- Malet, J-P., Maquaire, O. & Calais, E. 2002. The use of Global Positioning System techniques for the continuous monitoring of landslides: application to the Super-Sauze Earthflow (Alpes-de-Haute-Provence, France). *Geomorphology* 43: 33-54.
- Marwick, B. 2008. What attributes are important for the measurement of assemblage reduction intensity? Results from an experimental stone artefact assemblage with relevance to the Hoabinhian of mainland Southeast Asia. *Journal of Archaeological Science* 35: 1189-1200.
- Mason, R.J. 1962. *Prehistory of the Transvaal: A Record of Human Activity*. Johannesburg: Witwatersrand University Press.
- Mason, R.J. 1965. Makapansgat Limeworks fractured stone objects and natural fracture in Africa. *The South African Archaeological Bulletin* 20: 3-17.
- Mason, R.J. 1988. *Cave of Hearths, Makapansgat, Transvaal*. Johannesburg: University of the Witwatersrand.
- Matmon, A., Ron, H., Chazan, M., Porat, N. & Horwitz, L.K. 2012. Reconstructing the history of sediment deposition in caves: a case study from Wonderwerk Cave, South Africa. *Geological Society of America Bulletin* 124: 611-625.
- McBrearty, S. 1990. Consider the humble termite: termites as agents of post-depositional disturbance at African archaeological sites. *Journal of Archaeological Science* 17: 111-143.
- McBrearty, S. 1999. The archaeology of the Kapthurin Formation. In: Andrews, P. & Banham, P. (eds) *Late Cenozoic Environments and Hominid Evolution: A Tribute to Bill Bishop*: 143-156. London: Geological Society.

- McBrearty, S., Bishop, L.C. & Kingston, J.D. 1996. Variability in traces of Middle Pleistocene hominid behaviour in the Kapthurin Formation, Kenya. *Journal of Human Evolution* 30: 563-580.
- McBrearty, S., Bishop, L., Plummer, T., Dewar, R. & Conard, N. 1998. Tools underfoot: human trampling as an agent of lithic artifact edge modification. *American Antiquity* 63: 108-129.
- McBrearty, S. & Tryon, C. 2006. From Acheulean to Middle Stone Age in the Kapthurin Formation, Kenya. In: Hovers, E & Kuhn S. (eds) *Transitions Before the Transition: Evolution and Stability in the Middle Paleolithic and Middle Stone Age*: 257-277. New York: Springer Publishing.
- McDougall, I. & Brown, F.H. 2006. Precise $^{40}\text{Ar}/^{39}\text{Ar}$ geochronology for the upper Koobi Fora Formation, Turkana Basin, northern Kenya. *Journal of the Geological Society* 163: 205-220.
- McMillan, I.K. 1990. A foraminiferal biostratigraphy and chronostratigraphy for the Pliocene to Pleistocene Upper Algoa Group, Eastern Cape, South Africa. *South African Journal of Geology* 93: 622-644.
- McMillan, I.K. 1999. The Foraminifera of the late Valanginian to Hauterivian (Early Cretaceous) Sundays River Formation of the Algoa Basin, Eastern Cape Province, South Africa. *Annals of South African Museum* 106: 1-120.
- McMillan, I.K. 2003. The Foraminifera of the Late Valanginian to Hauterivian (Early Cretaceous) Sundays River Formation of the Algoa Basin, Eastern Cape Province, South Africa. *Annals of the South Africa Museum* 106:1-274.
- McNabb, J. 2001. The shape of things to come. A speculative essay on the role of the Victoria West phenomenon at Canteen Koppie, during the South African Earlier Stone Age. In: Milliken, S. & Cook, J. (eds) *A Very Remote Period Indeed*: 37-46. Oxford: Oxbow Books.
- McNabb, J. 2009. The ESA stone tool assemblage from the Cave of Hearths, Beds 1-3. In: McNabb, J. & Sinclair, A. (eds) *The Cave of Hearths Makapan Middle Pleistocene Research Project: Field Research by Anthony Sinclair and Patrick Quinney, 1996-2001*: 75-104. Oxford: Archeopress.
- McNabb, J. & Beaumont, P. 2011a. *A Report on the Archaeological Assemblages from Excavations by Peter Beaumont at Canteen Koppie, Northern Cape, South Africa*. Oxford: BAR International Series.

- McNabb, J. & Beaumont, P. 2011b. Excavations in the Acheulean levels at the Earlier Stone Age site of Canteen Koppie, Northern Province, South Africa. *Proceedings of the Prehistoric Society* 78: 51-71.
- McNabb, J., Binyon, F. & Hazelwood, L. 2004. The large cutting tools from the South African Acheulean and the question of social traditions. *Current Anthropology* 45: 653-677.
- McNabb, J. & Sinclair, A. 2009a. *The Cave of Hearths Makapan Middle Pleistocene Research Project: Field Research by Anthony Sinclair and Patrick Quinney, 1996-2001*. Oxford: Archeopress.
- McNabb, J. & Sinclair, A. 2009b. An overview of the archaeological history of the Cave of Hearths and its lithic assemblages. In: McNabb, J. & Sinclair, A. (eds) *The Cave of Hearths Makapan Middle Pleistocene Research Project: Field Research by Anthony Sinclair and Patrick Quinney, 1996-2001*: 12-28. Oxford: Archeopress.
- McNabb, J., Sinclair, A. & Underhill, D. 2009. Overview and broader significance of the ESA and MSA at the Cave of Hearths. In: McNabb, J. & Sinclair, A. (eds) *The Cave of Hearths Makapan Middle Pleistocene Research Project: Field Research by Anthony Sinclair and Patrick Quinney, 1996-2001*: 150-163. Oxford: Archeopress.
- McPherron, S.J.P. 2005. Artifact orientations and site formation processes from total station proveniences. *Journal of Archaeological Science* 32: 1003-1014.
- Millane, R.P., Weir, M.I. & Smart, G.M. 2006. Automated analysis of imbrication and flow direction in alluvial sediments using laser-scan data. *Journal of Sedimentary Research* 76: 1049-1055.
- Mills, H.H. 1984. Clast orientation in Mount St. Helens debris flow deposits: North Fork Toutle River, Washington. *Journal of Sedimentary Petrology* 54: 626-634.
- Mills, S.C. & Grab, S.W. 2005. Debris ridges along the southern Drakensberg escarpment as evidence for Quaternary glaciation in southern Africa. *Quaternary International* 129: 61-73.
- Mills, S.C., Grab, S.W. & Carr, S.J. 2009. Recognition and palaeoclimatic implications of late Quaternary niche glaciation in eastern Lesotho. *Journal of Quaternary Science* 24: 647-663.

- Mishra, S., Gaillard, C., Deo, S., Singh, M., Abbas, R. & Agrawal, N. 2010. Large Flake Acheulian in India: implications for understanding lower Pleistocene human dispersals. *Quaternary International* 223-224: 271-272.
- Mitchell, P. 2002. *The Archaeology of Southern Africa*. Cambridge: Cambridge University Press.
- Moeyersons, J. 1978. The behaviour of stones and stone implements, buried in consolidating and creeping Kalahari Sands. *Earth Surface Processes and Landforms* 3: 115-128.
- Mokokwe, W.D. 2005. Goldsmith's: a preliminary study of a newly discovered Pleistocene site near Sterkfontein. Unpublished MSc dissertation. Johannesburg: University of the Witwatersrand.
- Moolman, H.J. & Cowling, R.M. 1994. The impact of elephant and goat grazing on the endemic flora of South African succulent thicket. *Biological Conservation* 68: 53-61.
- Mora, R. & de la Torre, I. 2005. Percussion tools in Olduvai Beds I and II (Tanzania): implications for early human activities. *Journal of Anthropological Archaeology* 24: 179-192.
- Morgan, L.E., Renne, P.R., Kieffer, G., Piperno, M., Gallotti, R. & Raynal, J.P. 2012. A chronological framework for a long and persistent archaeological record: Melka Kunture, Ethiopia. *Journal of Human Evolution* 62: 104-115.
- Mortimer, B. 2012. The Sand River Canyon develops as bridge washes away for 3rd time (consulted August 2015): <http://stfrancischronicle.com/2012/10/21/the-sand-river-canyon-develops-as-bridge-washes-away-for-3rd-time-photo-gallery/>
- Morton, A.G.T. 2004. *Archaeological Site Formation: Understanding Lake Margin Contexts*. Oxford: BAR International Series.
- Mosher, D.C., Moran, K. & Hiscott, R.N. 1994. Late Quaternary sediment, sediment mass flow processes and slope stability on the Scotian Slope, Canada. *Sedimentology* 41: 1039-1061.
- Muir, R.A., Bordy, E.M. & Prevec, R. 2015. Lower Cretaceous deposit reveals first evidence of a post-wildfire debris flow in the Kirkwood Formation, Algoa Basin, Eastern Cape, South Africa. *Cretaceous Research* 56: 161-179.
- Munga, J.U. 2014. Morphological variability in Acheulean handaxes from Kariandusi and Lewa Downs archaeological sites in Kenya. Unpublished MA dissertation. Nairobi: University of Nairobi.

- Naden, P.S. & Brayshaw, A.C. 1987. Small- and medium-scale bedforms in gravel bed rivers. In: Richards, K. (ed) *River Channels: Environment and Process*: 249-271. Oxford: Basil Blackwell.
- Negash, A., Shackley, M.S. & Alene, M. 2006. Source provenance of obsidian artefacts from the Early Stone Age (ESA) site of Melka Konture, Ethiopia. *Journal of Archaeological Science* 33: 1647-1650.
- Netterberg, F. 1974. Observations on calcretes at some archaeological and palaeontological sites in South Africa. *Goodwin Series, Progress in Later Cenozoic Studies in South Africa* 2: 20-24.
- Nielsen, A.E. 1991. Trampling the archaeological record: an experimental study. *American Antiquity* 56: 483-503.
- Nishimura, M., 2005. Attribute analysis of the Hoabinhian Industry: implications from a comparative study of Bung Cave and Xom Trai Cave, northern Vietnam. *Journal of Southeast Asian Archaeology* 25: 81-104.
- Noll, M.P. 2000. Components of Acheulean lithic assemblage variability at Olorgesailie, Kenya. Unpublished PhD thesis. Illinois: University of Illinois.
- Noll, M.P. & Petraglia, M.D. 2003. Acheulean bifaces and early human behavioural patterns in East Africa and South India. In: Soressi, M. & Dibble, H.L. (eds) *Multiple Approaches to the Study of Bifacial Technologies*: 31-53. Pennsylvania: University of Pennsylvania.
- Norman, N. & Whitfield, G. 2006. *Geological Journeys: A Traveller's Guide to South Africa's Rocks and Landforms*. Cape Town: Struik Publishers and Council for Geoscience.
- Obanawa, H. & Matsukura, Y. 2006. Mathematical modelling of talus development. *Computers & Geosciences* 32: 1461-1478.
- Ogola, C.A. 2009a. The Sterkfontein Western Breccias: stratigraphy, fauna and artefacts. Unpublished PhD thesis. Johannesburg: University of the Witwatersrand.
- Ogola, C.A. 2009b. The taphonomy of the Cave of Hearths Acheulean faunal assemblage. In: McNabb, J. & Sinclair, A. (eds) *The Cave of Hearths Makapan Middle Pleistocene Research Project: Field Research by Anthony Sinclair and Patrick Quinney, 1996-2001*: 65-74. Oxford: Archeopress.
- Pappu, S. 1996. Reinvestigation of the prehistoric archaeological record in the Kortallayar Basin, Tamil Nadu. *Man and Environment* 1: 1-23.

- Pappu, S., Gunnell, Y., Akhilesh, K., Braucher, R., Taieb, M., Demory, F. & Thouveny, N. 2011. Early Pleistocene presence of Acheulian hominins in South India. *Science* 331: 1596-1599.
- Parsons, J.D., While, K.X. & Simoni, A. 2001. Experimental study of the grain-flow, fluid-mud transition in debris flows. *The Journal of Geology* 109: 427-447.
- Partridge, T.C. 1997. Late Neogene uplift in eastern and southern Africa and its paleoclimatic implications. In: Ruddiman, W.F. (ed) *Tectonic Uplift and Climatic Change*: 63-86. New York: Plenum Press.
- Partridge, T.C. 1998. Of diamonds, dinosaurs, and diastrophism: 150 million years of landscape evolution in southern Africa. *South African Journal of Geology* 3: 167-184.
- Partridge, T.C. & Maud, R.R. 1987. Geomorphic evolution of southern Africa since the Mesozoic. *South African Journal of Geology* 90: 179-208.
- Parush, Y., Assaf, E., Slon, V., Gopher, A. & Barkai, R. 2015. Looking for sharp edges: modes of flint recycling at Middle Pleistocene Qesem Cave, Israel. *Quaternary International* 361: 61-87.
- Perez, F.L. 1989. Talus fabric and particle morphology on Lassen Peak, California. *Geografiska Annaler. Series A, Physical Geography* 71: 43-57.
- Peters, C.R., Blumenshine, R.J., Hay, R.L., Livingstone, D.A., Marean, C.W., Harrison, T., Armour-Chelu, M., Andrews, P., Bernor, R., Bonnefille, R. & Werdelin, L. 2008. Paleoecology of the Serengeti-Mara Ecosystem. In: Sinclair, A., Packer, C., Mduma, S.A.R. & Fryxell, J.R. (eds) *Serengeti III: Humans Impacts on Ecosystem Dynamics*: 47-94. Chicago: University of Chicago Press.
- Petraglia, M.D. & Potts, R. 1994. Water flow and the formation of Early Pleistocene artefact sites in Olduvai Gorge, Tanzania. *Journal of Anthropological Archaeology* 13: 228-254.
- Petts, G. & Foster, I. 1985. *Rivers and Landscape*. London: Edward Arnold Publishers.
- Phillipson, D.W. 2005. *African Archaeology, Third Edition*. Cambridge: Cambridge University Press.
- Phillipson, L. 1997. Edge modification as an indicator of function and handedness of Acheulean handaxes from Kariandusi, Kenya. *Lithic Technology* 22: 171-183.

- Pickering, T.R. 2006. Subsistence behaviour of South African Pleistocene hominids. *South African Journal of Science* 102: 205-210.
- Pickering, T.R., Domínguez-Rodrigo, M., Egeland, C.P. & Brain, C.K. 2004. New data and ideas on the foraging behaviour of Early Stone Age hominids at Swartkrans Cave, South Africa. *South African Journal of Science* 100: 215-219.
- Pickering, T.R., Domínguez-Rodrigo, M., Egeland, C.P. & Brain, C.K. 2007. Carcass foraging by early hominids at Swartkrans Cave (South Africa): a new investigation of the zooarchaeology and taphonomy of Member 3. In: Pickering, T.R., Schick, K. & Toth, N. (eds) *African Taphonomy: A Tribute to the Career of C.K. "Bob" Brain*: 233-253. Indiana: Stone Age Institute Press.
- Pickering, T.R., Egeland, C.P., Domínguez-Rodrigo, M., Brain, C.K. & Schnell, A.G. 2008. Testing the 'shift in the balance of power' hypothesis at Swartkrans, South Africa: hominid cave use and subsistence behaviour in the Early Pleistocene. *Journal of Anthropological Archaeology* 27: 30-45.
- Pickering, T.R., Heaton, J.L., Clarke, R.J., Sutton, M.B., Brain, C.K. & Kuman, K. 2012. New hominid fossils from Member 1 of the Swartkrans formation, South Africa. *Journal of Human Evolution* 62: 618-628.
- Pickering, T.R. & Kramers, J.D. 2010. Re-appraisal of the stratigraphy and determination of new U-Pb dates for the Sterkfontein hominin site, South Africa. *Journal of Human Evolution* 59: 70-86.
- Pollarolo, L., Susino, G., Kuman, K. & Bruxelles, L. 2010. Acheulean artefacts at Maropeng in the Cradle of Humankind World Heritage Site, Gauteng Province, South Africa. *South African Archaeological Bulletin* 65: 3-12.
- Porat, N., Chazan, M., Grün, R., Aubert, M., Eisenmann, V. & Horwitz, L.K. 2010. New radiometric ages for the Fauresmith Industry from Kathu Pan, southern Africa: implications for the Earlier to Middle Stone Age transition. *Journal of Archaeological Science* 37: 269-283.
- Postma, G. 1986. Classification for sediment gravity-flow deposits based on flow conditions during sedimentation. *Geology* 14: 291-294.
- Potts, R. 1989. Olorgesailie: new excavations and findings in Early and Middle Pleistocene contexts, southern Kenya Rift Valley. *Journal of Human Evolution* 18: 477-484.

- Potts, R., Behrensmeyer, A.K., Deino, A., Ditchfield, P. & Clark, J. 2004. Small Mid-Pleistocene hominin associated with East African Acheulean Technology. *Science* 305: 75-78.
- Potts, R., Behrensmeyer, A.K. & Ditchfield, P. 1999. Palaeolandscape variation and Early Pleistocene hominid activities: Members 1 and 7, Olorgesailie Formation, Kenya. *Journal of Human Evolution* 37: 747-788.
- Quade, J., Levin, N., Semaw, S., Stout, D., Renne, P., Rogers, M.J. & Simpson, S. 2004. Paleoenvironments of the earliest stone toolmakers, Gona, Ethiopia. *Geological Society of America Bulletin* 116: 1529-1544.
- Quansah, C. 1981. The effect of soil type, slope, rain intensity and their interactions on splash detachment and transport. *Journal of Soil Science* 32: 215-224.
- Quinn, R.L., Lepre, C.J., Feibel, C.S., Wright, J.D., Mortlock, R.A., Harmand, S., Brugal, J.P. & Roche, H. 2013. Pedogenic carbonate stable isotopic evidence for wooded habitat preference of early Pleistocene tool-makers in the Turkana Basin. *Journal of Human Evolution* 65: 65-78.
- Raynal, J.P., Kieffer, G., Bardin, G. & Papy, G. 2004a. Garba IV and the Melka Kunture Formation. A preliminary lithostratigraphic approach. In: Chavaillon, J. & Piperno, M. (eds) *Studies on the Early Palaeolithic Site of Melka Kunture, Ethiopia*: 137-166. Firenze: Origines, Istituto Italiano di Preistoria e Protostoria.
- Raynal, J.P., Sbihi Alaoui, F.Z., Geraads, D., Magoga, L. & Mohib, A. 2001. The earliest occupation of North-Africa: the Moroccan perspective. *Quaternary International* 75: 65-75.
- Raynal, J.P., Sbihi Alaoui, F.Z., Magoga, L., Mohib, A., & Zouak, M. 2004b. The Lower Palaeolithic sequence of Atlantic Morocco revisited after recent excavations at Casablanca. *Bulletin d'Archéologie marocaine, Institut National des Sciences de l'Archéologie et du patrimoine*: 44-76.
- Raynal, J.P. & Texier, J.P. 1989. Decouverte d'Acheuleen ancien dans la carriere Thomas I a Casablanca et probleme de l'anciennete de la presence humaine au Maroc. *Comptes rendus de l'Academie des Sciences Paris* 308: 1743-1749.
- Reed, K.E. 1997. Early hominid evolution and ecological change through the African Plio-Pleistocene. *Journal of Human Evolution* 32: 289-322.

- Rich, T.H.V., Molnar, R.E., & Rich, P.V. 1983. Fossil vertebrates from the Late Jurassic or Early Cretaceous Kirkwood Formation, Algoa Basin, South Africa. *Transactions of the Geological Society of South Africa* 86: 281-291.
- Rightmire, G.P. 1983. The Lake Ndutu cranium and early *Homo sapiens* in Africa. *American Journal of Physical Anthropology* 61: 245-54.
- Rightmire, G.P. 1990. *The Evolution of Homo erectus: Comparative Anatomical Studies of an Extinct Human Species*. Cambridge: Cambridge University Press.
- Rightmire, G.P. 1998. Human evolution in the Middle Pleistocene: the role of *Homo heidelbergensis*. *Evolutionary Anthropology* 6: 218-227.
- Roche, H., Brugal, J.P., Delagnes, A., Feibel, C., Harmand, S., Kibunjia, M., Prat, S. & Texier, P.J. 2003. Les sites archéologiques plio-pléistocènes de la formation de Nachukui, Ouest-Turkana, Kenya: bilan synthétique 1997-2001. *Comptes Rendus Palevol* 2: 663-673.
- Roche, H. & Kibunjia, M. 1994. Les sites archéologiques plio-pléistocènes de la formation de Nachukui, West Turkana, Kenya. *Comptes rendus de l'Académie des Sciences Paris* 318: 1145-1151.
- Roe, D.A. 1964. The British Lower and Middle Paleolithic: some problems. Methods of study and preliminary results. *Proceedings of the Prehistoric Society* 30: 245-267.
- Roe, D.A. 1994a. A metrical analysis of selected sets of handaxes and cleavers from Olduvai Gorge. In: Leakey, M.D. & Roe, D.A. (eds) *Olduvai Gorge Volume 5: Excavations in Beds III, IV and the Masek Beds, 1968-1971*: 146-234. Cambridge: Cambridge University Press.
- Roe, D.A. 1994b. Summary and overview. In: Leakey, M.D. & Roe, D.A. (eds) *Olduvai Gorge Volume 5: Excavations in Beds III, IV and the Masek Beds, 1968-1971*: 299-310. Cambridge: Cambridge University Press.
- Rogers, M.J., Harris, J.W.K. & Feibel, C.S. 1994. Changing patterns of land use by Plio-Pleistocene hominids in the Lake Turkana Basin. *Journal of Human Evolution* 27: 139-158.
- Ross, C.F., Sues, H-D. & de Klerk, W.J. 1999. Lepidosaurian remains from the lower Cretaceous Kirkwood Formation of South Africa. *Journal of Vertebrate Paleontology* 19: 21-27.
- Rots, V. & Plisson, H. 2014. Projectiles and the abuse of the use-wear method in a search for impact. *Journal of Archaeological Science* 48: 154-165.

- Ruddock, A. 1948. Terraces in the lower part of the Sundays River Valley, Cape Province. *Transactions of the Royal Society of South Africa*. 31: 347-370.
- Ruddock, A. 1957: A note on the relation between Chelles-Archeul implements and Quaternary river terraces in the valleys of the Coega and Sundays Rivers, Cape Province. *South African Journal of Science*. 53: 373-377.
- Ruddock, A. 1968: Cenozoic sea-levels and diastrophism in a region bordering Algoa Bay. *Transactions of the Geological Society of South Africa* 71: 209-233.
- Sampson, C.G. 1974. *The Stone Age Archaeology of Southern Africa*. New York: Academic Press.
- Sass, O. & Krautblatter, M. 2007. Debris flow-dominated and rockfall-dominated talus slopes: genetic models derived from GPR measurements. *Geomorphology* 86: 176-192.
- Schackley, M. L. 1974. Stream abrasion of flint implements. *Nature* 248: 501-502.
- Schick, K.D. 1984. Processes of Palaeolithic site formation: an experimental study. Unpublished PhD thesis. Berkeley: University of California.
- Schick, K.D. 1987. Modeling the formation of Early Stone Age artifact concentrations. *Journal of Human Evolution* 16: 789-807.
- Schick, K.D. 1991. On making behavioural inferences from early archaeological sites. In: Clark, J.D. (ed) *Cultural Beginnings*: 79-107. Bonn: Dr. Rudolf Habelt GMBH.
- Schick, K.D. 1997. Experimental studies of site-formation processes. In: Isaac, G.I. & Isaac, B. (eds) *Koobi Fora Research Project: Volume 5, Plio-Pleistocene Archaeology*: 244-261. Oxford: Clarendon Press.
- Schick, K.D. & Clark, J.D. 2000. Acheulean archaeology of the Western Middle Awash. In: de Heinzelin, J., Clark, J.D., Schick, K.D. & Gilbert, W.H. (eds) *The Acheulean and the Plio-Pleistocene Deposits of the Middle Awash Valley, Ethiopia*: 123-181. Tervuren: Royal Museum of Central Africa.
- Schiffer, M.B. 1983. Toward the identification of formation processes. *American Antiquity* 48: 675-706.
- Schwartz, G.T. 2012. Growth, development, and life history throughout the evolution of *Homo*. *Current Anthropology* 53: S395-S408.
- Semaw, S. 2000. The World's oldest stone artefacts from Gona, Ethiopia: their implications for understanding stone technology and patterns of human

- evolution between 2.6–1.5 Million Years Ago. *Journal of Archaeological Science* 27: 1197-1214.
- Semaw, S., Rogers, M. & Stout, D. 2009. The Oldowan-Acheulian Transition: is there a "Developed Oldowan" artifact tradition? In: Camps, M. & Chauhan, P (eds) *Sourcebook of Paleolithic Transitions: Methods, Theories, and Interpretations*: 173-193. New York: Springer.
- Sharon, G. 2006. Acheulian large flake industries: technology, chronology, distribution and significance. Unpublished PhD thesis. Jerusalem: Hebrew University of Jerusalem.
- Sharon, G. 2008. The impact of raw material on Acheulian large flake production. *Journal of Archaeological Science* 35: 1329-1344.
- Sharon, G. 2010. Large flake Acheulian. *Quaternary International* 223-224: 226-233.
- Sharon, G., Alpers-Afil, N. & Goren-Inbar, N. 2011. Cultural conservatism and variability in the Acheulean sequence at Gesher Benot Ya-aqov. *Journal of Human Evolution* 60: 387-397.
- Sharon, G. & Beaumont, P. 2006. Victoria West: a highly standardised prepared core technology. In: Goren-Inbar, N. & Sharon, G. (eds) *Axe Age: Acheulian Tool-making from Quarry to Discard*: 181-199. London: Equinox Publishing Ltd.
- Shea, J. J. 1999. Artifact abrasion, fluvial processes, and “living floors” from the Early Palaeolithic site of ‘Ubeidiya (Jordan Valley, Israel). *Geoarchaeology: An International Journal* 14: 191-207.
- Shimokawa, E. 1997. Observation and measurement for debris flow. In: Armanini, A. & Michiue, M. (eds) *Recent Developments on Debris Flows*: 1-6. New York: Springer.
- Shipton, C. 2011. Taphonomy and behaviour at the Acheulean site of Kariandusi, Kenya. *African Archaeological Review* 28: 141-155.
- Shipton, C. & Petraglia, M.D. 2010. Inter-continental variation in Acheulean bifaces. In: Norton, C.J. & Braun, D.R. (eds) *Asian Palaeoanthropology: From Africa to China and Beyond*: 49-55. London: Springer Science and Business Media.
- Shone, R.W. 1978. A case of lateral gradation between the Kirkwood and Sundays River Formations, Algoa Basin. *Transactions of the Geological Society of South Africa* 81: 319-326.
- Shone, R.W. 1986. A new Ophiuroid from the Sundays River Formation (Lower Cretaceous), South Africa. *Journal of Paleontology* 60: 904-910.

- Sikes, N.E., Potts, R. & Behrensmeyer, A.K. 1999. Early Pleistocene habitat in Member 1 Olorgesailie based on palaeosol stable isotopes. *Journal of Human Evolution* 37: 721-746.
- Singer R. 1954. The Saldanha skull from Hopefield, South Africa. *American Journal of Physical Anthropology* 12: 345-362.
- Singer, R. & Crawford, J.R. 1958. The significance of the archaeological discoveries at Hopefield, South Africa. *The Journal of the Royal Anthropological Institute of Great Britain and Ireland* 88: 11-19.
- Slattery, M.C. & Bryan, R.B. 1992. Laboratory experiments on surface seal development and its effect on interrill erosion processes. *Journal of Soil Science* 43: 517-529.
- Smith, B.H., 1993. The physiological age of KNM-WT 15000. In: Leakey, R. & Walker, A. (eds) *The Nariokotome Homo erectus Skeleton*: 195-220. Cambridge: Harvard University Press.
- Smith, H.F. & Grine, F.E. 2008. Cladistic analysis of early *Homo* crania from Swartkrans and Sterkfontein, South Africa. *Journal of Human Evolution* 54: 684-704.
- Spies, D. 2012. Record beating rain in Mandela Bay (consulted August 2015): <http://www.metronewspaper.co.za/2012/10/22/record-beating-rain-in-mandela-bay/>
- Stein, J.K. 1983. Earthworm activity: a source of potential disturbance of archaeological sediments. *American Antiquity* 48: 277-289.
- Stein, J.K. 2001. A review of site formation processes and their relevance to Geoarchaeology. In: Goldberg, P., Holliday, V.T. & Reid Ferring, C. (eds) *Earth Sciences and Archaeology*: 37-51. London: Kluwer Academic/Plenum Publishers.
- Stein, J.K. & Teltser, P.A. 1989. Size distributions of artifact classes: combining macro- and micro-fractions. *Geoarchaeology: An International Journal* 4: 1-30.
- Steininger, C.M. & Berger, L.R. 2001. Taxonomic affinity of a new specimen from Coopers, South Africa. *American Journal of Physical Anthropology Supplement* 30: 291.
- Stern, N. 1993. The structure of the Lower Pleistocene archaeological record: a case study from the Koobi Fora Formation. *Current Anthropology* 34: 201-225.

- Stiles, D. 1979. Early Acheulean and Developed Oldowan. *Current Anthropology* 20: 126-129.
- Stratford, D.J. 2011. The underground central deposits of the Sterkfontein Caves, South Africa. Unpublished PhD thesis. Johannesburg: University of the Witwatersrand.
- Susman, R.L., de Ruiter, D. & Brain, C.K. 2001. Recently identified postcranial remains of *Paranthropus* and early *Homo* from Swartkrans Cave, South Africa. *Journal of Human Evolution* 41: 607-629.
- Sutton, M. 2012. The archaeology of Swartkrans Cave, Gauteng, South Africa: new excavations of Members 1 and 4. Unpublished PhD thesis. Johannesburg: University of the Witwatersrand.
- Suwa, G., Asfaw, B., Haile-Selassie, Y., White, T., Katoh, S., WoldeGabriel, G., Hart, W.K., Nakaya, H. & Beyene, Y. 2007. Early Pleistocene *Homo erectus* fossils from Konso, southern Ethiopia. *Anthropological Science* 115: 133-151.
- Tallon, P.W.J. 1976. The stratigraphy, paleoenvironments and geomorphology of the Pleistocene Kapthurin Formation, Kenya. Unpublished PhD thesis. London: Queen Mary College.
- Tallon, P.W.J. 1978. Geological setting of the hominid fossils and Acheulian artifacts from the Kapthurin Formation, Baringo District, Kenya. In: Bishop, W.W. (ed) *Geological Background to Fossil Man*: 361-373. Edinburgh: Scottish Academic Press.
- Tamrat, E., Thouveny, N., Taïeb, M. & Opdyke, N.D. 1995. Revised magnetostratigraphy of the Plio-Pleistocene sedimentary sequence of the Olduvai Formation (Tanzania). *Palaeogeography, Palaeoclimatology, Palaeoecology* 114: 273-283.
- Tandon, S.K. & Kumar, R. 1981. Gravel fabric in a sub-Himalayan braided stream. *Sedimentary Geology* 28: 133-152.
- Texier, P.J. 1995. The Oldowan assemblage from NY 18 site at Nyabusosi (Toro-Uganda). *Comptes Rendus Academy of Science* 320: 647-653.
- Thomas, D.S.G. 1987. Discrimination of depositional environments, using sedimentary characteristics, in the Mega Kalahari, central Southern Africa. In Frostick, L.E. & Reid, I. (eds) *Desert Sediments, Ancient and Modern*: 293-306. London: Geological Society Special Publication 35.

- Thompson, E. 2009. Acheulean artefact accumulation and early hominin land use, Garden Route Casino Road, Pinnacle Point, South Africa. *Geoarchaeology: An International Journal* 24: 402-428.
- Tixier, J. 1957 Le hachereau dans l'Acheuléen Nord-Africain – notes typologiques. *Congrès préhistorique de France - Compte-rendu de la XVème session* 1956: 914-923.
- Toth, N. 1985. Oldowan reassessed: a close look at early stone artifacts. *Journal of Archaeological Science* 12: 101-120.
- Toth, N. 1987. Behavioural inferences from Early Stone artefact assemblages: an experimental model. *Journal of Human Evolution* 16: 763-787.
- Tryon, C.A. 2003. The Acheulean to Middle Stone Age transition: tephrostratigraphic context for archaeological change in the Kapthurin Formation, Kenya. Unpublished PhD thesis. Connecticut: University of Connecticut.
- Tryon, C.A. 2006. "Early" Middle Stone Age lithic technology of the Kapthurin Formation (Kenya). *Current Anthropology* 47: 367-375.
- Tryon, C.A. & McBrearty, S. 2002. Tephrostratigraphy and the Acheulean to Middle Stone Age transition in the Kapthurin Formation, Kenya. *Journal of Human Evolution* 42: 211-235.
- Tryon, C.A. & McBrearty, S. 2006. Tephrostratigraphy of the Bedded Tuff Member (Kapthurin Formation, Kenya) and the nature of archaeological change in the later Middle Pleistocene. *Quaternary Research* 65: 492-507.
- Tryon, C.A., McBrearty, S. & Texier, P.J. 2005. Levallois lithic technology from the Kapthurin Formation, Kenya: Acheulean origin and Middle Stone Age diversity. *African Archaeological Review* 22: 199-229.
- Tryon, C.A. & Potts, R. 2011. Approaches for understanding flake production in the African Acheulean. *PaleoAnthropology* 2011: 376-389.
- Underdown, S. 2006. How the word 'hominid' evolved to include hominin. *Nature* 444: 680.
- Underhill, D. 2007. Subjectivity inherent in by-eye symmetry judgments and the large cutting tools at the Cave of Hearths, Limpopo Province, South Africa. *Paper from the Institute of Archaeology* 18: 101-113.
- Van Peer, P. 1992. *The Levallois Reduction Strategy*. Madison: Prehistory Press.
- van Riet Lowe, C. 1954. The Cave of Hearths. *The South African Archaeological Bulletin* 9: 25-29.

- Vaquero, M., Bargalló, A., Chacón, M.G., Romagnoli, F. & Sañudo, P. 2015. Lithic recycling in a Middle Palaeolithic expedient context: evidence from the Abric Romaní (Capellades, Spain). *Quaternary International* 361: 212-228.
- Ventura, E., Nearing, M.A., Amore, E. & Norton, L.D. 2002. The study of detachment and deposition on a hillslope using a magnetic tracer. *Catena* 48: 149-161.
- Ventura, E., Nearing, M.A. & Norton, L.D. 2001. Developing a magnetic tracer to study soil erosion. *Catena* 43: 277-291.
- Vermeersch, P.M. & Bubenik, S. 1997. Postdepositional artefact scattering in a podzol. Processes and consequences for late Palaeolithic and Mesolithic sites. *Anthropologie* 2: 119-130.
- Villa, P. & Courtin, J. 1983. The interpretation of stratified sites: a view from underground. *Journal of Archaeological Science* 10: 267-281.
- Vrba, E.S. 1975. Some evidence of chronology and palaeoecology of Sterkfontein, Swartkrans and Kromdraai from the fossil Bovidae. *Nature* 254: 301-304.
- Wadley, L. 2015. Those marvellous millennia: the Middle Stone Age of Southern Africa. *Azania: Archaeological Research in Africa* 50: 155-226.
- Walter, M.J. & Trauth, M.H. 2013. A MATLAB based orientation analysis of Acheulean handaxe accumulations in Olorgesailie and Kariandusi, Kenya Rift. *Journal of Human Evolution* 64: 569-581.
- Watson, V. 1993. Composition of the Swartkrans bone accumulations in terms of skeletal parts and animals represented. In: Brain, C.K. (ed) *Swartkrans: A Cave's Chronicle of Early Man*: 35-74. Pretoria: Transvaal Museum.
- White, M., Ashton, N. & Scott, B. 2011. The emergence, diversity and significance of Mode 3 (Prepared Core) Technologies. In: Ashton, N., Lewis, S.G. & Stringer, C. (eds) *The Ancient Human Occupation of Britain*: 53-65. London: Elsevier.
- Wilkins, J. & Chazan, M. 2012. Blade production ~500 thousand years ago at Kathu Pan 1, South Africa: support for a multiple origins hypothesis for early Middle Pleistocene blade technologies. *Journal of Archaeological Science* 39: 1883-1900.
- Wilkins, J., Schoville, B.J., Brown, K.S. & Chazan, M. 2012. Evidence for early hafted hunting technology. *Science* 338: 942-946.
- Wilkins, J., Schoville, B.J., Brown, K.S. & Chazan, M. 2015. Kathu Pan 1 points and the assemblage-scale, probabilistic approach: a response to Rots and Plisson,

“Projectiles and the abuse of the use-wear method in a search for impact.”

Journal of Archaeological Science 54: 294-299.

WoldeGabriel, G., Gilbert, W.H., Hart, W.K., Renne, P.R. & Ambrose, S.H. 2008.

Geology and Geochronology. In: Gilbert, W. & Asfaw, B. (eds) *Homo erectus: Pleistocene Evidence from the Middle Awash, Ethiopia*: 13-44. California: University of California Press.

Wood, B. & Harrison, T. 2011. The evolutionary context of the first hominins. *Nature* 470: 347-352.

Wright, R. & Anderson, B. 1982. The importance of sediment gravity flow to sediment transport and sorting in the glacial marine environment: Eastern Weddell Sea, Antarctica. *Geological Society of American Bulletin* 93: 951-963.

Yagishita, K. & Jopling, A.V. 1983. Grain fabric of planar cross-bedding formed by lateral accretion, Caledon outwash, Ontario, Canada. *The Journal of Geology* 91: 599-606.

Zhang, G-H., Liu, B-Y., Liu, G-B., He, X-W. & Nearing, M.A. 2003. Detachment of undisturbed soil by shallow flow. *Soil Science Society of America Journal* 67: 713-719.

Appendix A

Data excluded from Chapter 4.3

Table 1. Bernol Farm LCT technological measurements, by type (n=11).

Artefact number	Type	Weight (g)	1 (mm)	2 (mm)	3 (mm)	4 (mm)	5 (mm)	6 (mm)	7 (mm)	8 (mm)	9 (mm)	10 (mm)	11 (mm)
Bernol-LL-1	Pick	963.47	165.0	108.0	75.0	61.0	102.6	94.1	20.1	48.6	62.0	57.2	40.0
Bernol-LL-3	Biface	148.91	79.0	53.0	55.0	48.6	51.3	43.7	21.8	37.9	40.0	25.5	48.0
Bernol-LL-13	Handaxe	221.96	102.0	67.0	45.0	41.9	60.8	63.5	17.1	25.3	32.0	34.9	27.0
Bernol-LL-14	Handaxe	220.31	104.0	64.0	30.0	41.0	61.1	60.8	19.2	27.8	33.0	33.1	17.0
Bernol-LL-20	Handaxe	364.26	120.0	74.0	40.0	46.0	66.8	72.1	23.5	33.4	48.0	46.8	21.0

Artefact number	Type	Weight (g)	1 (mm)	2 (mm)	3 (mm)	4 (mm)
Bernol-LL-6	Cleaver	906.86	171.0	102.0	109.2	58.0
Bernol-LL-7	Cleaver	257.30	95.0	67.0	52.9	43.0
Bernol-LL-9	Cleaver	378.01	136.0	88.0	37.0	39.0
Bernol-LL-10	Cleaver	119.90	90.0	51.0	34.2	27.0
Bernol-LL-12	Cleaver	999.28	173.0	96.0	62.0	72.6
Bernol-LL-15	Cleaver	186.70	96.0	64.0	52.5	30.0

Table 1 continued...

Handaxe measurements
1: Maximum length (L)
2: Maximum width (W)
3: Location of maximum width
4: Width at upper fifth
5: Width at half length
6: Width at lower fifth
7: Thickness at upper fifth
8: Thickness at half length
9: Maximum thickness (T)
10: Thickness at lower fifth
11: Location of maximum thickness

Cleaver measurements
1: Maximum length (L)
2: Maximum width (W)
3: Edge length
4: Maximum thickness (T)

Table 2. Bernol Farm LCT size ratio data (W, L and T as in Table 1 above).

Artefact number	Type	Size ratio		
		W/L	L/W (elongation)	T/W (refinement)
Bernol-LL-1	Pick	0.65	1.53	0.57
Bernol-LL-3	Biface	0.67	1.49	0.75
Bernol-LL-13	Handaxe	0.66	1.52	0.48
Bernol-LL-14	Handaxe	0.62	1.63	0.52
Bernol-LL-20	Handaxe	0.62	1.62	0.65
Bernol-LL-6	Cleaver	0.60	1.68	0.57
Bernol-LL-7	Cleaver	0.71	1.42	0.64
Bernol-LL-9	Cleaver	0.65	1.55	0.44
Bernol-LL-10	Cleaver	0.57	1.76	0.53
Bernol-LL-12	Cleaver	0.55	1.80	0.76
Bernol-LL-15	Cleaver	0.67	1.50	0.47

Table 3. Additional LCT size data averages for Bernol Farm.

Bernol Farm LCTs (n=11)		Pick (n=1)	Biface (n=1)	Handaxe (n=3)	Cleaver (n=6)
Edge length (mm)	Min	-	-	-	34.20
	Median	-	-	-	52.70
	Max	-	-	-	109.20
	Mean	-	-	-	57.97
	SD	-	-	-	27.21
Location of max width (mm)	Min	75.00	55.00	30.00	-
	Median	-	-	40.00	-
	Max	75.00	55.00	45.00	-
	Mean	-	-	38.33	-
	SD	-	-	7.64	-
Width at upper fifth (mm)	Min	61.00	48.60	41.00	-
	Median	-	-	41.90	-
	Max	61.00	48.60	46.00	-
	Mean	-	-	42.97	-
	SD	-	-	2.67	-
Width at half length (mm)	Min	102.60	51.30	60.80	-
	Median	-	-	61.10	-
	Max	102.60	51.30	66.80	-
	Mean	-	-	62.90	-
	SD	-	-	3.38	-

Table 3 continued...

Bernol Farm LCTs (n=11)		Pick (n=1)	Biface (n=1)	Handaxe (n=3)	Cleaver (n=6)
Width at lower fifth (mm)	Min	94.10	43.70	60.80	-
	Median	-	-	63.50	-
	Max	94.10	43.70	72.10	-
	Mean	-	-	65.47	-
	SD	-	-	5.90	-
Thickness at upper fifth (mm)	Min	20.10	21.80	17.10	-
	Median	-	-	19.20	-
	Max	20.10	21.80	23.50	-
	Mean	-	-	19.93	-
	SD	-	-	3.26	-
Thickness at half length (mm)	Min	48.60	37.90	25.30	-
	Median	-	-	27.80	-
	Max	48.60	37.90	33.40	-
	Mean	-	-	28.83	-
	SD	-	-	4.15	-
Thickness at lower fifth (mm)	Min	57.20	25.50	33.10	-
	Median	-	-	34.90	-
	Max	57.20	25.50	46.80	-
	Mean	-	-	38.27	-
	SD	-	-	7.44	-
Location of max thickness (mm)	Min	40.00	48.00	17.00	-
	Median	-	-	21.00	-
	Max	40.00	48.00	27.00	-
	Mean	-	-	21.67	-
	SD	-	-	5.03	-

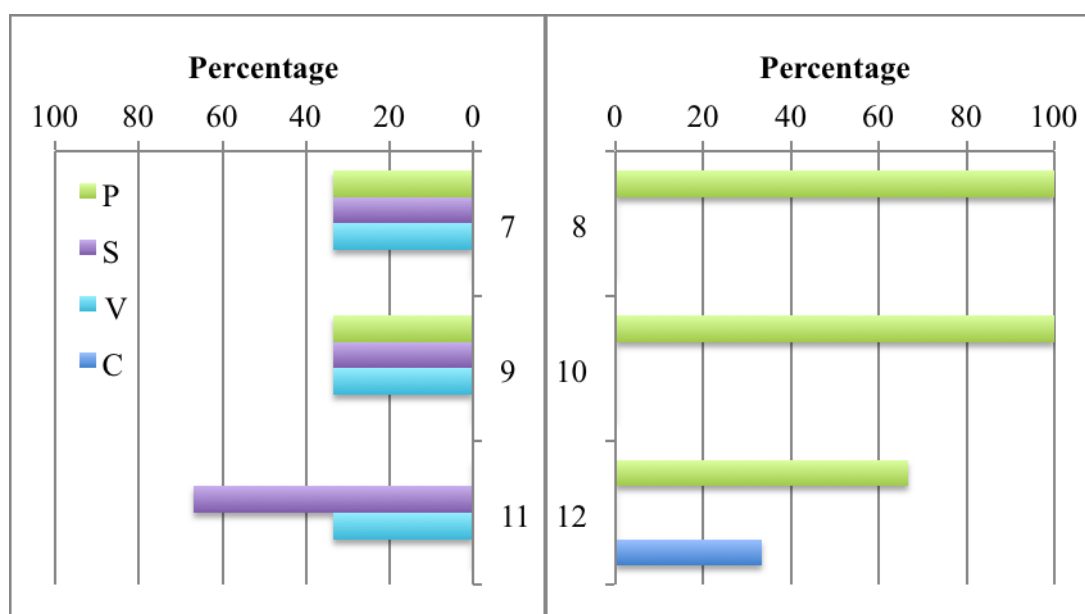
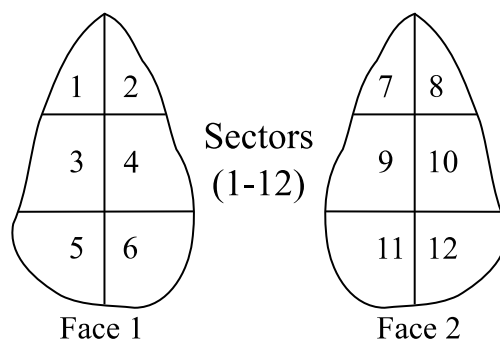
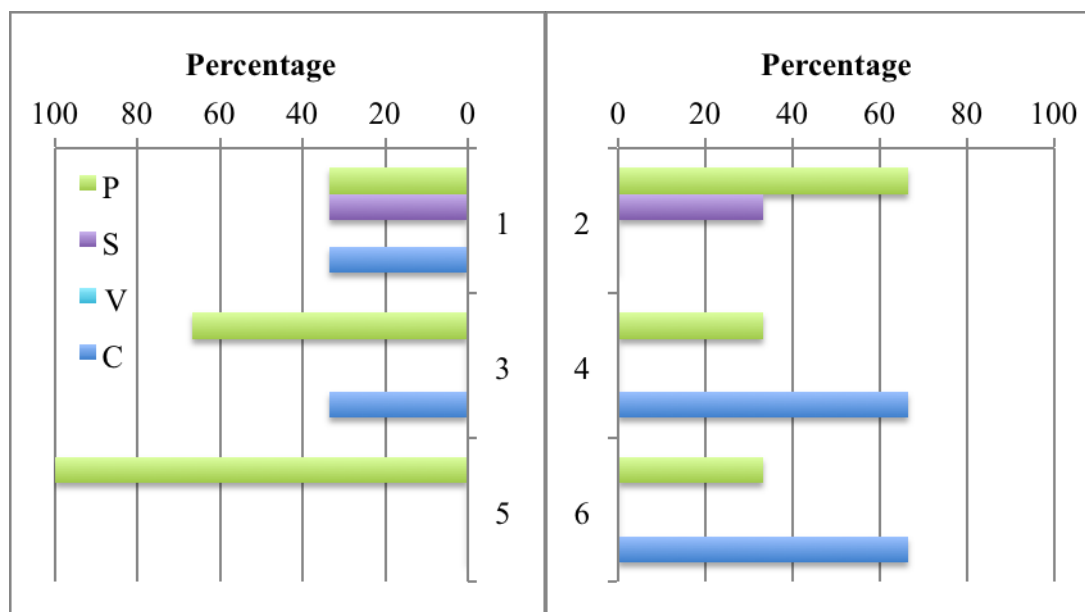


Figure 1. Flaking location for the Bernol Farm handaxe sample (n=3). P: primary; S: secondary; V: ventral/no working; C: cortical. For flake blanks the dorsal surface is recorded first (face 1, upper graphs) and the ventral second (face 2, lower graphs).

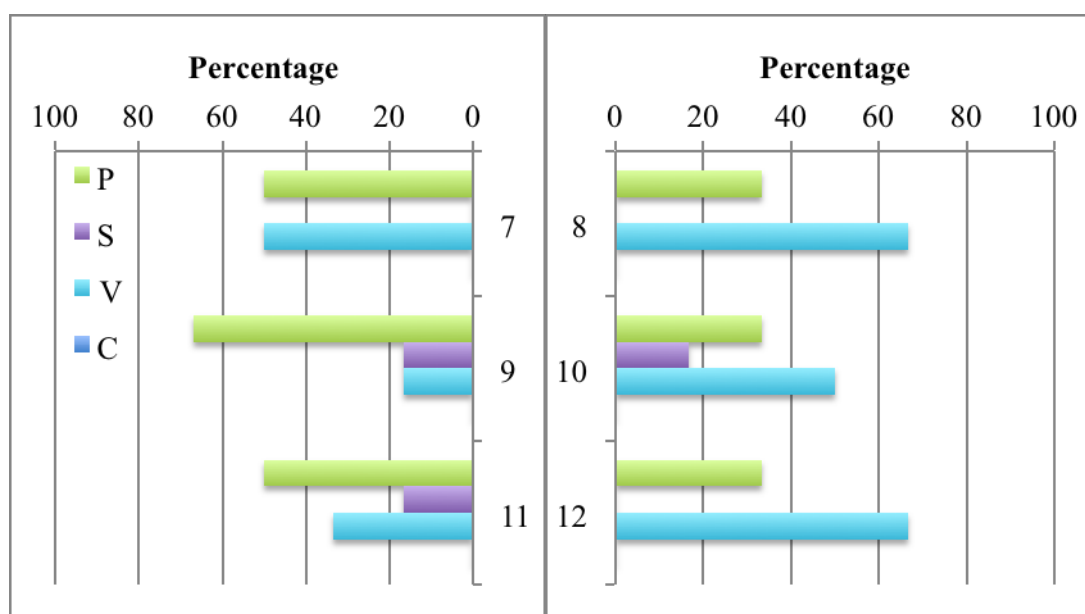
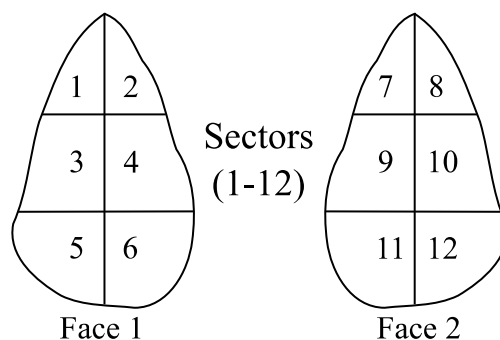
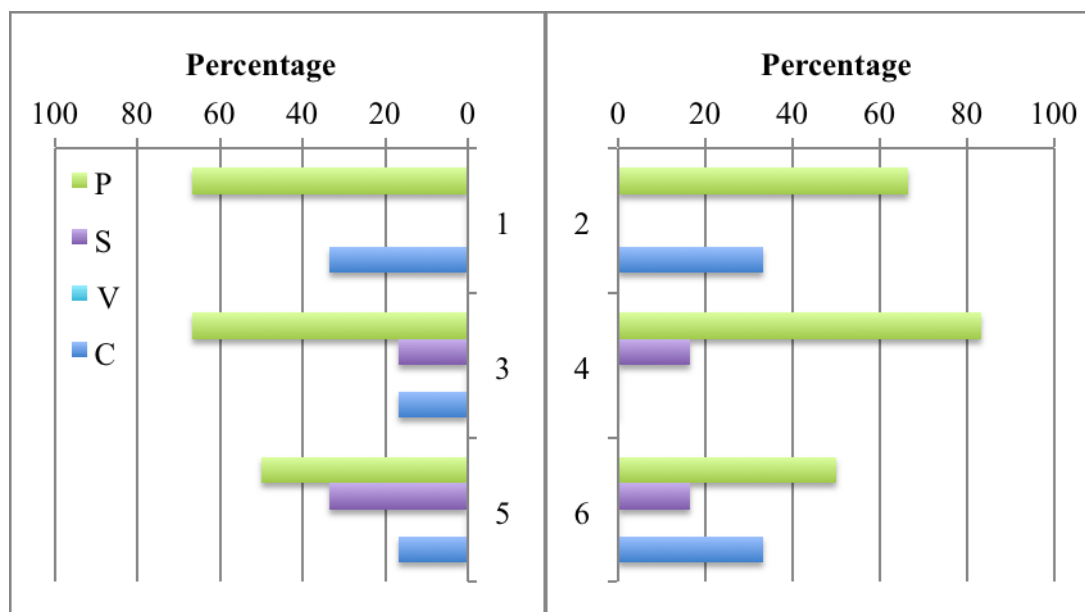


Figure 2. Flaking location for the Bernol Farm cleaver sample (n=6). P: primary; S: secondary; V: ventral/no working; C: cortical. For flake blanks the dorsal surface is recorded first (face 1, upper graphs) and the ventral second (face 2, lower graphs).

Appendix B

Data excluded from Chapter 4.4

Table 1. Colluvial assemblage flake measurements, by raw material (n=446). Grey blocks indicate where sample is <15 pieces.

Flake measurement data (mm)		Raw materials					
		Quartzite	Siltstone	Hornfels	Lava	Silcrete	Claystone
Length	Mean	43.3	46.8	39.1	42	32.5	-
	SD	18.6	21.1	17.2	-	16.3	-
Width	Mean	43	48.2	36.9	47	30.3	-
	SD	16.6	17.5	16	-	16.2	-
Thickness	Mean	12.9	13.9	10	11	12.3	-
	SD	6.8	5.3	5.5	-	-	-
Platform thickness	Mean	10	10.8	8.2	10.4	12.3	-
	SD	5.5	6.1	5.3	-	-	-
Length & width	Technological flake length and width following Isaac & Keller 1968						
Thickness	Technological flake thickness at midpoint following Dibble 1997						
Platform thickness	Platform thickness at point of percussion following Dibble 1997						

Table 2. Flake measurements for the debris flow assemblage, by raw material (n=2208). Grey blocks indicate where sample is <15 pieces.

Flake measurement data (mm)		Raw materials						
		Quartzite	Siltstone	Silt-qzte	Hornfels	Lava	Silcrete	Claystone
Length	Mean	44.4	48	37	36.7	37.5	53.5	47.3
	SD	20.1	19.7	-	14.8	9.2	19.1	12.3
Width	Mean	46	50.1	35.5	34.8	30	67	44.5
	SD	23.3	24.6	9.2	12.4	-	-	11.9
Thickness	Mean	13	13.3	-	9.2	8.7	26.1	11.8
	SD	7.5	8	-	4.8	-	-	4
Platform thickness	Mean	10.9	9.4	-	8.3	2.8	23.2	12.1
	SD	7.1	7.5	-	4.1	-	-	3
Length & width	Technological flake length and width following Isaac & Keller 1968							
Thickness	Technological flake thickness at midpoint following Dibble 1997							
Platform thickness	Platform thickness at point of percussion following Dibble 1997							

Table 3. Colluvial assemblage complete flake measurements, by flaking axis (n=134).

Complete flake measurement data (mm)		Flaking axis		
		Corner	End	Side
Maximum length	Mean	-	53	48.1
	SD	-	22.9	16.8
Length	Mean	-	49.3	35.7
	SD	-	21.9	13.6
Width	Mean	-	39	45.3
	SD	-	17.2	15.2
Thickness	Mean	-	13	11.4
	SD	-	7.5	5.8
Platform thickness	Mean	-	9.1	9.4
	SD	-	5.4	5.1
Platform width	Mean	-	23.7	30.1
	SD	-	11.1	12.8
Weight (g)	Mean	-	54	31
	SD	-	92.3	36.6
Length and width	Technological flake length and width following Isaac & Keller 1968			
Thickness	Technological flake thickness at midpoint following Dibble 1997			
Platform thickness	Platform thickness at point of percussion following Dibble 1997			
Flaking axis	Technological flaking axis following Isaac & Keller 1968			

Table 4. Debris flow assemblage complete flake measurements, by flaking axis (n=335).

Complete flake measurement data (mm)		Flaking axis		
		Corner	End	Side
Maximum length	Mean	-	51	51
	SD	-	21.6	23
Length	Mean	-	47.4	37.2
	SD	-	20	17
Width	Mean	-	37.5	47.9
	SD	-	18	21.5
Thickness	Mean	-	11.7	12.1
	SD	-	6.7	7.8
Platform thickness	Mean	-	9.1	10.6
	SD	-	5.4	7.6
Platform width	Mean	-	23.4	33
	SD	-	10.4	17.3
Weight (g)	Mean	-	43.9	42.9
	SD	-	87.8	80.6
Length and width	Technological flake length and width following Isaac & Keller 1968			
Thickness	Technological flake thickness at midpoint following Dibble 1997			
Platform thickness	Platform thickness at point of percussion following Dibble 1997			
Flaking axis	Technological flaking axis following Isaac & Keller 1968			

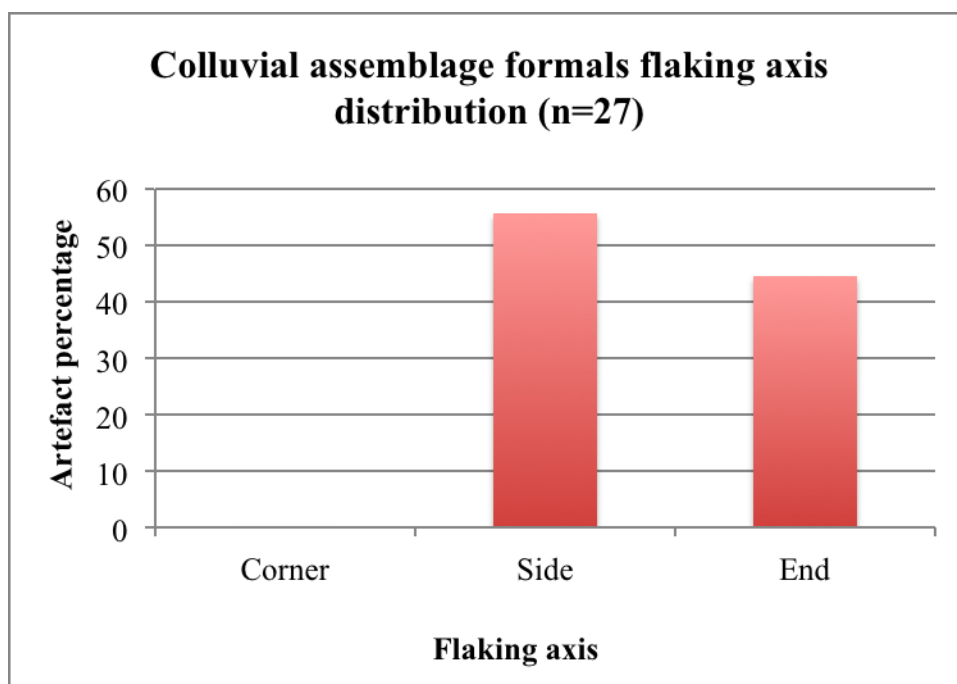
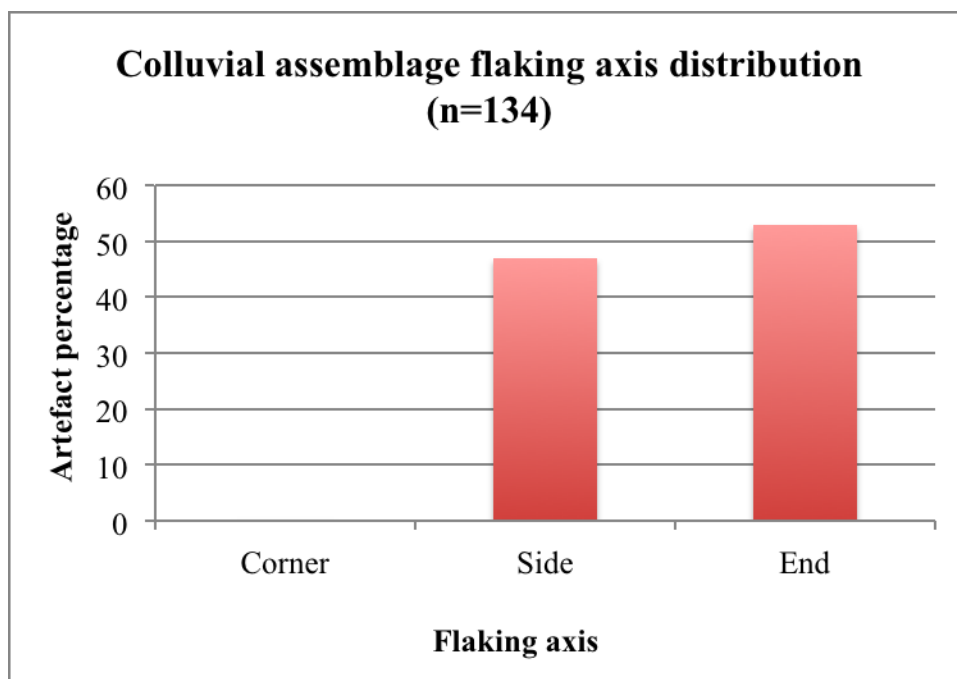


Figure 1. Colluvial assemblage flaking axis distribution (following Isaac & Keller 1968) for complete flakes and formal tools on complete flakes.

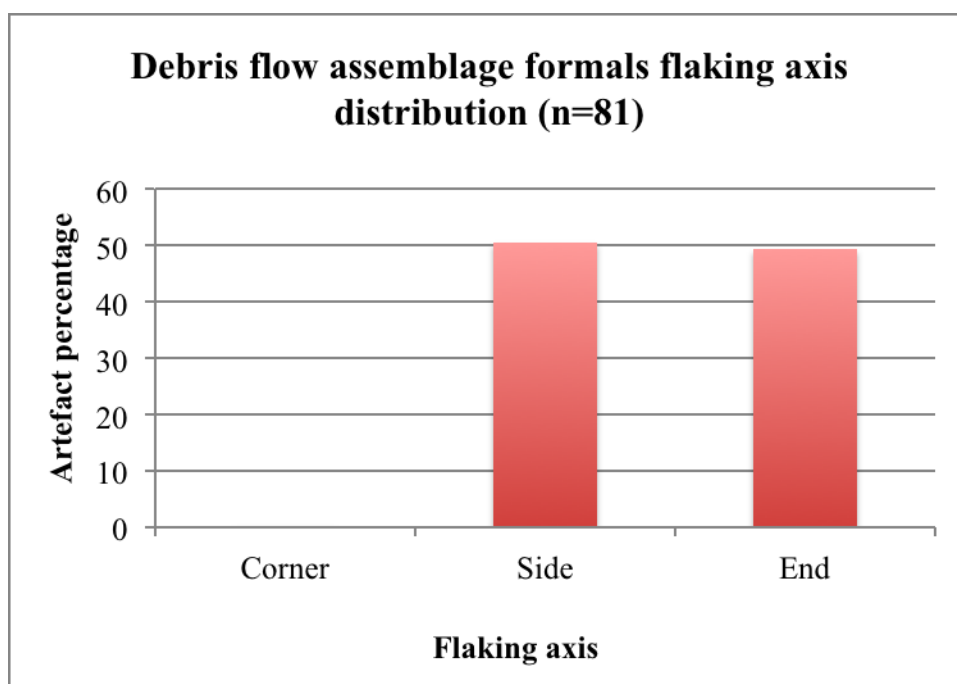
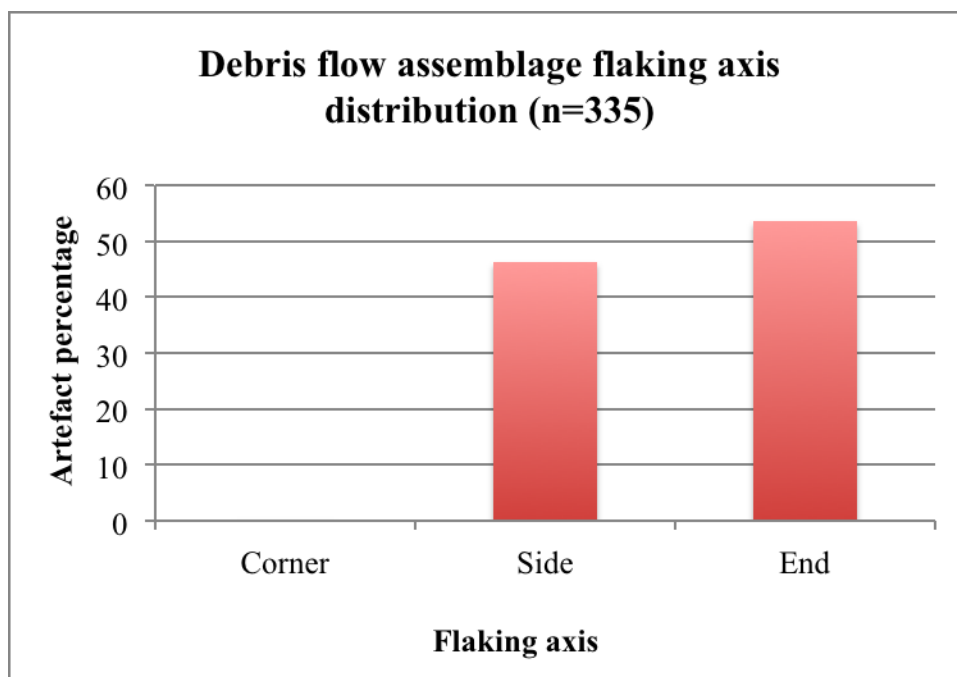


Figure 2. Debris flow assemblage flaking axis distribution (following Isaac & Keller 1968) for complete flakes and formal tools on complete flakes.

Table 5. Colluvial assemblage flaking axis by raw material.

Raw material	Flaking axis n=161 (Isaac & Keller 1968)					
	Side (n=78)		End (n=83)		Total	
	N	%	N	%	N	%
Quartzite	62	48.4	66	51.6	128	100
Siltstone	8	50	8	50	16	100
Hornfels	6	40	9	60	15	100
Lava	1	100	0	0	1	100
Silcrete	1	100	0	0	1	100

Table 6. Debris flow assemblage flaking axis by raw material.

Raw material	Flaking axis n=416 (Isaac & Keller 1968)					
	Side (n=196)		End (n=220)		Total	
	N	%	N	%	N	%
Quartzite	146	48.7	154	51.3	300	100
Siltstone	20	50	20	50	40	100
Hornfels	26	37.7	43	62.3	69	100
Lava	0	0	1	100	1	100
Silcrete	1	100	0	0	1	100
Claystone	3	60	2	40	5	100

Table 7. Colluvial assemblage LCT technological measurements, by type and raw material (n=11).

Type	Raw material	Weight (g)	1 (mm)	2 (mm)	3 (mm)	4 (mm)	5 (mm)	6 (mm)	7 (mm)	8 (mm)	9 (mm)	10 (mm)	11 (mm)
Pick	Quartzite	650.99	132.0	81.0	40.0	55.6	80.2	77.7	33.3	66.0	79.0	60.1	30.0
Pick	Quartzite	113.91	97.0	45.2	17.0	25.4	40.1	41.6	14.4	30.5	31.0	27.6	37.0
Biface	Quartzite	98.39	73.0	44.0	31.0	30.1	37.9	37.9	17.6	23.7	27.0	24.1	24.0
Biface	Quartzite	262.64	108.0	73.0	34.0	40.7	61.8	63.3	33.2	28.8	32.0	29.4	31.0
Handaxe	Quartzite	188.65	99.0	67.0	39.0	42.1	65.0	59.6	16.1	28.9	32.0	30.1	12.0
Handaxe	Quartzite	889.93	185.0	102.0	70.0	57.3	92.3	70.0	28.5	41.6	43.0	40.9	60.0
Handaxe	Siltstone	671.03	180.0	93.0	75.0	57.1	93.4	76.4	19.6	38.0	41.0	38.3	80.0
Handaxe	Siltstone	556.37	116.0	78.0	70.0	65.1	79.6	72.1	33.6	56.8	57.0	49.9	53.0

Type	Raw material	Weight (g)	1 (mm)	2 (mm)	3 (mm)	4 (mm)
Cleaver	Quartzite	521.37	118.0	84.0	48.1	50.0
Cleaver	Quartzite	274.42	95.0	72.0	38.0	70.3
Cleaver	Siltstone	596.94	154.0	89.0	108.7	40.0

Handaxe measurements
1: Maximum length (L)
2: Maximum width (W)
3: Location of maximum width
4: Width at upper fifth
5: Width at half length
6: Width at lower fifth
7: Thickness at upper fifth
8: Thickness at half length
9: Maximum thickness (T)
10: Thickness at lower fifth
11: Location of maximum thickness

Cleaver measurements
1: Maximum length (L)
2: Maximum width (W)
3: Edge length
4: Maximum thickness (T)

Table 8. Debris flow assemblage LCT technological measurements, by type and raw material (n=32).

Type	Raw material	Weight (g)	1 (mm)	2 (mm)	3 (mm)	4 (mm)	5 (mm)	6 (mm)	7 (mm)	8 (mm)	9 (mm)	10 (mm)	11 (mm)
Pick	Quartzite	303.35	102.0	59.0	38.0	43.4	54.1	58.1	35.1	44.5	46.0	40.2	30.0
Pick	Quartzite	94.58	77.0	51.0	30.0	33.2	50.6	40.2	16.7	25.1	25.1	16.8	27.0
Pick	Quartzite	226.57	116.0	67.0	49.0	42.0	66.6	50.5	21.7	37.5	41.0	33.8	40.0
Pick	Siltstone	529.86	124.0	90.0	60.0	45.8	86.2	62.6	29.7	48.0	49.0	40.5	42.0
Pick	Siltstone	279.16	113.0	67.0	30.0	31.9	60.8	69.3	18.8	27.7	37.0	35.9	15.0
Biface	Quartzite	67.86	64.5	47.5	25.0	27.0	44.7	46.9	15.5	23.4	23.4	19.9	27.0
Biface	Quartzite	97.28	63.0	52.0	30.0	43.5	53.4	49.9	16.8	26.3	27.0	25.7	10.0
Biface	Siltstone	381.57	123.0	81.5	61.0	56.5	81.1	51.2	27.1	33.6	34.0	23.2	68.0
Handaxe	Quartzite	483.06	140.0	86.5	77.0	63.3	84.2	81.7	17.9	32.7	36.0	34.0	28.0
Handaxe	Quartzite	150.05	73.0	70.0	27.0	43.3	64.0	68.0	19.6	23.9	30.0	29.5	13.0
Handaxe	Quartzite	151.32	97.0	68.0	40.0	41.0	64.1	61.6	10.6	21.9	25.0	21.8	22.0
Handaxe	Quartzite	72.42	80.0	50.0	20.0	27.3	47.5	46.0	11.4	16.0	16.0	13.4	37.0
Handaxe	Quartzite	411.77	143.0	82.5	50.0	46.0	66.4	69.8	22.3	44.4	46.5	35.7	77.0
Handaxe	Quartzite	110.71	83.0	57.0	40.0	37.2	56.5	47.2	20.2	25.0	25.0	18.2	50.0
Handaxe	Quartzite	133.93	79.0	50.0	11.0	35.4	46.5	49.2	22.7	30.6	30.6	28.4	10.0
Handaxe	Quartzite	247.85	103.0	76.0	35.0	44.9	70.6	63.5	23.5	27.6	28.0	25.7	40.0
Handaxe	Quartzite	98.36	74.0	51.5	35.0	30.8	51.7	46.6	16.2	24.1	25.0	24.2	26.0
Handaxe	Siltstone	642.98	155.0	80.0	99.0	57.7	82.0	61.7	26.0	49.2	50.0	49.2	38.0
Handaxe	Siltstone	448.50	112.0	83.0	52.0	54.8	81.2	60.3	29.6	41.0	41.0	38.1	45.0
Handaxe	Siltstone	533.71	133.0	88.5	75.0	51.0	84.8	52.3	31.4	44.8	44.8	38.4	57.0

Table 8 continued...

Type	Raw material	Weight (g)	1 (mm)	2 (mm)	3 (mm)	4 (mm)
Cleaver	Quartzite	703.02	141.0	89.0	38.1	61.0
Cleaver	Quartzite	104.82	77.0	50.0	45.2	24.0
Cleaver	Quartzite	226.85	113.0	71.0	39.8	28.0
Cleaver	Quartzite	234.98	102.5	72.0	39.8	32.0
Cleaver	Quartzite	429.26	132.0	80.0	29.2	41.0
Cleaver	Quartzite	415.11	113.0	80.0	32.7	53.0
Cleaver	Quartzite	188.98	100.0	65.0	27.6	30.0
Cleaver	Quartzite	236.20	100.0	73.0	39.1	35.0
Cleaver	Quartzite	415.83	106.0	68.0	31.5	55.5
Cleaver	Siltstone	550.67	127.0	97.0	39.9	49.0
Cleaver	Siltstone	497.36	120.0	80.0	64.4	45.0
Cleaver	Siltstone	578.98	140.0	89.0	60.8	42.0

Handaxe measurements
1: Maximum length (L)
2: Maximum width (W)
3: Location of maximum width
4: Width at upper fifth
5: Width at half length
6: Width at lower fifth
7: Thickness at upper fifth
8: Thickness at half length
9: Maximum thickness (T)
10: Thickness at lower fifth
11: Location of maximum thickness

Cleaver measurements
1: Maximum length (L)
2: Maximum width (W)
3: Edge length
4: Maximum thickness (T)

Table 9. Colluvial assemblage LCT size ratio data (W, L and T as in Tables 7 & 8).

Type	Raw material	Size ratio		
		W/L	L/W (elongation)	T/W (refinement)
Pick	Quartzite	0.61	1.63	0.98
Pick	Quartzite	0.47	2.15	0.69
Biface	Quartzite	0.60	1.66	0.61
Biface	Quartzite	0.68	1.48	0.44
Handaxe	Quartzite	0.68	1.48	0.48
Handaxe	Quartzite	0.55	1.81	0.42
Handaxe	Siltstone	0.52	1.94	0.44
Handaxe	Siltstone	0.67	1.49	0.73
Cleaver	Quartzite	0.71	1.40	0.60
Cleaver	Quartzite	0.76	1.32	0.98
Cleaver	Siltstone	0.58	1.73	0.45

Table 10. Debris flow assemblage LCT size ratio data (W, L and T as in Tables 7 & 8).

Type	Raw material	Size ratio		
		W/L	L/W (elongation)	T/W (refinement)
Pick	Quartzite	0.58	1.73	0.78
Pick	Quartzite	0.66	1.51	0.49
Pick	Quartzite	0.58	1.73	0.61
Pick	Siltstone	0.73	1.38	0.54
Pick	Siltstone	0.59	1.69	0.55
Biface	Quartzite	0.83	1.21	0.52
Biface	Quartzite	0.74	1.36	0.49
Biface	Siltstone	0.66	1.51	0.42
Handaxe	Quartzite	0.62	1.62	0.42
Handaxe	Quartzite	0.96	1.04	0.43
Handaxe	Quartzite	0.70	1.43	0.37
Handaxe	Quartzite	0.63	1.60	0.32
Handaxe	Quartzite	0.58	1.73	0.56
Handaxe	Quartzite	0.69	1.46	0.44
Handaxe	Quartzite	0.63	1.58	0.61
Handaxe	Quartzite	0.74	1.36	0.37
Handaxe	Quartzite	0.70	1.44	0.49
Handaxe	Siltstone	0.52	1.94	0.63
Handaxe	Siltstone	0.74	1.35	0.49
Handaxe	Siltstone	0.67	1.50	0.51

Table 10 continued...

Type	Raw material	Size ratio		
		W/L	L/W (elongation)	T/W (refinement)
Cleaver	Quartzite	0.63	1.58	0.69
Cleaver	Quartzite	0.65	1.54	0.48
Cleaver	Quartzite	0.63	1.59	0.39
Cleaver	Quartzite	0.70	1.42	0.44
Cleaver	Quartzite	0.61	1.65	0.51
Cleaver	Quartzite	0.71	1.41	0.66
Cleaver	Quartzite	0.65	1.54	0.46
Cleaver	Quartzite	0.73	1.37	0.48
Cleaver	Quartzite	0.64	1.56	0.82
Cleaver	Siltstone	0.76	1.31	0.51
Cleaver	Siltstone	0.67	1.50	0.56
Cleaver	Siltstone	0.64	1.57	0.47

Table 11. Additional LCT size data averages for the colluvial assemblage.

Colluvial assemblage (n=11)		Pick (n=2)	Biface (n=2)	Handaxe (n=4)		Cleaver (n=3)	
		Quartzite	Quartzite	Quartzite	Siltstone	Quartzite	Siltstone
Edge length (mm)	Min	-	-	-	-	38.00	108.70
	Median	-	-	-	-	43.05	-
	Max	-	-	-	-	48.10	108.70
	Mean	-	-	-	-	43.05	-
	SD	-	-	-	-	7.14	-
Location of max width (mm)	Min	17.00	31.00	39.00	70.00	-	-
	Median	28.50	32.50	54.50	72.50	-	-
	Max	40.00	34.00	70.00	75.00	-	-
	Mean	28.50	32.50	54.50	72.50	-	-
	SD	16.26	2.12	21.92	3.54	-	-
Width at upper fifth (mm)	Min	25.40	30.10	42.10	57.10	-	-
	Median	40.50	35.40	49.70	61.10	-	-
	Max	55.60	40.70	57.30	65.10	-	-
	Mean	40.50	35.40	49.70	61.10	-	-
	SD	21.35	7.50	10.75	5.66	-	-
Width at half length (mm)	Min	40.10	37.90	65.00	79.60	-	-
	Median	60.15	49.85	78.65	86.50	-	-
	Max	80.20	61.80	92.30	93.40	-	-
	Mean	60.15	49.85	78.65	86.50	-	-
	SD	28.35	16.90	19.30	9.76	-	-

Table 11 continued...

Colluvial assemblage (n=11)		Pick (n=2)	Biface (n=2)	Handaxe (n=4)		Cleaver (n=3)	
		Quartzite	Quartzite	Quartzite	Siltstone	Quartzite	Siltstone
Width at lower fifth (mm)	Min	41.60	37.90	59.60	72.10	-	-
	Median	59.65	50.60	64.80	74.25	-	-
	Max	77.70	63.30	70.00	76.40	-	-
	Mean	59.65	50.60	64.80	74.25	-	-
	SD	25.53	17.96	7.35	3.04	-	-
Thickness at upper fifth (mm)	Min	14.40	17.60	16.10	19.60	-	-
	Median	23.85	25.40	22.30	26.60	-	-
	Max	33.30	33.20	28.50	33.60	-	-
	Mean	23.85	25.40	22.30	26.60	-	-
	SD	13.36	11.03	8.77	9.90	-	-
Thickness at half length (mm)	Min	30.50	23.70	28.90	38.00	-	-
	Median	48.25	26.25	35.25	47.40	-	-
	Max	66.00	28.80	41.60	56.80	-	-
	Mean	48.25	26.25	35.25	47.40	-	-
	SD	25.10	3.61	8.98	13.29	-	-
Thickness at lower fifth (mm)	Min	27.60	24.10	30.10	38.30	-	-
	Median	43.85	26.75	35.50	44.10	-	-
	Max	60.10	29.40	40.90	49.90	-	-
	Mean	43.85	26.75	35.50	44.10	-	-
	SD	22.98	3.75	7.64	8.20	-	-
Location of max thickness (mm)	Min	30.00	24.00	12.00	53.00	-	-
	Median	33.50	27.50	36.00	66.50	-	-
	Max	37.00	31.00	60.00	80.00	-	-
	Mean	33.50	27.50	36.00	66.50	-	-
	SD	4.95	4.95	33.94	19.09	-	-

Table 12. Additional LCT size data averages for the debris flow assemblage.

Debris flow assemblage (n=32)		Pick (n=5)		Biface (n=3)		Handaxe (n=12)		Cleaver (n=12)	
		Quartzite	Siltstone	Quartzite	Siltstone	Quartzite	Siltstone	Quartzite	Siltstone
Edge length (mm)	Min	-	-	-	-	-	-	27.60	39.90
	Median	-	-	-	-	-	-	38.10	60.80
	Max	-	-	-	-	-	-	45.20	64.40
	Mean	-	-	-	-	-	-	35.89	55.03
	SD	-	-	-	-	-	-	5.87	13.23
Location of max width (mm)	Min	30.00	30.00	25.00	61.00	11.00	52.00	-	-
	Median	38.00	45.00	27.50	-	35.00	75.00	-	-
	Max	49.00	60.00	30.00	61.00	77.00	99.00	-	-
	Mean	39.00	45.00	27.50	-	37.22	75.33	-	-
	SD	9.54	21.21	3.54	-	18.91	23.50	-	-
Width at upper fifth (mm)	Min	33.20	31.90	27.00	56.50	27.30	51.00	-	-
	Median	42.00	38.85	35.25	-	41.00	54.80	-	-
	Max	43.40	45.80	43.50	56.50	63.30	57.70	-	-
	Mean	39.53	38.85	35.25	-	41.02	54.50	-	-
	SD	5.53	9.83	11.67	-	10.49	3.36	-	-
Width at half length (mm)	Min	50.60	60.80	44.70	81.10	46.50	81.20	-	-
	Median	54.10	73.50	49.05	-	64.00	82.00	-	-
	Max	66.60	86.20	53.40	81.10	84.20	84.80	-	-
	Mean	57.10	73.50	49.05	-	61.28	82.67	-	-
	SD	8.41	17.96	6.15	-	12.13	1.89	-	-
Width at lower fifth (mm)	Min	40.20	62.60	46.90	51.20	46.00	52.30	-	-
	Median	50.50	65.95	48.40	-	61.60	60.30	-	-
	Max	58.10	69.30	49.90	51.20	81.70	61.70	-	-
	Mean	49.60	65.95	48.40	-	59.29	58.10	-	-
	SD	8.98	4.74	2.12	-	12.73	5.07	-	-

Table 12 continued...

Debris flow assemblage (n=32)		Pick (n=5)		Biface (n=3)		Handaxe (n=12)		Cleaver (n=12)	
		Quartzite	Siltstone	Quartzite	Siltstone	Quartzite	Siltstone	Quartzite	Siltstone
Thickness at upper fifth (mm)	Min	16.70	18.80	15.50	27.10	10.60	26.00	-	-
	Median	21.70	24.25	16.15	-	19.60	29.60	-	-
	Max	35.10	29.70	16.80	27.10	23.50	31.40	-	-
	Mean	24.50	24.25	16.15	-	18.27	29.00	-	-
	SD	9.51	7.71	0.92	-	4.73	2.75	-	-
Thickness at half length (mm)	Min	25.10	27.70	23.40	33.60	16.00	41.00	-	-
	Median	37.50	37.85	24.85	-	25.00	44.80	-	-
	Max	44.50	48.00	26.30	33.60	44.40	49.20	-	-
	Mean	35.70	37.85	24.85	-	27.36	45.00	-	-
	SD	9.82	14.35	2.05	-	8.03	4.10	-	-
Thickness at lower fifth (mm)	Min	16.80	35.90	19.90	23.20	13.40	38.10	-	-
	Median	33.80	38.20	22.80	-	25.70	38.40	-	-
	Max	40.20	40.50	25.70	23.20	35.70	49.20	-	-
	Mean	30.27	38.20	22.80	-	25.66	41.90	-	-
	SD	12.09	3.25	4.10	-	7.21	6.32	-	-
Location of max thickness (mm)	Min	27.00	15.00	10.00	68.00	10.00	38.00	-	-
	Median	30.00	28.50	18.50	-	28.00	45.00	-	-
	Max	40.00	42.00	27.00	68.00	77.00	57.00	-	-
	Mean	32.33	28.50	18.50	-	33.67	46.67	-	-
	SD	6.81	19.09	12.02	-	20.65	9.61	-	-